CARBAPENEMASES IN GRAM-NEGATIVE BACTERIA: A GLOBAL HEALTH THREAT AND THERAPEUTIC CHALLENGE

EDITED BY: Mullika Traidej Chomnawang, Che-Hsin Lee and Mary Marquart
PUBLISHED IN: Frontiers in Microbiology

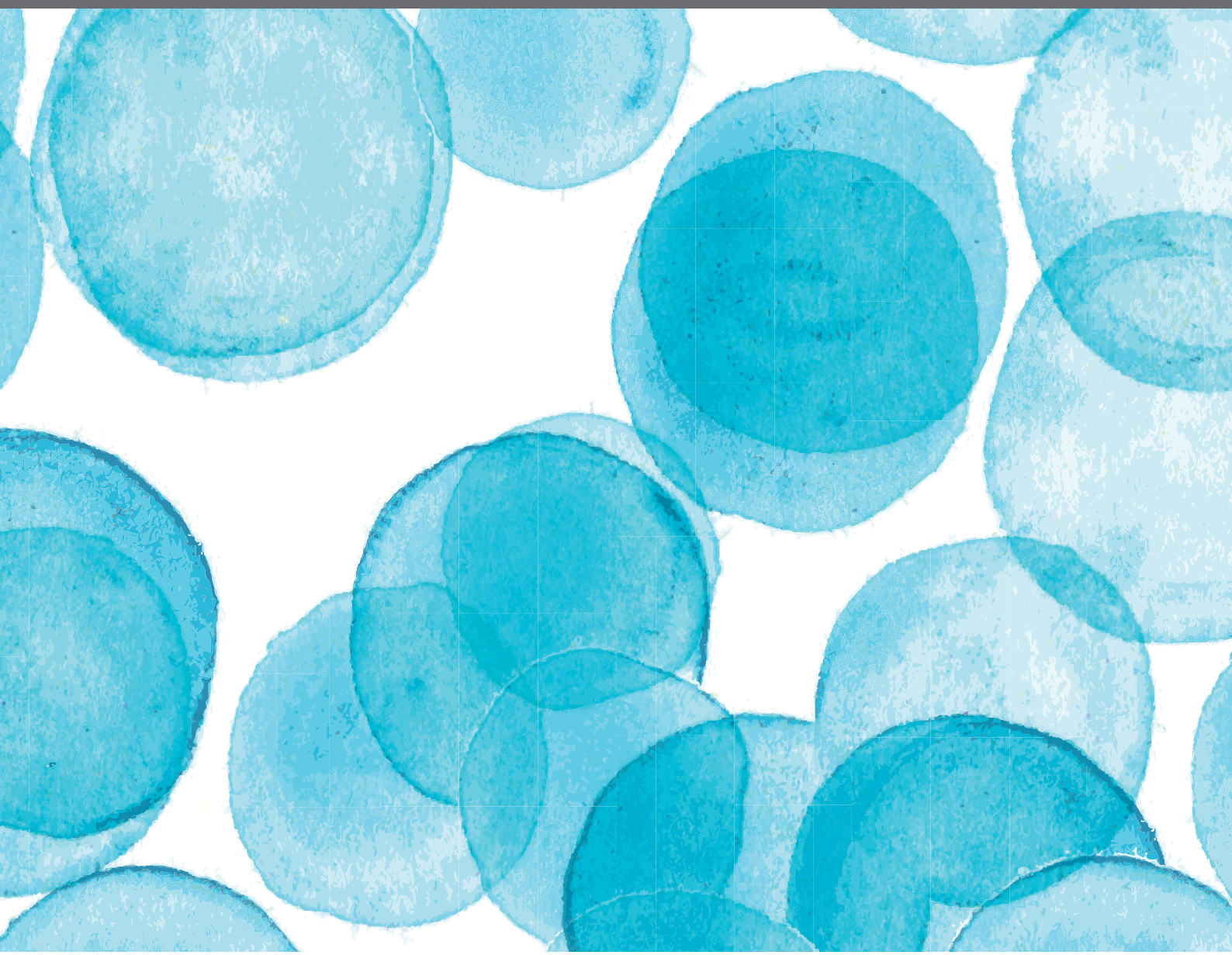

frontiers Research Topics

ISSN 1664-8714
ISBN 978-2-88976-415-0
DOI 10.3389/978-2-88976-415-0

About Frontiers

Frontiers is more than just an open-access publisher of scholarly articles: it is a pioneering approach to the world of academia, radically improving the way scholarly research is managed. The grand vision of Frontiers is a world where all people have an equal opportunity to seek, share and generate knowledge. Frontiers provides immediate and permanent online open access to all its publications, but this alone is not enough to realize our grand goals.

Frontiers Journal Series

The Frontiers Journal Series is a multi-tier and interdisciplinary set of open-access, online journals, promising a paradigm shift from the current review, selection and dissemination processes in academic publishing. All Frontiers journals are driven by researchers for researchers; therefore, they constitute a service to the scholarly community. At the same time, the Frontiers Journal Series operates on a revolutionary invention, the tiered publishing system, initially addressing specific communities of scholars, and gradually climbing up to broader public understanding, thus serving the interests of the lay society, too.

Dedication to Quality

Each Frontiers article is a landmark of the highest quality, thanks to genuinely collaborative interactions between authors and review editors, who include some of the world's best academicians. Research must be certified by peers before entering a stream of knowledge that may eventually reach the public - and shape society; therefore, Frontiers only applies the most rigorous and unbiased reviews.
Frontiers revolutionizes research publishing by freely delivering the most outstanding research, evaluated with no bias from both the academic and social point of view. By applying the most advanced information technologies, Frontiers is catapulting scholarly publishing into a new generation.

What are Frontiers Research Topics?

Frontiers Research Topics are very popular trademarks of the Frontiers Journals Series: they are collections of at least ten articles, all centered on a particular subject. With their unique mix of varied contributions from Original Research to Review Articles, Frontiers Research Topics unify the most influential researchers, the latest key findings and historical advances in a hot research area! Find out more on how to host your own Frontiers Research Topic or contribute to one as an author by contacting the Frontiers Editorial Office: frontiersin.org/about/contact

CARBAPENEMASES IN GRAM-NEGATIVE BACTERIA: A GLOBAL HEALTH THREAT AND THERAPEUTIC CHALLENGE

Topic Editors:
Mullika Traidej Chomnawang, Mahidol University, Thailand
Che-Hsin Lee, National Sun Yat-sen University, Taiwan
Mary Marquart, University of Mississippi Medical Center, United States

Citation: Chomnawang, M. T., Lee, C.-H., Marquart, M., eds. (2022). Carbapenemases in Gram-negative Bacteria: A Global Health Threat and Therapeutic Challenge. Lausanne: Frontiers Media SA.
doi: 10.3389/978-2-88976-415-0

Table of Contents

frontiers in Microbiology

ORIGINAL RESEARCH
published: 28 May 2021
doi: 10.3389/fmicb.2021.670202

A Potential High-Risk Clone of *Pseudomonas aeruginosa* ST463

Yanyan Hu[1†], Wenjing Peng[2†], Yifan Wu[2], Hui Li[3], Qi Wang[1], Huahua Yi[4], Rong Zhang[1], Bing Shao[3] and Kui Zhu[2*]*

[1] Clinical Microbiology Laboratory, The Second Affiliated Hospital of Zhejiang University, School of Medicine, Zhejiang University, Hangzhou, China, [2] National Center for Veterinary Drug Safety Evaluation, College of Veterinary Medicine, China Agricultural University, Beijing, China, [3] Beijing Key Laboratory of Diagnostic and Traceability Technologies for Food Poisoning, Beijing Center for Disease Prevention and Control, Beijing, China, [4] Department of Respiratory and Critical Care Medicine, Ruijin Hospital, Shanghai Jiao Tong University School of Medicine, Shanghai, China

Pseudomonas aeruginosa is one of the most common opportunistic pathogens, which causes severe nosocomial infections because of its well-known multidrug-resistance and hypervirulence. It is critical to curate routinely the epidemic *P. aeruginosa* clones encountered in the clinic. The aim of the present study was to investigate the connection between virulence factors and antimicrobial resistance profiles in epidemic clones. Herein, we found that ST463 (O4), ST1212 (O11), and ST244 (O5) were prevalent in 30 isolates derived from non-cystic fibrosis patients, based on multilocus sequence type (MLST) and serotype analysis. All isolates were multidrug-resistant (MDR) and each was resistance to at least three classes of antibiotics in antimicrobial susceptibility tests, which was consistent with the presence of the abundant resistance genes, such as bla_{OXA-50}, bla_{PAO}, *aph*(3′), *catB7*, *fosA*, *crpP*, and bla_{KPC-2}. Notably, all bla_{KPC-2} genes were located between IS*Kpn6*-like and IS*Kpn8*-like mobile genetic elements. In addition, classical exotoxins encoded by *exoU*, *exoS*, and *pldA* were present in 43.44% (13/40), 83.33% (25/30), and 70% (21/30) of the isolates, respectively. The expression of *phz* operons encoding the typical toxin, pyocyanin, was observed in 60% of isolates (18/30) and was quantified using triple quadrupole liquid chromatograph mass (LC/MS) assays. Interestingly, compared with other MLST types, all ST463 isolates harbored *exoU*, *exoS* and *pldA*, and produced pyocyanin ranging from 0.2 to 3.2 μg/mL. Finally, we evaluated the potential toxicity of these isolates using hemolysis tests and *Galleria mellonella* larvae infection models. The results showed that ST463 isolates were more virulent than other isolates. In conclusion, pyocyanin-producing ST463 *P. aeruginosa*, carrying diverse virulence genes, is a potential high-risk clone.

Keywords: hypervirulence, multi-drug resistance, pyocyanin, ST463, *Pseudomonas aeruginosa*

OPEN ACCESS

Edited by:
Mary Marquart, University of Mississippi Medical Center, United States

Reviewed by:
Rodolpho M. Albano, Rio de Janeiro State University, Brazil
Anusak Kerdsin, Kasetsart University, Thailand

***Correspondence:**
Bing Shao
shaobingch@sina.com
Kui Zhu
zhuk@cau.edu.cn

[†] These authors have contributed equally to this work

Specialty section:
This article was submitted to Antimicrobials, Resistance and Chemotherapy, a section of the journal Frontiers in Microbiology

Received: *20 February 2021*
Accepted: *20 April 2021*
Published: *28 May 2021*

Citation:
Hu Y, Peng W, Wu Y, Li H, Wang Q, Yi H, Zhang R, Shao B and Zhu K (2021) A Potential High-Risk Clone of Pseudomonas aeruginosa ST463. Front. Microbiol. 12:670202. doi: 10.3389/fmicb.2021.670202

INTRODUCTION

Pseudomonas aeruginosa is one of the most common gram-negative pathogens and is associated with ubiquitously acute and chronic infections, especially cystic fibrosis (Ji et al., 2013). The worldwide spread of *P. aeruginosa* poses a threat to global public health (Tacconelli et al., 2018). *P. aeruginosa* exhibits various mechanisms of antimicrobial resistance, including the use of efflux pumps, biofilm formation, an impermeable outer membrane, an adaptable genome,

antibiotic-inactivating enzymes, mobile resistance genes, and target mutations (Curran et al., 2018; Horcajada et al., 2019; Zhu et al., 2019). Recently, the increasing incidence of multidrug resistance (MDR), particularly for carbapenems, has induced a new crisis involving nosocomial *P. aeruginosa* infections (Curran et al., 2018; Horna et al., 2019).

Various virulence factors have been demonstrated to contribute to *P. aeruginosa* infection. For example, type III effectors (exotoxins ExoS, ExoT, ExoY, and ExoU), type VI effectors (PldA), adherence factors (type IV pili, flagella), alginate, elastase, and biosurfactant rhamnolipid (Karatuna and Yagci, 2010; Boulant et al., 2018; Luo et al., 2019) play crucial roles in mortality (Juan et al., 2017). It should be noted that ExoU-positive *P. aeruginosa* is more likely to be resistant to multiple antibiotics, such as carbapenems, cephalosporins, fluoroquinolones, and aminoglycosides (Hu et al., 2017), which further exacerbates infections and increases mortality (Horna et al., 2019). Interestingly, *exoU* has been reported to be mutually exclusive with *exoS*, a common gene in *P. aeruginosa* (Vareechon et al., 2017). Nevertheless, the coexistence of *exoS* and *exoU* enhances antibiotic resistance in *P. aeruginosa* (Horna et al., 2019). Moreover, pyocyanin, belonging to the family of phenazines, is the key virulence factor in *P. aeruginosa*. Pyocyanin is synthesized from chorismic acid through a series of biosynthetic enzymes encoded by the *phz* gene cluster (**Supplementary Figure 1**). Previous studies showed that pyocyanin can not only promote the pathogenicity to host cells by disrupting electron transport, cellular respiration, and energy metabolism (Rada and Leto, 2013), but also modulates bacterial physiology, such as survival, iron acquisition, biofilm formation, and antibiotic tolerance (Chincholkar and Thomashow, 2014; Zhu et al., 2019).

Recently, numerous epidemic *P. aeruginosa* strains have been described worldwide. For instance, ST175, ST235, and ST111 are high-risk clones with MDR profiles, among which ST235 is highly associated with *exoU* (Cholley et al., 2014). Infections caused by such strains often have a worse prognosis than infections with other strains. The combination of MDR and virulence factors always restricts the implementation of therapeutic options, thus there is an urgent need to investigate resistance and virulence characteristics to combat *P. aeruginosa* infections. The misuse and overuse of antibiotics, serving as a dominant driving force of resistance, might further shape the evolutionary trajectory of *P. aeruginosa* in the clinic and the environment. To date, the correlations between the presences of virulence factors, antibiotic resistance, and the genotype of *P. aeruginosa* in non-cystic fibrosis patients remain unclear. The present work investigated and characterized epidemic clones in a non-outbreak situation to shed light on the treatment options for *P. aeruginosa*-associated infections.

MATERIALS AND METHODS

Bacterial Isolation

Thirty *P. aeruginosa* isolates were collected from 30 non-CF patients from the Second Affiliated Hospital of Zhejiang University School of Medicine from 2009 to 2018. The Second Affiliated Hospital of Zhejiang University School of Medicine is a general hospital with 3,200 beds, in which carbapenem-resistant *P. aeruginosa* (CRPA) had reached to 38.9% according to recent hospital surveillance. Thirty CRPA strains were randomly chosen from our previously sequenced genomes based on the sample source, isolation time, virulence factor, sequence type (ST), and carbapenemase genes. Specifically, the isolates were collected from sputum (n = 13), CVC (central vascular catheter, n = 3), blood (n = 3), urine (n = 3), feces (n = 3), pus (n = 4), and one sample with an unknown source. Detailed clinical information is shown in **Supplementary Table 1**. Before the experiments, all the isolates were re-identified using Matrix-assisted laser desorption/ionization-time of flight mass spectrometry (Bruker Daltonics, Billerica, MA, United States).

Antimicrobial Susceptibility Testing

All isolates were tested with 16 kinds of antimicrobials, including aminoglycosides (amikacin, gentamicin, and tobramycin), β-lactam combination agents (ceftazidime-avibactam, cefoperazone-sulbactam, and piperacillin-tazobactam), cephems (ceftazidime, cefepime), monobactam (aztreonam), carbapenems (imipenem, meropenem), polymyxin (colistin, polymyxin B), and fluoroquinolones (ciprofloxacin, levofloxacin, and lomefloxacin). The minimum inhibitory concentrations (MICs) of the isolates were determined using the classic micro-broth dilution method following the operations in the Clinical and Laboratory Standards Institute's performance standards (CLSI M100-S29) (Wayne, 2019). *P. aeruginosa* strain ATCC 27853 was chosen as a standard control for the antimicrobial susceptibility tests.

Extraction of Pyocyanin

P. aeruginosa isolates were cultured on Luria-Bertani (LB) agar plates for 12 h, after which a single colony was selected for culture in LB broth at 37°C with 200 rpm shaking for 16 h. After centrifugation 13,000 × *g*, the supernatant was collected, extracted twice with chloroform (5:3 v/v), and vortexed. The chloroform phase was kept after centrifugation (5,000 × *g*, 10 min) and mixed with 0.2 M HCl (3:1 v/v). The red phase was collected after centrifugation (5,000 × *g*, 10 min), extracted with one-third the volume of chloroform containing $NaHCO_3$, and the chloroform phase (blue) was collected (El-Zawawy and Ali, 2016). The extract was dissolved with 90% acetonitrile for high performance liquid chromatography (HPLC)-mass spectrometry (MS) detection. The HPLC-MS apparatus (Shimadzu, HPLC/MS-8045, Kyoto, Japan) was equipped with a Shim-pack GIST-HP C18 column (2.1 mm × 50 mm, 3 μm, Shimadzu) at an oven temperature of 35°C and a flow-rate of 0.3 mL/min. The gradient program was applied with the mobile phase consisting of solvent A (0.1% formic acid in acetonitrile) and solvent B (0.1% formic acid in water) as follows: 95–70% of B for 0–5.00 min, 70–50% of B for 5.00–5.10 min, 50–30% of B for 5.10–7.10 min, 30–0% of B for 7.10–11.10 min, held at 0% B for 11.10–13.00 min, 0–95% of B for 13.00–14.00 min, and maintained at 95% B for 14.00–16.00 min. The positive electrospray ionization

(ESI+) mode was chosen to analyze pyocyanin. The MS parameters for pyocyanin are shown in **Supplementary Table 2**. The MS acquisition parameters used were as follows: gas temperature, 300°C; drying gas, 10 L/min; heating Gas, 10 L/min; DL Temperature, 250°C; heat block temperature, 400°C; second pole collision gas, argon gas; and CID gas volt, 17 kPa.

Toxicity Evaluation

P. aeruginosa isolates were incubated in brain heart infusion (BHI) agar containing 5% sheep blood for hemolytic experiments. Virulence genes were analyzed by using BLAST software (SRST2 Toolkit version 0.2.0; Inouye et al., 2014), and the database of virulence genes at the NCBI. The virulence of *P. aeruginosa* isolates was evaluated *in vivo* using the *Galleria mellonella* larval infection model, and eight strains (1615, 1802, E211-2, 1608, 1617, 1104, ZR16, and 1109) were selected to analyze their characteristics. Strains 1617 (ST1212), 1104 (ST244), ZR16 (ST463), and 1109 (ST463) are pyocyanin-producing isolates, and 1615 (ST1076), 1608 (ST1212), 1802 (ST1212), and E211-2 (ST274) are pyocyanin-negative isolates. PA14 was used as a reference strain for pyocyanin expression, and its mutant ΔPA (*phz* genes cluster deleted) (Dietrich et al., 2013) was used as a negative control to evaluate the contribution of pyocyanin to the pathogenicity of *P. aeruginosa*. To prepare the inoculum, bacteria were grown for 12 h at 37°C with 200 rpm shaking, washed in sterile phosphate-buffered saline (PBS) after centrifugation at 3,000 × *g*, and then adjusted to a final concentration of 10^5 colony forming units (CFU)/mL using a Nephelometer (Merieux, Nürtingen, Germany). A 10 μL aliquot of suspended strains (10^3 CFU of bacteria) was injected into each larva and incubated at 37°C. Larvae were considered as dead if they did not respond to touch. The survival rates of *G. mellonella* larvae were recorded. The statistical analysis in this study is performed using GraphPad Prism 8 (GraphPad Inc., La Jolla, CA, United States). Continuous variables were described using the mean ± SD and categorical variables as the number (percentage). *T*-tests were conducted to assess the normal distribution of continuous data, while the Chi-squared or Fisher's exact test were used to assess the categorical data. A *P*-value < 0.05 was considered statistically significant.

DNA Extraction and Genetic Analysis

Genomic DNA of all 30 isolates was extracted using a Wizard genomic DNA purification kit (Promega, Beijing, China) according to the manufacturer's instructions. The genomic DNA was then sequenced using the Illumina HiSeq X10 platform (Illumina, San Diego, CA, United States) with the 150-bp paired-end strategy. Raw reads were trimmed and assembled to contigs using SPAdes version 3.11.1 (Bankevich et al., 2012). Assembled contigs were analyzed *via* the Center for Genomic Epidemiology website to screen for the presence of acquired antimicrobial resistance genes (ARGs)[1] (Boolchandani et al., 2019). The multilocus sequence type (MLST)[2] (Larsen et al., 2012) and serotype[3] (Thrane et al., 2016) were also determined. Virulence-associated genes and mobile genetic elements (MGEs) were collected from the NCBI database and were identified using SRST2 Toolkit version 0.2.0. The genomes of the 27 pyocyanin-producing isolates were obtained from the *Pseudomonas* Genome Database[4]. The phylogenetic tree was analyzed using Parsnp in the Harvest package based on the core genome sequences of the eight *P. aeruginosa* ST463 strains (Schürch et al., 2018). The tree was then visualized using the online tool iTOL (Cui et al., 2020).

RESULTS

Clinical Characteristics of *P. aeruginosa* Isolates

MLST and serotype analysis revealed that all the isolates belonged to 14 MLST types: ST463 (8/30), ST244 (4/30), ST1212 (4/30), ST1076 (3/30), ST274 (2/30), ST769 (1/30), ST782 (1/30), ST3080 (1/30), ST235 (1/30), ST836 (1/30), ST260 (1/30), ST2438 (1/30), ST494 (1/30), and ST508 (1/30); and six serotypes: O5 (5/30), O6 (4/30), O10 (1/30), O11 (8/30), O3 (4/30), and O4 (8/30). The most prevalent ST type was ST463 (8/30), followed by ST1212 (4/30) and ST244 (4/30). Consistent with previous observations (Parkins et al., 2018; Horcajada et al., 2019), *P. aeruginosa* ST463 strains were associated with serotype O4, while ST244 was associated with serotype O5. The connections between serotypes and STs in other isolates are displayed in **Supplementary Table 1**. These data indicated that the sequence diversity of *P. aeruginosa* clones was high among the patients.

Antimicrobial Resistance

Among all *P. aeruginosa* isolates, the antimicrobial resistance rates of ceftazidime-avibactam, cefoperazone-sulbactam, piperacillin-tazobactam, ceftazidime, cefepime, aztreonam, imipenem, meropenem, ciprofloxacin, levofloxacin, and lomefloxacin were 3.33% (1/30), 96.67% (29/30), 76.67% (23/30), 66.67% (20/30), 80% (24/30), 73.33% (22/30), 90% (27/30), 86.67% (26/30), 56.67% (17/30), 70% (21/30), and 96.67% (29/30), respectively (**Table 1** and **Figure 1A**). Generally, there was a high proportion of resistance against the combinations of β-lactams because of the presence of intrinsic resistant genes $bla_{\mathrm{OXA-50}}$ and bla_{PAO}. Remarkably, carbapenem-resistance genes ($bla_{\mathrm{KPC-2}}$, $bla_{\mathrm{GES-1}}$, and $bla_{\mathrm{IMP-9}}$) were identified in 60% of the isolates (18/30, comprising 16 $bla_{\mathrm{KPC-2}}$, 1 $bla_{\mathrm{GES-1}}$, and 1 $bla_{\mathrm{IMP-9}}$) (**Figure 1B**). In all 16 strains, bla_{KPC} was flanked by IS*Kpn6*-like and IS*Kpn8* mobile genetic elements (MGEs). In addition, aminoglycoside-resistance genes [*aph*(3′) or *aac*(3)-IId, *aac*(6′)-IIb] were present in all isolates. The fluoroquinolone-resistance gene (*crpP*) was harbored by 63.33% of the isolates (19/30). In addition, some MGEs, such as *intI*1,

[1]https://cge.cbs.dtu.dk/services/ResFinder/

[2]https://cge.cbs.dtu.dk/services/MLST/

[3]https://cge.cbs.dtu.dk/services/PAst-1.0/

[4]http://www.pseudomonas.com

TABLE 1 | Antibiotic susceptibility profiles of *P. aeruginosa*.

Antimicrobial agents	MIC range (μg/mL)	MIC_{50} (μg/mL)	MIC_{90} (μg/mL)	Susceptible %	Intermediate %	Resistant %
AMK	0.5– > 64	2	>64	80.00	3.33	16.67
GM	1– > 64	2	>64	73.33	0	26.67
TOB	≤0.25– > 128	≤0.25	>128	73.33	0	26.67
CZA	≤1/4–128/4	4/4	8/4	96.67	0	3.33
SCF	8/4– > 256/4	256/4	>256/4	0	3.33	96.67
TZP	≤8/4– > 256/4	256/4	>256/4	13.33	10	76.67
CAZ	≤4–256	64	128	26.67	6,67	66.67
FEP	≤4– > 256	256	>256	10	10	80
ATM	≤8– > 256	256	>256	13.33	13.33	73.33
IMP	4– > 256	128	>256	0	10	90
MEM	2– > 256	128	>256	10.00	3.33	86.67
CST	1–4	1	2	96.67	0	3.33
PB	1–4	1	2	96.67	3.33	0
CIP	0.125–32	4	16	36.67	6.67	56.67
LEV	≤0.5–64	8	64	10	20	70
LOM	1– > 32	32	>32	3.33	0	96.67

AMK, amikacin; GM, gentamicin; TOB, tobramycin; CZA, ceftazidime-avibactam; SCF, cefperazone-sulbactam; TZP, piperacillin-tazobactam; CAZ, ceftazidime; FEP, cefepime; ATM, aztreonam; IMP, imipenem; MEM, meropenem; CST, colistin; PB, polymyxin B; CIP, ciprofloxacin; LEV, levofloxacin; LOM, lomefloxacin.

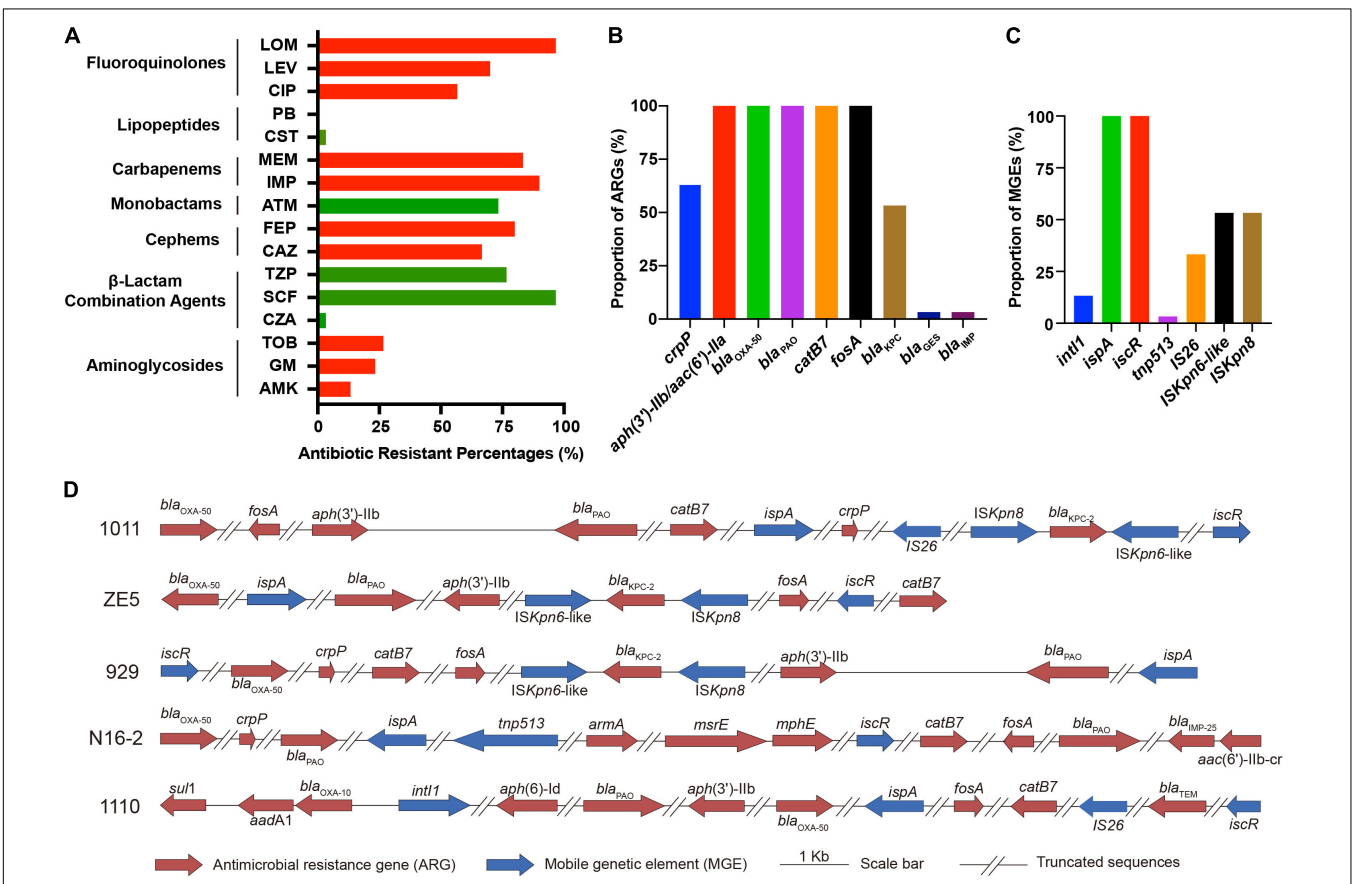

FIGURE 1 | Phenotypical and genetic profiles of antimicrobial resistance in *P. aeruginosa* isolates. **(A)** Antibiotic resistance profiles. Proportion of antimicrobial resistance genes (ARGs) **(B)** and mobile genetic elements (MGEs) **(C)** in the isolates. **(D)** Schematic diagram of representative ARGs and MGEs in five isolates. The bla_{KPC-2} genes in *P. aeruginosa* 1011, ZE5, and 929 are surrounded by IS*Kpn6*-like, IS*Kpn8*, and other MGEs (*ispA*, *iscR*). *P. aeruginosa* N16-2 harbors MGEs *ispA*, *tnp513*; and *P. aeruginosa* 1110 harbors *intI1*, IS*26*, *iscR*. All strains share similar patterns.

ispA, *iscR*, *tnp513*, and IS*26* were associated with diverse ARGs (**Figures 1C,D**).

Virulence Factors

To determine the toxin-producing capacity of these isolates, we first carried out hemolysis tests, which showed that 33.33% of the isolates (10/30) displayed β-hemolysis (**Figure 2B**). Subsequently, we performed further characterization of the virulence in these isolates based on whole-genome sequencing analysis. The main virulence factors included mucoid related alginate (*algA*), T3SS effectors (*toxA*, *exoS*, *exoT*, *exoU*, and *exoY*), adherence factors (flagella, *fliC*, and *fliA*), quorum sensing gene (*lasI*), Type IV pili (*pil*P), rhamnolipid (*rhlA*), phenazine biosynthetic genes (*phzA-H*, *phzM*, and *phzS*), and the T6SS effector (*pldA*). All strains harbored *exoT*, *pilP*, *rhlA*, and *algA*, and 96.67% (29/30) of the strains carried *exoY*. Meanwhile, the prevalence rates of other factors, such as *lasI*, *toxA*, *exoS*, *fliC*, and *fliA* were 90, 80, 83.33, 73.33, and 86.67%, respectively (**Figure 2A**), suggesting that such genes are probably related to bacterial colonization and pathogenesis. Additionally, *exoU* and *pldA* were identified in 43.33% (13/30) and 70% (21/30) of the strains, respectively (**Figure 2C**). Intriguingly, all ST463 (O4) strains possessed exotoxin genes *exoU*, *exoS*, and *pldA*. Finally, 60% (18/30) of the strains produced pyocyanin *in vitro*, ranging from 0.02 to 3.2 μg/mL, based on triple quadrupole liquid chromatograph mass (LC/MS) analysis (**Supplementary Figure 2** and **Supplementary Table 2**). Remarkably, all ST463 strains expressed high levels of pyocyanin (0.2–3.2 μg/mL), with an average of 1.48 μg/mL. Therefore, we deduced that ST463 (O4) might be a potential high-risk *P. aeruginosa* clone because of its high production of pyocyanin.

To explore whether there are any relationships between ST types and pyocyanin production in *P. aeruginosa*, we collected 27 genomes of pyocyanin-positive isolates from the *Pseudomonas* Genome Database (**Supplementary Table 3**.). We found that there was no common ST type that produced pyocyanin (**Table 2**). Taken together, these results suggested a positive connection between pyocyanin production and ST463-type *P. aeruginosa* strains.

To further evaluate the virulence potential of ST463, particularly the contribution of pyocyanin to survival rates, eight clinical isolates, 1615, 1802, E211-2, 1608, 1617, 1104, ZR16, and 1109 with different pyocyanin production levels, were used to challenge *G. mellonella* larvae. *P. aeruginosa* PA14, with high pyocyanin production and its mutant, *P. aeruginosa* ΔPA, with the deletion of pyocyanin producing *phz* genes (Zhu et al., 2019), were used as reference strains. We observed that the isolates that produced high levels of pyocyanin (*P. aeruginosa* 1617, 1104, ZR16, and 1109) induced higher mortality than those without pyocyanin production (*P. aeruginosa* 1615, 1802, E211-2, and 1608) (**Figure 2D**). This was in agreement with the finding that *P. aeruginosa* PA14 was more toxic to the larvae than *P. aeruginosa* ΔPA, indicating that pyocyanin plays an important role in the pathogenicity of *P. aeruginosa*-associated infections. Notably, the ST463 type isolates (*P. aeruginosa* ZR16 and 1109) exhibited higher virulence than *P. aeruginosa* PA14 and the other clinical isolates tested in this study. Altogether, these findings demonstrated that

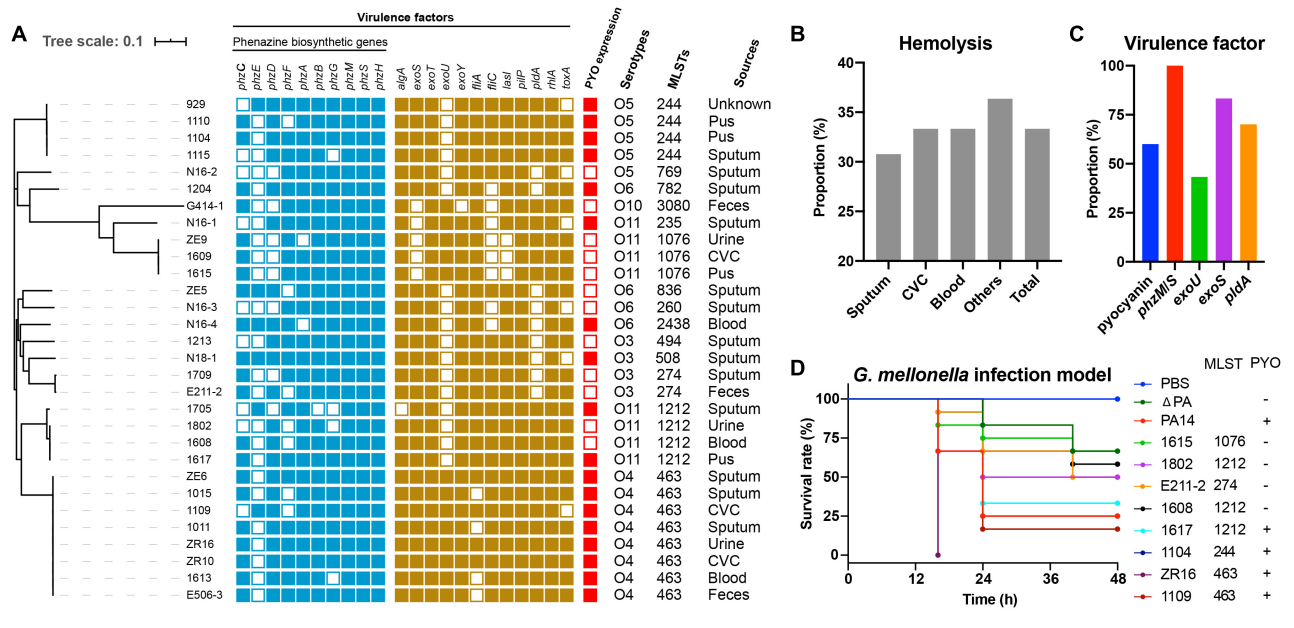

FIGURE 2 | Assessment of the potential toxicity of *P. aeruginosa* isolates. **(A)** Phylogenetic tree and characteristics of all isolates. CVC, Central Venous Catheter; **(B)** Hemolysis proportion of different sampling sources. **(C)** The proportion of antimicrobial resistance-associated virulence factors, such as biosynthetic genes, *exoU*, *exoS*, *pldA*; and pyocyanin expression. **(D)** Larval survival rates in the *G. mellonella* infection model. Each isolate was challenged with 12 larvae for 48 h, with three biological replicates.

P. aeruginosa ST463, with high pyocyanin production, is a high-risk clone in patients, suggesting that more attention should be paid to the control of the dissemination of such clones in the clinic.

TABLE 2 | Information of pyocyanin-producing *P. aeruginosa* strains.

Strains	MLST	Source	Year	References
U018A	852	CF patient	2003	Cullen et al., 2015
2192	9	CF patient	2008	Cullen et al., 2015
39177	27	Cornea	2011	Cullen et al., 2015
Pr335	27	Hospital environment	1997	Cullen et al., 2015
M10	549	Surface water	2014	Cullen et al., 2015
AMT0023-30	1,394	CF patient	2010	Cullen et al., 2015
IST27	Unknown	CF patient	1996	Cullen et al., 2015
89	1,822	CF patient	2009	Caldwell et al., 2009
ID4365	560	Soil	2008	Rane et al., 2008
148	Unknown	Dolphin, gastric juice	2014	Grosso-Becerra et al., 2014
A5803	1,567	Pneumonia patient	2007	Cullen et al., 2015
LMG14084	316	Water	1960–1964	Cullen et al., 2015
39016	2,613	Cornea	2011	Cullen et al., 2015
40	2,238	CF patient	2009	Cullen et al., 2015
LES400	146	CF patient	2002	Cullen et al., 2015
LESB58	146	CF patient	1998	Cullen et al., 2015
M18	1,239	Rhizosphere	2005	Li et al., 2008
17	179	CF patient	2009	Caldwell et al., 2009
KK1	155	CF patient	2012	Cullen et al., 2015
57P31PA	274	COP patient	2009	Cullen et al., 2015
679	198	Non-CF patient, Urine	2011	Cullen et al., 2015
C3719	Unknown	CF patient	2000	Cullen et al., 2015
DK2	386	CF patient	1973	Cullen et al., 2015
TBCF10839	234	CF patient	2013	Cullen et al., 2015
1709-12	111	Non-CF patient	2004	Cullen et al., 2015
AMT0060-1	111	CF patient	2010	Cullen et al., 2015
AMT0060-3	111	CF patient	2010	Cullen et al., 2015

MLST, multilocus sequence type; CF, cystic fibrosis; COP, chronic obstructive pulmonary; CVC, central venous catheter.

DISCUSSION

The increasing prevalence of chronic and hospital-acquired infections produced by MDR or extensively drug resistant (XDR) *P. aeruginosa* strains is associated with the increasing prevalence of transferable resistance determinants, particularly against carbapenemases and extended-spectrum β-lactamases (ESBLs) (Oliver et al., 2015). In this study, high proportions of antibiotic resistance (66.67–96.67% to the combinations of β-lactams, except CZA; 86.67–90% to carbapenems, 56.67–96.67% to fluoroquinolones, 66.67–80% to cephems, and 73.33% to monobactams) were mainly caused by the presence of multiple resistance genes. CZA is a novel approved combination in China in 2019, which is used to treat severe infections associated with CRPA. CZA is inactive against metallo-β-lactamases-producing stains, while is quite active against KPC-producing isolates (Horcajada et al., 2019). Our results confirmed that the bla_{IMP}-positive isolate (N16-2) is the only CZA-resistant strain among the *P. aeruginosa* isolates tested. Given the extensive usage of CZA, CZA-resistant KPC-producing *Klebsiella pneumoniae* has been reported in different countries, caused by a point mutation of the bla_{KPC-2} gene (Gaibani et al., 2019; Hemarajata and Humphries, 2019). Therefore, it is crucial to identify the resistance mechanism before the regimens to improve antibiotic efficacy are considered. The widespread carbapenemases are metallo-β-lactamases of VIM- (Verona imipenemase) and IMP- (imipenemase) types in *P. aeruginosa* (Boulant et al., 2018). Notably, there were 16 KPC-strains (KPC-2) among the 18 carbapenemase-producing isolates in our study, which was consistent with our previous findings that *P. aeruginosa*, especially ST463, is a new carrier of bla_{KPC-2} surrounded by the MGEs IS*Kpn6*-like and IS*Kpn8* (Hu et al., 2015).

Epidemic outbreaks of *P. aeruginosa* MDR/XDR high-risk clones within hospital environments typically belong to ST111 (serotype O11), ST175 (serotype O4), and ST235 (serotype O12) (Horcajada et al., 2019). ST235 has been identified worldwide as being associated with $exoS^{-}/exoU^{+}$ (Maatallah et al., 2011) and the carbapenemases VIM, IMP, FIM, and NDM (Maatallah et al., 2011; Juan et al., 2017). Frequently, ST175 is observed to be a producer of VIM-2, whereas ST111 can produce KPC-2 carbapenemase (Oliver et al., 2015). Compared with these MDR/XDR isolates, ST244 is another large clonal complex frequently detected globally (Oliver et al., 2015; Horcajada et al., 2019). Our collection contained one ST235 and four ST244 isolates, while ST463 is the most prevalent clone associated with serotype O4. Although *exoS* and *exoU* are often mutually exclusive (Vareechon et al., 2017), we identified the coexistence of *exoS* and *exoU* in all eight ST463 strains. Together with the observation that all ST463 strains produce high levels of pyocyanin and cause high toxicity in infection models, these results suggested that clinical ST463 *P. aeruginosa* is probably a high-risk clone that might cause serious threats to human health because of its integrated MDR and virulence factors.

CONCLUSION

The present study indicated that clinical *P. aeruginosa* poses a potential threat to human health because of the presence of multiple virulence factors and antibiotic resistance genes. The results suggested that the strain ST463 most likely emerged as a hypervirulent clone of *P. aeruginosa* as a result of a unique combination of pyocyanin production and virulence genes, including *exoU*$^{+}$/*exoS*$^{+}$, and *pldA*. Additionally, our study proves that the utility of genome sequencing in understanding and monitoring the epidemiology of clinically significant nosocomial clones, which will lead to improved control strategies. Nevertheless, the dissemination, evolution, and fitness cost of clone ST463 remain unclear.

DATA AVAILABILITY STATEMENT

Illumina sequences generated and used in this study are deposited and available at the NCBI website under BioProject ID: PRJNA716108 and part of PRJNA648026. All *P. aeruginosa* isolates (30) are available at https://www.ncbi.nlm.nih.gov/genome/. The specific BioSample accessions are listed in **Supplementary Table 1**. All other data generated or analyzed during this study are included in this article and it's **Supplementary File**.

ETHICS STATEMENT

The studies involving human participants were reviewed and Ethical approval was approved by the Ethics Committee of The Second Affiliated Hospital of Zhejiang University, School of Medicine (Number: 2020-319). Written informed consent for participation was not required for this study in accordance with the national legislation and the institutional requirements.

AUTHOR CONTRIBUTIONS

KZ: conceptualization. HL, QW, and HY: methodology. RZ, KZ, and BS: validation. YH and WP: formal analysis and writing-original draft preparation. YW: data curation. KZ and BS: writing-review and editing. YH, RZ, and ZK: funding acquisition. All authors have read and agreed to the published version of the manuscript.

FUNDING

This work was supported by the National Key Research and Development Program of China (2017YFC1600305), the Natural Science Foundation of Zhejiang Province (LY20H200006), and the National Natural Science Foundation of China (81861138052).

SUPPLEMENTARY MATERIAL

The Supplementary Material for this article can be found online at: https://www.frontiersin.org/articles/10.3389/fmicb.2021.670202/full#supplementary-material

REFERENCES

Bankevich, A., Nurk, S., Antipov, D., Gurevich, A. A., Dvorkin, M., Kulikov, A. S., et al. (2012). Spades: a new genome assembly algorithm and its applications to single-cell sequencing. *J. Comput. Biol.* 19, 455–477. doi: 10.1089/cmb.2012.0021

Boolchandani, M., D'souza, A. W., and Dantas, G. (2019). Sequencing-based methods and resources to study antimicrobial resistance. *Nat. Rev. Genet.* 20, 356–370.

Boulant, T., Boudehen, Y. M., Filloux, A., Plesiat, P., Naas, T., and Dortet, L. (2018). Higher prevalence of PldA, a *Pseudomonas aeruginosa* trans-kingdom H2-Type VI secretion system effector, in clinical isolates responsible for acute infections and in multidrug resistant strains. *Front. Microbiol.* 9:2578. doi: 10.3389/fmicb.2018.02578

Caldwell, C. C., Chen, Y., Goetzmann, H. S., Hao, Y., Borchers, M. T., Hassett, D. J., et al. (2009). *Pseudomonas aeruginosa* exotoxin pyocyanin causes cystic fibrosis airway pathogenesis. *Am. J. Pathol.* 175, 2473–2488. doi: 10.2353/ajpath.2009.090166

Chincholkar, S., and Thomashow, L. S. (2014). *Microbial Phenazines: Biosynthesis, agriculture and health*. Switzerland: Springer.

Cholley, P., Ka, R., Guyeux, C., Thouverez, M., Guessennd, N., Ghebremedhin, B., et al. (2014). Population structure of clinical *Pseudomonas aeruginosa* from west and central african countries. *PLoS One* 9:e107008. doi: 10.1371/journal.pone.0107008

Cui, Y., Wang, S., Ding, S., Shen, J., and Zhu, K. (2020). Toxins and mobile antimicrobial resistance genes in *Bacillus* probiotics constitute a potential risk for one health. *J. Hazard. Mater.* 382:121266. doi: 10.1016/j.jhazmat.2019.121266

Cullen, L., Weiser, R., Olszak, T., Maldonado, R. F., Moreira, A. S., Slachmuylders, L., et al. (2015). Phenotypic characterization of an international *Pseudomonas aeruginosa* reference panel: strains of cystic fibrosis (CF) origin show less in vivo virulence than non-CF strains. *Microbiology* 161, 1961–1977. doi: 10.1099/mic.0.000155

Curran, C. S., Bolig, T., and Torabi-Parizi, P. (2018). Mechanisms and targeted therapies for *Pseudomonas aeruginosa* lung infection. *Am. J. Respir. Crit. Care Med.* 197, 708–727.

Dietrich, L. E. P., Okegbe, C., Price-Whelan, A., Sakhtah, H., HunterR, C., and Newman, D. K. (2013). Bacterial community morphogenesis is intimately linked to the intracellular redox state. *J. Bacteriol.* 197, 1371–1380. doi: 10.1128/jb.02273-12

El-Zawawy, N. A., and Ali, S. S. (2016). Pyocyanin as anti-tyrosinase and anti tinea corporis: a novel treatment study. *Microb. Pathog.* 100, 213–220. doi: 10.1016/j.micpath.2016.09.013

Gaibani, P., Carla Re, M., Campoli, C., Viale, P., and Ambretti, S. (2019). Bloodstream infection caused by KPC-producing *Klebsiella pneumoniae* resistant to ceftazidime/avibactam: epidemiology and genomic characterization. *Clin. Microbiol. Infect.* 26, e516.e1–.e516.e4.

Grosso-Becerra, M. V., Santos-Medellin, C., Gonzalez-Valdez, A., Mendez, J. L., Delgado, G., Morales-Espinosa, R., et al. (2014). *Pseudomonas aeruginosa* clinical and environmental isolates constitute a single population with high phenotypic diversity. *BMC Genom.* 15:318. doi: 10.1186/1471-2164-15-318

Hemarajata, P., and Humphries, R. M. (2019). Ceftazidime/avibactam resistance associated with L169P mutation in the omega loop of KPC-2. *J. Antimicrob. Chemother.* 74, 1241–1243. doi: 10.1093/jac/dkz026

Horcajada, J. P., Montero, M., Oliver, A., Sorli, L., Luque, S., Gomez-Zorrilla, S., et al. (2019). Epidemiology and treatment of multidrug-resistant and extensively drug-resistant *Pseudomonas aeruginosa* infections. *Clin. Microbiol. Rev.* 32, e19–e31.

Horna, G., Amaro, C., Palacios, A., Guerra, H., and Ruiz, J. (2019). High frequency of the exoU+/exoS+ genotype associated with multidrug-resistant "high-risk

clones" of *Pseudomonas aeruginosa* clinical isolates from peruvian hospitals. *Sci. Rep.* 9:10874.

Hu, P., Chen, J., Chen, Y., Zhou, T., Xu, X., and Pei, X. (2017). Molecular epidemiology, resistance, and virulence properties of *Pseudomonas aeruginosa* cross-colonization clonal isolates in the non-outbreak setting. *Infect. Genet. Evol.* 55, 288–296. doi: 10.1016/j.meegid.2017.09.010

Hu, Y. Y., Gu, D. X., Cai, J. C., Zhou, H. W., and Zhang, R. (2015). Emergence of KPC-2-producing *Pseudomonas aeruginosa* sequence type 463 isolates in hangzhou, china. *Antimicrob. Agents Chemother.* 59, 2914–2917. doi: 10.1128/aac.04903-14

Inouye, M., Dashnow, H., Raven, L. A., Schultz, M. B., Pope, B. J., Tomita, T., et al. (2014). Srst2: rapid genomic surveillance for public health and hospital microbiology labs. *Genome Med.* 6:90.

Ji, J., Wang, J., Zhou, Z., Wang, H., Jiang, Y., and Yu, Y. (2013). *Multilocus* sequence typing reveals genetic diversity of carbapenem- or ceftazidime-nonsusceptible *Pseudomonas aeruginosa* in china. *Antimicrob. Agents Chemother.* 57, 5697–5700. doi: 10.1128/aac.00970-13

Juan, C., Pena, C., and Oliver, A. (2017). Host and pathogen biomarkers for severe *Pseudomonas aeruginosa* infections. *J. Infect. Dis.* 215, S44–S51.

Karatuna, O., and Yagci, A. (2010). Analysis of quorum sensing-dependent virulence factor production and its relationship with antimicrobial susceptibility in *Pseudomonas aeruginosa* respiratory isolates. *Clin. Microbiol. Infect.* 16, 1770–1775. doi: 10.1111/j.1469-0691.2010.03177.x

Larsen, M. V., Cosentino, S., Rasmussen, S., Friis, C., Hasman, H., Marvig, R. L., et al. (2012). *Multilocus* sequence typing of total-genome-sequenced bacteria. *J. Clin. Microbiol.* 50, 1355–1361. doi: 10.1128/jcm.06094-11

Li, Y., Jiang, H., Xu, Y., and Zhang, X. (2008). Optimization of nutrient components for enhanced phenazine-1-carboxylic acid production by gacA-inactivated *Pseudomonas* sp. M18G using response surface method. *Appl. Microbiol. Biotechnol.* 77, 1207–1217. doi: 10.1007/s00253-007-1213-4

Luo, R. G., Miao, X. Y., Luo, L. L., Mao, B., Yu, F. Y., and Xu, J. F. (2019). Presence of pldA and exoU in mucoid *Pseudomonas aeruginosa* is associated with high risk of exacerbations in non-cystic fibrosis bronchiectasis patients. *Clin. Microbiol. Infect.* 25, 601–606. doi: 10.1016/j.cmi.2018.07.008

Maatallah, M., Cheriaa, J., Backhrouf, A., Iversen, A., Grundmann, H., Do, T., et al. (2011). Population structure of *Pseudomonas aeruginosa* from five mediterranean countries: evidence for frequent recombination and epidemic occurrence of CC235. *PLoS One* 6:e25617. doi: 10.1371/journal.pone.0025617

Oliver, A., Mulet, X., Lopez-Causape, C., and Juan, C. (2015). The increasing threat of *Pseudomonas aeruginosa* high-risk clones. *Drug Resist. Updat.* 2, 41–59. doi: 10.1016/j.drup.2015.08.002

Parkins, M. D., Somayaji, R., and Waters, V. J. (2018). Epidemiology, biology, and impact of clonal *Pseudomonas aeruginosa* infections in cystic fibrosis. *Clin. Microbiol. Rev.* 37, e18–e19.

Rada, B., and Leto, T. L. (2013). Pyocyanin effects on respiratory epithelium: relevance in *Pseudomonas aeruginosa* airway infections. *Trends Microbiol.* 21, 73–81. doi: 10.1016/j.tim.2012.10.004

Rane, M. R., Sarode, P. D., Chaudhari, B. L., and Chincholkar, S. B. (2008). Exploring antagonistic metabolites of established biocontrol agent of marine origin. *Appl. Biochem. Biotechnol.* 151, 665–675. doi: 10.1007/s12010-008-8288-y

Schürch, A. C., Arredondo-Alonso, S., Willems, R. J. L., and Goering, R. V. (2018). Whole genome sequencing options for bacterial strain typing and epidemiologic analysis based on single nucleotide polymorphism versus gene-by-gene-based approaches. *Clin. Microbiol. Infect.* 24, 350–354. doi: 10.1016/j.cmi.2017.12.016

Tacconelli, E., Carrara, E., Savoldi, A., Harbarth, S., Mendelson, M., Monnet, D. L., et al. (2018). Discovery, research, and development of new antibiotics: the WHO priority list of antibiotic-resistant bacteria and tuberculosis. *Lancet Infect. Dis.* 18, 318–327.

Thrane, S. W., Taylor, V. L., Lund, O., Lam, J. S., and Jelsbak, L. (2016). Application of whole-genome sequencing data for O-specific antigen analysis andin silicoserotyping of *Pseudomonas aeruginosa* isolates. *J. Clin. Microbiol.* 54, 1782–1788. doi: 10.1128/jcm.00349-16

Vareechon, C., Zmina, S. E., Karmakar, M., Pearlman, E., and Rietsch, A. (2017). *Pseudomonas aeruginosa* effector ExoS inhibits ROS production in human neutrophils. *Cell Host Microbe* 21, 611–618. doi: 10.1016/j.chom.2017.04.001

Wayne, P. (2019). *Performance standards for antimicrobial susceptibility testing; 29th informational supplement. CLSI document M100-S29*. Maryland, USA: Clinical and Laboratory Standards Institute.

Zhu, K., Chen, S., Sysoeva, T. A., and You, L. (2019). Universal antibiotic tolerance arising from antibiotic-triggered accumulation of pyocyanin in *Pseudomonas aeruginosa*. *PLoS Biol.* 17:e3000573. doi: 10.1371/journal.pbio.3000573

Conflict of Interest: The authors declare that the research was conducted in the absence of any commercial or financial relationships that could be construed as a potential conflict of interest.

frontiers in Microbiology

ORIGINAL RESEARCH
published: 18 June 2021
doi: 10.3389/fmicb.2021.676113

First Report of Coexistence of *bla*$_{SFO-1}$ and *bla*$_{NDM-1}$ β-Lactamase Genes as Well as Colistin Resistance Gene *mcr-9* in a Transferrable Plasmid of a Clinical Isolate of *Enterobacter hormaechei*

Wenxiu Ai[1†], Ying Zhou[2,3†], Bingjie Wang[2,3], Qing Zhan[2,3], Longhua Hu[4], Yanlei Xu[2,3], Yinjuan Guo[2,3], Liangxing Wang[1], Fangyou Yu[2,3*] and Xiaolong Li[5*]*

[1] Department of Respiratory Medicine, The First Affiliated Hospital of Wenzhou Medical University, Wenzhou, China, [2] Department of Clinical Laboratory Medicine, Shanghai Pulmonary Hospital, Tongji University School of Medicine, Shanghai, China, [3] Shanghai Key Laboratory of Tuberculosis, Shanghai Pulmonary Hospital, Tongji University School of Medicine, Shanghai, China, [4] Jiangxi Provincial Key Laboratory of Medicine, Clinical Laboratory of the Second Affiliated Hospital of Nanchang University, Nanchang, China, [5] Department of Clinical Laboratory, The First Affiliated Hospital of Wenzhou Medical University, Wenzhou, China

Many antimicrobial resistance genes usually located on transferable plasmids are responsible for multiple antimicrobial resistance among multidrug-resistant (MDR) Gram-negative bacteria. The aim of this study is to characterize a carbapenemase-producing *Enterobacter hormaechei* 1575 isolate from the blood sample in a tertiary hospital in Wuhan, Hubei Province, China. Antimicrobial susceptibility test showed that 1575 was an MDR isolate. The whole genome sequencing (WGS) and comparative genomics were used to deeply analyze the molecular information of the 1575 and to explore the location and structure of antibiotic resistance genes. The three key resistance genes (*bla*$_{SFO-1}$, *bla*$_{NDM-1}$, and *mcr-9*) were verified by PCR, and the amplicons were subsequently sequenced. Moreover, the conjugation assay was also performed to determine the transferability of those resistance genes. Plasmid files were determined by the S1 nuclease pulsed-field gel electrophoresis (S1-PFGE). WGS revealed that p1575-1 plasmid was a conjugative plasmid that possessed the rare coexistence of *bla*$_{SFO-1}$, *bla*$_{NDM-1}$, and *mcr-9* genes and complete conjugative systems. And p1575-1 belonged to the plasmid incompatibility group IncHI2 and multilocus sequence typing ST102. Meanwhile, the pMLST type of p1575-1 was IncHI2-ST1. Conjugation assay proved that the MDR p1575-1 plasmid could be transferred to other recipients. S1-PFGE confirmed the location of plasmid with molecular weight of 342,447 bp. All these three resistant genes were flanked by various mobile elements, indicating that the *bla*$_{SFO-1}$, *bla*$_{NDM-1}$,

OPEN ACCESS

Edited by:
Che-Hsin Lee, National Sun Yat-sen University, Taiwan

Reviewed by:
Linda Falgenhauer, University of Giessen, Germany
Cheng-Yen Kao, National Yangming University, Taiwan

***Correspondence:**
Liangxing Wang
38805@163.com
Fangyou Yu
wzjxyfy@163.com
Xiaolong Li
lixiaolongcq@163.com

[†] These authors have contributed equally to this work

Specialty section:
This article was submitted to Antimicrobials, Resistance and Chemotherapy, a section of the journal Frontiers in Microbiology

Received: *04 March 2021*
Accepted: *27 April 2021*
Published: *18 June 2021*

Citation:
Ai W, Zhou Y, Wang B, Zhan Q, Hu L, Xu Y, Guo Y, Wang L, Yu F and Li X (2021) First Report of Coexistence of bla$_{SFO-1}$ and bla$_{NDM-1}$ β-Lactamase Genes as Well as Colistin Resistance Gene mcr-9 in a Transferrable Plasmid of a Clinical Isolate of Enterobacter hormaechei. Front. Microbiol. 12:676113. doi: 10.3389/fmicb.2021.676113

and *mcr-9* could be transferred not only by the p1575-1 plasmid but also by these mobile elements. Taken together, we report for the first time the coexistence of bla_{SFO-1}, bla_{NDM-1}, and *mcr-9* on a transferable plasmid in a MDR clinical isolate *E. hormaechei*, which indicates the possibility of horizontal transfer of antibiotic resistance genes.

Keywords: *Enterobacter hormaechei*, plasmid, bla_{SFO-1}, bla_{NDM-1}, *mcr-9*, IncHI2, WGS, mobile elements

INTRODUCTION

Carbapenem-resistant Enterobacteriaceae (CRE) has recently emerged as a serious threat to modern healthcare, challenging our present antibiotic treatment strategy (Chen et al., 2014). Moreover, the carbapenem-resistant and extended-spectrum β-lactamase (ESBL)-producing Enterobacteriaceae are also classified as the "priority pathogens" by the World Health Organization in 2017 (WHO, 2017; Tacconelli et al., 2018). Among all these Enterobacteriaceae isolates, *Enterobacter hormaechei* is a notorious nosocomial pathogen contributing to various infections, such as bacteremia, endocarditis, and lower respiratory, urinary tract, and intra-abdominal infections (Xu et al., 2015).

Recently, reports about the coexistence of a rare ESBL gene bla_{SFO-1} and carbapenemase genes were increased (Zhou et al., 2020). New Delhi metallo-lactamase (NDM-1), a β-lactam hydrolase, constitutes a critical and growingly important medical issue, since its resistance trait compromises the efficacy of almost all lactams (except aztreonam), including carbapenems (Dortet et al., 2014). Compared with other broad-spectrum β-lactamase, the bla_{SFO-1} gene is a low-incidence antimicrobial resistance gene and usually not subject to systematic monitoring, which puts it at risk of being missed (Zhao et al., 2015; Zhou et al., 2020). With the increase of infections caused by carbapenemase-producing bacteria and the lack of novel antibiotics (Gurjar, 2015), polymyxins have become the last-resort therapies in the treatment of infections caused by this kind of multidrug-resistant (MDR) bacterial (Olaitan et al., 2014; Yilmaz et al., 2016). Thus, once the strains are resistant to both carbapenems and polymyxins, the treatment will be very tough. The first plasmid-mediated colistin resistance gene *mcr-1* was identified in China from the plasmid of *Escherichia coli* and *Klebsiella pneumoniae* in IncI2 (Liu et al., 2016). *mcr-1* remains the main plasmid-mediated myxobacteria resistance gene, but *mcr-2* to *mcr-8* has been identified in different species in humans and animals (Wang et al., 2018; Nang et al., 2019). *mcr-9* has also been identified in Swedish ESBL isolates, including *Enterobacter cloacae*, *E. coli*, *Klebsiella acidophilus*, and *Citrobacter freundii* (Börjesson et al., 2020). Of particular concern is the spread of *mcr* genes into CRE, which would create strains that are potentially pan-drug resistant (PDR). So mobile colistin-resistant genes (*mcr*) have become an increasing public health concern.

It is common for the coexistence of mcr-9 with carbapenemases, such as bla_{NDM-1}, bla_{VIM-4}, and bla_{IMP-4} (Chavda et al., 2019; Chen et al., 2020). However, in this study, we found a clinical isolate of carbapenem-resistant *E. hormaechei*, which possessed the rare coexistence of bla_{SFO-1}, bla_{NDM-1}, and *mcr-9* genes. And we also explored the molecular basis for antibiotic resistance of this strain.

MATERIALS AND METHODS

Bacterial Isolation and Identification

The *E. hormaechei* 1575 was isolated from the blood sample in a tertiary hospital in Wuhan, Hubei Province, China. The cultured bacteria were stored in glycerol broth at 80°C. And then samples were cultured on Colombian blood Agar plate and identified by matrix-assisted laser desorption/ionization time of flight mass spectrometry (MALDI-TOF MS) according to the manufacturer's instructions and also by whole genome sequencing (WGS) (discussed below). *Escherichia coli* American Type Culture Collection (ATCC) 25922 was used as control strains for the identification of the species.

Antimicrobial Susceptibility Testing

A total of 17 antimicrobial agents were tested, including imipenem (Ipm), meropenem (Mer), piperacillin–tazobactam (P/T), ceftazidime–avibactam (Caz/Avi), aztreonam (Azt), cefoxitin (Fox), cefotaxime (Ctx), cefepime (Cpe), ceftazidime (Caz), gentamicin (Gen), amikacin (AMK), ciprofloxacin (Cip), sulfamethoxazole (CoSMZ), tetracycline (Te), minocycline (Min), tigecycline (TGC), and polymyxin B (PB). The minimum inhibitory concentrations (MICs) of antimicrobial agents for the bacteria tested were determined using the broth microdilution method, and the susceptibility breakpoints were interpreted in accordance with the Clinical and Laboratory Standards Institute (CLSI) guideline (Clinical and Laboratory Standards Institute (CLSI), 2020), except for tigecycline and colistin, for which we used the European Committee on Antimicrobial Susceptibility Testing (EUCAST) breakpoints (Clinical and Laboratory Standards Institute (CLSI), 2020; EUCAST, 2020). AST was repeated three times in our study. *E. coli* ATCC 25922 was used as a control strain for the AST.

Carbapenemase Phenotype Confirmation Testing

The modified carbapenem inactivation test (mCIM) was performed, according to CLSI 2020 standards [Clinical and Laboratory Standards Institute (CLSI), 2020], to verify carbapenemase production by the isolate. The tested strain 1575 was incubated with a meropenem disk (10 μg, OXOID, United Kingdom) immersed in the 2 ml of TSB suspension at 37°C for 4 h. *E. coli* ATCC 25922 was used as an indicator and with its 0.5 McFarland suspension uniformly coated on

the Mueller Hinton Agar (MHA) plate. After the plate was dried for 3–10 min, the meropenem disk was removed from the suspension, and the excess medium was squeezed out. It was then placed on the MHA plate and incubated at 37°C for 18–24 h.

Whole Genome Sequencing and Bioinformatics Analysis

Bacterial genomic DNA was isolated using the UltraClean Microbial Kit (Qiagen, NW, Germany) and sequenced from a sheared DNA library with average size of 15 kb (ranged from 10 to 20 kb) on a PacBio RSII sequencer (Pacific Biosciences, CA, United States), as well as a paired-end library with an average insert size of 350 bp (ranged from 150 to 600 kb) on a HiSeq sequencer (Illumina, CA, United States). Sequencing libraries were constructed using the NEBNext® Ultra™ II DNA Library Prep Kit for Illumina® (second-generation sequencing) and the SMRTbell® Express Template Prep Kit 2.0 kit (third-generation sequencing) and then loaded onto NovaSeq S4 flowcell and SMRT Cell 8 M DNA sequencing chip, respectively. The paired-end short Illumina reads were used to correct the long PacBio reads utilizing proovread (Hackl et al., 2014), and then the corrected PacBio reads were assembled *de novo* utilizing SMARTdenovo[1]. Antimicrobial resistance genes were identified by ResFinder 3.2 available at Center for Genomic Epidemiology[2]. The plasmid incompatibility groups, pMLST, and multilocus sequence typing (MLST) were identified by PlasmidFinder 2.1[3], pMLST 2.0[4], and MLST 2.0 software[5], respectively. To verify whether the plasmid was also a conjugative plasmid, we used the OriT Finder website[6] to conduct a detailed analysis of the conjugation module. The IS elements can be directly determined from the known website[7]. We used blast[8] to determine similar plasmids by comparing their coverages and identities. The circular representation of p1575 was generated with CGview[9]. The plasmid linear graph was analyzed by Easyfig software[10].

PCR Amplifications and Sequencing

The isolate was verified for the presence of bla_{SFO-1}-positive strains using PCR with the primers bla_{SFO-1}-forward and bla_{SFO-1}-reverse. Meanwhile, the other carbapenemase genes responsible for carbapenem resistance (bla_{KPC}, bla_{VIM}, bla_{GES}, bla_{IMP}, bla_{SPM}, bla_{OXA-23}, bla_{OXA-48}, bla_{SME}, bla_{SIM}, and bla_{NDM}) (Queenan and Bush, 2007; Nordmann et al., 2011) and the colistin resistance gene *mcr-9* were also detected by PCR. The DNA fragments were analyzed using gel electrophoresis on 1% agarose gels, and the amplicons were subsequently sequenced on both strands by TSINGKE sequencing (**Table 1**).

[1]https://github.com/ruanjue/smartdenovo
[2]https://cge.cbs.dtu.dk/services/ResFinder/
[3]https://cge.cbs.dtu.dk/services/PlasmidFinder/
[4]https://cge.cbs.dtu.dk/services/pMLST/
[5]https://cge.cbs.dtu.dk/services/MLST/
[6]https://bioinfo-mml.sjtu.edu.cn/oriTfinder/
[7]https://www-is.biotoul.fr/
[8]https://blast.ncbi.nlm.nih.gov/Blast.cgi
[9]http://stothard.afns.ualberta.ca/cgview_server/
[10]http://mjsull.github.io/Easyfig/

Conjugation Experiment

The horizontal transferability of bla_{SFO-1}, bla_{NDM-1}, and *mcr-9* was examined using conjugation assay. The *E. hormaechei* 1575 was used as donor strain, and the *E. coli* EC600 (rifampicin-resistant) was used as the recipient strain. The donors and recipients were cultured to the logarithmic phase (OD600 = 0.4–0.6), mixed in a 1:1 ratio, centrifuged at 8,000 *g* for 1 min, and resuspended them in 20 μl of Luria Bertani (LB) broth. The resuspension was spotted on the LB plates and incubated overnight at 37°C. The spots were then transferred to 15-ml centrifuge tubes and washed with 3 ml of LB broth. Subsequently, the serial dilutions were plated onto MH agar plates containing cefotaxime (8 μg/ml) and rifampicin (200 μg/ml). The donor cells and recipient cells were used separately as controls to ensure the effectiveness of the screening plate antibiotics. All transconjugants were confirmed by PCR for the presence of bla_{SFO-1}, bla_{NDM-1}, and *mcr-9* genes. Transconjugants were subjected to susceptibility assays. The conjugation frequency was calculated as the number of transconjugants per donor cell.

S1 Pulsed-Field Gel Electrophoresis

S1 pulsed-field gel electrophoresis (S1-PFGE) was performed to obtain plasmid profiles in donor strains, recipient strains, and transconjugants, as described previously (Chen et al., 2011). Briefly, the isolates were embedded in 10 g/L of Seakem Gold gel, digested with endonuclease S1 nuclease (Takara, Dalian, China), and subjected to pulsed-field gel electrophoresis (parameters: 14°C, voltage 6 V/cm, electric field angle 120°, conversion time 4.0–40 s, and electrophoresis 19 h). The genomic DNA of *Salmonella enterica* serovar Braenderup H9812 strain cut with *Xba*I was used as a control standard strain and a molecular size marker.

Nucleotide Accession Number

The complete nucleotide sequences of the chromosome of 1575, p1575-1, and p1575-2 were deposited as GenBank accession numbers CP068287, CP068288, and CP068289, respectively.

RESULTS

Enterobacter hormaechei 1575 Was a Multidrug-Resistant Strain and Produced Carbapenemase

To clarify the antibiotic-resistant phenotype of *E. hormaechei* 1575, we tested the susceptibility of 17 antibiotics in this strain. As the results showed (**Table 2**), *E. hormaechei* 1575 was resistant to all β-lactam antibiotics (cephalosporins, carbapenems, penicillins, and monocyclic β-lactams), aminoglycosides, quinolones, and tetracycline. We found that 1575 was only susceptible to tigecycline, amikacin, and polymyxin B. Notably, for the ceftazidime–avibactam, a novel carbapenemase inhibitor, this isolate also exhibited high-level resistance.

Since *E. hormaechei* 1575 was resistant to both carbapenems and ceftazidime–avibactam, we used the mCIM assay to test preliminary whether this isolate produces carbapenemases. The

TABLE 1 | Primers used in this study.

Amplicon	Product size (bp)	Temperature (°C)	Primer (5′–3′)	
			Forward	Reverse
bla_{SFO-1}	796	53	TTCTGCTGTGGCTGAGTG	TGATGGTCGCTACGGTTAT
mcr-9	730	50.3	TTCCCTTTGTTCTGGTTG	TACTCGGTGCGATTCATA

TABLE 2 | Antimicrobial drug susceptibility profiles.

Drug class	Antibiotic	MIC (mg/L)/antimicrobial susceptibility			
		1575	S/I/R	p1575-1-EC600	EC600
Carbapenems	Ipm	4	R	8	≤0.5
	Mer	>16	R	8	≤0.5
β-Lactam/β-lactamase	P/T	>128/4	R	64/4	≤4/4
Inhibitor complexes	Caz/Avi	>32/4	R	>32/4	≤0.25/4
Monocyclic β-lactam	Azt	>32	R	16	≤1
Cephalosporin	Fox	>32	R	16	4
	Ctx	>64	R	>64	≤1
	Cpe	>16	R	>16	≤0.5
	Caz	>32	R	>32	≤1
Fluoroquinolones	Cip	1	R	2	≤0.25
Folate metabolic pathway	CoSMZ	>2/38	-	>2/38	≤0.5/9.5
Inhibitors	Te	>16	R	>16	≤1
Tetracyclines	Min	>8	-	>8	≤2
	TGC	1	S	≤0.25	≤0.25
Polymyxin B	PB	2	S	2	≤0.5
Aminoglycosides	Gen	>16	R	>16	≤0.5
	AMK	≤2	S	≤2	≤2

MIC, minimum inhibitory concentration; S, susceptible; R, resistant; I, intermediate; Ipm, imipenem; Mer, meropenem; P/T, piperacillin–tazobactam; Caz/Avi, ceftazidime–avibactam; Azt, aztreonam; Fox, cefoxitin; Ctx, cefotaxime; Cpe, cefepime; Caz, ceftazidime; Cip, ciprofloxacin; CoSMZ, sulfamethoxazole; Te, tetracycline; Min, minocycline; TGC, tigecycline; PB, polymyxin B; Gen, gentamicin; AMK, amikacin.

result showed that *E. hormaechei* 1575 was positive for the mCIM assay, indicating that the isolate produced carbapenemases. Combining this strain with resistance to ceftazidime–avibactam, we speculated that *E. hormaechei* 1575 produced metallo-carbapenemase.

Enterobacter hormaechei 1575 Co-harboring bla_{SFO-1}, bla_{NDM-1}, and *mcr-9* Resistance Genes

Through the resistance phenotype assays, we evaluated the clinical treatment challenges brought by this strain. Here, we continued to explore the associated molecular mechanism that contributed to such phenotype.

We used WGS to deeply mine the genomic information of the MDR bacteria. We found two plasmids in this isolate (named p1575-1 and p1575-2); and p1575-1 (CP068288) was larger with approximately 342,447 bp and sheltered multiple antibiotic resistance genes, especially including β-lactam resistance genes bla_{SFO-1}, bla_{NDM-1}, and colistin resistance gene *mcr-9* (**Table 3**). Besides, consistent with its multidrug resistance phenotype, p1575-1 also had multiple genes mediating resistance to quinolone (*qnrS1*), aminoglycosides [*aac(3)-IId*, *aph(3′)-Ia*, and *aph(6)-Id*], β-lactams (bla_{TEM-1B} and bla_{LAP-2}), bleomycin ble_{MBL}, trimethoprims (*dfrA14* and *dfrA19*), and MLS—macrolide [*mph(A)*] and tetracycline [*tet(D)*]. p1575-2 was a small plasmid of approximately 1,699 bp, with no resistance genes located on. We found the antibiotic-resistant plasmid by second-generation sequencing and further analyzed it by third-generation sequencing. Then we applied the PCR assay to verify these resistance genes. In addition, MLST analysis showed that *E. hormaechei* 1575 belonged to clone group ST102.

TABLE 3 | General features, antimicrobial resistance genes, and mobile genetic elements of plasmids p1575-1 and p1575-2.

Location	Features	
	Size (bp)	Antimicrobial resistance genes
Chromosome	4,687,233	bla_{ACT-5}, fosA
Plasmid-1	342,447	bla_{SFO-1}, *mcr-9*, bla_{NDM-1}, bla_{TEM-1B}, *qnrS1*, *tet(D)*, ble_{MBL}, bla_{LAP-2} *aac(3)-IId*, *aph(3′)-Ia*, *aph(6)-Id*, *mph(A)*, *dfrA14*, *dfrA19*
Plasmid-2	1,699	NA

NA, not applicable.

Comparative Genomics of the Plasmid p1575-1 Carrying bla_{SFO-1}, bla_{NDM-1}, and *mcr-9*

We have known that the plasmid p1575-1 was the key plasmid for the contribution of the MDR phenotype; thus, exploring the characteristics of p1575-1 is the key to elucidating the spread of such bacteria and the mechanism of antibiotic resistance. p1575-1 is a 342,447-bp circular molecule with an average G + C content of 47.93% and was predicted to encode a total of 386 coding sequences (CDSs). Through the PlasmidFinder (see text footnote 3) and pMLST website (see text footnote 4), p1575-1 was typed as IncHI2 with Double Locus Sequence Type DLST1. To verify whether the p1575-1 plasmid was also a conjugative plasmid, we used the OriT Finder website (see text footnote 6) to conduct a detailed analysis of the conjugation module. Through the analysis, we identified the complete conjugative modules on the plasmid p1575-1, including the origin of transfer site (oriT), relaxase gene, gene encoding type IV coupling protein (T4CP), and gene cluster for bacterial type IV secretion system (T4SS) (**Table 4**). These results strongly suggested that p1575-1 is an MDR plasmid that can be transferred autonomously (**Figure 1**).

Moreover, we obtained three plasmids from the National Center for Biotechnology Information (NCBI) GenBank database for comparative analysis with our target plasmids. We found that p1575-1 had high homology with pNIHE14-1904-*mcr9* (GenBank accession no. LC570845.1) from *E. hormaechei*, with 91% query coverage and 99.97% sequence similarity. The other two plasmids held only 89% query coverage (pECL-90-2, CP061746.1) and 88% query coverage (pIHI2-323, CP049189.1) (**Figure 2A**). These results also suggested that these plasmids might have evolved from a single ancestor, or one might have evolved from the other. Finally, the pNIHE14-1904-*mcr9* was chosen as the reference plasmid for genome analysis, because of the high query coverage and sequence similarity (**Figure 2B**).

TABLE 4 | Type IV secretion system components.

Type	P1575-1	
	Location	**Gene/locus tag**
OriT	141410–141661	-
Relaxase	143413–146559	ORF1_174
T4CP	36707–37702	ORF1_45
T4SS	36707–47032	ORF1_45ORF1_46 ORF1_47ORF1_48 ORF1_49 ORF1_50 ORF1_51 ORF1_52 ORF1_53 ORF1_54 ORF1_56
T4SS	130105–148643	ORF1_162 ORF1_166 ORF1_167 ORF1_168 ORF1_175
T4SS	287738–297020	ORF1_350 ORF1_352 ORF1_353 ORF1_355 ORF1_356
T4SS	315507–325118	ORF1_371 ORF1_372 ORF1_375 ORF1_377 ORF1_378 ORF1_379 ORF1_380

T4CP, type IV coupling protein; T4SS, type IV secretion system; ORF, open reading frame.

The conjugative system of p1575-1 shared greater than 99% identity to that of pNIHE14-1904-*mcr9*, which in turn confirmed that the p1575-1 plasmid was a conjugative IncHI2 plasmid. Moreover, two IS*26* units were found on p1575-1. The first was the IS*26*–bla_{SFO-1}–IS*26* transposable unit containing the SFO-1 ESBL gene (bla_{SFO-1}) (**Figure 3A**). The other was the IS*26*–bla_{LAP-2}–*qnrS1*–IS*26* module (**Figure 3D**) with two resistance genes included (bla_{LAP-2} and *qnrS1*). Remarkably, only p1575-1 plasmid harbored the second MDR gene IS*26* unit compared with other three IncHI2 plasmids.

Overall, these findings revealed that the p1575-1 plasmid was an MDR conjugative plasmid, which carried three key resistance genes (bla_{SFO-1}, bla_{NDM-1}, and *mcr-9*) and complete conjugative systems.

p1575-1 Plasmid Could Transfer bla_{SFO-1}, bla_{NDM-1}, and *mcr-9* Genes

We found that the p1575-1 plasmid carried complete conjugative systems. Hence, we applied the conjugation assay to prove whether the MDR p1575-1 plasmid could infect other strains autonomously by conjugation. We identified that p1575-1 was able to be transferred to the rifampicin-resistant *Escherichia coli* EC600 *via* conjugation, p1575-1-EC600; and the conjugation frequency was estimated at (0.5–2) $\times$ 10^{-6} per donor cell. Then S1-PFGE revealed that *E. hormaechei* 1575 and p1575-1-EC600 contained the large plasmid (p1575-1) (336.5–398.4 kb) (**Figure 4**), consistent with the result of WGS. Besides, another plasmid (named p1575-2) was also found by WGS, a small plasmid approximately 1,699 bp, with no resistance genes on and could not be detected by S1-PFGE. Transconjugants were subjected to susceptibility assays. The antimicrobial susceptibility patterns are shown in **Table 2**. The transconjugants showed similar antibiotic susceptibility profile to the donor strain *E. hormaechei* 1575. The MICs of transconjugants were decreased compared with those of 1575, but they were both sensitive to tigecycline.

Mobile Genetic Elements Associated With bla_{SFO-1}, bla_{NDM-1}, and *mcr-9*

Besides an in-depth analysis of the characteristics of MDR plasmids, we also analyzed the mobile elements flanking the resistant genes.

Our results showed that bla_{SFO-1} was located on a 7,258-bp IS*26* unit (IS*26*–*traX*-*ampR*-bla_{SFO-1}-IS*26*) (**Figure 3A**). Genetic mapping of bla_{SFO-1} revealed that IS*26* and *ampR* were upstream and downstream of bla_{SFO-1}, respectively. Tn*3* family, Tn*3* transposase DDE domain protein, and IncF plasmid conjugative transfer pilin acetylase, *traX*, were located downstream of *ampR*. Genetic mapping of bla_{NDM-1} revealed that the insertion sequence IS*3000* was interrupted by the insertion of a truncated ΔIS*Aba125* element. A bleomycin resistance gene, ble_{MBL}, and dsbD, encoded oxidoreductase superfamily protein, were downstream of bla_{NDM-1} (**Figure 3B**). For bla_{NDM-1}, a high similar genetic pattern was also observed in other plasmids, pNDM-BTR (McGann et al., 2015)

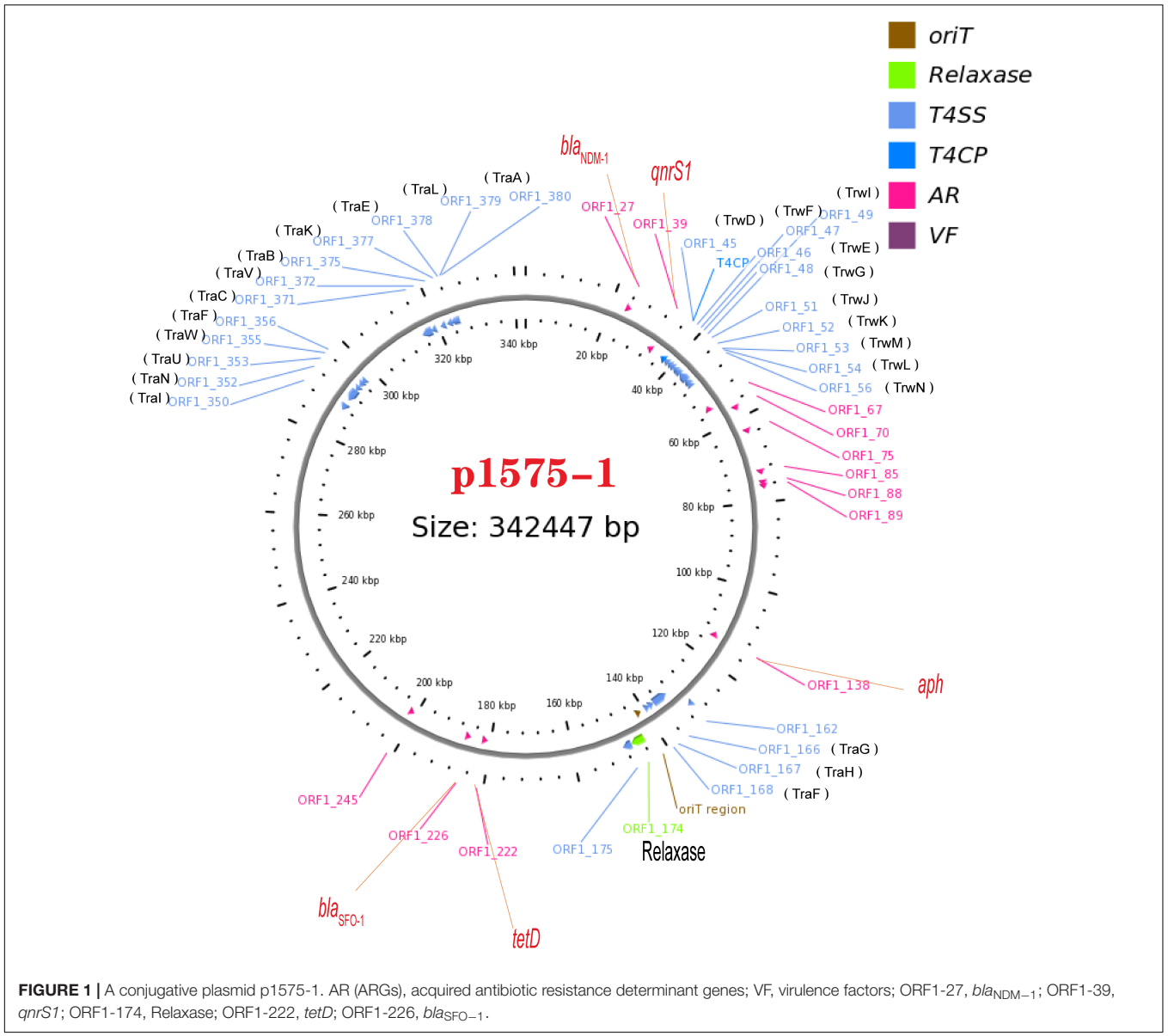

FIGURE 1 | A conjugative plasmid p1575-1. AR (ARGs), acquired antibiotic resistance determinant genes; VF, virulence factors; ORF1-27, bla_{NDM-1}; ORF1-39, *qnrS1*; ORF1-174, Relaxase; ORF1-222, *tetD*; ORF1-226, bla_{SFO-1}.

(GenBank accession number KF534788, IncN1) and pNDM1-CBG (accession number CP046118, unpublished). In plasmid 1575-1, IS*5* family transposase (IS*903B*) was located upstream of *mcr-9.1*, whereas *wbuC*, IS*1R*, *sil*, *mocR*, IS*26*, and *tnsDCBA* were located downstream (**Figure 3C**). Besides, there were many other insertion sequences on the backbone where *mcr-9* was located. However, *qseB* and *qseC* regulatory genes were not found in association with the *mcr-9* gene.

DISCUSSION

The spread of *bla*NDM-1 among bacterial pathogens is of concern not only because of resistance to carbapenems but also because such pathogens typically are resistant to multiple antimicrobial drug classes, which leaves few treatment choices available (Kumarasamy et al., 2010; Moellering, 2010; Walsh, 2010). Not like the *bla*NDM-1, which receives widespread attention, the bla_{SFO-1} gene is not included in the routine surveillance, but it could be an effective weapon that various gram-negative bacteria could use to resist β-lactams (Matsumoto and Inoue, 1999); therefore, the prevalence of the coexistence of the bla_{SFO-1} gene and carbapenemase genes might be underestimated. Some studies reported the coexistence of bla_{SFO-1} and bla_{NDM-1} β-lactamase genes and fosfomycin resistance gene *fosA3* in *Escherichia coli* clinical isolate (Zhao et al., 2015) and the co-occurrence of *mcr-9* and bla_{NDM-1} in *Enterobacter cloacae* (Yuan et al., 2019; Faccone et al., 2020; Lin et al., 2020). However, in this study, we not only found the coexistence of *mcr-9* and bla_{NDM-1}, but also a rare gene bla_{SFO-1} was detected on the same transferable plasmid. The presence of bla_{SFO-1} might confer resistance to more antibiotics.

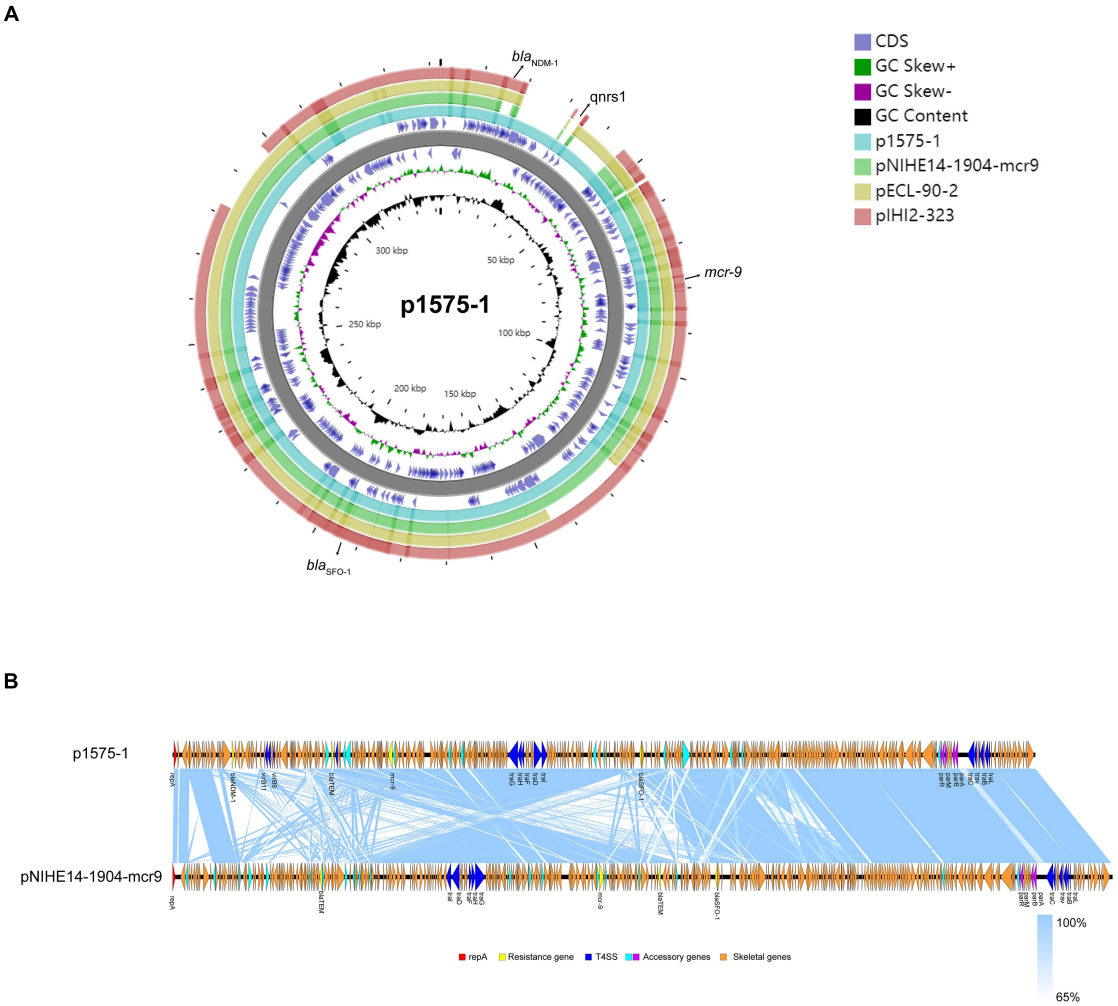

FIGURE 2 | (A) Ring diagram representation of plasmid p1575-1. From the inside to the outside, the first circle represents the scale; the second circle represents GC content; the third circle represents the GC skew; the fourth and sixth circles represent the COG to which each CDS belongs; the fifth circle represents the backbone; the seventh to 10th circles represent p1575-1, pNIHE14-1904-mcr9, pECL-90-2, and pIHI2-323, respectively. GC, guanine + cytosine; bla_{SFO-1}, extended-spectrum β-lactamases (ESBLs); bla_{NDM-1}, New Delhi metallo-β-lactamase-1 gene; *mcr-9*, colistin resistance gene; *qnrs1*, fluoroquinolones gene. **(B)** Comparative analysis of the *mcr-9*-harboring plasmid characterized in this study with closely related plasmid pNIHE14-1904-*mcr9*. Open reading frames (ORFs) are portrayed by arrows and are depicted in different colors based on their predicted gene functions. The genes associated with the T4SS are indicated by dark blue arrows, while the genes involved in replication are indicated by red arrows. Resistance genes are indicated by yellow arrows, and accessory genes are indicated by light blue and purple arrows. Orange arrows represent the skeletal gene of the plasmid, and blue shading denotes shared regions of homology among different plasmids.

mcr is a family of genes found to promote colistin resistance in bacteria. As we all know, polymyxin antibiotic would be a good choice for bla_{NDM-1}-positive strains, but we found *mcr-9* (Börjesson et al., 2020) in *E. hormaechei* 1575, which could reduce the sensitivity of the strain to polymyxin and increase its clinical menacing. Notably, the novel antibiotic ceftazidime–avibactam was also ineffective against 1575. Tigecycline is a last-resort antibiotic that is used to treat severe infections caused by extensively drug-resistant bacteria (Tasina et al., 2011) and may be used as a therapeutic drug for 1575. All these results indicated the *E. hormaechei* 1575 was MDR isolates and could only choose limited antibiotics. The presence of drug resistance genes strongly correlated with resistant phenotypes. The *E. hormaechei* 1575 was confirmed to produce carbapenemase. At the same time, two cases of MDR *E. cloacae* isolates had been reported to be ST102 in China (Cao et al., 2017), and this kind of strain was also found in our study. High attention should be given to its subsequent epidemic.

Previous studies showed that multiple resistance transfer of plasmids could result from rare gene capture events mediated by different mobile genetic elements, clustering, and combinatorial evolution of resistance genes and related mobile elements (Partridge and Tsafnat, 2018). Through the WGS and comparative genomics, we clarified that the key to mediating the antibiotic resistance of this strain was the p1575-1 resistant plasmid. The p1575-1 identified in this study was an IncHI2

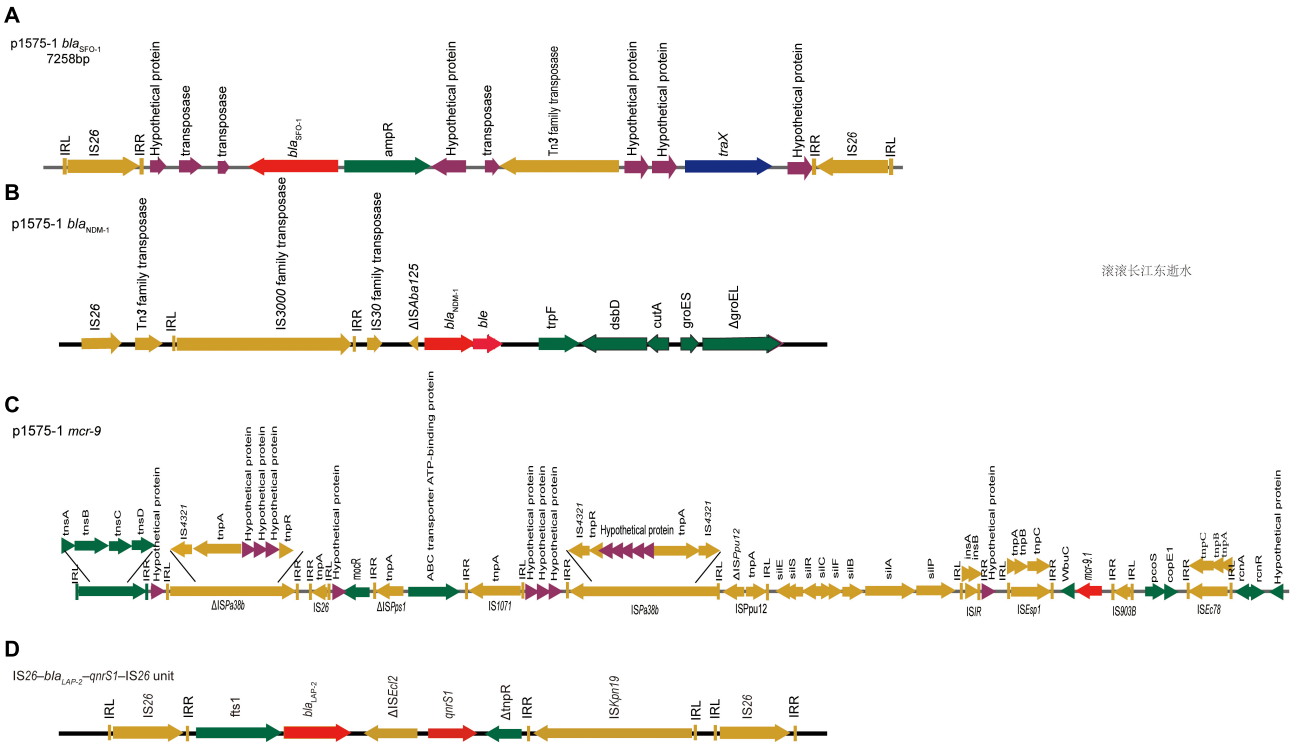

FIGURE 3 | bla_{SFO-1}, bla_{NDM-1}, and *mcr-9* gene contigs. Genetic environments surrounding the bla_{NDM-1}, bla_{SFO-1} and *mcr-9* genes in plasmid p1575-1. **(A)** The DNA fragments flanking the bla_{SFO-1} gene in plasmid p1575-1. **(B)** The DNA fragments flanking the bla_{NDM-1} gene in plasmid p1575-1. **(C)** The DNA fragments flanking the *mcr-9* gene in plasmid p1575-1. **(D)** The *IS26*–bla_{LAP-2}–*qnrS1*–*IS26* module. Colored arrows indicate open reading frames, with dark green, dark yellow, dark blue, purple, and red arrows representing other genes, mobile and accessory elements, the individual conjugation-related genes, hypothetical proteins and transposases, and antibiotic resistance genes, respectively.

conjugative plasmid, representing one of the most frequently encountered plasmid types in Enterobacteriaceae (Carattoli, 2009). Notably, IncHI2 plasmids are also broad-host-range, large (>250 kb) conjugative plasmids that mobilize metal and drug resistance genes within gram-negative pathogens (Bertrand et al., 2006; Novais et al., 2006; Roy Chowdhury et al., 2019). Meanwhile, IncHI2-ST1 plasmids always contributed to the dissemination of carbapenemase-encoding genes and are also reported frequently to play a critical role in the evolution of complex resistance phenotypes within disease-causing strains of Enterobacteriaceae (Roy Chowdhury et al., 2019). Moreover, IncHI2 plasmids contain the conjugal transfer gene regions *tra1* and *tra2*, likely contributing to the spread of resistance in the environment (Sherburne et al., 2000). In this study, we analyzed the conjugative modules of the p1575-1 plasmid and evaluated its mobility with conjugation assay. Like the classical IncHI2 plasmids, the p1575-1 plasmid held a complete conjugative system, and the conjugation frequencies ranged from 0.5×10^{-6} to 2×10^{-6} per donor cell. The IncHI2-type conjugative plasmids harboring *mcr-9* were also discovered previously, and the conjugation frequencies of those plasmid were 10^{-4} (Lin et al., 2020) or 2.03×10^{-7} (-5.42×10^{-8}) (Cha et al., 2020), which were similar to our findings. Through the analysis, we identified the complete conjugative modules on the plasmid p1575-1, strongly suggesting that p1575-1 could be transferred autonomously. In addition to the conjugative plasmids, the capture, accumulation, and dissemination of resistance genes are largely due to the actions of mobile genetic elements, including insertion sequences, transposons, gene cassettes, and integrons. In this study, we found that all these three resistance genes were flanked by several mobile elements. The bla_{SFO-1} was located in an *IS26* composite transposon. *IS6* family elements *IS26* have played a pivotal role in the dissemination of resistance determinants in Gram-negative bacteria; thus, bla_{SFO-1} held the potential to transfer to other strains. AmpR, a class of DNA-binding regulatory protein, belongs to the LysR family of transcriptional regulators (Henikoff et al., 1988; Bartowsky and Normark, 1993). AmpR is confirmed to be a transcriptional activator in the presence of certain β-lactam antibiotics in the culture medium and a repressor in their absence (Lindberg et al., 1988). The presence of *ampR* seems to be a disadvantage for the host strain because *E. cloacae* become highly resistant to β-lactams (Matsumoto and Inoue, 1999). The movement of *IS26* is originally demonstrated to occur by replicative transposition. Moreover, the *bla*SFO-1 genes in previous identifications were located on non-conjugative plasmids (Guo et al., 2012). In our study, the conjugative bla_{SFO-1}-bla_{NDM-1}-*mcr-9*-bearing plasmid belonged to IncHI2, which is a kind of broad-host-range mobile plasmid and might greatly accelerate the dissemination of the bla_{SFO-1} genes. Previous reports showed that the

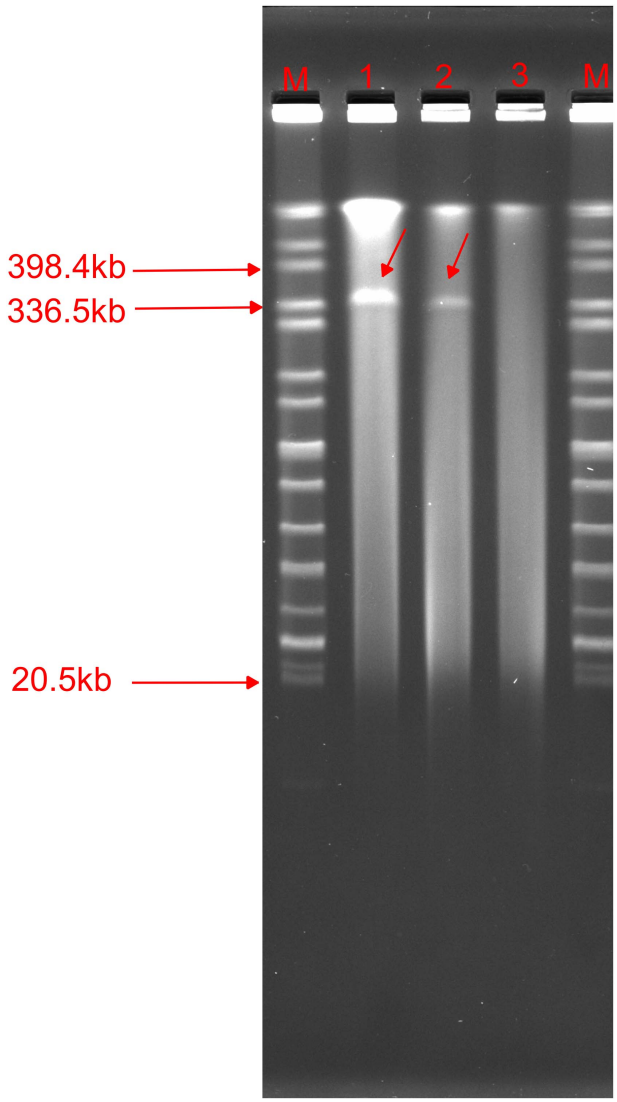

FIGURE 4 | S1-nuclease pulsed-field gel electrophoresis profiles. M, *Salmonella enterica* serotype Braenderup strain H9812; 1,1575; 2, p1575-1-EC600; 3, EC600.

bla_{NDM-1} genes in Enterobacteriaceae were usually on 50- to 200-kb plasmids belonging to IncL/M, IncHI1, IncFIIs, IncF, or untypable (Ahmad et al., 2018). IS*Aba125* and Tn*125* are always associated with the bla_{NDM-1} gene. Upstream of the bla_{NDM-1} gene, a truncated insertion sequence, IS*Aba125*, was identified, which provides a promoter for the expression of bla_{NDM-1} (Carattoli et al., 2012), and the presence of *ble* and Δ*tnpA* genes suggests a possible hypothesis that bla_{NDM-1} originates from *Acinetobacter baumannii* (Poirel et al., 2012; Toleman et al., 2012). Besides, phosphoribosylanthranilate isomerase gene *trpF* was identified in the downstream sequences of the ble_{MBL} gene (Liu et al., 2013). In addition, *qnrS1* in IS*26*–bla_{LAP-2}–*qnrS1*–IS*26* unit (3D) was also found, consistent with our AST results. In the IncHI2 plasmid, the *mcr-9* allele always inserted an IS*903B* element and an IS*Esp1*, encoding a cupin fold metalloprotein, *wbuC* family (Yuan et al., 2019; Börjesson et al., 2020), which was consistent with our results. Because *mcr-9.1* was located between IS*903B* and IS*26*, these flanking sequences can also be potentially transferred to other bacteria along with *mcr-9.1*. All results indicated that the resistant plasmid carried by *E. hormaechei* 1575 can be spontaneously transmitted to other strains through conjugation, which had great potential to cause clinical epidemics. *qseB* and *qseC* regulatory genes were found in association with the *mcr-9* gene and played an important role in mediating polymyxin resistance (Chavda et al., 2019; Kieffer et al., 2019). The lack of two key regulators (*qseB* and *qseC*) may explain why *E. hormaechei* 1575 carrying *mcr-9* did not exhibit a high resistance level to colistin (MIC, 2 μg/ml). Serious importance needs to be taken on this phenomenon.

In this study, all the resistant genes located on the p1575-1 plasmid were found to be chimeric with multiple IS sequences and various mobile elements, indicating that bla_{SFO-1}, bla_{NDM-1}, and *mcr-9* could be transferred not only by the p1575-1 plasmid but also by these mobile genes.

CONCLUSION

In this study, we report the coexistence of bla_{SFO-1}, bla_{NDM-1}, and *mcr-9* encoding one transferable IncHI2 plasmid in an *E. hormaechei* isolate. The co-occurrence of bla_{SFO-1}, bla_{NDM-1}, and *mcr-9* (as well as many associated resistance genes) caused *E. hormaechei* 1575 to be highly resistant not only to carbapenems but also to novel antibiotic ceftazidime–avibactam. At the same time, enough attention should be given to the dissemination of colistin resistance genes *mcr-9*, as polymyxin has been considered to be the "last-resort" antibiotic to treat human infections caused by CRE. Yet more worryingly, these genes are associated with various mobile elements and conjugative plasmids. The presence of multiple mobile elements indicates that horizontal gene transfer events play a key role in the acquisition of antibiotic resistance and the evolution of plasmids. Future studies are necessary to evaluate the prevalence of these plasmids among clinical isolates in China and other countries.

DATA AVAILABILITY STATEMENT

The datasets presented in this study can be found in online repositories. The names of the repository/repositories and accession number(s) can be found in the article/supplementary material.

ETHICS STATEMENT

As the *E. hormaechei* clinical isolate in this study was part of the routine hospital laboratory procedure, the Ethics Committee of the Shanghai Pulmonary Hospital of Tongji University School of Medicine approved our study.

AUTHOR CONTRIBUTIONS

All authors contributed to data analysis and drafting or revising the article, gave the final approval of the version to be published, and agreed to be accountable for all aspects of the work.

FUNDING

This study was supported by grants from the Jiangxi Provincial Department of Science and Technology, China (20181BBG70030) covering the each section of this study, including the design of the study and collection, analysis, and interpretation of the data and manuscript preparation.

ACKNOWLEDGMENTS

The authors thank the excellent technical assistance provided by Fangzhou Chen.

REFERENCES

Ahmad, N., Khalid, S., Ali, S., and Khan, A. (2018). blaOccurrence of Variants Among *Enterobacteriaceae* from a neonatal intensive care unit in a Northern India hospital. *Front. Microbiol.* 9:407. doi: 10.3389/fmicb.2018.00407

Bartowsky, E., and Normark, S. (1993). Interactions of wild-type and mutant AmpR of *Citrobacter freundii* with target DNA. *Mol. Microbiol.* 10, 555–565. doi: 10.1111/j.1365-2958.1993.tb00927.x

Bertrand, S., Weill, F., Cloeckaert, A., Vrints, M., Mairiaux, E., Praud, K., et al. (2006). Clonal emergence of extended-spectrum beta-lactamase (CTX-M-2)-producing *Salmonella enterica* serovar Virchow isolates with reduced susceptibilities to ciprofloxacin among poultry and humans in Belgium and France (2000 to 2003). *J. Clin. Microbiol.* 44, 2897–2903. doi: 10.1128/jcm.02549-05

Börjesson, S., Greko, C., Myrenas, M., Landén, A., Nilsson, O., and Pedersen, K. (2020). A link between the newly described colistin resistance gene mcr-9 and clinical *Enterobacteriaceae* isolates carrying bla from horses in Sweden. *J. Glob. Antimicrob. Resist.* 20, 285–289. doi: 10.1016/j.jgar.2019.08.007

Cao, X., Cheng, L., Zhang, Z., Ning, M., Zhou, W., Zhang, K., et al. (2017). Survey of clinical extended-spectrum beta-lactamase-producing *enterobacter cloacae* isolates in a Chinese tertiary hospital, 2012-2014. *Microb. Drug. Resist. (Larchmont, N.Y.)* 23, 83–89. doi: 10.1089/mdr.2015.0128

Carattoli, A. (2009). Resistance plasmid families in *Enterobacteriaceae*. *Antimicrob. Agents Chemother.* 53, 2227–2238. doi: 10.1128/aac.01707-08

Carattoli, A., Villa, L., Poirel, L., Bonnin, R., and Nordmann, P. (2012). Evolution of IncA/C blaCMY-2-carrying plasmids by acquisition of the blaNDM-1 carbapenemase gene. *Antimicrob. Agents Chemother.* 56, 783–786. doi: 10.1128/aac.05116-11

Cha, M. H., Woo, G. J., Lee, W., Kim, S. H., Woo, J. H., Kim, J., et al. (2020). Emergence of transferable mcr-9 gene-carrying colistin-resistant *Salmonella enterica* Dessau ST14 isolated from retail chicken meat in Korea. *Foodborne Pathog Dis.* 17, 720–727. doi: 10.1089/fpd.2020.2810

Chavda, K. D., Westblade, L. F., Satlin, M. J., Hemmert, A. C., Castanheira, M., Jenkins, S. G., et al. (2019). First report of bla (VIM-4)- and mcr-9-Coharboring *Enterobacter* species isolated from a pediatric patient. *mSphere* 4:e00629-19. doi: 10.1128/mSphere.00629-19

Chen, L., Mathema, B., Chavda, K., DeLeo, F., Bonomo, R., and Kreiswirth, B. (2014). Carbapenemase-producing *Klebsiella pneumoniae*: molecular and genetic decoding. *Trends Microbiol.* 22, 686–696. doi: 10.1016/j.tim.2014.09.003

Chen, W., Hu, Z., Wang, S., Huang, D., Wang, W., Cao, X., et al. (2020). Characterization of a clinical *Enterobacter* hormaechei strain belonging to epidemic clone ST418 co-carrying blaNDM-1, blaIMP-4 and mcr-9.1. *bioRxiv [preprint]* 2020.2009.2025.314500. doi: 10.1101/2020.09.25.314500

Chen, Y., Zhou, Z., Jiang, Y., and Yu, Y. (2011). Emergence of NDM-1-producing *Acinetobacter baumannii* in China. *J. Antimicrob. Chemothe.* 66, 1255–1259. doi: 10.1093/jac/dkr082

Clinical and Laboratory Standards Institute (CLSI) (2020). *Performance Standards for Antimicrobial Susceptibility Testing. CLSI supplement M100*, 30th Edn. Wayne: Clinical and Laboratory Standards Institute.

Dortet, L., Poirel, L., and Nordmann, P. (2014). Worldwide dissemination of the NDM-type carbapenemases in Gram-negative bacteria. *BioMed. Res. Int.* 2014:249856. doi: 10.1155/2014/249856

EUCAST (2020). *Breakpoint Tables for Interpretation of MICs and Zone Diameters. Version 10.0*. Available online at: http://www.eucast.org (accessed January 20, 2020).

Faccone, D., Martino, F., Albornoz, E., Gomez, S., Corso, A., and Petroni, A. (2020). Plasmid carrying mcr-9 from an extensively drug-resistant NDM-1-producing Klebsiella quasipneumoniae subsp. quasipneumoniae clinical isolate. *Infect. Genet. Evol. : J. Mol. Epidemiol. Evol. Genet. Infect. Dis.* 81:104273. doi: 10.1016/j.meegid.2020.104273

Guo, Q., Wang, P., Ma, Y., Yang, Y., Ye, X., and Wang, M. (2012). Co-production of SFO-1 and DHA-1 β-lactamases and 16S rRNA methylase ArmA in clinical isolates of *Klebsiella pneumoniae*. *J. Antimicrob. Chemother.* 67, 2361–2366. doi: 10.1093/jac/dks244

Gurjar, M. (2015). Colistin for lung infection: an update. *J. Intens. Care* 3:3. doi: 10.1186/s40560-015-0072-9

Hackl, T., Hedrich, R., Schultz, J., and Förster, F. (2014). proovread: large-scale high-accuracy PacBio correction through iterative short read consensus. *Bioinformatics (Oxford, England)* 30, 3004–3011. doi: 10.1093/bioinformatics/btu392

Henikoff, S., Haughn, G., Calvo, J., and Wallace, J. (1988). A large family of bacterial activator proteins. *Proc. Natl. Acad. Sci. U.S.A.* 85, 6602–6606. doi: 10.1073/pnas.85.18.6602

Kieffer, N., Royer, G., Decousser, J. W., Bourrel, A. S., Palmieri, M., Ortiz De La Rosa, J. M., et al. (2019). mcr-9, an inducible gene encoding an acquired phosphoethanolamine transferase in *Escherichia coli*, and its origin. *Antimicrob. Agents Chemother.* 63, e965–e919. doi: 10.1128/aac.00965-19

Kumarasamy, K., Toleman, M., Walsh, T., Bagaria, J., Butt, F., Balakrishnan, R., et al. (2010). Emergence of a new antibiotic resistance mechanism in India, Pakistan, and the UK: a molecular, biological, and epidemiological study. *Lancet Infect. Dis.* 10, 597–602. doi: 10.1016/s1473-3099(10)70143-2

Lin, M., Yang, Y., Yang, Y., Chen, G., He, R., Wu, Y., et al. (2020). mcr-9Co-occurrence of and in isolated from a patient with bloodstream infection. *Infect. Drug Resist.* 13, 1397–1402. doi: 10.2147/idr.S248342

Lindberg, F., Lindquist, S., and Normark, S. (1988). Genetic basis of induction and overproduction of chromosomal class I beta-lactamase in nonfastidious gram-negative bacilli. *Rev. Infect. Dis.* 10, 782–785. doi: 10.1093/clinids/10.4.782

Liu, Y., Wang, Y., Walsh, T., Yi, L., Zhang, R., Spencer, J., et al. (2016). Emergence of plasmid-mediated colistin resistance mechanism MCR-1 in animals and human beings in China: a microbiological and molecular biological study. *Lancet Infect. Dis.* 16, 161–168. doi: 10.1016/s1473-3099(15)00424-7

Liu, Z., Li, W., Wang, J., Pan, J., Sun, S., Yu, Y., et al. (2013). Identification and characterization of the first *Escherichia coli* strain carrying NDM-1 gene in China. *PLoS ONE* 8:e66666. doi: 10.1371/journal.pone.0066666

Matsumoto, Y., and Inoue, M. (1999). Characterization of SFO-1, a plasmid-mediated inducible class A beta-lactamase from *Enterobacter cloacae*. *Antimicrob. Agents Chemother.* 43, 307–313. doi: 10.1128/aac.43.2.307

McGann, P., Snesrud, E., Ong, A., Appalla, L., Koren, M., Kwak, Y., et al. (2015). War wound treatment complications due to transfer of an IncN plasmid harboring bla(OXA-181) from *Morganella morganii* to CTX-M-27-producing sequence type 131 *Escherichia coli*. *Antimicrob. Agents Chemother.* 59, 3556–3562. doi: 10.1128/aac.04442-14

Moellering, R. (2010). NDM-1–a cause for worldwide concern. *New England J. Med.* 363, 2377–2379. doi: 10.1056/NEJMp1011715

Nang, S., Li, J., and Velkov, T. (2019). mcrThe rise and spread of plasmid-mediated polymyxin resistance. *Crit. Rev. Microbiol.* 45, 131–161. doi: 10.1080/1040841x.2018.1492902

Nordmann, P., Poirel, L., Carrër, A., Toleman, M., and Walsh, T. (2011). How to detect NDM-1 producers. *J. Clin. Microbiol.* 49, 718–721. doi: 10.1128/jcm.01773-10

Novais, A., Cantón, R., Valverde, A., Machado, E., Galán, J., Peixe, L., et al. (2006). Dissemination and persistence of blaCTX-M-9 are linked to class 1 integrons containing CR1 associated with defective transposon derivatives from Tn402 located in early antibiotic resistance plasmids of IncHI2, IncP1-alpha, and IncFI groups. *Antimicrob. Agents Chemother.* 50, 2741–2750. doi: 10.1128/aac.00274-06

Olaitan, A., Morand, S., and Rolain, J. (2014). Mechanisms of polymyxin resistance: acquired and intrinsic resistance in bacteria. *Front. Microbiol.* 5:643. doi: 10.3389/fmicb.2014.00643

Partridge, S., and Tsafnat, G. (2018). Automated annotation of mobile antibiotic resistance in Gram-negative bacteria: the Multiple Antibiotic Resistance Annotator (MARA) and database. *J. Antimicrob. Chemother.* 73, 883–890. doi: 10.1093/jac/dkx513

Poirel, L., Bonnin, R., Boulanger, A., Schrenzel, J., Kaase, M., and Nordmann, P. (2012). Tn125-related acquisition of blaNDM-like genes in *Acinetobacter baumannii*. *Antimicrob. Agents Chemother.* 56, 1087–1089. doi: 10.1128/aac.05620-11

Queenan, A., and Bush, K. (2007). Carbapenemases: the versatile beta-lactamases. *Clin. Microbiol. Rev.* 20, 440–458. doi: 10.1128/cmr.00001-07 table of contents,

Roy Chowdhury, P., Fourment, M., DeMaere, M., Monahan, L., Merlino, J., Gottlieb, T., et al. (2019). Identification of a novel lineage of plasmids within phylogenetically diverse subclades of IncHI2-ST1 plasmids. *Plasmid* 102, 56–61. doi: 10.1016/j.plasmid.2019.03.002

Sherburne, C., Lawley, T., Gilmour, M., Blattner, F., Burland, V., Grotbeck, E., et al. (2000). The complete DNA sequence and analysis of R27, a large IncHI plasmid from *Salmonella* typhi that is temperature sensitive for transfer. *Nucleic Acids Res.* 28, 2177–2186. doi: 10.1093/nar/28.10.2177

Tacconelli, E., Carrara, E., Savoldi, A., Harbarth, S., Mendelson, M., Monnet, D., et al. (2018). Discovery, research, and development of new antibiotics: the WHO priority list of antibiotic-resistant bacteria and tuberculosis. *Lancet Infect. Dis.* 18, 318–327. doi: 10.1016/s1473-3099(17)30753-3

Tasina, E., Haidich, A. B., Kokkali, S., and Arvanitidou, M. (2011). Efficacy and safety of tigecycline for the treatment of infectious diseases: a meta-analysis. *Lancet Infect. Dis.* 11, 834–844. doi: 10.1016/s1473-3099(11)70177-3

Toleman, M., Spencer, J., Jones, L., and Walsh, T. (2012). blaNDM-1 is a chimera likely constructed in *Acinetobacter baumannii*. *Antimicrob. Agents Chemother.* 56, 2773–2776. doi: 10.1128/aac.06297-11

Walsh, T. (2010). Emerging carbapenemases: a global perspective. *Int. J. Antimicrob. Agents*, 36S3, S8–S14. doi: 10.1016/s0924-8579(10)70004-2

Wang, X., Wang, Y., Zhou, Y., Li, J., Yin, W., Wang, S., et al. (2018). Emergence of a novel mobile colistin resistance gene, mcr-8, in NDM-producing *Klebsiella pneumoniae*. *Emerg. Microbes Infect.* 7:122. doi: 10.1038/s41426-018-0124-z

WHO. (2017). *WHO Publishes List of Bacteria for Which New Antibiotics are Urgently Needed*. Geneva: World Health Organization.

Xu, Y., Liu, Y., Liu, Y., Pei, J., Yao, S., and Cheng, C. (2015). Bacteriophage therapy against Enterobacteriaceae. *Virol. Sin.* 30, 11–18. doi: 10.1007/s12250-014-3543-6

Yilmaz, G., Dizbay, M., Guven, T., Pullukcu, H., Tasbakan, M., Guzel, O., et al. (2016). Risk factors for infection with colistin-resistant gram-negative microorganisms: a multicenter study. *Ann. Saudi Med.* 36, 216–222. doi: 10.5144/0256-4947.2016.216

Yuan, Y., Li, Y., Wang, G., Li, C., Xiang, L., She, J., et al. (2019). *Enterobacter* hormaecheiCoproduction Of MCR-9 And NDM-1 By colistin-resistant isolated from bloodstream infection. *Infect. Drug Resist.* 12, 2979–2985. doi: 10.2147/idr.S217168

Zhao, J., Zhu, Y., Li, Y., Mu, X., You, L., Xu, C., et al. (2015). Coexistence of SFO-1 and NDM-1 β-lactamase genes and fosfomycin resistance gene fosA3 in an *Escherichia coli* clinical isolate. *FEMS Microbiol. Lett.* 362, 1–7. doi: 10.1093/femsle/fnu018

Zhou, K., Zhou, Y., Zhang, C., Song, J., Cao, X., Yu, X., et al. (2020). Dissemination of a 'rare' extended-spectrum β-lactamase gene bla(SFO-1) mediated by epidemic clones of carbapenemase-producing *Enterobacter* hormaechei in China. *Int J Antimicrob. Agents* 56:106079. doi: 10.1016/j.ijantimicag.2020.106079

Conflict of Interest: The authors declare that the research was conducted in the absence of any commercial or financial relationships that could be construed as a potential conflict of interest.

frontiers in Microbiology

ORIGINAL RESEARCH
published: 07 July 2021
doi: 10.3389/fmicb.2021.663033

High Prevalence of Extended-Spectrum Beta-Lactamases in *Escherichia coli* Strains Collected From Strictly Defined Community-Acquired Urinary Tract Infections in Adults in China: A Multicenter Prospective Clinical Microbiological and Molecular Study

*Peiyao Jia[1,2†], Ying Zhu[1,2†], Xue Li[1,3†], Timothy Kudinha[4,5], Yang Yang[1], Ge Zhang[1], Jingjia Zhang[1], Yingchun Xu[1] and Qiwen Yang[1]**

[1] Department of Clinical Laboratory, State Key Laboratory of Complex Severe and Rare Diseases, Peking Union Medical College Hospital, Chinese Academy of Medical Sciences and Peking Union Medical College, Beijing, China, [2] Graduate School, Peking Union Medical College, Chinese Academy of Medical Sciences, Beijing, China, [3] Department of Clinical Laboratory, Beijing Anzhen Hospital, Capital Medical University, Beijing, China, [4] School of Biomedical Sciences, Charles Sturt University, Orange, NSW, Australia, [5] NSW Health Pathology, Regional and Rural, Orange Hospital, Orange, NSW, Australia

Objective: The objective of the study was to investigate the antimicrobial susceptibility and extended-spectrum beta-lactamase (ESBL) positive rates of *Escherichia coli* from community-acquired urinary tract infections (CA-UTIs) in Chinese hospitals.

Materials and Methods: A total of 809 *E. coli* isolates from CA-UTIs in 10 hospitals (5 tertiary and 5 secondary hospitals) from different regions in China were collected during the period 2016–2017 according to the strict inclusion criteria. Antimicrobial susceptibility testing was carried out by standard broth microdilution method. Isolates were categorized as ESBL-positive, ESBL-negative, and ESBL-uncertain groups according to the CLSI recommended phenotypic screening method. ESBL and AmpC genes were amplified and sequenced on ESBL-positive and ESBL-uncertain isolates.

Results: The antimicrobial agents with susceptibility rates of greater than 95% included imipenem (99.9%), colistin (99.6%), ertapenem (98.9%), amikacin (98.3%), cefmetazole (97.9%), nitrofurantoin (96%), and fosfomycin (95.4%). However, susceptibilities to cephalosporins (varying from 58.6% to 74.9%) and levofloxacin (48.8%) were relatively low. In the phenotypic detection of ESBLs, ESBL-positive isolates made up 38.07% of *E. coli* strains isolated from CA-UTIs, while 2.97% were ESBL-uncertain. Antimicrobial susceptibilities of imipenem, cefmetazole, colistin, ertapenem, amikacin, and nitrofurantoin against ESBL-producing *E. coli* strains were greater than 90%. The percentage of ESBL-producing strains was higher in male (53.6%) than in female patients (35.2%) ($p < 0.001$). CTX-M-14 (31.8%) was the major CTX-M variant in the

OPEN ACCESS

Edited by:
Mary Marquart, University of Mississippi Medical Center, United States

Reviewed by:
Leila Vali, Kuwait University, Kuwait
Mariana Carmen Chifiriuc, University of Bucharest, Romania

***Correspondence:**
Qiwen Yang
yangqiwen81@vip.163.com

† These authors have contributed equally to this work

Specialty section:
This article was submitted to Antimicrobials, Resistance and Chemotherapy, a section of the journal Frontiers in Microbiology

Received: *02 February 2021*
Accepted: *26 May 2021*
Published: *07 July 2021*

Citation:
Jia P, Zhu Y, Li X, Kudinha T, Yang Y, Zhang G, Zhang J, Xu Y and Yang Q (2021) High Prevalence of Extended-Spectrum Beta-Lactamases in Escherichia coli Strains Collected From Strictly Defined Community-Acquired Urinary Tract Infections in Adults in China: A Multicenter Prospective Clinical Microbiological and Molecular Study. Front. Microbiol. 12:663033. doi: 10.3389/fmicb.2021.663033

ESBL-producing *E. coli*, followed by CTX-M-55 (23.4%), CTX-M-15 (17.5%), and CTX-M-27 (13.3%). The prevalence of carbapenem-resistant *E. coli* among CA-UTI isolates was 0.25% (2/809).

Conclusion: Our study indicated high prevalence of ESBL in *E. coli* strains from strictly defined community-acquired urinary tract infections in adults in China. Imipenem, colistin, ertapenem, amikacin, and nitrofurantoin were the most active antimicrobials against ESBL-positive *E. coli* isolates. $bla_{CTX-M-14}$ is the predominant *esbl* gene in ESBL-producing and ESBL-uncertain strains. Our study indicated that the use of cephalosporins and fluoroquinolone needs to be restricted for empirical treatment of CA-UTIs in China.

Keywords: community-acquired urinary tract infections, *Escherichia coli*, extended-spectrum beta-lactamase, antibiotic resistance, empirical treatment, CTX-M

INTRODUCTION

Escherichia coli (E. coli) is a common pathogen of community-acquired infections such as intra-abdominal infection, urinary tract infection (UTI), and pelvic inflammatory disease. UTI is one of the most common bacterial infectious diseases of humans. Over 85% of community-acquired urinary tract infections (CA-UTIs) have been attributed to *E. coli* infection (Espínola et al., 2011). Increasing trend in extended-spectrum beta-lactamase (ESBL) rates was seen among isolates from CA-UTIs in many regions; the antimicrobial resistance surveillance program in China showed that the proportion of ESBL-producing *E. coli* in community-acquired infections ranges from 45.2 to 68.2% (Yun et al., 2014; Fupin et al., 2017), in Canada, from 9.1 to 14.1%, and in the United States, from 6.5% in 2010 to 16.0% in 2014 (Lob et al., 2016). In some European countries, the prevalence of ESBL-producing *E. coli* isolated from CA-UTIs is currently lower than 5% (van Driel et al., 2019; Richelsen et al., 2020; Larramendy et al., 2021), but can reach up to 23.6% in Spanish, 38.2% in Turkey, and 34.6% in Iran (Arana et al., 2017; Koksal et al., 2017; Naziri et al., 2020). Most of the discrepancy in ESBL prevalence rates between studies might be related to geographical difference. However, the inclusion and exclusion criteria of isolates is also an important factor, which may over- or underestimate the ESBL rates or antimicrobial resistance in community-acquired infections. Studying the antimicrobial resistance patterns of *E. coli* in real community-acquired infections is important not only for understanding the resistance status but also for choosing the most appropriate empirical antimicrobial therapy for CA-UTIs (Lob et al., 2015). The real ESBL rate and molecular epidemiology in CA-UTIs in China is unclear.

The aim of this study was to investigate the real ESBL status and antimicrobial susceptibility of *E. coli* isolates strictly collected from CA-UTIs in China.

MATERIALS AND METHODS

Clinical Isolates

During the period 2016–2017, a total of 809 *E. coli* isolates from CA-UTIs were consecutively collected from 10 hospitals located in the following regions of China: northeastern (121 isolates), northern (179 isolates), central (172 isolates), western (159 isolates), and eastern (178 isolates). The specific geographical distribution is shown in **Figure 1**. The 10 hospitals included 5 tertiary hospitals (Peking Union Medical College Hospital; Sichuan Provincial People's Hospital; Tongji Hospital, Tongji Medical College Huazhong University of Science and Technology; The First Affiliated Hospital, College of Medicine, Zhejiang University; and Shengjing Hospital of China Medical University) and 5 secondary hospitals located in the same provinces as the 5 tertiary hospitals (Beijing Pinggu Hospital; Sichuan Science City Hospital; Zaoyang First People's Hospital; Zhuji People's Hospital of Zhejiang Province; and Dalian Hospital, Shengjing Hospital of China Medical University).

Isolates were strictly chosen by using the following inclusion and exclusion criteria to ensure all cases were community-acquired patients.

Inclusion Criteria

(1) All *E. coli* isolates were cultured from urines of adult UTI patients (>18 years old) from outpatient clinic/emergency department or admitted to a hospital in less than 48 h. (2) Isolates were cultured from uncomplicated UTI, such as acute cystitis, acute pyelonephritis, with evidence support of clinical symptoms, urine routine test, and/or imaging examination. (3) Isolates were infection-related pathogens cultured from qualified urine specimens with bacteria quantification of $> 10^5$ CFU/ml.

Exclusion Criteria

Isolates from patients with the following conditions were excluded; (1) patients with invasive devices (such as various venous catheters, urethral catheters, intubations, and artificial implants, etc.); (2) immunocompromised patients (e.g., patients who had received glucocorticoid, radiotherapy, and chemotherapy within 6 months); (3) patients with a history of surgery, hemodialysis/abdominal dialysis, hospitalization, and community clinic/health center hospitalization within the previous 1 year; (4) using broad-spectrum antibiotics within 3 months prior to infection; (5) patients with chronic urinary tract infections (previously isolated from the same

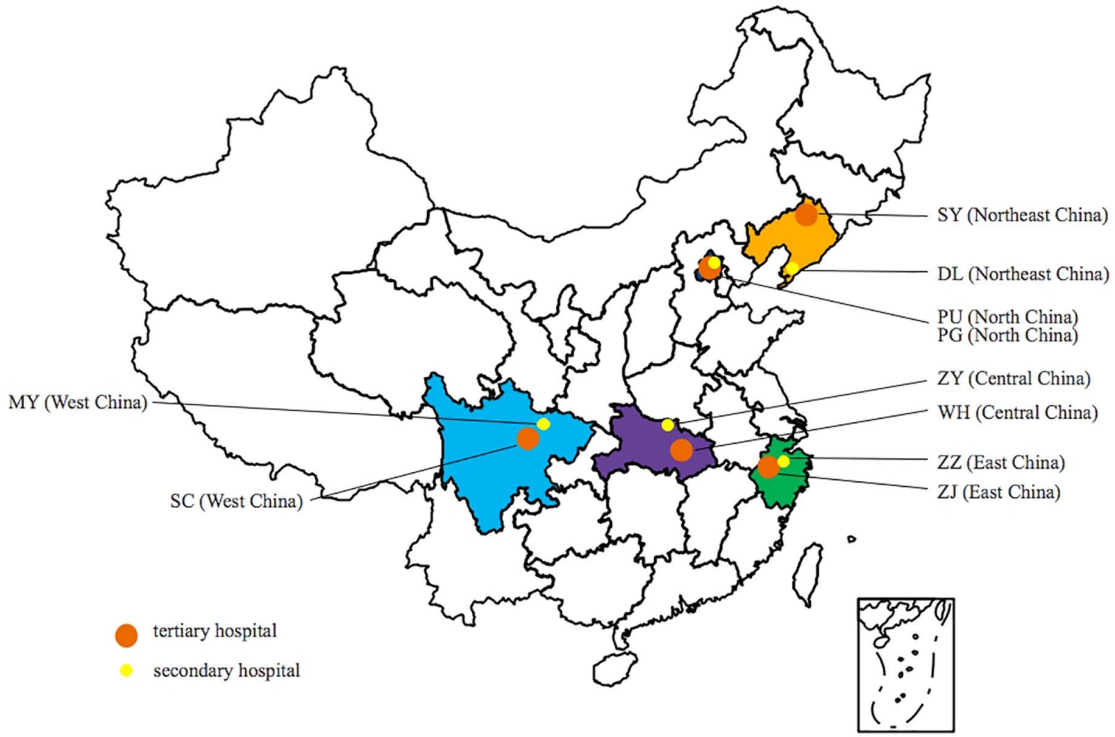

FIGURE 1 | Geographical distribution of hospitals participating in the study. PU, Peking Union Medical College Hospital; PG, Beijing Pinggu Hospital; SY, Shengjing Hospital of China Medical University; DL, Dalian Hospital; ZZ, Zhuji People's Hospital of Zhejiang Province; ZJ, The First Affiliated Hospital College of Medical Zhejiang University; WH, Tongji Hospital; ZY, First Peoples Hospital of Zaoyang; SC, Sichuan Provincial People's Hospital; and MY, Sichuan Science City Hospital.

type of specimen); (6) isolates implicated in healthcare-associated infections and recurrent UTIs (recurrences of uncomplicated and/or complicated UTIs, with a frequency of at least three UTIs/year or two UTIs in the last 6 months); (7) environmental samples or cultures for infection control purposes; and (8) duplicate isolates (the same species from the same patient).

Antimicrobial Susceptibility Test Method

Minimum inhibitory concentration determination for all antimicrobial agents, except fosfomycin, was performed using the microdilution broth method as per Clinical and Laboratory Standards Institute (CLSI) guidelines (CLSI, 2020). MICs of fosfomycin were determined by agar dilution method (25 μg/ml of glucose-6-phosphate was added in Mueller–Hinton agar). Seventeen antimicrobial agents were analyzed, including cefazolin (CZO), ceftriaxone (CRO), ceftazidime (CAZ), cefepime (FEP), cefoperazone/sulbactam (CSL, 2:1), imipenem (IPM), ertapenem (ETP), amikacin (AMK), levofloxacin (LVX), cefmetazole (CMZ), trimethoprim/sulfamethoxazole (SXT, 1:19), colistin (COL), fosfomycin (FOS), cefotaxime (CTX), cefotaxime/clavulanic acid (CTC), ceftazidime/clavulanic acid (CCV), and nitrofurantoin (NIT). For each batch of MIC testing, reference strains *E. coli* ATCC 25922 and *P. aeruginosa* ATCC 27853 were used as quality control organisms.

Phenotypic Detection of Extended-Spectrum β-Lactamases

Phenotypic identification of ESBL in *E. coli* was carried out by CLSI-recommended methods (CLSI, 2020). If cefotaxime or ceftazidime MIC of an isolate was $\geq$ 2 μg/ml each, the MICs of cefotaxime + clavulanic acid (4 μg/ml) or ceftazidime + clavulanic acid (4 μg/ml) were comparatively determined. ESBL production was defined as a greater than or equal to eightfold decrease in MICs for cefotaxime or ceftazidime when tested in combination with clavulanic acid, compared with their MICs without clavulanic acid. ESBL-negative isolates were defined as isolates with cefotaxime or ceftazidime MICs of $\leq$ 1 μg/ml. ESBL-uncertain isolates were defined as isolates with cefotaxime or ceftazidime MICs of $\geq$ 2 μg/ml, but did not exhibit a greater than or equal to eightfold decrease in MICs for cefotaxime or ceftazidime after a combination with clavulanic acid, compared with their MICs alone.

Characterization of Antibiotic Resistance Genes

The main *esbl* and *ampC* genes, including bla_{TEM}, bla_{SHV}, $bla_{CTX-M-1}$ group, $bla_{CTX-M-2}$ group, $bla_{CTX-M-9}$ group, bla_{DHA}, bla_{CMY}, and bla_{ACT}, were determined using polymerase chain (PCR) reaction method on the strains with ESBL-producing and ESBL-uncertain phenotype. The positive

amplicons were sequenced and aligned by blastn web[1]. Primers used in this study are listed in **Table 1**.

Statistical Analysis

The results of antimicrobial susceptibility testing were analyzed by the WHONET5.6 program. Ninety-five percent confidence intervals were calculated using the adjusted Wald method; comparison of ESBL rates between tertiary and secondary hospital, in demographic characteristics and clinical features, was assessed using Chi-square test. Analyses were performed using SPSS version 25.0 (IBM Corporation), and p-values < 0.05 were considered statistically significant.

RESULTS

Features of the Isolates

A total of 809 *E. coli* isolates from community-acquired adult urinary tract infections (CA-UTIs) were collected during the period 2016–2017. Most infections were lower UTIs (96.8%, 783/809), which included 5 cases of urethritis and 778 cases of cystitis. Upper UTIs accounted for 3.2% (26/809) including eight acute pyelonephritis, four hydronephrosis, seven kidney stones, and seven ureteral calculus. Isolates from female patients accounted for 85% of the total isolates. The ages of patients were as follows: 18–45 years, 31.8%; 46–65 years, 38.8%, and $\geq$ 66 years, 29.4%.

In vitro Susceptibility of *Escherichia coli* Isolates From Community-Acquired Adult Urinary Tract Infections

Among the 809 *E. coli* isolates studied, 308 (38.07%) were ESBL-producing strains, 477 (58.96%) were ESBL-negative, and 24 (2.97%) were ESBL-uncertain. The antimicrobial agents with susceptibility rates of greater than 95% included imipenem (99.9%), colistin (99.6%), ertapenem (98.9%), amikacin (98.3%), cefmetazole (97.9%), nitrofurantoin (96%), and fosfomycin (95.4%). However, the susceptibility rates to cephalosporins were relatively low, ranging from 58.6 to 74.9%. The antimicrobial susceptibility for all isolates is summarized in **Table 2**.

We investigated ESBL differences between isolates from secondary hospitals and tertiary hospitals. Overall, there was no major difference in the proportion of ESBL-positive isolates (37.66% in secondary hospitals vs. 38.44% in tertiary hospitals) or ESBL-uncertain strains (3.12% in secondary hospitals vs. 2.83% in tertiary hospitals) (**Figure 2**). However, we found some differences, although very small, in the distribution of ESBLs by geographic region. Relatively higher percentages of ESBL rate were found in the northeast (46.3%), central (43.6%), and west (43.4%) China, compared with the sites in the north (30.2%) and east (30.3%) of China (**Figure 2**).

In general, *E. coli* isolates collected from secondary and tertiary hospitals showed high susceptibility rates to most antibiotics as follows: imipenem (100% vs. 99.8%), colistin (100% vs. 99.3%), ertapenem (99.5% vs. 98.3%), amikacin (98.4% vs. 98.1%), cefmetazole (97.9% vs. 97.9%), fosfomycin (95.8% vs. 95.0%), and nitrofurantoin (94% vs. 97.9%). Furthermore, cefoperazone/sulbactam showed high activity against strains isolated from secondary and tertiary hospitals, with a susceptibility rate of 90.4% and 87.7%. The susceptibilities to cephalosporins in isolates collected from tertiary hospitals varied from 58.0 to 75.5%.

Characterization of Extended-Spectrum Beta-Lactamase and AmpC Genes

Polymerase chain was performed on 332 ESBL-producing and ESBL-uncertain isolates to determine the presence of EBSL and AmpC. The results are shown in **Figure 3**. The major β-lactamase family detected in the ESBL-producing *E. coli* strains was CTX-M-9 group (149/308, 48.4%), followed by the

[1]http://blast.ncbi.nlm.nih.gov/Blast.cgi

TABLE 1 | Polymerase chain reaction (PCR) primers used for detecting antibiotic resistance genes.

Target		Primer sequences (5′ to 3′)	Annealing temp. (°C)	Fragment size (bp)	References
TEM	Forward	ATAAAATTCTTGAAGACGAAA	55	1,079	Yang et al., 2015
	Reverse	GACAGTTAGCAATGCTTAATCA			
SHV	Forward	CCGGGTTATTCTTATTTGTCGCT	56	928	Lee et al., 2006
	Reverse	TAGCGTTGCCAGTGCTCG			
CTX-M-1 group	Forward	CGTCACGCTGTTGTTAGGAA	56	823	Yang et al., 2015
	Reverse	ACCGTCGGTGACGATTTTAG			
CTX-M-2 group	Forward	ATGATGACTCAGAGCATTCG	65	832	Yang et al., 2015
	Reverse	TCCCGACGGCTTTCCGCCTT			
CTX-M-9 group	Forward	AAAAATGATTGAAAGGTGGT	56	1,242	Yang et al., 2015
	Reverse	GTGAAGAAGGTGTTGCTGAC			
DHA-1	Forward	CTGATGAAAAAATCGTTATC	56	1,141	Giakkoupi et al., 2006
	Reverse	ATTCCAGTGCACTCAAAATA			
CMY	Forward	TGTCAACACGGTGCAAATCA	56	1,346	Armand-Lefèvre et al., 2003
	Reverse	AGCAACGACGGGCAAAATG			
ACT-1	Forward	CGAACGAATCATTATTCAGCACCG	56	1,518	Reisbig and Hanson, 2002
	Reverse	CGGCAATGTTTACTACACAGCG			

TABLE 2 | The antimicrobial susceptibilities of 809 *Escherichia coli* strains isolated from community-acquired urinary tract infection (CA-UTI) in China.

Antibiotic	All isolates (*n* = 809)						ESBL-producing and ESBL-uncertain isolates (*n* = 332)					
	%R	%I	%S	MIC50 (μg/ml)	MIC90 (μg/ml)	MIC range (μg/ml)	%R	%I	%S	MIC50 (μg/ml)	MIC90 (μg/ml)	MIC range (μg/ml)
Imipenem	0.1		99.9	0.125	0.125	0.03–16	0.3		99.7	0.12	0.25	0.03–16
Colistin	0.4		99.6	0.5	0.5	0.12–8	0.6		99.4	0.5	0.5	0.12–4
Ertapenem	0.2	0.9	98.9	0.016	0.125	0.008–32	0.6	2.1	97.3	0.03	0.25	0.008–32
Amikacin	1.2	0.5	98.3	2	4	0.25–512	3	0.6	96.4	2	8	1–512
Cefmetazole	1.4	0.7	97.9	1	4	0.06–256	2.4	1.5	96.1	1	8	0.06–256
Nitrofurantoin	1.6	2.3	96	16	32	0.5–256	2.7	4.2	93.1	16	32	4–256
Fosfomycin	3.6	1	95.4	1	16	0.25–512	8.4	1.5	90.1	2	64	0.5–512
Cefoperazone/sulbactam	3.5	7.5	89	1	32	0.06–256	8.1	18.1	73.8	16	32	0.06–256
Ceftazidime	20.4	4.7	74.9	0.25	32	0.03–64	49.7	11.4	38.9	8	64	0.12–64
Cefepime	31.5	3.5	65	0.064	64	0.016–64	76.8	8.4	14.8	64	64	0.03–64
Ceftriaxone	38.3	0.2	61.4	0.064	64	0.016–64	93.1	0.6	6.3	64	64	0.016–64
Cefotaxime	38.3	0.4	61.3	0.064	64	0.016–64	93.4	0.9	5.7	64	64	0.03–64
Cefazolin	41.4		58.6	4	32	1–32	93.1		6.9	32	32	1–32
Levofloxacin	50.2	1	48.8	2	16	0.016–64	72.3	0.6	27.1	8	16	0.016–64
Trimethoprim/sulfamethoxazole	55.6		44.4	8	8	0.25–8	68.7		31.3	8	8	0.25–8

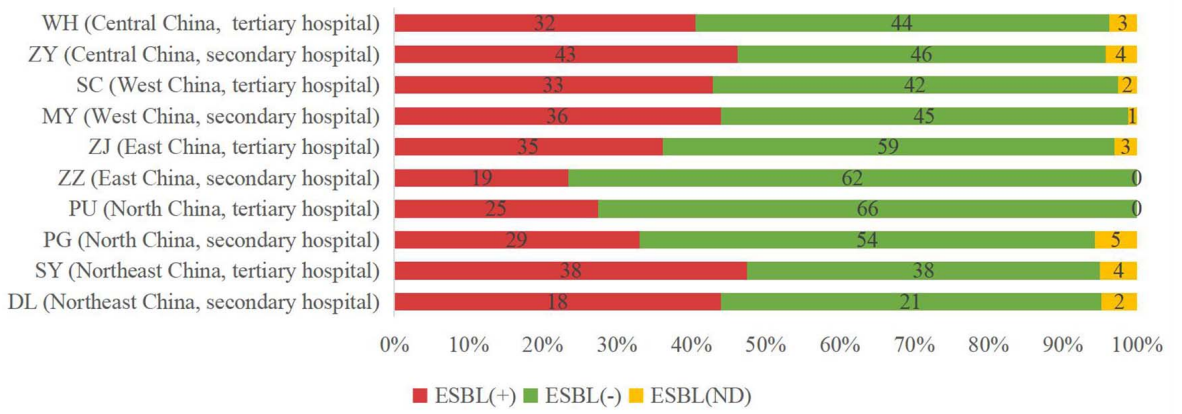

FIGURE 2 | Incidence of extended-spectrum beta-lactamase (ESBL)-producing strains in different sites of China. ESBL (+), ESBL-positive isolates; ESBL (–), ESBL-negative isolates; and ESBL (ND), ESBL-uncertain isolates.

CTX-M-1 group (136/308, 44.2%). The CTX-M-2 group was not detected. bla_{CMY-2} was detected in one isolate. Overall, 7 bla_{CTX-M} subtypes were detected: $bla_{CTX-M-14}$ (98 isolates, 31.8%), $bla_{CTX-M-55}$ (72 isolates, 23.4%), $bla_{CTX-M-15}$ (54 isolates, 17.5%), $bla_{CTX-M-27}$ (41 isolates, 13.3%), $bla_{CTX-M-65}$ (10 isolates, 3.2%), $bla_{CTX-M-3}$ (5 isolates, 1.6%), $bla_{CTX-M-64}$ (4 isolates, 1.3%), and $bla_{CTX-M-79}$ (1 isolates, 0.3%). Among the bla_{CTX-M} subtypes, two different variants were detected in 20/332 isolates (6.0%), most of which were $bla_{CTX-M-14}$ and $bla_{CTX-M-15}$ (7 isolates), $bla_{CTX-M-14}$ and $bla_{CTX-M-55}$ (7 isolates).

Among ESBL-uncertain isolates, bla_{CMY} was the most common AmpC gene (18/24, 75%), consisting of bla_{CMY-2} (15 isolates, including 2 isolates coexisting with $bla_{CTX-M-14}$), bla_{CMY-42} (2 isolates coexisted with $bla_{CTX-M-15}$), and bla_{CMY-34} (1 isolate). bla_{TEM-1} was determined in eight strains (33.3%, 1 isolate coexisted with $bla_{CTX-M-55}$). In five strains (20.8%), no ESBL genes were determined.

In vitro Susceptibility of *Escherichia coli* Strains With Different Extended-Spectrum Beta-Lactamase Phenotypes

Extended-spectrum beta-lactamase producing *E. coli* strains exhibited susceptibility rates of over 92% to imipenem (100%), cefmetazole (99.4%), colistin (99.4%), ertapenem (98.4%), amikacin (97.1%), and nitrofurantoin (92.9%). The susceptibility rates of ESBL-negative isolates against all the antimicrobial agents were higher than 90%, except levofloxacin (63.9%) and trimethoprim/sulfamethoxazole (53.5%). On the other hand, ESBL-uncertain isolates showed high susceptibility rates

to colistin (100%)], imipenem (95.8%), fosfomycin (95.8%), and nitrofurantoin (95.8%). The susceptibility rate differences between ESBL-producing and ESBL-negative isolates were greater for cephalosporins (**Figure 4**), including cefotaxime (6.2% vs. 100%), ceftriaxone (6.5% vs. 99.8%), cefazolin (7.1% vs. 94.5%), and cefepime (9.7% vs. 100%).

Comparison of the Antimicrobial Susceptibility Rates of *Escherichia coli* Isolates by Hospital Level, Demographic Characteristics, and Clinical Features

We observed that gender was a significant factor influencing antimicrobial susceptibility, with a significantly higher rate of ESBL-producing strains in male (53.6%) than in female patients (35.2%) ($p < 0.001$). Cephalosporins exhibited higher rates of *in vitro* activity against *E. coli* strains from female than from male patients ($p < 0.05$), including cefazolin, ceftazidime, ceftriaxone, cefotaxime, cefoperazone/sulbactam, and cefepime (**Figure 5** and **Table 3**). There was no significant difference in antimicrobial susceptibility and *esbl* genes between *E. coli* strains from tertiary and secondary hospitals, between the age groups of 18 and 65 and over 65 years, or between upper and lower UTIs. The major CTX-M variant in northeast China, west China, and central China was CTX-M-14, followed by CTX-M-15, CTX-M-55, and CTX-M-27. While in north China, the major variant was CTX-M-15 (13/59, 22.03%), in east China, the secondary variant was CTX-M-27 (12/57, 21.05%). The CTX-M genotypes included high rates of CTX-M-14 followed by CTX-M-55, CTX-M-15, and CTX-M-27, which was similar between isolates from tertiary hospitals and from secondary hospitals. There existed a difference in the distribution of CTX-M variants; CTX-M-15 had a larger proportion than CTX-M-55 among male patients and patients over 65 years of age (**Figure 3**).

Community-Acquired Carbapenem-Resistant Strains

In this study, two strains were identified as community-acquired carbapenem resistant. The two carbapenem-resistant *Enterobacteriaceae* (CRE) strains (MYU26 and SYU04) were resistant to almost all β-lactam antibiotics tested, with only three antimicrobial agents exhibiting potent activity against them, including colistin (MYU26: MIC $\leq$ 0.12, SYU04: MIC = 0.5), fosfomycin (MYU26: MIC = 1, SYU04: MIC = 4), and tigecycline (MYU26 and SYU04: MICs $\leq$ 0.06). MYU26 carried the $bla_{CTX-M-15}$ and bla_{CMY-42} genes and SYU04 carried the bla_{CMY-2} gene. No carbapenemase genes were detected.

DISCUSSION

Our analysis of stringently selected *E. coli* isolates from CA-UTIs, collected in China during the period 2016–2017, revealed a relatively lower ESBL rate (38.07%) than previously reported in 2012 (68.6%) and 2014 (59.1%) in a study from The Study for Monitoring Antimicrobial Resistance Trends (SMART) surveillance program (Yang et al., 2017). However, another study in China (Zhang et al., 2019) found no significant difference in the rates of ESBLs among *E. coli* isolates from HA and CA UTIs, and the ESBL rate in that study was 48.8% among CA-UTI *E. coli* isolates during the period 2016–2017, which is higher than in the present study. In Asia, the proportion of ESBL-producing *E. coli*

TABLE 3 | Comparison of the antimicrobial susceptibility rates of *E. coli* isolates in hospital level, demographic characteristics, and clinical features.

Antibiotic	Hospital level (%)			Age (%)			Gender (%)			Infection sites (%)		
	Tertiary hospital, *n* = 424	Secondary hospital, *n* = 385	*p*-Value	18–65, *n* = 571	> 65, *n* = 238	*p*-Value	Male, *n* = 123	Female, *n* = 686	*p*-Value	Upper urinary tract, *n* = 26	Lower urinary tract, *n* = 783	*p*-Value
ESBL rate (%)	37.7	35.3	0.985	38	38.2	0.998	53.6	35.2	< 0.001*	26.9	38.4	0.490
Imipenem	99.8	100	1	100	99.6	0.294	100	99.9	1	100	99.9	1
Ertapenem	98.3	99.5	0.153	99.6	97.1	0.005*	98.4	99	0.488	100	98.9	1
Colistin	99.3	100	0.251	99.6	99.6	1	99.2	99.7	0.391	100	99.6	1
Amikacin	98.1	98.4	0.908	98.6	97.5	0.139	96.7	98.5	0.089	100	98.2	1
Cefmetazole	97.9	97.9	1	98.2	97.1	0.440	99.2	97.7	0.871	96.2	98	0.425
Nitrofurantoin	97.9	94	0.017*	96.3	95.4	0.767	95.1	96.2	0.297	96.2	96	0.442
Fosfomycin	95	95.8	0.818	95.3	95.8	0.564	94.3	95.6	0.198	96.2	95.4	0.273
Cefoperazone/sulbactam	87.7	90.4	0.399	90.2	86.1	0.232	78.9	90.8	0.001*	92.3	88.9	1
Ceftazidime	75.5	74.3	0.910	75	74.8	0.954	65	76.7	0.023*	76.9	74.8	0.964
Cefepime	64.4	65.7	0.862	65.3	64.3	0.281	49.6	67.8	< 0.001*	76.9	64.6	0.390
Ceftriaxone	60.6	62.3	0.302	61.5	61.3	0.770	43.9	64.6	< 0.001*	69.2	61.2	0.573
Cefotaxime	60.8	61.8	0.207	61.5	60.9	0.974	43.9	64.4	< 0.001*	69.2	61	0.587
Cefazolin	58	59.2	0.729	58.8	58	0.821	44.7	61.1	0.001*	61.5	58.5	0.756
Levofloxacin	46.9	50.9	0.330	50.8	44.1	0.105	46.3	49.3	0.374	46.2	48.9	0.323
Trimethoprim/sulfamethoxazole	45.8	42.9	0.407	43.8	45.8	0.599	46.3	44	0.634	34.6	44.7	0.309

*$p < 0.05$.

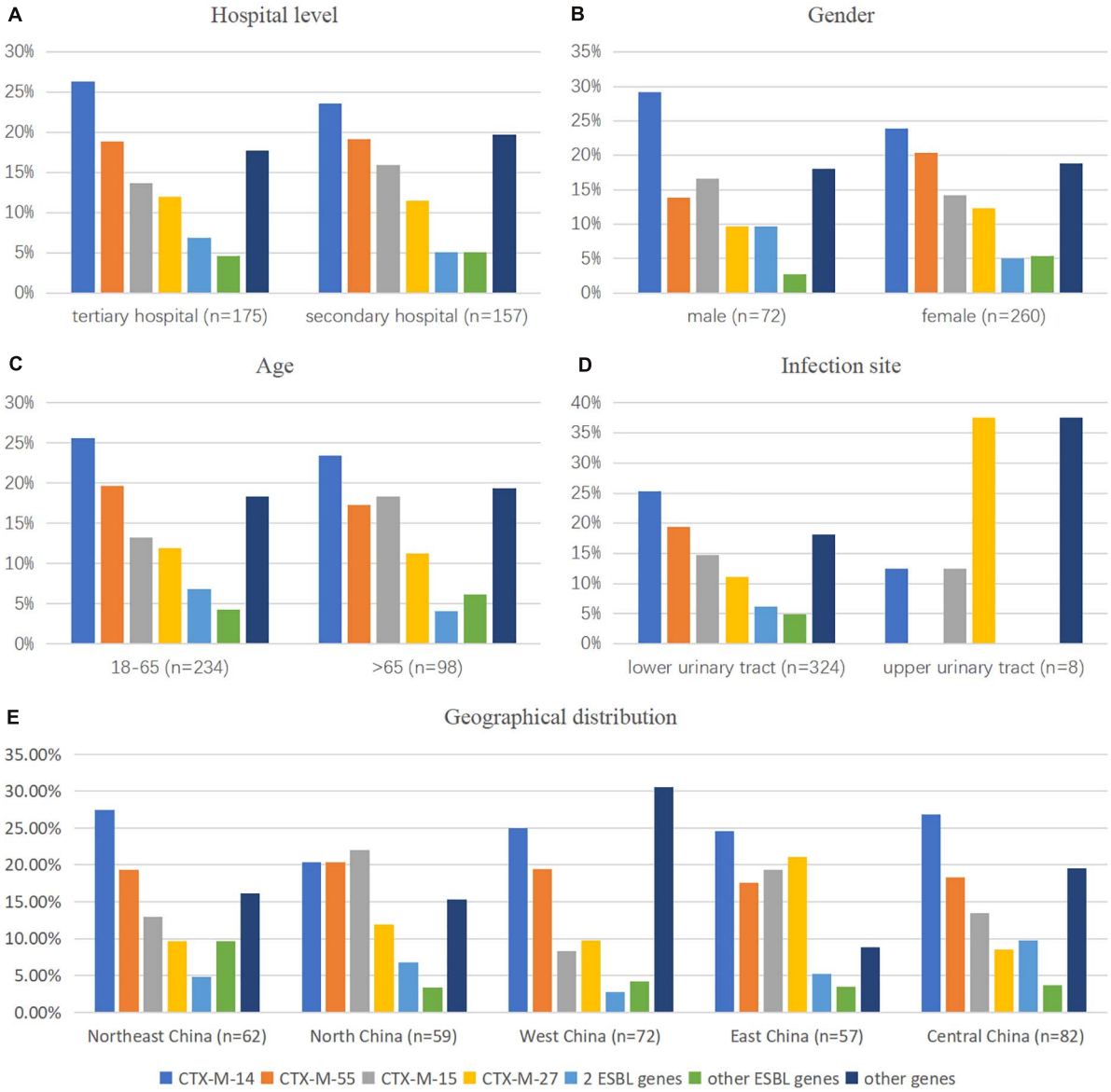

FIGURE 3 | Comparison of the CTX-M gene pattern of *E. coli* isolates by **(A)** hospital category, **(B,C,E)** demographic characteristics, and **(D)** clinical features. *2 ESBL genes*: CTX-M-1 coexisted with CTX-M-9 groups; *other ESBL genes*: genes that existed in less than 10 isolates in this study, such as CTX-M-3 (n = 5), CTX-M-64 (n = 3), CTX-M-65 (n = 9), and CTX-M-79 (n = 1); *other genes*: isolates with genes except ESBL genes detected in this study.

isolates was 4.1% in patients with acute uncomplicated cystitis in Japan (Hayami et al., 2019), with 10.8% rates in CA-UTI *E. coli* isolates in Korea (Park et al., 2017). In Europe, the frequency of ESBL-producing CA-UTI *E. coli* strains ranged from 2.2 to 24% (Yılmaz et al., 2016; Chervet et al., 2018; van Driel et al., 2019). In North America, the rates varied from 14.1% in Canada and 16.0% in the UnitedStates to 31.3% in Mexico (Lob et al., 2016; Galindo-Méndez, 2018). The difference in the prevalence of ESBLs among different studies may be due to population source of the isolates.

Our results show that CTX-M-14, CTX-M-55, and CTX-M-15 are the most dominant CTX-M variants in the ESBL-producing *E. coli*, followed by CTX-M-27, CTX-M-3, CTX-M-65, CTX-M-64, and CTX-M-79. CMY-2 is the major β-lactamase in the ESBL-uncertain *E. coli*. In different regions, the CTX-M variant pattern is different. In north China, CTX-M-15 (22.03%), CTX-M-14, and CTX-M-55 (20.34%) were distributed equally in the ESBL-producing and uncertain (phenotype) isolates, while in other regions, CTX-M-14 was the major variant with over 24% rate, and the rates of CTX-M-15 and CTX-M-55 were less than 20%. In east China, CTX-M-27 (21.05%) was the secondary variant that exceeded CTX-M-15 (19.3%) and CTX-M-55 (17.54%). In addition, another report also shows that CTX-M-27 has become more prevalent in East and Southeast Asia (Chong et al., 2018). Among the isolates from lower urinary tract infections, $bla_{CTX-M-14}$ was the most common ESBL gene

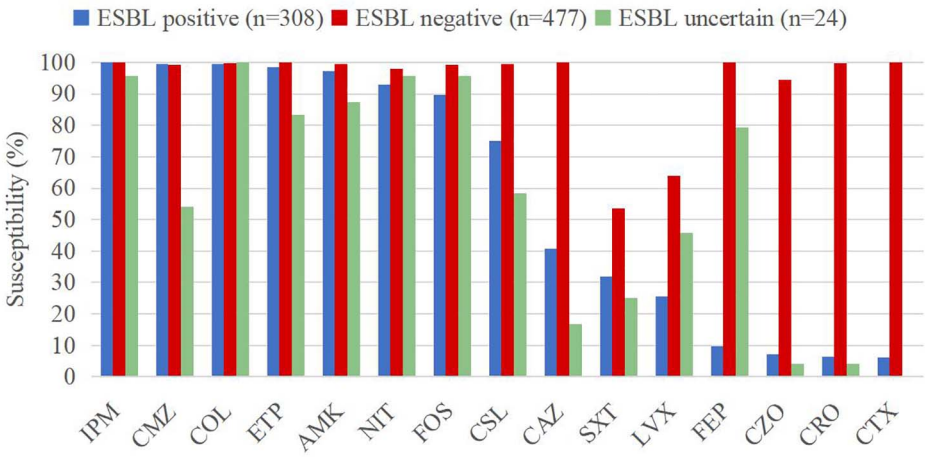

FIGURE 4 | Susceptibility rates of CA-UTI *Escherichia coli* strains with different ESBL phenotypes. IMP, imipenem; ETP, ertapenem; COL, colistin; AMK, amikacin; CMZ, cefmetazole; NIT, nitrofurantoin; FOS, fosfomycin; CSL, cefoperazone/sulbactam; CAZ, ceftazidime; FEP, cefepime; CRO, ceftriaxone; CTX, cefotaxime; CZO, cefazolin; LVX, levofloxacin; and SXT, trimethoprim/sulfamethoxazole.

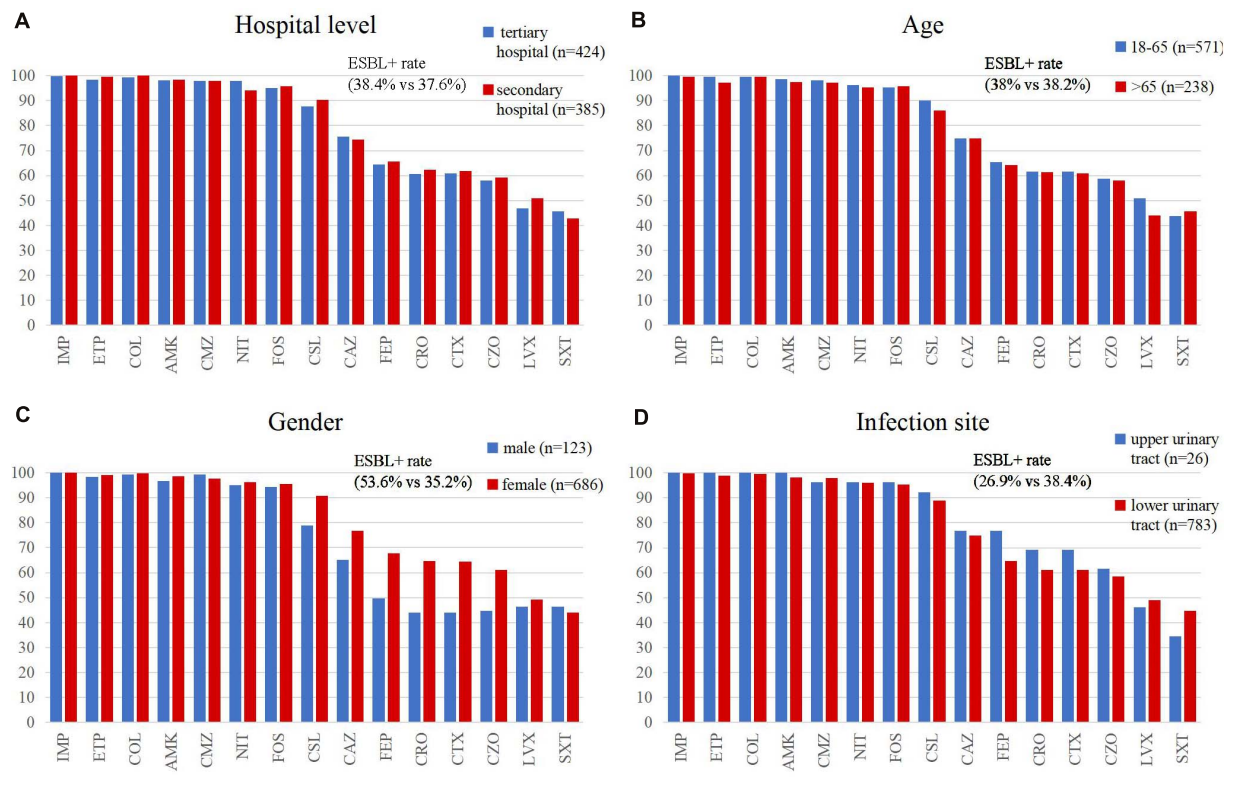

FIGURE 5 | Comparison of the antimicrobial susceptibility rates of *E. coli* isolates by **(A)** hospital category, **(B,C)** demographic characteristics, and **(D)** clinical features. IMP, imipenem; ETP, ertapenem; COL, colistin; AMK, amikacin; CMZ, cefmetazole; NIT, nitrofurantoin; FOS, fosfomycin; CSL, cefoperazone/sulbactam; CAZ, ceftazidime; FEP, cefepime; CRO, ceftriaxone; CTX, cefotaxime; CZO, cefazolin; LVX, levofloxacin; and SXT, trimethoprim/sulfamethoxazole.

type, which was different from upper urinary tract infections (the main gene was $bla_{CTX-M-27}$), but it may not be comprehensive since the number of isolates was extremely low in upper urinary tract infections ($n = 8$).

Most of CTX-Ms, such as CTX-M-14, CTX-M-3, and CTX-M-65, exhibit powerful activity against cefotaxime and ceftriaxone but not ceftazidime. Some CTX-Ms, such as CTX-M-15, CTX-M-27, CTX-M-55, and CTX-M-64, exhibit

enhanced catalytic efficiencies against ceftazidime (Zhao and Hu, 2013). In our study, the rate of ceftazidime-resistant isolates (49.7%) corresponds to the rate of isolates that carried CTX-M-15/55/27 (48.8%). In addition, among the ESBL-producing and uncertain (phenotype) isolates, the rates of ceftriaxone/cefotaxime/cefazolin-resistant were 93.1%, 93.4%, and 93.1%, respectively. Although CTX-M can be inhibited by β-lactamase inhibitors as sulbactam, clavulanate, and tazobactam, the susceptibility rate of cefoperazone/sulbactam was only 73.8%. Moreover, most of ESBL-uncertain isolates carried CMY-2, which cannot be inhibited by β-lactamase inhibitors. For these isolates, fosfomycin would be useful for the empirical treatment of acute cystitis since it had high rates of activity, with a susceptibility rate of over 90%.

The common antimicrobial drugs for treating acute uncomplicated cystitis include fosfomycin, nitrofurantoin, trimethoprim/sulfamethoxazole, and β-lactams, including cephalexin, cefaclor, and amoxicillin/clavulanate. Besides, β-lactams and quinolones are recommended as renal excretion-type antibiotics for acute uncomplicated pyelonephritis (Choe et al., 2018). However, the two old antibiotics, fosfomycin and nitrofurantoin, which achieve high urinary concentrations and minimal toxicity, are not often used in China (Qiao et al., 2013), yet *E. coli* accounts for the majority of pathogens causing CA-UTIs (Qiao et al., 2013; Yang et al., 2017). It is important to understand the activity of β-lactams and quinolones against *E. coli* strains to guide empirical antimicrobial therapy decision making.

In the European Association of Urology guidelines updated in 2020, cephalosporins are recommended for oral empirical treatment of uncomplicated pyelonephritis and as alternative antimicrobials for therapy in uncomplicated cystitis (Bonkat et al., 2020). However, in the present study, cephalosporins had poor activity against ESBL-producing *E. coli* strains. Susceptibility rates of *E. coli* to the first-, third-, and fourth-generation cephalosporins were lower than 80%, among which, the susceptibility rates were 76.9% (for strains that caused pyelonephritis) and 74.8% (for strains that caused lower urinary tract infections) for ceftazidime, 69.2% and 61% for cefotaxime, 69.2% and 61.2% for ceftriaxone, and 76.9% and 64.6% for cefepime, respectively, which indicate that these agents might not be the optimum medications for empirical UTI therapies.

In the present study, the proportion of ESBL-non-producing *E. coli* isolates was 73.1% in pyelonephritis and 61.6% in lower UTIs, which is consistent with the cephalosporin susceptibility rates. Genes that encode for ESBLs are usually found on large plasmids accompanied by genetic determinants of resistance against multiple classes of antibiotics, such as aminoglycosides, sulfonamides, and fluoroquinolones (Lee et al., 2012; Bader et al., 2017). Our study also investigated the differences in ESBL carriage rates and cephalosporin susceptibility rates between males and females. Significantly higher ESBL and cephalosporin resistance rates were found in *E. coli* isolates from men. ESBL rates range from 30.2% to 46.3% in different regions of China, with northeast, central, and west China having higher rates in *E. coli*. The choice of cephalosporins for treatment of UTIs should be based on local prevalence of ESBL-producing isolate data.

Fluoroquinolones and cephalosporins are antimicrobial agents that can be recommended for oral empirical treatment of uncomplicated pyelonephritis. Meanwhile, ciprofloxacin, levofloxacin, and ofloxacin are not recommended in the treatment of uncomplicated cystitis. However, quinolone use has been compromised by the high resistance rates to most bacterial pathogens (Kim and Hooper, 2014), with a 50.2% resistance rate reported in this study higher than the rates reported in patients with acute uncomplicated cystitis in Japan (6.4%) (Yılmaz et al., 2016). Quinolone resistance mechanisms are multiple and complicated. Chromosomal gene mutation including *gyrA*, *gyrB*, *parC*, and *parE* genes, reduce binding of the drug to the enzyme–DNA complex. Furthermore, overexpression of native efflux pumps localized in the bacterial membrane may cause resistance to quinolones and other antimicrobials. Additionally, plasmid-mediated quinolone resistance determinants can encode additional antimicrobial resistances and transfer multidrug resistance to a variety of antimicrobials, including quinolones (Hooper and Jacoby, 2015). Through these resistance mechanisms, the number of quinolone-resistant bacterial strains has grown steadily over the years. A previous study reported that S83L/D87N in *gyrA* and S80I in *parC* were the most common topoisomerase mutations in ESBL-producing *E. coli* isolates from the community (Ni et al., 2016). In addition, the majority of UTIs in the present study were uncomplicated cystitis (96%, 778/809) for which fluoroquinolones are not recommended for treatment. Thus, in this case, the use of fluoroquinolones for empiric treatment of UTIs should be restricted.

Although carbapenems are not recommended as the first-line treatment for uncomplicated cystitis and pyelonephritis (Bonkat et al., 2020), the carbapenems exhibited high *in vitro* activity against ESBL-producing *E. coli* in the present study, with a susceptibility rate of 100% for imipenem and 98.4% for ertapenem. Given the relatively high ESBL rates in CA-UTIs in the present study, and the low susceptibility rates to beta-lactam and fluoroquinolones, carbapenems can be considered for empiric therapy in patients with suspected ESBL-producing and multidrug-resistant (MDR) bacterial strains (Essack, 2000; Paterson, 2000; Livermore et al., 2001). On the other hand, in order to maintain the activity of carbapenems, it is necessary to replace carbapenems by other antimicrobials once the susceptibilities to antimicrobial agents have been confirmed. Carbapenem-resistant *E. coli* (CREc) constituted 0.25% (2/809) of the CA-UTI *E. coli* isolates studied, which is consistent with previous reports. Findings from previous studies indicate an increase in the prevalence of community-acquired CRE in Taiwan (Lai et al., 2013; Tang et al., 2016). CA-CREs have also been described in the southeastern part of the United States (Thaden et al., 2014), suggesting widespread distribution of the organism in the community, and patients infected with CA-CRE have more urinary tract infections (Tang et al., 2016). The two patients with CREc were both elderly and female, which is in agreement with previous findings (Tang et al., 2016). In this study, amikacin colistin, fosfomycin, and tigecycline exhibited potent activity against CREs, suggesting that colistin, fosfomycin, tigecycline, and aminoglycosides could be treatment choices for UTIs caused by CRE (Bader et al., 2017).

As with majority of the studies, a limitation in this study was the lack of genomic analysis such as multilocus sequence typing (MLST). Since all the isolates were collected from 10 different regions in China and the number per site was no more than 100, there was a high possibility that these isolates were sporadic and rarely clonal outbreak. From other studies, we learned that ST131, ST69, ST95, and ST73 were the dominant sequence types (STs) in *E. coli* isolated from urinary tract infections (Riley, 2014; Yamaji et al., 2018; Kot, 2019). Among multidrug-resistance *E. coli* isolates associated with CA-UTIs, ST131 and ST69 were predominant in Australia and Saudi Arabia (Alghoribi et al., 2015; Rogers et al., 2015); however, ST648, ST224, ST38, and ST405 also occurred in China (Cao et al., 2011, 2014).

This study also found that two of three colistin-resistant *E. coli* isolates carried $bla_{CTX-M-14}$ and bla_{TEM-1} genes but were susceptible to carbapenems, which is consistent with a previous study (Jiang et al., 2020). The results suggest we need to attach great importance to the management of MDR Gram-negative bacteria. This study showed the real ESBL rates and genotype distribution in community-acquired UTIs through strict selection criteria, since the strategies for treatment of hospital- and community-acquired UTIs are different. Besides, some UTIs might not represent genuine community acquisition if the patients were admitted to a hospital before infection. Hence, this strictly defined clinical epidemiological study in CA-UTIs will help the clinicians to better understand the antimicrobial resistance status and select empiric antimicrobial agents.

CONCLUSION

Our findings show that ESBLs are still a significant issue in *E. coli* isolates from CA-UTI in China, with an average prevalence of 38.07%. Higher rates of ESBL among the *E. coli* strains were confined to the northeast, central, and west parts of China. The choice of antimicrobial agents for the treatment of CA-UTIs should be based on local surveillance data. Use of fluoroquinolones for empiric treatment of UTIs should be restricted due to high resistance rate. Carbapenems can be used empirically for highly suspected ESBL-producing and MDR strains. However, the occurrence of CRE in the community is a cause for concern.

DATA AVAILABILITY STATEMENT

The original contributions presented in the study are included in the article/supplementary material, further inquiries can be directed to the corresponding author/s.

ETHICS STATEMENT

The protocol has been reviewed by the human research Ethics Committee of the Institutional Review Board (IRB) of the Peking Union Medical College Hospital (Ethics Approval Number: S-K136). This project did not involve any patient information nor did it affect the normal diagnosis and treatment of patients, and after consultation with the IRB, formal ethical approval was reviewed and waived, and written patient consent was not required.

AUTHOR CONTRIBUTIONS

QY conceived and designed the experiments. YY, GZ, and JZ performed the experiments. PJ, XL, and YZ analyzed the data and wrote the manuscript. TK, YX, and QY reviewed the manuscript and polished the language. All authors read and approved the final manuscript.

FUNDING

This study was supported by the National Natural Science Foundation of China (82072318) and National Key Research and Development Program of China (2018YFE0101800 and 2018YFC1200105). This study was also supported by the China Pharmacists Association, Beijing Key Clinical Specialty for Laboratory Medicine—Excellent Project (No. ZK201000).

REFERENCES

Alghoribi, M. F., Gibreel, T. M., Farnham, G., Al Johani, S. M., Balkhy, H. H., and Upton, M. (2015). Antibiotic-resistant ST38, ST131 and ST405 strains are the leading uropathogenic *Escherichia coli* clones in Riyadh, Saudi Arabia. *J. Antimicrob. Chemother.* 70, 2757–2762. doi: 10.1093/jac/dkv188

Arana, D. M., Rubio, M., and Alós, J. I. (2017). Evolution of antibiotic multiresistance in *Escherichia coli* and *Klebsiella pneumoniae* isolates from urinary tract infections: a 12-year analysis (2003-2014). *Enferm. Infecc. Microbiol. Clin.* 35, 293–298. doi: 10.1016/j.eimc.2016.02.018

Armand-Lefèvre, L., Leflon-Guibout, V., Bredin, J., Barguellil, F., Amor, A., Pagès, J. M., et al. (2003). Imipenem resistance in *Salmonella enterica* serovar Wien related to porin loss and CMY-4 beta-lactamase production. *Antimicrob. Agents Chemother.* 47, 1165–1168. doi: 10.1128/aac.47.3.1165-1168.2003

Bader, M. S., Loeb, M., and Brooks, A. A. (2017). An update on the management of urinary tract infections in the era of antimicrobial resistance. *Postgrad. Med.* 129, 242–258. doi: 10.1080/00325481.2017.1246055

Bonkat, G., Bartoletti, R., Bruyére, F., Cai, T., Geerlings, S. E., Köves, B., et al. (2020). EAU Guidelines on Urological Infections 2020 [Online]. (Arnhem: European Association of Urology Guidelines Office). Available online at: http://uroweb.org/guideline/urological-infections/

Cao, X., Cavaco, L. M., Lv, Y., Li, Y., Zheng, B., Wang, P., et al. (2011). Molecular characterization and antimicrobial susceptibility testing of *Escherichia coli* isolates from patients with urinary tract infections in 20 Chinese hospitals. *J. Clin. Microbiol.* 49, 2496–2501. doi: 10.1128/jcm.02503-10

Cao, X., Zhang, Z., Shen, H., Ning, M., Chen, J., Wei, H., et al. (2014). Genotypic characteristics of multidrug-resistant *Escherichia coli* isolates associated with urinary tract infections. *APMIS* 122, 1088–1095. doi: 10.1111/apm.12260

Chervet, D., Lortholary, O., Zahar, J. R., Dufougeray, A., Pilmis, B., and Partouche, H. (2018). Antimicrobial resistance in community-acquired urinary tract infections in Paris in 2015. *Med. Mal. Infect.* 48, 188–192. doi: 10.1016/j.medmal.2017.09.013

Choe, H. S., Lee, S. J., Yang, S. S., Hamasuna, R., Yamamoto, S., Cho, Y. H., et al. (2018). Summary of the UAA-AAUS guidelines for urinary tract infections. *Int. J. Urol.* 25, 175–185. doi: 10.1111/iju.13493

Chong, Y., Shimoda, S., and Shimono, N. (2018). Current epidemiology, genetic evolution and clinical impact of extended-spectrum β-lactamase-producing *Escherichia coli* and *Klebsiella pneumoniae*. *Infect. Genet. Evol.* 61, 185–188. doi: 10.1016/j.meegid.2018.04.005

CLSI (2020). *Performance Standards for Antimicrobial Susceptibility Testing, Document M100*, 30th Edn. Wayne, PA: Clinical and Laboratory Standards Institute.

Espínola, M., García, A., Somodevilla, Á, Martínez, M., Guiu, A., Correa, A., et al. (2011). Antibiotic susceptibility of *Escherichia coli* strains causing community-acquired urinary tract infection. *Clin. Microbiol. Infect.* 17:S690. doi: 10.1111/j.1469-0691.2011.03559.x

Essack, S. Y. (2000). Treatment options for extended-spectrum beta-lactamase-producers. *FEMS Microbiol. Lett.* 190, 181–184. doi: 10.1111/j.1574-6968.2000.tb09283.x

Fupin, H. U., Yan, G. U. O., Demei, Z. H. U., Fu, W., Xiaofei, J., Yingchun, X. U., et al. (2017). CHINET surveillance of bacterial resistance across China: report of the results in 2016. *Chin. J. Infect. Chemother.* 17, 481–491. doi: 10.16718/j.1009-7708.2017.05.001

Galindo-Méndez, M. (2018). Molecular characterization and antimicrobial susceptibility pattern of extended-spectrum β-lactamase-producing *Escherichia coli* as cause of community acquired urinary tract infection. *Rev. Chilena Infectol.* 35, 29–35. doi: 10.4067/s0716-10182018000100029

Giakkoupi, P., Tambic-Andrasevic, A., Vourli, S., Skrlin, J., Sestan-Crnek, S., Tzouvelekis, L. S., et al. (2006). Transferable DHA-1 cephalosporinase in *Escherichia coli*. *Int. J. Antimicrob. Agents* 27, 77–80. doi: 10.1016/j.ijantimicag.2005.09.013

Hayami, H., Takahashi, S., Ishikawa, K., Yasuda, M., Yamamoto, S., Wada, K., et al. (2019). Second nationwide surveillance of bacterial pathogens in patients with acute uncomplicated cystitis conducted by Japanese Surveillance Committee from 2015 to 2016: antimicrobial susceptibility of *Escherichia coli*, *Klebsiella pneumoniae*, and Staphylococcus saprophyticus. *J. Infect. Chemother.* 25, 413–422. doi: 10.1016/j.jiac.2019.02.021

Hooper, D. C., and Jacoby, G. A. (2015). Mechanisms of drug resistance: quinolone resistance. *Ann. N. Y. Acad. Sci.* 1354, 12–31. doi: 10.1111/nyas.12830

Jiang, B., Du, P., Jia, P., Liu, E., Kudinha, T., Zhang, H., et al. (2020). Antimicrobial susceptibility and virulence of mcr-1-positive *Enterobacteriaceae* in China, a multicenter longitudinal epidemiological study. *Front. Microbiol.* 11:1611. doi: 10.3389/fmicb.2020.01611

Kim, E. S., and Hooper, D. C. (2014). Clinical importance and epidemiology of quinolone resistance. *Infect. Chemother.* 46, 226–238. doi: 10.3947/ic.2014.46.4.226

Koksal, I., Yilmaz, G., Unal, S., Zarakolu, P., Korten, V., Mulazimoglu, L., et al. (2017). Epidemiology and susceptibility of pathogens from SMART 2011-12 Turkey: evaluation of hospital-acquired versus community-acquired urinary tract infections and ICU- versus non-ICU-associated intra-abdominal infections. *J. Antimicrob. Chemother.* 72, 1364–1372. doi: 10.1093/jac/dkw574

Kot, B. (2019). Antibiotic resistance among uropathogenic *Escherichia coli*. *Pol. J. Microbiol.* 68, 403–415. doi: 10.33073/pjm-2019-048

Lai, C. C., Wu, U. I., Wang, J. T., and Chang, S. C. (2013). Prevalence of carbapenemase-producing *Enterobacteriaceae* and its impact on clinical outcomes at a teaching hospital in Taiwan. *J. Formos. Med. Assoc.* 112, 492–496. doi: 10.1016/j.jfma.2012.09.021

Larramendy, S., Gaultier, A., Fournier, J. P., Caillon, J., Moret, L., and Beaudeau, F. (2021). Local characteristics associated with higher prevalence of ESBL-producing *Escherichia coli* in community-acquired urinary tract infections: an observational, cross-sectional study. *J. Antimicrob. Chemother.* 76, 789–795. doi: 10.1093/jac/dkaa514

Lee, J. H., Bae, I. K., and Lee, S. H. (2012). New definitions of extended-spectrum β-lactamase conferring worldwide emerging antibiotic resistance. *Med. Res. Rev.* 32, 216–232. doi: 10.1002/med.20210

Lee, Y. H., Cho, B., Bae, I. K., Chang, C. L., and Jeong, S. H. (2006). *Klebsiella pneumoniae* strains carrying the chromosomal SHV-11 beta-lactamase gene produce the plasmid-mediated SHV-12 extended-spectrum beta-lactamase more frequently than those carrying the chromosomal SHV-1 beta-lactamase gene. *J. Antimicrob. Chemother.* 57, 1259–1261. doi: 10.1093/jac/dkl115

Livermore, D. M., Oakton, K. J., Carter, M. W., and Warner, M. (2001). Activity of ertapenem (MK-0826) versus *Enterobacteriaceae* with potent beta-lactamases. *Antimicrob. Agents Chemother.* 45, 2831–2837. doi: 10.1128/aac.45.10.2831-2837.2001

Lob, S. H., Kazmierczak, K. M., Badal, R. E., Hackel, M. A., Bouchillon, S. K., Biedenbach, D. J., et al. (2015). Trends in susceptibility of *Escherichia coli* from intra-abdominal infections to ertapenem and comparators in the United States according to data from the SMART program, 2009 to 2013. *Antimicrob. Agents Chemother.* 59, 3606–3610. doi: 10.1128/aac.05186-14

Lob, S. H., Nicolle, L. E., Hoban, D. J., Kazmierczak, K. M., Badal, R. E., and Sahm, D. F. (2016). Susceptibility patterns and ESBL rates of *Escherichia coli* from urinary tract infections in Canada and the United States, SMART 2010-2014. *Diagn Microbiol. Infect. Dis.* 85, 459–465. doi: 10.1016/j.diagmicrobio.2016.04.022

Naziri, Z., Derakhshandeh, A., Soltani Borchaloee, A., Poormaleknia, M., and Azimzadeh, N. (2020). Treatment failure in urinary tract infections: a warning witness for virulent multi-drug resistant ESBL- producing *Escherichia coli*. *Infect. Drug Resist.* 13, 1839–1850. doi: 10.2147/idr.S256131

Ni, Q., Tian, Y., Zhang, L., Jiang, C., Dong, D., Li, Z., et al. (2016). Prevalence and quinolone resistance of fecal carriage of extended-spectrum β-lactamase-producing *Escherichia coli* in 6 communities and 2 physical examination center populations in Shanghai, China. *Diagn Microbiol. Infect. Dis.* 86, 428–433. doi: 10.1016/j.diagmicrobio.2016.07.010

Park, J. J., Seo, Y. B., and Lee, J. (2017). Antimicrobial susceptibilities of *Enterobacteriaceae* in community-acquired urinary tract infections during a 5-year period: a single hospital study in Korea. *Infect. Chemother.* 49, 184–193. doi: 10.3947/ic.2017.49.3.184

Paterson, D. L. (2000). Recommendation for treatment of severe infections caused by *Enterobacteriaceae* producing extended-spectrum beta-lactamases (ESBLs). *Clin. Microbiol. Infect.* 6, 460–463. doi: 10.1046/j.1469-0691.2000.00107.x

Qiao, L. D., Chen, S., Yang, Y., Zhang, K., Zheng, B., Guo, H. F., et al. (2013). Characteristics of urinary tract infection pathogens and their in vitro susceptibility to antimicrobial agents in China: data from a multicenter study. *BMJ Open* 3:e004152. doi: 10.1136/bmjopen-2013-004152

Reisbig, M. D., and Hanson, N. D. (2002). The ACT-1 plasmid-encoded AmpC beta-lactamase is inducible: detection in a complex beta-lactamase background. *J. Antimicrob. Chemother.* 49, 557–560. doi: 10.1093/jac/49.3.557

Richelsen, R., Smit, J., Anru, P. L., Schønheyder, H. C., and Nielsen, H. (2020). Incidence of community-onset extended-spectrum β-lactamase-producing *Escherichia coli* and *Klebsiella pneumoniae* infections: an 11-year population-based study in Denmark. *Infect. Dis. (Lond.)* 52, 547–556. doi: 10.1080/23744235.2020.1763452

Riley, L. W. (2014). Pandemic lineages of extraintestinal pathogenic *Escherichia coli*. *Clin. Microbiol. Infect.* 20, 380–390. doi: 10.1111/1469-0691.12646

Rogers, B. A., Ingram, P. R., Runnegar, N., Pitman, M. C., Freeman, J. T., Athan, E., et al. (2015). Sequence type 131 fimH30 and fimH41 subclones amongst *Escherichia coli* isolates in Australia and New Zealand. *Int. J. Antimicrob. Agents* 45, 351–358. doi: 10.1016/j.ijantimicag.2014.11.015

Tang, H. J., Hsieh, C. F., Chang, P. C., Chen, J. J., Lin, Y. H., Lai, C. C., et al. (2016). Clinical significance of community- and healthcare-acquired carbapenem-resistant *Enterobacteriaceae* isolates. *PLoS One* 11:e0151897. doi: 10.1371/journal.pone.0151897

Thaden, J. T., Lewis, S. S., Hazen, K. C., Huslage, K., Fowler, V. G. Jr., Moehring, R. W., et al. (2014). Rising rates of carbapenem-resistant *enterobacteriaceae* in community hospitals: a mixed-methods review of epidemiology and microbiology practices in a network of community hospitals in the southeastern United States. *Infect. Control Hosp. Epidemiol.* 35, 978–983. doi: 10.1086/677157

van Driel, A. A., Notermans, D. W., Meima, A., Mulder, M., Donker, G. A., Stobberingh, E. E., et al. (2019). Antibiotic resistance of *Escherichia coli* isolated from uncomplicated UTI in general practice patients over a 10-year period. *Eur. J. Clin. Microbiol. Infect. Dis.* 38, 2151–2158. doi: 10.1007/s10096-019-03655-3

Yamaji, R., Rubin, J., Thys, E., Friedman, C. R., and Riley, L. W. (2018). Persistent pandemic lineages of uropathogenic *Escherichia coli* in a college community from 1999 to 2017. *J. Clin. Microbiol.* 56:e01834-17. doi: 10.1128/jcm.01834-17

Yang, Q., Zhang, H., Cheng, J., Xu, Z., Xu, Y., Cao, B., et al. (2015). In vitro activity of flomoxef and comparators against *Escherichia coli*, *Klebsiella pneumoniae* and *Proteus mirabilis* producing extended-spectrum β-lactamases in China. *Int. J. Antimicrob. Agents* 45, 485–490. doi: 10.1016/j.ijantimicag.2014.11.012

Yang, Q., Zhang, H., Wang, Y., Xu, Z., Zhang, G., Chen, X., et al. (2017). Antimicrobial susceptibilities of aerobic and facultative gram-negative bacilli isolated from Chinese patients with urinary tract infections between 2010 and 2014. *BMC Infect. Dis.* 17:192. doi: 10.1186/s12879-017-2296-x

Yılmaz, N., Ağuş, N., Bayram, A., Şamlıoğlu, P., Şirin, M. C., Derici, Y. K., et al. (2016). Antimicrobial susceptibilities of *Escherichia coli* isolates as agents of community-acquired urinary tract infection (2008-2014). *Turk J. Urol.* 42, 32–36. doi: 10.5152/tud.2016.90836

Yun, L., Yuan, L., Feng, X., Xiu-zhen, Z., Yun-jian, H., Ting, Y., et al. (2014). Antimicrobial susceptibility surveillance of gram-negative bacterial from Mohnarin 2011-20112. *Chin. J. Clin. Pharmacol.* 30, 260–277.

Zhang, H., Johnson, A., Zhang, G., Yang, Y., Zhang, J., Li, D., et al. (2019). Susceptibilities of Gram-negative bacilli from hospital- and community-acquired intra-abdominal and urinary tract infections: a 2016-2017 update of the Chinese SMART study. *Infect. Drug Resist.* 12, 905–914. doi: 10.2147/idr.S203572

Zhao, W. H., and Hu, Z. Q. (2013). Epidemiology and genetics of CTX-M extended-spectrum β-lactamases in Gram-negative bacteria. *Crit. Rev. Microbiol.* 39, 79–101. doi: 10.3109/1040841x.2012.691460

Conflict of Interest: The authors declare that the research was conducted in the absence of any commercial or financial relationships that could be construed as a potential conflict of interest.

frontiers in Microbiology

ORIGINAL RESEARCH
published: 27 August 2021
doi: 10.3389/fmicb.2021.701513

KPC-2-Producing Carbapenem-Resistant *Klebsiella pneumoniae* of the Uncommon ST29 Type Carrying OXA-926, a Novel Narrow-Spectrum OXA β-Lactamase

Lina Liu[1†], Yu Feng[1†], Li Wei[2], Yuling Xiao[3] and Zhiyong Zong[1,2,4,5]*

[1] Center for Pathogen Research, West China Hospital, Sichuan University, Chengdu, China, [2] Department of Infection Control, West China Hospital, Sichuan University, Chengdu, China, [3] Laboratory of Clinical Microbiology, Department of Laboratory Medicine, West China Hospital, Sichuan University, Chengdu, China, [4] Center of Infectious Diseases, West China Hospital, Sichuan University, Chengdu, China, [5] Division of Infectious Diseases, State Key Laboratory of Biotherapy, Chengdu, China

OPEN ACCESS

Edited by:
Mullika Traidej Chomnawang, Mahidol University, Thailand

Reviewed by:
Chaitra Shankar, Christian Medical College & Hospital, India
Mehmet Demirci, Kirklareli University, Turkey

***Correspondence:**
Zhiyong Zong
zongzhiy@scu.edu.cn

[†] *These authors have contributed equally to this work*

Specialty section:
This article was submitted to Antimicrobials, Resistance and Chemotherapy, a section of the journal Frontiers in Microbiology

Received: *28 April 2021*
Accepted: *30 July 2021*
Published: *27 August 2021*

Citation:
Liu L, Feng Y, Wei L, Xiao Y and Zong Z (2021) KPC-2-Producing Carbapenem-Resistant Klebsiella pneumoniae of the Uncommon ST29 Type Carrying OXA-926, a Novel Narrow-Spectrum OXA β-Lactamase. Front. Microbiol. 12:701513. doi: 10.3389/fmicb.2021.701513

We isolated and characterized a carbapenem-resistant *Klebsiella pneumoniae* (CRKP) clinical strain from blood carrying a novel bla_{OXA} gene, $bla_{OXA-926}$, and belonging to ST29, an uncommon CRKP type. The strain, 130002, was genome sequenced using both short- and long-read sequencing and has a 94.9-kb self-transmissible IncFII plasmid carrying bla_{KPC-2}. *K. pneumoniae* genomes of the ST29 complex (ST29 and its single-allele variants) were retrieved and were subjected to single nucleotide polymorphism-based phylogenomic analysis. A total of 157 genomes of the ST29 complex were identified. This complex is commonly associated with extended-spectrum β-lactamase-encoding genes, in particular, $bla_{CTX-M-15}$ but rarely has carbapenemase genes. The novel plasmid-encoded β-lactamase-encoding gene $bla_{OXA-926}$ was identified on a 117.8-kb IncFIA-IncFII plasmid, which was transferrable in the presence of the bla_{KPC-2}-carrying plasmid. $bla_{OXA-926}$ was cloned and MICs of β-lactams in the transformants were determined using microdilution. OXA-926 has a narrow spectrum conferring reduced susceptibility only to piperacillin, piperacillin-tazobactam, and cephalothin. Avibactam cannot fully inhibit OXA-926. $bla_{OXA-926}$ and its variants have been seen in *Klebsiella* strains in Asia and Brazil. OXA-926 is the closest in sequence identity (89.9%) to a chromosome-encoding OXA-type enzyme of *Variovorax guangxiensis*. In conclusion, OXA-926 is novel plasmid-borne narrow-spectrum β-lactamase that cannot be fully inhibited by avibactam. It is likely that $bla_{OXA-926}$ originates from a species closely related to *V. guangxiensis* and was introduced into *Klebsiella* > 10 years ago.

Keywords: *Klebsiella pneumoniae*, carbapenem resistance, β-lactamase, OXA, plasmid

INTRODUCTION

Resistance to β-lactam agents such as penicillins, cephalosporins, and carbapenems in the *Enterobacteriaceae*, one of the most common human pathogens, is mainly due to the production of hydrolyzing enzymes called β-lactamases. β-Lactamases can be divided into classes A, B, C, and D based on amino acid homology (Hall and Barlow, 2005). Class A, C, and D enzymes are also termed serine β-lactamases as they possess a serine at the active site, while class B enzymes require a metal ion for activity and are therefore called metallo-β-lactamases. OXA (oxacillinase) is a large group of class D β-lactamases with a remarkably varied spectrum against β-lactam agents from narrow-spectrum (hydrolyzing penicillins only, e.g., OXA-1) to extended-spectrum (with ability to hydrolyze 3rd generation cephalosporins, e.g., OXA-11) and carbapenemases (e.g., OXA-23 and OXA-48) (Evans and Amyes, 2014). A number of bacterial species, e.g., *Acinetobacter baumannii* and *Pseudomonas aeruginosa* contain intrinsic OXA-encoding genes bla_{OXA} in their chromosomes, while many bla_{OXA} genes are carried by plasmids (Evans and Amyes, 2014). In this study, we found a bla_{OXA} gene encoding a novel OXA enzyme in a carbapenem-resistant *Klebsiella pneumoniae* (CRKP) clinical strain and determined its active spectrum. We also found that this strain belongs to ST29, an uncommon CRKP type. CRKP has emerged worldwide as a significant human health challenge (World Health Organization, 2017). The global dissemination of CRKP is mainly due to certain high-risk clones, in particular, ST 258 (Adler et al., 2014) and ST11 in China (Qi et al., 2011), but new CRKP lineages are continuously emerging. We, therefore, analyzed all available genomes of ST29 and found that this ST is commonly associated with the carriage of extended-spectrum β-lactamase-encoding genes rather than carbapenemases genes.

MATERIALS AND METHODS

The Study, the Strain, and Susceptibility Testing

Strain 130002 was recovered from the blood of an ICU patient in 2020 at West China Hospital as part of routine care. MICs of aztreonam, ceftazidime, ceftazidime-avibactam, cefepime, ertapenem, imipenem, meropenem, piperacillin-tazobactam, and colistin were determined using the broth microdilution method of the Clinical and Laboratory Standards Institute (CLSI) (CLSI, 2020). This study has been approved by the Ethical Committee of West China Hospital without the requirement of an informed consent due to the fact that no patient information is needed.

TABLE 1 | The allele profile of ST29 and its single-allele variants.

ST	*gapA*	*infB*	*mdh*	*pgi*	*phoE*	*rpoB*	*tonB*
29	2	3	2	2	6	4	4
193	2	3	2	2	48	4	4
465	2	3	2	2	9	4	4
711	2	61	2	2	6	4	4
723	2	3	2	2	131	4	4
985	10	3	2	2	6	4	4
1161	2	3	2	2	6	4	111
1271	2	3	2	2	4	4	4

The allele differences are highlighted.

Short- and Long-Read Whole Genome Sequencing and Analysis

Strain 130002 was subjected to whole genome sequencing using both a HiSeq X10 sequencer (Illumina; San Diego, CA, United States; 200×) and a MinION Sequencer (Nanopore; Oxford, United Kingdom). Genomic DNA was prepared using the QIAamp DNA Mini Kit (Qiagen, Hilden, Germany). Both short (Illumina) and long (Nanopore) reads were utilized to generate a *de novo* hybrid assembly using Unicycler (Wick et al., 2017) and Pilon (Walker et al., 2014). Sequence type (ST) was determined by querying the multilocus sequence typing database[1], while capsule (KL) typing was performed using Kleborate (Wyres et al., 2016). Antimicrobial resistance genes were identified from the genome sequences using the ABRicate program[2] to query the ResFinder database[3]. Replicon sequence types of IncF plasmids were determined using the pMLST[4]. Plasmid comparison was performed using BRIG (Alikhan et al., 2011) in the default settings. Insertion sequences were identified using ISFinder[5].

[1]http://bigsdb.pasteur.fr/klebsiella/klebsiella.html
[2]https://github.com/tseemann/abricate
[3]https://cge.cbs.dtu.dk/services/ResFinder/
[4]https://cge.cbs.dtu.dk/services/pMLST/
[5]https://www-is.biotoul.fr/

TABLE 2 | MIC (mg/L) of β-lactams for 130002 and *E. coli* BL21 expressing OXA-926 or not.

	130002	BL21::pET28a-OXA926	BL21::pET28a
Aztreonam	>256	0.03	0.03
Ampicillin	–	1	1
Ampicillin-sulbactam	–	1/0.5	0.5/0.25
Piperacillin	>256	32	0.5
Piperacillin-tazobactam	>256/4	16/4	1/4
Piperacillin-avibactam	8/4	4/4	0.5/4
Oxacillin	–	512	512
Cefazolin	–	0.5	0.5
Cephalothin	–	4	0.25
Cefuroxime	–	0.25	0.25
Ceftriaxone	–	0.03	0.03
Cefotaxime	–	≤0.015	≤0.015
Ceftazidime	32	0.06	0.06
Ceftazidime-avibactam	0.5/4	0.06/4	0.06/4
Cefepime	16	0.03	0.03
Cefoxitin	–	1	1
Ertapenem	>256	0.03	0.03
Imipenem	64	0.5	0.5
Meropenem	128	0.06	0.06
Colistin	1	–	–

TABLE 3 | The complete genome and antimicrobial resistance genes of isolate 013002.

	Accession no.	Size, bp	Replicon type	Genes mediating resistance to					
				β -lactam	Aminoglycoside	Quinolone	Fosfomycin	Sulfonamide	Tetracycline
Chromosome	CP064851	5,297,461	–	$bla_{SHV-187}$		*oqxA-B*	*fosA6*		*tet(34)*
p1_130002	CP064854	164,362	IncC2		*ant(2")-Ia*	*qnrA1*		*sul1*	
pKPC2_130002	CP064852	94,968	IncFII(Yp)_1_Yersenia	bla_{KPC-2}					
pOXA926_130002	CP064853	117,839	IncFIA(HI1)_1_HI1, IncFII_1_pKP91	$bla_{OXA-926}$					

Conjugation

Mating experiments were performed in broth and on filters with *Escherichia coli* J53 AizR (an azide resistant variant of J53) as the recipient at both 25 and 37°C, as described previously (Coque et al., 2002). Potential transconjugants were selected on LB agar plates containing 16/4 mg/L of piperacillin-tazobactam and 150 mg/L of sodium azide. The presence of bla_{KPC-2} and $bla_{OXA-926}$ in the transconjugants was confirmed by PCR with primers KPC-up1/KPC-dw1 (5′-CCTAGCTCCACCTTCAAACAA/GTGAGGGCGAAGGTTAAATG) (Zhang et al., 2012) and OXA926-Fw/OXA926-Rev (see below), respectively, and subsequent Sanger sequencing.

Cloning of $bla_{OXA-926}$ and Function Characterization

To determine the activity of OXA-926, the 807-bp complete coding sequence of $bla_{OXA-926}$ was amplified from strain 130002 using primers OXA926-Fw/Rev (5′-CCGGATCCATGTGCAATCGCATCCTCCA/CCCTCGAGTCAATGGTCGATGGCTGGCA; restriction sites are underlined). PCR amplicons and the vector pET-28a (Fenghbio; Changsha, China) were digested using *BamH*I and *Xho*I (New England Biolabs, Ipswich, MA, United States) and were then ligated to the pET-28a vector using T4 ligase (New England Biolabs) to construct pET28a-OXA926. The constructed plasmid was transformed into *E. coli* strain BL21 by chemical, as described before (Sambrook and Russell, 2001). Potential transformants containing pET28a-OXA926 were selected on Luria–Bertani agar plates (Sigma; St. Louis, MO, United States) containing 50 mg/L of kanamycin. Colonies on plates were screened for $bla_{OXA-926}$ by PCR using primers OXA926-Fw/Rev and subsequent Sanger sequencing. The empty vector pET-28a was also transformed into BL21 for control.

MICs of aztreonam, ampicillin, ampicillin-sulbactam, piperacillin, piperacillin-tazobactam, oxacillin, cefazolin, cephalothin, cefuroxime, ceftriaxone, cefotaxime, ceftazidime, ceftazidime-avibactam, cefepime, cefoxitin, ertapenem, imipenem, and meropenem for the transformant containing pET28a-OXA926 (BL21::pET28a-OXA926) were determined as described above. MICs of piperacillin in the presence of 4 mg/L of avibactam were also determined based on the methods to determine MICs of ceftazidime-avibactam (CLSI, 2020).

Protein Analysis

The secondary structure of OXA-926 β-lactamase was predicted using the neural network based web service JPred4 (Drozdetskiy et al., 2015) with the default settings. The origin of OXA-926 was investigated using BlastP[6].

Phylogenomic Analysis of the ST29 Complex

All complete and draft genomes of *K. pneumoniae* belonging to the ST29 complex including ST29 and its single-allele variants, i.e., ST193, 465, 711, 723, 985, 1161, and 1271 (the allele profile of these STs is shown in **Table 1**) were retrieved from GenBank

[6]https://blast.ncbi.nlm.nih.gov/blast.cgi

including the SRA database (accessed during May 2020). The genome sequences were mapped against the complete genome of 130002 for single nucleotide polymorphisms (SNP) calling using Snippy v4.6.0[7] with the default settings. Gubbins v2.4.1 (Croucher et al., 2015) was used for recombination filtering prior to the phylogenomic reconstruction using RAxML v8.2.12 (Stamatakis, 2014) under the GTRGAMMA model and a 1,000-bootstrap test. Trees were annotated and viewed in iTOL v5.7 (Letunic and Bork, 2019) and FigTree v1.4.4[8]. As there are up to 1,048 SNPs between the genomes of ST29 and its single-allele variants (see below), suggesting a significant phylogenetic divergence, we, therefore, did not include the double-allele variants of ST29 for analysis.

Retrieval of *bla*$_{OXA-926}$-Carrying Strains From GenBank

Draft and complete genome sequences deposited in GenBank were screened by BlastN (see text footnote 6) for the presence of *bla*$_{OXA-926}$. Metadata of *bla*$_{OXA-926}$-carrying strains including host species and countries and year of isolation were retrieved.

[7]https://github.com/tseemann/snippy
[8]https://github.com/rambaut/figtree

RESULTS AND DISCUSSION

CRKP Strain 130002 Belongs to ST29, an Uncommon CRKP Type

Strain 130002 was resistant to aztreonam, ceftazidime, cefepime, ertapenem, imipenem, meropenem, and piperacillin-tazobactam but was susceptible to ceftazidime-avibactam and was intermediate to colistin (**Table 2**). The complete genome sequence of strain 130002 was obtained by *de novo* hybrid assembly of both short (Illumina) and long (Nanopore) reads and had a 5.3-Mb circular chromosome with three plasmids (**Table 3**). Strain 130002 belongs to ST29, an uncommon CRKP type, and the KL62 capsule type.

The ST29 Complex of *K. pneumoniae* Is Widely Distributed and Commonly Associated With *bla*$_{CTX-M}$ Genes but Rarely With Carbapenemase Genes

As ST29 is an uncommon type of CRKP, we retrieved all genomes of *K. pneumoniae* belonging to the ST29 complex including ST29 and its single-allele variants (ST193, 465, 711, 723, 985, 1161, and 1271) from GenBank. A total of 157

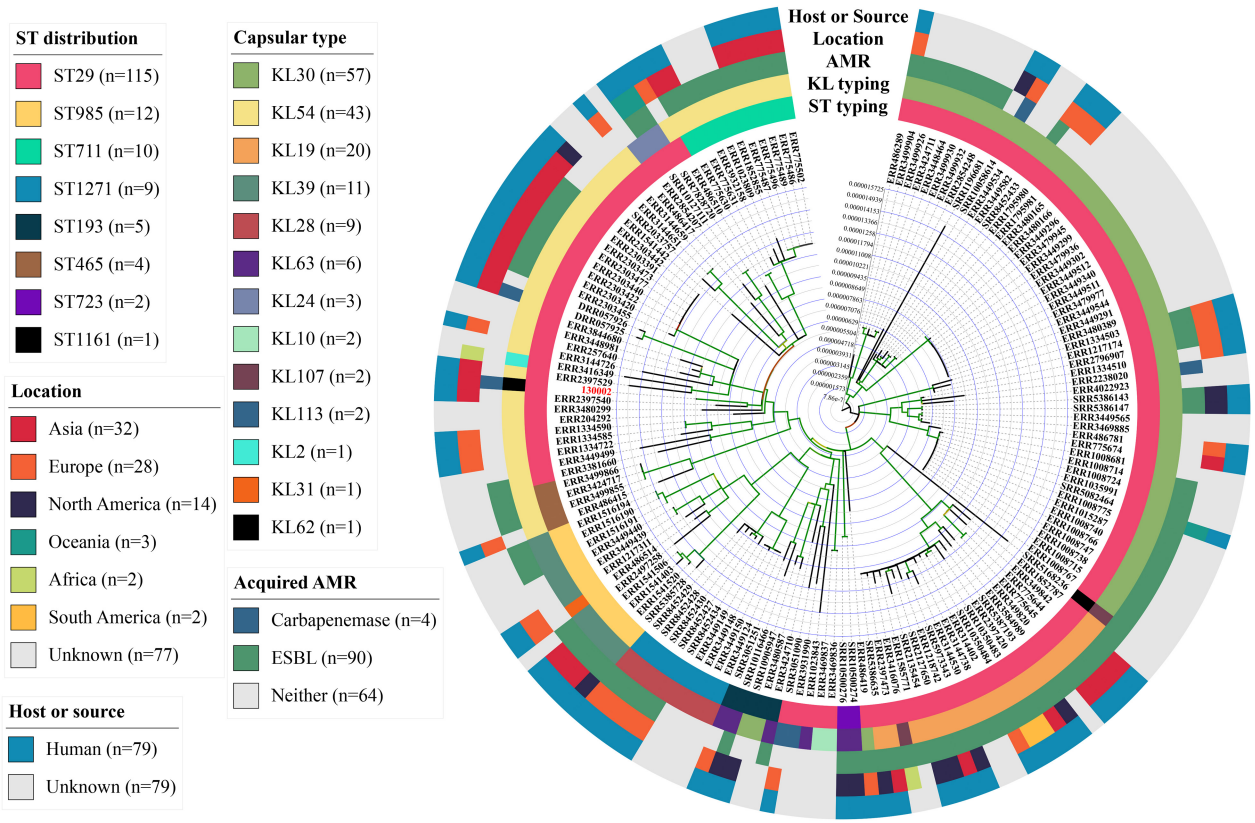

FIGURE 1 | Phylogenomic tree of *K. pneumoniae* strains of the ST29 complex. This phylogenomic tree of 130002 and 157 genomes of the ST29 complex is based on SNP calling using Snippy v4.6.0 and filtering recombination using Gubbins v2.4.1. The phylogeny was inferred using RAxML v8.2.12 under the GTRGAMMA model with a 1,000-bootstrap test and is annotated and viewed in iTOL v5.7 and FigTree v1.4.4. More information of the genomes is provided in **Supplementary Datasheet 1**.

genomes were identified and strains of the ST29 complex have been identified in all continents but Antarctica (**Supplementary Datasheet 1**). Most strains (57.3%, 90/157) of the ST29 complex carried genes encoding extended-spectrum β-lactamases (ESBL), in particular, $bla_{CTX-M-15}$ (n = 69), while only four strains had carbapenemase genes (bla_{KPC-2}, bla_{KPC-3}, or bla_{IMP-19}; **Supplementary Datasheet 1**). Strains of the ST29 complex were assigned to 13 capsular types (KL2, 10, 19, 24, 28, 30, 31, 33, 54, 62, 63, 107, and 113; **Figure 1**), while 130002 is the only strain of KL62. There was a maximum of 1,048 SNPs between strains of the ST29 complex (**Supplementary Datasheet 2**), suggesting that the complex is diverse in clonal background. Strain 130002 had a range of 258–904 SNPs with other strains of the ST29 complex (**Supplementary Datasheet 2**) and is most closely related to ST29 KL54 strain 4300STDY6470438 (accession no. ERR2397540) recovered from an unspecified human sample in Thailand in 2016 (**Figure 1**).

130002 Has a bla_{KPC-2} and bla_{OXA} Gene Encoding a Novel Narrow-Spectrum β-Lactamase OXA-926

Strain 130002 contains three β-lactamase-encoding genes including narrow-spectrum β-lactamase gene $bla_{SHV-187}$ (Tian et al., 2020) on chromosome, carbapenemase gene bla_{KPC-2} on a 94.9-kb IncFII plasmid of the Y6:A-:B- type (designated pKPC2_130002), and a novel bla_{OXA} gene on a 117.8-kb plasmid containing both IncFIA and IncFII replicons (designated pOXA926_130002; **Table 3**). pKPC2_130002 shows the closest similarity among the sequenced plasmids to pKPC2_020019 (accession no. CP028554), an 89.7-kb Y6:A-:B-type bla_{KPC-2}-carrying plasmid from a *Klebsiella variicola* strain recovered from a hospital of a neighboring city (Meishan, 80 km away from Chengdu) in 2017, with a 94% coverage and 99.93% identity (**Figure 2**). On pKPC2_130002 and pKPC2_020019, bla_{KPC-2} is located in a non-Tn*4401* element containing a transposase-encoding *tnpA* gene of an unnamed transposon of the Tn*3* family at upstream and another *tnpA* of an unnamed transposon of the Tn*As1* family at downstream (**Figure 2**). Transconjugants containing bla_{KPC-2} were obtained at a frequency of 1×10^{-4} (transconjugant per recipient), illustrating that pKPC2_130002 is readily self-transmissible. The findings above show that strain 130002 emerged as a CRKP by acquiring a self-transmissible bla_{KPC-2}-carrying plasmid.

The bla_{OXA} gene encodes an OXA enzyme that shows the closest similarity to OXA-459 with a 59.1% amino acid (aa) identity (143/242 aa) and 90.3% coverage (242/268 aa) among all known OXA enzymes in the Bacterial Antimicrobial Resistance

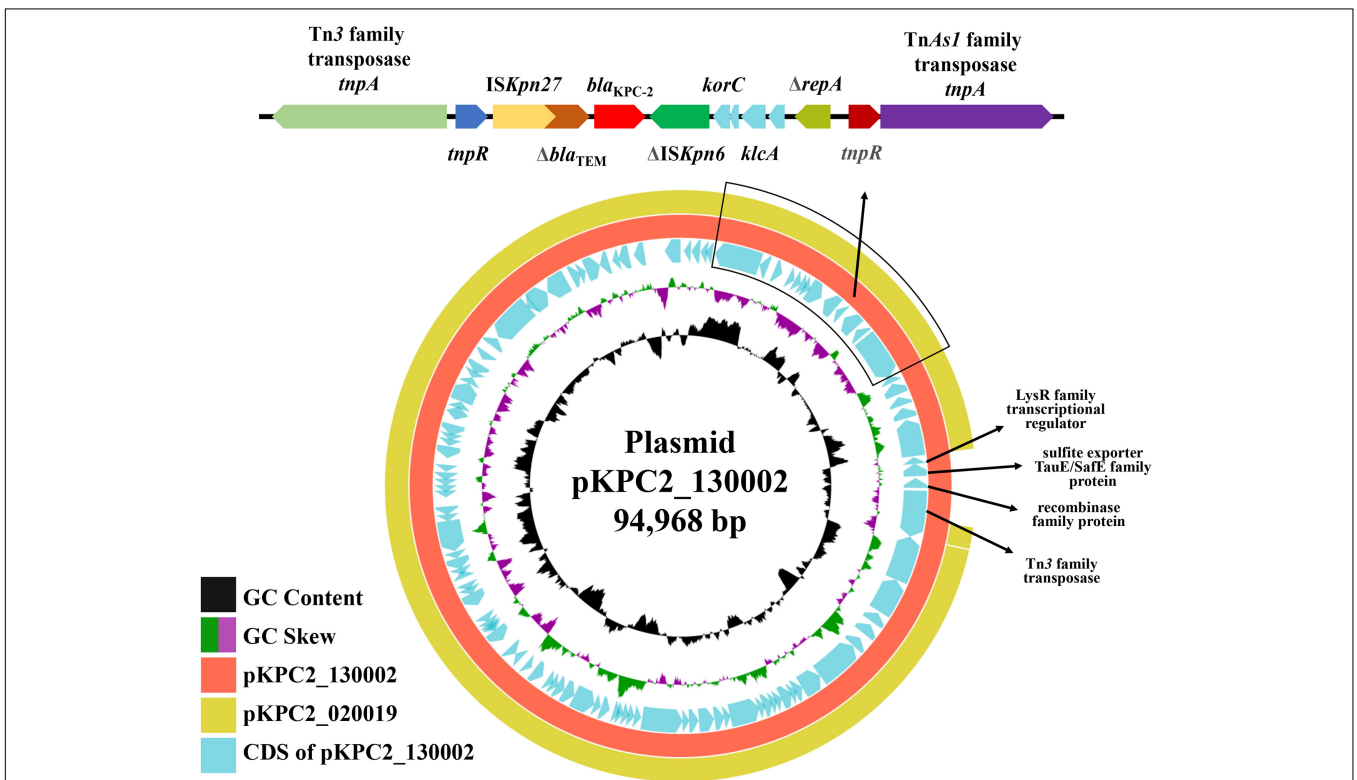

FIGURE 2 | Alignment of pKPC2_130002 with pKPC2_020019. pKPC2_130002 is a 94.9-kb IncFII plasmid of the Y6:A-:B- type and has bla_{KPC-2}. pKPC2_130002 is the closest to pKPC2_020019 (accession no. CP028554), an 89.7-kb Y6:A-:B-type bla_{KPC-2}-carrying plasmid from a *K. variicola* strain recovered in a hospital of a neighbor city (Meishan, 80 km away from Chengdu) in 2017, with a 94% coverage and 99.93% identity. Comparing with pKPC2_130002, pKPC2_020019 lacks several protein-encoding genes with the products being indicated. On pKPC2_130002 and pKPC2_020019, bla_{KPC-2} is located in a non-Tn*4401* element containing a transposase-encoding *tnpA* gene of an unnamed transposon of the Tn*3* family at upstream and another *tnpA* of an unnamed transposon of the Tn*As1* family at downstream. This comparison was performed using BRIG (Alikhan et al., 2011) in the default settings.

Reference Gene Database[9]. OXA-459 is one of the OXA-114-like enzymes intrinsic to *Achromobacter* spp. The findings above suggest that this OXA is a novel enzyme and is assigned OXA-926 by the Pathogen Detection group of GenBank, National Center for Biotechnology Information. OXA enzymes are very diverse in amino acid sequences and can be assigned to various subfamilies (Evans and Amyes, 2014; Yoon and Jeong, 2021). A ≥73.1% amino acid identity has been recently proposed as the cutoff to define OXA subfamilies (Yoon and Jeong, 2021) and, therefore, OXA-926 represents a novel subfamily. The secondary structure of OXA-926 contains seven α helixes, six β sheets, and four 3_{10}-helixes (**Figure 3**).

bla$_{OXA-926}$ was successfully cloned into vector pET28a, generating pET28a-OXA926. Among the β-lactams tested, only the MICs of piperacillin, piperacillin-tazobactam, and cephalothin for the transformant containing pET28a-OXA926 (BL21::pET28a-OXA926) were increased by ≥four-fold as compared with those for the transformant containing pET-28a (BL21::pET28a) (**Table 2**). This suggests that OXA-926 exhibits activity against piperacillin and such activities cannot be inhibited by tazobactam, a class A (not class D) β-lactamase inhibitor. As avibactam is a non-β-lactam β-lactamase inhibitor able to inhibit classes A, C, and D β-lactamases, we, therefore, determined the MICs of piperacillin in the presence of 4 mg/L of avibactam. In the presence of avibactam, MIC of piperacillin decreased from 32 to 4 mg/L for BL21::pET28a-OXA926 but was still 8-fold of that for BL21::pET28a (0.5 mg/L). This suggests that avibactam is able to provide protection for β-lactams from the hydrolysis OXA-926 to a certain extent but cannot fully inhibit OXA-926.

pOXA926_130002 has a K4 IncFII allele and a novel IncFIA allele closest to the FIA_10 type with a 98.7% identity (378/383 nucleotides). pOXA926_130002 was the closest, with a 56% coverage and 97.1% identity (**Figure 4**), to pRHBSTW-00167_2 [accession no. CP058119; containing a K4 IncFII allele and a FIA_10 type IncFIA allele (K4:A10:B-) plus an IncR replicon] of *Klebsiella michiganensis* strain RHBSTW-00167 recovered from freshwater in the United Kingdom in 2017. By Blast, there is only one *bla*$_{OXA-926}$-carrying plasmid, p15WZ-82_res (accession no. CP032357), with a complete sequence available in GenBank (**Table 4**). p15WZ-82_res was recovered from a *K. variicola* clinical strain in an unspecified place in China in 2015. This plasmid contains a K4 IncFII allele and a K (pCAV1099-114 type) IncFIB allele but no IncFIA allele (K4:A-:B-; pCAV1099-114 type IncFIB was not included in the IncF pMLST scheme). pOXA926_130002 had a 53% coverage and 99.0% identity with p15WZ-82_res (**Figure 4**). Transconjugants containing both *bla*$_{KPC-2}$ and *bla*$_{OXA-926}$ were obtained but those containing *bla*$_{OXA-926}$ alone were not, suggesting that pOXA926_130002 was not self-transmissible. Nonetheless, pOXA926_130002 was able to be transferred in the presence of pKPC2_130002 at a frequency of 1×10^{-6} (transconjugant per recipient). On pOXA926_130002, there are no mobile genetic elements including insertion sequences and transposons present in the immediate upstream and downstream of *bla*$_{OXA-926}$.

[9]https://www.ncbi.nlm.nih.gov/bioproject/PRJNA313047

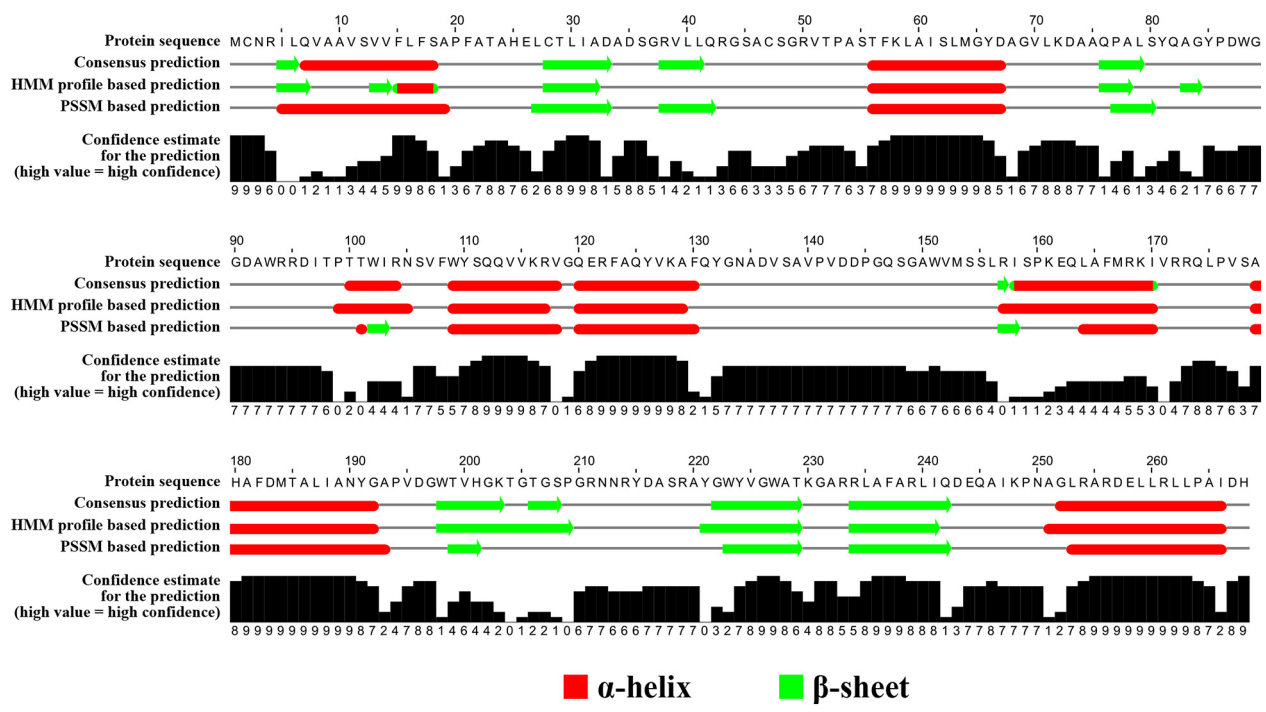

FIGURE 3 | Secondary structure of OXA-926. The secondary structure was predicted using the neural network-based web service JPred4 (Drozdetskiy et al., 2015) with the default settings. Secondary structure elements, α helixes, β sheets, and 3_{10}-helixes (representing by η), are indicated. β-strands are rendered as arrows, and strict α- and β-turns are shown as TTT and TT letters, respectively.

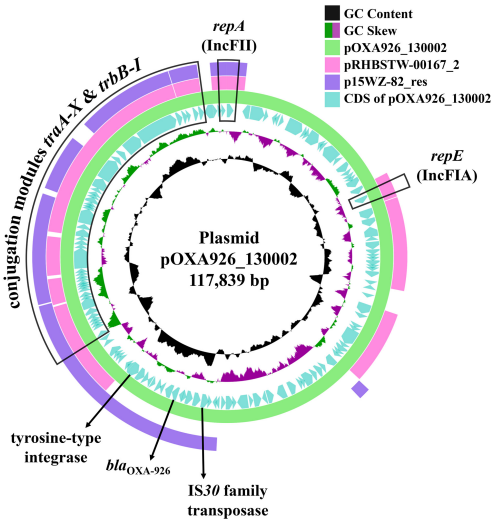

FIGURE 4 | Alignment of pOXA926_130002 with RHBSTW-00167_2 and p15WZ-82_res. pOXA926_130002 is a 117.8-kb IncF plasmid and has $bla_{OXA-926}$. Plasmid replication initiation-encoding genes *repA* of the IncFII replicon and *repE* of the IncFIA replicon and the conjugation module containing multiple genes (*traA* to *traX* and *trbB* to *trbI*) are indicated. A gene encoding the transpose of an IS*30* family insertion sequence at upstream of $bla_{OXA-926}$ and a gene encoding a tyrosine recombinase-like integrase at downstream are also shown. pOXA926_130002 is the closest (56% coverage and 97.1% identity) to pRHBSTW-00167_2 (accession no. CP058119), a 223.8-kb K4:A10:B- type IncF plasmid with an additional IncR replicon of an *K. michiganensis* strain recovered in United Kingdom in 2017. pRHBSTW-00167_2 has no $bla_{OXA-926}$, while p15WZ-82_res (accession no. CP032357) is another $bla_{OXA-926}$-carrying plasmid of a *K. variicola* clinical strain recovered from an unspecified place in China in 2015. p15WZ-82_res belongs to the K4:A-:B- IncF type and also contains a K (pCAV1099-114 type) IncFIB allele. pOXA926_130002 had a 53% coverage and 99.0% identity with p15WZ-82_res.

Nonetheless, an unnamed novel insertion sequence of the IS*30* family was found 3,137 bp upstream of $bla_{OXA-926}$ but no additional insertion sequences of the IS*30* family to form a composite transposon were present on pOXA926_130002 (**Figure 4**). A tyrosine recombinase-like integrase-encoding gene was present 4,984 bp downstream of $bla_{OXA-926}$ (**Figure 4**) but no crossover sites (recombination sites), which are required for recombination mediated by this type of integrases are found. No additional tyrosine recombinase-like integrase-encoding gene was present upstream of $bla_{OXA-926}$. Therefore, the mechanism for mobilizing $bla_{OXA-926}$ remains to be elucidated and warrants further study.

$bla_{OXA-926}$ May Originate From a Species Closely Related to *Variovorax*

BlastP shows that OXA-926 is the closest to a chromosome-encoding OXA-type enzyme of *Variovorax guangxiensis* (accession no. WP_184634888) with a 100% coverage and 89.9% (241/268) aa identity and is also similar to another chromosome-encoding OXA-type enzyme of *Variovorax gossypii* (accession no. WP_126469733) with a 98.9% (265/268) coverage and 85.4% (229/268) aa identity. *Variovorax* is a genus of the family *Comamonadaceae* within the order *Burkholderiales* (Taxonomy ID 34072 in NCBI). This suggests that $bla_{OXA-926}$ originates from a yet unknown species likely within the genus *Variovorax*.

$bla_{OXA-926}$ Has Been Present in *Klebsiella* for More Than 10 Years

In GenBank, $bla_{OXA-926}$ was found in one plasmid of *Klebsiella variicola* (GenBank accession no. CP032357) and seven *Klebsiella* draft genomes, including four *K. pneumoniae* and three *K. variicola* (**Table 4**). Four of the eight *Klebsiella* strains have detailed information available, revealing that the strains were recovered from China and Japan as far back as 2008. In addition, a variant of $bla_{OXA-926}$ encoding an OXA enzyme with 97.01% (260/268) aa identity with OXA-926 was found in one *Klebsiella michiganensis* from Malaysia and two *K. variicola* from Brazil (**Table 4**). These findings suggest that $bla_{OXA-926}$ has been circulating in *Klebsiella* spp. for more than a decade and has spread to multiple countries.

TABLE 4 | Genomes containing $bla_{OXA-926}$ or $bla_{OXA-926}$-like genes in GenBank[a].

Isolate	OXA	Species	aa identity, %	Accession no.	Country	Collection year	Host: sample type
TUM14060	OXA-926	*Klebsiella pneumoniae*	100	BIIN00000000	Japan	2013	Human :–
4300STDY6470463	OXA-926	*Klebsiella pneumoniae*	100	UFFP00000000	Thailand	2016	Human: –
4300STDY6470462	OXA-926	*Klebsiella pneumoniae*	100	UFFK00000000	Thailand	2016	Human: –
4300STDY6470402	OXA-926	*Klebsiella pneumoniae*	100	UFDU00000000	Thailand	2016	Human: –
15WZ-82	OXA-926	*Klebsiella variicola*	100	CP032357[c]	China	2015	Human: –
K022	OXA-926	*Klebsiella variicola*	100	JACNNG000000000	China	2008	Human: –
TUM14096	OXA-926	*Klebsiella variicola*	100	BIJX00000000	Japan	2014	Human: –
ZKP186	OXA-926	*Klebsiella variicola*	100	CABWXA000000000	China	2017	Human: –
R8A	OXA-926-like[b]	*Klebsiella michiganensis*	97.02	JNCH00000000	Malaysia	2013	Human: dental plaque
Kv104	OXA-926-like[b]	*Klebsiella variicola*	97.02	JAAQPW000000000	Brazil	2017	Human: blood
Kv97	OXA-926-like[b]	*Klebsiella variicola*	97.02	JAAQPV000000000	Brazil	2017	Human: urine

[a] *$bla_{OXA-926}$-like genes refer to those with ≥90% nucleotide identity with $bla_{OXA-926}$.*
[b] *The three OXA-926-like are identical in aa sequence.*
[c] *In strain 15WZ-82, $bla_{OXA-926}$ is carried on a plasmid, p15WZ-82_res, containing a K4 IncFII allele and a K (pCAV1099-114) IncFIB allele but no IncFIA allele.*

CONCLUSION

We found a CRKP strain of an uncommon sequence and capsular type. Carbapenem resistance of this strain was due to the acquisition of a self-transmissible plasmid carrying bla_{KPC-2}. We also found a novel plasmid-borne narrow-spectrum β-lactamase-encoding gene, $bla_{OXA-926}$, able to confer a reduced susceptibility to piperacillin and piperacillin-tazobactam which cannot be fully inhibited by avibactam. It is likely that $bla_{OXA-926}$ originates from a yet unknown species within the genus *Variovorax* of the order *Burkholderiales*.

DATA AVAILABILITY STATEMENT

The complete coding sequence of $bla_{OXA-926}$ has been deposited into GenBank under accession no. MT767688. The complete sequence of the chromosome and plasmids of strain 130002 has been deposited into GenBank under the accession no. CP064851-CP064854.

AUTHOR CONTRIBUTIONS

ZZ designed the study. LL, LW, and YX performed the experiments. LL, YF, and ZZ performed the analysis. LL, YF, and ZZ drafted the manuscript. All authors contributed to the article and approved the submitted version.

FUNDING

This work was supported by grants from the National Natural Science Foundation of China (project no. 81861138055) and West China Hospital of Sichuan University (1.3.5 project for disciplines of excellence, project no. ZYYC08006; and grant no. 312190022).

ACKNOWLEDGMENTS

We are grateful to Yanqiao Gong and Hongxia Wen at West China Hospital for collecting the strain. We thank Alan McNally at the University of Birmingham, United Kingdom for the helpful discussion and critical proofreading.

SUPPLEMENTARY MATERIAL

The Supplementary Material for this article can be found online at: https://www.frontiersin.org/articles/10.3389/fmicb.2021.701513/full#supplementary-material

REFERENCES

Adler, A., Hussein, O., Ben-David, D., Masarwa, S., Navon-Venezia, S., Schwaber, M. J., et al. (2014). Persistence of *Klebsiella pneumoniae* ST258 as the predominant clone of carbapenemase-producing *Enterobacteriaceae* in post-acute-care hospitals in Israel, 2008-13. *J. Antimicrob. Chemother.* 70, 89–92. doi: 10.1093/jac/dku333

Alikhan, N. F., Petty, N. K., Ben Zakour, N. L., and Beatson, S. A. (2011). BLAST Ring Image Generator (BRIG): simple prokaryote genome comparisons. *BMC Genomics* 12:402. doi: 10.1186/1471-2164-12-402

CLSI (2020). *Performance Standards for Antimicrobial Susceptibility Testing; Thirtieth Informational Supplement. M100-S30*. Wayne, PA: Clinical and Laboratory Standards Institute.

Coque, T. M., Oliver, A., Perez-Diaz, J. C., Baquero, F., and Canton, R. (2002). Genes encoding TEM-4, SHV-2, and CTX-M-10 extended-spectrum β-lactamases are carried by multiple *Klebsiella pneumoniae* clones in a single hospital (Madrid, 1989 to 2000). *Antimicrob. Agents Chemother.* 46, 500–510. doi: 10.1128/aac.46.2.500-510.2002

Croucher, N. J., Page, A. J., Connor, T. R., Delaney, A. J., Keane, J. A., Bentley, S. D., et al. (2015). Rapid phylogenetic analysis of large samples of recombinant bacterial whole genome sequences using Gubbins. *Nucleic Acids Res.* 43:e15. doi: 10.1093/nar/gku1196

Drozdetskiy, A., Cole, C., Procter, J., and Barton, G. J. (2015). JPred4: a protein secondary structure prediction server. *Nucleic Acids Res.* 43, W389–W394. doi: 10.1093/nar/gkv332

Evans, B. A., and Amyes, S. G. (2014). OXA β-lactamases. *Clin. Microbiol. Rev.* 27, 241–263. doi: 10.1128/CMR.00117-13

Hall, B. G., and Barlow, M. (2005). Revised Ambler classification of β-lactamases. *J. Antimicrob. Chemother.* 55, 1050–1051. doi: 10.1093/jac/dki130

Letunic, I., and Bork, P. (2019). Interactive Tree Of Life (iTOL) v4: recent updates and new developments. *Nucleic Acids Res.* 47, W256–W259. doi: 10.1093/nar/gkz239

Qi, Y., Wei, Z., Ji, S., Du, X., Shen, P., and Yu, Y. (2011). ST11, the dominant clone of KPC-producing *Klebsiella pneumoniae* in China. *J. Antimicrob. Chemother.* 66, 307–312. doi: 10.1093/jac/dkq431

Sambrook, J., and Russell, D. W. (2001). *Molecular Cloning. A Laboratory Manual*. Cold Spring Harbour, NY: Cold Spring Harbour Laboratory Press.

Stamatakis, A. (2014). RAxML version 8: a tool for phylogenetic analysis and post-analysis of large phylogenies. *Bioinformatics* 30, 1312–1313. doi: 10.1093/bioinformatics/btu033

Tian, X., Wang, Q., Perlaza-Jimenez, L., Zheng, X., Zhao, Y., Dhanasekaran, V., et al. (2020). First description of antimicrobial resistance in carbapenem-susceptible *Klebsiella pneumoniae* after imipenem treatment, driven by outer membrane remodeling. *BMC Microbiol.* 20:218. doi: 10.1186/s12866-020-01898-1

Walker, B. J., Abeel, T., Shea, T., Priest, M., Abouelliel, A., Sakthikumar, S., et al. (2014). Pilon: an integrated tool for comprehensive microbial variant detection and genome assembly improvement. *PLoS One* 9:e112963. doi: 10.1371/journal.pone.0112963

Wick, R. R., Judd, L. M., Gorrie, C. L., and Holt, K. E. (2017). Unicycler: resolving bacterial genome assemblies from short and long sequencing reads. *PLoS Comput. Biol.* 13:e1005595. doi: 10.1371/journal.pcbi.1005595

World Health Organization (2017). *Global Priority List of Antibiotic-Resistant Bacteria to Guide Research, Discovery, and Development of New Antibiotics*. Geneva: World Health Organization.

Wyres, K. L., Wick, R. R., Gorrie, C., Jenney, A., Follador, R., Thomson, N. R., et al. (2016). Identification of *Klebsiella* capsule synthesis loci from whole genome data. *Microb. Genom.* 2:e000102. doi: 10.1099/mgen.0.000102

Yoon, E. J., and Jeong, S. H. (2021). Class D β-lactamases. *J. Antimicrob. Chemother.* 76, 836–864. doi: 10.1093/jac/dkaa513

Zhang, X., Lu, X., and Zong, Z. (2012). *Enterobacteriaceae* producing the KPC-2 carbapenemase from hospital sewage. *Diagn. Microbiol. Infect. Dis.* 73, 204–206. doi: 10.1016/j.diagmicrobio.2012.02.007

Conflict of Interest: The authors declare that the research was conducted in the absence of any commercial or financial relationships that could be construed as a potential conflict of interest.

Publisher's Note: All claims expressed in this article are solely those of the authors and do not necessarily represent those of their affiliated organizations, or those of the publisher, the editors and the reviewers. Any product that may be evaluated in this article, or claim that may be made by its manufacturer, is not guaranteed or endorsed by the publisher.

frontiers in Microbiology

ORIGINAL RESEARCH
published: 01 October 2021
doi: 10.3389/fmicb.2021.743312

First Report of *bla*$_{IMP-4}$ and *bla*$_{SRT-2}$ Coproducing *Serratia marcescens* Clinical Isolate in China

Xiangning Huang[1†], Siquan Shen[2,3†], Qingyu Shi[2,3], Li Ding[2,3], Shi Wu[2,3], Renru Han[2,3], Xun Zhou[2,3], Hua Yu[1] and Fupin Hu[2,3*]*

[1] Department of Laboratory Medicine, Sichuan Provincial People's Hospital, University of Electronic Science and Technology of China, Chengdu, China, [2] Huashan Hospital, Institute of Antibiotics, Fudan University, Shanghai, China, [3] Key Laboratory of Clinical Pharmacology of Antibiotics, Ministry of Health, Shanghai, China

OPEN ACCESS

Edited by:
Mary Marquart,
University of Mississippi Medical Center, United States

Reviewed by:
Hua Zhou,
Zhejiang University, China
Hanna Evelina Sidjabat,
Griffith University, Australia
Hong-wei Zhou,
Zhejiang University, China

***Correspondence:**
Hua Yu
yvhua2002@163.com
Fupin Hu
hufupin@fudan.edu.cn

[†] These authors have contributed equally to this work and share senior authorship

Specialty section:
This article was submitted to Antimicrobials, Resistance and Chemotherapy, a section of the journal Frontiers in Microbiology

Received: 18 July 2021
Accepted: 01 September 2021
Published: 01 October 2021

Citation:
Huang X, Shen S, Shi Q, Ding L, Wu S, Han R, Zhou X, Yu H and Hu F (2021) First Report of bla$_{IMP-4}$ and bla$_{SRT-2}$ Coproducing Serratia marcescens Clinical Isolate in China. Front. Microbiol. 12:743312. doi: 10.3389/fmicb.2021.743312

Carbapenem-resistant *Enterobacterales* (CRE) has become a major therapeutic concern in clinical settings, and carbapenemase genes have been widely reported in various bacteria. In *Serratia marcescens*, class A group carbapenemases including SME and KPC were mostly identified. However, there are few reports of metallo-β-lactamase-producing *S. marcescens.* Here, we isolated a carbapenem-resistant *S. marcescens* (S378) from a patient with asymptomatic urinary tract infection which was then identified as an IMP-4-producing *S. marcescens* at a tertiary hospital in Sichuan Province in southwest of China. The species were identified using MALDI-TOF MS, and carbapenemase-encoding genes were detected using PCR and DNA sequencing. The results of antimicrobial susceptibility testing by broth microdilution method indicated that the isolate *S. marc*escens S378 was resistant to meropenem (MIC = 32 μg/ml) and imipenem (MIC = 64 μg/ml) and intermediate to aztreonam (MIC = 8 μg/ml). The complete genomic sequence of *S. marcescens* was identified using Illumina (Illumina, San Diego, CA, United States) short-read sequencing (150 bp paired-end reads); five resistance genes had been identified, including *bla*$_{IMP-4}$, *bla*$_{SRT-2}$, *aac(6′)-Ic*, *qnrS1*, and *tet(41)*. Conjugation experiments indicated that the *bla*$_{IMP-4}$-carrying plasmid pS378P was conjugative. Complete sequence analysis of the plasmid pS378P bearing *bla*$_{IMP-4}$ revealed that it was a 48,780-bp IncN-type plasmid with an average GC content of 50% and was nearly identical to pP378-IMP (99% nucleotide identity and query coverage).

Keywords: ***Serratia marcescens***, ***bla*$_{IMP-4}$**, ***bla*$_{SRT-2}$**, **IncN plasmid, class 1 integron**

INTRODUCTION

S. marcescens is recognized to be an important nosocomial pathogen and is usually associated with outbreaks in neonatal wards (Mahlen, 2011; Millán-Lou et al., 2021). The infection caused by *S. marcescens* can cause nosocomial infection, affecting several parts of the body, such as the meninges, blood, and lungs, leading to a series of infections like central nervous system infections, blood infections (including endocarditis), and nosocomial pneumonia (Mahlen, 2011; da Silva et al., 2021). The emergence of multidrug-resistant (MDR) *S. marcescens* strains poses a serious threat to public health. One important feature of *S. marcescens* is its intrinsic and acquired resistance to a large number of antibiotics including ampicillin, nitrofurantoin, tetracycline,

macrolides, cefuroxime, cephamycin, fluoroquinolone, and colistin (Sandner-Miranda et al., 2018). The identification of carbapenem-resistant *S. marcescens* in patients might pose potential spread into the hospital environment and/or to other patients. For example, in 2020, the outbreak of KPC-3-producing *S. marcescens* among nursing institutions in the United States made it very difficult for clinical treatment (Jimenez et al., 2020). The spread of carbapenem-resistant *S. marcescens* in a hospital environment is a worrying problem.

The metallo-β-lactamases (MBLs) can hydrolyze nearly all β-lactams, and their activities cannot be inhibited by clinically available β-lactamase inhibitors including avibactam, relebactam, and vaborbactam (Wu et al., 2019; Boyd et al., 2020). IMP-type MBLs were the earliest transferable carbapenemases reported in Gram-negative bacteria (Watanabe et al., 1991). Until now, more than 82 variants of *bla*$_{IMP}$ have been identified,[1] *bla*$_{IMP-4}$, as the most reported IMP variant, has often been found in class 1 integrons and carried by multiple plasmid types like HI2, L/M, A/C, and N for dissemination (Lai et al., 2017; Wang et al., 2018; Roberts et al., 2020). However, unlike NDM-type MBLs, *bla*$_{IMP}$ was not commonly detected among CRE from China (Zhang et al., 2017; Wang et al., 2018; Han et al., 2020). According to a longitudinal large-scale CRE Study in China from 2012 to 2016 (65 hospitals in 25 provinces were included), the common species carrying *bla*$_{IMP-4}$ were *Enterobacter cloacae*, *Escherichia coli*, *Klebsiella pneumoniae*, and *Citrobacter freundii* (Wang et al., 2018). In 2005, the first clinical isolate of *bla*$_{IMP-4}$-positive *S. marcescens* was identified in Australia (Peleg et al., 2005). In this study, we reported a *bla*$_{IMP-4}$ and *bla*$_{SRT-2}$ positive *S. marcescens* containing an IncN-type plasmid in China.

MATERIALS AND METHODS

Strains and Antimicrobial Susceptibility Testing

A carbapenem-resistant *S. marcescens* (S378) was isolated from a urine sample from a patient with asymptomatic urinary tract infection at a tertiary hospital in Sichuan Province in southwest of China. Species identification was performed using MALDI-TOF MS (bioMérieux, France). Phenotypic and genotypic detection of carbapenemases was performed using imipenem-EDTA double-disk synergy test and *NG*-Test Carba 5, respectively. The existence of the carbapenemase genes (KPC, NDM, OXA, IMP, and VIM) was confirmed by PCR-based sequencing, as previously described (Gülmez et al., 2008; Woodford et al., 2008; Feng et al., 2016; Ferreira et al., 2020; Solgi et al., 2020; Nikibakhsh et al., 2021). The broth microdilution method recommended by the Clinical and Laboratory Standards Institute (CLSI) was used as a reference for determining the minimal inhibition concentration with quality control and interpretation of the results according to CLSI M100-31th breakpoints for all agents with the exception of tigecycline, polymyxin, and cefoperazone–sulbactam (Clinical and Laboratory Standards Institute, 2021). Cefepime–zidebactam and cefepime–tazobactam referred to criteria for cefepime in CLSI. Tigecycline MICs were interpreted using US FDA MIC breakpoints for *Enterobacterales* (FDA, 2021), and polymyxin MICs were interpreted using the European Committee for Antimicrobial Susceptibility Testing (EUCAST) MIC breakpoints for *Enterobacterales*. *E. coli* ATCC 25922 and *Pseudomonas aeruginosa* ATCC 27853 were used as controls for testing antimicrobial susceptibility.

Conjugation and Plasmid Sequencing

A conjugation experiment was performed to explore the transferability of the plasmid. Briefly, the *bla*$_{IMP-4}$-positive isolate *S. marc*escens S378 was used as the donor, while the *E. coli* J53 (azide resistant) was used as the recipient strain. Conjugants were selected on Mueller–Hinton (MH) agar supplemented with azide (100 μg/ml) and ampicillin (50 μg/ml). The presence of the *bla*$_{IMP-4}$ gene and other resistance genes in conjugants was confirmed by antimicrobial susceptibility, PCR, and DNA sequencing. The plasmids of the *bla*$_{IMP-4}$-containing conjugants were extracted using the Qiagen Midi kit (Qiagen, Hilden, Germany) and sequenced using Illumina NovaSeq (Illumina, San Diego, CA, United States) short-read sequencing (150-bp paired-end reads). The sequencing reads were trimmed with sickle (GitHub) and *de novo* assembled using SPAdes 3.12.0. To evaluate and compare the assembly results, Pilon 1.18 is used for basic calibration. Open reading frame prediction and annotation were done with RAST version 2.0[2] and BLAST[3] at NCBI; the plasmid replicon was determined using the PCR-based replicon typing method (Carattoli et al., 2005). Plasmid comparisons were performed using BRIG[4] (Alikhan et al., 2011).

Whole-Genome Sequencing and Bioinformatics Analysis

Genomic DNA was extracted using a Genomic DNA Isolation Kit (Qiagen, Hilden, Germany) and sequenced using Illumina (Illumina, San Diego, CA, United States) short-read sequencing (150-bp paired-end reads). Sequences were *de novo* assembled using SPAdes 3.12.0. Antimicrobial resistance gene analysis and draft genome annotation were performed using BacWGSTdb.[5]

RESULTS

Overview of the *bla*$_{IMP-4}$-Positive Isolates

S. marcescens S378 was isolated from a urine specimen of a 76-year-old male patient who was admitted to the hospital for treatment of chronic obstructive pulmonary disease. During hospitalization, the patient was dizzy accompanied by shortness of breath and aggravated after activity. CT showed inflammatory changes in the lungs. The patient suffered from subarachnoid hemorrhage and has been cured. Comorbidities of the elderly patient included diabetes mellitus II, hypertension, acute cerebral

[1] http://www.ncbi.nlm.nih.gov/pathogens/beta-lactamase-data-resources/

[2] https://rast.nmpdr.org

[3] https://blast.ncbi.nlm.nih.gov/Blast.cgi

[4] http://brig.sourceforge.net

[5] http://bacdb.cn/BacWGSTdb/analysis_single.php

infarction, occlusion of right internal carotid artery, chronic obstructive pulmonary disease, and asymptomatic urinary tract infection. The interventional operation was performed for this patient to deal with acute cerebral infarction, and on the third day after the operation, he developed a fever and one extended-spectrum β-lactamase-negative *K. pneumoniae* was isolated from the sputum. With suspicion of pneumonia, the patient was started administering intravenous moxalactam (1 g Q12) for 5 days and ceftazidime (1 g Q8h) for 4 days. Subsequently, the patient's body temperature returned to normal and the infection was controlled. On the 20th day, *S. marc*escens S378 was isolated from the urine causing asymptomatic urinary tract infection. No antibiotic was given for this strain because this *Serratia marcescens* was considered to only colonize in the urinary tract. The patient was recovered and discharged 26 days after admission.

The antimicrobial susceptibility profiles of *S. marc*escens S378 are presented in **Table 1**. The isolate was susceptible to tigecycline (MIC = 0.5 μg/ml), amikacin (MIC = 16 μg/ml), and Trimethoprim-sulfamethoxazole (MIC ≤ 0.25 μg/L), intermediate to aztreonam (MIC = 8 μg/ml), but resistant to cefoperazone–sulbactam (MICs > 128 μg/ml), meropenem (MIC = 32 μg/ml), imipenem (MIC = 64 μg/ml), ceftazidime-avibactam (MIC ≥ 32 μg/ml), levofloxacin (MIC = 2 μg/ml), and ciprofloxacin (MIC = 1 μg/ml).

Carbapenemase-Encoding Genes and Conjugation Experiments

PCR-based sequencing demonstrated the presence of bla_{IMP-4} in *S. marcescens* strain S378. The bla_{IMP-4}-carrying plasmid was successfully transferred from *S. marcescens* strain S378 to *E. coli* J53, making the conjugants resistant to ceftazidime and ceftazidime–avibactam but intermediate to imipenem and meropenem. Compared with the recipient *E. coli* J53, the meropenem, imipenem, and ceftazidime–avibactam MICs of conjugants increased at least 60-, 8-, and 256-fold, respectively (**Table 1**).

Whole-Genome Sequencing Analysis

According to the whole-genome sequencing (WGS) analysis, many resistance genes had been identified, including the β-lactamase genes bla_{IMP-4} and bla_{SRT-2}, the aminoglycoside resistance genes *aac(6′)-Ic*, the fluoroquinolone resistance gene *qnrS1*, and the tetracycline resistance gene *tet(41)*. According to the sequencing results of pS378P, it was a 48,780-bp plasmid (**Figure 1**), belonging to the IncN type, with an average GC content of 50%. This targeted plasmid contained 43 open reading frames (ORFs). Only two resistance genes were identified in pS378P, bla_{IMP-4}, and *qnrS1*, conferring resistance to carbapenems and quinolones, respectively. Blast comparison indicates that pS378P in this study shares extensive similarity with pP378-IMP (99% nucleotide identity and query coverage), an IncN-type bla_{IMP-4} carrying plasmid with the length of 51,207 bp in a carbapenem-resistant *P. aeruginosa* strain P378 isolated from a teaching hospital in Chongqing China in 2016 (Feng et al., 2016). Like the source of our strain, they were all isolated from urine specimen. pP378-IMP and pS378P both possess the conserved IncN1-type backbone regions, the *tra* genes and *kikA-korB* for conjugal transfer, and IS*1* remnant (**Figure 1**). There are two major genetic differences between the backbones of pS378P and pP378-IMP. First, pP378-IMP contains an intact anti-restriction gene combination ccgA I, ccgAII, ccgC, and ccgD (located *around* the 4.1–4.6-kb nucleotide positions of pP378-IMP), while only ccgAI and ccgAII genes were found in pS378P. Second, compared with the plasmid pP378-IMP, the class one integron in pS378P is incomplete that an insertion sequence, *IS*6100, was truncated (**Figure 2**).

DISCUSSION

According to a previous epidemiological study, the most frequent carbapenemases found in *S. marcescens* species belong to the class A group, including chromosomal location SME type or KPC-2 (Dabos et al., 2019). bla_{SRT-2}, an AmpC-type β-lactamase gene, was first reported in a *S. marcescens* strain in 2004. Almost all subsequent reports about it are related to *S. marcescens*. Moreover, in *S. marcescens*, bla_{SRT-2} often appears with different resistance genes, such as $bla_{CTX-M-3}$, bla_{TEM-1}, aminoglycoside AAC (6′)-Ic, and bla_{KPC-2} (Wu et al., 2004; Yu et al., 2008; Srinivasan and Rajamohan, 2019; Quezada-Aguiluz et al., 2020). bla_{IMP-4} was first identified in *Acinetobacter* spp. in 2001 from Hong Kong, China (Chu et al., 2001), and had spread rapidly around the world (Espedido et al., 2008; Lee et al., 2017, 2018; Ghaith et al., 2018), but unlike KPC-type and NDM-type carbapenemases

TABLE 1 | Susceptibility of *S. marcescens* clinical isolate, conjugant and recipient to antimicrobial agents.

Strains	β-Lactamase genes	MIC (mg/l)															
		CZA	IPM	MEM	CAZ	FEP	TZP	CSL	ATM	AMK	FPZ	FPT	SXT	LEV	CIP	TGC	POL
S. marcescens S378	bla_{IMP-4}, bla_{SRT-2}	>32	64	32	>32	>128	>256	>128	8	16	4	>64	≤0.25	2	1	0.5	>16
E. coli S378-C	bla_{IMP-4}	>64	2	2	>32	8	8	64	≤1	≤1	0.125	8	≤0.25	1	1	0.25	0.25
E. coli J53	–	0.25	0.25	≤0.03	0.5	≤0.06	4	≤1	≤1	≤1	0.06	≤0.03	≤0.25	0.125	≤0.06	0.125	0.25

CZA, ceftazidime-avibactam; IPM, Imipenem; MEM, meropenem; CAZ, ceftazidime; FEP, cefepime; TZP, piperacillin-tazobactam; CSL, cefoperazone-sulbactam; ATM, aztreonam; AMK, amikacin; FPZ, cefepime-zidebactam; FPT, cefepime-tazobactam; SXT, trimethoprim-sulfamethoxazole; LEV, levofloxacin; CIP, ciprofloxacin; TGC, tigecycline; POL, polymyxin B.

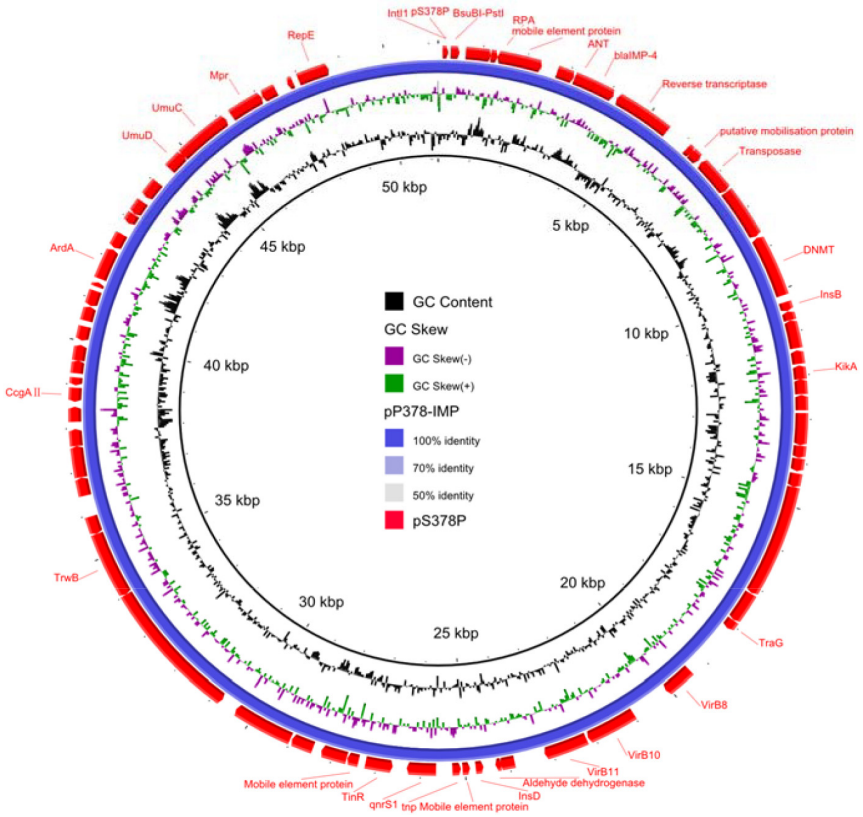

FIGURE 1 | Circular comparison between plasmid pS378P (MZ643942, in this study) and plasmid pP378-IMP (KX711879). The different colors indicated different plasmids and are listed in the color key.

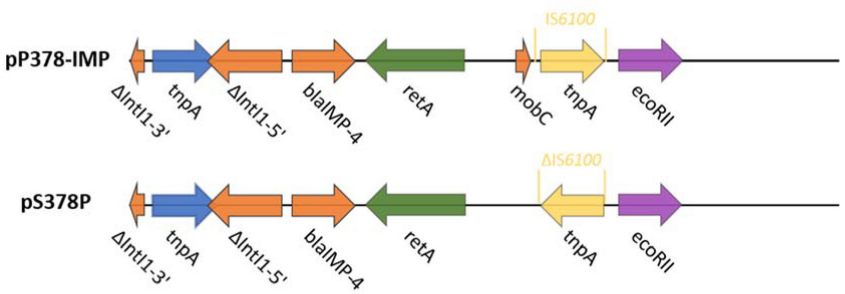

FIGURE 2 | Plasmid accessory resistance regions. The genetic environment comparison of *bla*$_{IMP-4}$ between pP378-IMP and pS378P. Genes are denoted by arrows and colored based on gene function classification.

among CRE (NDM-type MBL remains predominant), *bla*$_{IMP-4}$ has not been frequently detected, especially in *S. marcescens* (Xiong et al., 2016; Han et al., 2020). In 2018, the first report of *bla*$_{IMP-4}$- and *bla*$_{VIM-2}$-producing *S. marcescens* was published in Egypt (Ghaith et al., 2018). This is a clinical retrospective study. A total of 40 strains of *S. marcescens* were isolated from March to August 2015, of which 42.5% was IMP-4-positive and 37.5% was VIM-2-positive. Just like the strain in our study, they all showed resistance to meropenem and ceftazidime. Our study demonstrates the emergence of carbapenemase-producing *S. marcescens*, expressing *bla*$_{IMP-4}$ and *bla*$_{SRT-2}$ β-lactamase genes in China.

S. marcescens is featured by its rapid acquisition of antibiotic resistance, mainly due to the acquisition of plasmid (Mahlen, 2011). However, comprehensive analysis for the genome sequence carrying *bla*$_{IMP-4}$ is rare. According to current reports, although different types of plasmids had been detected, the IncN type remains predominant in China, especially for the transmission of *bla*$_{IMP-4}$ in recent years, and this type of plasmid usually presents a broad host range (Feng et al., 2016;

Wang et al., 2017; Xu et al., 2020), compared with the most identical plasmid pP378-IMP. The strains in both studies all harbored a conjugative bla_{IMP-4}-carrying plasmid, which accounts for the carbapenem resistance phenotype. In both plasmids, the bla_{IMP-4} gene was found in class 1 integron, identical to the IMP-4-carrying plasmids before (Xu et al., 2020; Liu et al., 2021). Class 1 integrons are responsible for the transmission of the bla_{IMP} gene; so far, many Class 1 integrons carrying the bla_{IMP-4} gene have been reported, such as In 809, 823, 1,456, 1,460, and 1,589 (Lee et al., 2017; Matsumura et al., 2017; Wang et al., 2017; Dolejska et al., 2018). In addition to integrons and the conjugative plasmids, the insertion sequence also plays an important role in the transmission of resistant genes. Previous studies about bla_{IMP-4}-carrying plasmids emphasized the role of the IS*26* mobile element, which may play an important role in the dissemination of IMP-4 in different plasmids (Xu et al., 2020; Liu et al., 2021); the corresponding situation also exists in our strains. Timely determination of the resistance mechanism and the transmission mechanism of resistance genes is very important for clinical anti-infective treatment and controlling the wide spread of these multi-drug resistant bacteria.

CONCLUSION

In summary, we first identified a bla_{IMP-4} and bla_{SRT-2} co-positive *S. marcescens* strain from a human urine sample in China. The patient was accompanied by many underlying diseases such as diabetes, emphysema, diabetic peripheral neuropathy, and atherosclerosis, and multiple antimicrobial substances were used in the course of treatment; since such risk factors for MDR bacteria are commonly present in high-risk populations, it seems justified to screen Gram-negative bacilli for carbapenemases in these patients with high-risk factors based on our routine antimicrobial susceptibility testing and molecular biotechnology. Moreover, to date, *S. marcescens* and many other *Enterobacteriaceae* bacteria that are not often reported might still be a neglected source of undetected carbapenemase allocation.

DATA AVAILABILITY STATEMENT

The datasets presented in this study can be found in online repositories. The names of the repository/repositories and accession number(s) can be found below: GenBank MZ643942.

ETHICS STATEMENT

The study protocol was approved by the Institutional Review Board of Huashan Hospital, Fudan University (No. 2018-408).

AUTHOR CONTRIBUTIONS

FH and HY designed the study. SS and XH collected clinical samples and performed the experiments. LD, SW, RH, and XZ analyzed the data. SS and XH wrote the manuscript. All authors contributed to the article and approved the submitted version.

FUNDING

This work was supported by the National Mega-project for Innovative Drugs (2019ZX09721001-006-004), the National Natural Science Foundation of China (81871690), the Shanghai Antimicrobial Surveillance Network (3030231003), and the China Antimicrobial Surveillance Network (2018QD100). The funders had no role in the study design, data collection and analysis, decision to publish, or preparation of the manuscript.

REFERENCES

Alikhan, N. F., Petty, N. K., Ben Zakour, N. L., and Beatson, S. A. (2011). BLAST Ring Image Generator (BRIG): simple prokaryote genome comparisons. *BMC Genomics* 12:402. doi: 10.1186/1471-2164-12-402

Boyd, S. E., Livermore, D. M., Hooper, D. C., and Hope, W. W. (2020). Metallo-β-lactamases: structure, function, epidemiology, treatment options, and the development pipeline. *Antimicrob. Agents Chemother.* 64:e00397-e20. doi: 10.1128/aac.00397-20

Carattoli, A., Bertini, A., Villa, L., Falbo, V., Hopkins, K. L., and Threlfall, E. J. (2005). Identification of plasmids by PCR-based replicon typing. *J. Microbiol. Methods* 63, 219–228.

Chu, Y. W., Afzal-Shah, M., Houang, E. T., Palepou, M. I., Lyon, D. J., Woodford, N., et al. (2001). IMP-4, a novel metallo-beta-lactamase from nosocomial *Acinetobacter spp.* Collected in Hong Kong between 1994 and 1998. *Antimicrob. Agents Chemother.* 45, 710–714. doi: 10.1128/aac.45.3.710-714.2001

Clinical and Laboratory Standards Institute (2021). *Performance Standards for Antimicrobial Susceptibility Testing, CLSI Supplement M100*, 31th Edn. Wayne, PA: Clinical and Laboratory Standards Institute.

da Silva, K. E., Rossato, L., Jorge, S., de Oliveira, N. R., Kremer, F. S., Campos, V. F., et al. (2021). Three challenging cases of infections by multidrug-resistant *Serratia marcescens* in patients admitted to intensive care units. *Braz. J. Microbiol.* 52, 1341–1345. doi: 10.1007/s42770-021-477-474

Dabos, L., Patiño-Navarrete, R., Nastro, M., Famiglietti, A., Glaser, P., Rodriguez, C. H., et al. (2019). SME-4-producing *Serratia marcescens* from Argentina belonging to clade 2 of the *S. Marcescens* phylogeny. *J. Antimicrob. Chemother.* 74, 1836–1841. doi: 10.1093/jac/dkz115

Dolejska, M., Papagiannitsis, C., Medvecky, M., Davidova-Gerzova, L., and Valcek, A. J. A. (2018). Characterization of the complete nucleotide sequences of IMP-4-encoding plasmids, belonging to diverse inc families, recovered from *Enterobacteriaceae* isolates of wildlife origin. *Antimicrob. Agents Chemother.* 62:e2434-e17. doi: 10.1128/aac.02434-17

Espedido, B. A., Partridge, S. R., and Iredell, J. R. (2008). bla_{IMP-4} in different genetic contexts in *Enterobacteriaceae* isolates from Australia. *Antimicrob. Agents Chemother.* 52, 2984–2987. doi: 10.1128/aac.01634-07

FDA (2021). *Tigecycline-Injection Products*. Available online at: https://www.fda.gov/drugs/development-resources/tigecycline-injection-products.

Feng, W., Zhou, D., Wang, Q., Luo, W., Zhang, D., Sun, Q., et al. (2016). Dissemination of IMP-4-encoding pIMP-HZ1-related plasmids among *Klebsiella pneumoniae* and *Pseudomonas aeruginosa* in a Chinese teaching hospital. *Sci. Rep.* 6:33419. doi: 10.1038/srep33419

Ferreira, R. L., Rezende, G. S., Damas, M. S. F., Oliveira-Silva, M., Pitondo-Silva, A., Brito, M. C. A., et al. (2020). Characterization of KPC-producing *Serratia marcescens* in an intensive care unit of a Brazilian tertiary hospital. *Front. Microbiol.* 11:956. doi: 10.3389/fmicb.2020.00956

Ghaith, D. M., Zafer, M. M., Ismail, D. K., Al-Agamy, M. H., Bohol, M. F. F., Al-Qahtani, A., et al. (2018). First reported nosocomial outbreak of *Serratia*

marcescens harboring bla_{IMP-4} and bla_{VIM-2} in a neonatal intensive care unit in Cairo, Egypt. *Infect. Drug Resist.* 11, 2211–2217. doi: 10.2147/idr.S174869

Gülmez, D., Woodford, N., Palepou, M. F., Mushtaq, S., Metan, G., Yakupogullari, Y., et al. (2008). Carbapenem-resistant *Escherichia coli* and *Klebsiella pneumoniae* isolates from Turkey with OXA-48-like carbapenemases and outer membrane protein loss. *Int. J. Antimicrob. Agents* 31, 523–526. doi: 10.1016/j.ijantimicag.2008.01.017

Han, R., Shi, Q., Wu, S., Yin, D., Peng, M., Dong, D., et al. (2020). Dissemination of carbapenemases (KPC, NDM, OXA-48, IMP, and VIM) among carbapenem-resistant *Enterobacteriaceae* isolated from adult and children patients in China. *Front. Cell. Infect. Microbiol.* 10:314. doi: 10.3389/fcimb.2020.00314

Jimenez, A., Abbo, L. M., Martinez, O., Shukla, B., Sposato, K., Iovleva, A., et al. (2020). KPC-3-producing *Serratia marcescens* outbreak between acute and long-term care facilities, Florida, USA. *Emerg. Infect. Dis.* 26, 2746–2750. doi: 10.3201/eid2611.202203

Lai, K., Ma, Y., Guo, L., An, J., Ye, L., and Yang, J. (2017). Molecular characterization of clinical IMP-producing *Klebsiella pneumoniae* isolates from a Chinese tertiary Hospital. *Ann. Clin. Microbiol. Antimicrob.* 16:42. doi: 10.1186/s12941-017-0218-9

Lee, J. H., Bae, I. K., Lee, C. H., and Jeong, S. (2017). Molecular characteristics of first IMP-4-producing *Enterobacter cloacae* sequence type 74 and 194 in Korea. *Front. Microbiol.* 8:2343. doi: 10.3389/fmicb.2017.02343

Lee, J. H., Lee, C. H., and Bae, I. K. (2018). Emergence of IMP-4-producing *Enterobacter aerogenes* clinical isolate. *Clin. Lab.* 64, 1323–1326. doi: 10.7754/Clin.Lab.2018.180211

Liu, W., Dong, H., Yan, T., Liu, X., Cheng, J., Liu, C., et al. (2021). Molecular characterization of bla_{IMP-4}-carrying *Enterobacterales* in henan province of china. *Front. Microbiol.* 12:626160. doi: 10.3389/fmicb.2021.626160

Mahlen, S. D. (2011). *Serratia* infections: from military experiments to current practice. *Clin. Microbiol. Rev.* 24, 755–791. doi: 10.1128/cmr.00017-11

Matsumura, Y., Peirano, G., Motyl, M. R., Adams, M. D., Chen, L., Kreiswirth, B., et al. (2017). Global molecular epidemiology of IMP-producing *Enterobacteriaceae*. *Antimicrob. Agents Chemother.* 61:e02729-16.

Millán-Lou, M. I., López, C., Bueno, J., Pérez-Laguna, V., Lapresta, C., Fuertes, M. E., et al. (2021). Successful control of *Serratia marcescens* outbreak in a neonatal unit of a tertiary-care hospital in Spain. *Enferm. Infecc. Microbiol. Clin.* 16:S0213-005X(21)00186-5. doi: 10.1016/j.eimc.2021.05.003

Nikibakhsh, M., Firoozeh, F., Badmasti, F., Kabir, K., and Zibaei, M. (2021). Molecular study of metallo-β-lactamases and integrons in *Acinetobacter baumannii* isolates from burn patients. *BMC Infect. Dis.* 21:782. doi: 10.1186/s12879-021-06513-w

Peleg, A. Y., Franklin, C., Bell, J. M., and Spelman, D. W. (2005). Dissemination of the metallo-beta-lactamase gene bla_{IMP-4} among gram-negative pathogens in a clinical setting in Australia. *Clin. Infect. Dis.* 41, 1549–1556. doi: 10.1086/497831

Quezada-Aguiluz, M., Lincopan, N., Cerdeira, L., Fuga, B., Silva, F., Barrera, B., et al. (2020). Draft genome sequence of a multidrug-resistant KPC-2 and SRT-2 co-producing *Serratia marcescens* strain isolated from a hospitalised patient in Chile. *J. Glob. Antimicrob. Resist.* 21, 1–2. doi: 10.1016/j.jgar.2020.02.004

Roberts, L. W., Catchpoole, E., Jennison, A. V., Bergh, H., Hume, A., Heney, C., et al. (2020). Genomic analysis of carbapenemase-producing *Enterobacteriaceae* in Queensland reveals widespread transmission of bla_{IMP-4} on an IncHI2 plasmid. *Microb. Genom.* 6:e000321. doi: 10.1099/mgen.0.000321

Sandner-Miranda, L., Vinuesa, P., Cravioto, A., and Morales-Espinosa, R. (2018). The genomic basis of intrinsic and acquired antibiotic resistance in the genus *Serratia*. *Front Microbiol* 9:828. doi: 10.3389/fmicb.2018.00828

Solgi, H., Nematzadeh, S., Giske, C. G., Badmasti, F., Westerlund, F., Lin, Y. L., et al. (2020). Molecular epidemiology of OXA-48 and NDM-1 producing *Enterobacterales* species at a university hospital in Tehran, Iran, Between 2015 and 2016. *Front. Microbiol.* 11:936. doi: 10.3389/fmicb.2020.00936

Srinivasan, V. B., and Rajamohan, G. (2019). Genome analysis of urease positive *Serratia marcescens*, co-producing SRT-2 and AAC(6′)-Ic with multidrug efflux pumps for antimicrobial resistance. *Genomics* 111, 653–660. doi: 10.1016/j.ygeno.2018.04.001

Wang, Q., Wang, X., Wang, J., Ouyang, P., Jin, C., Wang, R., et al. (2018). Phenotypic and genotypic characterization of carbapenem-resistant *Enterobacteriaceae*: data from a longitudinal large-scale CRE study in China (2012-2016). *Clin. Infect. Dis.* 67(Suppl. 2), S196–S205. doi: 10.1093/cid/ciy660

Wang, Y., Lo, W.-U., Lai, R. W.-M., Tse, C. W.-S., Lee, R. A., Luk, W.-K., et al. (2017). IncN ST7 epidemic plasmid carrying bla_{IMP-4} in *Enterobacteriaceae* isolates with epidemiological links to multiple geographical areas in China. *J. Antimicrob. Chemother.* 72, 99–103. doi: 10.1093/jac/dkw353

Watanabe, M., Iyobe, S., Inoue, M., and Mitsuhashi, S. (1991). Transferable imipenem resistance in *Pseudomonas aeruginosa*. *Antimicrob. Agents Chemother.* 35, 147–151. doi: 10.1128/aac.35.1.147

Woodford, N., Zhang, J., Warner, M., Kaufmann, M. E., Matos, J., Macdonald, A., et al. (2008). Arrival of *Klebsiella pneumoniae* producing KPC carbapenemase in the United Kingdom. *J. Antimicrob. Chemother.* 62, 1261–1264. doi: 10.1093/jac/dkn396

Wu, L. T., Tsou, M. F., Wu, H. J., Chen, H. E., Chuang, Y. C., and Yu, W. L. (2004). Survey of CTX-M-3 extended-spectrum beta-lactamase (ESBL) among cefotaxime-resistant *Serratia marcescens* at a medical center in middle Taiwan. *Diagn. Microbiol. Infect. Dis.* 49, 125–129. doi: 10.1016/j.diagmicrobio.2004.02.004

Wu, W., Feng, Y., Tang, G., Qiao, F., McNally, A., and Zong, Z. (2019). NDM metallo-β-lactamases and their bacterial producers in health care settings. *Clin. Microbiol. Rev.* 32, e00115-18. doi: 10.1128/cmr.00115-18

Xiong, J., Déraspe, M., Iqbal, N., Ma, J., Jamieson, F. B., Wasserscheid, J., et al. (2016). Genome and plasmid analysis of bla_{IMP-4}-carrying *Citrobacter freundii* B38. *Antimicrob. Agents Chemother.* 60, 6719–6725. doi: 10.1128/aac.00588-16

Xu, J., Lin, W., Chen, Y., and He, F. (2020). Characterization of an IMP-4-producing *Klebsiella pneumoniae* ST1873 strain recovered from an infant with a bloodstream infection in China. *Infect. Drug Resist.* 13, 773–779. doi: 10.2147/idr.S247341

Yu, W. L., Ko, W. C., Cheng, K. C., Chen, H. E., Lee, C. C., and Chuang, Y. C. (2008). Institutional spread of clonally related *Serratia marcescens* isolates with a novel *AmpC* cephalosporinase (S4): a 4-year experience in Taiwan. *Diagn. Microbiol. Infect. Dis.* 61, 460–467. doi: 10.1016/j.diagmicrobio.2008.03.010

Zhang, R., Liu, L., Zhou, H., Chan, E. W., Li, J., Fang, Y., et al. (2017). Nationwide surveillance of clinical carbapenem-resistant *Enterobacteriaceae* (CRE) strains in China. *EBioMedicine* 19, 98–106. doi: 10.1016/j.ebiom.2017.04.032

Conflict of Interest: The authors declare that the research was conducted in the absence of any commercial or financial relationships that could be construed as a potential conflict of interest.

Publisher's Note: All claims expressed in this article are solely those of the authors and do not necessarily represent those of their affiliated organizations, or those of the publisher, the editors and the reviewers. Any product that may be evaluated in this article, or claim that may be made by its manufacturer, is not guaranteed or endorsed by the publisher.

frontiers in Microbiology

ORIGINAL RESEARCH
published: 14 October 2021
doi: 10.3389/fmicb.2021.670535

Targeted Delivery of Narrow-Spectrum Protein Antibiotics to the Lower Gastrointestinal Tract in a Murine Model of *Escherichia coli* Colonization

Nuria Carpena[1], Kerry Richards[2], Teresita D. J. Bello Gonzalez[1], Alberto Bravo-Blas[1], Nicholas G. Housden[3], Konstantinos Gerasimidis[1], Simon W. F. Milling[1], Gillian Douce[1], Danish J. Malik[2] and Daniel Walker[1]**

[1]College of Medical, Veterinary and Life Sciences, University of Glasgow, Glasgow, United Kingdom, [2]Chemical Engineering Department, Loughborough University, Loughborough, United Kingdom, [3]Department of Biochemistry, University of Oxford, Oxford, United Kingdom

Bacteriocins are narrow-spectrum protein antibiotics that could potentially be used to engineer the human gut microbiota. However, technologies for targeted delivery of proteins to the lower gastrointestinal (GI) tract in preclinical animal models are currently lacking. In this work, we have developed methods for the microencapsulation of *Escherichia coli* targeting bacteriocins, colicin E9 and Ia, in a pH responsive formulation to allow their targeted delivery and controlled release in an *in vivo* murine model of *E. coli* colonization. Membrane emulsification was used to produce a water-in-oil emulsion with the water-soluble polymer subsequently cross-linked to produce hydrogel microcapsules. The microcapsule fabrication process allowed control of the size of the drug delivery system and a near 100% yield of the encapsulated therapeutic cargo. pH-triggered release of the encapsulated colicins was achieved using a widely available pH-responsive anionic copolymer in combination with alginate biopolymers. *In vivo* experiments using a murine *E. coli* intestinal colonization model demonstrated that oral delivery of the encapsulated colicins resulted in a significant decrease in intestinal colonization and reduction in *E. coli* shedding in the feces of the animals. Employing controlled release drug delivery systems such as that described here is essential to enable delivery of new protein therapeutics or other biological interventions for testing within small animal models of infection. Such approaches may have considerable value for the future development of strategies to engineer the human gut microbiota, which is central to health and disease.

Keywords: antibiotic resistance, bacteriocins, drug delivery, hydrogels, membrane emulsification, microbiome engineering

OPEN ACCESS

Edited by:
Mary Marquart,
University of Mississippi Medical Center, United States

Reviewed by:
Juan C. Cruz,
University of Los Andes, Colombia
Xiujuan Zhang,
Dalian University of Technology, China

***Correspondence:**
Daniel Walker
daniel.walker@glasgow.ac.uk
Danish J. Malik
d.j.malik@lboro.ac.uk

Specialty section:
This article was submitted to Antimicrobials, Resistance and Chemotherapy, a section of the journal Frontiers in Microbiology

Received: *21 February 2021*
Accepted: *21 September 2021*
Published: *14 October 2021*

Citation:
Carpena N, Richards K, Bello Gonzalez TDJ, Bravo-Blas A, Housden NG, Gerasimidis K, Milling SWF, Douce G, Malik DJ and Walker D (2021) Targeted Delivery of Narrow-Spectrum Protein Antibiotics to the Lower Gastrointestinal Tract in a Murine Model of Escherichia coli Colonization. Front. Microbiol. 12:670535. doi: 10.3389/fmicb.2021.670535

INTRODUCTION

The global rise in infections attributed to antibiotic-resistant Gram-negative bacteria poses a serious public health threat. Foremost among the Gram-negative pathogens are *Escherichia coli*, *Klebsiella pneumoniae* for which clinical isolates with extensive drug resistance, including to antibiotics of last resort such as carbapenems, are frequently encountered (Logan and Weinstein, 2017). Together with other generally drug-resistant bacterial species, such as Enterococci, these bacteria can be problematic in the hospital environment as they can dominate the microbiota of patients treated with broad spectrum antibiotics and may subsequently cause serious nosocomial infections (Ravi et al., 2019). In addition, Gram-negative bacteria are frequently present at elevated levels in dysbiotic microbiota associated with non-infectious chronic disease, where proteobacteria such as *E. coli* are generally overrepresented. For example, increased levels of *E. coli*, specifically adherent-invasive *E. coli* (AIEC), are associated with Crohn's disease (CD), an incurable form of inflammatory bowel disease (Darfeuille-Michaud et al., 2004; Lloyd-Price et al., 2019). New strategies are therefore required to target problematic gram-negative bacteria within the human microbiota.

Narrow-spectrum protein bacteriocins are emerging as promising alternative antibiotics and could be utilized to target specific pathogenic bacteria in the complex microbial community of the human microbiota, sparing the key eubiotic organisms (Brown et al., 2015; McCaughey et al., 2016; Six et al., 2020). The best studied of the protein bacteriocins are the colicins, which specifically target *E. coli* and strains of other closely related bacterial species (Cascales et al., 2007). The narrow killing spectrum of colicin-like bacteriocins is dictated by the numerous protein–protein interactions involved in the import of these 40–70 kDa toxins (Kleanthous, 2010; Behrens et al., 2019). Colicins, and other protein bacteriocins, deliver a single cytotoxic activity that either depolarizes the inner membrane, hydrolyses DNA or RNA in the cytoplasm or abolishes cell wall biosynthesis in the periplasm. Colicin E9, for example, is a non-specific DNase and colicin Ia forms voltage-gated ion-conducting channels in the cytoplasmic membrane (Pommer et al., 2001; Jakes and Finkelstein, 2010).

Bacteriocins are deployed naturally by both commensal and pathogenic organisms to augment niche colonization through the displacement of closely related bacteria. Colicins have been shown to play a direct role in the success of pathogenic *Salmonella* competing against commensal *E. coli* in enteric blooms and were a contributory factor in the success and spread of *Shigella sonnei* in Vietnam (Holt et al., 2013; Nedialkova et al., 2014). However, although these studies demonstrate that colicins can be successfully deployed within the environment of the gastrointestinal (GI) tract when produced *in situ*, it has also been demonstrated that colicins are highly susceptible to degradation by the proteases deployed in the stomach and small intestine to digest proteins (Schulz et al., 2015). Therefore, to utilize purified bacteriocins as orally dosed therapeutics, choice of a delivery formulation that protects against proteolysis in the upper GI tract but allows release in the lower GI tract will be essential.

In this work, we explore the potential of orally dosed colicin E9 and Ia to target bacteria in the lower GI tract. To protect colicins during transit through the upper GI tract and to enable controlled release of high doses of active agent in the lower GI tract, we encapsulated purified colicin E9 and Ia in pH-responsive microcapsules. Oral dosing demonstrated that active encapsulated colicins can be delivered to the lower GI tract in a murine *E. coli* colonization model.

MATERIALS AND METHODS

Bacterial Strains and Purification of Recombinant Colicins

For colicin overexpression, plasmids based on pET21a encoding the genes for the colicin E9-Im9 complex with a C-terminal His6-tag on the immunity protein and colicin Ia carrying a C-terminal His6-tag were transformed into *E. coli* BL21 (DE3) pLysS (Promega). Cells were grown in Luria–Bertani Broth media (LB) supplemented with ampicillin (100 μg ml^{-1}), until the OD_{600} reached 0.6. The cultures were induced with 0.1 mM IPTG β-D thiogalactopyranoside (IPTG) for 20 h at 28°C to express colicin Ia and with 1 mM IPTG for 3 h at 37°C to express colicin E9. After induction, cells were harvested by centrifugation (5,000 rpm for 15 min) at 4°C. Cell pellets were re-suspended in lysis buffer (50 mM Tris, 200 mM NaCl pH 7.5) supplemented with DNAse I (1 μg/ml, Sigma-Aldrich), lysozyme (1 mg/ml, Sigma-Aldrich), and protease inhibitor tablet (cOmplete™, EDTA-free Protease Inhibitor Cocktail, Sigma-Aldrich) and lysed by sonication for 15 cycles (15 s on, 45 s off). Cell debris was removed by centrifugation (18,000 rpm for 20 min at 4°C), and supernatants were filtered through 0.22 μm syringe filters and applied to a His trap™ HP column (GE healthcare). The columns were washed using a modified lysis buffer containing 20 mM imidazole, followed by a 50 mM imidazole wash. Finally, the proteins were eluted with 500 mM imidazole. Colicins isolated by nickel affinity chromatography were concentrated and further purified by size exclusion chromatography, Superdex HiLoad 26/600 Superdex 200 pg. column (GE Healthcare), in 50 mM Tris-HCl 200 mM NaCl pH 7.5 solution. The protein concentrations were determined by ultraviolet absorption at 280 nm, using the extinction coefficient of 0.807 M^{-1} cm^{-1} for E9-Im9 and 0.855 M^{-1} cm^{-1} for colicin Ia.

To determine colicin killing activity and for *in vivo* experiments a spontaneous streptomycin resistant mutant of the AIEC reference strain LF82, an ileal CD mucosa-associated isolate (Darfeuille-Michaud et al., 2004) was selected following treatment with this antibiotic and transformed with the p16S*lux* plasmid which contains the erythromycin resistance cassette (*erm*AM). This strain, *E. coli* LF82StrR, was grown on LB agar plates, or in LB broth with shaking at 37°C with the addition of ampicillin (100 μg ml^{-1}) and erythromycin (500 μg ml^{-1}). Before infection, bacteria from overnight cultures were diluted 1:100 in fresh media and grown to an OD_{600} of 0.65, which is equivalent to approximately 1×10^9 c.f.u/ml. Subsequently, cultures were harvested, washed and resuspended in PBS. For *in vivo*

experiments, counts of challenge dose were plated before and after infection to determine viable bacterial numbers.

Colicin Killing Activity Assay

Colicin killing activity was determined using a spot test. Briefly, aliquots (100 µl) of overnight cultured LF82StrR were transferred into 5 ml of soft agar (0.8% w/v); the mixture was then poured onto an LB agar plate (1.5% w/v) supplemented with 100 mM bipyridine. An aliquot (10 µl) of colicin (1 mg/ml) was spotted onto the soft agar layer seeded with cultured bacteria. After overnight incubation at 37°C, plates were visualized for colicin sensitivity observed as clear zones of lysis of the overlaid strains. To evaluate the hydrogel encapsulated colicins, 10 mg of the colicin E9 or Ia hydrogels were resuspended with 1 ml of PBS (pH 6.8) and incubated for 24 h. An aliquot (10 µl) of hydrogels was spotted onto the soft agar layer seeded with cultured bacteria. After overnight incubation at 37°C, plates were visualized for colicin sensitivity observed as clear zones of lysis of the overlaid strains.

Murine *E. coli* LF82 Colonization Model

All procedures were performed in strict accordance with the Animals (Scientific Procedures) Act 1986 with specific approval granted by the Home Office, United Kingdom (PPL60/8797; P64BCA712). Food and water were provided *ad libitum,* and animals were kept at a constant room temperature of 20–22°C *with a 12 h light/dark cycle*. Eight- to ten-week-old, pathogen-free C57/BL6 female mice (The Jackson Laboratory, Envigo) were pre-treated by a single oral administration of the broad-spectrum antibiotic streptomycin (20 mg, intragastric per mouse) to disrupt normal resident bacterial flora in the gastrointestinal tract (Wadolkowski et al., 1988). Before the administration of the LF82StrpR strain, fecal pellets were collected, plated on LB agar plates with streptomycin (100 µg ml^{-1}) and erythromycin (500 µg ml^{-1}) and incubated at 37°C. No colonies were detected in any of the streptomycin treated mice. Mice were then orally challenged with approx. 1×10^9 cfu of LF82StrpR or 0.1 ml PBS (control group) 24 h post-antibiotic treatment. LF82StrpR colonization was monitored by analysis of bacterial recovery on selective LB plates of fresh fecal material collected from individual animals.

Colonization Evaluation in Stool and Tissues

Fresh stool samples were collected from infected mice 1, 2, 3, and 4 days post-LF82 challenge to determine bacterial fecal shedding. Fecal pellets standardized to a concentration of 100 mg ml^{-1} in PBS were homogenized and serial 10-fold dilutions performed. About 10 µl of diluted samples was plated on Eosin Methylene Blue (EMB) differential medium agar containing ampicillin (100 µg ml^{-1}) and erythromycin (500 µg ml^{-1}) and incubated at 37°C overnight. Ileum, caecum, and colon samples were collected 4 days post-infection in cold PBS at necropsy and homogenized using Tissue Master 125 Homogenizer (OMNI International). Homogenate tissues were serially diluted and plated on EMB agar containing ampicillin (100 µg ml^{-1}) and erythromycin (500 µg ml^{-1}). Colonies were counted after 24–48 h of incubation at 37°C and expressed as c.f.u. per gram of tissue.

Delivery of Colicin by Direct Injection in *E. coli* LF82 Colonized Mice

The above murine colonization model was used to assess the efficacy of a colicin E9/Ia in reducing LF82 levels in the lower GI tract after a single treatment administration of colicin by direct injection in the caecum. Four days after LF82 challenge, mice were treated with 50 µl of a combination of E9 and Ia (0.5 mg ml^{-1}) or 50 µl of PBS (control group), directly injected into the caecum after laparotomy. Animals were maintained under inhalation anesthesia with isoflurane (Abbott Labs, Abbott Park, IL) during surgery and were allowed to fully recover. Three hours post-treatment, mice were killed and LF82StrpR colonization levels of the different regions of the GI tract (ileum, ceacum, and colon) and fecal content were assessed. For bacterial counts, tissue samples were washed thoroughly with PBS prior to homogenization to eliminate fecal content and non-adhered bacteria. For fecal samples, fecal pellets from the colon were homogenized.

Treatment of *E. coli* LF82 Colonized Mice With Encapsulated Colicins

C57/BL6 animals were treated as described above for the murine colonization model, with the addition of dextran sulfate sodium (DSS) which was added to drinking water at a concentration of 2.5% 3 days before the LF82 challenge. This concentration of DSS was maintained for 3 days (renewed daily) and caused mild symptoms of colitis which improved LF82 adherence to the mucosal layer. Three days after LF82StrpR challenge, mice were orally treated with two doses of colicins per day, delivered 7 h apart, with 200 µl of hydrogel particles containing colicins E9 and Ia (0.5 mg each) or control hydrogel particles by gavage in a delivery buffer (sodium acetate buffer, 2% Tween 20, 50% glucose, pH 3.8). Animals were treated for a total of 3 days. On the fourth day, mice were culled by cervical dislocation and LF82StrR colonization levels of the different parts of the GI tract and fecal content were assessed as detailed above.

Measurement of Gastrointestinal Luminal pH

The impact of exposure of gut tissue to the low pH of the delivery buffer was determined *ex vivo* following aseptically extraction of the luminal contents from the small intestine, caecum, and colon. Tissue and luminal contents were then placed in 1 ml of sterile PBS, delivery buffer (200 mM sodium acetate buffer, 2% Tween 20, 50% glucose, pH 3.8), or sterile water. Organs and luminal contents were incubated, and pH measurements were acquired 2 h later. Data represent pH values (mean ± SD) in each buffer.

Chemical Reagents Used to Prepare Hydrogel Microcapsules With Encapsulated Colicins

Water-in-oil emulsion production employed a continuous (oil) phase composed of Miglyol 840 (Safic Alcan, Warrington, United Kingdom), a propylene glycol diester of saturated plant

fatty acids and Polyglycerol polyricinoleate (PGPR, Aston Chemicals Ltd., Aylesbury, United Kingdom), an emulsifier made from glycerol and fatty acids. The aqueous dispersed phase contained a pH responsive polymer, Eudragit L 100-55 (Evonik, Germany), which is an anionic copolymer based on ethyl acrylate and methacrylic acid. Medium viscosity alginate (Sigma-Aldrich, Dorset) was added to the dispersed phase. Sodium chloride, sodium hydroxide, and p-toluenesulfonic acid (pTSA) were all purchased from Fisher Scientific, Loughborough, United Kingdom.

Production of Encapsulated Colicins in Microcapsules Using Membrane Emulsification

The continuous (oil) phase was produced by preparing a solution of miglyol and castor oil (9:1, respectively) with the addition of 5% PGPR to lower the interfacial tension between water and oil. The dispersed phase was composed of 10% (w/v) Eudragit polymer L100-55 dissolved in an alkaline solution, typically produced in 40 ml batches with 4 ml of 4 M NaOH, 36 ml de-ionized water (dH2O), and 4 g L100-55. This solution was mixed with a magnetic stirring bar at room temperature until the solution appeared clear. Subsequently, pre-weighed alginate powder was added at a final concentration of 1% (w/v) and mixed with a magnetic stirring bar overnight or until completely dissolution. Immediately before the membrane emulsification process commenced, colicin was added (typically E9: 100 mg, Ia: 80 mg). The solution was mixed gently using a magnetic stirrer for 5 min to disperse the colicin in the polymer solution. Each colicin was encapsulated separately to allow accurate enumeration of the amount of each colicin administered to the animals.

Aqueous colicin containing droplets were produced as a water-in-oil (W/O) emulsion using a membrane emulsification dispersion cell LDC-1 (Micropore Technologies Ltd., Redcar, United Kingdom). A stainless-steel membrane was utilized with circular, uniformly spaced 40 µm micropore arrays. Initially, the membrane was coated in 1H,1H,2H,2H-Perfluorodecyltriethoxysilane (Sigma-Aldrich, Gilingham, United Kingdom) resulting in a hydrophobic surface to prevent water droplets from spreading on the membrane surface. The dispersed phase was used to fill the cavity below the membrane using a syringe pump (Harvard Apparatus United Kingdom, Kent). About 50 ml of continuous phase was added above the membrane into the cylindrical glass chamber. A paddle blade stirrer was used to create shear on the membrane surface using a controlled rotation rate of 250 revolution per minute (rpm). About 5 ml of the dispersed phase was then pumped upwards through the membrane at a flow rate of 25 ml h^{-1} to produce a W/O emulsion in the glass chamber (**Figure 1**).

After the entire volume of the dispersed phase had passed through the membrane and into the oil phase, protonation of the polymer was carried out to precipitate the polymer resulting in formation of the microcapsules. The water-in-oil emulsion was added to acidified oil (Miglyol with 0.05 M pTSA and 5% PGPR) in an excess volume. The emulsion in acidified oil was placed into a beaker and stirred using axial mixing at 100 rpm for 6 h at a controlled temperature of 25°C using a water bath.

After the TSA step, the W/O emulsion was added to hexane. The amount of hexane to emulsion proportion was 50:50 (v/v) in a beaker. The TSA-treated microcapsules formed a precipitate at the bottom of the beaker. The hexane was then discarded and the microcapsules washed with 2% Tween-20 in deionized water (pH 4). The sample was gently stirrer at 60 rpm using a magnetic stirrer throughout this resuspension step to produce a well-dispersed sample and to avoid formation of aggregates. 1 M $CaCl_2$ was then added to the solution to cross-link the alginate (final working concentration 0.1 M), then mixed using a three-bladed impeller at 100 rpm for 1 h. The microcapsules were then washed three times with 2% Tween solution (pH 4) and stored in 10 ml of this solution in a refrigerator (4°C).

Characterization of the Particle Size Distribution of the W/O Emulsion and the Final Cross-Linked Microcapsules

Throughout the encapsulation process, samples were imaged using a high-speed camera (Micro C100 Phantom Ametek, United Kingdom) which was connected to a microscope (Nikon Eclipse E200). A x 10 magnification lens was used to view each sample, and these images were captured through connection to a laptop and use of the Phantom Camera Control software (PCC 3.1). The size distribution of the droplets and microcapsules were measured using a Coulter LS series 130 instrument (Beckmann Coulter Inc). About 15 ml of miglyol +5% PGPR was placed into the coulter sample chamber. Typically, 100 µl of emulsion was added until the obscuration level measured was between 8 and 12%. For microcapsule particle size characterization, 15 ml of 2% (v/v) tween in deionized water (pH 4) was used as the sample diluent and 100 µl of suspended particles was added until the correct obscuration level was reached. Three repetitions of each measurement were taken and results averaged to produce the final size distribution curves (**Supplementary Figure S1**).

Measuring the Activity of Encapsulated Colicin in Eudragit L100-55 Hydrogel Microcapsules

To test the colicin activity of colicin encapsulated in hydrogel microcapsules and evaluate the release kinetics, 0.1 g of the hydrogels (containing either E9 or Ia) was weighed and exposed to 1 ml of Sorensen's buffer, pH 5.5. Samples were taken over a period of 2 h by removing 10 µl of supernatant and serially diluting with 90 µl of sterile Sorensen's buffer to measure the release kinetics of colicin from the capsules. The absorbance (OD_{280nm}) was measured using a UV spectrophotometer. Using the extinction coefficient and quartz cuvette path length, the colicin concentration was enumerated at each time point. The viability of the colicin after release from the microparticles was confirmed using the double-layer agar method, with *E. coli* LF82 as the indicator strain, and compared to colicin stocks before encapsulation.

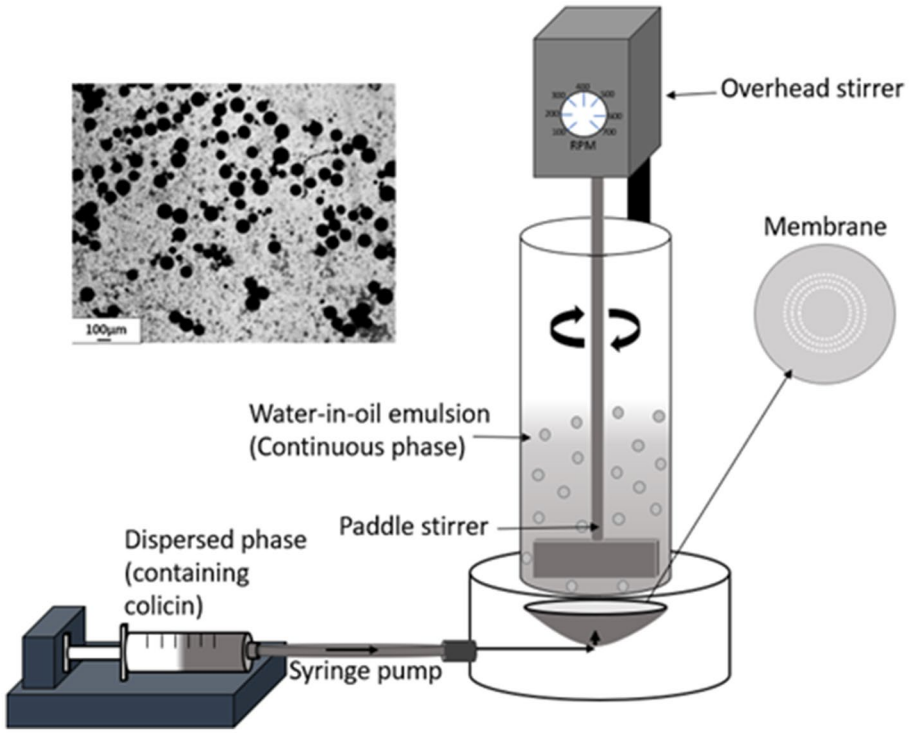

FIGURE 1 | Schematic representation of the membrane emulsification process. The aqueous phase containing the dissolved colicins in the polymer formulation was pumped through a microporous membrane. The stainless-steel membrane had 40 µm uniform circular pores arranged in a ring format located at an optimal radial position where the rotating paddle stirrer provides maximum surface shear for aqueous droplet detachment. At low liquid flow rates, interfacial forces dominate, the drop grows before finally detaching from the membrane surface due to the surface shear caused by the dispersed phase flowing across the membrane surface and the droplets are carried away into the bulk continuous oil phase. The image (top left) shows the prepared microcapsules after exposure to TSA and alginate cross-linking.

This allowed assessment of colicin activity following encapsulation using the microcapsule production process and that the released colicin retained its *E. coli* killing potency. The acid stability of the colicin containing hydrogels was tested using the same method indicated above, with exposure to 0.2 M NaCl (pH 2.5) for 2 h simulating exposure to mouse gastric fluid before colicin release from the capsules in Sorensen's buffer (pH 5.5).

Sample Preparation for the Ion Microscopy

Critical point drying (CPD) and freeze-drying methods were used to prepare the hydrogel samples for ion microscopy. The particles were freeze-dried (VirTis Wizard 2.0, SP Scientific, New York, United States) for 24 h at 50 Pa pressure and −20°C. Dried powder was applied directly on the carbon tape, which was attached to the sample stub. To analyze the morphology of the hydrogel particles, both freeze-dried and critical-point-dried hydrogels were examined with ion microscopy. Zeiss Orion NanoFab (University of Jyväskylä) with He^+ beam and acceleration voltage 35 kV, 0.20 pA current, 32 line averages, and 1 µs dwell time was used for He^+ imaging. For cutting, an about 20-pA Ne^+ beam with 10 kV acceleration voltage was used. Milling was carried out using a 45 degrees tilted angle by setting the reduced raster scan rectangle over the area to be removed and scanning until the material disappeared. After cutting, the sample stage was rotated 180° and the cross section was imaged with a He^+ beam. Flood gun charge compensation was used during both milling and imaging.

Statistics

Data are expressed as means and SD. Due to small sample sizes, nonparametric tests were used for analysis. Two-tailed Mann–Whitney U tests with a significance threshold of $p \leq 0.05$ were used to analyze the specific sample pairs for significant differences. Mice colonization data are represented using Tukey's box-and-whisker plot. All statistical tests were performed with GraphPad Prism software, version 8.0c. All mice, including outliers, were included in the statistical analysis.

RESULTS

In vivo Colicin Activity After Direct Administration to the Lower GI Tract

Colicins have been shown to be highly sensitive to proteolytic cleavage in conditions found in the stomach and small intestine (Schulz et al., 2015). However, little is known about their stability and activity in the lower GI tract. To determine if colicins retain killing activity against *E. coli* in the environment

of the lower GI tract, a combination of colicin IA and E9 were injected directly, during laparotomy, into the caecum of mice pre-colonized with the adherent-invasive *E. coli* strain LF82. This model is widely used in the study of CD and enables relatively stable colonization of the lower GI tract, including the colon and ileum, which are the major sites of AIEC colonization and inflammation in this condition (Darfeuille-Michaud et al., 2004). Colicin E9 and Ia were selected for testing since they show broad activity against a panel of AIEC and commensal strains isolated from CD patients and healthy controls, respectively.

After streptomycin treatment to disrupt the endogenous microbiota, mice were infected with LF82 and 4-days post-infection were treated with a single dose of colicin E9/IA or PBS for the control group (**Figure 2A**). Three hours post-treatment mice were killed, and AIEC colony forming units were determined in tissue of the ileum, caecum, and colon and fecal content of the colon. Colicin E9/IA administered by direct injection resulted in significant reductions in LF82 levels in the ileum (1.9 log units), caecum (1.7 log units), colon (1.5 log units), and in the fecal content (1.5 log units), relative to PBS-treated controls (**Figure 2B**). Thus, a single dose of colicin E9/Ia is able to reduce *E. coli* levels in the lower GI tract. These data indicate that if colicins can be formulated to protect them from the high levels of proteolytic activity associated with the stomach and small intestine, then a highly targeted killing activity of *E. coli* could be achieved through delivery of these protein antibiotics to the lower GI tract.

Colicin Formulation for Lower GI Tract Delivery

To formulate colicins for lower GI tract delivery, we attempted to encapsulate colicin E9 and Ia in pH-responsive hydrogel microcapsules consisting of a commercially available mixture of synthetic polymer containing ethyl acrylate and methacrylic acid monomers combined with seaweed derived alginate biopolymer (**Supplementary Figure S2**). This technique has previously been used to formulate enteric bacteriophages for gastrointestinal applications affording protection from acidic pH and enzymatic stresses. Controlled release relies on dissociation of carboxylic acid groups when the pH rises above 5 (**Supplementary Figure S2**). Based on our own measurements of pH from mouse stomach tissue samples (*in vivo* studies reported below), these range from pH 3.8–5.4 depending on the diluent medium used. In contrast, the pH of the small intestine, caecum, and colon tissue samples was above pH 5.5 when either PBS or water was used as the diluent. Using the mildly acidic delivery buffer (pH 3.8) as the diluent resulted in considerably lower measured pH values. Freeze-dried microparticles appeared as spheres with a smooth and uniform surface (**Supplementary Figure S2C**, left). CPD-dried microparticles displayed a sponge-like surface (**Supplementary Figure S2C**, right). The internal structure was found to be porous with an interconnected network of much smaller pores.

Colicins E9 and Ia were encapsulated by membrane emulsification yielding small microcapsules around 100 μm in diameter, which when suspended in a buffer were suitable for delivery to mice *via* oral gavage using a 20 gauge gavage tube (**Figure 1**). The dispersed phase alginate concentrations were varied to determine the concentration with optimal viscosity levels for controlled production of 100 μm beads (**Supplementary Figure S3**). Initial analysis confirmed 1% (w/v) alginate produced approximately 100 μm microcapsules, whereas 0.5% (w/v) alginate produced mean diameters of ~35 μm with high CV values of ~80%. 2% (w/v) alginate caused membrane fouling and reduced encapsulation efficiency. The size distribution of the emulsion droplets and the resulting cross-linked hydrogel microcapsules were similar although a slight shrinkage in the size of the microparticles was observed upon gelation (**Supplementary Figure S1**). The yield of the encapsulated colicins in the hydrogel microcapsules was high, with no measurable loss in activity due to the encapsulation process as measured following release in simulated intestinal fluid at pH 5.5 (**Figure 3**). The polymer L100-55 was selected due to its pH triggered dissolution at solution pH 5 and above. The amount of encapsulated E9 released at pH 5.5 from the hydrogel capsules was ~80 mg/g, whereas that of Ia was ~70 mg/g which was almost 100% of the colicin added to the polymer solution for fabrication of the microcapsules (**Figure 3**). The release kinetics were similar for the two batches of microcapsules with 50% of the encapsulated colicin released in the first 30 min and over 90% released within 90 min of the hydrogel microcapsules being exposed to the pH 5.5 buffer. Exposure of the hydrogels to acidic buffer (pH 2.5) mimicking harsh simulated gastric fluid (SGF) conditions in the mouse stomach for 2 h resulted in a modest reduction in the activity of the encapsulated colicin in the microcapsules with released amounts falling to ~70 mg/g for E9 and ~60 mg/g for Ia. Over 90% of the encapsulated colicin was still released from the acid exposed microcapsules within 90 min. The *in vitro* data confirm the colicin was encapsulated within the alginate/Eudragit matrix. As the microcapsules were exposed to acidic buffer and the colicin retained lytic activity after capsule dissolution as the pH increased, this verifies the colicin resides inside of the microcapsule. The hydrogel capsules used for the *in vivo* experiments were not pre-exposed to SGF.

Hydrogel microcapsules were shipped in a cool box from Loughborough (United Kingdom) to Glasgow (United Kingdom) for testing in the *in vivo* mouse model and were immediately stored in the fridge upon arrival. Samples were evaluated *in vivo* within a week of manufacture. A significant reduction in the activity of colicin was observed during this transportation and storage period. Measured protein values prior to administration of the capsules to the animals showed around 30 mg/g for both Ia and E9 given that 10 mg of capsules was dissolved in 1 ml of buffer, and this resulted in a measured concentration of 0.3 mg/ml (**Figure 4A**). The killing activity of the released colicins from the hydrogels was similar to that of free colicin and the released colicin showing activity on plates with clear zones indicating cell death (**Figures 4B,C**).

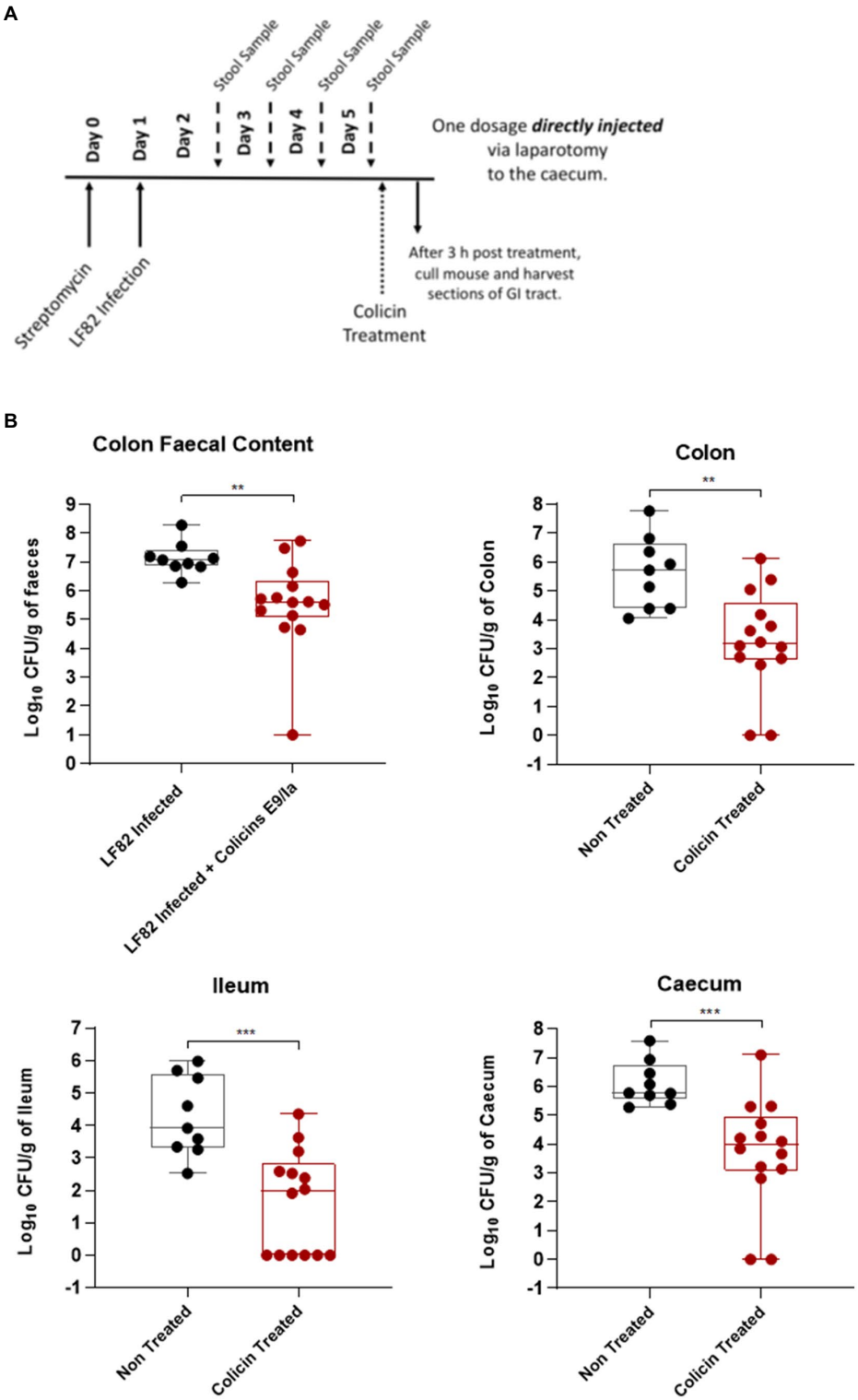

FIGURE 2 | Direct administration of a colicin cocktail reduces levels of LF82 colonization of infected mice. An *Escherichia coli* LF82StrpR murine infection model was used to assess the efficacy of a colicin cocktail treatment directly administered to the caecum *via* laparotomy. Four days after LF82StrpR challenge, mice were treated with the administration *via* laparotomy of 50 µl of a combination of E9 and Ia (0.5 mg ml^{-1} each) or 50 µl of PBS (control group). **(A)** Experimental scheme. **(B)** Levels of LF82StrpR strain in both control (black, $n = 10$) and colicin treated (red, $n = 14$) groups for the different sections of the GI tract. Statistical analysis was carried out for each subset using a Mann–Whitney test between LF82StrpR infected and colicin-treated groups. $^{**}p < 0.002$, $^{***}p < 0.0004$.

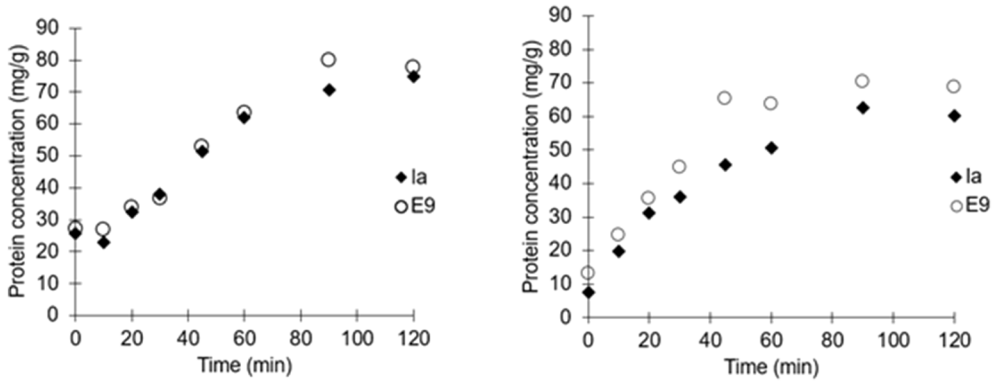

FIGURE 3 | Release kinetics of individually encapsulated colicins Ia and E9. Microcapsules exposed to simulated intestinal fluid buffer (SIF) at pH 5.5 (Left). Release kinetics of individually encapsulated colicins Ia and E9 in microcapsules exposed to simulated gastric fluid (SCF; pH 2.5) for 2 h followed by release in SIF at pH 5.5 (Right).

In vivo Colicin Activity After Repeat Dose Oral Administration of Colicin Containing Hydrogels

To determine the ability of colicin microcapsules to reduce *E. coli* levels in the lower GI tract, hydrogel microcapsules were administered twice daily to LF82 colonized mice beginning 1 day after LF82 administration (**Figure 5A**). Mice treated with colicin containing microcapsules shed significantly lower amounts of *E. coli* (median cfu values) in feces compared with the control group, which were administered empty microcapsules, on all days following treatment: day 2 (0.9 log units lower), day 3 (1.2 log units), and day 4 (0.9 log units; **Figure 5B**). At 4-days post-LF82 administration, mice were killed and LF82 levels in tissue samples from the lower GI tract were determined. Significant decreases in LF82 levels (median cfu values) were found in tissue samples from mice treated with colicin microcapsules in the ileum (2.5 log units), caecum (1.5 log units), and colon (1.7 log units) relative to control mice (**Figure 5C**). Interestingly, no colonies were isolated in a number of tissue samples and in fecal samples from day 4, indicating that eradication of *E. coli* may be feasible on prolonged colicin treatment.

DISCUSSION

In this work, we have demonstrated that colicins can be successfully formulated in hydrogel microcapsules in an active form and that formulated colicin is able to reduce *E. coli* levels in a murine colonization model. The membrane emulsification process resulted in controlled fabrication of hydrogel capsules, which were relatively uniform in size and were small enough to be administered *via* oral gavage to mice (**Figure 1**). The encapsulation process resulted in a high yield of encapsulated colicin and the process of manufacturing the hydrogel capsules did not affect colicin activity upon release. The capsules displayed pH responsive characteristics suitable for targeted delivery of the therapeutic cargo in response to changes in pH (**Figure 3**). The design of the particles to deliver a slow rate of release allowed delivery of the encapsulated colicin to different parts of the GI tract given the relatively small differences in pH values observed in the mouse lower GI tract (McConnell et al., 2008). For human therapeutic applications, other methacrylate polymers, e.g., L100 (pH 6) or S100 (pH 7) could be used to target delivery in response to more significant differences in pH (Vinner et al., 2019). Polymers which may release encapsulated cargo based on the presence of virulence factors in the environment could potentially be a more sophisticated targeted approach (Bean et al., 2014).

Previous published colicin encapsulation research is limited to encapsulation in pectin hydrogel beads with low reported encapsulation efficiency of ~1%. The encapsulated beads were administered orally to mice, and after 6 days of treatment, no significant differences reported in CFU/g fecal matter between treated and non-treated mice (Brown, 2015). This may be attributed to the lack of targeted delivery and limited stability of colicins exposed to the gastric environmental conditions. Membrane emulsification process used in the present study has previously been used for encapsulation of phage biotherapeutics. Encapsulated phages were shown to be released at defined pH values dependent on the type of pH-responsive polymer used in the formulation and phages shown to withstand gastric acid exposure at pH 1.5 for up to 2 h (Richards and Malik, 2021).

The polymers used for the microcapsule fabrication are routinely used in food formulations and for enteric delivery applications (Evonik healthcare). The polymers utilized for colicin encapsulation have regulatory approval for healthcare applications and are generally regarded as safe (GRAS) for human consumption by the US FDA. The safety of alginic acid has extensively been researched and recognized as posing no toxicity risks in mammals. JECFA (1993) reviewed alginate toxicology literature and summarized there were no toxic effects when tested in rats at levels up to 13,500 mg sodium alginate/kg body weight (bw) per day (JECFA, 1993). No carcinogenic effects were reported at 37,500 mg sodium alginate/kg bodyweight per day in mice (Rychen et al., 2017). Furthermore, Eudragit polymers were tested for effects on the nervous system through

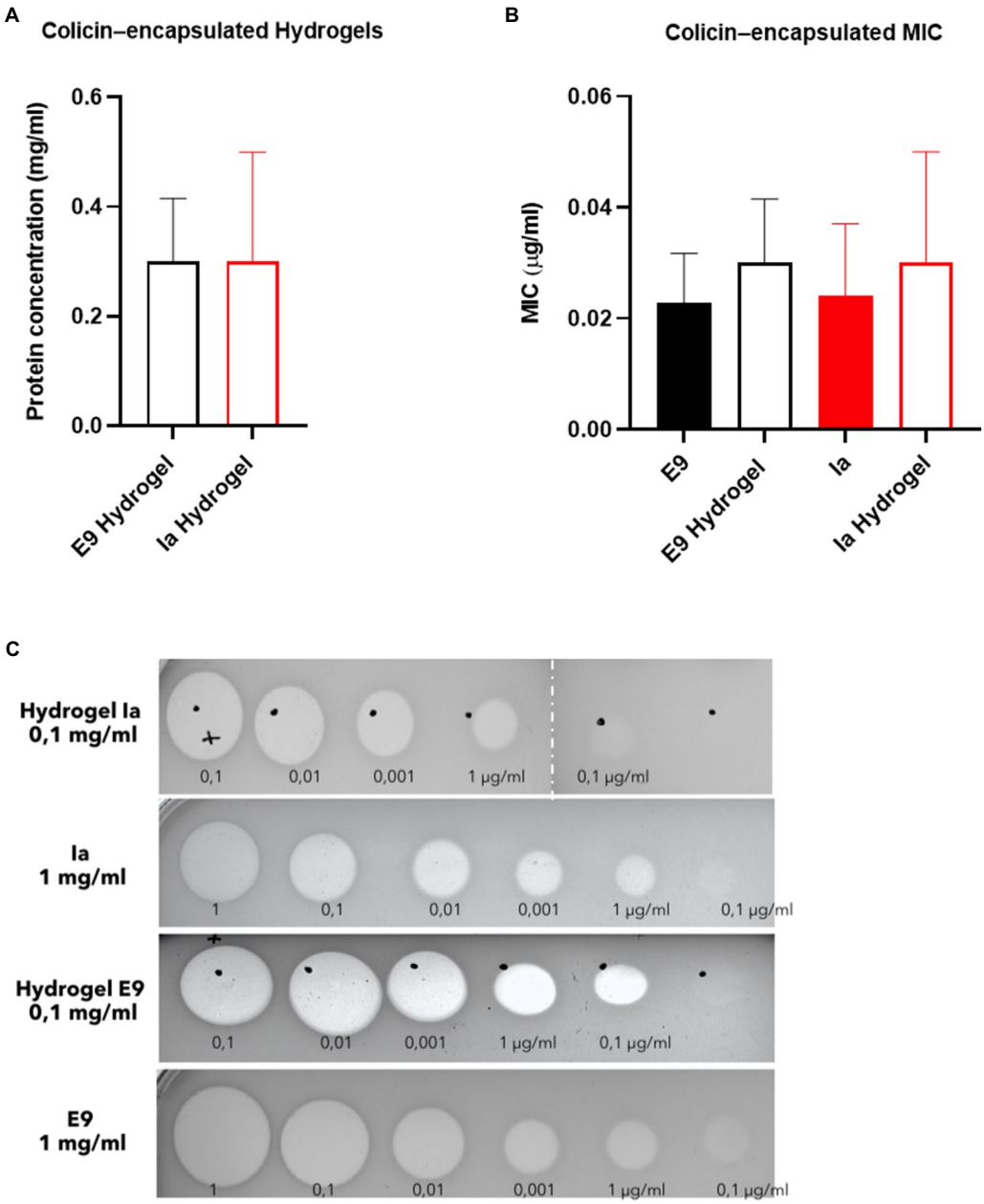

FIGURE 4 | Killing activity of hydrogel-encapsulated colicins. **(A)** Levels of encapsulated protein (mg/ml) after suspension. **(B)** Minimum inhibitory concentration (MIC) and **(C)** inhibition of growth of *E. coli* LF82StrpR by colicins E9 and Ia and hydrogel-encapsulated colicin E9 and Ia. Clear zones indicate cell death. Data represent four different experiments (mean ± SD). Statistical analysis was carried out for each subset using a Mann–Whitney test between the control protein and the hydrogel particles and no significant differences were found. Hydrogel microcapsules that did not contain encapsulated colicins showed no bactericidal activity.

nanoparticle administration to rats either orally or intraperitoneally. Animals were killed at timepoints up to 3 weeks. Histological examination determined a normal histological picture and insignificant changes, thus concluding diminutive toxic effects on the brain (Abdel-Wahhab et al., 2017).

Small rodent animal models are routinely used in preclinical testing of drugs and vaccines due to their size and low cost. pH responsive drug delivery platforms rely on defined changes in physiological pH along the GI tract to trigger release of therapeutic cargo. Encapsulation of therapeutic agents may overcome delivery issues such as degradation of the therapeutic upon exposure to stomach acidity or due to enzymatic activity, and colicins are particularly susceptible to proteolysis-related degradation (Schulz et al., 2015). Polymethacrylate and cellulose-based enteric capsules are routinely used for delivery of drugs or vaccines to the GI tract by dissolving only when the pH of the environment exceeds a threshold level. Knowledge of the gut pH of the mouse is critical in selecting the appropriate

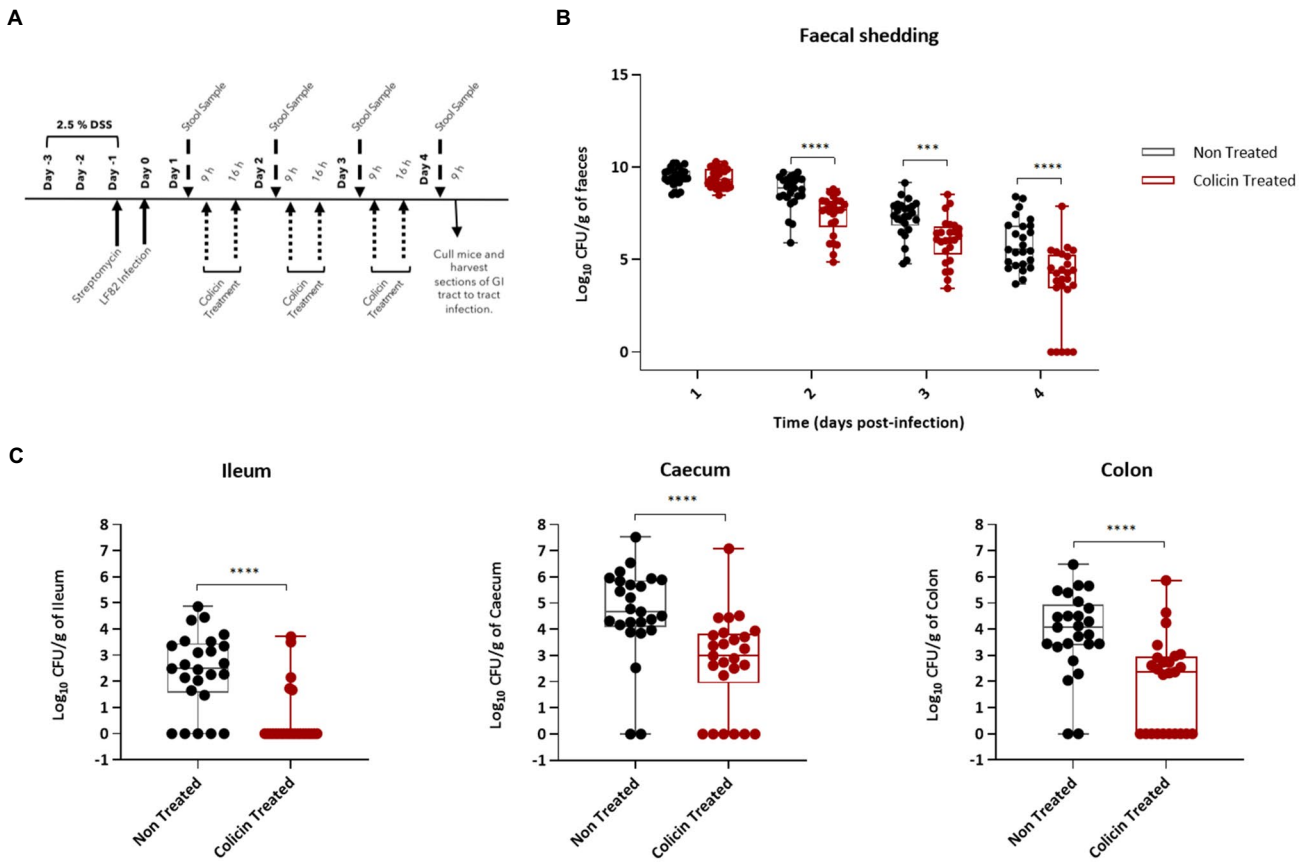

FIGURE 5 | Reduction in LF82 colonization of the lower gastrointestinal (GI) tract in infected mice treated with hydrogel-encapsulated colicins. An *E. coli* LF82 murine infection model was used to assess the efficacy of the hydrogel encapsulated treatment using a combination of E9 and Ia. Day one post-bacterial challenge, mice were treated by oral administration of 200 µl of colicin E9 and Ia (dose of 0.5 mg each of E9 and Ia) containing hydrogel in a slurry with PBS or 200 µl of colicin free hydrogel slurry (control group). **(A)** Experimental scheme. **(B)** Tukey boxplot of fecal shedding of *E. coli* LF82StrpR. **(C)** Levels of LF82StrpR strain in both control (black, $n = 25$) and colicin treated (red, $n = 25$) groups for the different sections of the GI tract. Statistical analysis was carried out for each subset using a Mann–Whitney test between LF82StrpR infected and colicin-treated groups. $^{***}p < 0.0004$, $^{****}p < 0.0001$.

polymer for formulation of microcapsules for targeted delivery and controlled release. The residence time of the capsules and the fluid content of the GI tract are other critical factors in targeted delivery of the therapeutic agent at the site of infection. The moderately acidic pH values of the stomach tissue samples measured in the present study were low enough to prevent colicin release from the microcapsules in the stomach. The pH of the small intestine, caecum, and colon tissue samples was found to be higher than pH 5.5 albeit when the diluent used may have influenced the measured pH values. A pH above pH 5 is suitably high for dissolution of the fabricated L100-55/alginate hydrogel microcapsules, resulting in the successful release of the encapsulated colicin cargo in the lower GI tract in the mice. Previous studies in which measurement of mouse GI tract pH was performed indicated variability in measured pH between individual animals with mean values of stomach pH around pH 4, and pH 5 for intestinal tract tissue samples, using undiluted tissue contents (McConnell et al., 2008). Drug formulations are often given to animals by oral gavage with the dose volume determined by the stomach volume of the animal and typically, doses not exceeding 0.4 ml are recommended for studies in mice (Wolfensohn and Lloyd, 1994). We used 0.2 ml of buffer with suspended hydrogels in this study. Previous studies have reported that very low levels of fluid, less that 1 ml, are present within the mouse gastrointestinal tract (McConnell et al., 2008). Noninvasive studies of GI transit times in mice suggest oral administered microcapsules may pass through into the small intestine within 1 h of ingestion, with a total transit time of 6 h to the colon (Padmanabhan et al., 2013). The *in vitro* data reported here (**Figure 3**) showed the release kinetics of colicin over a 2 h period from the hydrogel microcapsules would be sufficient to allow encapsulated colicin to be released in the lower GI tract. The low water content of the mouse GI tract and the relatively low intestinal pH may further slow the rate of release *in vivo* which may result in a significant dose of the encapsulated colicin cargo being released much lower in the GI tract.

Significant *in vivo* reduction in bacterial counts (cfu/ml) in all GI tract tissue samples suggests that encapsulation of

the colicins in the microcapsules could serve as a useful strategy for evaluating the therapeutic potential of protein antibiotics, which may otherwise degrade due to exposure to the harsh environmental conditions in the stomach and along the GI tract. The capacity to administer protein antibiotics to the lower GI tract offers opportunities for the deployment of these narrow-spectrum antibiotics for re-engineering of the gut microbiota through selective targeting of specific bacterial species. This may be particularly useful in decolonization of the gut microbiota of potential pathogens such as drug-resistant resistant Enterobacteriaceae that may be dominant and cause disease.

DATA AVAILABILITY STATEMENT

The raw data supporting the conclusions of this article will be made available by the authors, without undue reservation.

ETHICS STATEMENT

The animal study was reviewed and approved by University of Glasgow Ethics Committee, License number: Home Office, United Kingdom (PPL60/8797 and P64BCA712).

AUTHOR CONTRIBUTIONS

NC, KR, DM, and DW contributed to conception and design of the study and wrote the first draft of the manuscript. NC performed the statistical analysis. All authors contributed to manuscript revision, read, and approved the submitted version.

FUNDING

DM acknowledges funding from the UK Engineering and Physical Sciences Research Council (Grant No. EP/M027341/1), "Tackling Antimicrobial Resistance: An Interdisciplinary Approach." KR acknowledges a Loughborough University PhD studentship. DW acknowledges funding from Scottish Enterprise (Grant No. PS7305CA55), the MRC (Grant No. MC_PC_15039), and the Wellcome Trust (Grant No. 201505/Z/16/Z).

ACKNOWLEDGMENTS

We thank Colin Kleanthous for the gift of the colicin Ia expression plasmid used in this work. We also thank Miika Leppanen (Department of Physics, University of Jyväskylä, Jyväskylä, Finland) for carrying out the Helium Ion Microscopy.

SUPPLEMENTARY MATERIAL

The Supplementary Material for this article can be found online at: https://www.frontiersin.org/articles/10.3389/fmicb.2021.670535/full#supplementary-material

Supplementary Figure S1 | Particle size distributions of the water-in-oil (W/O) emulsion droplets and the final cross-linked hydrogel microcapsules. The differential volume distributions **(A)** and cumulative volume distributions **(B)** are shown, respectively. Droplets refer to the initial (W/O) emulsion prior to cross-linking (gelation), whereas the particles refer to the final hydrogel microcapsules produced after L100 precipitation due to protonation in TSA and the alginate cross-linking in calcium chloride.

Supplementary Figure S2 | Mechanism of encapsulation and pH-triggered release action. The capsules were initially fabricated using membrane emulsification **(A)** the alginate and L100-55 polymer chains form the internal capsule structure. The L100-55 was protonated through incubation in 0.05 M TSA + Miglyol +5% (w/v) PGPR. The capsules were then cross-linked using 0.1 M $CaCl_2$ as the calcium ions cross-link the alginate chains forming an eggbox-like structure. The polymer chains dissociate upon exposure to pH 5.5 and above and the colicin subsequently released. **(B)** L100-55 chemical structure. **(C)** SEM imaging showing Freeze-dried L100-55 microcapsules (left) and Helium Ion Microscopy image (right) of the internal Eudragit-Alginate matrix. A microcapsule having particle size about 10 μm was cut in half using a Ne^+ beam and after 180° rotation imaged with He^+. A CPD-dried microparticle was milled with the Ne^+ beam. After 180° rotation, the cut surface was imaged with He^+. Higher magnification image of the cross section showing internal porous matrix of the polymer. Schematic **(A,B)** created with BioRender.com.

Supplementary Figure S3 | Effect of alginate concentration on W/O emulsion droplet characteristics. Emulsions were produced using a membrane with 40 μm pores arranged as a ringed array. The dispersed phase was composed of either 0.5, 1, or 2% (w/v) medium viscosity alginate with 10% (w/v) L100-D55 polymer dissolved in dH_2O. The continuous phase was composed of miglyol +5% (v/v) PGPR. A flow rate of 25 ml/h was used along with a stirrer speed of 300 RPM. Emulsions were produced in 55 ml batches, 50 ml continuous phase +5 ml dispersed phase. **(A)** Mean particle diameters are displayed as columns; coefficient of variation values is presented as data points corresponding to the secondary axis. Emulsions were tested on the LS coulter immediately after production. **(B)** Optical images taken immediately after emulsion production using the Nikon Phantom camera and the 10x magnification lens. (i) displays the emulsion produced using 0.5% (w/v) alginate, (ii) 1% (w/v) alginate.

REFERENCES

Abdel-Wahhab, M. A., Joubert, O., Khadrawy, Y. A., Safar, R., El-Nekeety, A. A., Ronzani, C., et al. (2017). Preliminary safety assessment of Eudragit® polymers nanoparticles administration in the rat brain. *J. Appl. Pharm. Sci.* 7, 176–185. doi: 10.7324/JAPS.2017.70726

Bean, J. E., Alves, D. R., Laabei, M., Esteban, P. P., Thet, N. T., Enright, M. C., et al. (2014). Triggered release of bacteriophage K from agarose/hyaluronan hydrogel matrixes by staphylococcus aureus virulence factors. *Chem. Mater.* 26, 7201–7208. doi: 10.1021/cm503974g

Behrens, H. M., Lowe, E. D., Gault, J., Housden, N. G., Kaminska, R., Moritz Weber, T., et al. (2019). Pyocin S5 import into *Pseudomonas aeruginosa* reveals a generic mode of bacteriocin transport. bioRxiv [Preprint]. doi: 10.1101/856047

Brown, C. L. (2015). The development of colicins as novel antimicrobials against crohn's disease associated adherent-invasive *Escherichia coli*. PhD thesis. University of Glasgow. Available at: https://eleanor.lib.gla.ac.uk/record=b3153152

Brown, C. L., Smith, K., Wall, D. M., and Walker, D. (2015). Activity of species-specific antibiotics against crohn's disease-associated adherent-invasive *Escherichia coli*. *Inflamm. Bowel Dis.* 21, 2372–2382. doi: 10.1097/MIB.0000000000000488

Cascales, E., Buchanan, S. K., Duche, D., Kleanthous, C., Lloubes, R., Postle, K., et al. (2007). Colicin biology. *Microbiol. Mol. Biol. Rev.* 71, 158–229. doi: 10.1128/MMBR.00036-06

Darfeuille-Michaud, A., Boudeau, J., Bulois, P., Neut, C., Glasser, A. L., Barnich, N., et al. (2004). High prevalence of adherent-invasive *Escherichia coli* associated

with ileal mucosa in crohn's disease. *Gastroenterology* 127, 412–421. doi: 10.1053/j.gastro.2004.04.061

Holt, K. E., Thieu Nga, T. V., Thanh, D. P., Vinh, H., Kim, D. W., Vu Tra, M. P., et al. (2013). Tracking the establishment of local endemic populations of an emergent enteric pathogen. *Proc. Natl. Acad. Sci. U. S. A.* 110, 17522–17527. doi: 10.1073/pnas.1308632110

Jakes, K. S., and Finkelstein, A. (2010). The colicin Ia receptor, Cir, is also the translocator for colicin Ia. *Mol. Microbiol.* 75, 567–578. doi: 10.1111/j.1365-2958.2009.06966.x

JECFA (1993). Alginic acid and its ammonium; calcium; potassium and sodium salts. (Join FAO/WHO Expert Committee on Food Additives). 755.

Kleanthous, C. (2010). Swimming against the tide: progress and challenges in our understanding of colicin translocation. *Nat. Rev. Microbiol.* 8, 843–848. doi: 10.1038/nrmicro2454

Lloyd-Price, J., Arze, C., Ananthakrishnan, A. N., Schirmer, M., Avila-Pacheco, J., Poon, T. W., et al. (2019). Multi-omics of the gut microbial ecosystem in inflammatory bowel diseases. *Nature* 569, 655–662. doi: 10.1038/s41586-019-1237-9

Logan, L. K., and Weinstein, R. A. (2017). The epidemiology of carbapenem-resistant enterobacteriaceae: the impact and evolution of a global menace. *J. Infect. Dis.* 215, S28–S36. doi: 10.1093/infdis/jiw282

McCaughey, L. C., Ritchie, N. D., Douce, G. R., Evans, T. J., and Walker, D. (2016). Efficacy of species-specific protein antibiotics in a murine model of acute *Pseudomonas aeruginosa* lung infection. *Sci. Rep.* 6:30201. doi: 10.1038/srep30201

McConnell, E. L., Basit, A. W., and Murdan, S. (2008). Measurements of rat and mouse gastrointestinal pH, fluid and lymphoid tissue, and implications for in-vivo experiments. *J. Pharm. Pharmacol.* 60, 63–70. doi: 10.1211/jpp.60.1.0008

Nedialkova, L. P., Denzler, R., Koeppel, M. B., Diehl, M., Ring, D., Wille, T., et al. (2014). Inflammation fuels colicin Ib-dependent competition of Salmonella serovar Typhimurium and *E. coli* in enterobacterial blooms. *PLoS Pathog.* 10:e1003844. doi:10.1371/journal.ppat.1003844

Padmanabhan, P., Grosse, J., Asad, A. B. M. A., Radda, G. K., and Golay, X. (2013). Gastrointestinal transit measurements in mice with 99mTc-DTPA-labeled activated charcoal using NanoSPECT-CT. *EJNMMI Res.* 3:60. doi: 10.1186/2191-219X-3-60

Pommer, A. J., Cal, S., Keeble, A. H., Walker, D., Evans, S. J., Kühlmann, U. C., et al. (2001). Mechanism and cleavage specificity of the H-N-H endonuclease colicin E9. *J. Mol. Biol.* 314, 735–749. doi: 10.1006/jmbi.2001.5189

Ravi, A., Halstead, F. D., Bamford, A., Casey, A., Thomson, N. M., Van Schaik, W., et al. (2019). Loss of microbial diversity and pathogen domination of the gut microbiota in critically ill patients. *Microb. Genomics* 5:e000293. doi: 10.1099/mgen.0.000293

Richards, K., and Malik, D. J. (2021). Microencapsulation of bacteriophages using membrane emulsification in different pH-triggered controlled release formulations for oral administration. *Pharmaceuticals* 14:424. doi: 10.3390/ph14050424

Rychen, G., Aquilina, G., Azimonti, G., Bampidis, V., Bastos, M. L., Bories, G., et al. (2017). Safety and efficacy of sodium and potassium alginate for pets, other non food-producing animals and fish. *EFSA J.* 15:e04945. doi: 10.2903/j.efsa.2017.4945

Schulz, S., Stephan, A., Hahn, S., Bortesi, L., Jarczowski, F., Bettmann, U., et al. (2015). Broad and efficient control of major foodborne pathogenic strains of *Escherichia coli* by mixtures of plant-produced colicins. *Proc. Natl. Acad. Sci. U. S. A.* 112, E5454–E5460. doi: 10.1073/pnas.1513311112

Six, A., Mosbahi, K., Barge, M., Kleanthous, C., Evans, T., and Walker, D. (2020). Pyocin efficacy in a murine model of *Pseudomonas aeruginosa* sepsis. bioRxiv [Preprint]. doi: 10.1101/2020.03.27.011908

Vinner, G. K., Richards, K., Leppanen, M., Sagona, A. P., and Malik, D. J. (2019). Microencapsulation of enteric bacteriophages in a pH-responsive solid oral dosage formulation using a scalable membrane emulsification process. *Pharmaceutics* 11:475. doi: 10.3390/pharmaceutics11090475

Wadolkowski, E. A., Laux, D. C., and Cohen, P. S. (1988). Colonization of the streptomycin-treated mouse large intestine by a human fecal *Escherichia coli* strain: role of adhesion to mucosal receptors. *Infect. Immun.* 56, 1036–1043. doi: 10.1128/iai.56.5.1036-1043.1988

Wolfensohn, S., and Lloyd, M. (1994). *Handbook of Laboratory Animal Management*. Oxford: Oxford University Press.

Conflict of Interest: The authors declare that the research was conducted in the absence of any commercial or financial relationships that could be construed as a potential conflict of interest.

Publisher's Note: All claims expressed in this article are solely those of the authors and do not necessarily represent those of their affiliated organizations, or those of the publisher, the editors and the reviewers. Any product that may be evaluated in this article, or claim that may be made by its manufacturer, is not guaranteed or endorsed by the publisher.

frontiers in Microbiology

ORIGINAL RESEARCH
published: 14 October 2021
doi: 10.3389/fmicb.2021.737828

Preponderance of *bla*$_{KPC}$-Carrying Carbapenem-Resistant Enterobacterales Among Fecal Isolates From Community Food Handlers in Kuwait

*Ola H. Moghnia, Vincent O. Rotimi and Noura A. Al-Sweih**

Department of Microbiology, Faculty of Medicine, Kuwait University, Kuwait City, Kuwait

OPEN ACCESS

Edited by:
Che-Hsin Lee,
National Sun Yat-sen University,
Taiwan

Reviewed by:
Xiaogang Xu,
Fudan University, China
Michael P. Ryan,
University of Limerick, Ireland

***Correspondence:**
Noura A. Al-Sweih
nourah.alsuwaih@ku.edu.kw

Specialty section:
This article was submitted to Antimicrobials, Resistance and Chemotherapy, a section of the journal Frontiers in Microbiology

Received: *07 July 2021*
Accepted: *14 September 2021*
Published: *14 October 2021*

Citation:
Moghnia OH, Rotimi VO and Al-Sweih NA (2021) Preponderance of bla$_{KPC}$-Carrying Carbapenem-Resistant Enterobacterales Among Fecal Isolates From Community Food Handlers in Kuwait. Front. Microbiol. 12:737828. doi: 10.3389/fmicb.2021.737828

Carbapenem-resistant Enterobacterales (CRE) are pathogens that have been found in several countries, with a significant public health concern. Characterizing the mode of resistance and determining the prevailing clones are vital to the epidemiology of CRE in our community. This study was conducted to characterize the molecular mode of resistance and to determine the clonality of the CRE fecal isolates among community food handlers (FHs) vs. infected control patients (ICPs) in Kuwait. Fecal CRE isolates obtained from FHs and ICPs from September 2016 to September 2018 were analyzed for their resistance genes. Gene characterization was carried out by polymerase chain reaction (PCR) assays and sequencing. Clonality of isolates was established by multilocus sequence typing (MLST). Of the 681 and 95 isolates of the family Enterobacterales isolated from FHs and ICPs, 425 (62.4%) and 16 (16.8%) were *Escherichia coli*, and 18 (2.6%) and 69 (72.6%) were *Klebsiella pneumoniae*, respectively. A total of 36 isolates were CRE with a prevalence of 5.3% among FH isolates and 87 (91.6%) among the ICPs. Of these, carbapenemase genes were detected in 22 (61.1%) and 65 (74.7%) isolates, respectively ($p < 0.05$). The detected specific genes among FHs and ICPs were positive for *bla*$_{KPC}$ 19 (86.4%) and 35 (40.2%), and *bla*$_{OXA}$ 10 (45.5%) and 59 (67.8%), in addition to *bla*$_{NDM}$ 2 (9.1%) and 32 (36.8%), respectively. MLST assays of the *E. coli* and *K. pneumoniae* isolates revealed considerable genetic diversity and polyclonality as well as demonstrated multiple known ST types and eight novel sequence types. The study revealed a relatively high number of CRE harboring predominantly *bla*$_{KPC}$-mediated CRE among the community FH isolates vs. predominant *bla*$_{OXA}$ genes among the ICPs. Those heterogeneous CRE isolates raise concerns and mandate more efforts toward molecular surveillance. A multinational study is recommended to monitor the spread of genes mediating CRE in the community of Arabian Peninsula countries.

Keywords: *bla*$_{KPC}$, carbapenem-resistant Enterobacterales, food handlers, rectal colonization, molecular characterization

INTRODUCTION

Carbapenems have been used as effective and drugs of choice over the years to treat life-threatening nosocomial infections, particularly bloodstream infections, transplant-related infections, ventilator-associated infections, and infections in hospitalized patients in intensive care units, in addition to infections caused by extended-spectrum β-lactamases and AmpC-producing species of the family Enterobacterales. With an increase in the number of people exposed to antibiotics, the intestinal microflora remains a selective pressure for multidrug-resistant (MDR) bacteria due to the milieu of antibiotics consumed by patients. Enterobacterales are inhabitants of the intestinal flora and are among the most common human pathogens causing community and healthcare-associated infections. They have the propensity to acquire genetic material through horizontal gene transfer. The emergence of carbapenem-resistant Enterobacterales (CRE) is an increasing threat to global health. The primary mechanism of resistance is the production of carbapenemases. In the past years, the worldwide spread of CRE and the mechanism of resistance in these isolates attracted much attention because of their rapid global transmission and limited therapeutic options for the infections caused, posing an urgent threat to the efficacy of carbapenem antibiotics. KPC genes have spread internationally among Gram-negative bacteria in China, Greece, Italy, Poland, Colombia, Argentina, Brazil, and some states in the United States but not in Kuwait (Munoz-Price et al., 2013; Stoesser et al., 2017; Cienfuegos-Gallet et al., 2019). Other carbapenemases, such as OXA-48, are present in Turkey and North Africa (Temkin et al., 2014). The Indian subcontinent is endemic for NDM variants and acts as a reservoir of these carbapenemases and other inactivating enzymes such as KPC and OXA-181 (Nordmann and Poirel, 2014). A few studies have been conducted in our hospitals to determine the prevalence and burden of CRE in the country. A report documenting cases of nosocomial acquisition of two NDM-1 producing *Klebsiella pneumoniae* isolates in Indian and indigenous Kuwaiti patients, who had no history of travel, was published in 2012 by Jamal et al. (2012). Other reports have highlighted the emergence of VIM-4 and NDM-1-producing Enterobacterales in Kuwait (Jamal et al., 2013, 2015). Food handlers (FHs) who are considered an important link in the chain from farm to fork are at high risk of being CRE colonized or infected. Those unrecognized workers may serve as a reservoir for CRE transmission and play an essential role in spreading these organisms in community as well as healthcare settings. At the same time, FHs have an important integral part in the community in preventing food contamination. This largely depends on their health status and hygiene practices, which may occur at any point in the journey from the producer to the consumer. Studies have found that poor personal hygiene could be a potential source of infections and may serve as a reservoir of genes for antimicrobial resistance in organisms (Luo et al., 2011). Early detection of carriers or colonizers facilitates the rapid establishment of contact precautions to prevent acquiring CRE. The emergence of CRE as a global problem was extensively studied in healthcare settings. Delineation of genes encoding carbapenemase production in CRE colonizing the rectum of FHs has never been explored in community settings. Therefore, the present study aimed to evaluate the prevalence of genes mediating carbapenemase production in CRE isolates circulating among FH population in the community of Kuwait.

MATERIALS AND METHODS

Study Design

This study was conducted between September 2016 and September 2018 among FHs working catering establishments in the community. In addition, clinically proven infected control patients (ICPs) were admitted to four teaching hospitals, including Mubarak Al-Kabeer (MAK), Farwaniya (FAH), Ibn-Sina (ISH), and Al Babtain (BabH) Hospitals, and were investigated as the control group. A descriptive analysis of demographic characteristics and predisposing factors of a healthy population of volunteer FHs was performed previously (Moghnia et al., 2021a).

Bacterial Isolates

Non-duplicate 405 fecal samples and 92 rectal swabs were collected from FHs and ICPs, respectively. Fecal samples were prospectively self-collected by FHs in privacy, following instructions, in a clean, dry screw-top container. Then, a sterile cotton-wool swab with 5 ml of Amies gel transport medium (Copan, Brescia, Italy) was dipped into the stool specimen collected from each of the FHs. In addition, rectal swabs were collected from ICPs. Then, swabs were immediately inoculated on freshly prepared MacConkey agar and blood agar plates (Oxoid, Basingstoke, Hants, United Kingdom). The plates were incubated in an aerobic incubator (Gallenkamp, Widnes, England) at 37°C for 18–24 h. A pure colony of CRE isolate was selected from each sample and cultured into a new MacConkey agar plate to obtain pure growth, and then the plate was incubated at 37°C for 18–24 h.

CRE isolates were identified to the species level by the Gram-negative identification card on VITEK 2 ID automated System (bioMérieux, Marcy l'Etoile, France). The minimum inhibitory concentrations (MICs) of the antibiotics tested that inhibited 90% (MIC90) and 50% (MIC50) of the isolates were determined using both E-test (bioMérieux, Marcy l'Etoile, France) and agar dilution methods according to the manufacturer's instruction as previously described (Moghnia et al., 2021b) according to the Clinical Laboratory Standards Institute interpretative criteria. Carbapenem resistance isolate was defined as an Enterobacterales isolate that was non-susceptible to at least one of the carbapenems with MIC of > 0.5 μg/ml for ertapenem, or > 1 μg/ml for imipenem and meropenem (CLSI [Clinical and Laboratory Standard Institute], 2018).

Indirect Carbapenemase Test

The carbapenemase production (OXA, KPC, NDM, IMP, and VIM) of CRE isolates from FHs and infected control group was investigated with indirect carbapenemase test MAST®ICT (Mast Diagnostic, France) according to the manufacturer's instruction.

Polymerase Chain Reaction Analysis of Carbapenemase and Sequencing

The presence of genes encoding the carbapenemases was detected by PCR amplification assays using previously published primers (Sigma-Aldrich, Darmstadt, Germany) designed to detect bla_{KPC}, bla_{OXA} (Poirel et al., 2011), bla_{NDM} (Ellem et al., 2011), bla_{VIM}, bla_{IMP} (Toleman et al., 2003), and bla_{SIM} (Lee et al., 2003). These primers as well as the PCR cycling conditions are reported in **Table 1**. Sequencing of the amplicons was performed to identify *bla* variants using the GeneAmp PCR system 9700 by cycle sequencing with ABI Prism BigDye terminator V3.1 Ready Reaction Cycle Sequencing Kit (Applied Biosystems, Foster City, CA, United States). The sequencing results were determined using software from the National Center for Biotechnology Information.[1]

Multilocus Sequence Typing

Random selection of carbapenem-resistant *Escherichia coli* and *K. pneumoniae* isolates harboring carbapenemases encoding genes from FHs and ICPs were performed to understand the clonal relatedness of these isolates. Carbapenem-resistant *E. coli* ($n = 13$) isolates including FHs ($n = 7$) and ICPs ($n = 6$) isolates as well as *K. pneumoniae* isolates ($n = 14$) including FHs ($n = 7$) and ICPs ($n = 7$) isolates were assigned to multilocus sequence typing (MLST) method as described previously (Diancourt et al., 2005; Wirth et al., 2006). Allelic profiles (obtained from the pattern of allele numbers) for seven gene fragments of each isolate were obtained by comparing with corresponding allele available in MLST *E. coli* database,[2] as well as in MLST *K. pneumoniae* database[3] following website instruction. The sequence type (ST) of each isolate was determined by combining seven allelic profiles. The MLST data, based on the allele number for the seven gene fragments for each isolate, were used for constructing strain relatedness dendrogram by minimum spanning trees using BioNumerics software (version 6.1; Applied Maths, Kortrijk, Belgium).

Comparative goeBURST analysis was performed to determine the diversity of the *E. coli* and *K. pneumoniae* isolates against the entire *E. coli* and *K. pneumoniae* database and to reveal their relationships with all publicly available STs. STs were clustered into clonal complexes (CCs) using the goeBURST algorithm of the Phyloviz software.[4] The goeBURST assigned each ST that shared at least five of seven identical alleles into a single CC.

Statistical Criteria

Data were tabulated and analyzed using IBM SPSS Statistics v.25.0 (IBM Corp., Armonk, NY, United States). Significance was determined by Pearson's chi-squared test (χ^2) to test associations between two categorical variable CRE isolates expressing carbapenemase genes from FHs and ICPs and evaluate how likely it is that there is any observed genetic difference in

[1] www.ncbi.nlm.nih.gov

[2] https://pubmlst.org/mlst/

[3] https://bigsdb.pasteur.fr/klebsiella/

[4] http://www.phyloviz.net/goeburst/

TABLE 1 | Primer sets used for PCR amplification of carbapenem-resistance genes and their expected amplicon size.

Gene	Primer sequences	Amplicon size (bp)	PCR cycling conditions (reference)
bla_{KPC}	F: CGTCTAGTTCTGCTGTCTTG R:CTTGTCATCCTTGTTAGGCG	798	Heat activation of polymerase at 95°C for 15 min, then initial denaturation at 94°C for 10 min, followed by 35 cycles of denaturation at 94°C for 30 s, annealing at 52°C for 40 s, and elongation at 72°C for 50 s, followed by a final elongation step at 72°C for 5 min (Poirel et al., 2011)
bla_{OXA}	F: GCGTGGTTAAGGATGAACAC R: CATCAAGTTCAACCCAACCG	438	
bla_{NDM}	F: CTTCCAACGGTTTGATCGTC R: ATTGGCATAAGTCGCAAT CC	206	Heat activation of polymerase at 95°C for 15 min, then initial denaturation at 95°C for 5 min, followed by 30 cycles of denaturation at 95°C for 2 min, annealing at 60°C for 1 min, and elongation at 72°C for 1 min, followed by a final elongation step at 72°C for 5 min (Ellem et al., 2011)
bla_{IMP}	F: ATGAGCAAGTTATCTTAGTATTC R: GCTGCAACGACTTGTTAG	765	Heat activation of polymerase at 95°C for 15 min, then initial denaturation at 95°C for 5 min, followed by 30 cycles of denaturation at 95°C for 2 min, annealing at 50°C for 1 min, and elongation at 68°C for 1 min, followed by a final elongation step at 68°C for 5 min (Toleman et al., 2003)
bla_{VIM}	F: TTATGGAGCAGCAACGATGT R: CGAATG CGCAGCACCAGG	621	Heat activation of polymerase at 95°C for 15 min, then initial denaturation at 95°C for 5 min, followed by 30 cycles of denaturation at 95°C for 1 min, annealing at 59°C for 1 min, and elongation at 68°C for 1 min, followed by a final elongation step at 68°C for 5 min (Toleman et al., 2003)
bla_{SIM}	F: TACAAGGGATTC GGCATC G R: TAATGGCCTGTTCCCATGTG	571	Heat activation of polymerase at 95°C for 15 min, then initial denaturation at 94°C for 5 min, followed by 25 cycles of denaturation at 94°C for 30 s, annealing at 52°C for 1 min, and elongation at 68°C for 1 min, followed by a final elongation step at 68°C for 5 min (Lee et al., 2003)

The direction of the primer is indicated at the end of the primer name, as follows: F, forward (5′–3′) and R, reverse (3′–3′).KPC, Klebsiella pneumoniae carbapenemase; OXA, oxacillinase; NDM, New Delhi metallo-β-lactamase; IMP, imipenem-resistant Pseudomonas; VIM, Verona integron-encoded metallo-β-lactamase; SIM, Seoul imipenemase.

the species level. The threshold for statistical significance was a p-value of < 0.05.

RESULTS

Demographic Characteristics

A total of 405 samples and 92 samples were collected from FHs and ICPs, respectively. A total of 31 FHs and 84 ICPs were found to be colonized with CRE. The CRE colonization rates were 31/405 (7.6%) and 84/92 (91.3%) among FHs and ICPs, respectively. The non-Arab ethnic group constituted 26/31 (83.8%) of the FH CRE colonizers. The Southeast Asians represented the highest proportion among FHs, and the nationalities were as follows: 14 (45.2%), nine (29%), one (3.2%), two (6.5%), and five (16.1%) were Indians, Filipinos, Siri Lankans, Bangladeshis, and Egyptians. On the other hand, the Arab ethnic group constituted 63/84 (75%) of the ICP CRE colonizers. The top five nationalities were Kuwaitis, 36 (43%); Egyptians, nine (11%); Indians, six (7%); Jordanians, five (6%); Iranians, five (6%); and others, 23 (27%).

Bacterial Isolates

Microbiological cultures yielded 681 and 95 isolates of the family Enterobacterales recovered from FHs and ICPs, respectively. *E. coli* isolates of 425 (62.4%) were the most predominant, followed by *K. pneumoniae* isolates of 18 (2.6%) among FHs, whereas the predominant isolates among ICPs were *K. pneumoniae* accounting for 69 (72.6%), followed by *E. coli* of 16 (16.8%). A total of 36/681 and 87/95 were CRE isolates giving prevalence rates of 5.3 and 91.5% among FHs and ICPs, respectively. The breakdown of the CRE isolates among CRE colonized FHs and ICPs is shown in **Table 2**. *E. coli* isolates represent 15 (41.7%) and 15 (17.3%) ($p = 0.004$) among FHs and ICPs, respectively, in addition to *K. pneumoniae* isolates representing 8 (22.2%) and 65 (74.7%) ($p = 0.001$) among FHs and ICPs, respectively. Other isolates represent 13 (36%) and 7 (8%) ($p = 0.001$) among FHs and ICPs, respectively.

TABLE 2 | Carbapenem-resistant Enterobacterales (CRE) isolates from food handlers and infected control patients.

Bacteria	Number (%) of CRE isolates		*p*-value
	FHs (*N* = 36)	ICPs (*N* = 87)	
Escherichia coli	15 (41.7)	15 (17.3)	0.004*
Klebsiella pneumoniae	8 (22.2)	65 (74.7)	0.001*
Enterobacter cloacae	3 (8.3)	4 (4.7)	0.41
Kluyvera spp.	2 (5.5)	0 (0)	
Citrobacter freundii	1 (2.8)	1 (1.2)	0.51
Citrobacter youngae	1 (2.8)	0 (0)	
Escherichia fergusonii	1 (2.8)	0 (0)	
Morganella morganii	1 (2.8)	0 (0)	
Pantoea spp.	1 (2.8)	1 (1.2)	0.51
Proteus vulgaris	1 (2.8)	0 (0)	
Providencia rettegri	1 (2.8)	0 (0)	
Serratia marcescens	1 (2.8)	1 (1.2)	0.51

FHs, food handlers; ICPs, infected control patients.
**p-value is significant.*

Indirect Carbapenemase Test

All CRE isolates were tested with MAST® Indirect Carbapenemase Test (ICT). Carbapenemase production was detected in 15 (41.6%) of the FHs ($n = 36$) and 44 (50.5%) of the control group ($n = 87$). Positive carbapenemase production was indicated when there is a distortion of the zone around the tip of the ICT, as shown in **Figure 1**.

Carbapenemase Genes

Twenty-two (61.1%) out of 36 CRE isolates were recovered from FHs, and 65 (74.7%) out of 87 CRE isolates from ICPs harbored one, two, or three carbapenemase-mediating genes, as shown in **Table 3**. The detection of *bla* genes among FHs and ICPs was as follows: 54 CRE isolates harbored single genes, and of these, 15 (68.2%) and 39 (60%) isolates were from FHs and ICPs, respectively. In addition to the coexistence of two genes that were observed in 28 CRE isolates, of these, 5 (22.7%) and 23 (35.4%) were from FHs and ICPs, respectively. Five CRE isolates were in combination with three genes, and of these, 2 (9%) and 3 (4.6%) were from FHs and ICPs, respectively. There are no statistical differences between the FHs and ICPs groups.

In **Table 4**, the predominant CRE genes harbored by FHs 22/36 (61.1%) and ICPs 65/87 (74.7%) isolates were as follows: the occurrence of bla_{OXA} genes was observed in all isolates of FHs 10/22 (45.5%) whereas 44/65 (67.7%) isolates among ICPs ($p = 0.06$). The presence of bla_{KPC} genes was detected in 19/22 (86%) and 26/65 (40%) from FHs and ICPs ($p = 0.0001$), respectively. The presence of bla_{NDM} genes was identified in 2/22 (9.1%) and 24/65 (36.9%) isolates from FHs and ICPs ($p = 0.01$), respectively.

As demonstrated in **Table 4**, sequence analysis of *K. pneumoniae*, *E. coli*, and other isolates harboring bla_{OXA}, bla_{KPC}, and bla_{NDM} recovered from FHs and ICPs shows the following. Allelic variants of bla_{OXA} as $bla_{\mathrm{OXA-48}}$ genes were positive for 5/22 (22.7%) and 10/65 (15.3%) *K. pneumoniae* isolates from FHs and ICPs, respectively. Among ICPs alone, 18/65 (27.6%) and 1/65 (1.5%) *K. pneumoniae* isolates carried $bla_{\mathrm{OXA-181}}$ and $bla_{\mathrm{OXA-232}}$, respectively.

The allelic variants of *E. coli* isolates, 4/22 (18%) and 11/65 (17%), were harbored by $bla_{\mathrm{OXA-48}}$ genes among FHs and ICPs, respectively. One *E. coli* isolate out of 65 CRE isolates (1.5%) harbored $bla_{\mathrm{OXA-181}}$ gene among ICPs. The sequenced variants among other isolates showed that $bla_{\mathrm{OXA-48}}$ gene was detected in a single *Citrobacter freundii* isolate out of 22 CRE isolates (4.5%) from FHs and 2/65 (3%) *Enterobacter cloacae* and *Serratia marcescens* isolates from ICPs. In addition, $bla_{\mathrm{OXA-181}}$ was detected in an *E. cloacae* isolate out of 65 CRE isolates (1.5%) from ICPs.

Eleven (57.9%) of 19 randomly selected bla_{KPC}-positive isolates from FHs were sequenced. $bla_{\mathrm{KPC-18}}$ genes were harbored by 5/22 (22.7%) *K. pneumoniae* isolates from FHs. In addition, 3/22 (13.6%) and 14/65 (21.5%) *K. pneumoniae* isolates carried $bla_{\mathrm{KPC-2}}$ gene from FHs and ICPs, respectively, while

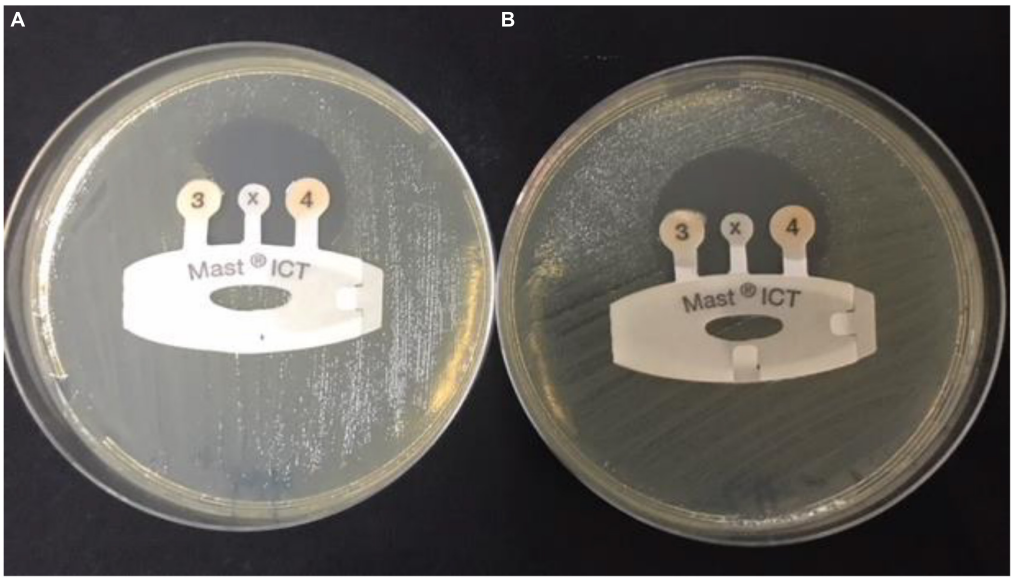

FIGURE 1 | Detection of carbapenemases in carbapenem-resistant Enterobacteriaceae sample by indirect carbapenemase test (ICT). **(A)** Positive CRE sample: ICT positive, showing carbapenemase production and distortion of the zone around tip 3. **(B)** Negative sample: ICT negative, showing no carbapenemases production and formation of a regular, circular zone of inhibition around the indicator tip 3. CRE, carbapenem-resistant Enterobacterales.

bla_{KPC-29} was detected in 2/65 (3%) *K. pneumoniae* isolates among ICPs only. The sequenced variants of bla_{KPC} among *E. coli* isolates showed the following: 4 (6%), 1 (1.5%), and 2 (3%) out of 65 CRE *E. coli* isolates harbored bla_{KPC-18}, bla_{KPC-2}, and bla_{KPC-20} among ICPs, respectively. However, bla_{KPC-29} was harbored by 2/22 (9%) *E. coli* isolates among FHs only. The sequenced variants of bla_{KPC} among other isolates showed the following: bla_{KPC-2} was harbored by 1/22 (4.5%) *E. cloacae* from FHs and 3/65 (4.6%) including *E. cloacae*, *S. marcescens*, and *Pantoea* isolates from ICPs.

The sequenced variants of the bla_{NDM} among *K. pneumoniae* isolates yielded bla_{NDM-1} gene carried by one *K. pneumoniae* isolate (4.5%) out of 22 CRE isolates from FHs and 17/65 (26%) from ICPs. Furthermore, one *K. pneumoniae* isolate (1.5%) carried bla_{NDM-6} and bla_{NDM-7} out of 65 CRE isolates from ICPs. Of the *E. coli* isolates that carried bla_{NDM} genes, 1/22 (4.5%) harbored bla_{NDM-7} among FHs only, while bla_{NDM-1}, bla_{NDM-5}, and bla_{NDM-6} were harbored by 3 (4.6%), 1 (1.5%), and 1 (1.5%) *E. coli* isolates out of 65 CRE isolates from ICPs alone, respectively.

TABLE 3 | Prevalence of mediating carbapenem resistance genes in isolates from food handlers and infected control patients.

Carbapenemase genes detection	Number (%) of CRE isolates		
	FHs ($N = 36$)	ICPs ($N = 87$)	*p*-value
Total number of gene detected	22 (61.1)	65 (74.7)	0.13
Single gene	15 (68.2)	39 (60)	0.49
bla_{OXA}	3 (20)	21 (53.8)	0.05
bla_{NDM}	0	10 (25.7)	
bla_{KPC}	12 (80)	8 (20.5)	0.05
Dual genes	5 (22.7)	23 (35.4)	0.27
bla_{OXA}/bla_{KPC}	5 (100)	12 (52.2)	
bla_{OXA}/bla_{NDM}	0	8 (34.8)	
bla_{NDM}/bla_{KPC}	0	3 (13)	
Triple genes	2 (9)	3 (4.6)	
$bla_{OXA}/bla_{NDM}/bla_{KPC}$			0.43

FHs, food handlers; ICPs, infected control patients.

Clonal Relatedness of Isolates

Clonal relationships of 27 CRE isolates that carried either bla_{OXA} or bla_{KPC} or bla_{NDM} genes from FHs and ICPs were genotyped by MLST. **Figure 2** demonstrates the selected carbapenem-resistant *E. coli* isolates from FHs. Those isolates were found to belong to seven unique STs with the following types: ST38, ST295, ST10, ST1415, and ST1876. Those STs were considered genotypically distinct. In addition to two novel STs, STN1, and STN2 lineages were found for the first time in this study. The CCs assigned *E. coli* isolates of FHs into five CCs consisting of ST1876, which belongs to CC538; ST295, CC295; ST10, CC10; ST1415, CC1415; and ST38, CC38. Out of the six *E. coli* isolates analyzed among ICPs, four known ST types were yielded—ST10276, ST405, ST69, and ST410—besides two novel STs, STN3 and STN4. The four *E. coli* ST isolates were assigned into different CCs, as follows: ST410 to CC23; ST10276, CC405; ST405, CC405; and ST69, CC69. According to the dendrogram, two clones including ST type ST10276 and ST405 with similar CC (CC405) were considered to be closely related clones with the coexistence of bla_{OXA}/bla_{KPC} carbapenemase genes. Another closely related two isolates belonged to the newly described ST types STN3 and ST410.

TABLE 4 | Proportion of CRE isolates expressing carbapenemase gene variants among food handlers and infected control patients.

Carbapenemase genes	Number (%) of CRE isolates expressing carbapenemase genes		
	FHs	ICPs	*p*-value
Overall isolates	22 (61.1)	65 (74.7)	
bla_{OXA} (54)	10 (45.5)	44 (67.7)	0.06
bla_{KPC} (45)	19 (86.4)	26 (40)	0.0001*
bla_{NDM} (26)	2 (9.1)	24 (36.9)	0.01*
Klebsiella pneumoniae (52)	7 (32)	45 (69)	0.004*
bla_{OXA}			
bla_{OXA-48} (15)	5 (22.7)	10 (15.3)	0.006*
$bla_{OXA-181}$ (18)	0	18 (27.6)	
$bla_{OXA-232}$ (1)	0	1 (1.5)	
bla_{KPC}			
bla_{KPC} (1)	1 (4.5)	0	
bla_{KPC-18} (5)	5 (22.7)	0	
bla_{KPC-2} (17)	3 (13.6)	14 (21.5)	0.4
bla_{KPC-29} (2)	0	2 (3)	
bla_{KPC-20} (0)	0	0	
bla_{NDM}			
bla_{NDM-1} (18)	1 (4.5)	17 (26)	0.06
bla_{NDM-5} (0)	0	0	
bla_{NDM-6} (1)	0	1 (1.5)	
bla_{NDM-7} (1)	0	1 (1.5)	
Escherichia coli (26)	11 (50)	15 (23)	0.01*
bla_{OXA}			
bla_{OXA-48} (15)	4 (18)	11 (17)	0.8
$bla_{OXA-181}$ (1)	0	1 (1.5)	
$bla_{OXA-232}$ (0)	0	0	
bla_{KPC}			
bla_{KPC} (4)	4 (18)	0	
bla_{KPC-18} (4)	0	4 (6)	
bla_{KPC-2} (1)	0	1 (1.5)	
bla_{KPC-29} (2)	2 (9)	0	
bla_{KPC-20} (2)	0	2 (3)	
bla_{NDM}			
bla_{NDM-1} (3)	0	3 (4.6)	
bla_{NDM-5} (1)	0	1 (1.5)	
bla_{NDM-6} (1)	0	1 (1.5)	
bla_{NDM-7} (1)	1 (4.5)	0	
Others (9)*	4 (18)	5 (8)	0.16
bla_{OXA}			
bla_{OXA-48} (3)	1 (4.5)	2 (3)	0.7
$bla_{OXA-181}$ (1)	0	1 (1.5)	
$bla_{OXA-232}$ (0)	0	0	
bla_{KPC}			
bla_{KPC} (3)	3 (13.6)	0	
bla_{KPC-18} (0)	0	0	
bla_{KPC-2} (4)	1 (4.5)	3 (4.6)	0.9
bla_{KPC-29} (0)	0	0	
bla_{KPC-20} (0)	0	0	
bla_{NDM}			
bla_{NDM-1} (0)	0	0	
bla_{NDM-5} (0)	0	0	
bla_{NDM-6} (0)	0	0	
bla_{NDM-7} (0)	0	0	

CRE, carbapenem-resistant Enterobacterales; FHs, food handlers; ICPs, infected control patients.

**Others = Enterobacter cloacae (5), Serratia marcescens (2), Pantoea (1), Citrobacter freundii (1), Kluyvera (1), and Escherichia fergusonii (1).*

Figure 3 shows that the MLST analysis of representative carbapenem-resistant *K. pneumoniae* isolates obtained from FHs revealed seven different STs. The four known ST types were as follows: ST461, ST268, ST25, and ST2389. In addition, three novel combinations of alleles and thus undescribed STs designated ST3495, ST3496, and ST3497 were assigned by Pasteur Institute MLST database. Those STs were considered genotypically distinct. The CCs assigned *K. pneumoniae* isolates into five CCs, as follows: ST461, CC461; ST3497, CC1155; ST268, CC268; ST25, CC65; and ST2389, CC2274. However, *K. pneumoniae* isolates obtained from ICPs revealed five different and known STs, which were as follows: ST37, ST2059, ST147, ST1880, and ST231. In addition to one novel ST identified for the first time in this study, submitted to the Pasteur Institute MLST scheme and given a new designation ST4743. The analysis of goeBURST assigned *K. pneumoniae* isolates into five CCs: ST37 belonged to CC37; ST2059, CC138; ST231, CC43; ST147, CC147; and ST1880, CC147. Two identical isolates that belonged to ST231 with CC43 were isolated from two Kuwaiti ICPs admitted to MAK Hospital; isolates K429 and K430 co-harbored dual genes $bla_{OXA-232}/bla_{KPC-2}$ and $bla_{OXA-181}/bla_{KPC-2}$, respectively. Moreover, there are two related isolates ST147 and ST1880, with similar CC (CC147) harboring in combination genes bla_{NDM-1} and bla_{KPC-2}. Those isolates were isolated from Egyptian and Kuwaiti ICPs admitted to MAK Hospital.

DISCUSSION

In this study, we described the occurrence of the CRE isolates among FHs in our community. Unrecognized personnel working in commercial food services colonized with CRE and unsafe food handling could be potential sources of antimicrobial resistance dissemination. Molecular characteristics of the CRE isolates revealed that not all the isolates that were resistant to the carbapenems harbored the carbapenemase-encoding genes, demonstrated by the fact that only 61.1 and 74.7% of CRE were positive among the FHs and ICPs isolates, respectively. The most plausible explanation is that these negative CRE isolates probably expressed different resistance mechanisms other than carbapenemase-encoding genes not evaluated in this study. One of the most important findings of this study is the high preponderance of bla_{KPC}, representing 86.4% of the genes found among FHs isolates with various variants like bla_{KPC-18}, bla_{KPC-2}, and bla_{KPC-29} for the first time in Kuwait and very uncommon in the neighboring countries. Previously, it has been shown that the majority of the genes described in clinical isolates from Kuwait and Gulf Cooperation Council (GCC) region were bla_{OXA} and bla_{NDM} and anecdotal reports of clinical isolates of KPC-producing CRE. Most of the patients from whom these carbapenemase genes were found have so far been patients transferred from hospitals abroad (Zowawi et al., 2013, 2014; Sonnevend et al., 2015). Encountering a large number of isolates harboring bla_{KPC} in the current study suggested that there might be wide dissemination of this gene in our country. This gene has been predominantly found in *K. pneumoniae* all over the world, but in our study, it was also found in other isolates such

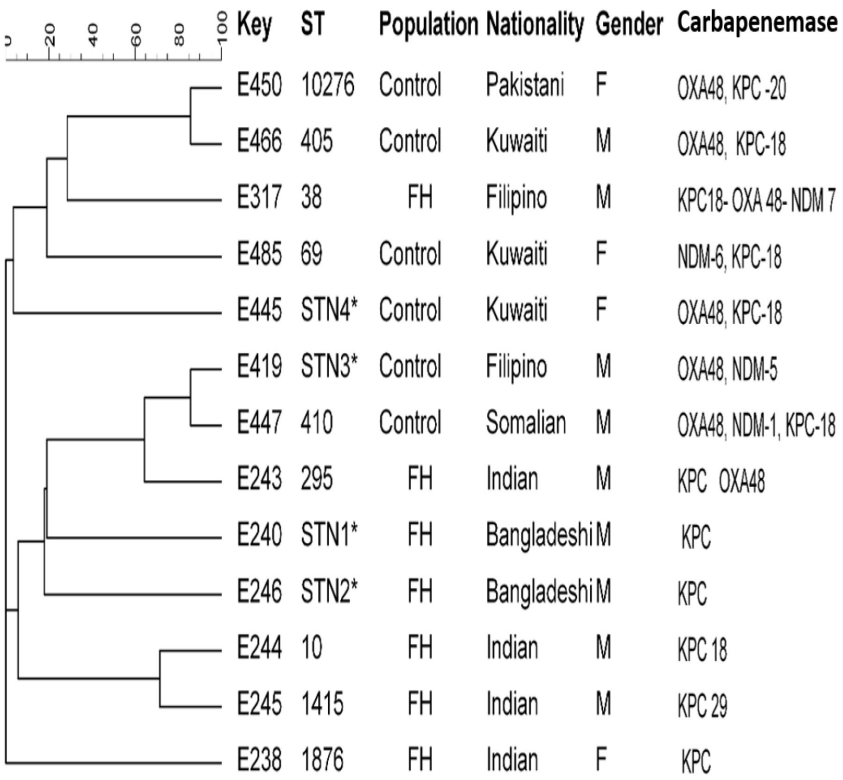

FIGURE 2 | Dendrogram of *Escherichia coli* obtained from food handlers and infected control patients showing clonal relatedness demonstrated by cluster analysis based on their MLST. The characteristics of the major clones generated using minimum spanning trees by BioNumerics software v6.1 (Applied Maths, Kortrijk, Belgium) are also highlighted. Similarity in the isolates is presented in percentages using the scale bar in the upper left corner. In the Key column, E represents *E. coli*, STs = sequence type; population = food handler (FH) and infected control patients; nationality; gender F = female, male = male; and carbapenemases. MLST, multilocus sequence typing.

as *E. coli*, *E. cloacae*, *S. marcescens*, and *Pantoea*. This finding is similar to that obtained in previous studies that documented the presence of bla_{KPC} genes in many clinical isolates of *E. coli*, *Enterobacter* spp., *Salmonella enterica*, *Proteus mirabilis*, and *C. freundii* (Queenan and Bush, 2007).

Other interesting findings in our study included a high number of rectal isolates harboring $bla_{\mathrm{OXA-181}}$ gene among the ICP population as well as the FHs. This confirms an earlier report by Al Fadhli et al. (2020) heralding the emergence of this gene among the family Enterobacterales colonizing the gastrointestinal tract of patients in our hospitals, a phenomenon hitherto confined to the Indian subcontinent (Castanheira et al., 2011) from where it has apparently spread to other parts of the world (Rojas et al., 2017).

Interestingly, we detected five *K. pneumoniae* isolates co-producing $bla_{\mathrm{NDM-1}}$/$bla_{\mathrm{OXA-181}}$. Similarly, the presence of the combination of OXA-181 and NDM-5-producing CRE was reported in India in 2011 encountered in patients admitted to hospitals (Castanheira et al., 2011). Finding this combination in *K. pneumoniae*, like ours, has only been reported in two isolates carrying both $bla_{\mathrm{OXA-181}}$ and $bla_{\mathrm{NDM-1}}$ or $bla_{\mathrm{NDM-5}}$ isolated from epidemiologically unrelated patients in Singapore in 2013 (Balm et al., 2013). Furthermore, the occurrence of $bla_{\mathrm{OXA-181}}$ gene in association with other carbapenemase genes as $bla_{\mathrm{KPC-2}}$ in *K. pneumoniae* isolates was found in the present study. This is the first of such findings in Kuwait, which can be a serious concern. It should be noted that in our study, a novel milieu of OXA48-like carbapenemase, as OXA-232, was detected in *K. pneumoniae* isolates from Kuwaiti patients with ST231. This is in line with a previous report in South India that found $bla_{\mathrm{OXA-232}}$ variant in 35 (71%) *K. pneumoniae* isolates, and ST231 was the predominant ST in 22 isolates (45%) (Shankar et al., 2019).

According to previous reports from Kuwait, $bla_{\mathrm{NDM-1}}$ is by far the most prevalent gene mediating resistance to carbapenems in clinical isolates of CRE (Jamal et al., 2012, 2013, 2016). In our current study, a relatively high proportion of *K. pneumoniae* isolates in ICPs harbored this gene as well as a few *E. coli* isolates. However, this gene was found in only one isolate in FHs. It is conceivable that perhaps this gene is also confined to the hospital, where it is gradually being replaced by $bla_{\mathrm{OXA-181}}$. A few new variants of bla_{NDM}, $bla_{\mathrm{NDM-5}}$, $bla_{\mathrm{NDM-6}}$, and $bla_{\mathrm{NDM-7}}$, were detected in a few of the *K. pneumoniae* and *E. coli* isolates, particularly among the ICP group. Thus, our finding is concordant with the reports of previous studies, which demonstrated that these variants are present in a low level in clinical isolates in the Arabian Peninsula (Pal et al., 2017). A spillover of this gene from the

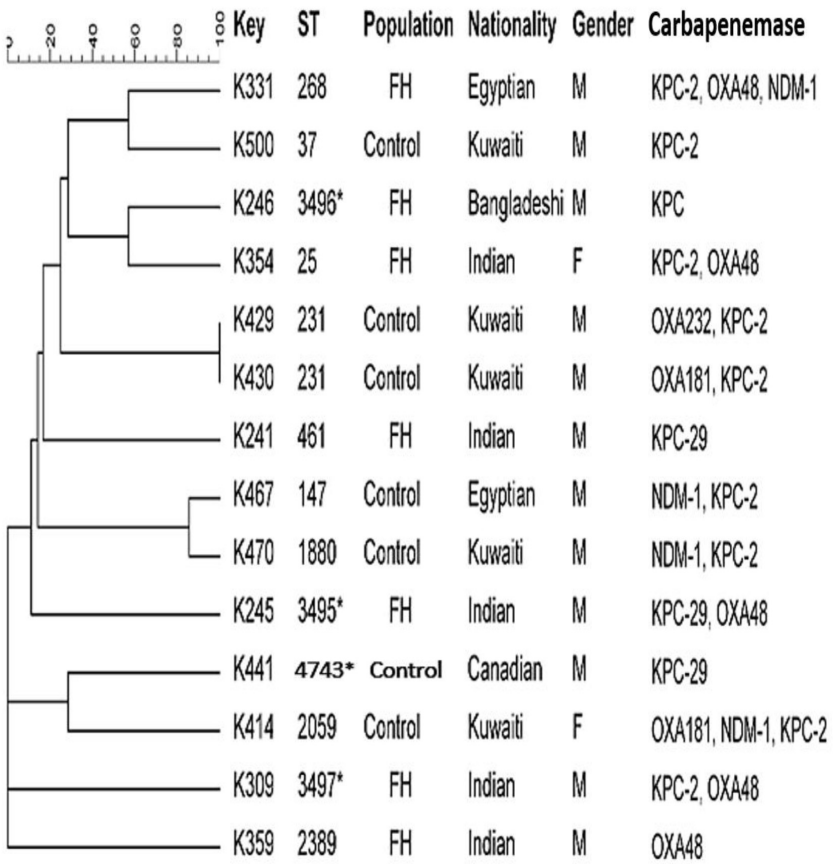

FIGURE 3 | Dendrogram of *Klebsiella pneumoniae* obtained from food handlers and infected control patients showing clonal relatedness demonstrated by cluster analysis based on their MLST. The characteristics of the major clones generated using minimum spanning trees by BioNumerics software v6.1 (Applied Maths, Kortrijk, Belgium) are also highlighted. Similarity in the isolates is presented in percentages using the scale bar in the upper left corner. In the Key column, K represents *K. pneumoniae*, STs = sequence type; population = food handler (FH) and infected control patients; nationality; gender F = female, male = male; and carbapenemases. MLST, multilocus sequence typing.

rectal site into clinical isolates may herald a dangerous resistance trend in the country.

MLST of *E. coli* CRE isolates showed polyclonality with a diverse set of known STs with their CCs circulating among FHs, and two novel STs linked with KPC-producing isolates from Bangladeshi FHs national were typed. These individuals had a history of travel during the last 3 months and lived in the same district in Kuwait. In this study, an isolate belonging to ST10 type detected in Indian FHs has been related to various diseases caused by Enteroaggregative *E. coli* (Chattaway et al., 2014) in the past. In addition, ST295, detected in this study, has also been previously described in a study in Nigeria by Adesina et al. (2019), associating this clone to MDR extra-intestinal pathogenic *E. coli*. In our study, isolates belonging to ST10276 type obtained from a 60-year-old Pakistani female patient admitted to MAK Hospital and ST405 isolated from a Kuwaiti male patient admitted to ISH were closely related to and shared the same CC405 with the coexistence of $bla_{\mathrm{OXA-48}}$ and $bla_{\mathrm{KPC-18}}$ carbapenemase genes. Other related isolates with the novel STN3 were isolated from a Filipino male patient and ST410 from a Somalian male patient admitted to MAK Hospital. The international clones ST38 and ST405 harboring triple carbapenemases $bla_{\mathrm{KPC-18}}/bla_{\mathrm{OXA-48}}/bla_{\mathrm{NDM-7}}$ genes were isolated from the ICP group in this study. This is in line with previous studies that reported *E. coli* isolates that belonged to ST38 and ST405 were encountered in patients in 2015 in Kuwait (Jamal et al., 2015) and Saudi Arabia (Alghoribi et al., 2015).

Carbapenem-resistant *K. pneumoniae* strains obtained from the ICP group were assigned to several STs with their CCs. It is noteworthy that there were two isolates from the ICP group in MAK Hospital with identical STs ST231 with CC43 carrying dual $bla_{\mathrm{OXA}}/bla_{\mathrm{KPC}}$ genes. There were also two related isolates with > 95% similarity, in the same hospital, that belonged to different ST types ST147 and ST1880, sharing the same CC147 that harbored dual $bla_{\mathrm{NDM}}/bla_{\mathrm{KPC}}$ genes. This suggested that clonal dissemination might have occurred. Thus, different STs appeared to carry diverse drug-resistant profiles. It is important to note that some STs found among the rectal isolates in our study were different from the previously described ST types, such as ST677, ST16, ST107, ST485, ST1593, ST1592, and ST1594, among clinical isolates circulating in Kuwait (Jamal et al., 2015). The novel ST type ST3496 that harbored bla_{KPC} gene was recognized

for the first time in a Bangladeshi FH who had a history of travel to his home country during the previous 3 months. In addition, the novel ST4743 was recognized for the first time in a Canadian patient who was admitted to MAK Hospital. The diversity of clones could be related to an increasing number of expatriate employees from diverse geographical areas working in Kuwait coupled with their constant movement to and from other parts of the world. The diverse genetic background of these resistant genes is presumably related to importation from different geographical regions, mainly from workers from South Asia. Many of these workers work in food vending establishments, which may explain, in part, the possible introduction of CRE isolates harboring a variety of encoding genes into the population over time. Therefore, it is our speculation at this time that some clones are probably expanding among these healthy subjects who work in the same Governorate and a large population of clients who may carry such strains to others. Adding to that, an increased number of Kuwait nationals travel abroad seeking medical treatment and are often re-admitted to local hospitals upon their return. This also creates opportunities for importing different CRE clones from other countries, thereby expanding the CRE population in the country's hospitals.

A limitation of this study is that we did not investigate all carbapenemase resistance genes and other mechanisms of resistance.

CONCLUSION

In conclusion, the study contributes to our understanding of the molecular epidemiology of CRE in the community of Kuwait. Our study revealed high prevalence rates of CRE rectal colonization among FHs and ICPs. The commonest mediating genes were *bla*KPC among FH isolates and *bla*OXA-types among patients' isolates. Therefore, the emergence of KPC-carrying Enterobacterales in the healthy human population in the food industry is an unusual finding representing the first of such findings in our country. These results raise significant public health concerns in Kuwait hospitals and the community and highlight the need for necessary vigilance to detect community-acquired CRE isolates. Emphasis on the importance of continuous surveillance of the CRE strains to detect the introduction of new strains into the community and healthcare systems to avoid a trend toward endemicity is highly recommended. Further studies involving whole-genome sequencing (WGS) analysis should help to unravel the other possible mechanisms of resistance.

DATA AVAILABILITY STATEMENT

The original contributions presented in the study are included in the article/supplementary material, further inquiries can be directed to the corresponding author/s.

ETHICS STATEMENT

The studies involving human participants were reviewed and approved by Institutional approval was secured from the Joint Committee for the Protection of Human Subjects in Research, Health Sciences Center, Kuwait University before commencing the data collection. In addition, authorizing Medical Ethics Committee of the Food and Nutrition Administration, Ministry of Health, Kuwait (permit number. 299/2015) was granted. Specimens collection was conducted according to the Declaration of Helsinki and with particular institutional ethical and professional standards. Written informed consent was taken from all participants. The patients/participants provided their written informed consent to participate in this study.

AUTHOR CONTRIBUTIONS

OM, NA-S, and VR: conceptualization, methodology, software, formal analysis, investigation, resources, and visualization. NA-S and VR: validation, data curation, writing—review and editing, and supervision. OM: writing—original draft preparation. NA-S: project administration. NA-S and OM: funding acquisition. All authors have read and agreed to the published version of the manuscript.

FUNDING

This work was supported by the Research Sector Kuwait University (YM 07/15).

ACKNOWLEDGMENTS

We thank to the Public Health Department, Ministry of Health, for their cooperation and to the food handlers who participated in the study. We thank to Dr. Mohammad Asadzadeh from the Microbiology Department for his sincere assistance in the MLST analysis.

REFERENCES

Adesina, T., Nwinyi, O., De, N., Akinnola, O., and Omonigbehin, E. (2019). First detection of carbapenem-resistant *Escherichia fergusonii* strains harbouring beta-lactamase genes from clinical samples. *Pathogens (Basel, Switzerland)* 8, 164–176. doi: 10.3390/pathogens8040164

Al Fadhli, A. H., Jamal, W. Y., and Rotimi, V. O. (2020). Prevalence of carbapenem-resistant *Enterobacteriaceae* and emergence of high rectal colonization rates of blaOXA-181-positive isolates in patients admitted to two major hospital intensive care units in Kuwait. *PLoS One* 15:e0241971. doi: 10.1371/journal.pone.0241971

Alghoribi, M. F., Gibreel, T. M., Farnham, G., Al Johani, S. M., Balkhy, H. H., Upton, M., et al. (2015). Antibiotic-resistant ST38, ST131 and ST405 strains are the leading uropathogenic *Escherichia coli* clones in Riyadh, Saudi Arabia. *J. Antimicrob. Chemother.* 70, 2757–2762. doi: 10.1093/jac/dkv188

Balm, M. N., La, M. V., Krishnan, P., Jureen, R., Lin, R. T., and Teo, J. W. (2013). Emergence of *Klebsiella pneumoniae* co-producing NDM-type and OXA-181 carbapenemases. *Clin. Microbiol. Infect.* 19, E421–E423.

Castanheira, M., Deshpande, L. M., Mathai, D., Bell, J. M., Jones, R. N., Mendes, R. E., et al. (2011). Early dissemination of NDM-1-and OXA-181-producing *Enterobacteriaceae* in Indian hospitals: report from the SENTRY Antimicrobial Surveillance Program, 2006-2007. *Antimicrob. Agents Chemother.* 55, 1274–1278. doi: 10.1128/aac.01497-10

Chattaway, M. A., Jenkins, C., Rajendram, D., Cravioto, A., Talukder, K. A., Dallman, T., et al. (2014). Enteroaggregative *Escherichia coli* have evolved independently as distinct complexes within the *E. coli* population with varying ability to cause disease. *PLoS One* 9:e112967. doi: 10.1371/journal.pone.0112967

Cienfuegos-Gallet, A. V., Ocampo de Los Ríos, A. M., Sierra Viana, P., Ramirez Brinez, F., Restrepo Castro, C., Roncancio Villamil, G., et al. (2019). Risk factors and survival of patients infected with carbapenem-resistant *Klebsiella pneumoniae* in a KPC endemic setting: a case-control and cohort study. *BMC Infect. Dis.* 19:830. doi: 10.1186/s12879-019-4461-x

CLSI [Clinical and Laboratory Standard Institute] (2018). *Performance Standards for Antimicrobial Susceptibility Testing, Twenty-Eighth Informational Supplement CLSI publication 2018; M100–S28*. Wayne, PA: CLSI.

Diancourt, L., Passet, V., Verhoef, J., Grimont, P. A., and Brisse, S. (2005). Multilocus sequence typing of *Klebsiella pneumoniae* nosocomial isolates. *J. Clin. Microbiol.* 43, 4178–4182. doi: 10.1128/jcm.43.8.4178-4182.2005

Ellem, J., Partridge, S. R., and Iredell, J. R. (2011). Efficient direct extended-spectrum β-lactamase detection by multiplex real-time PCR: accurate assignment of phenotype by use of a limited set of genetic markers. *J. Clin. Microbiol.* 49, 3074–3077. doi: 10.1128/jcm.02647-10

Jamal, W. Y., Albert, M. J., and Rotimi, V. O. (2016). High prevalence of New Delhi metallo-β-lactamase-1 (NDM-1) producers among carbapenem-resistant *Enterobacteriaceae* in Kuwait. *PLoS One* 11:e0152638. doi: 10.1371/journal.pone.0152638

Jamal, W. Y., Albert, M. J., Khodakhast, F., Poirel, L., and Rotimi, V. O. (2015). Emergence of new sequence type OXA-48 carbapenemase-producing *Enterobacteriaceae* in Kuwait. *Microb. Drug Resist.* 21, 329–334. doi: 10.1089/mdr.2014.0123

Jamal, W., Rotimi, V. O., Albert, M. J., Khodakhast, F., Nordmann, P., and Poirel, L. (2013). High prevalence of VIM-4 and NDM-1 metallo-β-lactamase among carbapenem-resistant *Enterobacteriaceae*. *J. Med. Microbiol.* 62, 1239–1244. doi: 10.1099/jmm.0.059915-0

Jamal, W., Rotimi, V., Albert, M. J., Khodakhast, F., Udo, E., Poirel, L., et al. (2012). Emergence of nosocomial New Delhi metallo-β-lactamase-1 (NDM-1)-producing *Klebsiella pneumoniae* in patients admitted to a tertiary care hospital in Kuwait. *Int. J. Antimicrob. Agents* 39, 177–185.

Lee, K., Lee, W. G., Uh, Y., Ha, G. Y., Cho, J., Chong, Y., et al. (2003). VIM- and IMP-type metallo-beta-lactamase-producing *Pseudomonas* spp. and *Acinetobacter* spp. in Korean hospitals. *Emerg. Infect. Dis.* 9, 868–871.

Luo, Y., Cui, S., Li, J., Yang, J., Lin, L., Hu, C., et al. (2011). Characterization of *Escherichia coli* isolates from healthy food handlers in hospital. *Microb. Drug Resist.* 17, 443–448.

Moghnia, O. H., Rotimi, V. O., and Al-Sweih, N. A. (2021a). Evaluating food safety compliance and hygiene practices of food handlers working in community and healthcare settings in Kuwait. *Int. J. Environ. Res.d Public Health* 18:1586. doi: 10.3390/ijerph18041586

Moghnia, O. H., Rotimi, V. O., and Al-Sweih, N. A. (2021b). Monitoring antibiotic resistance profiles of faecal isolates of *Enterobacteriaceae* and the prevalence of carbapenem-resistant isolates among food handlers in Kuwait. *J. Glob. Antimicrob. Resist.* 25, 370–376. doi: 10.1016/j.jgar.2021.04.009

Munoz-Price, L. S., Poirel, L., Bonomo, R. A., Schwaber, M. J., Daikos, G. L., Cormican, M., et al. (2013). Clinical epidemiology of the global expansion of *Klebsiella pneumoniae* carbapenemases. *Lancet Infect. Dis.* 13, 785–796. doi: 10.1016/s1473-3099(13)70190-7

Nordmann, P., and Poirel, L. (2014). The difficult-to-control spread of carbapenemase producers among *Enterobacteriaceae* worldwide. *Clin. Microbiol. Infect.* 20, 821–830. doi: 10.1111/1469-0691.12719

Pal, T., Ghazawi, A., Darwish, D., Villa, L., Carattoli, A., Hashmey, R., et al. (2017). Characterization of NDM-7 carbapenemase-producing *Escherichia coli* isolates in the Arabian Peninsula. *Microb. Drug Resist.* 23, 871–878. doi: 10.1089/mdr.2016.0216

Poirel, L., Walsh, T. R., Cuvillier, V., and Nordmann, P. (2011). Multiplex PCR for detection of acquired carbapenemase genes. *Diagn. Microbiol. Infect. Dis.* 70, 119–123. doi: 10.1016/j.diagmicrobio.2010.12.002

Queenan, A. M., and Bush, K. (2007). Carbapenemases: the versatile beta-lactamases. *Clin. Microbiol. Rev.* 20, 440–458. doi: 10.1128/cmr.00001-07

Rojas, L. J., Hujer, A. M., Rudin, S. D., Wright, M. S., Domitrovic, T. N., Marshall, S. H., et al. (2017). NDM-5 and OXA-181 beta-lactamases, a significant threat continues to spread in the americas. *Antimicrob. Agents .Chemother.* 61:e00454–17.

Shankar, C., Mathur, P., Venkatesan, M., Pragasam, A. K., Anandan, S., Khurana, S., et al. (2019). Rapidly disseminating blaOXA-232 carrying *Klebsiella pneumoniae* belonging to ST231 in India: multiple and varied mobile genetic elements. *BMC Microbiol.* 19:137. doi: 10.1186/s12866-019-1513-8

Sonnevend, A., Ghazawi, A. A., Hashmey, R., Jamal, W., Rotimi, V. O., Shibl, A. M., et al. (2015). Characterization of carbapenem-resistant *Enterobacteriaceae* with high rate of autochthonous transmission in the Arabian Peninsula. *PLoS One* 10:e0131372. doi: 10.1371/journal.pone.0131372

Stoesser, N., Sheppard, A. E., Peirano, G., Anson, L. W., Pankhurst, L., Sebra, R., et al. (2017). Genomic epidemiology of global *Klebsiella pneumoniae* carbapenemase (KPC)-producing *Escherichia coli*. *Sci. Rep.* 7, 5917–5927.

Temkin, E., Adler, A., Lerner, A., and Carmeli, Y. (2014). Carbapenem-resistant *Enterobacteriaceae*: biology, epidemiology, and management. *Ann. N. Y. Acad. Sci.* 1323, 22–42. doi: 10.1111/nyas.12537

Toleman, M. A., Biedenbach, D., Bennett, D., Jones, R. N., and Walsh, T. R. (2003). Genetic characterization of a novel metallo-β-lactamase gene, bla IMP-13, harboured by a novel Tn 5051-type transposon disseminating carbapenemase genes in Europe: report from the SENTRY worldwide antimicrobial surveillance programme. *J. Antimicrob. Chemother.* 52, 583–590. doi: 10.1093/jac/dkg410

Wirth, T., Falush, D., Lan, R., Colles, F., Mensa, P., Wieler, L. H., et al. (2006). Sex and virulence in *Escherichia coli*: an evolutionary perspective. *Mol. Microbiol.* 60, 1136–1151. doi: 10.1111/j.1365-2958.2006.05172.x

Zowawi, H. M., Balkhy, H. H., Walsh, T. R., and Paterson, D. L. (2013). β-Lactamase production in key gram-negative pathogen isolates from the Arabian Peninsula. *Clin. Microbiol. Rev.* 26, 361–380. doi: 10.1128/cmr.00096-12

Zowawi, H. M., Sartor, A. L., Balkhy, H. H., Walsh, T. R., Al Johani, S. M., Al Jindan, R. Y., et al. (2014). Molecular characterization of carbapenemase-producing *Escherichia coli* and *Klebsiella pneumoniae* in the countries of the Gulf cooperation council: dominance of OXA-48 and NDM producers. *Antimicrob. Agents Chemother.* 58, 3085–3090. doi: 10.1128/aac.02050-13

Conflict of Interest: The authors declare that the research was conducted in the absence of any commercial or financial relationships that could be construed as a potential conflict of interest.

Publisher's Note: All claims expressed in this article are solely those of the authors and do not necessarily represent those of their affiliated organizations, or those of the publisher, the editors and the reviewers. Any product that may be evaluated in this article, or claim that may be made by its manufacturer, is not guaranteed or endorsed by the publisher.

frontiers in Microbiology

ORIGINAL RESEARCH
published: 10 November 2021
doi: 10.3389/fmicb.2021.741093

Deciphering the Epidemiological Characteristics and Molecular Features of *bla*$_{KPC-2}$- or *bla*$_{NDM-1}$-Positive *Klebsiella pneumoniae* Isolates in a Newly Established Hospital

Ruifei Chen[1†], Ziyi Liu[2,3†], Poshi Xu[1], Xinkun Qi[1], Shangshang Qin[4], Zhiqiang Wang[2] and Ruichao Li[2,3*]*

[1] Department of Clinical Laboratory, Henan Provincial People's Hospital, Department of Clinical Laboratory of Central China Fuwai Hospital, Central China Fuwai Hospital of Zhengzhou University, Zhengzhou, China, [2] Jiangsu Co-innovation Center for Prevention and Control of Important Animal Infectious Diseases and Zoonoses, College of Veterinary Medicine, Yangzhou University, Yangzhou, China, [3] Institute of Comparative Medicine, Yangzhou University, Yangzhou, China, [4] School of Pharmaceutical Sciences, Zhengzhou University, Zhengzhou, China

OPEN ACCESS

Edited by:
Che-Hsin Lee,
National Sun Yat-sen University, Taiwan

Reviewed by:
Subhasree Roy,
National Institute of Cholera and Enteric Diseases (ICMR), India
Anusak Kerdsin,
Kasetsart University, Thailand

***Correspondence:**
Zhiqiang Wang
zqwang@yzu.edu.cn
Ruichao Li
rchl88@yzu.edu.cn

† These authors have contributed equally to this work

Specialty section:
This article was submitted to Antimicrobials, Resistance and Chemotherapy, a section of the journal Frontiers in Microbiology

Received: 14 July 2021
Accepted: 27 September 2021
Published: 10 November 2021

Citation:
Chen R, Liu Z, Xu P, Qi X, Qin S, Wang Z and Li R (2021) Deciphering the Epidemiological Characteristics and Molecular Features of bla$_{KPC-2}$- or bla$_{NDM-1}$-Positive Klebsiella pneumoniae Isolates in a Newly Established Hospital. Front. Microbiol. 12:741093. doi: 10.3389/fmicb.2021.741093

The emergence of hypervirulent carbapenem-resistant *Klebsiella pneumoniae* (hv-CRKP) was regarded as an emerging threat in clinical settings. Here, we investigated the prevalence of CRKP strains among inpatients in a new hospital over 1 year since its inception with various techniques, and carried out a WGS-based phylogenetic study to dissect the genomic background of these isolates. The genomes of three representative *bla*$_{NDM-1}$-positive strains and the plasmids of four *bla*$_{KPC-2}$-positive strains were selected for Nanopore long-read sequencing to resolve the complicated MDR structures. Thirty-five CRKP strains were identified from 193 *K. pneumoniae* isolates, among which 30 strains (85.7%) harbored *bla*$_{KPC-2}$, whereas the remaining five strains (14.3%) were positive for *bla*$_{NDM-1}$. The antimicrobial resistance profiles of *bla*$_{NDM-1}$-positive isolates were narrower than that of *bla*$_{KPC-2}$-positive isolates. Five isolates including two *bla*$_{NDM-1}$-positive isolates and three *bla*$_{KPC-2}$-positive strains could successfully transfer the carbapenem resistance phenotype by conjugation. All CRKP strains were categorized into six known multilocus sequence types, with ST11 being the most prevalent type. Phylogenetic analysis demonstrated that the clonal spread of ST11 *bla*$_{KPC-2}$-positive isolates and local polyclonal spread of *bla*$_{NDM-1}$-positive isolates have existed in the hospital. The *bla*$_{NDM-1}$ gene was located on IncX3, IncFIB/IncHI1B, and IncHI5-like plasmids, of which IncFIB/IncHI1B plasmid has a novel structure. By contrast, all ST11 isolates shared the similar *bla*$_{KPC-2}$-bearing plasmid backbone, and 11 of them possessed pLVPK-like plasmids. In addition, *in silico* virulome analysis, *Galleria mellonella* larvae infection assay, and siderophore secretion revealed the hypervirulence potential of most *bla*$_{KPC-2}$-positive strains. Given that these isolates also had remarkable environmental adaptability, targeted measures should be implemented to prevent the grave consequences caused by hv-CRKP strains in nosocomial settings.

Keywords: *bla*$_{KPC-2}$, *bla*$_{NDM-1}$, whole-genome sequencing, hypervirulence, novel structure, new hospital

INTRODUCTION

Klebsiella pneumoniae is an important clinical pathogen that can cause severe hospital-acquired infections among immunocompromised patients (Pau et al., 2015). Nowadays, *K. pneumoniae* has evolved into two distinct pathotypes: hypervirulent *K. pneumoniae* and classical *K. pneumoniae* (cKp) (Shon et al., 2013). Both pathotypes are global challenges for nosocomial infections (Patel et al., 2014). Classical *K. pneumoniae* is capable of acquiring various antimicrobial resistance (AMR) genes, resulting in the emergence of multidrug-resistant (MDR) and extensively drug-resistant (XDR) strains (Navon-Venezia et al., 2017). The typical representation is carbapenem-resistant *K. pneumoniae* (CRKP). Hypervirulent *K. pneumoniae* can cause infections, such as liver abscesses, pneumoniae, meningitis, and endophthalmitis in healthy individuals, and the *rmpA* and *rmpA2* genes are associated with its pathogenicity (Shon et al., 2013). For a long time, *K. pneumoniae* did not simultaneously encode the phenotypes of MDR and hypervirulence (Yang et al., 2020b). However, in recent years, the convergence of carbapenem resistance and virulence in a single epidemic clone has been reported constantly, which becomes a serious public health issue (Chen and Kreiswirth, 2018; Wong et al., 2018a; Xie et al., 2020). The most representative clade is ST11-CR-HvKp detected in different regions of China (Wong et al., 2018b; Yao et al., 2018; Xu et al., 2019). A recent study successfully traced ST11-CR-HvKp and speculated that the stool may be a reservoir of it (Zheng et al., 2020). These findings revealed the subsistent dissemination of this clone among nosocomial systems.

Currently, *K. pneumoniae* carbapenemase (KPC) is one of the most clinically significant carbapenemase, and its rapid dissemination has become a public health threat globally (Chen et al., 2014). To date, 95 KPC variants have been identified[1]. The pandemic of KPC-producing *K. pneumoniae* is dominated by clonal group 258, which consists of ST258 and its single-locus variants ST11, ST340, and ST512 (Chen et al., 2014). ST258 is the major KPC-producing *K. pneumoniae* sequence type (ST) in North America, Latin America, and several countries in Europe, whereas ST11 prevails mainly in Asia and Latin America (Munoz-Price et al., 2013; Andrade et al., 2014). In China, a study revealed that bla_{KPC-2} was presented in 71% of 109 ertapenem-resistant *K. pneumoniae* isolates in a teaching hospital in Shanghai, and it was often detected along with CTX-M type ESBL enzymes (Chen et al., 2011). Besides, a retrospective observational study (2008–2018) of clinical CRKP isolates found the main CRKP ST was ST11, and bla_{KPC-2} was the most prevalent variant in Zhejiang, China (Hu et al., 2020). In addition, the bla_{NDM}-positive *K. pneumoniae* is another target for nosocomial infection control, which colonized in hospitals of China with high incidence (Qin et al., 2014). Therefore, it is necessary to recognize the dissemination characteristics and molecular features of CRKP. As the most prevalent area of CRKP, the detection rate of CRKP in Henan province reached 32.8% in 2019 according to China Antimicrobial Surveillance Network 2019 annual report[2]. Nevertheless, the epidemiological investigation of CRKP in newly established hospitals is still limited. To systematically study, the prevalence and transmission of CRKP in new hospitals are of guiding significance to evaluate the development trend of CRKP; hence, we aim to investigate the prevalence and genomic characterization of CRKP in a newly established hospital in China and further explore the underlying risk factors, viability, virulence, antibiotic resistance profiles and molecular characteristics of CRKP.

MATERIALS AND METHODS

Research Design

During March 2018–August 2019, seven kinds of samples including blood, ascitic fluid, sputum, bronchoalveolar fluid, wound secretion, urine, and ductus venosus of inpatients were collected from either public wards or intensive care units (ICUs) in a newly established hospital in Henan, China. The hospital that specializes in the treatment of cardiovascular diseases is a 1,000-bed tertiary hospital with 132 ICU beds and 34 public wards. Besides, the present study was approved by the Research Ethics Committee of Henan Provincial People's Hospital.

Bacterial Isolation and Identification

Collected samples were subjected to standard bacterial isolation procedure. The samples were streaked directly onto 5% sheep blood agar plate. Colonies of different morphologies were selected to perform subsequent purification and stocked at −80℃. The detection of carbapenemase-encoding genes was conducted by multiplex polymerase chain reaction (PCR) (Poirel et al., 2011; **Supplementary Table 1**), and laboratory-stored strains carrying the corresponding carbapenemase-encoding genes were used as the positive control. Species identification of the strains and subsequent antimicrobial susceptibility testing were conducted by BD Phoenix100 (Becton, Dickinson and Company, Franklin Lakes, NJ, United States) and verified by disk diffusion method. The minimum inhibitory concentrations of ciprofloxacin, levofloxacin, aztreonam, chloramphenicol, ampicillin, ampicillin–sulbactam, piperacillin, piperacillin–tazobactam, amoxicillin–clavulanic acid, gentamicin, amikacin, cefazolin, ceftazidime, cefotaxime, cefepime, meropenem, imipenem, trimethoprim-sulfamethoxazole, and tetracycline were interpreted based on the standard of the Clinical and Laboratory Standards Institute [CLSI] (2018) except tigecycline and polymyxin B, which followed the criteria of European Committee on Antimicrobial Susceptibility Testing (version 11.0)[3]. *Escherichia coli* ATCC25922 was used as the quality control strain.

Characterization of STs, Capsular Types, Virulence Genes, and Virulence Phenotype

To preliminarily distinguish the STs and capsular types and confirm the presence of the virulence-associated genes

[1]http://www.bldb.eu/BLDB.php?prot=A#KPC

[2]http://www.carss.cn/Report/Details?aId=770

[3]https://eucast.org/clinical_breakpoints/

including *rmpA*, *rmpA2*, *iroN*, and *iutA*, multiplex PCR analysis was performed as previously mentioned (Yu et al., 2018; **Supplementary Table 1**), and laboratory-stored strains carrying the corresponding genes were used as the positive control. Furthermore, the hypervirulence phenotype of *K. pneumoniae* was evaluated using string test and *Galleria mellonella* larvae infection assay. For string test, all isolates were inoculated onto 5% sheep blood agar and incubated at 37℃, and the cutoff criterion for positive was the viscous string longer than 5 mm (Shon et al., 2013). For *G. mellonella* larvae infection assay, larvae of approximately 300 mg were stored in a special box at 4℃ until being used. Overnight cultures of *K. pneumoniae* were washed and adjusted to 10^6 colony-forming units (CFU)/mL using phosphate-buffered saline (PBS). Ten larvae in each group were challenged with 10 μL of diluents, with ST11 clinical cKP HS11286 derivate YZ6 (Xie et al., 2018) used as the negative control. Infected larvae were incubated in sterilized Petri dishes at 37℃ for 72 h, and survival rate was recorded every 24 h. All experiments were repeated in triplicate.

Filter Mating Assay

Transferability of carbapenem resistance phenotype was determined using conjugation assay with a filter mating method. Thirty-five CRKPs were used as donor strains, and *K. pneumoniae* YZ6 Hyg^r was served as the recipient strain. Transconjugants were selected on LB agar plates supplemented with hygromycin (200 mg/L) and meropenem (2 mg/L). The transconjugants harboring carbapenemase encoding genes were confirmed by PCR and antimicrobial susceptibility testing.

Growth Curves

To investigate the fitness of CRKP isolates, growth curves of seventeen strains including 15 CRKP isolates in this study, YZ6 and ATCC700603 in LB broth were conducted according to standardized protocols using three technical replicates and three biological replicates. *Klebsiella pneumoniae* ATCC700603 and YZ6 were regarded as control strains (Schaufler et al., 2016). Growth rates were calculated as follows: $\mu = (\ln(\text{CFU/mL t1}) - \ln(\text{CFU/mL t0}))/\text{t1} - \text{t0}$.

Siderophore Secretion

We qualitatively detected siderophore secretion of CRKP isolates as previously described (Schwyn and Neilands, 1987). A single colony was transplanted into MKB solid medium for iron starvation treatment. After incubation for 24 h at 37℃, the bacterial suspension was adjusted to an OD600 of 0.6 by normal saline, and then 5 μL of suspension was placed on agar plates containing chrome azurol S-iron(III)-hexadecyltrimethylammonium bromide and incubated overnight at 37℃. The orange secretory ring around the colony indicated the production of siderophore. *Klebsiella pneumoniae* ATCC700603 and YZ6 were considered as control strains, and the experiment was repeated three times for each strain.

Biofilm Formation

Biofilm formation assays were conducted as previously mentioned (Ma et al., 2020). Overnight cultures of tested isolates were adjusted to a cell density equivalent to a 0.5 McFarland standard. Two hundred microliters of culture per well were transferred to a 96-well plate. After incubation at 37℃ for 2 days, cultures were discarded, and wells were washed twice with 200 μL PBS. The biofilms were fixed in methanol for 10 min. Subsequently, wells were stained with 1% crystal violet solution for 10 min and rinsed with PBS until colorless. Finally, biofilms were dissolved in 100 μL of 30% formic acid for 30 min, and biofilm formation was quantified by measuring the absorbance at OD590. *Klebsiella pneumoniae* ATCC700603 and YZ6 were used as control strains.

Human Serum Resistance

We evaluated the ability of human serum resistance as previously described (Heiden et al., 2020). Briefly, 5 μL of overnight culture was added to 495 μL LB fresh medium and incubated for 1.5 h at 37℃. Inoculum was resuspended with 1 mL of sterile 1 × PBS. Thirty microliters was mixed in triplicates with 270 μL 50% human serum in 96-well plates. Meanwhile, 30-μL mixture was sucked out from each well, serially diluted, placed on LB agar, and counted the next day. After incubation for 4 h at 37℃, 30 μL of mixture was subjected to the same procedure. Finally, the number of colonies of 0- and 4-h time points was compared to evaluate the survival ability of CRKP isolates in human serum. *Klebsiella pneumoniae* ATCC700603 and YZ6 were used as control strains.

Desiccation Resilience

Desiccation resilience assays were carried out according to previously methods (Heiden et al., 2020) with minor modified. Briefly, a single colony was cultured in LB broth until bacterial cells reached an OD600 value of 0.6–0.8. One hundred microliters of inoculum was serially diluted, plated on LB agar plates, and counted the next day. Meanwhile, another 100-μL inoculum was transferred to 96-well plates. Then, the plates were laid flat in a glass sterile dryer supplemented with desiccant and placed in a 37℃ incubator. After 6 days of drying, 100 μL/well fresh LB broth was readded in 96-well plates; the prepared 96-well plates were cultured with 200-rpm shaking at 37℃ for 3 h. At this point, 100 μL was collected, and the same procedure was performed to count the number of colonies. *Klebsiella pneumoniae* ATCC700603 and YZ6 were used as control strains.

Statistical Analysis

The data were presented using GraphPad Prism 8.3.0. After ensuring that the data were non–normally distributed, the non-parametric Kruskal–Wallis test was utilized to perform multiple comparisons among different groups. Bonferroni adjustment was applied; the corrected $p < 0.1$ was considered significant.

Genome Extraction and High-Throughput Sequencing

Genomic DNA of the 35 CRKP strains was extracted using the TIANamp bacterial DNA kit (TianGen, Beijing, China). The plasmids of four ST11 bla_{KPC-2}-positive strains, which were selected based on virulence test (C13, C26, C31, and C38), were

extracted using the Qiagen plasmid midi-kit (Qiagen, Germany). The extracted genomic DNA was evaluated by 1% agarose gel electrophoresis and quantified by the Qubit fluorometer and then subjected to short-read sequencing (2 × 150 bp) with the Illumina HiSeq 2500 platform. Subsequently, genomic DNAs of three bla_{NDM}-positive strains (C11, C39, and C20) from different branches and plasmids of four aforementioned strains were sequenced with the Oxford Nanopore Technologies MinION long-read platform with the RBK004 barcoding library preparation kit and MinION R9.4.1 flow cells as previously described (Wick et al., 2017; Li et al., 2018).

Bioinformatics Analysis and Phylogenomic Tree Construction

The short-read Illumina raw sequences of CRKP were quality filtered and assembled by SPAdes (Bankevich et al., 2012), and contigs less than 500 bp were discarded. The clone lineages, STs, insertion sequences, AMR determinants, and the virulence genes of CRKP were identified using online tools[4] and Kleborate tool (Wick et al., 2018). The phylogenetic trees of the comparison within CRKP in this study and the comparison between CRKP in this study and other strains in GenBank were constructed using Roary and FastTree based on SNPs of core genomes (Price et al., 2009; Page et al., 2015), and further visualization and modification were performed in iTOL[5]. Combining the formed tree file and the gene presence and absence file, a phylogenetic tree with a matrix describing the presence and absence of core and accessory genes was constructed. The sequences of 35 CRKP were compared against the classical virulence plasmid pLVPK (GenBank accession AY378100), and representative plasmid sequences were further plotted by GView web server[6] using pLVPK as reference sequence. The layout and output were edited in the GView Java stand-alone application obtained from results webpage. Genomic DNA with short-read Illumina and long-read Nanopore data was subjected to perform *de novo* hybrid assembly as described previously (Wick et al., 2017). The complete genome sequences were annotated using RAST[7] automatically and modified manually. BRIG and Easyfig were used to generate the genetic comparison figures (Alikhan et al., 2011).

Risk Factor Analysis

To analyze the risk factors responsible for the occurrence of CRKP, the clinical information of CRKP-carriers was compared to the non-carriers in terms of underwent different variables, which included gender, age, ICU, exposure to carbapenem during hospital stay, isolation season, and sample type. For all data, logistic regression analysis models were used to obtain odds ratios (ORs) and 95% confidence intervals (CIs) for analysis of independent risk factors associated with the occurrence of CRKP. Categorical variables were compared using χ^2 test or two-tailed Fisher exact test, with $p < 0.05$ considered statistically significant. All statistical analyses were processed in SPSS version 22.0.

Data Availability

The draft genome sequences of 32 CRKP isolates have been deposited in the GenBank database under BioProject accession no. PRJNA705380. The complete genome sequences of three bla_{NDM-1}-positive CRKP isolates obtained by hybrid assembly have been deposited in GenBank with accession numbers C11 (pending, deposited in figshare database temporarily), C20 (CP084103-CP084106), and C39 (CP061700-CP061702). The assembled plasmid sequences of four strains (C13, C26, C31, and C38) were deposited in the figshare database (https://doi.org/10.6084/m9.figshare.14199287.v5) for reference. Additional data that support the findings of this study are available from the corresponding authors upon reasonable request.

RESULTS

Characterization of Carbapenem-Resistant *Klebsiella pneumoniae*, Resistance Phenotypes, and Transferability

From March 2018 to August 2019, a total of 1,413 isolates were collected from different wards or ICUs of a newly established hospital in Henan province, China. In these isolates, *K. pneumoniae* (193, 14%) was the most prevalent species, followed by *Acinetobacter baumannii* [177 (13%)], *Pseudomonas aeruginosa* [158 (11%)], *E. coli* [116 (8%)], and *Staphylococcus aureus* [92 (7%)], which were the common nosocomial pathogens (**Supplementary Table 2**). *Klebsiella pneumoniae* isolates were from 18 different wards or ICUs in the hospital (**Supplementary Table 3**). PCR and Sanger sequencing identified 35 [of 193 (18.1%)] carbapenemase-producing *K. pneumoniae*. Among them, 30 isolates were positive for bla_{KPC-2}, whereas the remaining five isolates carried bla_{NDM-1}. All strains exhibited resistance to tested β-lactam antibiotics meropenem, imipenem, aztreonam, ampicillin, ampicillin–sulbactam, piperacillin, piperacillin–tazobactam, amoxicillin–clavulanic acid, cefazolin, ceftazidime, cefotaxime, and cefotaxime. Meanwhile, most strains were resistant to ciprofloxacin [30/35 (85.7%)], levofloxacin [30/35 (85.7%)], chloramphenicol [14/35 (40%)], gentamicin [33/35 (94.3%)], amikacin [25/35 (71.4%)], trimethoprim-sulfamethoxazole [21/35 (60%)], and tetracycline [20/35 (57.1%)], but remained susceptible to tigecycline [34/35 (97.1%)] and polymyxin B [35/35 (100%)] (**Supplementary Table 4**). To investigate the transferability of the carbapenemase-encoding genes, 35 strains were subjected to conjugation assay. However, only five isolates (C11, C12, C1, C29, and C21) including two bla_{NDM-1}-positive strains and three bla_{KPC-2}-positive strains could successfully transfer the carbapenem resistance phenotype to the recipient strain YZ6 Hyg^R, suggesting the carbapenemase-encoding genes of them were located on conjugative plasmids (**Figure 1**).

[4]https://cge.cbs.dtu.dk/services/

[5]http://itol.embl.de/login.cgi

[6]https://server.gview.ca/

[7]http://rast.nmpdr.org/

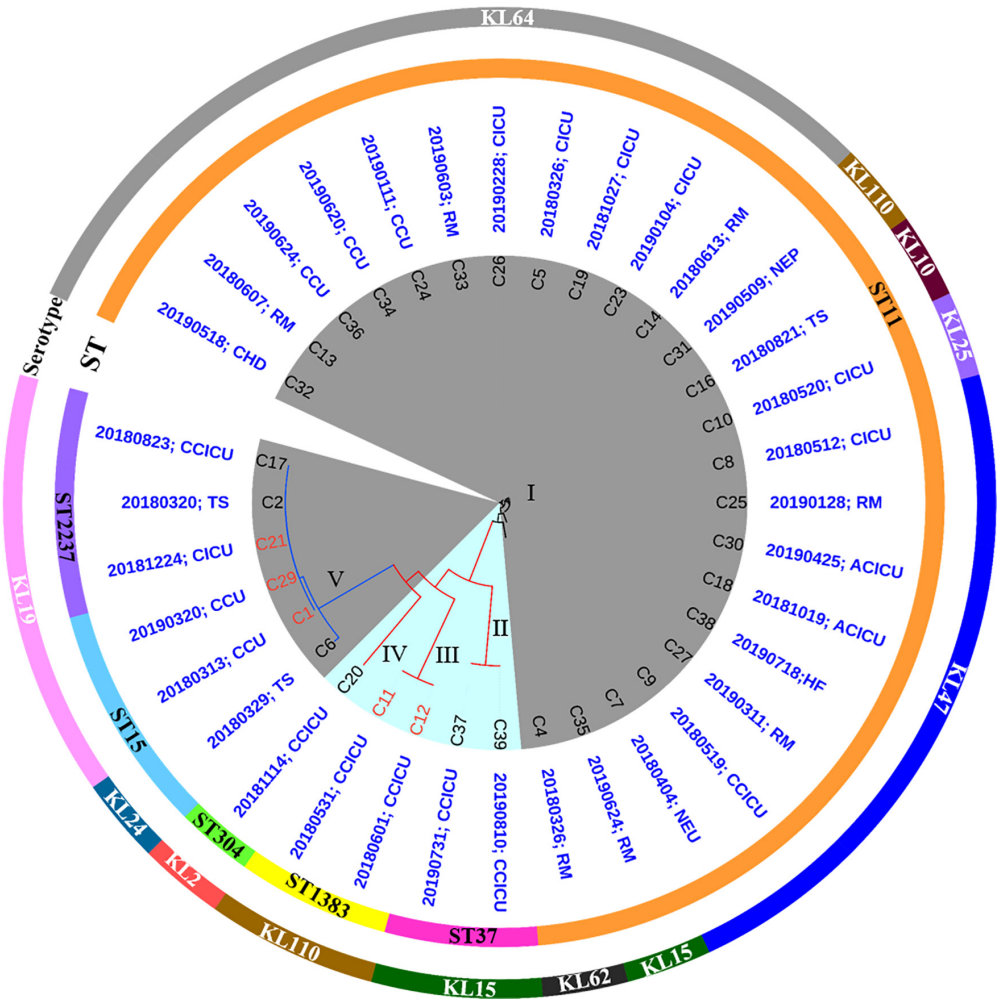

FIGURE 1 | Phylogenetic analysis of 35 CRKP isolates and their basic characterization. *bla*$_{NDM-1}$- and *bla*$_{KPC-2}$-positive strains are highlighted in blue and gray background, respectively. Circles outside the tree indicate the STs and serotypes of each strain. The isolation time and sites are shown in blue words (RM, respiratory medicine ward; CHD, coronary heart disease ward; CCU, coronary care unit; CICU, comprehensive intensive care unit; NEP, nephrology ward; TS, thoracic surgery ward; ACICU, adult cardiac intensive care unit; HF, heart failure ward; NEU, neurology ward; CCICU, children cardiac intensive care unit). The labels marked in red represent the carbapenem resistance phenotype could successfully transfer by conjugation.

Risk Factors Associated With the Emergence of Carbapenem-Resistant *Klebsiella pneumoniae*

To evaluate the risk factors accounting for the emergence of CRKP, clinical information without individual identification of patients was compared (**Supplementary Tables 5, 6**). Among 35 CRKP colonization cases ranged from 3 days to 80 years old, 66% (23/35) were male and 71.4% (25/35) were older than 50 years, suggesting CRKP tended to invade middle-aged and elder patients. Furthermore, colonization was observed in 10 different wards or ICUs. Among them, 60% (21/35) of cases were from ICUs. Besides, 71.4% (25/35) of patients used to experience carbapenem treatment. Comparing with the CRKP non-carriers, no significant differences were detected in gender, age, isolation season, ICU patients, and sample source groups, but the correlation was detected between carbapenem treatment history and being CRKP positive (p = 0.009) [OR = 3.453 (95% CI = 1.369–8.707)].

Multilocus ST Genotyping, Serotypes, and Phylogenetic Analysis of Carbapenem-Resistant *Klebsiella pneumoniae* Isolates

Analysis of genomic characteristics revealed that the *bla*$_{KPC-2}$-positive isolates belonged to three known STs (ST11, ST15, and ST2237), with ST11 being the most dominant type [24/30 (80%)]. In contrast to the *bla*$_{KPC-2}$-positive isolates, five *bla*$_{NDM-1}$-positive strains exhibited diverse STs including ST37, ST1383, and ST304. To our knowledge, ST1383 and ST304 *K. pneumoniae* strains were not associated with carbapenem resistance; especially, the ST304 type has never been reported to carry *bla*$_{NDM-1}$. Analysis of *wzi* locus revealed that seven

TABLE 1 | Summary of all carbapenem-resistant *Klebsiella pneumoniae* strains revealed by WGS data and virulence assay in this study.

Strains	STs/capsular types	Antimicrobial resistance genes	Virulence genes	String test	*Galleria mellonella* larvae infection (survival rate at 72 h)	Virulence score[b]
C13	ST11/KL64	*qnrS1*, *aadA2*, *rmtB*, $bla_{CTX-M-65}$, bla_{KPC-2}, bla_{SHV-12}, bla_{TEM-1B}, *catA2*, *dfrA14*, *fosA*, *sul2*, *tet*(A)	*Yersiniabactin*, *aerobactin*, *rmpA*, *rmpA2*	Negative	20%	4
C32	ST11/KL64	*qnrS1*, *rmtB*, $bla_{CTX-M-65}$, bla_{KPC-2}, bla_{SHV-12}, bla_{TEM-1B}, *catA2*, *fosA*, *sul2*, *tet*(A)	*Yersiniabactin*, *aerobactin*, *rmpA*, *rmpA2*	Negative	—[a]	4
C34	ST11/KL64	*qnrS1*, *aadA2*, *rmtB*, $bla_{CTX-M-65}$, bla_{KPC-2}, bla_{SHV-12}, bla_{TEM-1B}, *dfrA14*, *fosA*, *sul2*, *tet*(A)	*Yersiniabactin*, *aerobactin*, *rmpA*, *rmpA2*	Negative	—	4
C36	ST11/KL64	*qnrS1*, *aadA2*, *rmtB*, $bla_{CTX-M-65}$, bla_{KPC-2}, bla_{SHV-12}, bla_{TEM-1B}, *dfrA14*, *fosA*, *sul2*, *tet*(A)	*Yersiniabactin*, *aerobactin*, *rmpA*, *rmpA2*	Negative	—	4
C24	ST11/KL64	*qnrS1*, *aadA2*, *rmtB*, $bla_{CTX-M-65}$, bla_{KPC-2}, bla_{SHV-12}, bla_{TEM-1B}, *catA2*, *dfrA14*, *fosA*, *sul2*, *tet*(A)	*Yersiniabactin*, *aerobactin*, *rmpA*, *rmpA2*	Negative	—	4
C33	ST11/KL64	*qnrS1*, *aadA2*, $bla_{CTX-M-65}$, bla_{KPC-2}, bla_{SHV-11}, *fosA*, *sul2*, *tet*(A)	*Yersiniabactin*, *aerobactin*, *rmpA*, *rmpA2*	Negative	—	4
C26	ST11/KL64	*qnrS1*, *rmtB*, $bla_{CTX-M-65}$, bla_{KPC-2}, bla_{SHV-12}, bla_{TEM-1B}, *catA2*, *dfrA14*, *fosA*, *tet*(A)	*Yersiniabactin*, *aerobactin*, *rmpA2*	Positive	0%	4
C5	ST11/KL64	*qnrB4*, *aac(3)-IId*, *aadA2*, *armA*, bla_{DHA-1}, bla_{KPC-2}, bla_{SHV-11}, bla_{TEM-1B}, *catA2*, *fosA*, *mph*(A), *mph*(E), *msr*(E),	*Yersiniabactin*, *aerobactin*, *rmpA2*	Negative	—	4
C19	ST11/KL64	*aadA2*, *rmtB*, $bla_{CTX-M-65}$, bla_{KPC-2}, bla_{SHV-12}, bla_{TEM-1B}, *fosA*	*Yersiniabactin*, *aerobactin*, *Salmonchelin*, *rmpA*, *rmpA2*	Negative	0%	4
C14	ST11/KL64	*aadA2*, *rmtB*, $bla_{CTX-M-65}$, bla_{KPC-2}, bla_{SHV-12}, bla_{TEM-1B}, *fosA*	*Yersiniabactin*, *aerobactin*, *Salmonchelin*, *rmpA*, *rmpA2*	Negative	0%	4
C23	ST11/KL64	*aadA2*, *rmtB*, $bla_{CTX-M-65}$, bla_{KPC-2}, bla_{SHV-12}, bla_{TEM-1B}, *fosA, dfrA12, mph*(A)	*Yersiniabactin*, *aerobactin*, *rmpA2*	Negative	—	4
C31	ST11/KL110	*aadA2*, *rmtB*, $bla_{CTX-M-65}$, bla_{KPC-2}, bla_{SHV-12}, bla_{TEM-1B}, *fosA, dfrA12, mph*(A)	*Yersiniabactin*, *aerobactin*, *Salmonchelin*, *rmpA*, *rmpA2*	Negative	0%	4
C16	ST11/KL10	*ARR-3*, *oqxA*, *oqxB*, *aac(3)-IId*, *aac(6′)Ib*, *aadA16*, *aadA2*, *aph(3′)-Ia*, *strA*, *strB*, $bla_{CTX-M-15}$, bla_{KPC-2}, bla_{SHV-11}, *dfrA27*, *fosA*, *mph*(A), *tet*(A)	*Yersiniabactin*	Negative	—	1
C10	ST11/KL25	*qnrS1*, *oqxA*, *oqxB*, *aac(3)-IId*, *aadA2*, *rmtB*, *strA*, *strB*, $bla_{CTX-M-65}$, bla_{KPC-2}, bla_{SHV-11}, bla_{TEM-1B}, *catA2*, *dfrA14*, *fosA*, *sul2*, *tet*(A), *tet*(D)	*Yersiniabactin*	Negative	—	1
C8	ST11/KL47	*oqxA*, *oqxB*, *aadA2*, *rmtB*, $bla_{CTX-M-65}$, bla_{KPC-2}, bla_{SHV-11}, bla_{TEM-1B}, *catA2*, *fosA*	*Yersiniabactin*	Negative	—	1
C25	ST11/KL47	*qnrB6*, *qnrS1*, $bla_{CTX-M-3}$, bla_{KPC-2}, bla_{SHV-11}, bla_{TEM-1B}, *dfrA14*, *fosA*	*Yersiniabactin*	Negative	—	1
C18	ST11/KL47	*oqxA*, *oqxB*, *rmtB*, $bla_{CTX-M-65}$, bla_{KPC-2}, bla_{SHV-12}, bla_{TEM-1B}, *catA2*, *fosA*	*Yersiniabactin*, *aerobactin*, *rmpA2*	Negative	—	4
C30	ST11/KL47	*oqxA*, *oqxB*, *aadA2*, *rmtB*, $bla_{CTX-M-65}$, bla_{KPC-2}, bla_{SHV-11}, bla_{TEM-1B}, *catA2*, *fosA*, *mph*(E)	*Yersiniabactin*, *aerobactin*, *rmpA2*	Negative	—	4
C27	ST11/KL47	*oqxA*, *oqxB*, *aac(6′)Ib*, *aadA2*, *aph(3′)-Ia*, $bla_{CTX-M-15}$, $bla_{CTX-M-65}$, bla_{KPC-2}, bla_{OXA-1}, bla_{SHV-11}, bla_{TEM-1B}, *catA2*, *fosA*, *tet*(A)	*Yersiniabactin*, *aerobactin*, *rmpA2*	Negative	—	4
C38	ST11/KL47	*oqxA*, *oqxB*, *aac(6′)Ib*, *rmtB*, *aph(3′)-Ia*, $bla_{CTX-M-15}$, $bla_{CTX-M-65}$, bla_{KPC-2}, bla_{OXA-1}, bla_{SHV-11}, bla_{TEM-1B}, *catA2*, *fosA*, *tet*(A)	*Yersiniabactin*, *aerobactin*, *rmpA2*	Negative	0%	4
C7	ST11/KL47	*oqxA*, *oqxB*, *aac(6′)Ib*, *aadA2*, *rmtB*, *aph(3′)-Ia*, $bla_{CTX-M-15}$, $bla_{CTX-M-65}$, bla_{KPC-2}, bla_{OXA-1}, bla_{SHV-11}, bla_{TEM-1B}, *fosA*, *tet*(A)	*Yersiniabactin*, *aerobactin*, *rmpA2*	Negative	—	4

(Continued)

TABLE 1 | (Continued)

Strains	STs/capsular types	Antimicrobial resistance genes	Virulence genes	String test	*Galleria mellonella* larvae infection (survival rate at 72 h)	Virulence score[b]
C9	ST11/KL47	*oqxA*, *oqxB*, *aac(6′)Ib*, *rmtB*, *aph(3′)-Ia*, $bla_{CTX-M-65}$, bla_{KPC-2}, bla_{OXA-1}, bla_{SHV-11}, bla_{TEM-1B}, *fosA*, *tet*(A)	*Yersiniabactin*, *aerobactin*, *rmpA2*	Negative	—	4
C35	ST11/KL15	*oqxA*, *oqxB*, *aac(3)-IId*, bla_{KPC-2}, bla_{SHV-11}, *fosA*, *tet*(D)	*Yersiniabactin*	Negative	—	1
C4	ST11/KL62	*ARR-3*, *oqxA*, *oqxB*, *aac(3)-IId*, *aadA16*, *strA*, *strB*, $bla_{CTX-M-14}$, bla_{KPC-2}, bla_{SHV-11}, bla_{TEM-1B}, *dfrA27*, *fosA*, *mph*(A), *sul1*, *sul2*, *tet*(D)	*Yersiniabactin*	Negative	—	1
C37	ST37/KL15	*ARR-3*, *qnrA7*, *oqxA*, *oqxB*, *aac(3)-IId*, bla_{NDM-1}, bla_{SFO-1}-like, bla_{SHV-11}, bla_{TEM-1B}, bla_{VEB-3}, *dfrA27*, *fosA*, *mph*(A), *sul1*	*Yersiniabactin*	Negative	—	1
C39	ST37/KL15	*ARR-3*, *qnrA7*, *oqxA*, *oqxB*, *aac(3)-IId*, bla_{NDM-1}, bla_{SFO-1}-like, bla_{SHV-11}, bla_{TEM-1B}, bla_{VEB-3}, *dfrA27*, *fosA*, *mph*(A), *sul1*	*Yersiniabactin*	Negative	—	1
C11	ST1383/KL110	*oqxA*, *oqxB* bla_{NDM-1}, bla_{SHV-11}, *fosA*, bla_{SHV-12}	None	Negative	—	0
C12	ST1383/KL110	*oqxA*, *oqxB* bla_{NDM-1}, bla_{SHV-11}, *fosA*, bla_{SHV-12}	None	Negative	—	0
C20	ST304/KL2	*qnrS1*, *oqxA*, *oqxB*, *aac(3)-IId*, *aadA2*, $bla_{CTX-M-14}$, bla_{NDM-1}, bla_{SHV-11}, *fosA*	*Yersiniabactin*	Negative	—	1
C6	ST15/KL24	*qnrB4*, *oqxA*, *oqxB*, *aac(6′)-IIa*, aadA2, *armA*, bla_{KPC-2}, bla_{LEN15}, *dfrA14*, *fosA*, *mph*(E), *msr*(E), *sul1*, *sul2*	*Yersiniabactin*, *aerobactin*, *rmpA2*	Positive	0%	4
C1	ST15/KL19	*oqxA*, *oqxB*, *aac(3)-IId*, *aac(6′)Ib*, *aadA2*, *aph(3′)-Ia*, *strA*, *strB*, $bla_{CTX-M-15}$, bla_{DHA-1}, bla_{KPC-2}, bla_{OXA-1}, bla_{SHV-28}, bla_{TEM-1B}, *dfrA12*, *fosA*, *mph*(A), *sul1*, *sul2*	None	Negative	—	0
C29	ST15/KL19	*qnrB4*, *oqxA*, *oqxB*, *aac(3)-IId*, *aac(6′)Ib*, aadA2, *aph(3′)-Ia*, *armA*, $bla_{CTX-M-15}$, bla_{KPC-2}, bla_{OXA-1}, bla_{SHV-11}, bla_{TEM-1B}, *catA2*, *fosA*, *mph*(A), *mph*(E), *msr*(E), *sul1*	*Yersiniabactin*, *aerobactin*, *rmpA2*	Negative	0%	4
C21	ST2237/KL19	*qnrB4*, *oqxA*, *oqxB*, *aph(3′)-Ia*, *armA*, bla_{DHA-1}, bla_{KPC-2}, bla_{OXA-1}, bla_{SHV-11}, *fosA*, *mph*(E), *msr*(E), *sul1*	*Yersiniabactin*, *aerobactin*, *rmpA2*	Negative	—	4
C17	ST2237/KL19	*qnrB4*, *oqxA*, *oqxB*, *aac(3)-IId*, *aadA2*, *aph(3′)-Ia*, *armA*, bla_{DHA-1}, bla_{KPC-2}, bla_{SHV-11}, *dfrA12*, *fosA*, *mph*(A), *mph*(E), *msr*(E), *sul1*	*Yersiniabactin*, *aerobactin*, *rmpA2*	Negative	—	4
C2	ST2237/KL19	*qnrB4*, *oqxA*, *oqxB*, *aac(3)-IId*, *armA*, bla_{DHA-1}, bla_{KPC-2}, bla_{SHV-11}, *fosA*, *mph*(E), *msr*(E), *sul1*	*Yersiniabactin*, *aerobactin*, *rmpA2*	Negative	—	4

[a] *The strain was not selected for Galleria mellonella larvae infection assay.*

[b] *Virulence score is determined by Kleborate software; virulence increases with the score.*

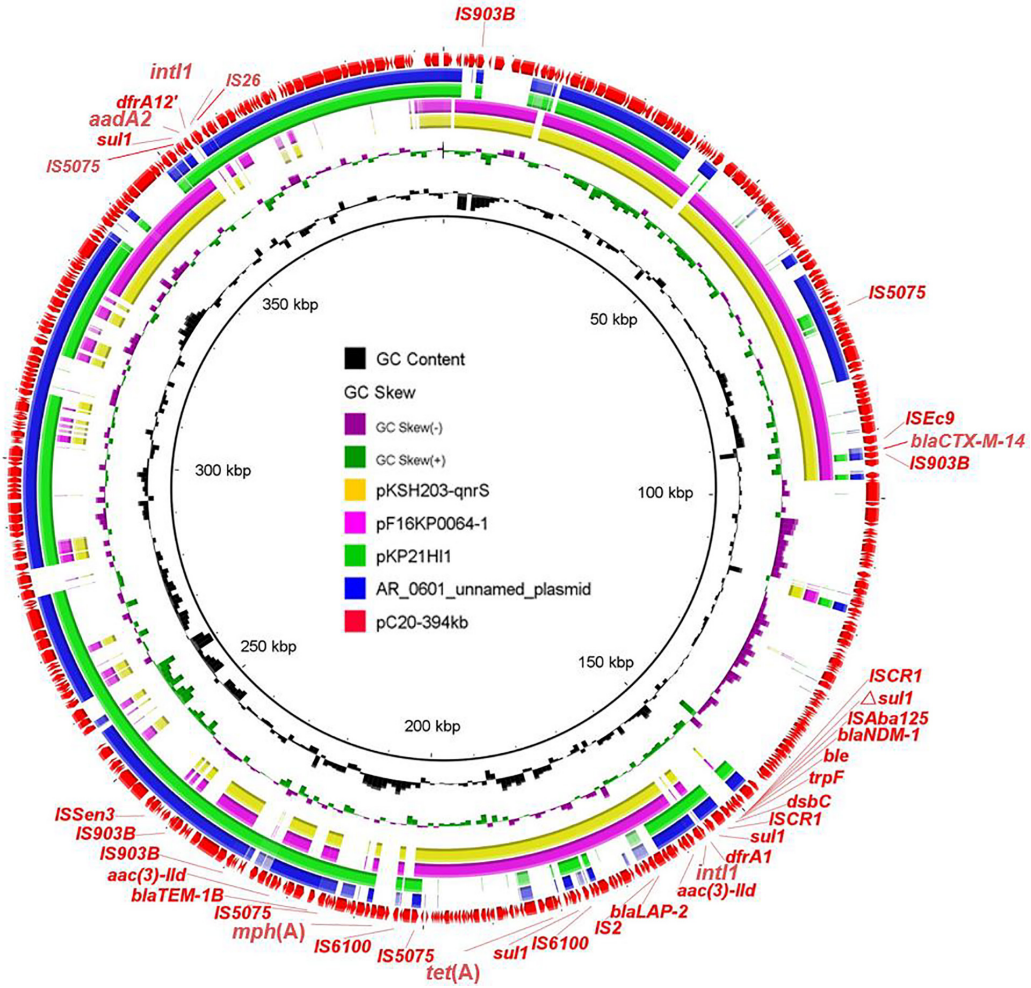

FIGURE 2 | Circular comparison of pC20-394 kb and four most related plasmids available in NCBI. The outmost circle shows the coding genes of pC20-394 kb.

different types (KL64, KL110, KL10, KL25, KL47, KL15, and KL62) existed in ST11 isolates, whereas KL24 and KL19 were identified in ST15 and ST2237 isolates. In addition, bla_{NDM-1}-positive strains possessed three serotypes including KL15, KL110, and KL2. Roary identified a total of 9,610 genes in pangenome, including core genes (n = 3,951), soft core genes (n = 156), shell genes (n = 2,100), and cloud genes (n = 3,403) (**Supplementary Figures 1, 2**). A maximum likelihood phylogenetic tree demonstrated that all strains were clustered into five clades. ST11 bla_{KPC-2}-positive isolates were grouped into cluster I, whereas the remaining bla_{KPC-2}-positive isolates including three ST15 strains and three ST2237 strains were assigned to cluster V, suggesting the clonal expansion of bla_{KPC-2}-positive isolates dominated by ST11 *K. pneumoniae* along with ST15 and ST2237 *K. pneumoniae* that existed in this hospital. By contrast, five bla_{NDM} positive isolates were classified into cluster II (two ST37 strains), III (two ST1383 strains), and IV (one ST304 strain), respectively. The diversity of multilocus ST showed that bla_{NDM}-carrying strains had polyclonal spread. However, the epidemic features were distinguished between bla_{KPC-2}-harboring and bla_{NDM-1}-harboring isolates, as the bla_{KPC-2}-harboring isolates were detected in 10 different wards and ICUs, whereas the bla_{NDM-1} strains were solely concentrated in children cardiac ICU. These findings suggested that the clonal spread of ST11 bla_{KPC-2}-positive isolates and local polyclonal spread of bla_{NDM-1}-positive isolates have existed in this hospital (**Figure 1**). Furthermore, the ST11 and ST15 CRKP strains reported in other studies (Liu et al., 2012; Li et al., 2020; Zheng et al., 2020) were also highly related to corresponding strains in this study. These strains derived from different hospitals in China, suggesting the CRKP involved in this study has been widely spread among the clinical settings (**Supplementary Figure 3**).

Resistome Analysis of Carbapenem-Resistant *Klebsiella pneumoniae* Isolates

Resistome analysis revealed that the bla_{KPC-2}-positive strains harbored more types of AMR genes than those found in

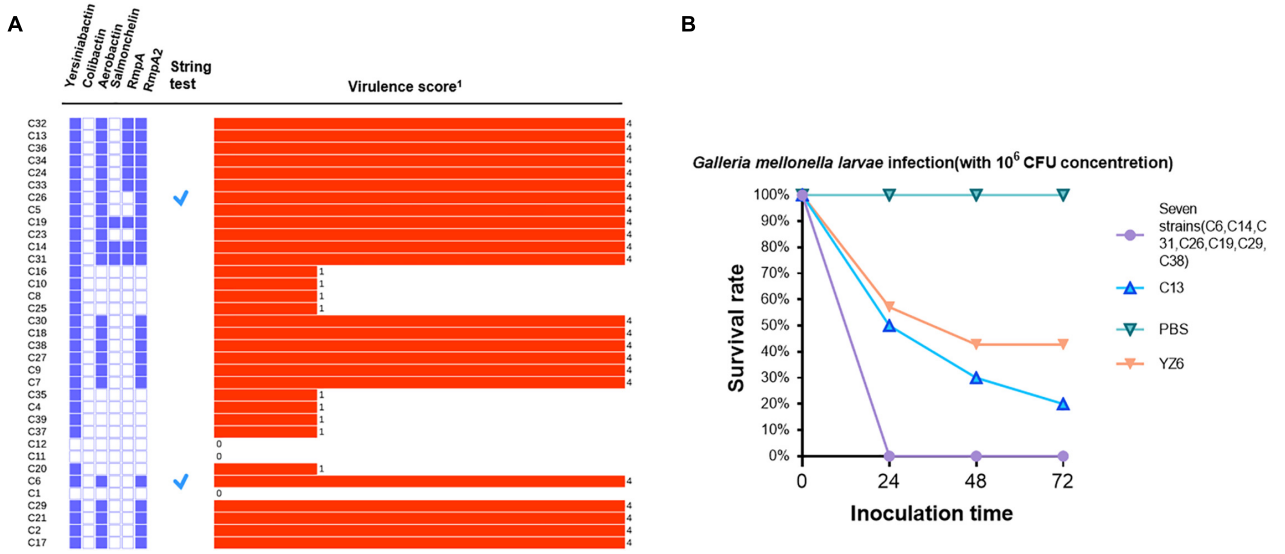

FIGURE 3 | (A) Virulence gene distribution, string test, and virulence scores of all CRKP isolates. The distribution of virulence factors is shown in purple solid (positive) and hollow (negative) rectangles. A tick represents positive result of string test, and the virulence score is shown by a red bar and marked with corresponding numbers in right. **(B)**. Virulence potential of eight CRKP strains in a *G. mellonella* larvae infection model. The effect of 1×10^6 CFU of each strain on survival was assessed in *G. mellonella* larvae. [1]Virulence score is determined by Kleborate software; virulence increases with the score.

bla_{NDM-1}-positive strains. Moreover, bla_{KPC-2}-positive strains possessed almost all classes of genes conferring resistance to aminoglycoside, quinolone, sulfonamide, fosfomycin, tetracycline, and β-lactam, with the most prevalent being *fosA*, bla_{TEM-1B}, *rmtB*, *aadA2*, and $bla_{CTX-M-65}$ genes, which implied that bla_{KPC-2} had potential risks of cotransmission with other AMR genes. However, the AMR profiles of bla_{NDM-1}-positive isolates were narrower than those of bla_{KPC-2}-positive isolates. They were resistant to β-lactam but still susceptible to other antibiotics including ciprofloxacin, levofloxacin, amikacin, polymyxin B, and tigecycline. Interestingly, three bla_{NDM-1}-positive strains carried rare ESBLs bla_{SFO-1}-like (with three bases mutation compared to bla_{SFO-1}) and bla_{VEB-3}, which were usually excluded from routine surveillance (**Table 1**).

Detailed Analysis of Novel bla_{NDM-1}-Bearing Plasmids From Strain C20

Five bla_{NDM-1}-positive strains were separated to three clades based on phylogenetic analysis; therefore, three representative isolates from different branches were selected (C11, C20, and C39) for further exploration of genetic structures via MinION Nanopore long-read sequencing. The results showed that bla_{NDM-1} was located on three distinct plasmids IncX3, IncFIB/IncHI1B, and IncHI5-like, respectively. In strain C11, bla_{NDM-1} was found in typical IncX3 plasmid, which disseminated in human or animal sources worldwide and severed as the major vehicle of bla_{NDM} transmission to evolve with the generation of new NDM variants (Wu et al., 2019). In addition to bla_{NDM-1}, the plasmid also carried bla_{SHV-12}. In strain C20, bla_{NDM-1}-bearing plasmid pC20-394 kb with 52.1% G + C content and 458 predicted ORF was 394 kb in size and possessed IncFIB and IncHI1B replicons. Apart from bla_{NDM-1}, this latter plasmid harbored ESBL genes $bla_{CTX-M-14}$, bla_{LAP-2}, and bla_{TEM-1B}; tetracycline resistance gene *tet*(A); aminoglycoside resistance genes *aadA2* and *aac(3)-IId*; sulfonamide resistance gene *sul1*; trimethoprim resistance genes *dfrA1* and *dfrA12*; and macrolide resistance gene *mph*(A). Except $bla_{CTX-M-14}$, *aadA2*, and *dfrA12* genes, the remaining AMR genes were in a 97-kb MDR region. Despite that the plasmid could not transfer by conjugation, the coselection of bla_{NDM-1} may occur because of the existence of abundant AMR genes. Two integrons were found in different positions. The common genetic structure ΔIS*Aba125*-bla_{NDM-1}-ble_{MBL}-*trpF*-*dsbC* was embedded in downstream of In*183*, generating the complex class I integron In*183*-IS*CR1*-bla_{NDM-1} structure. Another In*1248*-like integron with the genetic array *intI1*-*dfrA12*-*aadA2*-*qacE*Δ*1*-*sul1* was flanked by IS*26* and IS*5075*. BLASTn search of pC20-394 kb against the NCBI nr database showed that less homologous sequences were found between this plasmid and the known plasmids; the maximum similarity was 99% identical at 58% coverage (pAR-0161_plasmid_unnamed, CP028952) (**Figure 2** and **Supplementary Figure 4**). The emergence of novel bla_{NDM-1}-bearing MDR plasmid in ST304 *K. pneumoniae* C20 implied that the novel plasmid mediated the transmission of bla_{NDM-1} and expanded the host ranges of bla_{NDM-1}. Furthermore, the detailed analysis of IncHI5-like bla_{NDM-1}-bearing plasmid in C39 has been reported in another study; the plasmid was 334,893 bp in length and possessed a large MDR region, which contained abundant AMR genes and mobile elements (Liu et al., 2021).

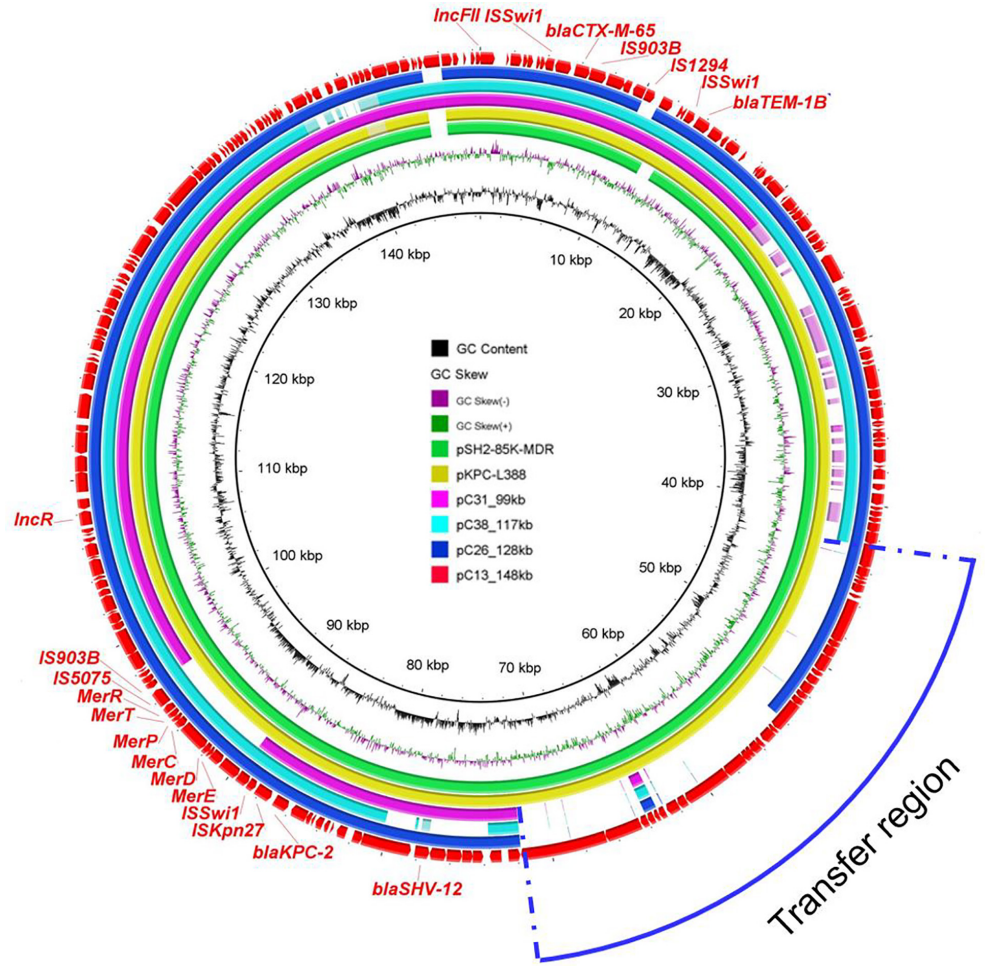

FIGURE 4 | Circular comparison between the four bla_{KPC-2}-bearing plasmids in this study and other most similar plasmids in the NCBI nr database. The plasmid pC13_148 kb was used as the reference in the outmost ring.

Genetic Characteristics and Virulence Phenotype of Carbapenem-Resistant *Klebsiella pneumoniae* Indicate the Emergence of bla_{KPC-2}-Positive Hypervirulent *Klebsiella pneumoniae*

A total of six classes of virulence factor analysis were conducted among these isolates. Fewer virulence genes were possessed by bla_{NDM-1}-positive strains than bla_{KPC-2}-positive isolates. In bla_{NDM-1}-positive strains, two isolates (C11 and C12) were not found to carry any virulence factors, whereas the remaining three isolates (C37, C39, and C20) harbored only one virulence factor yersiniabactin. Correspondingly, they also obtained lower virulence scores (**Figure 3A**). Analysis of the *ybt* locus revealed that 32 isolates were positive for the chromosomally encoded yersiniabactin, of which the dominant type was yersiniabactin lineage 9 within *ICEkp3* element distributed in all ST11-bla_{KPC-2} strains. Twenty-two bla_{KPC-2}-positive strains harbored aerobactin lineage *iuc1* with aerobactin ST1. Besides, three salmochelin-producing strains, nine *rmpA*-positive strains, and 23 *rmpA2*-positive strains were also detected in bla_{KPC-2}-positive strains. To get further insight into virulence phenotype of CRKP, all isolates were subjected to string test. The positive results were observed in C6 (ST15/KL24) and C26 (ST11/KL64). However, a negative string test could not predicate low virulence (Russo and Marr, 2019). Therefore, eight representative bla_{KPC-2}-positive strains from clusters I and V, which contained all bla_{KPC}-carrying strains, were conducted with *G. mellonella* larvae infection assay. Seven strains (C6, C14, C31, C26, C19, C29, and C38) resulted in 0% survival at 24 h with an inoculum of 10^6 CFU, and the survival rate was 20% after the infection of C13 at 72 h (**Figure 3B**). No deaths were observed in PBS treatment group, and the survival rate of negative control YZ6 was higher than the experimental group.

Comparative Analysis of Plasmids in ST11 bla_{KPC-2}-Positive Strains

In order to gain further insights into the genetic basis of virulence and antibiotic resistance of plasmids harbored by ST11

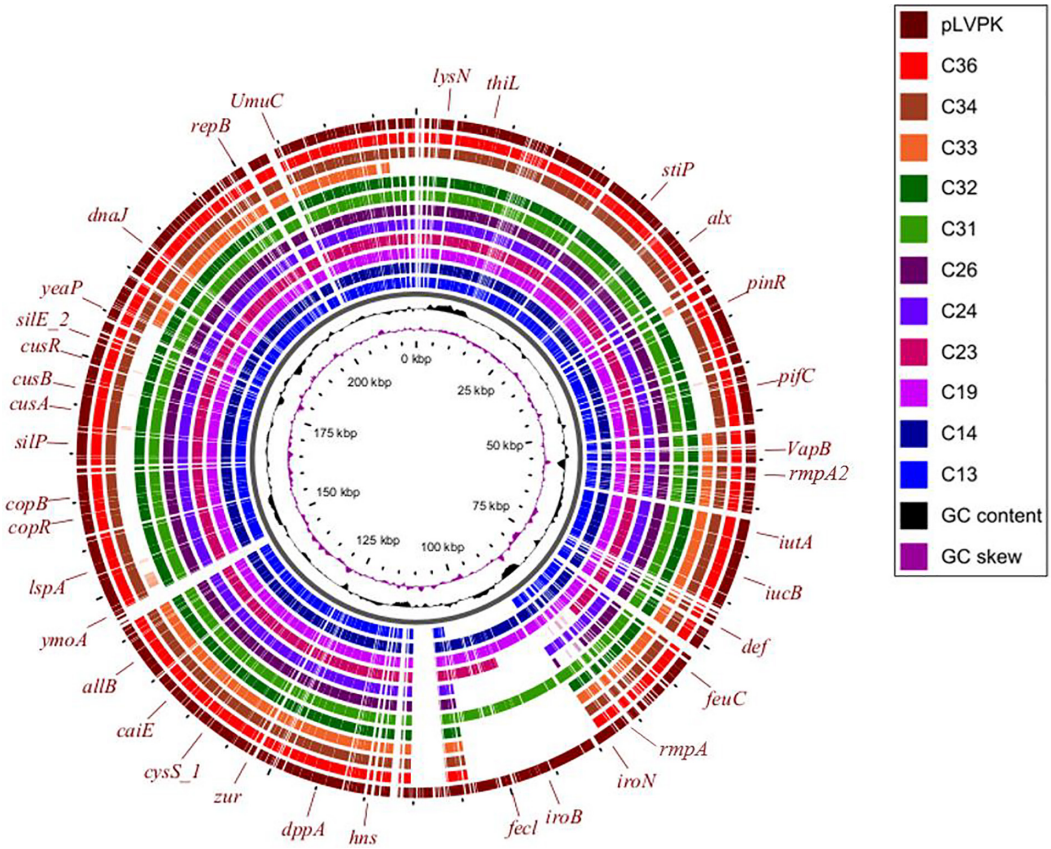

FIGURE 5 | Circular comparison between the classical virulence plasmid pLVPK and the assembled plasmid contigs based on Illumina short-read data of the other 11 CRKP strains in this study.

bla_{KPC-2}-positive isolates, plasmids of four ST11 strains (C13, C26, C31, and C38) were sequenced by MinION Nanopore sequencing platform. As the results showed, bla_{KPC-2}-bearing plasmids of C13, C26, C31, and C38 shared similar backbone. These plasmids ranged from 99 to 148 kb and were classified as IncFII/IncR plasmid. Among them, the largest plasmid pC13_148 kb harbored by C13 was 148,462 bp and carried genes related to plasmid replicon, maintenance, conjugative elements, and AMR genes including bla_{KPC-2}, $bla_{CTX-M-55}$, bla_{TEM-1B}, and bla_{SHV-12}. BLASTn analysis demonstrated that it was similar to pSH2-85K-MDR (MH643792) and pKPC-L388 (CP029225) from *K. pneumoniae*, indicating the universal prevalence of this plasmid among *K. pneumoniae* (**Figure 4**). Besides, more detailed analysis of the remaining bla_{KPC-2}-bearing plasmids in ST11 strains was performed using pC13_148 kb as reference. All ST11 isolates possessed this type of plasmid, with the absence of some specific regions. The bla_{KPC-2} gene was located on the same genetic context, flanked by genes belonging to the Tn*3*-based transposon family insertion sequences (IS*Kpn6* and IS*Kpn27*). Obviously, the deficiency of conjugation transfer region was observed in the majority of plasmids, which may explain why the bla_{KPC-2}-bearing plasmids of most ST11 strains were non-conjugative. However, several bla_{KPC-2}-bearing plasmids (C33, C32, C23, C19, and C14) with intact conjugation transfer regions were unable to be transferred successfully; the underlying mechanism warranted further study (**Supplementary Figure 5**).

Three virulence plasmids carried by C13, C26, and C31 were aligned well with classical virulence plasmid pLVPK (GenBank accession AY378100), a 219-kb plasmid that harbors *iroBCDN*, *iucABCD*, *rmpA*, and *rmpA2*. Furthermore, we found the similar plasmid structure presented in other eight ST11 strains based on Illumina-based contigs analysis (**Figure 5**).

Phenotypic Assays Proved the Carbapenem-Resistant *Klebsiella pneumoniae* Isolates Had Remarkable Environmental Adaptability

To evaluate indicators of survival in the clinical settings of CRKP isolates in this study, according to the previous literature (Heiden et al., 2020), the fitness, desiccant resilience, biofilm formation, human serum resistance, and siderophore secretion assays were performed. To facilitate the analysis of the results, a total of 17 strains covering 15 representative CRKP isolates in this study and two control strains were divided into five groups, including A group (nine bla_{KPC-2}-harboring ST11 strains), B (three bla_{KPC-2}-harboring ST15 or ST2237 strains), C (three

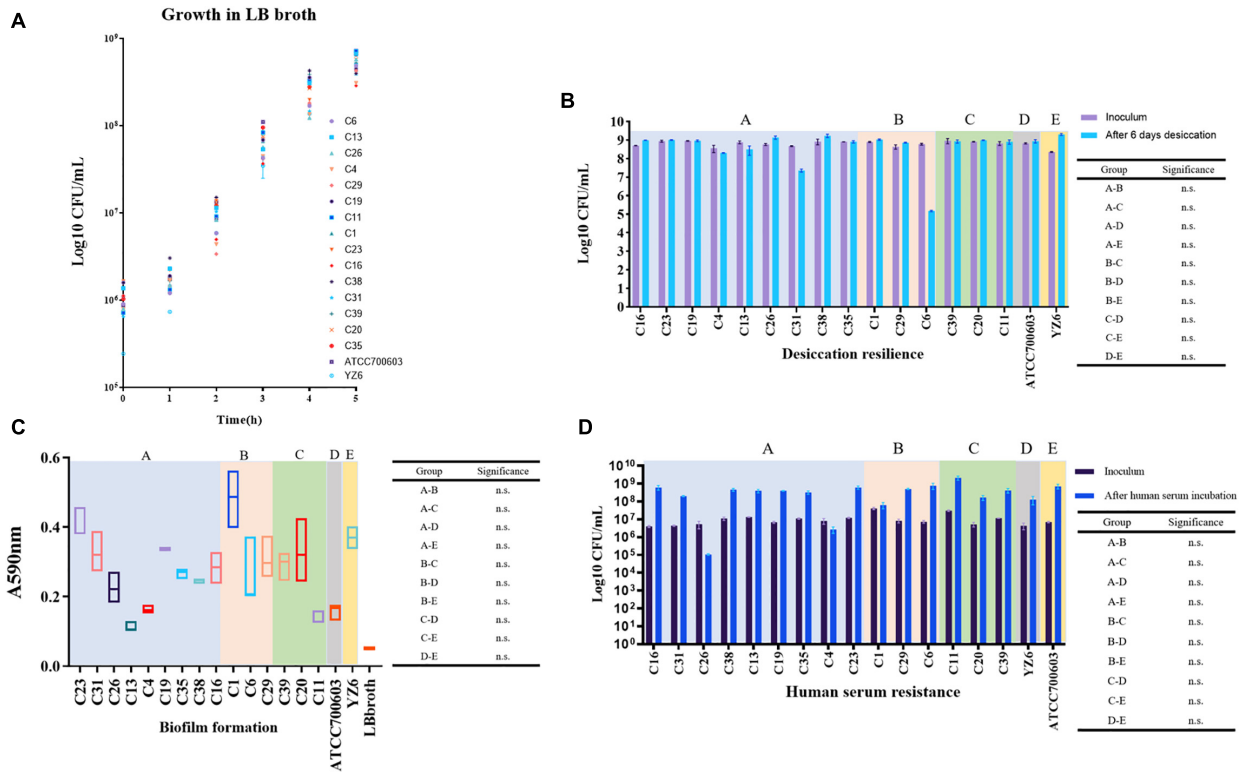

FIGURE 6 | Results of phenotypic experiments to evaluate the fitness and viability of CRKP. Five groups with background color in pale purple (**A:** *bla*$_{KPC-2}$-ST11 group), light pink (**B:** *bla*$_{KPC-2}$-ST15 and ST2237 group), green (**C:** *bla*$_{NDM-1}$-positive group), gray (**D:** standard strain ATCC700603), and yellow (**E:** YZ6), respectively. **(A)** Growth conditions of CRKP and control isolates over 5 h. **(B)** Comparison of the changes of CRKP and control isolates amount during desiccation. n.s., not significant. **(C)** Biofilm formation of CRKP and control isolates; the value represents the absorbance values at 590 nm. n.s., not significant. **(D)** Comparison of the changes of CRKP and control isolates amount incubation in human serum for 4 h. n.s., not significant.

bla$_{NDM-1}$-positive strains), D (*K. pneumoniae* ATCC700603), and E (clinical cKP HS11286 derivative YZ6).

We observed no significant difference in growth rates of the A, B, and C groups when compared to control groups. However, it was only found that the growth rate of the C group was significantly lower than that of group E at 2 h ($p = 0.044$ at 2 h) (**Supplementary Table 7**), which will be worth exploring further. Subsequently, we want to evaluate the performance of CRKP isolates under extreme dry environment, its capacity for biofilm formation, and the tolerance in human serum, which allowed us to assess the viability of CRKP in clinical settings and host. Desiccation resilience and human serum resistance experiments showed high survival rates of CRKP isolates under drying and human serum pressure. Comparable results were also obtained in biofilm formation, which suggested that these CRKP isolates will persist in this hospital for a long time, either under the clinical pressure or in patients (**Figure 6**).

Nevertheless, the siderophore secretion capacity of A group (*bla*$_{KPC-2}$-ST11) was significantly higher than C (*bla*$_{NDM-1}$-positive group, $p = 0.005$), D (standard *K. pneumoniae* ATCC700603, $p = 0.002$), and E (YZ6, $p = 0.005$), but no significant difference was found between the A and B groups. This might be the role of the presence of yersiniabactin, aerobactin, and salmochelin in ST11 *bla*$_{KPC-2}$-positive strains. However, the decreased siderophore secretion capacity was also observed in *bla*$_{KPC-2}$-harboring ST15 strain C1, as it exhibited quite smaller secretion zone in absence of those genes encoding siderophores (**Figure 7**).

DISCUSSION

Our study systematically demonstrated the emergence of CRKP in a newly established hospital. Among these CRKP strains, we found *bla*$_{KPC-2}$ harboring isolates with hypervirulence and multidrug resistance phenotype spread throughout the hospital for a long term, whereas *bla*$_{NDM-1}$ carrying strains with novel ST types and plasmids were detected only in children cardiac ICU. Importantly, these isolates showed superior adaptive ability in clinical environment and host, which was likely due to the strong biofilm formation capacity. As a reservoir of pathogenic bacteria, hospital is often regarded as an ideal setting to investigate the epidemic characteristics of MDR strains (Yang et al., 2013; Wang et al., 2019), especially *K. pneumoniae* (Hu et al., 2020).

We identified the risk factors responsible for the occurrence of CRKP. Not surprisingly, it was found that exposure to carbapenem was associated with the emergence of CRKP, which was consistent with the previous investigations of CRKP

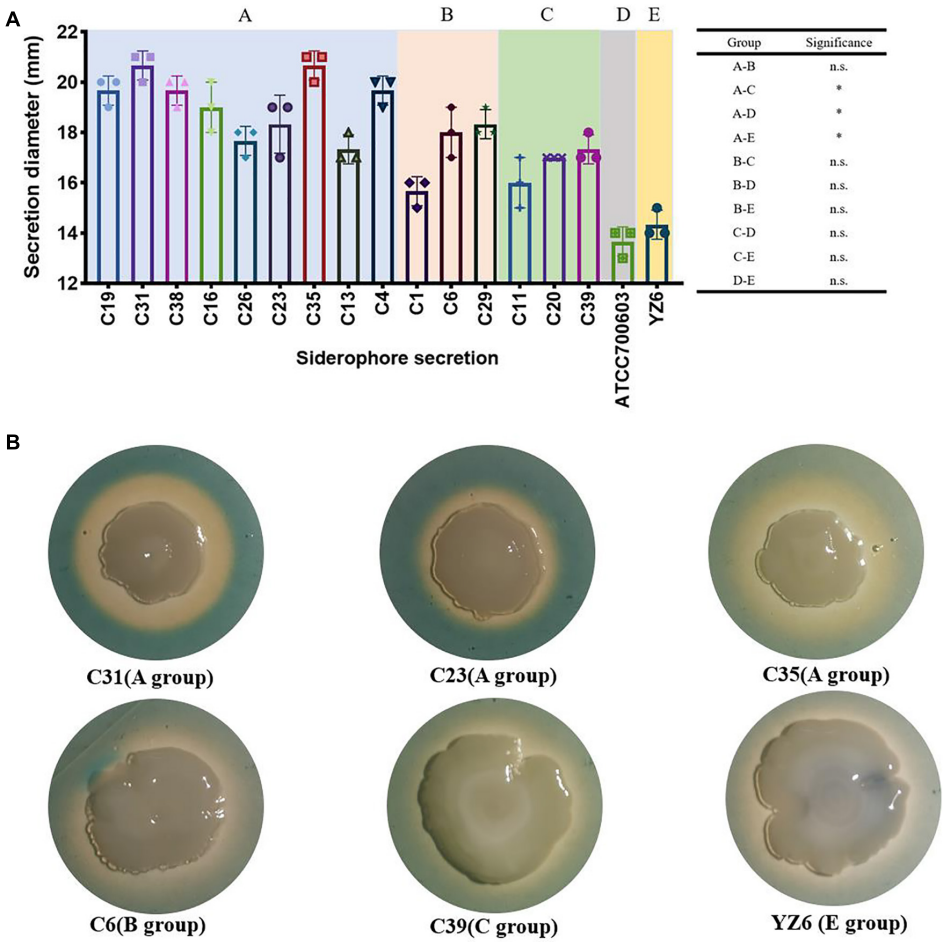

FIGURE 7 | Results of siderophore secretion experiments. **(A)** The siderophore secretion diameters (showed in millimeters) of CRKP and control isolates. n.s., not significant, $^{*}p < 0.01$. **(B)** The siderophore secretion zone of six representative isolates on CAS agar; the orange–yellow ring around the colonies indicates the siderophore secretion.

(Liu et al., 2019a) and carbapenem-resistant *P. aeruginosa* (Lee et al., 2017; Zhang et al., 2018). Furthermore, previous study pointed out that carbapenem use with insufficient infection control measure might increase the risk of colistin resistance in *K. pneumoniae* (Gundogdu et al., 2018). Therefore, prudent carbapenem use is vital to reduce the production of drug-resistant bacteria in clinical settings.

It was found that the ST11 bla_{KPC-2}-positive *K. pneumoniae* was the dominant strain in this hospital. However, the bla_{KPC-2}-bearing plasmids among them were unable to transfer, which may due to the absence of the conjugation transfer genes in most plasmids. The genetic context of bla_{KPC-2} shared the core structure with IS*Kpn27*-bla_{KPC-2}-IS*Kpn6*, suggesting that these mobile elements played a key role in the dissemination of bla_{KPC-2}. Virulence assay revealed that most of bla_{KPC-2}-positive strains were associated with hypervirulence, which could be mainly attributed to the existence of various virulence factors. Siderophore production was an important biomarker to distinguish hvKP and cKp (Russo et al., 2018). Generally, salmochelin, yersiniabactin, aerobactin, and enterobactin were regarded as typical siderophores to assist bacteria to acquire iron ion (Bachman et al., 2011) and involved in the virulence of Enterobacteriaceae and human infection (Schubert et al., 2000; Lam et al., 2018). The majority of bla_{KPC-2}-positive *K. pneumoniae* encoded siderophore yersiniabactin and aerobactin, causing the siderophore secretion to be significantly higher than that of control groups. In addition, some strains carried the mucoid phenotype regulators *rmpA* and *rmpA2*, yet they were not positive for string test. It may be attributed to the fact that the expression of hypermucoviscosity phenotype was a fine-tuned process, which needed the mutual assistance of multiple genes (Walker et al., 2019). Moreover, the distribution of virulence factors in bla_{KPC-2} isolates may be diverse. For example, two virulence factors *rmpA2* and aerobactin, which had been detected in Illumina data of C38 strain, were not found in the complete plasmid sequence, manifesting that these two genes were located on chromosome. By contrast, the pLVPK-like plasmid was detected in 11 ST11 bla_{KPC-2} isolates. This plasmid harbored a set of virulence genes, including *iroBCDN*, *iucABCD*,

rmpA, and *rmpA2*, indicating that the hypervirulent phenotypes of these strains were mediated by plasmids.

Unlike the traditional hypervirulent serotype KL1, KL2, and KL57, the major types of bla_{KPC-2}-positive strains in this study were KL47 and KL64. In the early years, there were few reports regarding KL47 and KL64 hypervirulent *K. pneumoniae*. However, in recent 2 years, reports began to emerge (Liu et al., 2019b; Xie et al., 2020; Yang et al., 2020a; Zhang et al., 2020), and most of them were found in China. A recent study demonstrated that ST11-KL64 and ST11-KL47 isolates with enhanced virulence and transmissibility have emerged and undergone local expansion in China (Zhou et al., 2020). Our study also highlighted the potential hypervirulence of these two serotypes; more attention should be focused on them in further investigation.

In this study, bla_{NDM-1}-positive CRKP occurred locally, as they were solely detected in children cardiac ICU with low virulence. The bla_{NDM-1} gene derived from pediatrics n China were frequently reported (Ding et al., 2019; Wang et al., 2020). *Klebsiella pneumoniae* was regarded as a key trafficker of AMR genes from environmental to clinical settings, and hundreds of mobile AMR genes have been found in this species (Wyres and Holt, 2018). Hence, it could explain why ST304 and ST1383 *K. pneumoniae* isolates were found to harbor bla_{NDM} in our study. Apart from IncX3 plasmid, bla_{NDM} was found in large MDR plasmids, including IncHI5-like and IncFIB/IncHI1B plasmids. The characteristics of IncFIB/IncHI1B plasmid harboring carbapenemase-encoding genes have been described previously (Matsumura et al., 2018). However, the structure of bla_{NDM-1}-bearing plasmid containing IncFIB/IncHI1B replicons in our study was novel. It was a megaplasmid and carried the resistance determinants to heavy metals and several conjugal transfer genes. Abundant insertion sequences and two integrons were distributed in different locations among accessory regions, which might drive the formation of the novel structure of this plasmid. These findings alert us that the surveillance of bla_{NDM-1} in nosocomial setting needs to be strengthened.

There are still some drawbacks in this study. First, the sample size was not enough to objectively elucidate the distribution of CRKP in a large region. Second, the results of this study may not be able to apply to other hospitals. Besides, the strategy of sample collection should be improved in future studies; in addition to patients, more attention should focus on the nosocomial environment and staffs.

CONCLUSION

The data presented in this study revealed two types of CRKP (bla_{KPC-2} and bla_{NDM-1}) with distinct epidemiological features occurring in a newly established hospital in Henan province. Carbapenem exposure was associated with emergence of CRKP. These strains with superior viability constitute substantial threats in clinical settings. The clonal spread of ST11 hypervirulent bla_{KPC-2}-positive *K. pneumoniae*, the occurrence of bla_{NDM-1}-positive *K. pneumoniae* with novel ST type, and the dissemination of novel carbapenemase-encoding plasmids should be included in future surveillance priorities.

DATA AVAILABILITY STATEMENT

The datasets presented in this study can be found in online repositories. The names of the repository/repositories and accession number(s) can be found in the article/ **Supplementary Material**.

AUTHOR CONTRIBUTIONS

RL and ZW designed and supervised the project. RC, ZL, PX, and XQ collected the strains, performed the experiments, and analyzed data. ZL, RL, and RC drafted the manuscript. RL and SQ revised the manuscript. All authors approved the final version for submission.

FUNDING

This work was supported by the Henan Province Medical Science and Technology Research Joint Construction Project (LHGJ20200073), the Natural Science Foundation of Jiangsu Province (BK20180900), the National Natural Science Foundation of China (U2004125), and the Priority Academic Program Development of Jiangsu Higher Education Institutions (PAPD).

ACKNOWLEDGMENTS

We are grateful to referees for critical comments to improve this manuscript.

SUPPLEMENTARY MATERIAL

The Supplementary Material for this article can be found online at: https://www.frontiersin.org/articles/10.3389/fmicb.2021.741093/full#supplementary-material

REFERENCES

Alikhan, N. F., Petty, N. K., Ben Zakour, N. L., and Beatson, S. A. (2011). BLAST Ring Image Generator (BRIG): simple prokaryote genome comparisons. *BMC Genomics* 12:402. doi: 10.1186/1471-2164-12-402

Andrade, L. N., Vitali, L., Gaspar, G. G., Bellissimo-Rodrigues, F., Martinez, R., and Darini, A. L. (2014). Expansion and evolution of a virulent, extensively drug-resistant (polymyxin B-resistant), QnrS1-, CTX-M- 2-, and KPC-2-producing *Klebsiella pneumoniae* ST11 international high-risk clone. *J. Clin. Microbiol.* 52, 2530–2535. doi: 10.1128/JCM.00088-14

Bachman, M. A., Oyler, J. E., Burns, S. H., Caza, M., Lepine, F., Dozois, C. M., et al. (2011). *Klebsiella pneumoniae* yersiniabactin promotes respiratory tract infection through evasion of lipocalin 2. *Infect. Immun.* 79, 3309–3316. doi: 10.1128/IAI.05114-11

Bankevich, A., Nurk, S., Antipov, D., Gurevich, A. A., Dvorkin, M., Kulikov, A. S., et al. (2012). SPAdes: a new genome assembly algorithm and its applications to single-cell sequencing. *J. Comput. Biol.* 19, 455–477. doi: 10.1089/cmb.2012.0021

Chen, L., and Kreiswirth, B. N. (2018). Convergence of carbapenem-resistance and hypervirulence in *Klebsiella pneumoniae*. *Lancet Infect. Dis.* 18, 2–3. doi: 10.1016/s1473-3099(17)30517-0

Chen, L., Mathema, B., Chavda, K. D., DeLeo, F. R., Bonomo, R. A., and Kreiswirth, B. N. (2014). Carbapenemase-producing *Klebsiella pneumoniae*: molecular and genetic decoding. *Trends Microbiol.* 22, 686–696. doi: 10.1016/j.tim.2014.09.003

Chen, S., Hu, F., Xu, X., Liu, Y., Wu, W., Zhu, D., et al. (2011). High prevalence of KPC-2-type carbapenemase coupled with CTX-M-type extended-spectrum beta-lactamases in carbapenem-resistant *Klebsiella pneumoniae* in a teaching hospital in China. *Antimicrob. Agents Chemother.* 55, 2493–2494. doi: 10.1128/AAC.00047-11

Clinical and Laboratory Standards Institute [CLSI] (2018). *Performance Standards for Antimicrobial Susceptibility Testing: Twenty-Fourth Informational Supplement, M100-S28*. Wayne, PA: CLSI.

Ding, Y., Wang, Y., Hsia, Y., Sharland, M., and Heath, P. T. (2019). Systematic review of carbapenem-resistant *Enterobacteriaceae* causing neonatal sepsis in China. *Ann. Clin. Microbiol. Antimicrob.* 18:36. doi: 10.1186/s12941-019-0334-9

Gundogdu, A., Ulu-Kilic, A., Kilic, H., Ozhan, E., Altun, D., Cakir, O., et al. (2018). Could frequent carbapenem use be a risk factor for colistin resistance? *Microb. Drug Resist.* 24, 774–781. doi: 10.1089/mdr.2016.0321

Heiden, S. E., Hubner, N. O., Bohnert, J. A., Heidecke, C. D., Kramer, A., Balau, V., et al. (2020). A *Klebsiella pneumoniae* ST307 outbreak clone from Germany demonstrates features of extensive drug resistance, hypermucoviscosity, and enhanced iron acquisition. *Genome Med.* 12:113. doi: 10.1186/s13073-020-00814-6

Hu, Y., Liu, C., Shen, Z., Zhou, H., Cao, J., Chen, S., et al. (2020). Prevalence, risk factors and molecular epidemiology of carbapenem-resistant *Klebsiella pneumoniae* in patients from Zhejiang, China, 2008-2018. *Emerg. Microbes Infect.* 9, 1771–1779. doi: 10.1080/22221751.2020.1799721

Lam, M. M. C., Wick, R. R., Wyres, K. L., Gorrie, C. L., Judd, L. M., Jenney, A. W. J., et al. (2018). Genetic diversity, mobilisation and spread of the yersiniabactin-encoding mobile element ICEKp in *Klebsiella pneumoniae* populations. *Microb. Genom.* 4:e000196. doi: 10.1099/mgen.0.000196

Lee, C. H., Su, T. Y., Ye, J. J., Hsu, P. C., Kuo, A. J., Chia, J. H., et al. (2017). Risk factors and clinical significance of bacteremia caused by *Pseudomonas aeruginosa* resistant only to carbapenems. *J. Microbiol. Immunol. Infect.* 50, 677–683. doi: 10.1016/j.jmii.2015.06.003

Li, R., Cheng, J., Dong, H., Li, L., Liu, W., Zhang, C., et al. (2020). Emergence of a novel conjugative hybrid virulence multidrug-resistant plasmid in extensively drug-resistant *Klebsiella pneumoniae* ST15. *Int. J. Antimicrob. Agents* 55:105952. doi: 10.1016/j.ijantimicag.2020.105952

Li, R., Xie, M., Dong, N., Lin, D., Yang, X., Wong, M. H. Y., et al. (2018). Efficient generation of complete sequences of MDR-encoding plasmids by rapid assembly of MinION barcoding sequencing data. *Gigascience* 7, 1–9. doi: 10.1093/gigascience/gix132

Liu, Z., Chen, R., Xu, P., Wang, Z., and Li, R. (2021). Characterization of a bla_{NDM-1}-Bearing IncHI5-like plasmid from *Klebsiella pneumoniae* of infant origin. *Front. Cell. Infect. Microbiol.* 11. doi: 10.3389/fcimb.2021.738053

Liu, J., Wang, H., Huang, Z., Tao, X., Li, J., Hu, Y., et al. (2019a). Risk factors and outcomes for carbapenem-resistant *Klebsiella pneumoniae* bacteremia in onco-hematological patients. *J. Infect. Dev. Ctries.* 13, 357–364. doi: 10.3855/jidc.11189

Liu, Z., Gu, Y., Li, X., Liu, Y., Ye, Y., Guan, S., et al. (2019b). Identification and characterization of NDM-1-producing hypervirulent (Hypermucoviscous) *Klebsiella pneumoniae* in China. *Ann. Lab. Med.* 39, 167–175. doi: 10.3343/alm.2019.39.2.167

Liu, P., Li, P., Jiang, X., Bi, D., Xie, Y., Tai, C., et al. (2012). Complete genome sequence of *Klebsiella pneumoniae* subsp. pneumoniae HS11286, a multidrug-resistant strain isolated from human sputum. *J. Bacteriol.* 194, 1841–1842. doi: 10.1128/JB.00043-12

Ma, T., Fu, J., Xie, N., Ma, S., Lei, L., Zhai, W., et al. (2020). Fitness cost of blaNDM-5-Carrying p3R-IncX3 plasmids in Wild-Type NDM-Free *Enterobacteriaceae*. *Microorganisms* 8:377. doi: 10.3390/microorganisms8030377

Matsumura, Y., Peirano, G., Bradford, P. A., Motyl, M. R., DeVinney, R., and Pitout, J. D. D. (2018). Genomic characterization of IMP and VIM carbapenemase-encoding transferable plasmids of *Enterobacteriaceae*. *J. Antimicrob. Chemother.* 73, 3034–3038. doi: 10.1093/jac/dky303

Munoz-Price, L. S., Poirel, L., Bonomo, R. A., Schwaber, M. J., Daikos, G. L., Cormican, M., et al. (2013). Clinical epidemiology of the global expansion of *Klebsiella pneumoniae* carbapenemases. *Lancet Infect. Dis.* 13, 785–796. doi: 10.1016/S1473-3099(13)70190-7

Navon-Venezia, S., Kondratyeva, K., and Carattoli, A. (2017). *Klebsiella pneumoniae*: a major worldwide source and shuttle for antibiotic resistance. *FEMS Microbiol. Rev.* 41, 252–275. doi: 10.1093/femsre/fux013

Page, A. J., Cummins, C. A., Hunt, M., Wong, V. K., Reuter, S., Holden, M. T., et al. (2015). Roary: rapid large-scale prokaryote pan genome analysis. *Bioinformatics* 31, 3691–3693. doi: 10.1093/bioinformatics/btv421

Patel, P. K., Russo, T. A., and Karchmer, A. W. (2014). Hypervirulent *Klebsiella pneumoniae*. *Open Forum Infect. Dis.* 1:ofu028. doi: 10.1093/ofid/ofu028

Pau, C. K., Ma, F. F., Ip, M., and You, J. H. (2015). Characteristics and outcomes of *Klebsiella pneumoniae* bacteraemia in Hong Kong. *Infect. Dis. (Lond.)* 47, 283–288. doi: 10.3109/00365548.2014.985710

Poirel, L., Walsh, T. R., Cuvillier, V., and Nordmann, P. (2011). Multiplex PCR for detection of acquired carbapenemase genes. *Diagn. Microbiol. Infect. Dis.* 70, 119–123. doi: 10.1016/j.diagmicrobio.2010.12.002

Price, M. N., Dehal, P. S., and Arkin, A. P. (2009). FastTree: computing large minimum evolution trees with profiles instead of a distance matrix. *Mol. Biol. Evol.* 26, 1641–1650. doi: 10.1093/molbev/msp077

Qin, S., Fu, Y., Zhang, Q., Qi, H., Wen, J. G., Xu, H., et al. (2014). High incidence and endemic spread of NDM-1-positive *Enterobacteriaceae* in Henan Province, China. *Antimicrob. Agents Chemother.* 58, 4275–4282. doi: 10.1128/AAC.02813-13

Russo, T. A., and Marr, C. M. (2019). Hypervirulent *Klebsiella pneumoniae*. *Clin. Microbiol. Rev.* 32:e00001-19. doi: 10.1128/CMR.00001-19

Russo, T. A., Olson, R., Fang, C. T., Stoesser, N., Miller, M., MacDonald, U., et al. (2018). Identification of biomarkers for differentiation of hypervirulent *Klebsiella pneumoniae* from classical *K. pneumoniae*. *J. Clin. Microbiol.* 56:e00776-18. doi: 10.1128/JCM.00776-18

Schaufler, K., Semmler, T., Pickard, D. J., de Toro, M., de la Cruz, F., Wieler, L. H., et al. (2016). Carriage of extended-spectrum beta-lactamase-plasmids does not reduce fitness but enhances virulence in some strains of pandemic *E. coli* Lineages. *Front. Microbiol.* 7:336. doi: 10.3389/fmicb.2016.00336

Schubert, S., Cuenca, S., Fischer, D., and Heesemann, J. (2000). High-pathogenicity island of Yersinia pestis in *enterobacteriaceae* isolated from blood cultures and urine samples: prevalence and functional expression. *J. Infect. Dis.* 182, 1268–1271. doi: 10.1086/315831

Schwyn, B., and Neilands, J. B. (1987). Universal chemical assay for the detection and determination of siderophores. *Anal. Biochem.* 160, 47–56. doi: 10.1016/0003-2697(87)90612-9

Shon, A. S., Bajwa, R. P., and Russo, T. A. (2013). Hypervirulent (hypermucoviscous) *Klebsiella pneumoniae*: a new and dangerous breed. *Virulence* 4, 107–118. doi: 10.4161/viru.22718

Walker, K. A., Miner, T. A., Palacios, M., Trzilova, D., Frederick, D. R., Broberg, C. A., et al. (2019). A *Klebsiella pneumoniae* regulatory mutant has reduced capsule expression but retains hypermucoviscosity. *mBio* 10:e00089-19. doi: 10.1128/mBio.00089-19

Wang, B., Pan, F., Wang, C., Zhao, W., Sun, Y., Zhang, T., et al. (2020). Molecular epidemiology of Carbapenem-resistant *Klebsiella pneumoniae* in a paediatric hospital in China. *Int. J. Infect. Dis.* 93, 311–319. doi: 10.1016/j.ijid.2020.02.009

Wang, R., Yang, Q., Zhang, S., Hong, Y., Zhang, M., and Jiang, S. (2019). Trends and correlation of antibiotic susceptibility and antibiotic consumption at a large teaching hospital in China (2007-2016): a surveillance study. *Ther. Clin. Risk Manag.* 15, 1019–1027. doi: 10.2147/TCRM.S210872

Wick, R. R., Heinz, E., Holt, K. E., and Wyres, K. L. (2018). Kaptive Web: user-friendly capsule and lipopolysaccharide serotype prediction for *Klebsiella* Genomes. *J. Clin. Microbiol.* 56:e00197-18. doi: 10.1128/JCM.00197-18

Wick, R. R., Judd, L. M., Gorrie, C. L., and Holt, K. E. (2017). Unicycler: resolving bacterial genome assemblies from short and long sequencing reads. *PLoS Comput. Biol.* 13:e1005595. doi: 10.1371/journal.pcbi.1005595

Wong, M. H. Y., Shum, H.-P., Chen, J. H. K., Man, M.-Y., Wu, A., Chan, E. W.-C., et al. (2018a). Emergence of carbapenem-resistant hypervirulent *Klebsiella pneumoniae*. *Lancet Infect. Dis.* 18:24. doi: 10.1016/s1473-3099(17)30629-1

Wong, M. H. Y., Shum, H. P., Chen, J. H. K., Man, M. Y., Wu, A., Chan, E. W., et al. (2018b). Emergence of carbapenem-resistant hypervirulent *Klebsiella pneumoniae*. *Lancet Infect. Dis.* 18:24. doi: 10.1016/S1473-3099(17)30629-1

Wu, W., Feng, Y., Tang, G., Qiao, F., McNally, A., and Zong, Z. (2019). NDM metallo-beta-lactamases and their bacterial producers in health care settings. *Clin. Microbiol. Rev.* 32:e00115-18. doi: 10.1128/CMR.00115-18

Wyres, K. L., and Holt, K. E. (2018). *Klebsiella pneumoniae* as a key trafficker of drug resistance genes from environmental to clinically important bacteria. *Curr. Opin. Microbiol.* 45, 131–139. doi: 10.1016/j.mib.2018.04.004

Xie, M., Dong, N., Chen, K., Yang, X., Ye, L., Chan, E. W., et al. (2020). A hybrid plasmid formed by recombination of a virulence plasmid and a resistance plasmid in *Klebsiella pneumoniae*. *J. Glob. Antimicrob. Resist*. 23, 466–470. doi: 10.1016/j.jgar.2020.10.018

Xie, Y., Tian, L., Li, G., Qu, H., Sun, J., Liang, W., et al. (2018). Emergence of the third-generation cephalosporin-resistant hypervirulent *Klebsiella pneumoniae* due to the acquisition of a self-transferable blaDHA-1-carrying plasmid by an ST23 strain. *Virulence* 9, 838–844. doi: 10.1080/21505594.2018.1456229

Xu, M., Fu, Y., Fang, Y., Xu, H., Kong, H., Liu, Y., et al. (2019). High prevalence of KPC-2-producing hypervirulent *Klebsiella pneumoniae* causing meningitis in Eastern China. *Infect. Drug. Resist.* 12, 641–653. doi: 10.2147/IDR.S191892

Yang, J., Ye, L., Guo, L., Zhao, Q., Chen, R., Luo, Y., et al. (2013). A nosocomial outbreak of KPC-2-producing *Klebsiella pneumoniae* in a Chinese hospital: dissemination of ST11 and emergence of ST37, ST392 and ST395. *Clin. Microbiol. Infect.* 19, E509–E515. doi: 10.1111/1469-0691.12275

Yang, Q., Jia, X., Zhou, M., Zhang, H., Yang, W., Kudinha, T., et al. (2020a). Emergence of ST11-K47 and ST11-K64 hypervirulent carbapenem-resistant *Klebsiella pneumoniae* in bacterial liver abscesses from China: a molecular, biological, and epidemiological study. *Emerg. Microbes Infect.* 9, 320–331. doi: 10.1080/22221751.2020.1721334

Yang, X., Dong, N., Chan, E. W., Zhang, R., and Chen, S. (2020b). Carbapenem resistance-encoding and virulence-encoding conjugative plasmids in *Klebsiella pneumoniae*. *Trends Microbiol.* 29, 65–83. doi: 10.1016/j.tim.2020.04.012

Yao, H., Qin, S., Chen, S., Shen, J., and Du, X. D. (2018). Emergence of carbapenem-resistant hypervirulent *Klebsiella pneumoniae*. *Lancet Infect. Dis.* 18:25. doi: 10.1016/S1473-3099(17)30628-X

Yu, F., Lv, J., Niu, S., Du, H., Tang, Y. W., Pitout, J. D. D., et al. (2018). Multiplex PCR analysis for rapid detection of *Klebsiella pneumoniae* carbapenem-resistant (sequence Type 258 [ST258] and ST11) and hypervirulent (ST23, ST65, ST86, and ST375) Strains. *J. Clin. Microbiol.* 56:e00731-18. doi: 10.1128/JCM.00731-18

Zhang, D., Cui, K., Wang, T., Shan, Y., Dong, H., Feng, W., et al. (2018). Risk factors for carbapenem-resistant *Pseudomonas aeruginosa* infection or colonization in a Chinese teaching hospital. *J. Infect. Dev. Ctries.* 12, 642–648. doi: 10.3855/jidc.10150

Zhang, Y., Jin, L., Ouyang, P., Wang, Q., Wang, R., Wang, J., et al. (2020). Evolution of hypervirulence in carbapenem-resistant *Klebsiella pneumoniae* in China: a multicentre, molecular epidemiological analysis. *J. Antimicrob. Chemother.* 75, 327–336. doi: 10.1093/jac/dkz446

Zheng, B., Xu, H., Lv, T., Guo, L., Xiao, Y., Huang, C., et al. (2020). Stool samples of acute diarrhea inpatients as a reservoir of ST11 hypervirulent KPC-2-producing *Klebsiella pneumoniae*. *mSystems* 5:e00498-20. doi: 10.1128/mSystems.00498-20

Zhou, K., Xiao, T., David, S., Wang, Q., Zhou, Y., Guo, L., et al. (2020). Novel subclone of carbapenem-resistant *Klebsiella pneumoniae* sequence Type 11 with enhanced virulence and transmissibility, China. *Emerg. Infect. Dis.* 26, 289–297. doi: 10.3201/eid2602.190594

Conflict of Interest: The authors declare that the research was conducted in the absence of any commercial or financial relationships that could be construed as a potential conflict of interest.

frontiers in Microbiology

ORIGINAL RESEARCH
published: 18 November 2021
doi: 10.3389/fmicb.2021.756410

Quantitative Insights Into β-Lactamase Inhibitor's Contribution in the Treatment of Carbapenemase-Producing Organisms With β-Lactams

*Yanfang Feng[1], Arend L. de Vos[1,2], Shakir Khan[1,3], Mary St. John[1,4] and Tayyaba Hasan[1,5]**

[1]Wellman Center for Photomedicine, Massachusetts General Hospital, Harvard Medical School, Boston, MA, United States, [2]Swammerdam Institute for Life Sciences, University of Amsterdam, Amsterdam, Netherlands, [3]Department of Physics, University of Massachusetts, Boston, MA, United States, [4]School of Arts and Sciences, Tufts University, Medford, MA, United States, [5]Health Sciences and Technology (Harvard-MIT), Cambridge, MA, United States

OPEN ACCESS

Edited by:
Mullika Traidej Chomnawang, Faculty of Pharmacy, Mahidol University, Thailand

Reviewed by:
Soojin Jang, Korea Pasteur Institute, South Korea
Krit Thirapanmethee, Mahidol University, Thailand

***Correspondence:**
Tayyaba Hasan
thasan@mgh.harvard.edu

Specialty section:
This article was submitted to Antimicrobials, Resistance and Chemotherapy, a section of the journal Frontiers in Microbiology

Received: *10 August 2021*
Accepted: *28 October 2021*
Published: *18 November 2021*

Citation:
Feng Y, de Vos AL, Khan S, St. John M and Hasan T (2021) Quantitative Insights Into β-Lactamase Inhibitor's Contribution in the Treatment of Carbapenemase-Producing Organisms With β-Lactams. Front. Microbiol. 12:756410. doi: 10.3389/fmicb.2021.756410

Objectives: Carbapenemase-producing organisms (CPOs) are associated with high mortality rates. The recent development of β-lactamase inhibitors (BLIs) has made it possible to control CPO infections safely and effectively with β-lactams (BLs). This study aims to explicate the quantitative relationship between BLI's β-lactamase inhibition and CPO's BL susceptibility restoration, thereby providing the infectious disease society practical scientific grounds for regulating the use of BL/BLI in CPO infection treatment.

Methods: A diverse collection of human CPO infection isolates was challenged by three structurally representative BLIs available in the clinic. The resultant β-lactamase inhibition, BL susceptibility restoration, and their correlation were followed quantitatively for each isolate by coupling FIBA (fluorescence identification of β-lactamase activity) and BL antibiotic susceptibility testing.

Results: The β-lactamase inhibition and BL susceptibility restoration are positively correlated among CPOs under the treatment of BLIs. Both of them are dependent on the target CPO's carbapenemase molecular identity. Of note, without sufficient β-lactamase inhibition, CPO's BL susceptibility restoration is universally low across all tested carbapenemase molecular groups. However, a high degree of β-lactamase inhibition would not necessarily lead to a substantial BL susceptibility restoration in CPO probably due to the existence of non-β-lactamase BL resistance mechanisms.

Conclusion: BL/BLI choice and dosing should be guided by quantitative tools that can evaluate the inhibition across the entire β-lactamase background of the CPO upon the BLI administion. Furthermore, rapid molecular diagnostics for BL/BLI resistances, especially those sensitive to β-lactamase independent BL resistance mechanisms, should be exploited to prevent ineffective BL/BLI treatment.

Keywords: carbapenemase, β-lactamase inhibitor, antimicrobial stewardship, β-lactam antibiotics, carbapenem resistance

INTRODUCTION

Carbapenemase-producing organisms (CPOs) are multidrug-resistant pathogens associated with high mortality rates (13.3–67%; Tamma et al., 2017). The recent development of β-lactamase inhibitors (BLIs) that could inhibit carbapenemases, the most potent type of β-lactamases, has made it possible to control CPO infections safely and effectively with β-lactam (BL) antibiotics (Cui et al., 2019; El Hafi et al., 2019; Sheu et al., 2019; Pogue et al., 2020). Unfortunately, recent clinical data have emerged demonstrating that treatment failures and subsequent bacterial resistance development may occur in CPO treatments with BLs and novel BLIs, necessitating further development of guidelines on rational use of BLs and BLIs for CPO infections (Shields et al., 2016; Cui et al., 2020).

Clinically, BLIs are available together with β-lactam antibiotics (BLs) at fixed dosages, forming the so-called BL/BLI agents. The rational choice of BL/BLI for CPO infections could appear straightforward according to the knowledge of each BLI's carbapenemase inhibitory spectrum and carbapenemase type(s) of the CPO. However, whether the desired anti-CPO effect of the chosen BL/BLI agent could be achieved across diverse pathogens by a fixed BLI dosage is still of great concern for the infectious disease society (Spellberg and Bonomo, 2016) due to the large variety of CPO carbapenemase molecular structures and expression statuses. Moreover, many CPO co-produce other β-lactamases, including extended-spectrum β-lactamase (ESBL) and AmpC β-lactamase, both of which can reduce BLI activity (Ferreira et al., 2020; Shields and Doi, 2020). Additionally, the further complicating effects of other BL resistance mechanisms unrelated to β-lactamase (e.g., efflux pump overproduction, drug target alterations and porin mutations) and their influence on CPO response to BL/BLI agents remain unclear (Karumathil et al., 2018; Nicolas-Chanoine et al., 2018; Nordmann and Poirel, 2019; Black et al., 2020).

Our technology, fluorescence identification of β-lactamase activity (FIBA), has now enabled the quantification of β-lactamase activity in CPO regardless of their β-lactamase backgrounds (Sallum et al., 2010; Erdem et al., 2014; Khan et al., 2014; Feng et al., 2020, 2021). It uses β-lactamase enzyme-activated fluorophore (β-LEAF), which turns from dark to fluorescent when cleaved by β-lactamases, such as penicillinases, ESBL, AmpC β-lactamases, and carbapenemases. Therefore, the fluorescence increase rate (R) of β-LEAF is a direct measure of the activity of bacterial β-lactamases, and R is decreased as the β-lactamase activity is inhibited by BLIs. By coupling FIBA with BL susceptibility detection, this study aims to explicate the quantitative relationship between β-lactamase inhibition and BL susceptibility restoration in CPO under BLI treatment, thereby providing a detailed insight into the contribution of BLIs in CPO treatment with BLs. To this end, a diverse collection of human CPO infection isolates was challenged by three structurally representative BLIs available in the clinic (clavulanate, vaborbactam, and avibactam) to generate broadly applicable conclusions. The resultant β-lactamase inhibition, BL susceptibility restoration, and their quantitative correlation were investigated for different carbapenemase molecular groups to assist the future development of the current carbapenemase molecular type-derived BL/BLI administration guidelines for CPO infections.

MATERIALS AND METHODS

Bacterial Isolates, BL and BLIs

Bacterial isolates of human CPO infection were acquired from the CDC and FDA Antibiotic Resistance Isolate Bank. The BL resistance mechanisms, including the β-lactamase production, were identified by analyzing the whole genome sequence of the isolates with the Resistance Gene Identifier of the Comprehensive Antibiotic Resistance Database (McArthur et al., 2013; Alcock et al., 2020). The information of the genome sequences (i.e., sequence accession numbers) of the tested isolates was provided by the CDC and FDA Antibiotic Resistance Isolate Bank, and is available on the official website of this isolate bank. Three BLIs (clavulanate, vaborbactam, avibactam) and their clinically combined partner BLs (amoxicillin for clavulanate; meropenem for vaborbactam; ceftazidime for avibactam) were purchased from Sigma-Aldrich. To facilitate comparison, all BLIs were tested at the same concentration attainable in patient plasma (50 μm) (Carlier et al., 2013; Nicolau et al., 2015; Lee et al., 2019).

Quantification of β-Lactamase Inhibition

BLI's β-lactamase inhibition was quantified by β-lactamase inhibition index (BI), which is defined as the ratio of β-lactamase activity with and without BLI. The β-lactamase activity was measured by FIBA as previously described (Feng et al., 2021). Briefly, bacterial culture was exposed to β-lactamase enzyme-activated fluorophore (β-LEAF), and the fluorescence increase rate (R), which is the direct measure of the β-lactamase activity, was then acquired by monitoring the β-LEAF fluorescence every 10 s for 10 min with an excitation wavelength of 450 nm and an emission wavelength of 510 nm at 37°C. Thus, BI could be acquired by the equation below:

$$BI = R^{\text{without BLI}} / R^{\text{with BLI}}$$

BL Susceptibility Restoration

The BL susceptibility, with and without the three tested BLIs, was determined by measuring the minimal inhibitory concentration (MIC) with the broth microdilution method following the Clinical and Laboratory Standards Institute guidelines. The MIC reduction of BL due to the addition of BLI was defined as the BL susceptibility restoration in response to the tested BLI. An isolate with BL MIC reduced 4-fold was considered sensitized toward the tested BL by the inclusion of the tested BLI.

Statistical Analysis

Data analysis was performed in R (v3.6.3). BI and BL susceptibility restoration was compared among BLIs using Kruskal-Wallis

followed by *post hoc* pairwise Dunn testing. The quantitative correlation of BI with the ratio of sensitized isolates for each BLI was analyzed by the polynomial regression model. All statistical analyses were considered significant at a value of $p < 0.05$.

RESULTS

This study tested CPO infection isolates from 15 different species, including *Pseudomonas aeruginosa*, *Acinetobacter baumannii*, and 13 *Enterobacteriaceae* species, as shown in **Tables 1**–**3**. These isolates produce a range of carbapenemase molecular classes commonly found in clinic, including Class A carbapenemases ($n = 43$, **Table 1**), Class B carbapenemases ($n = 45$, **Table 2**), and Class D carbapenemases ($n = 73$, **Table 3**). Besides carbapenemases, many of the tested isolates co-produce non-carbapenemase β-lactamases, such as ESBL (59%) and AmpC β-lactamase (84%), reflecting CPO's "complex β-lactamase background" encountered in clinic. In addition to β-lactamase, other β-lactam resistance mechanisms, such as overexpression of efflux pumps, inactivation of drug target, and porin mutations, are also found among most of the tested isolates (**Tables 1**–**3**), illustrating the multifactorial nature of BL resistance in CPO.

Upon the same BLI exposure, the β-lactamase inhibition, quantified by BI, varies widely from one isolate to another

TABLE 1 | Class A carbapenemase-producing isolates included in this study.

Carba subtype	Species	BL susceptibility (With/without BLI)			Other BL resistance Mechanisms		
		AMX/CA	MPN/VB	CFZ/AV	Efflux pumps	Reduced permeability	Target alteration
KPC	*C. freundii*	>1024/>1024	512/≤0.5	>1024/≤0.5	Y	Y	Y
	E. cloacae	>1024/1024	32/32	>1024/4	Y	Y	Y
		>1024/>1024	256/≤0.5	>1024/≤0.5	Y	Y	Y
		>1024/>1024	64/≤0.5	1024/≤0.5	Y	Y	Y
		>1024/>1024	>1024/1	>1024/256	Y	Y	Y
		>1024/>1024	64/≤0.5	1024/≤0.5	Y	Y	Y
		>1024/>1024	64/≤0.5	512/1	–	–	–
		>1024/>1024	128/≤0.5	>1024/2	–	–	–
		>1024/>1024	64/≤0.5	>1024/2	–	–	–
		>1024/>1024	256/1	>1024/2	–	–	–
	E. coli	>1024/1024	16/≤0.5	≤0.5/≤0.5	Y	Y	Y
		>1024/>1024	128/64	>1024/4	Y	Y	Y
		>1024/>1024	16/≤0.5	>1024/≤0.5	Y	Y	Y
		>1024/>1024	128/≤0.5	256/≤0.5	–	–	–
	K. oxytoca	>1024/1024	32/≤0.5	>1024/≤0.5	Y	Y	Y
	K. ozaenae	>1024/>1024	256/≤0.5	128/≤0.5	Y	Y	Y
	K. pneumoniae	>1024/>1024	1024/16	>1024/1024	Y	Y	Y
		>1024/>1024	1024/≤0.5	256/≤0.5	Y	Y	Y
		>1024/>1024	1024/16	>1024/8	Y	Y	Y
		>1024/>1024	>1024/128	>1024/8	Y	Y	Y
		>1024/>1024	1024/16	>1024/8	Y	Y	Y
		>1024/>1024	1024/2	>1024/8	Y	Y	Y
		>1024/>1024	>1024/64	>1024/1024	Y	Y	Y
		>1024/>1024	>1024/32	>1024/>1024	Y	Y	Y
		>1024/>1024	512/8	512/2	Y	Y	Y
		>1024/4	32/8	1024/≤0.5	Y	Y	Y
		>1024/>1024	128/≤0.5	128/≤0.5	–	–	–
		>1024/>1024	4/≤0.5	512/≤0.5	–	–	–
		256/256	128/≤0.5	16/≤0.5	–	–	–
		>1024/>1024	256/4	128/2	–	–	–
		>1024/>1024	1024/8	>1024/2	–	–	–
		>1024/>1024	256/4	>1024/1	–	–	–
		>1024/>1024	1024/32	>1024/1	–	–	–
		>1024/>1024	512/16	1024/2	–	–	–
		>1024/>1024	128/≤0.5	>1024/0.5	–	–	–
		>1024/256	512/4	256/1	–	–	–
		>1024/>1024	128/2	1024/1	–	–	–
		>1024/>1024	64/1	64/≤0.5	–	–	–
		>1024/>1024	64/≤0.5	256/≤0.5	–	–	–
	M. morganii	>1024/>1024	16/≤0.5	>1024/2	Y	N	Y
	P. mirabilis	>1024/>1024	256/128	>1024/1024	Y	N	Y
		512/64	4/4	128/128	Y	N	Y

Carba, carbapenemase; β-lactams (BLs) tested include CA (clavulanate), VB (vaborbactam), AV (avibactam); Partner β-lactamase inhibitors (BLIs) tested include CA (clavulanate), VB (vaborbactam), AV (avibactam); –, Not available.

TABLE 2 | Class B carbapenemase-producing isolates included in this study.

Carba subtype	Species	BL susceptibility (With/without BLI)			Other BL resistance Mechanisms		
		AMX/CA	MPN/VB	CFZ/AV	Efflux pumps	Reduced permeability	Target alteration
IMP	*K. aerogenes*	>1024/≤0.5	32/32	1024/64	Y	Y	Y
	K. pneumoniae	>1024/>1024	128/128	>1024/>1024	Y	Y	Y
	P. aeruginosa	>1024/>1024	1024/1024	>1024/1024	Y	N	Y
		>1024/>1024	>1024/>1024	>1024/>1024	Y	N	Y
NDM	*A. baumannii*	>1024/>128	512/512	>1024/>1024	Y	N	N
	C. freundii	>1024/>1024	>1024/>1024	>1024/1024	Y	Y	Y
	E. coli	>1024/>1024	>1024/>1024	>1024/>1024	Y	Y	Y
		>1024/>1024	>1024/>1024	>1024/>1024	Y	Y	Y
		>1024/>1024	8/≤0.5	>1024/1024	Y	Y	Y
		>1024/>1024	512/512	>1024/≤0.5	Y	Y	Y
		>1024/>1024	256/256	>1024/>1024	Y	Y	Y
		>1024/>1024	1024/1024	>1024/>1024	Y	Y	Y
		>1024/>1024	1024/1024	>1024/>1024	Y	Y	Y
		>1024/>1024	>1024/>1024	>1024/>1024	Y	Y	Y
		>1024/≤0.5	1024/1024	>1024/≤0.5	Y	Y	Y
		>1024/≤0.5	>1024/>1024	>1024/≤0.5	Y	Y	Y
		>1024/>1024	512/512	>1024/>1024	Y	Y	Y
	K. pneumoniae	>1024/512	512/512	>1024/>1024	Y	Y	Y
		>1024/>1024	1024/1024	>1024/512	Y	Y	Y
		>1024/>1024	256/256	>1024/>1024	Y	Y	Y
		>1024/>1024	>1024/>1024	>1024/>1024	Y	Y	Y
		>1024/>1024	>1024/>1024	1024/1024	Y	Y	Y
		>1024/≤0.5	512/512	>1024/256	Y	Y	Y
		>1024/>1024	1024/1024	>1024/>1024	Y	Y	Y
		>1024/>1024	512/512	>1024/>1024	Y	Y	Y
		>1024/>1024	1024/1024	>1024/>1024	Y	Y	Y
		>1024/>1024	>1024/>1024	>1024/>1024	Y	Y	Y
		>1024/>1024	512/512	>1024/512	Y	Y	Y
		>1024/>1024	1024/1024	>1024/>1024	Y	Y	Y
	M. morganii	>1024/>1024	16/8	>1024/>1024	Y	N	Y
	P. mirabilis	>1024/>1024	512/512	>1024/>1024	Y	N	Y
	*P. rett*geri	>1024/>1024	>1024/>1024	>1024/>1024	Y	N	Y
	S. senftenberg	>1024/>1024	1024/1024	>1024/>1024	Y	Y	Y
SPM	*P. aeruginosa*	>1024/>1024	>1024/>1024	>1024/>1024	Y	N	Y
VIM	*E. cloacae*	>1024/>1024	>1024/>1024	>1024/>1024	Y	Y	Y
	K. pneumoniae	>1024/>1024	>1024/>1024	>1024/>1024	Y	Y	Y
		>1024/>1024	>1024/>1024	>1024/>1024	N	N	N
		>1024/>1024	>1024/>1024	128/128	Y	Y	Y
		>1024/>1024	>1024/>1024	>1024/>1024	Y	Y	Y
	P. aeruginosa	>1024/>1024	>1024/>1024	>1024/>1024	Y	N	Y
		>1024/>1024	512/512	256/128	Y	N	Y
		>1024/>1024	>1024/1024	>1024/>1024	Y	N	Y
		>1024/>1024	512/512	>1024/64	Y	N	Y
		>1024/>1024	256/256	64/16	Y	N	Y

Carba, carbapenemase; β-lactams (BLs) tested include CA (clavulanate), VB (vaborbactam), AV (avibactam); Partner β-lactamase inhibitors (BLIs) tested include CA (clavulanate), VB (vaborbactam), AV (avibactam).

within the same carbapenemase molecular group of CPO (**Figure 1A**). Despite the individual heterogeneity, each carbapenemase molecular group of CPO has its own superior BLI (s): KPC isolates have high BIs induced by avibactam/vaborbactam and a lower BI led by clavulanate; MBL isolates are overall resistant to all tested BLIs (BIs <0.5); among OXA isolates, the most potent β-lactamase inhibition is induced by avibactam followed by vaborbactam and clavulanate.

Same to the β-lactamase inhibition, the BL susceptibility restoration in response to each BLI has also shown a great extent of individual heterogeneity in the same carbapenemase molecular group of CPO (**Figure 1B**). Significantly, a higher degree of β-lactamase inhibition (**Figure 1A**) is often corresponding to a bigger scale of partner BL MIC reduction (**Figure 1B**). For example, avibactam and vaborbactam, which lead to a stronger β-lactamase inhibition compared to clavulanate among KPC islates, result in a bigger decrease of partner BL MIC versus clavulanate among KPC isolates. As the most potent BLI for OXA type of CPO isolates, avibactam result in the highest partner BL MIC reduction in comparison with the other two tested BLIs among the

TABLE 3 | Class D Carbapenemase-producing isolates included in this study.

Carba Subtype	Species	BL susceptibility (With/without BLI)			Other BL resistance Mechanisms		
		AMX/CA	MPN/VB	CFZ/AV	Efflux pumps	Reduced permeability	Target alteration
OXA	*A. baumannii*	>1024/>1024	256/256	128/2	Y	N	N
		>1024/>1024	128/128	128/4	Y	N	N
		>1024/>1024	1024/1024	>1024/>1024	Y	N	N
		>1024/>1024	64/64	256/≤0.5	Y	Y	Y
		>1024/>1024	>1024/>1024	>1024/2	Y	N	N
		>1024/>1024	64/64	>1024/4	Y	N	N
		>1024/>1024	64/64	>1024/8	Y	N	N
		>1024/>1024	8/8	16/≤0.5	Y	N	N
		>1024/>1024	32/16	>1024/2	Y	N	N
		>1024/>1024	64/4	512/8	Y	N	N
		>1024/128	512/512	>1024/>1024	Y	N	N
		>1024/>1024	128/128	128/8	Y	N	N
		>1024/>1024	128/128	64/8	Y	N	N
	C. freundii	>1024/>1024	>1024/>1024	>1024/1024	Y	Y	Y
	E. cloacae	>1024/8	512/512	>1024/>1024	Y	Y	Y
		>1024/>1024	256/≤0.5	>1024/≤0.5	Y	Y	Y
		>1024/>1024	64/≤0.5	1024/≤0.5	Y	Y	Y
		>1024/>1024	>1024/1	>1024/256	Y	Y	Y
		>1024/>1024	64/≤0.5	>1024/≤0.5	Y	Y	Y
	E. coli	>1024/>1024	>1024/>1024	>1024/>1024	Y	Y	Y
		>1024/>1024	>1024/>1024	>1024/>1024	Y	Y	Y
		>1024/1024	16/≤0.5	≤0.5/≤0.5	Y	Y	Y
		>1024/>1024	512/512	>1024/≤0.5	Y	Y	Y
		>1024/>1024	256/256	>1024/>1024	Y	Y	Y
		>1024/>1024	1024/1024	>1024/>1024	Y	Y	Y
		>1024/>1024	1024/1024	>1024/>1024	Y	Y	Y
	K. aerogenes	>1024/≤0.5	32/32	1024/64	Y	Y	Y
	K. ozaenae	>1024/>1024	256/≤0.5	128/≤0.5	Y	Y	Y
	K. pneumoniae	>1024/>1024	64/64	>1024/≤0.5	Y	Y	Y
		>1024/>1024	>1024/>1024	>1024/>1024	Y	Y	Y
		>1024/512	512/512	>1024/>1024	Y	Y	Y
		>1024/>1024	64/32	>1024/1	Y	Y	Y
		>1024/128	4/4	>1024/256	Y	Y	Y
		>1024/>1024	>1024/>1024	>1024/>1024	N	N	N
		>1024/>1024	1024/1024	>1024/512	Y	Y	Y
		>1024/>1024	1024/16	>1024/1024	Y	Y	Y
		-	-	-		Y	Y
		>1024/>1024	256/256	>1024/>1024	Y	Y	Y
		>1024/>1024	64/64	>1024/1	Y	Y	Y
		>1024/>1024	128/128	>1024/>1024	Y	Y	Y
		>1024/128	256/256	>1024/512	Y	Y	Y
		>1024/>1024	16/8	>1024/8	Y	Y	Y
		>1024/>1024	1024/2	>1024/8	Y	Y	Y
		>1024/>1024	>1024/32	>1024/>1024	Y	Y	Y
		>1024/>1024	512/8	512/2	Y	Y	Y
		>1024/>1024	>1024/>1024	>1024/>1024	Y	Y	Y
		>1024/>1024	>1024/>1024	1024/1024		Y	Y
		>1024/>1024	512/16	>1024/>1024	Y	Y	Y
		>1024/>1024	1024/32	>1024/16	Y	Y	Y
		>1024/1024	8/2	>1024/16	Y	Y	Y
		>1024/≤0.5	512/512	>1024/256	Y	Y	Y
		>1024/>1024	1024/1024	>1024/>1024	Y	Y	Y
		>1024/>1024	512/512	>1024/>1024	Y	Y	Y
		>1024/>1024	1024/1024	>1024/>1024	Y	Y	Y
		>1024/>1024	>1024/>1024	>1024/>1024	Y	Y	Y
		>1024/>1024	512/512	>1024/512	Y	Y	Y
		>1024/>1024	1024/1024	>1024/>1024	Y	Y	Y
		>1024/>1024	64/32	≤0.5/≤0.5	Y	Y	Y
	M. morganii	>1024/>1024	16/8	>1024/>1024	Y	N	Y
	P. aeruginosa	>1024/>1024	>1024/>1024	>1024/>1024	Y	N	Y

(Continued)

Table 3 | Continued.

Carba Subtype	Species	BL susceptibility (With/without BLI)			Other BL resistance Mechanisms		
		AMX/CA	MPN/VB	CFZ/AV	Efflux pumps	Reduced permeability	Target alteration
		>1024/>1024	>1024/>1024	>1024/>1024	Y	N	Y
		>1024/>1024	256/16	>1024/1	Y	N	Y
		>1024/>1024	1024/1024	>1024/1024	Y	N	Y
		>1024/>1024	64/64	>1024/512	Y	N	Y
		>1024/>1024	64/64	16/4	Y	N	Y
		>1024/>1024	512/512	256/128	Y	N	Y
		>1024/>1024	>1024/>1024	>1024/>1024	Y	N	Y
		>1024/>1024	64/64	32/2	Y	N	Y
		>1024/>1024	>1024/1024	>1024/>1024	Y	N	Y
		>1024/>1024	512/512	>1024/64	Y	N	Y
		>1024/>1024	256/256	64/16	Y	N	Y
	P. mirabilis	512/64	4/4	128/128	Y	Y	Y

Carba, carbapenemase; β-lactams (BLs) tested include CA (clavulanate), VB (vaborbactam), AV (avibactam); Partner β-lactamase inhibitors (BLIs) tested include CA (clavulanate), VB (vaborbactam), AV (avibactam); –, Not available.

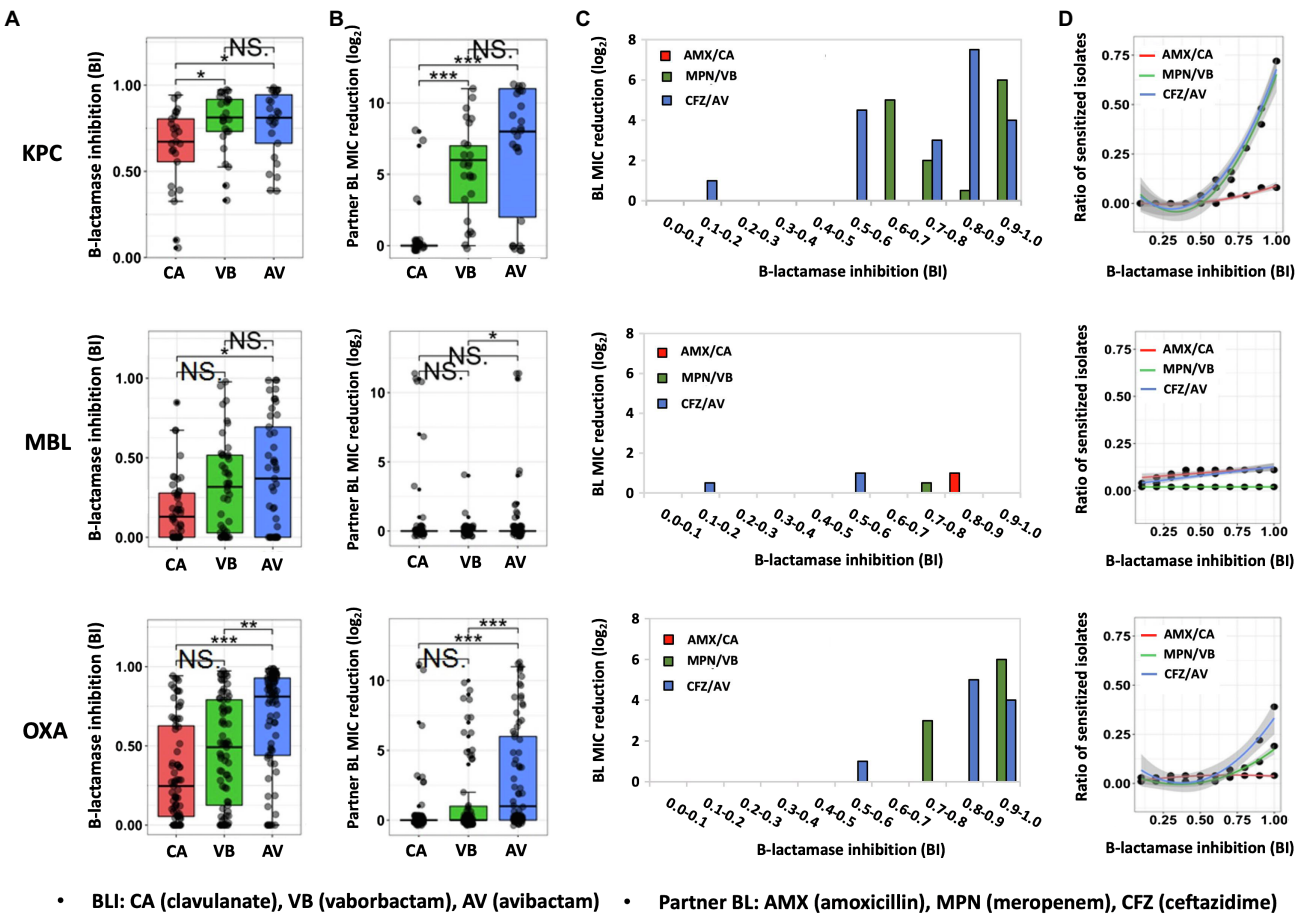

FIGURE 1 | Quantitative relationship between BLI's β-lactamase inhibition and its partner BL's susceptibility restoration in CPO human isolates. Distribution of β-lactamase inhibition **(A)** and the resulted partner BL susceptibility restoration **(B)** of three clinically representative BLIs (50 μM) in CPO human isolates containing KPC carbapenemase, MBL carbapenemase, OXA carbapenemase. Partner BL MIC reduction on average **(C)** and the ratio of sensitized isolates (BL MIC reduction ≥4 times) **(D)** by the function of β-lactamase inhibition among different molecular groups of CPO human isolates. BI, β-lactamase inhibition index; NS., no significant difference; *, significant difference (*P* value of <0.05); **, significant difference (*P* value of <0.01); ***, significant difference (*P* value of <0.001).

OXA-producing CPO. These data indicate that BLI's β-lactamase inhibitory efficacy is positively correlated with its partner BL's susceptibility restoration. Such correlation is further supported by the increase of the BL susceptibility restoration (**Figure 1C**) and the ratio of the sensitized isolates by the function of BI (**Figure 1D**) for both KPC-produing and OXA-producing CPOs.

It is noteworthy that the increase of β-lactamase inhibition of a BLI is not proportional to its partner BL's susceptibility restoration, as illustrated in **Figures 1C,D**. Significantly, when BI is low (<0.5), both the BL susceptibility restoration (**Figure 1C**) and the ratio of sensitized isolates (**Figure 1D**) are universally low for all BLI/CPO groups, suggesting that, without sufficient BLI dosing, there is no carbapenemase molecular identity-dependent superiority when choosing among BL/BLI agents. This is especially true for MBL isolates which none of the tested BLIs could effectively inhibit (median BIs, 0.1–0.4).

Intriguingly, even in isolates with a high degree of BLI-induced β-lactamase inhibition (BI>0.9), 50% (3/6) of CPO isolates had their MICs unchanged to amoxicillin, 50% (11/22) to ceftazidime and 35% (14/40) to meropenem. These isolates all carry additional BL resistance mechanisms besides β-lactamases, suggesting that BL resistance mechanisms independent of β-lactamase also play a significant role in the efficacy of BL/BLI to CPO. The non-proportional increase of the BL susceptibility by BLI's β-lactamase inhibition shown in **Figures 1C,D** further supports this conclusion.

DISCUSSION

By quantifying BLI-induced β-lactamase inhibition in diverse CPO isolates, this study demonstrated the variation of BLI activity with carbapenemase molecular classes, supporting the carbapenemase identity derived BL/BLI treatment guidelines currently proposed for CPO (Pogue et al., 2019). On the other hand, our data revealed the substantial BLI response heterogeneity from isolates within the same carbapenemase molecular group. Important contributors to this heterogeneity might include variations in carbapenemase subtype/expression status and the co-existence of non-carbapenemase β-lactamases among CPO (Bush and Bradford, 2020). Therefore, the choice of BL/BLI for CPO infection should be personalized upon the entire β-lactamase background, rather than the carbapenemase identity alone, perhaps by further exploiting genetic sequencing information or utilizing other quantitative β-lactamase inhibition assays like FIBA.

This study provides for the first time, a quantitative insight into the correlation between β-lactamase inhibition and BL activity restoration against CPOs. The positive correlation illustrated here supports BL/BLI agents as effective CPO treatments, in line with the results of several clinical trials recently performed (Van Duin et al., 2018; Pogue et al., 2020). Beyond this, our data demonstrate that the anti-CPO success of a BL/BLI depends on the completeness of a BLI's β-lactamase inhibition, motivating the need to alter BLI dosing to suit the specific β-lactamases in the clinical isolate. Therefore, BLI as an independent treatment adjuvant merits future consideration. To select the most suitable BLI, the structures and the resultant β-lactamase inhibitory mechanisms and profiles of the available BLIs have to be carefully compared in order to achieve the best clinical outcome. In addition, whether an BLI itself has antimicrobial activity besides β-lactamase inhibitory activity has also to be taken in account. To quantify the percentage of CPOs whose BL MICs are significantly changed by the introduction of BLIs, a CPO was considered sensitized by a BLI in this study if its BL MIC was reduced no less than 4 times after the BLI inclusion. However, it is of note that a reduction in the MIC by 4-fold or more may not be sufficient to change one CPO's clinical susceptibility as bacteria are classified as susceptible (potentially treatable) or resistant (probably not treatable) to a particular agent based on whether the MIC of this agent falls below or above a clinical breakpoint.

Our results, in line with other findings (Sun et al., 2017; Cabot et al., 2018; Dulyayangkul et al., 2020; Sadek et al., 2020; Gomis-Font et al., 2021), suggested that substantial β-lactamase inhibition generated by the use of BLI may not significantly improve the susceptibility of CPO toward its partner BL due to the presence of BL resistance mechanisms irrelated to β-lactamase production. Thus, besides BLI inhibitor efficacy, BL/BLI choice should also be customized based on the other relevant BL resistance mechanisms of CPO. However, the current molecular tests for BL resistance are still mainly based on the detection of the bacterial β-lactamase production (Evans et al., 2019). Therefore, deciphering the β-lactamase-independent BL resistance mechanisms that significantly influence a BL/BLI's efficacy to clinically significant pathogens, such as CPO, is urgently needed.

In summary, by quantitatively evaluating BLIs' contribution to CPO treatments with BLs, this study recommends personalization of BL/BLI usage based on the whole resistance backgrounds of the specific CPO case. Specifically, BLI choice and dosing should be guided by quantitative tools that can evaluate the inhibition across the entire β-lactamase background of the CPO upon BLI treatment. Furthermore, rapid molecular diagnostics for BLI resistances, especially those sensitive to non-β-lactamase resistance mechanisms, should be exploited to prevent ineffective BL/BLI treatment. Though the scope of this study was limited to CPO, the insights acquired here are adaptable to all bacterial pathogens for which BL/BLI agents could be effective.

DATA AVAILABILITY STATEMENT

The original contributions presented in the study are included in the article/supplementary material, further inquiries can be directed to the corresponding author.

AUTHOR CONTRIBUTIONS

YF conceived of the presented idea and drafted the manuscript. YF and AV conducted the experiments. SK and MJ performed the statistical analysis. TH supervised the project. All authors discussed the results and contributed to the finalization of the manuscript.

FUNDING

This study was supported by the Military Medicine Photonics Program from the US Department of Defense/Air Force (FA9550-16\1-0479), and the Netherlands Organization for Scientific Research (NWO) Rubicon program (452172009).

ACKNOWLEDGMENTS

The authors thank Jeff Gelfand for his constructive comments from the perspective of infectious diseases in clinical practice, Mark Vangel for his guidance on statistical analysis, and Akilan Palanisami for his constructive discussion on the data analysis and supports in manuscript writing.

REFERENCES

Alcock, B. P., Raphenya, A. R., Lau, T. T. Y., Tsang, K. K., Bouchard, M., Edalatmand, A., et al. (2020). CARD 2020: antibiotic resistome surveillance with the comprehensive antibiotic resistance database. *Nucleic Acids Res.* 48, D517–D525. doi: 10.1093/nar/gkz935

Black, C. A., So, W., Dallas, S. S., Gawrys, G., Benavides, R., Aguilar, S., et al. (2020). Predominance of non-carbapenemase producing Carbapenem-resistant Enterobacterales in South Texas. *Front. Microbiol.* 11:623574. doi: 10.3389/fmicb.2020.623574

Bush, K., and Bradford, P. A. (2020). Epidemiology of β-lactamase-producing pathogens. *Clin. Microbiol. Rev.* 33:e00047-19. doi: 10.1128/CMR.00047-19

Cabot, G., Florit-Mendoza, L., Sánchez-Diener, I., Zamorano, L., and Oliver, A. (2018). Deciphering β-lactamase-independent β-lactam resistance evolution trajectories in Pseudomonas aeruginosa. *J. Antimicrob. Chemother.* 73, 3322–3331. doi: 10.1093/jac/dky364

Carlier, M., Noë, M., De Waele, J. J., Stove, V., Verstraete, A. G., Lipman, J., et al. (2013). Population pharmacokinetics and dosing simulations of amoxicillin/clavulanic acid in critically ill patients. *J. Antimicrob. Chemother.* 68, 2600–2608. doi: 10.1093/jac/dkt240

Cui, X., Shan, B., Zhang, X., Qu, F., Jia, W., Huang, B., et al. (2020). Reduced Ceftazidime-avibactam susceptibility in KPC-producing Klebsiella pneumoniae From patients Without Ceftazidime-avibactam use history - A Multicenter study in China. *Front. Microbiol.* 11:1365. doi: 10.3389/fmicb.2020.01365

Cui, X., Zhang, H., and Du, H. (2019). Carbapenemases in Enterobacteriaceae: detection and antimicrobial therapy. *Front. Microbiol.* 10:1823. doi: 10.3389/fmicb.2019.01823

Dulyayangkul, P., Douglas, E. J. A., Lastovka, F., and Avison, M. B. (2020). Resistance to Ceftazidime/avibactam plus Meropenem/Vaborbactam when Both are used together is achieved in four steps in Metallo-β-lactamase-negative Klebsiella pneumoniae. *Antimicrob. Agents Chemother.* 64:e00409-20. doi: 10.1128/AAC.00409-20

El Hafi, B., Rasheed, S. S., Abou Fayad, A. G., Araj, G. F., and Matar, G. M. (2019). Evaluating the efficacies of Carbapenem/β-lactamase inhibitors Against Carbapenem-resistant gram-negative bacteria in vitro and in vivo. *Front. Microbiol.* 10:933. doi: 10.3389/fmicb.2019.00933

Erdem, S. S., Khan, S., Palanisami, A., and Hasan, T. (2014). Rapid, low-cost fluorescent assay of β-lactamase-derived antibiotic resistance and related antibiotic susceptibility. *J. Biomed. Opt.* 19:105007. doi: 10.1117/1.JBO.19.10.105007

Evans, S. R., Tran, T. T. T., Hujer, A. M., Hill, C. B., Hujer, K. M., Mediavilla, J. R., et al. (2019). Rapid molecular diagnostics to inform empiric use of Ceftazidime/avibactam and Ceftolozane/Tazobactam Against Pseudomonas aeruginosa: PRIMERS IV. *Clin. Infect. Dis. Off. Publ. Infect. Dis. Soc. Am.* 68, 1823–1830. doi: 10.1093/cid/ciy801

Feng, Y., Palanisami, A., Kuriakose, J., Pigula, M., Ashraf, S., and Hasan, T. (2020). Novel rapid test for detecting Carbapenemase. *Emerg. Infect. Dis.* 26, 793–795. doi: 10.3201/eid2604.181655

Feng, Y., Swain, J. W. R., Palanisami, A., Ashraf, S., and Hasan, T. (2021). One-step detection and classification of bacterial Carbapenemases in 10 minutes using fluorescence identification of β-lactamase activity. *J. Clin. Microbiol.* 59:e02517-20. doi: 10.1128/JCM.02517-20

Ferreira, R. L., Rezende, G. S., Damas, M. S. F., Oliveira-Silva, M., Pitondo-Silva, A., Brito, M. C. A., et al. (2020). Characterization of KPC-producing Serratia marcescens in an intensive care unit of a Brazilian tertiary hospital. *Front. Microbiol.* 11:956. doi: 10.3389/fmicb.2020.00956

Gomis-Font, M. A., Pitart, C., Del Barrio-Tofiño, E., Zboromyrska, Y., Cortes-Lara, S., Mulet, X., et al. (2021). Emergence of resistance to novel cephalosporin-β-lactamase inhibitor combinations through the modification of the Pseudomonas aeruginosa MexCD-OprJ efflux pump. *Antimicrob. Agents Chemother.* 65:e0008921. doi: 10.1128/AAC.00089-21

Karumathil, D. P., Nair, M. S., Gaffney, J., Kollanoor-Johny, A., and Venkitanarayanan, K. (2018). Trans-Cinnamaldehyde and eugenol increase Acinetobacter baumannii sensitivity to Beta-lactam antibiotics. *Front. Microbiol.* 9:1011. doi: 10.3389/fmicb.2018.01011

Khan, S., Sallum, U. W., Zheng, X., Nau, G. J., and Hasan, T. (2014). Rapid optical determination of β-lactamase and antibiotic activity. *BMC Microbiol.* 14:84. doi: 10.1186/1471-2180-14-84

Lee, Y., Kim, J., and Trinh, S. (2019). Meropenem-Vaborbactam (Vabomere™): Another option for Carbapenem-resistant Enterobacteriaceae. *P T Peer-Rev. J. Formul. Manag.* 44, 110–113.

McArthur, A. G., Waglechner, N., Nizam, F., Yan, A., Azad, M. A., Baylay, A. J., et al. (2013). The comprehensive antibiotic resistance database. *Antimicrob. Agents Chemother.* 57, 3348–3357. doi: 10.1128/AAC.00419-13

Nicolas-Chanoine, M.-H., Mayer, N., Guyot, K., Dumont, E., and Pagès, J.-M. (2018). Interplay Between membrane permeability and enzymatic barrier leads to antibiotic-dependent resistance in Klebsiella Pneumoniae. *Front. Microbiol.* 9:1422. doi: 10.3389/fmicb.2018.01422

Nicolau, D. P., Siew, L., Armstrong, J., Li, J., Edeki, T., Learoyd, M., et al. (2015). Phase 1 study assessing the steady-state concentration of ceftazidime and avibactam in plasma and epithelial lining fluid following two dosing regimens. *J. Antimicrob. Chemother.* 70, 2862–2869. doi: 10.1093/jac/dkv170

Nordmann, P., and Poirel, L. (2019). Epidemiology and diagnostics of Carbapenem resistance in gram-negative bacteria. *Clin. Infect. Dis. Off. Publ. Infect. Dis. Soc. Am.* 69, S521–S528. doi: 10.1093/cid/ciz824

Pogue, J. M., Bonomo, R. A., and Kaye, K. S. (2019). Ceftazidime/avibactam, Meropenem/Vaborbactam, or Both? Clinical and formulary considerations. *Clin. Infect. Dis. Off. Publ. Infect. Dis. Soc. Am.* 68, 519–524. doi: 10.1093/cid/ciy576

Pogue, J. M., Kaye, K. S., Veve, M. P., Patel, T. S., Gerlach, A. T., Davis, S. L., et al. (2020). Ceftolozane/Tazobactam vs Polymyxin or aminoglycoside-based regimens for the treatment of drug-resistant Pseudomonas aeruginosa. *Clin. Infect. Dis. Off. Publ. Infect. Dis. Soc. Am.* 71, 304–310. doi: 10.1093/cid/ciz816

Sadek, M., Juhas, M., Poirel, L., and Nordmann, P. (2020). Genetic features leading to reduced susceptibility to Aztreonam-avibactam among Metallo-β-lactamase-producing Escherichia coli isolates. *Antimicrob. Agents Chemother.* 64:e01659-20. doi: 10.1128/AAC.01659-20

Sallum, U. W., Zheng, X., Verma, S., and Hasan, T. (2010). Rapid functional definition of extended spectrum β-lactamase activity in bacterial cultures via competitive inhibition of fluorescent substrate cleavage. *Photochem. Photobiol.* 86, 1267–1271. doi: 10.1111/j.1751-1097.2010.00801.x

Sheu, C.-C., Chang, Y.-T., Lin, S.-Y., Chen, Y.-H., and Hsueh, P.-R. (2019). Infections caused by Carbapenem-resistant Enterobacteriaceae: An update on therapeutic options. *Front. Microbiol.* 10:80. doi: 10.3389/fmicb.2019.00080

Shields, R. K., and Doi, Y. (2020). Aztreonam combination therapy: An answer to Metallo-β-lactamase-producing gram-negative bacteria? *Clin. Infect. Dis. Off. Publ. Infect. Dis. Soc. Am.* 71, 1099–1101. doi: 10.1093/cid/ciz1159

Shields, R. K., Potoski, B. A., Haidar, G., Hao, B., Doi, Y., Chen, L., et al. (2016). Clinical outcomes, drug toxicity, and emergence of Ceftazidime-avibactam resistance Among patients treated for Carbapenem-resistant Enterobacteriaceae infections. *Clin. Infect. Dis. Off. Publ. Infect. Dis. Soc. Am.* 63, 1615–1618. doi: 10.1093/cid/ciw636

Spellberg, B., and Bonomo, R. A. (2016). Editorial commentary: Ceftazidime-avibactam and Carbapenem-resistant Enterobacteriaceae: "We're Gonna need a bigger boat.", *Clin. Infect. Dis. Off. Publ. Infect. Dis. Soc. Am.* 63, 1619–1621. doi: 10.1093/cid/ciw639

Sun, D., Rubio-Aparicio, D., Nelson, K., Dudley, M. N., and Lomovskaya, O. (2017). Meropenem-Vaborbactam resistance selection, resistance prevention, and molecular mechanisms in mutants of KPC-producing Klebsiella pneumoniae. *Antimicrob. Agents Chemother.* 61:e01694-17. doi: 10.1128/AAC.01694-17

Tamma, P. D., Goodman, K. E., Harris, A. D., Tekle, T., Roberts, A., Taiwo, A., et al. (2017). Comparing the outcomes of patients With Carbapenemase-producing and non-Carbapenemase-producing Carbapenem-resistant Enterobacteriaceae Bacteremia. *Clin. Infect. Dis. Off. Publ. Infect. Dis. Soc. Am.* 64, 257–264. doi: 10.1093/cid/ciw741

Van Duin, D., Lok, J. J., Earley, M., Cober, E., Richter, S. S., Perez, F., et al. (2018). Colistin versus Ceftazidime-avibactam in the treatment of infections due to Carbapenem-resistant Enterobacteriaceae. *Clin. Infect. Dis. Off. Publ. Infect. Dis. Soc. Am.* 66, 163–171. doi: 10.1093/cid/cix783

Conflict of Interest: The authors declare that the research was conducted in the absence of any commercial or financial relationships that could be construed as a potential conflict of interest.

Publisher's Note: All claims expressed in this article are solely those of the authors and do not necessarily represent those of their affiliated organizations, or those of the publisher, the editors and the reviewers. Any product that may be evaluated in this article, or claim that may be made by its manufacturer, is not guaranteed or endorsed by the publisher.

frontiers in Microbiology

ORIGINAL RESEARCH
published: 25 November 2021
doi: 10.3389/fmicb.2021.738812

The Monte Carlo Simulation of Three Antimicrobials for Empiric Treatment of Adult Bloodstream Infections With Carbapenem-Resistant Enterobacterales in China

Dongna Zou[1], Guangyue Yao[2], Chengwu Shen[1], Jinru Ji[3,4,5], Chaoqun Ying[3,4,5], Peipei Wang[3,4,5], Zhiying Liu[3,4,5], Jun Wang[1], Yan Jin[6] and Yonghong Xiao[3,4,5]**

[1] Department of Pharmacy, Shandong Provincial Hospital Affiliated to Shandong First Medical University, Jinan, China, [2] Cancer Therapy and Research Center, Shandong Provincial Hospital Affiliated to Shandong University, Jinan, China, [3] State Key Laboratory for Diagnosis and Treatment of Infectious Diseases, College of Medicine, The First Affiliated Hospital, Zhejiang University, Hangzhou, China, [4] National Clinical Research Center for Infectious Diseases, College of Medicine, The First Affiliated Hospital, Zhejiang University, Hangzhou, China, [5] Collaborative Innovation Center for Diagnosis and Treatment of Infectious Diseases, The First Affiliated Hospital, College of Medicine, Zhejiang University, Hangzhou, China, [6] Department of Clinical Laboratory, Shandong Provincial Hospital Affiliated to Shandong First Medical University, Jinan, China

OPEN ACCESS

Edited by:
Mary Marquart, University of Mississippi Medical Center, United States

Reviewed by:
Siqiang Niu, The First Affiliated Hospital of Chongqing Medical University, China
Thitima Wattanavijitkul, Chulalongkorn University, Thailand

***Correspondence:**
Yan Jin
sdjinyan@163.com
Yonghong Xiao
xiaoyonghong@zju.edu.cn

Specialty section:
This article was submitted to Antimicrobials, Resistance and Chemotherapy, a section of the journal Frontiers in Microbiology

Received: *09 July 2021*
Accepted: *25 October 2021*
Published: *25 November 2021*

Citation:
Zou D, Yao G, Shen C, Ji J, Ying C, Wang P, Liu Z, Wang J, Jin Y and Xiao Y (2021) The Monte Carlo Simulation of Three Antimicrobials for Empiric Treatment of Adult Bloodstream Infections With Carbapenem-Resistant Enterobacterales in China. Front. Microbiol. 12:738812. doi: 10.3389/fmicb.2021.738812

Introduction: The aim of this study was to predict and evaluate three antimicrobials for treatment of adult bloodstream infections (BSI) with carbapenem-resistant Enterobacterales (CRE) in China, so as to optimize the clinical dosing regimen further.

Methods: Antimicrobial susceptibility data of blood isolates were obtained from the Blood Bacterial Resistance Investigation Collaborative Systems in China. Monte Carlo simulation was conducted to estimate the probability target attainment (PTA) and cumulative fraction of response (CFR) of tigecycline, polymyxin B, and ceftazidime/avibactam against CRE.

Results: For the results of PTAs, tigecycline following administration of 50 mg every 12 h, 75 mg every 12 h, and 100 mg every 12 h achieved > 90% PTAs when minimum inhibitory concentration (MIC) was 0.25, 0.5, and 0.5 μg/mL, respectively; polymyxin B following administration of all tested regimens achieved > 90% PTAs when MIC was 1 μg/mL with CRE; ceftazidime/avibactam following administration of 1.25 g every 8 h, 2.5 g every 8 h achieved > 90% PTAs when MIC was 4 μg/mL, 8 μg/mL with CRE, respectively. As for CFR values of three antimicrobials, ceftazidime/avibactam achieved the lowest CFR values. The highest CFR value of ceftazidime/avibactam was 77.42%. For tigecycline and ceftazidime/avibactam, with simulated regimens daily dosing increase, the CFR values were both increased; the highest CFR of tigecycline values was 91.88%. For polymyxin B, the most aggressive dosage of 1.5 mg/kg every 12 h could provide the highest CFR values (82.69%) against CRE.

Conclusion: This study suggested that measurement of MICs and individualized therapy should be considered together to achieve the optimal drug exposure. In particular, pharmacokinetic and pharmacodynamic modeling based on local antimicrobial resistance data can provide valuable guidance for clinicians for the administration of empirical antibiotic treatments for BSIs.

Keywords: bloodstream infections, carbapenem-resistant Enterobacteriaceae, polymyxin B, ceftazidime/avibactam, tigecycline, Monte Carlo simulation

INTRODUCTION

Bacterial drug resistance is becoming more and more serious. The monitoring of drug-resistant bacteria and the management of antimicrobials have valued more attention from all over the world. Carbapenems are the most potent β-lactam family of antibiotics for the treatment of bacterial infections, especially Enterobacteriaceae infections (Rahal, 2008), and are regarded as the "last resort" in the treatment of Gram-negative bacterial infections (El-Gamal et al., 2017). Once strains are resistant to carbapenem, the treatment will face great difficulties.

However, in the past few decades, the isolation of carbapenem-resistant Enterobacterales (CRE) strains has greatly increased, which bring great difficulties and challenges in clinical treatment. In many countries in the world, such as Europe, Asia, South America, and North America, outbreaks caused by CRE have been reported. CRE has become a global public health threat now (Sievert et al., 2013). The US Centers for Disease Control and Prevention (CDC) also lists CRE as a threat to public health in 2015 (Centers for Disease Control and Prevention, 2013). According to the US CDC, the incidence of CRE increased from 1.2% in 2001 to 4.2% in 2011 (Little et al., 2012). Chen et al. (2021) reported that in a population-based study in seven states in the United States, CRE incidence was up to 2.93 per 100,000 persons. The complex resistance mechanisms have also brought more troubles to treatment, especially bloodstream infections (BSIs) with CRE, which have been rapidly spreading worldwide with a high mortality and pose a challenge to therapeutic decision-making (Tumbarello et al., 2012; Laupland and Church, 2014; Wu et al., 2020). As the most serious type of infections caused by CRE, BSI usually leads to a worse prognosis, longer hospital stay, and higher mortality (Neuwirth et al., 1995; Hussein et al., 2013). The fatality rate of patients with CRE infections was significantly different in different studies; the fatality rate of BSIs is 40–50% (Patel et al., 2008). According to the reports reported in the United States, Italy, Greece, and Spain, the mortality of CRE BSIs was 40–60% (Meatherall et al., 2009), and the fatality rate of BSIs in the population of neutropenia and hematological malignancies was as high as 69% (Satlin et al., 2013). Falagas et al. (2014) reported that their pooled analysis of the nine studies (985 patients) showed that the death rate was higher among CRE-infected than carbapenem-susceptible Enterobacterales (CSE)–infected patients. CRE-infected patients had an unadjusted number of deaths twofold higher than that for CSE-infected patients (Falagas et al., 2014). Compared with CSE, effective anti-infective treatment is often delayed because of the limited treatment of infections caused by CRE (Little et al., 2012), so the mortality of patients whose infections are caused by CRE is higher (Satlin et al., 2016; Averbuch et al., 2017).

The treatment of CRE infections is difficult, and the prognosis is poor; it brings great challenges to clinical treatment and nosocomial infection control. Previous study has been demonstrated that insufficient empirical antimicrobial therapy is independently associated with higher mortality in CRE BSIs (Tumbarello et al., 2012), especially in patients with inadequate initial dosing (Zarkotou et al., 2011). Thus, early administration of appropriate empirical antimicrobial therapy for BSIs with CRE is particularly important. Inappropriate antimicrobial therapy of CRE sensitive drugs may increase the selective pressure of antibacterial and increase the waste of medical resources (Dautzenberg et al., 2015; Lee and Lee, 2016). For critically ill patients, combining local pathogenic characteristics, drug sensitivity, and pharmacokinetic (PK) and pharmacodynamic (PD) characteristics of antimicrobial can improve the success rate of treatment.

To choose an optimal antibiotic or dosing regimen, susceptibility results, PK/PD factors, infection site, and patient factors (allergies or intolerances) should be considered to make an individualized treatment (Vasoo et al., 2015; Zhu et al., 2020). The combined use of the distributions of location-specific minimum inhibitory concentrations (MICs), different antibiotic regimens, and PK parameters derived from human studies via the application of PK/PD models with Monte Carlo simulation is a useful approach for predicting treatment outcomes (Bradley et al., 2003).

We examined the MIC distributions of CRE isolated from blood cultures of adults with BSIs from the Blood Bacterial Resistance Investigation Collaborative Systems (BRICS) in China, 2018–2019, as a basis for PK/PD modeling. We predicted and evaluated three antimicrobials (tigecycline, polymyxin B, and ceftazidime/avibactam) used to treat CRE-infected BSIs so as to identify the most appropriate antibiotics and dosage regimens for the empirical treatment of CRE-infected BSIs and to optimize the clinical dosing regimen further.

MATERIALS AND METHODS

Antimicrobials

Three antimicrobials and eight dosage regimens were selected for modeling, based on their common use for the treatment of CRE-infected BSIs in China (**Table 1**).

TABLE 1 | Antibiotic regimens used in the Monte Carlo simulations.

Antibiotic	Dose
Tigecycline	50 mg every 12 h
	75 mg every 12 h
	100 mg every 12 h
Polymyxin B	1.25 mg/kg every 12 h
	1.5 mg/kg every 12 h
	2.5 mg/kg per day continuous infusion
Ceftazidime/avibactam	1.25 g every 8 h
	2.5 g every 8 h

TABLE 2 | Pharmacokinetic parameters (means ± SDs) used in the Monte Carlo simulations.

Antibiotic	Cl_T (L/h)	Fu (%)	Vd (L)	References
Tigecycline	19.2 ± 7.76	—	—	Rubino et al., 2010
Polymyxin B	2.5 ± 0.4	—	—	Thamlikitkul et al., 2016
Ceftazidime/avibactam	7.53 ± 1.28	90	18.8 ± 6.54	Bensman et al., 2017

Cl_T, total body clearance; fu, fraction unbound; SDs, standard deviations; Vd, volume of distribution.

Bacterial Isolates

The data in the present study were from the National Bloodstream Infection BRICS platform in China (50 hospitals) for 2018 and 2019. Most of the hospitals included were the largest hospitals in each province. Six hundred fifty-three non-duplicate CRE species were isolated from blood cultures. Each laboratory of the 50 hospitals identified the species using standard biochemical methodology with an automated system (Vitec 2, bioMérieux, France; MicroScan walkAway-96, Siemens, United States; or Phoenix-100, BD, United States).

Minimum Inhibitory Concentration Determination

The MICs of tigecycline, polymyxin B, and ceftazidime/avibactam were determined by broth microdilution method or one of the three automated systems in accordance with the Clinical Laboratory Standards Institute (CLSI, 2019) guidelines.

PK/PD Model

All the PK data were obtained from previously published studies of infected and/or critically ill patients who had adequate renal function, shown in **Table 2**.

PD exposures were simulated as free drug (f) for ceftazidime/avibactam and as total drug for tigecycline and polymyxin B.

For the tigecycline and polymyxin B, PK exposures were measured by 24-h area under the curve (AUC_{24})/MIC > 6.96 and AUC/MIC ≥ 50, respectively, to be predictive of the clinical

TABLE 3 | MIC distributions for antimicrobials against all CRE isolated from blood specimens in China during 2018–2019.

MIC (mg/L)	No.[a]	Percentages of isolates by MIC												MIC_{50}	MIC_{90}	MIC range
Antibiotic		**0.03**	**0.06**	**0.125**	**0.25**	**0.5**	**1**	**2**	**4**	**8**	**16**	**32**	**64**			
CRE (*n* = 653)																
Tigecycline	646	1.39	1.86	10.22	39.16	20.12	21.83	4.49	0.62	0.31	0	0	0	0.25	1	0.03–8
Polymyxin B	650	0	0	0	4.77	54.31	22.92	12.15	2.15	1.08	1.38	1.23	0	0.5	2	0.25–32
Ceftazidime/avibactam	445	0	0.22	0.22	0.67	2.02	4.72	9.66	26.74	30.79	1.8	22.02	1.12	8	16	0.06–32

MIC, minimum inhibitory concentration; CRE, carbapenem-resistant Enterobacterales; MIC_{50}, 50% minimum inhibitory concentration; MIC_{90}, 90% minimum inhibitory concentration. [a]No., number of isolates in which antibiotic sensitivity was tested.

TABLE 4 | MIC distributions for antimicrobials against all CRE isolated from blood specimens in China during 2018–2019.

MIC (mg/L)	No.[a]	Percentages of isolates by MIC												MIC_{50}	MIC_{90}	MIC range
Antibiotic		**0.03**	**0.06**	**0.125**	**0.25**	**0.5**	**1**	**2**	**4**	**8**	**16**	**32**	**64**			
CRKP (*n* = 511)																
Tigecycline	511	0.98	1.57	9.59	33.86	22.31	25.64	4.89	0.78	0.39	0	0	0	0.5	1	0.03–8
Polymyxin B	511	0	0	0	4.11	57.73	20.94	11.35	2.15	0.98	1.76	0.98	0	0.5	–	0.25–32
Ceftazidime/avibactam	325	0	0.31	0.31	0	1.85	5.23	12.62	34.15	37.23	0.92	7.38	0	4	16	0.06–32
CREC (*n* = 83)																
Tigecycline	83	4.82	4.82	15.66	61.45	4.82	6.02	2.41	0	0	0	0	0	0.25	0.5	0.03–2.41
Polymyxin B	83	0	0	0	7.23	53.01	21.69	15.66	2.41	0	0	0	0	0.5	2	0.25–4
Ceftazidime/avibactam	61	0	0	0	0	3.28	3.28	1.64	6.56	24.59	6.56	54.1	0	32	32	0.5–54.1
CRE species except CRKP and CREC (*n* = 59).																
Tigecycline	52	0	0	8.93	55.36	23.21	8.93	3.57	0	0	0	0	0	0.25	1	0.125–2
Polymyxin B	56	0	0	0	6.67	28.33	41.67	13.33	1.67	3.33	0	5	0	1	2	0.25–32
Ceftazidime/avibactam	59	0	0	0	5.08	1.69	3.39	1.69	6.78	1.69	1.69	69.49	8.47	32	32	0.25–64

MIC, minimum inhibitory concentration; CRE, carbapenem-resistant Enterobacterales; MIC_{50}, 50% minimum inhibitory concentration; MIC_{90}, 90% minimum inhibitory concentration; [a]No., number of isolates in which antibiotic sensitivity was tested; CRKP, carbapenem-resistant Klebsiella pneumoniae; CREC, carbapenem-resistant Escherichia coli.

and microbiologic efficacy (Miglis et al., 2018; Wang et al., 2020). The steady-state AUC from 0 to 24 h ($AUC_{0-24\ h}$) was calculated according to the following equation: AUC_{0-24} = dose/Cl_T.

For ceftazidime/avibactam, PK exposures was measured by 50% fT > MIC (Wang et al., 2020), which was calculated using the following one-compartment intravenous infusion equation (Drusano et al., 2001). fu is the fraction of unbound drug, Vd is the volume of distribution in liters at steady state, MIC is the MIC, Cl_T is total body clearance, and DI is dosing interval.

$$\%fT > MIC = ln\left(\frac{Dose \times fu}{Vd \times MIC}\right) \times \frac{Vd}{CLt} \times \frac{100}{DI}$$

Monte Carlo Simulations

A 10,000-subject Monte Carlo simulation (Oracle Crystal Ball; version 11.1.2.4.400) was conducted for each antimicrobial regimen. PK data in the "PK/PD Model" section were used to determine the percentages of PK/PD target attainment (PTA) for a range of MICs from 0.03 to 64 mg/L. The probability of PTA, which represented the likelihood that an antimicrobial regimen will meet or exceed the target at a specific MIC, was assessed for each regimen. The cumulative fraction of response (CFR), which represented the expected population PTA for a specific drug dose and a specific population of microorganisms, was calculated for MIC distributions using weighted summation and calculated as follows (Drusano et al., 2001). A regimen that achieved more than 90% CFR against a population of organisms was considered optimal (Mouton et al., 2005).

$$CFR = \sum_{i=0}^{n} PT\,Ai \times Fi$$

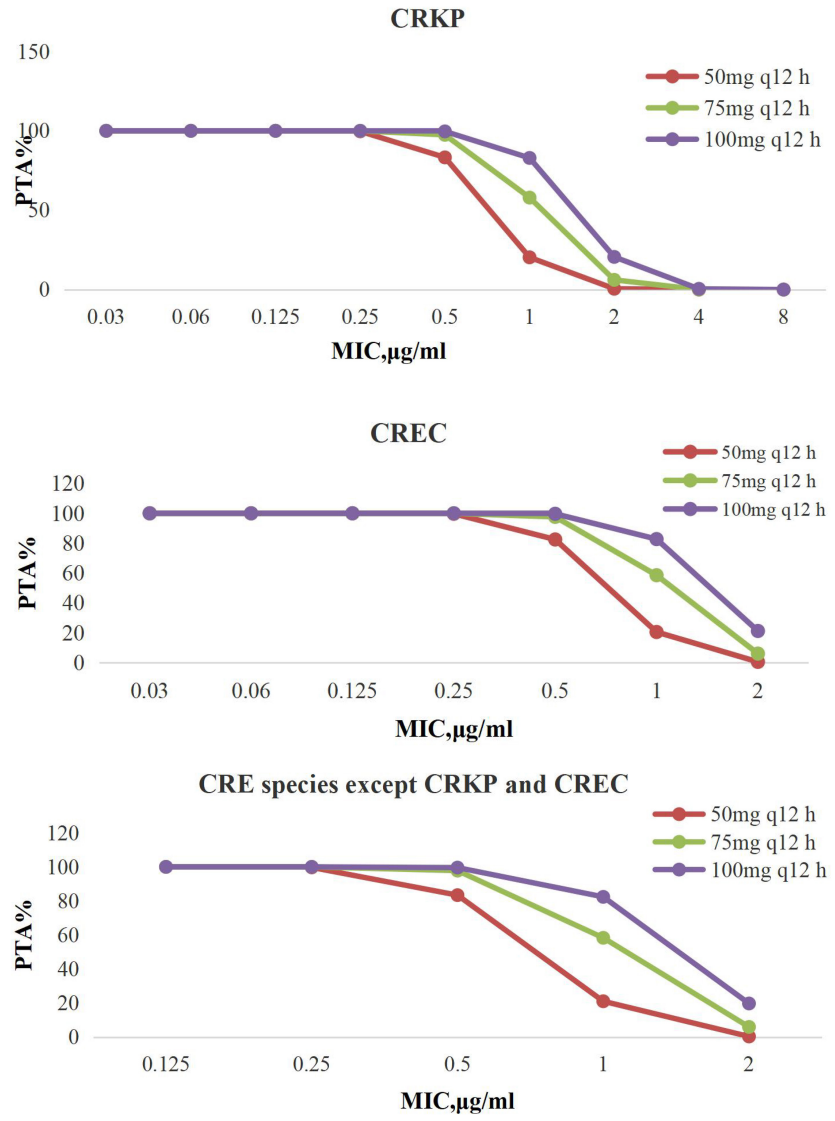

FIGURE 1 | PTA against CRE at MICs from 0.03 to 8 mg/L for tigecycline. PTA, probability target attainment; MIC, minimum inhibitory concentration; CRE, carbapenem-resistant Enterobacterales; CRKP, carbapenem-resistant *Klebsiella pneumoniae*; CREC, carbapenem-resistant *Escherichia coli*.

RESULTS

The Results of Susceptibility Testing

There were 653 non-duplicate CRE species isolated from blood cultures enrolled in our study during 2018 and 2019, including carbapenem-resistant *Klebsiella pneumoniae* (CRKP) (n = 511), carbapenem-resistant *Escherichia coli* (CREC) (n = 83), and other CRE species except CRKP and CREC (n = 59).

We analyzed the MIC data for all CRE and established discrete MIC distributions for each population based on MIC frequencies. **Tables 3**, **4** show the 50% MIC (MIC_{50}) and 90% MIC (MIC_{90}) percentage of isolates by MIC for each antimicrobial agent.

For tigecycline, the MIC_{50} and MIC_{90} against CRKP, which was the strain with the highest detection rate among all CREs, were 0.5 and 1 mg/L, whereas the value of MIC_{50} and MIC_{90} were 0.5 and 2 mg/L for polymyxin B, and 4 and 16 mg/L for ceftazidime/avibactam.

Probability Target Attainment

Targets of AUC_{24}/MIC > 6.96 are shown in **Figure 1**. Tigecycline following administration of 50 mg every 12 h, 75 mg every 12 h, and 100 mg every 12 h achieved > 90% PTAs when MIC was from 0.03 to 8 μg/mL.

The PTAs for polymyxin B regimens at specific MICs with targets of AUC/MIC ≥ 50 are shown in **Figure 2**. Polymyxin B following administration of 1.25 mg/kg every 12 h, 1.5 mg/kg every 12 h, and 2.5 mg/kg per day continuous infusion achieved > 90% PTAs when MIC was 1 μg/mL with CRE. No regimen achieved a 90% PTA with an MIC of 2 μg/mL.

The PTAs for ceftazidime/avibactam regimens at specific MICs with targets of 50% fT > MIC are shown in **Figure 3**. Ceftazidime/avibactam following administration of 1.25 g every 8 h, 2.5 g every 8 h achieved > 90% PTAs when MIC was 4 μg/mL, 8 μg/mL with CRE. No regimen of ceftazidime/avibactam achieved a 90% PTA with an MIC of 16 μg/mL with CRE.

Cumulative Fraction of Response

Tables 5, **6** show the CFR values for each antibiotic regimen based on the Monte Carlo simulations against CRE. As for CFR values of three antimicrobials, ceftazidime/avibactam achieved the lowest CFR values; the highest CFR value was 77.42%. For tigecycline and ceftazidime/avibactam, with simulated regimen improvement, the CFR values were both increased; the lowest

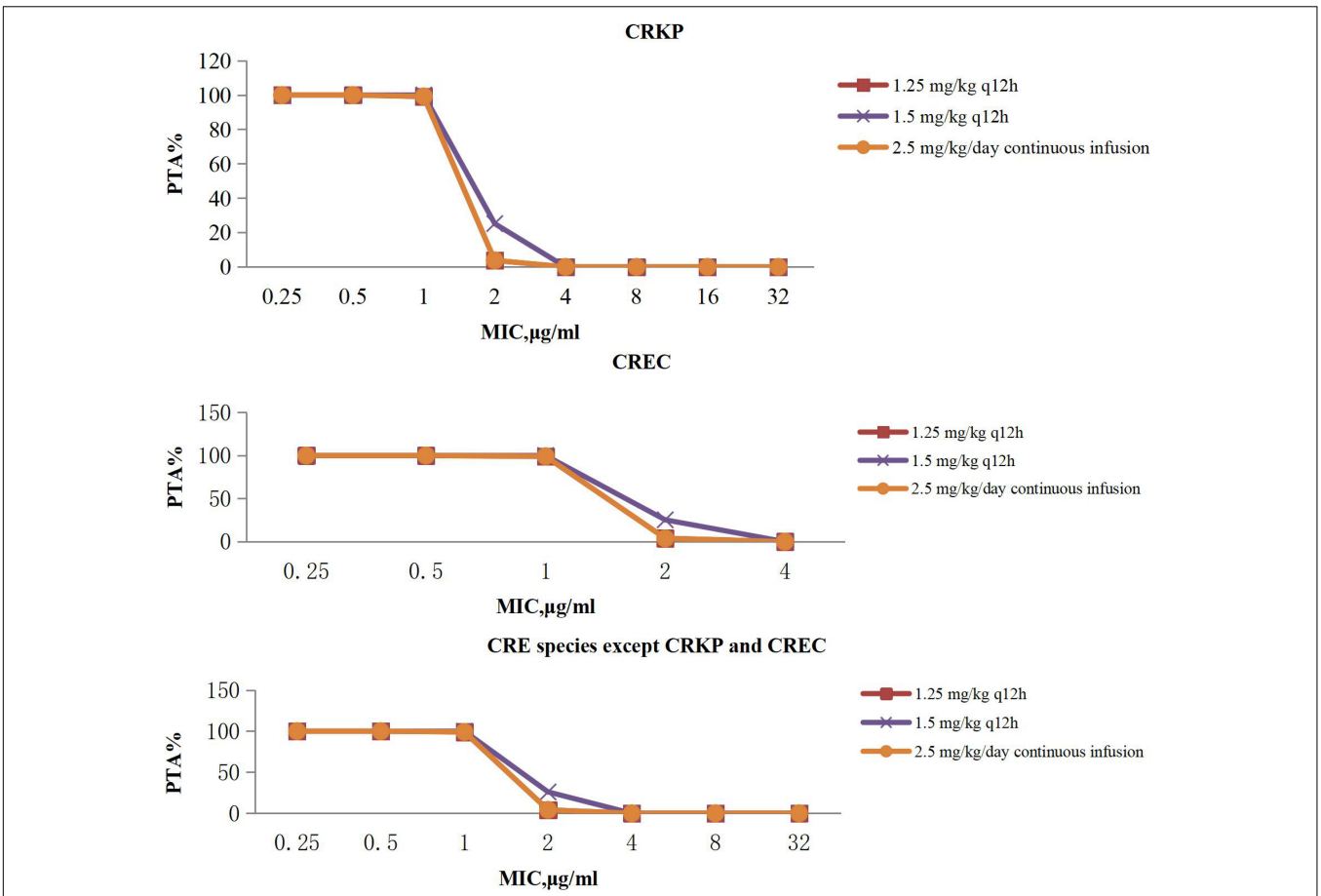

FIGURE 2 | PTA against CRE at MICs from 0.25 to 32 mg/L for polymyxin B. PTA, probability target attainment; MIC, minimum inhibitory concentration; CRE, carbapenem-resistant Enterobacterales; CRKP, carbapenem-resistant *Klebsiella pneumoniae*; CREC, carbapenem-resistant *Escherichia coli*.

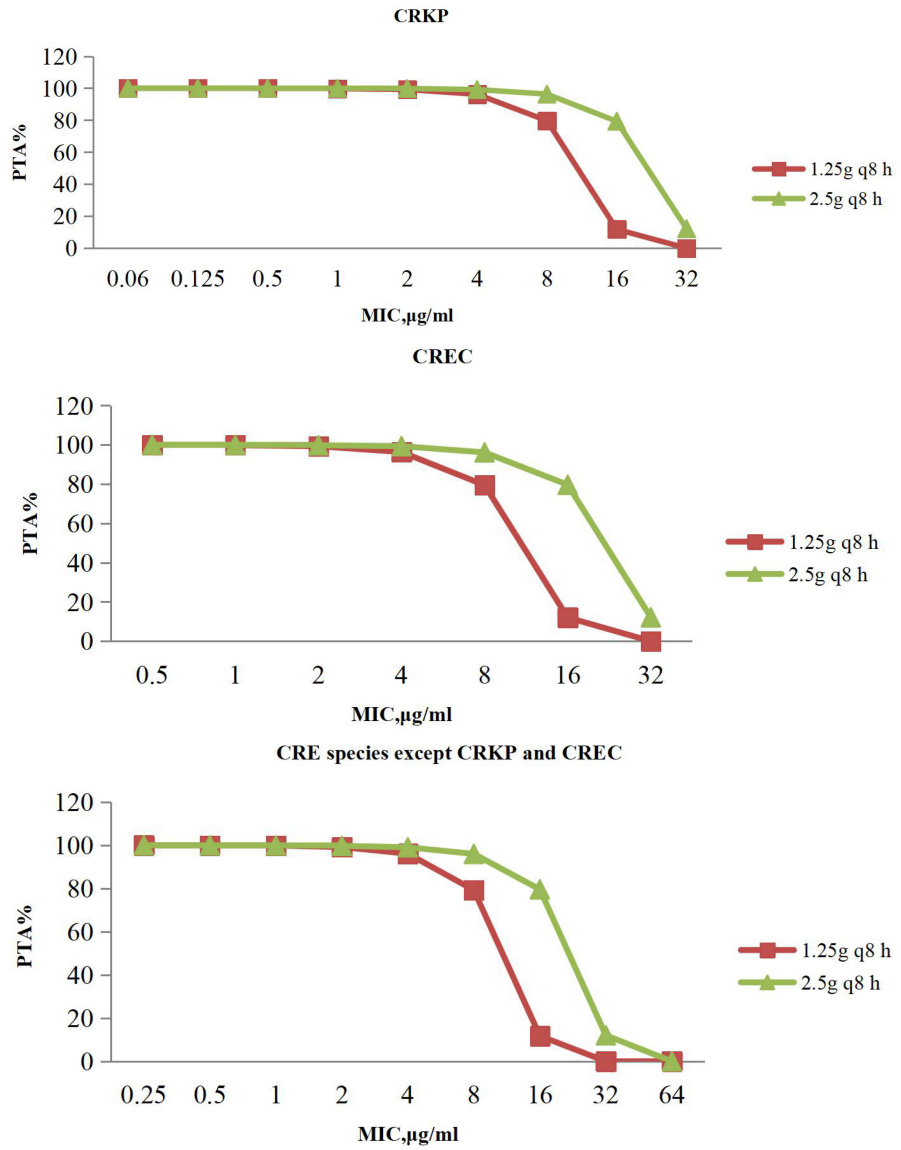

FIGURE 3 | PTA against CRE at MICs from 0.06 to 64 mg/L for ceftazidime/avibactam. PTA, probability target attainment; MIC, minimum inhibitory concentration; CRE, carbapenem-resistant Enterobacterales; CRKP, carbapenem-resistant *Klebsiella pneumoniae*; CREC, carbapenem-resistant *Escherichia coli*.

CFR of tigecycline values was 73.42%. It is worth noting that the CFR values of polymyxin B were neither very low nor very high; the lowest CFR value of polymyxin B was 80.89%; the most aggressive dosage of 1.5 mg/kg every 12 h provided CFR value of 82.69% against CRE.

DISCUSSION

Ceftazidime/avibactam is a novel β-lactam/β-lactamase inhibitor combination against CRE that inactivates Ambler class A, class C, and some class D β-lactamase–producing pathogens, including those producing *Klebsiella pneumoniae* carbapenemase and *OXA-48* carbapenemases, but not metallo-β-lactamases (Li et al., 2019), and it has improved survival in multidrug-resistant Gram-negative bacilli infections (Shields et al., 2016, 2017; Temkin et al., 2017; Tumbarello et al., 2019; Clerici et al., 2021). For treatment of all CRE, tigecycline, which is a novel antimicrobial agent with *in vitro* activity against most Gram-positive and Gram-negative pathogens, is mainly used for treatment of complicated skin, soft tissue, and intra-abdominal infections in adults (Babinchak et al., 2005; Ellis-Grosse et al., 2005; Pankey, 2005; Bhavnani et al., 2012; Bodmann et al., 2012). Polymyxin B is considered as the last line of defense against drug-resistant bacteria (Li et al., 2006; Zavascki et al., 2007; Landman et al., 2008; Yu et al., 2017; Nang et al., 2021). Our study analyzed the CRE data of the BRICS to evaluate the effectiveness of the three most commonly used antibacterial for

TABLE 5 | CFR values for three antibiotics against CRE.

Antimicrobials	Dosing regimens	CFR (%)
Tigecycline	50 mg every 12 h	73.42
	75 mg every 12 h	85.32
	100 mg every 12 h	91.88
Polymyxin B	1.25 mg/kg every 12 h	81.14
	1.5 mg/kg every 12 h	82.69
	2.5 mg/kg per day continuous infusion	80.89
Ceftazidime/avibactam	1.25 g every 8 h	66.59
	2.5 g every 8 h	77.42

CFR, cumulative fraction of response; CRE, carbapenem-resistant Enterobacterales.

TABLE 6 | CFR values for three antibiotics against CRE.

Antimicrobials	CRE	Dosing regimens	CFR (%)
Tigecycline	CRKP	50 mg every 12 h	69.22
		75 mg every 12 h	83.12
		100 mg every 12 h	91.15
	CREC	50 mg every 12 h	91.45
		75 mg every 12 h	95.53
		100 mg every 12 h	96.77
	CRE species except CRKP and CREC	50 mg every 12 h	85.14
		75 mg every 12 h	92.53
		100 mg every 12 h	95.62
Polymyxin B	CRKP	1.25 mg/kg every 12 h	82.84
		1.5 mg/kg every 12 h	86
		2.5 mg/kg per day continuous infusion	82.79
	CREC	1.25 mg/kg every 12 h	82.6
		1.5 mg/kg every 12 h	86.05
		2.5 mg/kg per day continuous infusion	82.3
	CRE species except CRKP and CREC	1.25 mg/kg every 12 h	77.05
		1.5 mg/kg every 12 h	79.99
		2.5 mg/kg per day continuous infusion	76.31
Ceftazidime/avibactam	CRKP	1.25 g every 8 h	82.48
		2.5 g every 8 h	91.78
	CREC	1.25 g every 8 h	67.79
		2.5 g every 8 h	86.33
	CRE species except CRKP and CREC	1.25 g every 8 h	19.63
		2.5 g every 8 h	29.12

CFR, cumulative fraction of response; CRE, carbapenem-resistant Enterobacterales; CRKP, carbapenem-resistant Klebsiella pneumoniae; CREC, carbapenem-resistant Escherichia coli.

BSIs with CRE in different dosing regimens using Monte Carlo simulations to model *in vivo* antibiotic pharmacodynamics, in the hope that empirical administration will help improve the survival rate of patients.

Ceftazidime/avibactam clinical breakpoints of susceptible MIC $\leq$ 8 mg/L have been assigned to CRE by CLSI, and the breakpoints of susceptible MIC $\leq$ 2 mg/L for tigecycline and polymyxin B were assigned to CRE by the US Food and Drug Administration and European Committee on Antimicrobial Susceptibility Testing.

From **Tables 3**, **4**, it could be known that 334 strains were sensitive to ceftazidime/avibactam in CRE, with a susceptibility rate of 75.06% (334/445), which was in line with the literature that the susceptibility rate of ceftazidime/avibactam was 75.0% (Zou et al., 2020), but it was higher than the results reported in 2020 [published by the China Antimicrobial Surveillance Network (CHINET) Study Group, the susceptibility of ceftazidime/avibactam against CRE was 61.4%] (Han et al., 2020); it could be attributed to the strict control of the application of antibacterial recent years. However, our research also revealed that the current MIC_{50} and MIC_{90} of ceftazidime/avibactam against CRE are significantly different with the literature reported (8 vs. 2 mg/L, 16 vs. 32 mg/L) (Han et al., 2020). This phenomenon needs further research. We also found that the MIC of CRE to ceftazidime/avibactam is up to 64 μg/mL, and high MIC of CRE accounts for a high proportion; for example, the percentage of MIC such as 32 μg/mL in other CRE species except CRKP and CREC is as high as 69.49%. This also explains why the CFR of ceftazidime/avibactam is low, which suggests that we empirically apply ceftazidime/avibactam to treat BSIs caused by other CREs and should be used cautiously.

Ceftazidime/avibactam PTA at MIC $\leq$ 8 and 16 mg/L ranged from 96.01 to 100% and 79.6–79.33% with the dosage of 2.5 g every 8 h, respectively; a similar finding has been observed in adults with complicated intra-abdominal infections, complicated urinary tract infections, and nosocomial pneumonia (Das et al., 2019). PTA was lower with the dosage of 1.25 g every 8 h, but still with high target attainment (>95%) against MICs $\leq$ 4 mg/ L. It was a limitation that the study lacked the enzymes of CRE, which reminded us that we should detect the enzymes produced by CRE of ceftazidime/avibactam-resistant in future work, so as to provide more targeted recommendations for clinical medication.

We also investigated that polymyxin B and tigecycline showed excellent antibacterial activity against CRE strains; 612 strains were sensitive to polymyxin B, with a susceptibility rate of 94.15% (612 /650); 640 strains were sensitive to tigecycline, with a susceptibility rate of 99.07% (640/646). The findings were consistent with the literature published by the CHINET Study Group (the susceptibility rates were 95.8 and 98.4% for polymyxin B and tigecycline, respectively) (Han et al., 2020). The data in the study were from the BRICS, covering most provinces in China, and the resistance of CRE was basically consistent with the relevant literature about the resistance of bacteria in China. It truly reflected the resistance of CRE in China, and it has a very high reference value.

For treatment of all CRE, tigecycline achieved the optimal CFRs (>90%) when tigecycline was given 100 mg every 12 h; particularly, it can achieve the satisfactory CFR values for CREC given any dosage regimen, which were in line with the literature that in their response to the high-dose tigecycline (200 mg

followed by 100 mg every 12 h), *E. coli* and *K. pneumoniae* showed CFRs greater than 90% (Wang et al., 2020). Our study is consistent with literature reports, when MIC was 1 μg/mL; the PTAs of standard dosing for CRKP, CREC, and other CRE species were 29.84, 29.86, and 28.39%, whereas the other regimen (100 mg every 12 h) PTA was ≥ 88%.

It is worth noting that MIC has a tendency to increase, and the highest MIC of CPKP to tigecycline had reached 8 μg/mL; strains with MIC as high as 2 μg/mL were also found in CREC and other CRE species. Studies have shown that when the MIC is 1 μg/mL, the conventional dosage of tigecycline is worthy of questions (Silvestri and van Saene, 2010), because peak serum levels of tigecycline are low (0.63–1.4 mg/mL) after standard dosing (100 mg followed by 50 mg every 12 h) due to its rapid movement from the bloodstream into tissues after administration (Yamashita et al., 2014), and another study showed that a high-dose tigecycline regimen (200 mg followed by 100 mg every 12 h) was a reasonable strategy for BSIs and other severe infections by CRE (Tumbarello et al., 2018). In general, the CFRs of tigecycline were higher, but because of a lack of exact PK/PD target in BSIs, we still have a suspicion about the efficacy of high-dose tigecycline regimen for use in BSIs with CRE; more prospective studies are needed to determine the clinical benefits of high-dose tigecycline for BSIs with CRE.

Polymyxin B PTA at MIC ≤ 1 mg/L showed excellent target attainment (>98%) at any dosage, whereas PTAs ranged from 3.78 to 25.97% at MIC 2 mg/L. For CRKP and CREC, the CFRs of all administration regimens of polymyxin B could reach 80% or more, and our research showed that polymyxin B could achieve moderate results under majority of conventional dosing regimens, whereas dosing regimens with a CFR between 80 and 90% were regarded as providing moderate probabilities of treatment success (Bradley et al., 2003). For other CRE species, the CFRs ranged from 76.31 to 79.99%, with no administration regimen achieving 90%. However, it is important to note that polymyxin poses a risk of nephrotoxicity (Vattimo M de et al., 2016; Liu et al., 2021; Zeng et al., 2021), especially when administered in large dosage. Data indicated that the tolerated maximum dosage of polymyxin B is 3 mg/kg per day (Liu et al., 2021), although the maximum dosage of polymyxin B is the most effective of all regimens according to simulation; attention should be paid to monitoring renal function when applied.

Monte Carlo simulation was applied in this study to predict the efficacy of three different drug administration regimens in the CRE BSI, without combining the host status, such as combination medication, whether there was hypoproteinemia, and so on, which will lead to different clinical results. In the future, more prospective studies are still needed to evaluate the therapeutic effects of the aforementioned dosing regimens.

CONCLUSION

Our study indicates that tigecycline and polymyxin B regimens have high CFR value of BSIs caused by CRE; ceftazidime/avibactam achieved the lowest CFR values among three antimicrobials. Tigecycline regimens were more effective against CRE than the other two antibiotics. For tigecycline and ceftazidime/avibactam, with simulated regimen improvement, the CFR values were both increased. We suggest that measurement of MICs and individualized therapy should be considered together to achieve the optimal drug exposure. In particular, PK and PD modeling based on local antimicrobial resistance data can provide valuable guidance for clinicians for the administration of empirical antibiotic treatments for BSIs.

DATA AVAILABILITY STATEMENT

The original contributions presented in the study are included in the article/supplementary material, further inquiries can be directed to the corresponding author/s.

AUTHOR CONTRIBUTIONS

YJ and YX were responsible for the study conception and design. DZ drafted the manuscript. GY, CS, JJ, CY, PW, ZL, and JW searched the literature. All authors contributed to the article and approved the submitted version.

FUNDING

This work was partially funded by grants from the Key Research and Development Program of Zhejiang Province (2021C03068), the Shandong Province Medical and Health Technology Development Plan (2019WS501), and the Special Funding for Clinical Pharmacy Research of Shandong Provincial Medical Association (YXH2021ZX008).

ACKNOWLEDGMENTS

We thank members of the National Bloodstream Infection Bacterial Resistance Surveillance (BRICS) platform in China: The First Affiliated Hospital, Zhejiang University School of Medicine, Hangzhou 310003, China; Clinical Laboratory, Lishui City Central Hospital, Lishui 323000, China; Clinical Laboratory, Affiliated Hospital of Binzhou Medical College, Binzhou 256603, China; Clinical Laboratory, the First People's Hospital of Lianyungang, Lianyungang 222002, China; Clinical Laboratory, First Affiliated Hospital of Anhui Medical University, Hefei 230022,China; Clinical Laboratory, Yijishan Hospital of Wannan Medical College, Wuhu 241001, China; Clinical Laboratory, Anhui Provincial Hospital, Hefei 230036, China; Clinical Laboratory, Wuhan Puren Hospital, Wuhan 430081, China; Clinical Laboratory, the First People's Hospital of Jingzhou, Jingzhou 434000, China; Clinical Laboratory, People's Hospital of Ningxia Hui Autonomous Region, Yinchuan 750021, China; Clinical Laboratory, Anyang District Hospital of Henan Province, Anyang 455000, China; Clinical Laboratory, the Second People's Hospital of Yunnan Province, Kunming 650021, China; Clinical Laboratory, Zhejiang Provincial Hospital of Traditional Chinese Medicine, Hangzhou 310006, China; Clinical Laboratory, People's Hospital of Huangshan City, Huangshan 245000, China; Clinical Laboratory, Mindong Hospital of Ningde City, Fu'an

355000, China; Clinical Laboratory, the Affiliated Hospital of Jining Medical University, Jining 272000, China; Clinical Laboratory, People's Hospital of Qingyang, Qingyang 745000, China; Clinical Laboratory, Tengzhou Centre People's Hospital, Tengzhou 277500, China; Clinical Laboratory, Lu'an People's Hospital, Lu'an 237000, China; Clinical Laboratory, Xinjiang Uygur Autonomous Region Youyi Hospital, Yili 835000, China; Clinical Laboratory, People's Hospital of Yichun City, Yichun 336000, China; Clinical Laboratory, Jiujiang No. 1 People's Hospital, Jiujiang 332000, China; Clinical Laboratory, Shandong Provincial Hosptial, Jinan 250021, China; Clinical Laboratory, Jingzhou Central Hospital, Jingzhou 434000, China; Clinical Laboratory, the First Affiliated Hospital of Gannan Medical University, Ganzhou 341000, China; Clinical Laboratory, the First Hospital of Putian City, Putian 351100, China; Clinical Laboratory, People's Hospital of Haining City, Haining 314400, China; Clinical Laboratory, Shengli Oilfield Central Hospital, Dongying 257034, China; Clinical Laboratory, the Affiliated Hongqi Hospital of Mudanjiang Medicine College, Mudanjiang 157011, China; Clinical Laboratory, the Affiliated Hospital of Ningbo Medical School, Ningbo 315211, China; Clinical Laboratory, Women's Hospital, Zhejiang University School of Medicine, Hangzhou 310006, China; Clinical Laboratory, the Forth Affiliated Hospital of Anhui Medical University, Hefei 230000, China; Clinical Laboratory, Tianchang City People's Hospital, Tianchang 239300, China; Clinical Laboratory, Shanxi Provincial People's Hospital, Xi'an 710068, China; Clinical Laboratory, the First Affiliated Hospital of Henan University of Science and Technology, Luoyang 471003, China; Clinical Laboratory, the Second People's Hospital of Jingzhou, Jingzhou 530031, China; Clinical Laboratory, Lu'anCivily Hospital, Lu'an 237000, China; Clinical Laboratory, the Second Affiliated Hospital of Bengbu Medicine College, Bengbu 233040, China; Clinical Laboratory, Huaihe Hospital of Henan University, Kaifeng 475000, China; Clinical Laboratory, Qilu Children's Hospital of Shandong University, Jinan 250022, China; Clinical Laboratory, Zigong Third People's Hospital, Zigong 643000, China; Clinical Laboratory, the Second Hospital of Shanxi Medical University, Taiyuan 030001, China; Clinical Laboratory, the People's Hospital of Lujiang, Chaohu 231500, China; Clinical Laboratory, the First People's Hospital of Jiayuguan, Jiayuguan 735100, China; Clinical Laboratory, the Third Hospital of Hefei, Hefei 230022, China; Clinical Laboratory, General Hospital of Northern Theater Command, Shenyang 110015, China; Clinical Laboratory, Xingang Hospital of Xinyu, Xinyu 338001, China; Clinical Laboratory, the First Affiliated Hospital of Xi'an Medical University, Xi'an 710077, China; Clinical Laboratory, Gansu Provincial Hospital of Traditional Chinese Medicine, Lanzhou 730699, China; Clinical Laboratory, First People's Hospital of Chenzhou, Chenzhou 423000, China.

REFERENCES

Averbuch, D., Tridello, G., Hoek, J., Mikulska, M., Akan, H., Yaòez San Segundo, L., et al. (2017). Antimicrobial resistancein gram-negative rods causing bacteremia in hematopoietic stem cell transplant recipients: intercontinental prospective study of the infectious diseases working party of the European bone marrow transplantation group. *Clin. Infect. Dis.* 65, 1819–1828. doi: 10.1093/cid/cix646

Babinchak, T., Ellis-Grosse, E., Dartois, N., Rose, G. M., Loh, E., Tigecycline 301 Study Group, et al. (2005). The efficacy and safety of tigecycline for the treatment of complicated intra-abdominal infections: analysis of pooled clinical trial data. *Clin. Infect. Dis.* 41(Suppl. 5), S354–S367. doi: 10.1086/431676

Bensman, T. J., Wang, J., Jayne, J., Fukushima, L., Rao, A. P., D'Argenio, D. Z., et al. (2017). Pharmacokinetic-pharmacodynamic target attainment analyses to determineoptimal dosing of ceftazidime-avibactamforthe treatment of acute pulmonary exacerbations in patients with cystic fibrosis. *Antimicrob. Agents Chemother.* 61:e00988-17. doi: 10.1128/AAC.00988-17

Bhavnani, S. M., Rubino, C. M., Hammel, J. P., Forrest, A., Dartois, N., Cooper, C. A., et al. (2012). Pharmacological and patient-specific response determinants in patients with hospital-acquired pneumonia treated with tigecycline. *Antimicrob. Agents Chemother.* 56, 1065–1072. doi: 10.1128/AAC.01615-10

Bodmann, K. F., Heizmann, W. R., von Eiff, C., Petrik, C., Löschmann, P. A., and Eckmann, C. (2012). Therapy of 1,025 severely ill patients with complicated infections in a German multicenter study: safety profile and efficacy of tigecycline in different treatment modalities. *Chemotherapy.* 58, 282–294. doi: 10.1159/000342451

Bradley, J. S., Dudley, M. N., and Drusano, G. L. (2003). Predicting efficacy of antiinfectives with pharmacodynamics and Monte Carlo simulation. *Pediatr. Infect. Dis J.* 22, 982–995. doi: 10.1097/01.inf.0000094940.81959.14

Centers for Disease Control and Prevention (2013). *Antibiotic Resistance Threats in the United States,2013[EB/OL]*. Available online at: http://www.cdc.gov/drugresistance/threat-report-2013/pdf/ar-threats-2013-508.pdf (accessed October 9, 2020)

Chen, H. Y., Jean, S. S., Lee, Y. L., Lu, M. C., Ko, W. C., Liu, P. Y., et al. (2021). Carbapenem-resistant enterobacterales in long-term care facilities: a global and narrative review. *Front. Cell. Infect. Microbiol.* 11:601968. doi: 10.3389/fcimb.2021.601968

Clerici, D., Oltolini, C., Greco, R., Ripa, M., Giglio, F., Mastaglio, S., et al. (2021). The place in therapy of ceftazidime/avibactam and ceftolozane/tazobactam in hematological patients with febrile neutropenia. *Int. J. Antimicrob. Agents* 57:106335. doi: 10.1016/j.ijantimicag.2021.106335

CLSI (2019). *Performance Standards for Antimicrobial Susceptibility Testing, Informational Supplement. CLSI Document M100-S29*, 29th Edn. Wayne, PA: Clinical and Laboratory Standards Institute.

Das, S., Li, J., Riccobene, T., Carrothers, T. J., Newell, P., Melnick, D., et al. (2019). Dose selection and validation for ceftazidime-avibactam in adults with complicated intra-abdominal infections, complicated urinary tract infections, and nosocomial pneumonia. *Antimicrob. Agents Chemother.* 63:e02187-18. doi: 10.1128/AAC.02187-18

Dautzenberg, M. J., Wekesa, A. N., Gniadkowski, M., Antoniadou, A., Giamarellou, H., Petrikkos, G. L., et al. (2015). The association between colonization with carbapenemase-producing Enterobacteriaceae and overall ICU mortality: an observational cohort study. *Crit. Care Med.* 43, 1170–1177. doi: 10.1097/CCM.0000000000001028

Drusano, G. L., Preston, S. L., Hardalo, C., Hare, R., Banfield, C., Andes, D., et al. (2001). Use of preclinical data for selection of a phase II/III dose for evernimicin and identification of a preclinical MIC breakpoint. *Antimicrob. Agents Chemother.* 45, 13–22. doi: 10.1128/AAC.45.1.13-22.2001

El-Gamal, M. I., Brahim, I., Hisham, N., Aladdin, R., Mohammed, H., and Bahaaeldin, A. (2017). Recent updates of carbapenem antibiotics. *Eur. J. Med. Chem.* 131, 185–195. doi: 10.1016/j.ejmech.2017.03.022

Ellis-Grosse, E. J., Babinchak, T., Dartois, N., Rose, G., Loh, E., Tigecycline 300 cSSSI Study Group, et al. (2005). The efficacy and safety of tigecycline in the treatment of skin and skin-structure infections: results of 2 double-blind phase 3 comparison studies with vancomycin-aztreonam. *Clin. Infect. Dis.* 41(Suppl. 5), S341–S353. doi: 10.1086/431675

Falagas, M. E., Tansarli, G. S., Karageorgopoulos, D. E., and Vardakas, K. Z. (2014). Deaths attributable to carbapenem-resistant Enterobacteriaceae infections. *Emerg. Infect. Dis.* 20, 1170–1175. doi: 10.3201/eid2007.121004

Han, R., Shi, Q., Wu, S., Yin, D., Peng, M., Dong, D., et al. (2020). Dissemination of carbapenemases (KPC, NDM, OXA-48, IMP, and VIM) among carbapenem-resistant Enterobacteriaceae isolated from adult and children patients in China. *Front. Cell. Infect. Microbiol.* 10:314. doi: 10.3389/fcimb.2020.00314

Hussein, K., Raz-Pasteur, A., Finkelstein, R., Neuberger, A., Shachor-Meyouhas, Y., Oren, I., et al. (2013). Impact of carbapenem resistance on the outcome of patients' hospital-acquired bacteraemia caused by *Klebsiella pneumoniae*. *J. Hosp. Infect.* 83, 307–313. doi: 10.1016/j.jhin.2012.10.012

Landman, D., Georgescu, C., Martin, D. A., and Quale, J. (2008). Polymyxins revisited. *Clin. Microbiol. Rev.* 21, 449–465. doi: 10.1128/CMR.00006-08

Laupland, K. B., and Church, D. L. (2014). Population-based epidemiology and microbiology of community-onset bloodstream infections. *Clin. Microbiol. Rev.* 27, 647–664. doi: 10.1128/CMR.00002-14

Lee, H., and Lee, H. (2016). Clinical and economic evaluation of multidrug-resistant *Acinetobacter baumannii* colonization in the intensive care unit. *Infect. Chemother.* 48, 174–180. doi: 10.3947/ic.2016.48.3.174

Li, J., Lovern, M., Green, M. L., Chiu, J., Zhou, D., Comisar, C., et al. (2019). Ceftazidime-avibactam population pharmacokinetic modeling and pharmacodynamic target attainment across adult indications and patient subgroups. *Clin. Transl. Sci.* 12, 151–163. doi: 10.1111/cts.12585

Li, J., Nation, R. L., Turnidge, J. D., Milne, R. W., Coulthard, K., Rayner, C. R., et al. (2006). Colistin: the re-emerging antibiotic for multidrug-resistant Gram-negative bacterial infections. *Lancet Infect. Dis.* 6, 589–601. doi: 10.1016/S1473-3099(06)70580-1

Little, M. L., Qin, X., Zerr, D. M., and Weissman, S. J. (2012). Molecular diversity in mechanisms of carbapenem resistance in paediatric Enterobacteriaceae. *Int. J. Antimicrob. Agents* 39, 52–57. doi: 10.1016/j.ijantimicag.2011.09.014

Liu, X., Chen, Y., Yang, H., Li, J., Yu, J., Yu, Z., et al. (2021). Acute toxicity is a dose-limiting factor for intravenouspolymyxin B: a safety and pharmacokinetic study in healthy Chinese subjects. *J. Infect.* 82, 207–215. doi: 10.1016/j.jinf.2021.01.006

Meatherall, B. L., Gregson, D., Ross, T., Pitout, J. D., and Laupland, K. B. (2009). Incidence, risk factors, and outcomes of *Klebsiella pneumoniae* bacteremia. *Am. J. Med.* 122, 866–873. doi: 10.1016/j.amjmed.2009.03.034

Miglis, C., Rhodes, N. J., Avedissian, S. N., Kubin, C. J., Yin, M. T., Nelson, B. C., et al. (2018). Population pharmacokinetics of polymyxin B in acutely ill adult patients. *Antimicrob. Agents Chemother.* 62:e01475-17. doi: 10.1128/AAC.01475-17

Mouton, J. W., Dudley, M. N., Cars, O., Derendorf, H., and Drusano, G. L. (2005). Standardization of pharmacokinetic/pharmacodynamic (PK/PD) terminology for anti-infective drugs: an update. *J. Antimicrob. Chemother.* 55, 601–607. doi: 10.1093/jac/dki079

Nang, S. C., Azad, M. A. K., Velkov, T., Zhou, Q. T., and Li, J. (2021). Rescuing the last-line polymyxins: achievements and challenges. *Pharmacol. Rev.* 73, 679–728. doi: 10.1124/pharmrev.120.000020

Neuwirth, C., Siébor, E., Duez, J. M., Péchinot, A., and Kazmierczak, A. (1995). Imipenem resistance in clinical isolates of *Proteus mirabilis* associated with alterations in penicillin-binding proteins. *J. Antimicrob. Chemother.* 36, 335–342. doi: 10.1093/jac/36.2.335

Pankey, G. A. (2005). Tigecycline. *J. Antimicrob. Chemother.* 56, 470–480. doi: 10.1093/jac/dki248

Patel, G., Huprikar, S., Factor, S. H., Jenkins, S. G., and Calfee, D. P. (2008). Outcomes of carbapenem-resistant *Klebsiella pneumoniae* infection and the impact of antimicrobial and adjunctive therapies. *Infect. Control Hosp. Epidemiol.* 29, 1099–1106. doi: 10.1086/592412

Rahal, J. J. (2008). The role of carbapenems in initial therapy for serious Gram-negative infections. *Crit. Care* 12(Suppl. 4):S5. doi: 10.1186/cc6821

Rubino, C. M., Forrest, A., Bhavnani, S. M., Dukart, G., Cooper, A., Korth-Bradley, J., et al. (2010). Tigecycline population pharmacokinetics in patients with community- or hospital-acquired pneumonia. *Antimicrob. Agents Chemother.* 54, 5180–5186. doi: 10.1128/AAC.01414-09

Satlin, M. J., Calfee, D. P., Chen, L., Fauntleroy, K. A., Wilson, S. J., Jenkins, S. G., et al. (2013). Emergence of carbapenem-resistant Enterobacteriaceae as causes of bloodstream infections in patients with hematologic malignancies. *Leuk. Lymphoma* 54, 799–806. doi: 10.3109/10428194.2012.723210

Satlin, M. J., Cohen, N., Ma, K. C., Gedrimaite, Z., Soave, R., Askin, G., et al. (2016). Bacteremia due to carbapenem-resistant Enterobacteriaceae in neutropenic patients with hematologic malignancies. *J. Infect.* 73, 336–345. doi: 10.1016/j.jinf.2016.07.002

Shields, R. K., Nguyen, M. H., Chen, L., Press, E. G., Potoski, B. A., Marini, R. V., et al. (2017). Ceftazidime-avibactam is superior to other treatment regimens against carbapenem-resistant *Klebsiella pneumoniae* bacteremia. *Antimicrob. Agents Chemother.* 61:e00883-17. doi: 10.1128/AAC.00883-17

Shields, R. K., Potoski, B. A., Haidar, G., Hao, B., Doi, Y., Chen, L., et al. (2016). Clinical outcomes, drug toxicity, and emergence of ceftazidime-avibactam resistance among patients treated for carbapenem-resistant Enterobacteriaceae infections. *Clin. Infect. Dis.* 63, 1615–1618. doi: 10.1093/cid/ciw636

Sievert, D. M., Ricks, P., Edwards, J. R., Schneider, A., Patel, J., Srinivasan, A., et al. (2013). Antimicrobial-resistant pathogens associated with healthcare-associated infections: summary of data reported to the National Healthcare Safety Network at the Centers for Disease Control and Prevention, 2009-2010. *Infect. Control Hosp. Epidemiol.* 34, 1–14. doi: 10.1086/668770

Silvestri, L., and van Saene, H. K. (2010). Hospital-acquired infections due to gram-negative bacteria. *N. Engl. J. Med.* 363, 1482–1484. doi: 10.1056/NEJMc1006641

Temkin, E., Torre-Cisneros, J., Beovic, B., Benito, N., Giannella, M., Gilarranz, R., et al. (2017). Ceftazidime-avibactam as salvage therapy for infections caused by carbapenem-resistant organisms. *Antmicrob. Agents Chemother.* 61:e01964-16. doi: 10.1128/AAC.01964-16

Thamlikitkul, V., Dubrovskaya, Y., Manchandani, P., Ngamprasertchai, T., Boonyasiri, A., Babic, J. T., et al. (2016). Dosing and pharmacokinetics of polymyxin B in patients with renal insufficiency. *Antimicrob. Agents Chemother.* 61:e01337-16. doi: 10.1128/AAC.01337-16

Tumbarello, M., Losito, A. R., and Giamarellou, H. (2018). Optimizing therapy in carbapenem-resistant Enterobacteriaceae infections. *Curr. Opin. Infect. Dis.* 31, 566–577. doi: 10.1097/QCO.0000000000000493

Tumbarello, M., Trecarichi, E. M., Corona, A., De Rosa, F. G., Bassetti, M., Mussini, C., et al. (2019). Efficacy of ceftazidime-avibactam salvage therapy in patients with infections caused by *Klebsiella pneumoniae* carbapenemase-producing *K. Pneumoniae*. *Clin. Infect. Dis.* 68, 355–364. doi: 10.1093/cid/ciy492

Tumbarello, M., Viale, P., Viscoli, C., Trecarichi, E. M., Tumietto, F., Marchese, A., et al. (2012). Predictors of mortality in bloodstream infections caused by *Klebsiella pneumoniae* carbapenemase-producing *K. pneumoniae*: importance of combination therapy. *Clin. Infect. Dis.* 55, 943–950. doi: 10.1093/cid/cis588

Vasoo, S., Barreto, J. N., and Tosh, P. K. (2015). Emerging issues in gram-negative bacterial resistance: an update for the practicing clinician. *Mayo Clin. Proc.* 90, 395–403. doi: 10.1016/j.mayocp.2014.12.002

Vattimo M de, F., Watanabe, M., da Fonseca, C. D., Neiva, L. B., Pessoa, E. A., and Borges, F. T. (2016). Polymyxin B nephrotoxicity: from organ to cell damage. *PLoS One* 11:e0161057. doi: 10.1371/journal.pone.0161057

Wang, C., Hao, W., Jin, Y., Shen, C., and Wang, B. (2020). Pharmacokinetic/pharmacodynamic modeling of seven antimicrobials for empiric treatment of adult bloodstream infections with gram-negative bacteria in China. *Microb Drug Resist.* 26, 1559–1567. doi: 10.1089/mdr.2019.0152

Wu, Y. E., Xu, H. Y., Shi, H. Y., van den Anker, J., Chen, X. Y., and Zhao, W. (2020). Carbapenem-resistant Enterobacteriaceae bloodstream infection treated successfully with high-dose meropenem in a preterm neonate. *Front. Pharmacol.* 11:566060. doi: 10.3389/fphar.2020.566060

Yamashita, N., Matschke, K., Gandhi, A., and Korth-Bradley, J. (2014). Tigecycline pharmacokinetics, tolerability, safety, and effect on intestinal microflora in healthy Japanese male subjects. *J. Clin. Pharmacol.* 54, 513–519. doi: 10.1002/jcph.236

Yu, Y., Fei, A., Wu, Z., Gao, C., and Pan, S. (2017). Intravenous polymyxins: revival with puzzle. *Biosci. Trends.* 11, 370–382. doi: 10.5582/bst.2017.01188

Zarkotou, O., Pournaras, S., Tselioti, P., Dragoumanos, V., Pitiriga, V., Ranellou, K., et al. (2011). Predictors of mortality in patients with bloodstream infections caused by KPC-producing *Klebsiella pneumoniae* and impact of appropriate antimicrobial treatment. *Clin. Microbiol. Infect.* 17, 1798–1803. doi: 10.1111/j.1469-0691.2011.03514.x

Zavascki, A. P., Goldani, L. Z., Li, J., and Nation, R. L. (2007). Polymyxin B for the treatment of multidrug-resistant pathogens: a critical review. *J. Antimicrob. Chemother.* 60, 1206–1215. doi: 10.1093/jac/dkm357

Zeng, H., Zeng, Z., Kong, X., Zhang, H., Chen, P., Luo, H., et al. (2021). Effectiveness and nephrotoxicity of intravenous polymyxin B in Chinese patients with MDR and XDR nosocomial pneumonia. *Front. Pharmacol.* 11:579069. doi: 10.3389/fphar.2020.579069

Zhu, W., Chu, Y., Zhang, J., Xian, W., Xu, X., and Liu, H. (2020). Pharmacokinetic and pharmacodynamic profiling of four antimicrobials against *Acinetobacter baumannii* infection. *Microb. Pathog.* 138:103809. doi: 10.1016/j.micpath.2019.103809

Zou, C., Wei, J., Shan, B., Chen, X., Wang, D., and Niu, S. (2020). In vitro activity of ceftazidime-avibactam and aztreonam-avibactam against carbapenem-resistant Enterobacteriaceae isolates collected from three secondary hospitals in Southwest China between 2018 and 2019. *Infect. Drug Resist.* 13, 3563–3568. doi: 10.2147/IDR.S273989

Conflict of Interest: The authors declare that the research was conducted in the absence of any commercial or financial relationships that could be construed as a potential conflict of interest.

frontiers in Microbiology

ORIGINAL RESEARCH
published: 13 December 2021
doi: 10.3389/fmicb.2021.779988

Edited by:
Che-Hsin Lee,
National Sun Yat-sen University,
Taiwan

Reviewed by:
Hua Zhou,
Zhejiang University, China
Chang-Ro Lee,
Myongji University, South Korea

***Correspondence:**
Andrea Lay-Hoon Kwa
andrea.kwa.l.h@sgh.com.sg

†Present address:
Nazira Fauzi,
Department of Infection Prevention, National University Hospital, Singapore, Singapore
Shannon Jing-Yi Lee, NovogeneAIT Pte Ltd., Singapore, Singapore
Yiying Cai, Programme in Health Services and Systems Research, Duke-National University of Singapore Medical School, Singapore, Singapore

Specialty section:
This article was submitted to Antimicrobials, Resistance and Chemotherapy, a section of the journal Frontiers in Microbiology

Received: *20 September 2021*
Accepted: *22 November 2021*
Published: *13 December 2021*

Citation:
Teo JQ, Fauzi N, Ho JJ, Tan SH, Lee SJ, Lim TP, Cai Y, Chang HY, Mohamed Yusoff N, Sim JH, Tan TT, Ong RT and Kwa AL (2021) In vitro Bactericidal Activities of Combination Antibiotic Therapies Against Carbapenem-Resistant Klebsiella pneumoniae With Different Carbapenemases and Sequence Types. Front. Microbiol. 12:779988. doi: 10.3389/fmicb.2021.779988

In vitro Bactericidal Activities of Combination Antibiotic Therapies Against Carbapenem-Resistant *Klebsiella pneumoniae* With Different Carbapenemases and Sequence Types

Jocelyn Qi-Min Teo[1,2], Nazira Fauzi[1†], Jayden Jun-Yuan Ho[1], Si Hui Tan[1], Shannon Jing-Yi Lee[1†], Tze Peng Lim[1,3,4], Yiying Cai[1†], Hong Yi Chang[1], Nurhayati Mohamed Yusoff[1], James Heng-Chiak Sim[5], Thuan Tong Tan[6], Rick Twee-Hee Ong[2] and Andrea Lay-Hoon Kwa[1,4,7]*

[1] Department of Pharmacy, Singapore General Hospital, Singapore, Singapore, [2] Saw Swee Hock School of Public Health, National University of Singapore and National University Health System, Singapore, Singapore, [3] Singhealth Duke-NUS Pathology Academic Clinical Programme, Singapore, Singapore, [4] Singhealth Duke-NUS Medicine Academic Clinical Programme, Singapore, Singapore, [5] Department of Microbiology, Singapore General Hospital, Singapore, Singapore, [6] Department of Infectious Diseases, Singapore General Hospital, Singapore, Singapore, [7] Emerging Infectious Diseases, Duke-National University of Singapore Medical School, Singapore, Singapore

Carbapenem-resistant *Klebsiella pneumoniae* (CRKP) is becoming increasingly problematic due to the limited effectiveness of new antimicrobials or other factors such as treatment cost. Thus, combination therapy remains a suitable treatment option. We aimed to evaluate the *in vitro* bactericidal activity of various antibiotic combinations against CRKP with different carbapenemase genotypes and sequence types (STs). Thirty-seven CRKP with various STs and carbapenemases were exposed to 11 antibiotic combinations (polymyxin B or tigecycline in combination with β-lactams including aztreonam, cefepime, piperacillin/tazobactam, doripenem, meropenem, and polymyxin B with tigecycline) in static time-kill studies (TKS) using clinically achievable concentrations. Out of the 407 isolate-combination pairs, only 146 (35.8%) were bactericidal (≥3 $\log_{10}$CFU/mL decrease from initial inoculum). Polymyxin B in combination with doripenem, meropenem, or cefepime was the most active, each demonstrating bactericidal activity in 27, 24, and 24 out of 37 isolates, respectively. Tigecycline in combination with β-lactams was rarely bactericidal. Aside from the lower frequency of bactericidal activity in the dual-carbapenemase producers, there was no apparent difference in combination activity among the strains with other carbapenemase types. In addition, bactericidal combinations were varied even in strains with similar STs, carbapenemases, and other genomic characteristics. Our findings demonstrate that

the bactericidal activity of antibiotic combinations is highly strain-specific likely owing to the complex interplay of carbapenem-resistance mechanisms, i.e., carbapenemase genotype alone cannot predict *in vitro* bactericidal activity. The availability of WGS information can help rationalize the activity of certain combinations. Further studies should explore the use of genomic markers with phenotypic information to predict combination activity.

Keywords: *in vitro*, bactericidal, combination, carbapenemase, enterobacterales, tigecycline, polymyxin

INTRODUCTION

Klebsiella pneumoniae are common Gram-negative pathogens that are implicated in a variety of infections including pneumonia, bloodstream infections, and skin/soft tissue infections. As one of the ESKAPE organisms, it possesses the ability to acquire multiple resistance mechanisms to the various drug classes and is a major contributor to nosocomial infections (Rice, 2010). Resistance to carbapenems, one of the last-line antimicrobial agents, in these bacteria has resulted in very limited treatment options for these infections. Although there are currently a few novel agents such as ceftazidime/avibactam and meropenem/vaborbactam, they are not universally active against all carbapenem-resistant *K. pneumoniae* (CRKP) and are cost-prohibitive or are not readily available in certain settings (Bush and Bradford, 2019). Treatment with antibiotic combinations is regarded as the optimal alternative, especially in patients with high mortality risks (Giannella et al., 2019). Multiple *in vitro* studies evaluating combination therapy in CRKP infections have been conducted with varying results (Lenhard et al., 2016). Previously, we have shown that antibiotic combinations were highly strain-specific in extensively drug-resistant NDM-producing *K. pneumoniae* (Lim et al., 2015), while *in vitro* synergy of double carbapenem combinations have been widely demonstrated, albeit primarily in KPC-producing *K. pneumoniae* (Bulik and Nicolau, 2011; Chua et al., 2015; Oliva et al., 2016).

The management of CRKP infections is complicated by the various mechanisms mediating carbapenem resistance which include: (1) production of carbapenemases (e.g., KPC, metallo-β-lactamases, OXA-48); (2) extended-spectrum β-lactamases (ESBLs) in combination with mutations that alter porin function or expression; and (3) overexpression of efflux pumps (Papp-Wallace et al., 2011). Even among the carbapenemases, there are differences in the types of substrates, the mechanisms of hydrolysis, and the hydrolytic activities of the active substrates (Queenan et al., 2010; Jeon et al., 2015). For instance, OXA carbapenemases have a weaker activity against carbapenems compared to the other carbapenemases (Queenan et al., 2010). Along with the type of antibiotics selected for combination therapy, this carbapenemase diversity may have implications in the efficacy of antibiotic combination therapy (Poirel et al., 2016). Hence, this study sought to evaluate the *in vitro* activity of various antibiotic combinations against CRKP with different carbapenemase genotypes.

MATERIALS AND METHODS

Bacterial Isolates

Thirty-seven CRKP isolates with varied carbapenemases were tested. The majority of these isolates were selected from an ongoing carbapenem resistance surveillance project conducted at a 1,800-bed public healthcare hospital since 2015. The remaining isolates were received at the hospital's pharmacy research laboratory for antibiotic combination testing, including isolates from various other local hospitals (Cai B. et al., 2016). These isolates were representative of difficult-to-treat infections encountered which will likely require combination therapy. They possessed highly resistant phenotypic profiles [carbapenem minimum inhibitory concentrations (MICs) $\geq$ 8 mg/L] and represented various high-risk international clones (e.g., ST11, ST17, ST14, ST20, ST147, and ST231) with varying carbapenemases.

Genus identity was determined at the hospital's microbiology laboratory as part of routine investigations using VITEK GNI+ cards (bioMérieux, Hazelwood, MO, United States). The isolates were stored at −70°C in Microbank^{TM} (Pro Lab Diagnostics Inc., Ontario, Canada) storage vials and sub-cultured twice on 5% blood agar plates (Thermo Fisher Scientific Microbiology, Malaysia) for 24 h at 35°C prior to each experiment.

This study is exempted from review by the Singhealth Centralized Institutional Review Board, as it is a retrospective study involving archival bacterial isolates, which does not fall under the Human Biomedical Research Act. No identifiable data were collected.

Antibiotics

Aztreonam, meropenem, and polymyxin B were purchased from Toronto Research Chemicals. Cefepime was purchased from Kemimac(s) Pte Ltd. Piperacillin/tazobactam and tigecycline were purchased from Sigma-Aldrich. Doripenem was obtained from Shionogi and Co. Aliquots of stock solutions of all antibiotics were prepared in sterile water and stored at −80°C. Before each experiment, the aliquots were thawed and diluted to the desired concentrations with cation-adjusted Mueller Hinton broth (Ca-MHB).

In vitro Susceptibility Testing

Carbapenem non-susceptibility was detected routinely at the microbiology laboratory using either disk diffusion testing or the

VITEK® 2 instrument. The minimum inhibitory concentrations (MICs) were determined in this study using customized commercial microbroth dilution panels (Trek Diagnostics, East Grinstead, United Kingdom). *E. coli* ATCC 25922 was used as the quality control strain. MICs were interpreted according to the Clinical and Laboratory Standards Institute (CLSI) guidelines, except for tigecycline which was interpreted according to the Food and Drug Administration (FDA) criteria for tigecycline (CLSI, 2020).

Molecular Characterization

CRKPs were routinely tested for the presence of carbapenemase genes either at the hospital's microbiological laboratory or at the National Public Health Laboratory using in-house polymerase chain reaction (PCR)-based assays or the Cepheid Xpert® Carba-R assay on the GeneXpert® device (Cepheid, Sunnyvale, CA, United States).

Genomic DNA was extracted from overnight bacterial cultures and purified with the Qiagen Blood DNeasy kit (Qiagen Inc., Valencia, CA, United States). The genomic DNA was then used to prepare libraries for paired-end whole-genome sequencing using the Illumina HiSeq or MiSeq instrument (Illumina, San Diego, CA), with a resultant sequencing depth of at least 50-fold. Sequence types (STs) were determined by performing a basic local alignment search tool (BLAST) search of the assembled contigs against multilocus sequence typing (MLST) databases[1], while other antimicrobial resistance features were characterized using the Kleborate tool (v.2.0.4)[2].

Static Time-Kill Studies

Modified TKS were performed on the isolates with the antibiotics singly and in two-antibiotic combinations using procedures described previously (Cai Y. et al., 2016; Cai et al., 2017) to examine the bactericidal activity. In brief, log-phase bacterial suspensions were diluted into 15 mL of fresh Ca-MHB to yield an initial inoculum of approximately 5 $\log_{10}$CFU/mL, which were then transferred to flat-bottomed sterile flasks containing 1 mL of antibiotic solutions and placed into a shaker water bath at 35°C.

A total of 11 combinations were tested—polymyxin B or tigecycline was tested in combination with five different β-lactams. Polymyxin B was also tested in combination with tigecycline. The concentrations utilized in this study were derived from clinically relevant unbound concentrations when maximum antibiotic doses were administered (**Supplementary Table 1**).

At 24 h, aliquots were obtained in duplicates from each flask. Total viable counts were enumerated visually by plating serial dilutions of the aliquots on Mueller-Hinton agar plates (Thermo Fisher Scientific, Singapore). The final limit of detection was 1.3 $\log_{10}$CFU/mL. Bactericidal activity was defined as a 3 $\log_{10}$ CFU/mL decrease (99.9% kill) in the colony count from the initial inoculum at 24 h (CLSI, 1999).

[1]https://pubmlst.org/databases/

[2]https://github.com/katholt/Kleborate

RESULTS

Isolate Characteristics

The phenotypic characteristics of the 37 isolates are presented in **Table 1**. All isolates had similar β-lactam phenotypic characteristics where there was phenotypic resistance to all β-lactams tested. The minimum inhibitory concentrations (MICs) to aztreonam, cefepime, and piperacillin-tazobactam were uniformly high (≥64 mg/L). Carbapenem MICs were also high in all isolates (8 to ≥ 32 mg/L, MIC_{50}: ≥ 32 mg/L). Polymyxin B and tigecycline resistance were observed in nine (24.3%) and four (10.8%) isolates, respectively, of which one isolate was resistant to both polymyxin B and tigecycline (EC301).

The genotypic characteristics are summarized in **Figure 1** (genotypic details of individual isolates are presented in **Supplementary Table 2**). A total of 14 different sequence types (STs) were included. All except two isolates were carbapenemase-producing. Among the various CRKP with differing carbapenemase genotypes, the majority harbored an extended-spectrum β-lactamase (ESBL), most commonly CTX-M-15, together with porin alteration. Out of the nine polymyxin-resistant isolates, MgrB mutations were detected in five of them. Tetracycline resistance *tet* genes were observed in 14 isolates which included both tigecycline-susceptible and -resistant isolates. None of the isolates harbored plasmid-mediated resistance genes associated with polymyxin (*mcr*) and tigecycline [*tet*(X)] resistance.

Static Time-Kill Studies Results

The activity of each antibiotic alone was limited against most of the strains except in two isolates (EC1642 and EC2096) where doripenem (corresponding to a high dose extended infusion regimen) resulted in a bactericidal kill; and in three isolates (EC1717, EC1812, and EC0172) where polymyxin B resulted in bactericidal kill (**Figure 1** and **Supplementary Table 3**). Consequently, doripenem- or polymyxin-containing combination regimens exhibited bactericidal killing against these isolates, respectively.

Of the 407 combinations evaluated, only 146 (35.9%) exhibited bactericidal killing at 24 h. Polymyxin with doripenem (27/37 isolates), meropenem (24/37 isolates), cefepime (24/37 isolates), and tigecycline (20/37 isolates) were the combinations exhibiting the highest bactericidal activities. Polymyxin B in combinations with the various β-lactams were more active (99/185 bactericidal activity, 53.5%) than tigecycline combinations (27/185 bactericidal activity, 14.6%), while polymyxin and tigecycline demonstrated bactericidal activities in 20/37 (54.0%) isolates.

Against polymyxin- and/or tigecycline-resistant isolates, only 32/121 (26.4%) combinations were bactericidal, while 114/286 (39.9%) combinations were bactericidal against isolates that remained susceptible to both polymyxin B and tigecycline. This indicates that combinations were less likely to be active in resistant isolates, suggesting that polymyxin or tigecycline resistance phenotypes could be predictive of the activity of polymyxin and tigecycline combinations, respectively. Only

TABLE 1 | Phenotypic characteristics (antibiotic susceptibilities) of 37 CRKP.

Strain	Carbapenemase	Minimum inhibitory concentrations (mg/L)			
		Doripenem	Meropenem	Polymyxin B	Tigecycline
EC1642	None	8	16	**≥16**	2
EC0283	None	16	16	2	2
EC0215	OXA-181	≥32	≥32	0.5	2
EC1717	OXA-181	≥32	≥32	0.5	2
EC2096	OXA-181	16	≥32	**8**	≤0.25
EC1277	OXA-181	16	≥32	0.5	0.5
EC1824	OXA-181	≥32	≥32	0.5	1
EC1812	OXA-181	≥32	≥32	0.5	1
EC0633	OXA-232	≥32	≥32	1	2
EC1902	OXA-232	≥32	≥32	**≥16**	1
EC0307	KPC-2	8	≥32	0.5	1
EC0301	KPC-2	≥32	≥32	**≥16**	**≥16**
EC2772	KPC-2	16	≥32	≤0.25	≤0.25
EC1470	KPC-2	≥32	≥32	**≥16**	2
EC2617	KPC-2	≥32	≥32	0.5	**8**
EC0174	NDM-1	≥32	≥32	0.5	2
EC0044	NDM-1	≥32	≥32	≤0.25	0.5
EC0466	NDM-1	≥32	≥32	2	**4**
EC0045	NDM-1	≥32	≥32	0.5	2
EC0177	NDM-1	≥32	≥32	0.5	2
EC0178	NDM-1	≥32	≥32	0.5	2
EC0334	NDM-1	≥32	≥32	2	0.5
EC1170	NDM-1	≥32	≥32	**8**	2
EC0172	NDM-1	≥32	≥32	0.5	≤0.25
EC0299	IMP-1	≥32	≥32	1	**4**
EC0360	NDM-1 + OXA-181	≥32	≥32	0.5	2
EC0564	NDM-1 + OXA-181	≥32	≥32	**8**	1
EC0567	NDM-1 + OXA-181	≥32	≥32	**8**	1
EC0391	NDM-1 + OXA-181	≥32	≥32	**8**	1
EC1488	NDM-1 + OXA-232	≥32	≥32	2	2
EC1522	NDM-1 + OXA-232	≥32	≥32	0.5	1
EC1645	NDM-1 + OXA-232	≥32	≥32	0.5	2
EC1655	NDM-1 + OXA-232	≥32	≥32	0.5	1
EC1678	NDM-1 + OXA-232	≥32	≥32	0.5	1
EC1729	NDM-1 + OXA-232	≥32	≥32	1	1
EC1792	NDM-1 + OXA-232	≥32	≥32	0.5	1
EC0462	NDM-1 + OXA-232	≥32	≥32	0.5	1

Aztreonam and piperacillin-tazobactam minimum inhibitory concentrations are not shown here as all isolates have values ≥ 64 mg/L (resistant phenotype). Values in bold denote polymyxin- and/or tigecycline-resistant isolates.

seven polymyxin B combinations retained bactericidal activity against polymyxin-resistant isolates (Polymyxin B + doripenem against EC1642, EC2096, EC1902; polymyxin B + meropenem against EC1642; polymyxin B + cefepime against EC2096 polymyxin B + tigecycline against EC1642, EC2096). Against tigecycline-resistant isolates, polymyxin + tigecycline was the only tigecycline-containing combination that exhibited bactericidal killing (EC2617 and EC0299).

Analyzing only the polymyxin B- and tigecycline-susceptible isolates where monotherapy was not bactericidal (22 isolates), our results did not reveal marked differences in bactericidal activity between isolates harboring OXA-48-like, KPC-2 or NDM-1 (**Supplementary Figure 1**). Polymyxin B with cefepime, doripenem, or meropenem was bactericidal against almost all of these isolates (except EC0283 where polymyxin + cefepime was not bactericidal). The remaining combinations were variable in activity. Against NDM and OXA dual producers, all combinations were variable in activity. This was despite dual carbapenemase-producing isolates belonging to the same ST and harboring similar genotypic characteristics (carbapenemases, β-lactamases, and porin genes), suggesting that STs were unlikely to predict any specific antibiotics in combination.

Interestingly, only four combinations (polymyxin with meropenem/doripenem or tigecycline with

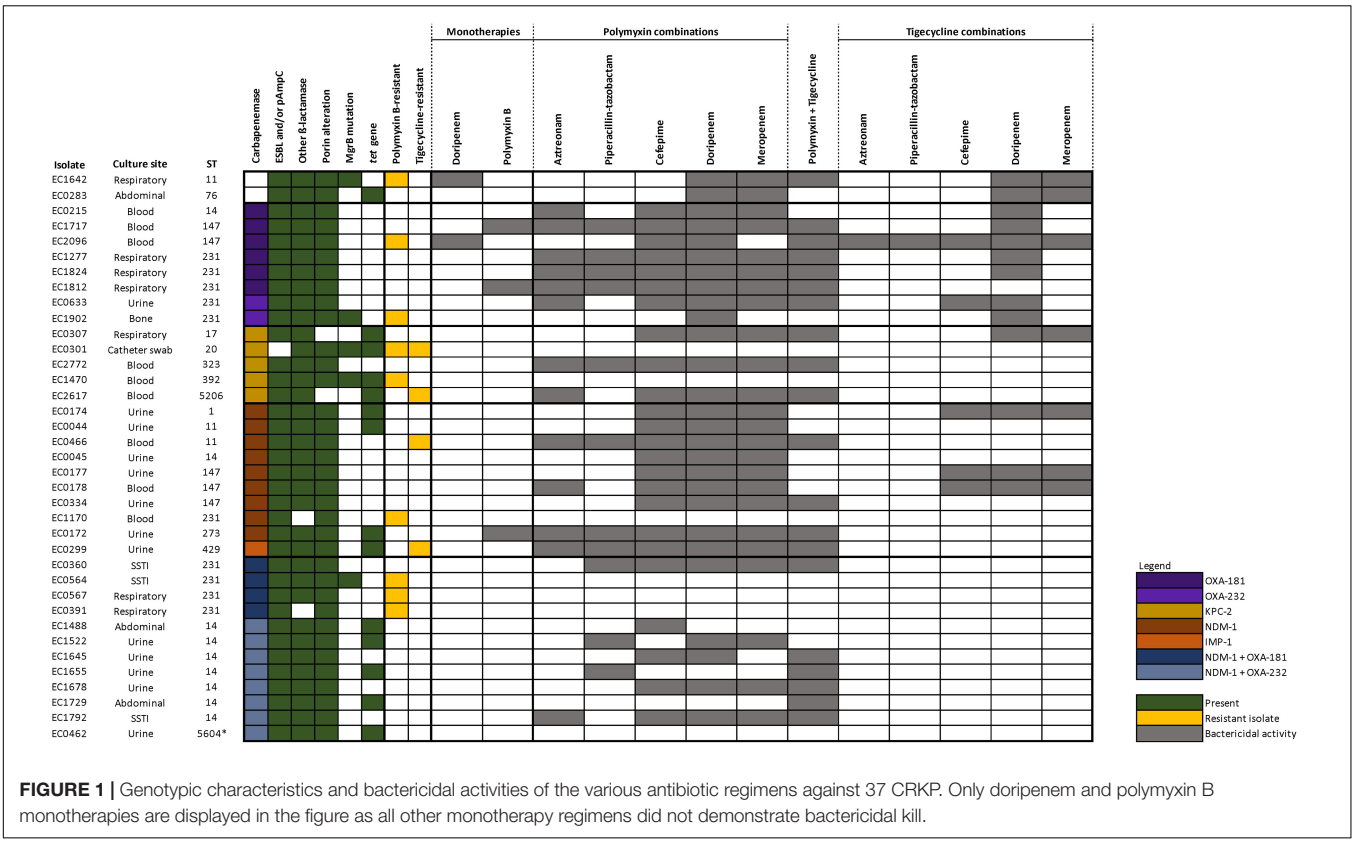

FIGURE 1 | Genotypic characteristics and bactericidal activities of the various antibiotic regimens against 37 CRKP. Only doripenem and polymyxin B monotherapies are displayed in the figure as all other monotherapy regimens did not demonstrate bactericidal kill.

meropenem/doripenem) were bactericidal against EC0283, which did not harbor any carbapenemase. In this study, we included CRKP (carbapenem MICs > 8 mg/L), which were isolates where most single antibiotic therapies including high-dose carbapenem extended infusions will likely fail; hence it is likely EC0283, while not a carbapenemase-producer, harbored higher levels of CTX-M-15 and a higher degree of porin loss to manifest the high carbapenem phenotypic resistance which could not be overcome by combination therapies.

DISCUSSION

CRKP infections are challenging to treat due to limited treatment options. Antibiotic combination therapy has been explored as a viable option in several *in vitro* studies, but available data are limited by the overrepresentation of KPC producers (Zusman et al., 2013). It is well known that the effectiveness of antibiotic combinations is not universal and tends to be unpredictable, rendering it extremely challenging to select an antibiotic combination regimen. Interactions observed when antibiotics are combined can range from antagonism to synergism rates up to 80% (Zusman et al., 2013; Lenhard et al., 2016; Mohammadi et al., 2017; Jiang et al., 2018). These interactions can be influenced by pathogen factors (species, susceptibility, and resistance mechanisms), antibiotic factors (number, classes, and concentration), and the testing methodology (Zusman et al., 2013). As the understanding of the mechanisms behind the bactericidal/synergistic/additive effect of combinations remains poor, we evaluated 37 CRKP isolates with differing carbapenemase genotypes against 11 two-antibiotic combinations in this study.

In our study, bactericidal activity was observed with at least one polymyxin-containing combination for the majority of the isolates. This result corroborates other *in vitro* studies where synergistic/bactericidal activity has been demonstrated with polymyxin B-containing combinations. Synergy rates between 30 and 59% for *K. pneumoniae* have been reported, and polymyxins in combination with carbapenems have demonstrated bactericidal activity in several *in vitro* studies (Zusman et al., 2013; Lenhard et al., 2016; Scudeller et al., 2021). The utility of polymyxin combinations has mechanistic plausibility. In Gram-negative bacteria like *K. pneumoniae*, most antibiotics enter the cell *via* porin channels in the outer membrane. Polymyxins' main mechanism of bacterial killing has been suggested to be the disruption/destabilization of the outer membrane (Trimble et al., 2016). There is evidence that synergism between polymyxin and other antibiotics occurs as a result of this membrane disruption, allowing the entry of the partner antibiotics into the bacterial cell (Rosenthal and Storm, 1977). However, it appears that bactericidal activity of polymyxin combinations is primarily limited to polymyxin-susceptible isolates in our study, unlike other reports which established combination activity in polymyxin-resistant strains (Jernigan et al., 2012). The difference in combination activities observed in our isolates with frank polymyxin B resistance

(mediated by MgrB mutations) might be related to differences in the mechanisms mediating polymyxin resistance.

In contrast, we did not observe good results with tigecycline-containing combinations, even in tigecycline-susceptible isolates. Previous studies have also demonstrated variable *in vitro* tigecycline activity (Pournaras et al., 2011). Antagonism has also been reported with tigecycline and meropenem/doripenem combinations (Bi et al., 2019). Tigecycline is a bacteriostatic drug that exerts its activity *via* ribosomal binding, leading to the prevention of protein synthesis and retardation of cell growth (Greer, 2006). Studies have demonstrated that tetracyclines affect cell division, leading to growth stasis forming the basis of antagonism when paired with bactericidal drugs such as β-lactams which are the most potent against actively dividing cells (Ocampo et al., 2014). This phenomenon, also known as phenotypic tolerance (Tuomanen, 1986), might explain the lack of activity in the tigecycline and β-lactam combinations assessed here, whereas tigecycline when paired with polymyxin still exhibit moderate activity (**Supplementary Table 3**). Contrary to our expectation of beta-lactam activity being inhibited/antagonized by the addition of tigecycline in tigecycline and beta-lactam combinations, we have also noticed higher 24-h bacterial counts of tigecycline combinations compared to tigecycline monotherapy. The mechanisms behind this antagonism warrant further exploration.

There was high variability in bactericidal activity of the various combinations in our isolates, emphasizing the high strain specificity of antibiotic combinations. It was suggested that genotypic information could be more predictive of combination antibiotic activities/interactions than the phenotypes alone (Shields et al., 2015; Wistrand-Yuen et al., 2020). Knowledge of the carbapenemase family can aid in the rationalization of therapeutic choices since the different carbapenemases have different substrate activities (Queenan and Bush, 2007; Livermore et al., 2020). In this study, aside from the poor bactericidal activity observed amongst the co-producers, we were unable to identify a clear trend among the isolates with the other carbapenemase types, indicating that the knowledge of carbapenemase types alone was a poor indicator of combination activity in our isolates.

The mechanisms of carbapenem resistance are complex and multi-factorial. Aside from being mediated by carbapenemase production, resistance may also result from various combinations of β-lactamases production, porin loss/downregulation, and efflux activity, leading to the same carbapenem resistance phenotype (Codjoe and Donkor, 2017). The availability of WGS results in this study shed some light on our observations. All of our isolates harbored at least one ESBL/plasmid AmpC, in addition to the carbapenemases which might have explained the higher frequency of bactericidal activity in doripenem, meropenem, and cefepime combinations since these β-lactams are generally more stable against ESBL production. We also noted that many of our isolates have porin mutations which may lead to decreased porin expression. The variability in combination effectiveness may be related to differentiation in the levels of porin expression, which was unfortunately not quantitated in this study. Given that the mechanism of combination antibiotic synergism/bactericidal effect is likely due to the increased effective entry of the antibiotic into the bacterial cell, combination therapy may likely be more effective in strains where phenotypic resistance is contributed to a larger extent by cell permeability which may then be "reversed" with antibiotic combinations. In light of this, further studies characterizing/quantitating porin expression and efflux activity may be useful to establish if genetic mechanisms related to cell permeability may be a better predictor of the bactericidal activity of the combination.

The complexity of mechanisms mediating carbapenem resistance has contributed to the difficulty in antibiotic combination selection. However, it is unlikely that there is a universal combination that is effective against all or even the majority of the CRKP strains, and knowledge of the genomic characteristics still only serves as a small step toward the rational selection of antibiotic combinations. Given that our local isolates tend to co-harbor ESBLs and are porin-deficient, partner antibiotics that are ESBL-stable and have better cell penetration profiles should be selected. In our study, polymyxin and doripenem appear to be the most reliable combination against the various types of CRKP. Aside from the better β-lactamase stability of doripenem compared to the other β-lactams like cefepime, aztreonam, and piperacillin-tazobactam, its pharmacodynamic and safety profile of doripenem has allowed the drug to be given at a high-dose prolonged infusion (concentration of doripenem used in this study corresponded to a 2 g every 8-hourly dosing regimen given as a 4-h prolonged infusion), which will likely result in a higher probability in achieving a longer $fT > MIC$ (Strawbridge and Nailor, 2016). Furthermore, doripenem MICs tended to be one to twofold lower compared to meropenem. It was also proposed that there might be improved *in vivo* efficacy compared to the other carbapenems due to a favorable immunological profile (enhanced neutrophil killing and reduced endotoxin release) (Hilliard et al., 2011). When taken together with other studies supporting the positive interactions with polymyxin-doripenem combinations (Deris et al., 2012; Jernigan et al., 2012; Lee and Burgess, 2013), this combination may be considered a rational choice for the treatment of CRKP infections, especially if other potentially active agents such as ceftazidime-avibactam are not available. Furthermore, this was the only combination that potentially exhibited activity against polymyxin-resistant strains.

This study is not without limitations. We utilized static time-kill studies to evaluate bactericidal activity, which may not correlate well with *in vivo* studies. The small sample size also limits the generalization of our results to the larger CRKP population. Ideally, further studies, including pharmacokinetic/pharmacodynamic models, animal models, and even clinical trials, should be conducted to verify if these *in vitro* observations may be translated to clinical utility. Nevertheless, the findings are in line and lend support to several other *in vitro* studies as discussed above. We hope the results here may serve as a proof of concept and provide a preliminary guide for rational antibiotic combination design, aiding to narrow down the potential combinations that will eventually be brought to large clinical trials.

CONCLUSION

The present study confirmed the high strain specificity of antibiotic combinations among CRKP with various carbapenemase genotypes. Bactericidal killing was observed with polymyxin combinations, in particular, polymyxin B with doripenem, against CRKP with varying carbapenemase genotypes. However, bactericidal killing was rare against polymyxin-resistant CRKP and those harboring more than one carbapenemase, suggesting that more efforts need to be directed at identifying therapeutic options for this group of pathogens. WGS provided genomic information about the bacterial resistome, which when taken together with pharmacokinetic/pharmacodynamic knowledge of the various antibiotics can guide the rational selection of combination antibiotic therapy. This approach will improve the chances of selecting a successful combination through identifying potential synergistic mechanisms and avoidance of antagonism. Future *in vitro* pharmacokinetic/pharmacodynamic studies should incorporate genomic characterization to facilitate comparisons between studies.

DATA AVAILABILITY STATEMENT

The datasets presented in this study can be found in online repositories. The names of the repository/repositories and accession number(s) can be found below: https://www.ncbi.nlm.nih.gov/, PRJNA577535.

AUTHOR CONTRIBUTIONS

JT conceived and designed the study, performed the laboratory work and data curation and data and bioinformatics analyses, and wrote the manuscript. NF, JH, and ST undertook the laboratory work and data curation. SL performed the molecular experiments. HC and NMY performed the time-kill studies and phenotypic characterization. TL and YC designed the experiments and reviewed the manuscript. JS provided the isolates, contributed to the implementation of the research, and reviewed the manuscript. TT reviewed the manuscript. RO supervised the bioinformatics analyses and reviewed the manuscript. AK conceived the study, reviewed the manuscript, and provided funding. All authors read and approved the final manuscript.

FUNDING

This study was supported by funding from the National Medical Research Council, Singapore (NMRC/CG/C005/2017, NMRC/CG/M011/2017, NMRC/TA/0056/2017, and NMRC/MOH-000018-00), the Biomedical Research Council, Singapore (IAF311018), and Singapore General Hospital Research Grant (SRG-OF#01/2016).

ACKNOWLEDGMENTS

We would like to thank Tang Cheng Yee for her excellent technical assistance in whole-genome sequencing analyses and the Singapore General Hospital of Microbiology and Pharmacy Research Laboratory for assisting in isolate collection. This work was presented, in part, at the 28th European Congress of Clinical Microbiology and Infectious Diseases (ECCMID), Madrid, Spain, April 21–24, 2018 (Presentation O0577).

SUPPLEMENTARY MATERIAL

The Supplementary Material for this article can be found online at: https://www.frontiersin.org/articles/10.3389/fmicb.2021.779988/full#supplementary-material

REFERENCES

Bi, S., Yao, X., Huang, C., Zheng, X., Xuan, T., Sheng, J., et al. (2019). Antagonistic effect between tigecycline and meropenem: successful management of KPC-producing *Klebsiella pneumoniae* infection. *Infection* 47, 497–500. doi: 10.1007/s15010-019-01274-w

Bulik, C. C., and Nicolau, D. P. (2011). Double-carbapenem therapy for carbapenemase-producing *Klebsiella pneumoniae*. *Antimicrob. Agents Chemother.* 55, 3002–3004. doi: 10.1128/AAC.01420-10

Bush, K., and Bradford, P. A. (2019). Interplay between beta-lactamases and new beta-lactamase inhibitors. *Nat. Rev. Microbiol.* 17, 295–306. doi: 10.1038/s41579-019-0159-8

Cai, B., Cai, Y., Liew, Y. X., Chua, N. G., Teo, J. Q., Lim, T. P., et al. (2016). Clinical Efficacy of polymyxin monotherapy versus nonvalidated polymyxin combination therapy versus validated polymyxin combination therapy in extensively drug-resistant gram-negative *Bacillus* infections. *Antimicrob. Agents Chemother.* 60, 4013–4022. doi: 10.1128/AAC.03064-15

Cai, Y., Lim, T. P., Teo, J., Sasikala, S., Lee, W., Hong, Y., et al. (2016). *In vitro* activity of polymyxin B in combination with various antibiotics against extensively drug-resistant *Enterobacter cloacae* with decreased susceptibility to polymyxin B. *Antimicrob. Agents Chemother.* 60, 5238–5246. doi: 10.1128/AAC.00270-16

Cai, Y., Lim, T. P., Teo, J. Q., Sasikala, S., Chan, E. C., Hong, Y. J., et al. (2017). Evaluating polymyxin B-based combinations against carbapenem-resistant *Escherichia coli* in time-kill studies and in a hollow-fiber infection model. *Antimicrob. Agents Chemother.* 61, e01509-16. doi: 10.1128/AAC.01509-16

Chua, N. G., Zhou, Y. P., Tan, T. T., Lingegowda, P. B., Lee, W., Lim, T. P., et al. (2015). Polymyxin B with dual carbapenem combination therapy against carbapenemase-producing *Klebsiella pneumoniae*. *J Infect* 70, 309–311. doi: 10.1016/j.jinf.2014.10.001

CLSI (1999). *Methods for Determining Bactericidal Activity of Antimicrobial Agents; Approved Guideline. CLSI document M26-A*. Wayne, PA: Clinical and Laboratory Standards Institute.

CLSI (2020). *Performance Standards for Antimicrobial Susceptibility Testing CLSI Supplement M100*, 30th Edn. Wayne, PA: Clinical and Laboratory Standards Institute.

Codjoe, F. S., and Donkor, E. S. (2017). Carbapenem resistance: a review. *Med Sci (Basel)* 6, 1. doi: 10.3390/medsci6010001

Deris, Z. Z., Yu, H. H., Davis, K., Soon, R. L., Jacob, J., Ku, C. K., et al. (2012). The combination of colistin and doripenem is synergistic against *Klebsiella pneumoniae* at multiple inocula and suppresses colistin resistance in an *in vitro* pharmacokinetic/pharmacodynamic model. *Antimicrob. Agents Chemother.* 56, 5103–5112. doi: 10.1128/AAC.01064-12

Giannella, M., Bartoletti, M., Gatti, M., and Viale, P. (2019). Advances in the therapy of bacterial bloodstream infections. *Clin. Microbiol. Infect.* 26, 158–167. doi: 10.1016/j.cmi.2019.11.001

Greer, N. D. (2006). Tigecycline (Tygacil): the first in the glycylcycline class of antibiotics. *Proc. (Bayl Univ Med Cent)* 19, 155–161. doi: 10.1080/08998280.2006.11928154

Hilliard, J. J., Melton, J. L., Hall, L., Abbanat, D., Fernandez, J., Ward, C. K., et al. (2011). Comparative effects of carbapenems on bacterial load and host immune response in a *Klebsiella pneumoniae* murine pneumonia model. *Antimicrob. Agents Chemother.* 55, 836–844. doi: 10.1128/AAC.00670-10

Jeon, J., Lee, J., Lee, J., Park, K., Karim, A., Lee, C.-R., et al. (2015). Structural basis for carbapenem-hydrolyzing mechanisms of carbapenemases conferring antibiotic resistance. *Int. J. Mol. Sci.* 16, 9654–9692. doi: 10.3390/ijms16059654

Jernigan, M. G., Press, E. G., Nguyen, M. H., Clancy, C. J., and Shields, R. K. (2012). The combination of doripenem and colistin is bactericidal and synergistic against colistin-resistant, carbapenemase-producing *Klebsiella pneumoniae*. *Antimicrob. Agents Chemother.* 56, 3395–3398. doi: 10.1128/AAC.06364-11

Jiang, Z., He, X., and Li, J. (2018). Synergy effect of meropenem-based combinations against *Acinetobacter baumannii*: a systematic review and meta-analysis. *Infect. Drug Resist.* 11, 1083–1095. doi: 10.2147/IDR.S172137

Lee, G. C., and Burgess, D. S. (2013). Polymyxins and doripenem combination against KPC-producing *Klebsiella pneumoniae*. *J. Clin. Med. Res.* 5, 97–100. doi: 10.4021/jocmr1220w

Lenhard, J. R., Nation, R. L., and Tsuji, B. T. (2016). Synergistic combinations of polymyxins. *Int. J. Antimicrob. Agents* 48, 607–613. doi: 10.1016/j.ijantimicag.2016.09.014

Lim, T. P., Cai, Y., Hong, Y., Chan, E. C., Suranthran, S., Teo, J. Q., et al. (2015). *In vitro* pharmacodynamics of various antibiotics in combination against extensively drug-resistant *Klebsiella pneumoniae*. *Antimicrob. Agents Chemother.* 59, 2515–2524. doi: 10.1128/aac.03639-14

Livermore, D. M., Nicolau, D. P., Hopkins, K. L., and Meunier, D. (2020). Carbapenem-resistant enterobacterales, carbapenem resistant organisms, carbapenemase-producing enterobacterales, and carbapenemase-producing organisms: terminology past its "Sell-By Date" in an era of new antibiotics and regional carbapenemase epidemiology. *Clin. Infect. Dis.* 71, 1776–1782. doi: 10.1093/cid/ciaa122

Mohammadi, M., Khayat, H., Sayehmiri, K., Soroush, S., Sayehmiri, F., Delfani, S., et al. (2017). Synergistic effect of colistin and rifampin against multidrug resistant *Acinetobacter baumannii*: a systematic review and meta-analysis. *Open Microbiol. J.* 11, 63–71. doi: 10.2174/1874285801711010063

Ocampo, P. S., Lazar, V., Papp, B., Arnoldini, M., Abel Zur Wiesch, P., Busa-Fekete, R., et al. (2014). Antagonism between bacteriostatic and bactericidal antibiotics is prevalent. *Antimicrob. Agents Chemother.* 58, 4573–4582. doi: 10.1128/AAC.02463-14

Oliva, A., Gizzi, F., Mascellino, M. T., Cipolla, A., D'abramo, A., D'agostino, C., et al. (2016). Bactericidal and synergistic activity of double-carbapenem regimen for infections caused by carbapenemase-producing *Klebsiella pneumoniae*. *Clin. Microbiol. Infect.* 22, 147–153. doi: 10.1016/j.cmi.2015.09.014

Papp-Wallace, K. M., Endimiani, A., Taracila, M. A., and Bonomo, R. A. (2011). Carbapenems: past, present, and future. *Antimicrob. Agents Chemother.* 55, 4943–4960. doi: 10.1128/AAC.00296-11

Poirel, L., Kieffer, N., and Nordmann, P. (2016). *In vitro* evaluation of dual carbapenem combinations against carbapenemase-producing *Enterobacteriaceae*. *J. Antimicrob. Chemother.* 71, 156–161. doi: 10.1093/jac/dkv294

Pournaras, S., Vrioni, G., Neou, E., Dendrinos, J., Dimitroulia, E., Poulou, A., et al. (2011). Activity of tigecycline alone and in combination with colistin and meropenem against *Klebsiella pneumoniae* carbapenemase (KPC)-producing *Enterobacteriaceae* strains by time-kill assay. *Int. J. Antimicrob. Agents* 37, 244–247. doi: 10.1016/j.ijantimicag.2010.10.031

Queenan, A. M., and Bush, K. (2007). Carbapenemases: the versatile beta-lactamases. *Clin. Microbiol. Rev.* 20, 440–458. doi: 10.1128/CMR.00001-07

Queenan, A. M., Shang, W., Flamm, R., and Bush, K. (2010). Hydrolysis and inhibition profiles of beta-lactamases from molecular classes A to D with doripenem, imipenem, and meropenem. *Antimicrob. Agents Chemother.* 54, 565–569. doi: 10.1128/AAC.01004-09

Rice, L. B. (2010). Progress and challenges in implementing the research on ESKAPE pathogens. *Infect. Control Hosp. Epidemiol.* 31(Suppl. 1), S7–S10. doi: 10.1086/655995

Rosenthal, K. S., and Storm, D. R. (1977). Disruption of the *Escherichia coli* outer membrane permeability barrier by immobilized polymyxin B. *J. Antibiot. (Tokyo)* 30, 1087–1092. doi: 10.7164/antibiotics.30.1087

Scudeller, L., Righi, E., Chiamenti, M., Bragantini, D., Menchinelli, G., Cattaneo, P., et al. (2021). Systematic review and meta-analysis of *in vitro* efficacy of antibiotic combination therapy against carbapenem-resistant Gram-negative bacilli. *Int. J. Antimicrob. Agents* 57, 106344. doi: 10.1016/j.ijantimicag.2021.106344

Shields, R. K., Nguyen, M. H., Potoski, B. A., Press, E. G., Chen, L., Kreiswirth, B. N., et al. (2015). Doripenem MICs and ompK36 porin genotypes of sequence type 258, KPC-producing *Klebsiella pneumoniae* may predict responses to carbapenem-colistin combination therapy among patients with bacteremia. *Antimicrob. Agents Chemother.* 59, 1797–1801. doi: 10.1128/AAC.03894-14

Strawbridge, S., and Nailor, M. D. (2016). Safety of high-dose doripenem in adult patients with cystic fibrosis. *Ther. Adv. Drug Saf.* 7, 89–93. doi: 10.1177/2042098616643708

Trimble, M. J., Mlynarcik, P., Kolar, M., and Hancock, R. E. (2016). Polymyxin: alternative mechanisms of action and resistance. *Cold Spring Harb. Perspect. Med.* 6, a025288. doi: 10.1101/cshperspect.a025288

Tuomanen, E. (1986). Phenotypic tolerance: the search for beta-lactam antibiotics that kill nongrowing bacteria. *Rev. Infect. Dis.* 8(Suppl. 3), S279–S291. doi: 10.1093/clinids/8.supplement_3.s279

Wistrand-Yuen, P., Olsson, A., Skarp, K. P., Friberg, L. E., Nielsen, E. I., Lagerback, P., et al. (2020). Evaluation of polymyxin B in combination with 13 other antibiotics against carbapenemase-producing *Klebsiella pneumoniae* in time-lapse microscopy and time-kill experiments. *Clin. Microbiol. Infect.* 26, 1214–1221. doi: 10.1016/j.cmi.2020.03.007

Zusman, O., Avni, T., Leibovici, L., Adler, A., Friberg, L., Stergiopoulou, T., et al. (2013). Systematic review and meta-analysis of *in vitro* synergy of polymyxins and carbapenems. *Antimicrob. Agents Chemother.* 57, 5104–5111.[endref] doi: 10.1128/AAC.01230-13

Conflict of Interest: AK received unrestricted funding for research from Pfizer Inc., and Merck Sharp and Dohme (I.A) Corp for investigator-initiated research studies which are not related to this study. The funders were not involved in the study design, collection, analysis, interpretation of data, the writing of this article or the decision to submit it for publication.

The remaining authors declare that the research was conducted in the absence of any commercial or financial relationships that could be construed as a potential conflict of interest.

frontiers in Microbiology

ORIGINAL RESEARCH
published: 14 December 2021
doi: 10.3389/fmicb.2021.777054

Intra- and Extra-Hospital Dissemination of IMP-22-Producing *Klebsiella pneumoniae* in Northern Portugal: The Breach of the Hospital Frontier Toward the Community

Daniela Gonçalves[1,2,3,4†], Pedro Cecílio[1†], Alberta Faustino[5], Carmen Iglesias[5], Fernando Branca[5], Alexandra Estrada[5] and Helena Ferreira[1,2]*

[1]Microbiology Laboratory - Biological Sciences Department, Faculty of Pharmacy, University of Porto, Porto, Portugal, [2]UCIBIO - Research Unit on Applied Molecular Biosciences, REQUIMTE, Porto, Portugal, [3]ISAVE - Instituto Superior de Saúde, Amares, Portugal, [4]CICS - Interdisciplinary Centre in Health Sciences, Amares, Portugal, [5]Clinical Pathology Service - Braga Hospital, Braga, Portugal

OPEN ACCESS

Edited by:
Mullika Traidej Chomnawang, Mahidol University, Thailand

Reviewed by:
Carlos Henrique Camargo, Adolfo Lutz Institute, Brazil
Ignasi Roca Subirà, Instituto Salud Global Barcelona (ISGlobal), Spain

***Correspondence:**
Helena Ferreira
hferr@ff.up.pt

[†]These authors have contributed equally to this work

Specialty section:
This article was submitted to Antimicrobials, Resistance and Chemotherapy, a section of the journal Frontiers in Microbiology

Received: 14 September 2021
Accepted: 16 November 2021
Published: 14 December 2021

Citation:
Gonçalves D, Cecílio P, Faustino A, Iglesias C, Branca F, Estrada A and Ferreira H (2021) Intra- and Extra-Hospital Dissemination of IMP-22-Producing Klebsiella pneumoniae in Northern Portugal: The Breach of the Hospital Frontier Toward the Community. Front. Microbiol. 12:777054. doi: 10.3389/fmicb.2021.777054

The emergence of infections (and colonization) with *Enterobacteriaceae*-producing carbapenemases is a threatening public health problem. In the last decades, we watched an isolated case becoming a brutal outbreak, a sporadic description becoming an endemic problem. The present study aims to highlight the dissemination of IMP-22-producing *Klebsiella pneumoniae* in the North of Portugal, through the phenotypic and genotypic characterization of isolates collected from hospitalized patients ($n = 5$) and out-patients of the emergency ward of the same acute care hospital ($n = 2$), and isolates responsible for the intestinal colonization of residents in a Long-Term Care Facility ($n = 4$). Pulsed-field gel electrophoresis (PFGE) results, associated with conjugation experiments pointed to a pattern of both vertical and horizontal dissemination. Overall, and complementing other studies that give relevance to IMP-22-producing *K. pneumoniae* in the clinical settings, here we show for the first time the public health threatening breach of the hospital frontier of this resistance threat, toward the community.

Keywords: *Klebsiella pneumoniae*, antimicrobial resistance, carbapenemases, metallo-β-lactamases, nosocomial infections, intestinal colonization, long-term care facilities

INTRODUCTION

Antimicrobial resistance is among the major public health problems of the 21st century. In 2015 the World Health Organization launched the "Global Action Plan on Antimicrobial Resistance" (giving great relevance to antibiotics) to respond to this global issue on five fronts (WHO, 2015). Still, each year, only in the United States and the European Union, 50,000 individuals die due to antibiotic therapy failure (CDC, 2019). Even considering the "last-line" treatment options for infections caused by resistant *Enterobacteriaceae*, carbapenems, we know today several enzymes that can effectively hydrolyze their β-lactam ring, and consequently, compromise their activity (Queenan and Bush, 2007).

Carbapenemases can be divided into two different groups according to their dependency on cations for enzyme activity: serine/non-metallo- (zinc-independent; classes A, C, and D) and metallo-carbapenemases (MBLs; zinc-dependent; class B; Queenan and Bush, 2007). Within the latter, a versatile family of beta-lactamases often associated with *Enterobacteriaceae*, the VIM, IMP, and NDM types are the most relevant carbapenemases globally (Poirel et al., 2011; Nordmann, 2014). Interestingly VIM and IMP are so well settled, that they are considered an endemic problem in the Mediterranean basin (Poirel et al., 2011; Pitout et al., 2015). However, in Portugal, the occurrence of MBL-producing *Enterobacteriaceae* in the clinical settings is apparently not common; only a few sporadic cases were reported, including a VIM-34-producing *Klebsiella pneumoniae* (Rodrigues et al., 2014) and a VIM-2-producing *Klebsiella oxytoca* (Conceicao et al., 2005). In fact, recent studies confirmed that among carbapenemase-producing *Enterobacteriaceae* (CPE), MBL-producing bacteria only represent 5% in Portugal (Manageiro et al., 2018; Gorgulho et al., 2020).

IMP-22 was first described in Italy in two non-related environmental strains of *Pseudomonas fluorescens* as well as in one clinical isolate of *Pseudomonas aeruginosa* (Pellegrini et al., 2009). Since the first description, the same enzyme was then described also in a *Pseudomonas* spp. single clinical isolate from Austria (Duljasz et al., 2009) and recently emerged in Spain, always in the clinics, associated first with *P. aeruginosa* (Viedma et al., 2012) and then mainly with *K. pneumoniae* (Miro et al., 2013; Pena et al., 2014) but also with *E. coli* (Ortega et al., 2016).

Here, we report and describe the successful installation of IMP-22-producing *K. pneumoniae* in a Portuguese acute care hospital (in the North of Portugal), due to both vertical and horizontal dissemination. Furthermore, we describe for the first time the breach of the hospital frontier, with the detection and characterization of an IMP-22-producing *K. pneumoniae* isolate, *via* the screening of intestinal colonizers of residents of a long-term care facility (LTCF). These results ultimately highlight the circulation of patients between hospital and extra-hospital care settings as the most probable justification for the "dissemination of multiresistant bacteria toward the community."

MATERIALS AND METHODS

Hospital Settings and Clinical Carbapenem-Resistant *K. pneumoniae* Isolates

This study was performed in the context of one of the largest acute care hospitals in the North of Portugal (705 beds), covering a population of 1.2 million people (hereafter called Hospital A). During a one-year study period (from March 2011 to May 2012) *K. pneumoniae* clinical isolates showing reduced susceptibility to carbapenems (imipenem or ertapenem or meropenem) were identified as part of routine diagnostics in the hospital Clinical Pathology Service. Isolates were collected from both inpatients admitted to the internal medicine service and from patients admitted to the hospital emergency ward.

Long-Term Care Facility and Carbapenem-Resistant *K. pneumoniae* Intestinal Colonizers

An extra-hospital healthcare institution for dependent and old people in the North of Portugal was studied. The LTCF with 54 beds has three different typologies of care: long-term maintenance (LTM, 22 beds), medium-term and rehabilitation (MTR, 22 beds), and palliative care (PC, 10 beds). The institution is located in the same geographic area as Hospital A (distance of 4 Km), and consequently, the circulation of patients between these two healthcare institutions occurs frequently.

Thirty-eight fecal samples from LTCF residents were collected between January and February 2012, suspended in Brain Heart Infusion (BHI; Oxoid, Hampshire, United Kingdom), and incubated overnight at 37°C. The enriched suspensions were then plated onto MacConkey agar plates (Oxoid, Hampshire, United Kingdom) supplemented with meropenem (1 mg/l). Isolates that grew in the selective media were re-inoculated in a new plate to exclude any satellite growers (maximum of four random colonies per plate).

Bacterial Identification and Antimicrobial Susceptibility Determination

The clinical isolates were identified using the Vitek® 2 automated system (bioMérieux, Marcy l'Étoile, France). Bacteria isolated as part of the intestinal colonization screening were identified using the bacterial identification biochemical galleries API® 20E and ID®32GN (bioMérieux).

The antimicrobial susceptibility of clinical isolates was assessed through the determination of the minimum inhibitory concentration (MIC) of different antimicrobial agents, performed using the Vitek® 2 (bioMérieux) and/or WalkAway (Beckman Coulter, Brea, CA, United States) automated systems. The MICs detected for ampicillin, piperacillin, ticarcillin, amoxicillin + clavulanic acid, piperacillin + tazobactam, ticarcillin + clavulanic acid, cephalothin, cefuroxime, ceftazidime, cefotaxime, cefepime, aztreonam, imipenem, ertapenem, meropenem (β-lactams), gentamicin, tobramycin, amikacin, minocycline, ciprofloxacin, levofloxacin, pefloxacin, nitrofurantoin, trimethoprim + sulfamethoxazole, and rifampicin (non-β-lactams) were interpreted into susceptible, intermediate susceptible or resistant according to the clinical and laboratory standards institute (CLSI) guidelines (Queenan and Bush, 2007; **Supplementary Table S1**). For isolates collected in the LTCF intestinal colonization screening, antimicrobial susceptibility was determined by disk-diffusion methods; susceptibility to both β-lactams [ampicillin (10 μg), amoxicillin + clavulanic acid (20 + 10 μg), ceftazidime (30 μg), cefotaxime (30 μg), cefepime (30 μg), cefoxitin (30 μg), aztreonam (30 μg), imipenem (10 μg), ertapenem (10 μg), and meropenem (10 μg)] and non-β-lactam antibiotics [streptomycin (10 μg), gentamicin (10 μg), netilmicin (30 μg), tobramycin (10 μg), amikacin (30 μg), tetracycline (30 μg), nalidixic acid (30 μg), ciprofloxacin (5 μg), nitrofurantoin (300 μg), chloramphenicol (30 μg), tigecycline (15 μg), and trimethoprim + sulfamethoxazole (1.25/23.75 μg)] was defined according to the CLSI guidelines (CLSI, 2013)

or the EUCAST criteria in the case of tigecycline[1] (**Supplementary Table S2**).

Carbapenemases Phenotypic Screening

An initial carbapenemase production screening (MBLs) was performed using the double disk synergism method (DDSM) - IMP (10 μg) versus IMP (10 μg) + EDTA (0,5 M), followed by the confirmatory MBL *E*-test IP/IPI [(MIC determination; IMP (4-256 μg/ml) versus IMP (1-364 μg/ml) + EDTA (constant level)] (bioMérieux, Marcy l'Étoile, France). The *E*-test was considered MBL suggestive when the MIC ratio of imipenem/imipenem plus EDTA was ≥8 and/or when the presence of a phantom zone or deformation of the inhibitory ellipse was observed. The modified hodge test (MHT) was performed in parallel, to screen for non-MBL carbapenemase production. Briefly, an imipenem disk (10 μg) was placed at the center of a Müeller-Hinton agar plate (Oxoid, Hampshire, United Kingdom), previously inoculated with *E. coli* ATCC 25922, and the clinical isolates were streaked heavily from the edge of the disk toward the edge of the plate. The MHT was considered positive when *E. coli* growth was observed within the usual inhibition zone of the imipenem disk (CLSI, 2013). As a final confirmatory step the biochemical Blue-Carba test was performed as described elsewhere (Pires et al., 2013).

Characterization of Antibiotic Resistance Genes

Total DNA was extracted from all isolates *via* the boiling of single bacterial colony suspensions for 10 min, followed by a 5 min centrifugation step at 15,000 rpm. The supernatant was then collected and stored at 4°C until further use. Relevant beta-lactamase [bla_{TEM}, $bla_{OXA,}$ bla_{SHV} (Dallenne et al., 2010), and $bla_{CTX\text{-}M\ group\ 1}$ (Machado et al., 2005)] and carbapenemase [bla_{VIM}, bla_{IMP}, bla_{KPC}, $bla_{OXA\text{-}48}$, and bla_{NDM} (Poirel et al., 2011)] genes were screened using the primers and amplification conditions described in the literature (Machado et al., 2005; Dallenne et al., 2010; Poirel et al., 2011; Goncalves et al., 2016; Teixeira et al., 2016). Whenever relevant, amplicons were sequenced using the ABI-PRISM 3100 automatic genetic analyzer (Thermo Fischer Scientific, Waltham, MA, United States). Sequence analysis and alignment were performed using the National Center for Biotechnology Information tool.[2] As a final confirmation step, IMP-22 specific primers were used (Pellegrini et al., 2009). A compilation of all primer sequences used in this study can be found in (Goncalves et al., 2016).

Determination of the Clonal Relationships *via* Pulsed-Field Gel Electrophoresis

The clonal relationships of the *K. pneumoniae* clinical isolates were studied *via* pulsed-field gel electrophoresis (PFGE), after total genomic DNA digestion with *XbaI* (Gautom, 1997). Briefly, carbapenem-resistant clinical isolates were cultured in brain heart infusion (BHI) for 24 h at 37°C, then "trapped" into 1.6% agarose plugs. A lysis step was performed at 54°C for 2 h (50 mm Tris, 50 mm EDTA, 1% N-lauryl-sarcosine, 0.1 mg/ml proteinase K, pH 8.0), followed by 2–3 washing cycles, and afterward, the digestion overnight with 30 U of *XbaI* at 37°C. Total DNA digests were separated on 1.0% agarose gels (SeaKem Gold Agarose, Lonza, Basel, Switzerland) *via* PFGE using the CHEFF DR III system (Bio-Rad Laboratories, Hercules, CA, United States) and the following conditions: electric field strength of 6 V/cm^2 (200 V), 14°C, and pulse time of 15 s–25 s for 16 h. After electrophoresis, the gels were stained with ethidium bromide (10 μg/ml) for 30 min and watched under a UV light (Bio-Rad Laboratories). Data analysis was performed using the BIONUMERICS software, version 8.0 (bioMérieux, Marcy l'Étoile, France); the UPGMA algorithm based on the Dice coefficient (1.0% band tolerance; 1.0% optimization) was applied. The PFGE profiles were defined on the basis of DNA banding patterns in accordance with the criteria defined by Tenover et al. (1995). Isolates with a pattern similarity profile above ≥80% were considered identical.

Horizontal Gene Transfer Assessment

Conjugation experiments were performed to investigate the transfer of carbapenem resistance determinants. *E. coli* HB101 (azide resistant, lactose-negative) was used as the recipient strain. Donor and recipient bacterial strains were individually grown overnight in Trypticase Soy Broth (TSB; Oxoid, Hampshire, United Kingdom) and drops of donor and recipient bacterial suspensions were then mixed on the surface of a Müeller-Hinton Agar plate (Oxoid) and re-incubated at 37°C for 24 h. The resulting bacterial growth was re-inoculated on Müeller-Hinton medium supplemented with meropenem or ceftazidime (10 mg/l) and azide (100 μg/ml) and incubated for a maximum of 72 h at 37°C. Growing colonies on the selective medium were randomly chosen and inoculated in MacConkey agar (Oxoid) to assess lactose fermentation. Lactose non-fermenters were subjected to antimicrobial susceptibility determination and to genotypic characterization as above stated.

Ethics Statement

This research was conducted in accordance with the Declaration of Helsinki Ethical Principles. This study was approved by the Ethics Committee of Hospital de Braga, Braga, Portugal. Additionally, human fecal sample collection was performed in accordance with the Good Clinical Practice guidelines; the LTCF direction provided the necessary authorization to conduct this study. Of note, all of the study participants provided written informed consent.

RESULTS

Hospital *K. pneumoniae* Isolates: Clinical Context

Eight carbapenem-resistant *K. pneumoniae* showing reduced susceptibility to at least one of the carbapenems tested were isolated from different biological samples of seven distinct hospitalized patients: five inpatients of the internal medicine

[1]http://www.eucast.org/clinicalbreakpoints/
[2]http://blast.ncbi.nlm.nih.gov/Blast.cgi

service of Hospital A and two patients admitted to the emergency ward of the same hospital. The most common type of biological sample from which these bacteria were isolated was sputum ($n = 5$), followed by urine ($n = 2$) and blood ($n = 1$; **Table 1**). Two of the carbapenem-resistant *K. pneumoniae* (isolates H13 and H50) were isolated from the same patient (patient 3) in different periods (December 2011 and April 2012, respectively; **Table 1**). The patients were mostly elderly (median age 74 years; range 36–92 years) with distinct underlying illnesses, namely urinary tract infection ($n = 1$), endocarditis ($n = 1$), renal insufficiency ($n = 2$), brain tumor ($n = 1$), nosocomial pneumonia ($n = 1$), acute pancreatitis ($n = 1$), respiratory insufficiency ($n = 2$), and bladder tumor ($n = 1$; **Table 1**). All of the patients had previous hospitalization history in Hospital A, with many of them spending prolonged periods at the internal medicine ward. Of note, patients 3, 6, and 7 received meropenem therapy during their hospitalization period (**Table 1**).

LTCF Carbapenem-Resistant *K. pneumoniae* Isolates: Contextualization

Four carbapenem-resistant *K. pneumoniae* isolates (10.53%, 4/38) with reduced susceptibility to imipenem were detected in fecal samples of residents of a LTCF (two different typologies of care; LTM, $n = 3$; MTR, $n = 1$; **Table 2**). The four residents colonized with carbapenem-resistant bacteria were mostly elderly (median age 72.5 years; range 63–82 years), with previous history of stroke ($n = 2$), stroke associated with other pathologies (endocarditis and pneumonia; $n = 1$), and chronic renal insufficiency ($n = 1$; **Table 2**). Three of them had recent hospitalization history in Hospital A: two spent prolonged periods in the internal medicine ward (residents A and D) while the third one was admitted to the orthopedics service (resident B). The fourth resident (C) had hospitalization history in three different hospitals in the same geographic area of Hospital A (one hospital in Braga district and two hospitals in Porto district; **Table 2**).

Antimicrobial Susceptibility Patterns of the Carbapenem-Resistant *K. pneumoniae* Isolates

All clinical isolates showed reduced susceptibility to meropenem (MIC ≥16; R). Additionally, of the set of clinical isolates analyzed, six presented resistance to Ertapenem, and two to imipenem (three others showed an intermediate phenotype; **Table 3**). Importantly, most of the clinical isolates also showed resistance to expanded-spectrum cephalosporins, other β-lactams and β-lactam/β-lactamase inhibitor combinations; additionally resistance to gentamycin ($n = 2$), tobramycin ($n = 5$), ciprofloxacin ($n = 6$), norfloxacin ($n = 1$), pefloxacin ($n = 1$), trimethoprim/sulfamethoxazole ($n = 7$), and tetracycline ($n = 6$) was also detected (**Table 3**).

The four intestinal colonization *K. pneumoniae* isolates also showed reduced susceptibility to imipenem (**Table 4**). Two of them also showed reduced susceptibility to ertapenem (isolates 22 and 24), with only one (isolate 22) showing resistance to the three carbapenems tested (imipenem, ertapenem, and meropenem). The majority of the intestinal isolates also showed resistance to expanded-spectrum cephalosporins ($n = 3$), other β-lactams ($n = 4$), β-lactam/β-lactamase inhibitor combinations ($n = 4$) as well as to non-β-lactam antibiotics, including

TABLE 1 | Hospital *K. pneumoniae* isolates: clinical context.

Patient Nr.	Date (month/year)	Isolate ID	Age/Sex	Hospital service	Biological products	Underlying diseases	Origin[a]	Treated with meropenem during hospital admission
1	March 2011	H7	92/F	Internal medicine	Blood culture	Urinary tract infection	Domicile	No
2	May 2011	H8	36/M	Internal medicine	Urine	Endocarditis	No residence identified	No
3	December 2011 (1st isolate)	H13	86/M	Internal medicine	Urine	Renal insufficiency	Domicile/LTCF	Yes
	April 2012 (2nd isolate)	H50		Internal medicine	Sputum			
4	December 2011	H15	77/F	Internal medicine	Sputum	Brain tumor and nosocomial pneumonia	Hospital B	No
5	January 2012	H40	80/M	Emergency ward	Sputum	Acute pancreatitis and respiratory insufficiency	Domicile	No
6	March 2012	H41	89/M	Emergency ward	Sputum	Renal and respiratory insufficiency	LTCF	Yes
7	May 2012	H52	56/M	Internal medicine	Sputum	Bladder tumor	Hospital C	Yes

F, female; M, male. [a]*origin of the patient before admission into Hospital A, hospitals B and C are different, but in the same geographic area of Hospital A.*

TABLE 2 | Extra-hospital carbapenem-resistant *K. pneumoniae* isolates: epidemiological contextualization.

LTCF resident code	Date (month/year)	Isolate ID	Age/Sex	LTCF typology	Underlying diseases	Resident origin[a]
A	February 2012	22	63/M	MTR	Stroke	Hospital A – IM
B	February 2012	34	80/F	LTM	Stroke	Hospital A – O
C	February 2012	31	65/F	LTM	Stroke, endocarditis pneumonia	Hospitals B, C and D[*]
D	February 2012	24	82/F	LTM	Chronic renal insufficiency	Hospital A – IM

F, female; IM, internal medicine ward; LTM, long-term maintenance; LTCF, long-term care facility; M, male; MTR, medium-term and rehabilitation; O, orthopedics service. [a]*origin of the resident before LTCF admission.*

[*]*hospitalization, in chronological order, in three different hospitals: hospital B - Braga district; hospitals C and D, Porto district.*

tetracycline ($n = 3$), trimethoprim/sulfamethoxazole ($n = 3$), nalidixic acid ($n = 4$), ciprofloxacin ($n = 4$), chloramphenicol ($n = 2$), and streptomycin ($n = 1$; **Table 4**).

Of note, all clinical and intestinal colonization *K. pneumoniae* isolates were defined as multidrug-resistant (MDR) in accordance with the definition proposed by Magiorakos and colleagues (non-susceptible to ≥1 agent in ≥3 antimicrobial categories; Magiorakos et al., 2012).

Characterization of the Carbapenem Resistance Mechanisms

Interestingly, the production of MBL in the context of all of the *K. pneumoniae* clinical isolates was initially defined as negative, as per the MBL *E*-test IP/IPI. Additionally, the results of the MHT were also negative for all of the clinical isolates. However, contrary to these findings, the results of the Blue-Carba test (all positive), suggested the expression of carbapenemases in all clinical isolates. Similarly, one of the intestinal colonization *K. pneumoniae* isolates was also determined as a carbapenemase producer, as per the results of the Blue-Carba test. Of note, according to the CLSI guidelines, extended-spectrum β-lactamase production was not detected, both in the clinical and intestinal colonization carbapenem-resistant isolates.

Finally, the $bla_{\text{IMP-22}}$ gene was detected *via* PCR followed by sequencing in all of the eight *K. pneumoniae* clinical isolates and in one of the carbapenem-resistant intestinal isolates, part of the commensal intestinal microbiota of one LTCF resident (isolate 22). PCR amplification was further confirmed using IMP-22 specific primers, supporting our sequencing results. No other carbapenemase genes were detected in the set of *K. pneumoniae* isolates.

Clonal Relationships of the IMP-22-Producing *K. pneumoniae* Isolates

For epidemiological purposes, since many different carbapenem-resistant isolates were isolated in a short period of time in Hospital A, next, we investigated the genetic relationships of the eight IMP-22-producing *K. pneumoniae* clinical isolates using PFGE. Three distinct PFGE profiles (I to III) were revealed. Importantly, six of the clinical isolates (namely H7, H8, H13, H15, H40, and H41) shared the same profile (profile I), indicating that these isolates are genetically identical and have the same origin (**Figure 1**). The two remaining isolates, H52 and H50 showed two different profiles (profiles II and III, respectively; **Figure 1**). Of note, the isolates belonging to the single major clone (clone I) were isolated from four patients admitted to the medicine ward (isolates H7, H8, H13, and H15), and two patients admitted to the emergency ward (isolates H40 and H41); however, these two patients had previously been admitted to the same hospital. Interestingly, the two isolates collected from the same patient showed different PFGE patterns: H13, with the predominant profile I, was isolated during a first prolonged stay in Hospital A, while H50, with a unique typing pattern unrelated to profile I, was isolated during a second hospitalization, after a period spent in an LTCF in the same geographic region of Hospital A (the same LTCF from which the IMP-22-producing *K. pneumoniae* intestinal colonizer was isolated).

IMP-22-Producing *K. pneumoniae* Isolates of the Dominant Clone Are Effectively Able to Horizontally Transfer the Carbapenem Resistance Determinant

Since the findings in the context of the patient from which two isolates were collected suggest the horizontal transfer of $bla_{\text{IMP-22}}$ (two different PFGE types), we further performed conjugation experiments. Importantly, our results confirmed the above hypothesis; we observed the transference not only of the carbapenem resistance determinant but also of resistance determinants to non-β-lactam antibiotics (**Table 3**; underlined), in the context of six clinical isolates (H7, H8, H13, H15, H40, and H41), all belonging to the single major clone. On the other hand, no conjugation was achieved in the context of the two remaining clones isolated from clinical samples, as well as of the carbapenem-resistant *K. pneumoniae* intestinal isolates. Importantly, the presence of the $bla_{\text{IMP-22}}$ gene in all of the trans-conjugants obtained was confirmed *via* PCR and sequencing.

DISCUSSION

Since the widespread use of carbapenems in the clinical settings, carbapenem-resistant *Enterobacteriaceae* have been increasingly detected worldwide (including in Portugal), not only in hospitals,

TABLE 3 | IMP-22-producing *K. pneumoniae* clinical isolates: phenotypic and genotypic antimicrobial susceptibility patterns.

Patient Nr.	Isolate ID	MICs of carbapenem antibiotics (mg/l)			MICs of other β-lactam antibiotics (mg/l)							Resistance to non-β-lactam antibiotics[a]	MBL E-test	Modified Hodge test	Blue-Carba test	Resistance determinants
		IPM	ETP	MEM	AMC	AMP	P/T	CAZ	CTX	FEP	ATM	FOX				
1	H7	2 I	4 R	≥16 R	≥32 R	≥32 R	≥32 I	≥64 R	8 R	–	≤1 S	8 R	TE, T/S	Negative	Negative	Positive	*blaIMP-22*
2	H8	≤1 S	≥8 R	≥16 R	>16/8 R	>16 R	8 S	≥64 R	>32 R	16 I	≤1 S	>16 R	TE, CIP, GM, TOB, PE, T/S	Negative	Negative	Positive	*blaIMP-22*
3	H13	≤1 S	≤1 S/I	≥16 R	16/8 I	>16 R	≤8S	≥16 R	≥16 R	8 S	–	≥16 R	TE, CIP, NOR, T/S	Negative	Negative	Positive	*blaIMP-22*
	H50	4 R	>1 R	≥16 R	≥32 R	≥32 R	64 I	≥64 R	16 R	–	–	–	CIP, TOB	Negative	Negative	Positive	*blaIMP-22*
4	H15	4 R	4 R	≥16 R	>16/8 R	>16 R	≤8S	>16 R	>16 R	8 S	–	>32 R	TE, CIP, TOB, T/S	Negative	Negative	Positive	*blaIMP-22*
5	H40	2 I	4 R	≥16 R	≥32 R	>16 R	8 S	≥64 R	≥64 R	16 I	≤1 S	≥64 R	TE, CIP, TOB, T/S	Negative	Negative	Positive	*blaIMP-22*
6	H41	2 I	>1 R	≥16 R	>16/8 R	>16 R	≤8S	>16 R	>32 R	8 S	–	>16 R	TE, CIP GM, TOB, T/S	Negative	Negative	Positive	*blaIMP-22*
7	H52	≤1 S	≤1 S/I	≥16 R	16/8 I	16 I	≤4S	16 I	>16 R	≤1 S	–	>16 R	T/S	Negative	Negative	Positive	*blaIMP-22*

IPM, imipenem; ETP, ertapenem; MEM, meropenem; AMC, amoxicillin + clavulanic acid; AMP, ampicillin; P/T, piperacillin + tazobactam; CAZ, ceftazidime; CTX, cefotaxime; FEP, cefepime; ATM, aztreonam; FOX, cefoxitin; TE, tetracycline; CIP, ciprofloxacin; GM, gentamicin; TOB, tobramycin; PE, pefloxacin; T/S, trimethoprim + sulfamethoxazole; NOR, norfloxacin. (a) - antibiotic resistance to non-β-lactamic antibiotics transferred by conjugation is underlined, (–) not evaluated.

FIGURE 1 | PFGE analysis of the IMP-22-producing *K. pneumoniae* clinical isolates. The clonal relationships between the eight *K. pneumoniae* clinical isolates were studied *via* pulsed-field gel electrophoresis (PFGE), after total genomic DNA digestion with *XbaI*. Cluster analysis was performed using the UPGMA algorithm based on the Dice coefficient (1.0% band tolerance; 1.0% optimization). The dendrogram obtained is shown, as are the isolated band patterns' used in the cluster analysis. Additionally, a similarity matrix is also provided. Together with both the dendrogram and the similarity matrix, a similarity scale (in percentage) is provided (distance or color code, respectively). Additionally, in the dendrogram, the cophenetic correlation values are given in each node, as is the standard deviation (in grey). The PFGE profiles were defined on the basis of DNA banding patterns in accordance with the criteria defined by Tenover et al. (1995); isolates with a pattern similarity profile above ≥80% (represented by the dashed red line in the dendrogram) were considered identical.

but also in extra-hospital healthcare institutions, as well as in the environment (Logan and Weinstein, 2017). Among these bacteria, *K. pneumoniae* are formidable nosocomial pathogens with the potential to acquire resistance to multiple antimicrobial agents and consequently associated with high mortality and morbidity; of note, the emergence of MDR *K. pneumoniae* in extra-hospital healthcare institutions in the community, including LTCF, has been more and more reported (Navon-Venezia et al., 2017). Here, we describe for the first time not only the emergence

TABLE 4 | Carbapenem-resistant intestinal colonization *K. pneumoniae* isolates: phenotypic and genotypic antimicrobial susceptibility features.

LTCF resident code	Isolate ID	Resistance to carbapenems	Resistance to non-β-lactam antibiotics	Blue-Carba test	Resistance determinants
A	22	IPM, ETP, MEM	TE, CIP, T/S, S, NA	Positive	*blaIMP-22*
B	34	IPM	CIP, T/S, NA, C	Negative	–
C	31	IPM	TE, CIP, NA	Negative	–
D	24	IPM, ETP	TE, CIP, T/S, NA, C	Negative	–

LTCF, long-term care facility; IPM, imipenem; ETP, ertapenem; MEM, meropenem; TE, tetracycline; CIP, ciprofloxacin; T/S, trimethoprim+sulfamethoxazole; S, streptomycin; NA, nalidixic acid; C, chloramphenicol; (–) negative.

of IMP-22-producing *K. pneumoniae* in an acute care hospital in the North of Portugal, but also, and more importantly, the breach of the hospital frontier toward the community, with the detection of one IMP-22-producing *K. pneumoniae* isolate as a component of the fecal microbiota of a resident of an extra-hospital health care setting (LTCF) in the same geographic area.

IMP-22 MBLs, first described associated with *Pseudomonas* spp. in different European countries are now emerging in *K. pneumoniae* in the Iberian Peninsula. In fact, the finding of the $bla_{\text{IMP-22}}$ gene in *P. fluorescens* environmental strains (Pellegrini et al., 2009) as well as in *P. aeruginosa*, *K. pneumoniae,* and *E. coli* (Duljasz et al., 2009; Pellegrini et al., 2009; Viedma et al., 2012; Miro et al., 2013; Pena et al., 2014; Ortega et al., 2016) clinical isolates in different European countries suggest the ongoing spread of this bla_{MBL} gene among Gram-negative bacteria. Importantly, our results support this notion and highlight the spread of this particular resistance determinant *via* both vertical and horizontal transmission, not only in the clinics but also in the community. Indeed, our results show a clonal spread of IMP-22-producing *K. pneumoniae* in the clinical settings, but also the possible plasmid-mediated spread of the $bla_{\text{IMP-22}}$ gene in both the clinics and the community. These data reflect the complexity of the spread of CPE alerting for the need for adequate infection control practices in all healthcare institutions.

Different clonal outbreaks caused by carbapenem-resistant *K. pneumoniae* have been reported in particular hospitals in Portugal; however, most if not all of the reported outbreaks were associated with non-metallo-carbapenemases (including KPC-3 and OXA-48; (Conceicao et al., 2005; Rodrigues et al., 2014; Vubil et al., 2017; Manageiro et al., 2018; Mendes et al., 2018; Aires-de-Sousa et al., 2019; Perdigao et al., 2019; Gorgulho et al., 2020; Guerra et al., 2020; Lopes et al., 2020). In fact, only around 5% of the reported CPE in Portugal are associated with metallo-carbapenemases (Manageiro et al., 2018; Gorgulho et al., 2020). Therefore, our report of an outbreak caused by IMP-22-producing *K. pneumoniae* has epidemiological relevance, complementing the landscape of carbapenemase-producing bacteria in Portugal. Of note, the first IMP-22-producing *K. pneumoniae* clinical isolate was detected in March 2011, and since then, during one-year period (till May 2012) seven more isolates were found in the same hospital (and one more in the community). These data may suggest the successful installation of such resistant bacteria in the North of Portugal, with public health implications.

The original source and potential route of transmission of these IMP-22-producing *K. pneumoniae* isolates (clinical and intestinal commensal) is not known. However, our results suggest a common source, at least considering the IMP-22-producing *K. pneumoniae* clinical isolates of the predominant clone. The link between most patients admitted to Hospital A was their stay in the medicine ward; therefore, it is not unreasonable to speculate that transmission occurred during the hospital stay. Of note, although the *K. pneumoniae* isolates from patients 5 and 6 were detected in the emergency ward, both patients were previously admitted for a long period to the medicine ward of Hospital A; after hospital discharge, patient 5 went home, and patient 6 went to an LTCF in the same geographic region (the facility where the IMP-22 positive intestinal colonizer strain was isolated), but then returned to Hospital A due to health status complications. Therefore, intestinal colonization of these patients with IMP-22-producing *K. pneumoniae* is a serious hypothesis to be considered, after hospital discharge. Importantly, our results are in line with the more and more recognized notion that extra-hospital care institutions are a highway for the escape of MDR bacteria from the hospitals to the community, as well as for the (re)-introduction of MDR bacteria into hospitals (Masgala et al., 2015; Mody et al., 2018).

Interestingly, our results also suggest that, although most transmission events were clonal, some of them were horizontal in nature. This was particularly clear in the context of patient number 3, with two different isolates (detected during two distinct hospitalizations) showing non-related PFGE profiles. This, together with the fact that we were able to obtain trans-conjugants with all of the clinical isolates from the predominant clone suggest that these *K. pneumoniae* isolates are able to disseminate this particular carbapenem resistance determinant. Our results are, therefore, worrisome, thinking on the possibility of the emergence of more fit IMP-22-producing *Enterobacteriaceae* and their installation in the clinics and the community, in Portugal and even abroad (depending on the dissemination success of the bacteria).

Remarkably, MBL detection, as per the *E*-test IP/IPI, was negative in the context of all IMP-22-producing isolates, highlighting the need for the use of adequate phenotypic approaches to detect these particular carbapenem-resistant strains. Although according to some reports there is still "no gold standard CPE detection method" (Berry et al., 2019), many recognize the genotypic approach (detection of carbapenemase-encoding genes) as the most suitable (Nordmann and Poirel, 2013). However, the diagnosis capacity is not homogeneous around the world; the COVID-19 pandemic

exposed the clear inequality-derived differences among countries (Giri and Rana, 2020; Millar, 2020). Therefore, phenotypic methods are still widely used as a primary approach to detect CPE. Importantly, our results highlight the need to use complementary (phenotypic) methods, to prevent the potential disregard of carbapenemase-producing strains, such as the IMP-22-producing *K. pneumoniae* isolates we report here; metallo-carbapenemase producers not detected using the standard *E*-test IP/IPI method (thus inadequate for the detection of IMP-22-producing *K. pneumoniae*), but detected using the Blue-Carba test. Of note, if possible, the genotypic determination of MBL is recommended in situations of reduced susceptibility to carbapenems, excluding imipenem. Altogether, our results alert for the need for the correct detection of CPE in routine clinical microbiology testing, to avoid outbreak installation.

The early identification of CPE in hospitalized patients and the implementation of adequate infection control measures are, thus, extremely important to prevent the persistence and spread of carbapenem-resistant bacteria (Magiorakos et al., 2017), such as the IMP-22-producing *K. pneumoniae* strains we report in this study, not only in the hospital settings but also in the community. In fact, after hospital discharge, patients can remain colonized and contribute for the dissemination of these MDR *K. pneumoniae* within extra-hospital care settings, namely, LTCF, and nursing homes (Chen et al., 2021). Therefore, the early identification of carriers and the implementation of adequate control strategies are essential to prevent nosocomial outbreaks. This is precisely what we show in this study. The individual colonized with the IMP-22-producing *K. pneumoniae* had previous hospitalization history in the medicine ward of the same acute care hospital where the clinical isolates were detected; therefore, our results suggest that this individual was colonized during hospitalization and served as a silent vehicle transporting the IMP-22-producing *K. pneumoniae* toward the community after discharge.

This study is not without limitations. First, antibiotic susceptibility of clinical and community isolates was assessed using two different methods, MIC determination, and disc-diffusion assays, respectively. However, for both methods, the CLSI/EUCAST guidelines were strictly followed. Second, the community isolate was not included in the analysis of clonal relationships. Therefore, we do not know whether this isolate belongs to the major clone, to one of the two single clones, or if it is a different clone; all of these options are possible. Third, although our results clearly suggest that the single clones were derived from horizontal dissemination events, this must yet be clearly shown. To address these limitations, we plan, in a follow-up study, to perform whole-genome sequencing of the isolates that will allow us to determine their MLST (and the clonal relationships of all of the isolates) and their resistome, as well as to perform detailed plasmid analyses and undoubtedly prove the horizontal transfer of the IMP-22 resistance determinant.

Altogether, our results align with the dogma that the presence of patients colonized with MDR *Enterobacteriaceae* in LTCF can represent a serious risk of dissemination and potential infection of elderly patients in the community, requiring, therefore strict epidemiological attention. In the future, as a preventive measure of the dissemination of multidrug-resistant bacteria, we suggest the active screening of intestinal colonization, both at hospital admission and hospital discharge, as well as, sporadically, in extra-hospital healthcare settings including LTCF and nursing homes; the detection of carbapenem-resistant bacteria at these stages will allow the implementation of rational infection control measures, with the potential to prevent outbreaks both in the clinics and the community.

DATA AVAILABILITY STATEMENT

The raw data supporting the conclusions of this article will be made available by the authors, without undue reservation.

ETHICS STATEMENT

This research was conducted in accordance with the Declaration of Helsinki Ethical Principles. This study was approved by the Ethics Committee of Hospital de Braga, Braga, Portugal. Additionally, human fecal sample collection was performed in accordance with the Good Clinical Practice guidelines; the LTCF direction provided the necessary authorization to conduct this study. Of note, all of the study participants provided written informed consent.

AUTHOR CONTRIBUTIONS

DG and HF conceived and designed the experiments. DG and PC performed the experiments and wrote the original draft. DG, PC, and HF analyzed the data. DG, PC, AF, CI, FB, AE, and HF critically discussed the results and critically revised and edited the paper. HF assured the funding and contributed with the reagents, materials, and analysis tools. AF, CI, FB, and AE provided the clinical strains. All authors approved the current version of this manuscript.

FUNDING

This study was supported by internal funding.

ACKNOWLEDGMENTS

The authors are grateful to Professor Laurent Poirel for generously providing the NDM and OXA-48 producing control strains and to Professor Luísa Peixe for access to the InfoQuest FP software.

SUPPLEMENTARY MATERIAL

The Supplementary Material for this article can be found online at: https://www.frontiersin.org/articles/10.3389/fmicb.2021.777054/full#supplementary-material

REFERENCES

Aires-de-Sousa, M., Ortiz de la Rosa, J. M., Goncalves, M. L., Pereira, A. L., Nordmann, P., and Poirel, L. (2019). Epidemiology of Carbapenemase-producing Klebsiella pneumoniae in a hospital, Portugal. *Emerg. Infect. Dis.* 25:1632. doi: 10.3201/eid2509.190656

Berry, C., Davies, K., Woodford, N., Wilcox, M., and Chilton, C. (2019). Survey of screening methods, rates and policies for the detection of carbapenemase-producing Enterobacteriaceae in English hospitals. *J. Hosp. Infect.* 101, 158–162. doi: 10.1016/j.jhin.2018.08.005

CDC (2019) Infographic: Antibiotic Resistance The Global Threat Available at: https://www.cdc.gov/globalhealth/infographics/antibiotic-resistance/antibiotic_resistance_global_threat.htm. (Accessed May 27, 2021).

Chen, H. Y., Jean, S. S., Lee, Y. L., Lu, M. C., Ko, W. C., Liu, P. Y., et al. (2021). Carbapenem-resistant Enterobacterales in long-term care facilities: A global and narrative review. *Front. Cell. Infect. Microbiol.* 11:601968. doi: 10.3389/fcimb.2021.601968

CLSI (2013). *Performance standards for antimicrobial susceptibility testing.* Wayne, PA: Clinical and Laboratory Standards Institute. Supplement M100-S23 p.

Conceicao, T., Brizio, A., Duarte, A., and Barros, R. (2005). First isolation of Bla(VIM-2) in *Klebsiella oxytoca* clinical isolates from Portugal. *Antimicrob. Agents Chemother.* 49:476. doi: 10.1128/AAC.49.1.476.2005

Dallenne, C., Da Costa, A., Decre, D., Favier, C., and Arlet, G. (2010). Development of a set of multiplex PCR assays for the detection of genes encoding important beta-lactamases in Enterobacteriaceae. *J. Antimicrob. Chemother.* 65, 490–495. doi: 10.1093/jac/dkp498

Duljasz, W., Gniadkowski, M., Sitter, S., Wojna, A., and Jebelean, C. (2009). First organisms with acquired metallo-beta-lactamases (IMP-13, IMP-22, and VIM-2) reported in Austria. *Antimicrob. Agents Chemother.* 53, 2221–2222. doi: 10.1128/AAC.01573-08

Gautom, R. K. (1997). Rapid pulsed-field gel electrophoresis protocol for typing of *Escherichia coli* O157:H7 and other gram-negative organisms in 1 day. *J. Clin. Microbiol.* 35, 2977–2980. doi: 10.1128/jcm.35.11.2977-2980.1997

Giri, A. K., and Rana, D. R. S. J. B. (2020). Charting the challenges behind the testing of COVID-19 in developing countries: Nepal as a case study. *Biosafety Health* 2:53. doi: 10.1016/j.bsheal.2020.05.002

Goncalves, D., Cecilio, P., and Ferreira, H. (2016). Nursing homes and long-term care facilities: reservoirs of CTX-M-15-producing *Escherichia coli* O25b-ST131 in Portugal. *J. Glob. Antimicrob. Resist.* 7, 69–71. doi: 10.1016/j.jgar.2016.08.001

Gorgulho, A., Grilo, A. M., de Figueiredo, M., and Selada, J. (2020). Carbapenemase-producing Enterobacteriaceae in a Portuguese hospital - a five-year retrospective study. *Germs* 10, 95–103. doi: 10.18683/germs.2020.1190

Guerra, A. M., Lira, A., Lameirao, A., Selaru, A., Abreu, G., Lopes, P., et al. (2020). Multiplicity of Carbapenemase-Producers Three Years after a KPC-3-Producing K. pneumoniae ST147-K64 Hospital Outbreak. *Antibiotics* 9:806. doi: 10.3390/antibiotics9110806

Logan, L. K., and Weinstein, R. A. (2017). The epidemiology of Carbapenem-resistant Enterobacteriaceae: The impact and evolution of a global menace. *J. Infect. Dis.* 215(suppl. 1), S28–S36. doi: 10.1093/infdis/jiw282

Lopes, E., Saavedra, M. J., Costa, E., de Lencastre, H., Poirel, L., and Aires-de-Sousa, M. (2020). Epidemiology of carbapenemase-producing Klebsiella pneumoniae in northern Portugal: predominance of KPC-2 and OXA-48. *J. Glob. Antimicrob. Resist.* 22, 349–353. doi: 10.1016/j.jgar.2020.04.007

Machado, E., Canton, R., Baquero, F., Galan, J. C., Rollan, A., Peixe, L., et al. (2005). Integron content of extended-spectrum-beta-lactamase-producing *Escherichia coli* strains over 12 years in a single hospital in Madrid, Spain. *Antimicrob Agents Chemother* 49, 1823–1829. doi: 10.1128/AAC.49.5.1823-1829.2005

Magiorakos, A. P., Burns, K., Rodriguez Bano, J., Borg, M., Daikos, G., Dumpis, U., et al. (2017). Infection prevention and control measures and tools for the prevention of entry of carbapenem-resistant Enterobacteriaceae into healthcare settings: guidance from the European Centre for Disease Prevention and Control. *Antimicrob. Resist. Infect. Control* 6:113. doi: 10.1186/s13756-017-0259-z

Magiorakos, A. P., Srinivasan, A., Carey, R. B., Carmeli, Y., Falagas, M. E., Giske, C. G., et al. (2012). Multidrug-resistant, extensively drug-resistant and pandrug-resistant bacteria: an international expert proposal for interim standard definitions for acquired resistance. *Clin. Microbiol. Infect.* 18, 268–281. doi: 10.1111/j.1469-0691.2011.03570.x

Manageiro, V., Romao, R., Moura, I. B., Sampaio, D. A., Vieira, L., Ferreira, E., et al. (2018). Molecular epidemiology and risk factors of Carbapenemase-producing Enterobacteriaceae isolates in Portuguese hospitals: results From European survey on Carbapenemase-producing Enterobacteriaceae (EuSCAPE). *Front. Microbiol.* 9:2834. doi: 10.3389/fmicb.2018.02834

Masgala, A., Kostaki, K., and Ioannnidis, I. (2015). Multi drug resistant gram negative pathogens in long term care facilities: ASteadily arising problem. *J. Infect. Dis. Diagno.* 1:101. doi: 10.4172/2576-389X.1000124

Mendes, A. C., Novais, A., Campos, J., Rodrigues, C., Santos, C., Antunes, P., et al. (2018). Mcr-1 in Carbapenemase-producing Klebsiella pneumoniae with hospitalized patients, Portugal, 2016-2017. *Emerg. Infect. Dis.* 24, 762–766. doi: 10.3201/eid2404.171787

Millar, M. (2020). "A capability perspective on antibiotic resistance, inequality, and child development," in *Ethics and Drug Resistance: Collective Responsibility for Global Public Health Public Health Ethics Analysis*. eds. E. Jamrozik and M. Selgelid (Cham, Switzerland: Springer).

Miro, E., Aguero, J., Larrosa, M. N., Fernandez, A., Conejo, M. C., Bou, G., et al. (2013). Prevalence and molecular epidemiology of acquired AmpC beta-lactamases and carbapenemases in Enterobacteriaceae isolates from 35 hospitals in Spain. *Eur. J. Clin. Microbiol. Infect. Dis.* 32, 253–259. doi: 10.1007/s10096-012-1737-0

Mody, L., Foxman, B., Bradley, S., McNamara, S., Lansing, B., Gibson, K., et al. (2018). Longitudinal assessment of multidrug-resistant organisms in newly admitted nursing facility patients: implications for an evolving population. *Clin. Infect. Dis.* 67, 837–844. doi: 10.1093/cid/ciy194

Navon-Venezia, S., Kondratyeva, K., and Carattoli, A. (2017). Klebsiella pneumoniae: a major worldwide source and shuttle for antibiotic resistance. *FEMS Microbiol. Rev.* 41, 252–275. doi: 10.1093/femsre/fux013

Nordmann, P. (2014). Carbapenemase-producing Enterobacteriaceae: overview of a major public health challenge. *Med. Mal. Infect.* 44, 51–56. doi: 10.1016/j.medmal.2013.11.007

Nordmann, P., and Poirel, L. (2013). Strategies for identification of carbapenemase-producing Enterobacteriaceae. *J. Antimicrob. Chemother.* 68, 487–489. doi: 10.1093/jac/dks426

Ortega, A., Saez, D., Bautista, V., Fernandez-Romero, S., Lara, N., Aracil, B., et al. (2016). Carbapenemase-producing *Escherichia coli* is becoming more prevalent in Spain mainly because of the polyclonal dissemination of OXA-48. *J. Antimicrob. Chemother.* 71, 2131–2138. doi: 10.1093/jac/dkw148

Pellegrini, C., Mercuri, P. S., Celenza, G., Galleni, M., Segatore, B., Sacchetti, E., et al. (2009). Identification of Bla(IMP-22) in pseudomonas spp. in urban wastewater and nosocomial environments: biochemical characterization of a new IMP metallo-enzyme variant and its genetic location. *J. Antimicrob. Chemother.* 63:901. doi: 10.1093/jac/dkp061

Pena, I., Picazo, J. J., Rodriguez-Avial, C., and Rodriguez-Avial, I. (2014). Carbapenemase-producing Enterobacteriaceae in a tertiary hospital in Madrid, Spain: high percentage of colistin resistance among VIM-1-producing Klebsiella pneumoniae ST11 isolates. *Int. J. Antimicrob. Agents* 43, 460–464. doi: 10.1016/j.ijantimicag.2014.01.021

Perdigao, J., Modesto, A., Pereira, A. L., Neto, O., Matos, V., Godinho, A., et al. (2019). Whole-genome sequencing resolves a polyclonal outbreak by extended-spectrum beta-lactam and carbapenem-resistant Klebsiella pneumoniae in a Portuguese tertiary-care hospital. *Microb. Genom* 7:349. doi: 10.1099/mgen.0.000349

Pires, J., Novais, A., and Peixe, L. (2013). Blue-carba, an easy biochemical test for detection of diverse carbapenemase producers directly from bacterial cultures. *J. Clin. Microbiol.* 51, 4281–4283. doi: 10.1128/JCM.01634-13

Pitout, J. D., Nordmann, P., and Poirel, L. (2015). Carbapenemase-producing Klebsiella pneumoniae, a key pathogen set for global nosocomial dominance. *Antimicrob. Agents Chemother.* 59, 5873–5884. doi: 10.1128/AAC.01019-15

Poirel, L., Walsh, T. R., Cuvillier, V., and Nordmann, P. (2011). Multiplex PCR for detection of acquired carbapenemase genes. *Diagn. Microbiol. Infect. Dis.* 70, 119–123. doi: 10.1016/j.diagmicrobio.2010.12.002

Queenan, A. M., and Bush, K. (2007). Carbapenemases: the versatile beta-lactamases. *Clin Microbiol Rev* 20, 440–458. doi: 10.1128/CMR.00001-07

Rodrigues, C., Novais, A., Machado, E., and Peixe, L. (2014). Detection of VIM-34, a novel VIM-1 variant identified in the intercontinental ST15 Klebsiella pneumoniae clone. *J. Antimicrob. Chemother.* 69, 274–275. doi: 10.1093/jac/dkt314

Teixeira, J. V., Cecilio, P., Goncalves, D., Vilar, V. J., Pinto, E., and Ferreira, H. N. (2016). Multidrug-resistant Enterobacteriaceae from indoor air of an urban wastewater treatment plant. *Environ. Monit. Assess.* 188:388. doi: 10.1007/s10661-016-5382-4

Tenover, F. C., Arbeit, R. D., Goering, R. V., Mickelsen, P. A., Murray, B. E., Persing, D. H., et al. (1995). Interpreting chromosomal DNA restriction patterns produced by pulsed-field gel electrophoresis: criteria for bacterial strain typing. *J. Clin. Microbiol.* 33, 2233–2239. doi: 10.1128/jcm.33.9.2233-2239.1995

Viedma, E., Juan, C., Villa, J., Barrado, L., Orellana, M. A., Sanz, F., et al. (2012). VIM-2-producing multidrug-resistant *Pseudomonas aeruginosa* ST175 clone, Spain. *Emerg. Infect. Dis* 18, 1235–1241. doi: 10.3201/eid1808.111234

Vubil, D., Figueiredo, R., Reis, T., Canha, C., Boaventura, L., and Das, G. J. (2017). Outbreak of KPC-3-producing ST15 and ST348 Klebsiella pneumoniae in a Portuguese hospital. *Epidemiol. Infect.* 145, 595–599. doi: 10.1017/S0950268816002442

WHO (2015). Global Action Plan on Antimicrobial Resistance. Available at: http://www.who.int/antimicrobial-resistance/publications/global-action-plan/en/ (Accessed April 27, 2021).

Conflict of Interest: The authors declare that the research was conducted in the absence of any commercial or financial relationships that could be construed as a potential conflict of interest.

Publisher's Note: All claims expressed in this article are solely those of the authors and do not necessarily represent those of their affiliated organizations, or those of the publisher, the editors and the reviewers. Any product that may be evaluated in this article, or claim that may be made by its manufacturer, is not guaranteed or endorsed by the publisher.

frontiers in Microbiology

ORIGINAL RESEARCH
published: 03 January 2022
doi: 10.3389/fmicb.2021.811263

The Co-occurrence of NDM-5, MCR-1, and FosA3-Encoding Plasmids Contributed to the Generation of Extensively Drug-Resistant *Klebsiella pneumoniae*

*Ying Zhou[1†], Wenxiu Ai[2†], Yanhua Cao[3†], Yinjuan Guo[1], Xiaocui Wu[1], Bingjie Wang[1], Lulin Rao[1], Yanlei Xu[1], Huilin Zhao[1], Xinyi Wang[1] and Fangyou Yu[4]**

[1] Department of Clinical Laboratory Medicine, Shanghai Pulmonary Hospital, School of Medicine, Tongji University, Shanghai, China, [2] Department of Respiratory Medicine, The First Affiliated Hospital of Wenzhou Medical University, Wenzhou, China, [3] Department of Respiratory Intensive Care Unit, Shanghai Pulmonary Hospital, School of Medicine, Tongji University, Shanghai, China, [4] Department of Laboratory Medicine, The First Affiliated Hospital of Wenzhou Medical University, Wenzhou, China

OPEN ACCESS

Edited by:
Che-Hsin Lee,
National Sun Yat-sen University, Taiwan

Reviewed by:
Prasanth Manohar,
Zhejiang University-University of Edinburgh Institute, China
Abinaya Badri,
Ginkgo BioWorks, United States

***Correspondence:**
Fangyou Yu
wzjxyfy@163.com

[†] These authors have contributed equally to this work

Specialty section:
This article was submitted to Antimicrobials, Resistance and Chemotherapy, a section of the journal Frontiers in Microbiology

Received: 08 November 2021
Accepted: 30 November 2021
Published: 03 January 2022

Citation:
Zhou Y, Ai W, Cao Y, Guo Y, Wu X, Wang B, Rao L, Xu Y, Zhao H, Wang X and Yu F (2022) The Co-occurrence of NDM-5, MCR-1, and FosA3-Encoding Plasmids Contributed to the Generation of Extensively Drug-Resistant Klebsiella pneumoniae. Front. Microbiol. 12:811263. doi: 10.3389/fmicb.2021.811263

The rise and global dissemination of extensively drug-resistant (XDR) bacteria are often related to plasmid-borne mobile antimicrobial resistance genes. Notably, isolates having multiple plasmids are often highly resistant to almost all the antibiotics available. In this study, we characterized an extensively drug-resistant *Klebsiella pneumoniae* 1678, which exhibited high-level resistance to almost all the available antibiotics. Through whole-genome sequencing (WGS), more than 20 resistant elements and 5 resistant plasmids were observed. Notably, the tigecycline resistance of *K. pneumoniae* 1678 was not related to the plasmid-borne *tetA* gene but associated with the overexpression of AcrAB and OqxAB efflux pumps, according to the susceptibility results of *tetA*-transformant and the related mRNA quantification of RND efflux pumps. Except for tigecycline resistance, three plasmids, mediating resistance to colistin, Fosfomycin, and ceftazidime–avibactam, respectively, were focused. Detailed comparative genetic analysis showed that all these plasmids belonged to dominated epidemic plasmids, and harbored completed conjugation systems. Results of conjugation assay indicated that these three plasmids not only could transfer to *E. coli* J53 with high conjugation frequencies, respectively, but also could co-transfer to *E. coli* J53 effectively, which was additionally confirmed by the S1-PFGE plasmids profile. Moreover, multiple insertion sequences (IS) and transposons (Tn) were also found surrounding the vital resistant genes, which may form several novel mechanisms involved in the resistant determinants' mobilization. Overall, we characterized and reported the uncommon co-existence and co-transferring of FosA3-, NDM-5, and MCR-1-encoding plasmids in a *K. pneumoniae* isolate, which may increase the risk of spread of these resistant phenotypes and needing great concern.

Keywords: *K. pneumoniae*, plasmid, *fosA3*, bla_{NDM-5}, *mcr-1*, mobile elements

INTRODUCTION

Carbapenem-resistant *Klebsiella pneumoniae* (CRKP) has recently emerged as a major class of bacterial pathogens that pose a significant threat to global public health, since it can cause high-fatal infections, and the treatment choices are very limited (Chen et al., 2014). The emergence of antibiotic resistance arises the development of several new antibiotics, such as tigecycline (Chopra, 2002) and ceftazidime–avibactam (Zhanel et al., 2013), and the re-evaluation of old antibiotics such as Fosfomycin and polymyxin as a potential regimen for treating such multidrug-resistant bacteria (Doi, 2019). Tigecycline, colistin, Fosfomycin, and ceftazidime–avibactam were considered as the most effective agents for the CRKP infection treatments, and were even regarded as the last "trump card" to defend against CRKP (Doi, 2019). However, clinical isolates resistant to those four antibiotics emerged frequently (Petrosillo et al., 2019; Fang et al., 2020; Yahav et al., 2020; Zurfluh et al., 2020; Yusuf et al., 2021). Hence, verifying the related mechanism and demonstrating the potential of the spread of these resistant phenotypes in clinical isolate are urgent, which are the vital clues to solve antibiotic resistance.

The acquisition of antibiotic resistance was always associated with mobile genetic elements (MGEs) such as conjugative and mobilizable plasmids and transposons (Partridge et al., 2018). In *Enterobacteriaceae*, Fosfomycin-modifying enzymes are the important factors to inactivate the Fosfomycin, genes encoding these enzymes (*fosA*) are frequently found on plasmids, transposons, or within integrons (Zurfluh et al., 2020). Lipopolysaccharide modifications are the key issues to reduce the antibiotic effect of polymyxin. In addition to the two-component systems (TCSs) *PhoP/PhoQ*, *PmrA/PmrB,* and *CrrA/CrrB* (Mcconville et al., 2020), the plasmid-mediated *mcr* genes (such as *mcr-1*) mediated enzymes are the most noteworthy way to modify lipopolysaccharides, which not only result in polymyxin resistance, but also result in the transferring of this antibiotic resistant-phenomena worldwide (Xiaomin et al., 2020). The tigecycline resistance is sometimes associated with the overexpression of the efflux pumps AcrAB and OqxAB (Bialek-Davenet et al., 2015). Meanwhile, mutations in tetracycline resistance factors, including efflux pumps (*tetA*, *tetB*, and *tetK*) (Foong et al., 2020; Xu et al., 2021) and other plasmid-borne tigecycline resistance genes, *tet(X)* (Sun et al., 2019) and *tmexCD-toprJ* (Hirabayashi et al., 2021), have also been reported to contribute to *K. pneumoniae* resistance to tigecycline. Although ceftazidime–avibactam (CAZ/AVI) exhibited remarkable inhibition to KPC carbapenemase, it is not active against Metallo-β-Lactamases (MBL)-producing bacteria, such as bla_{NDM}-positive isolates (Yang et al., 2020). Overall, since almost all the antibiotic resistance could be carried by various MGEs, once the bacteria obtain multiple resistant elements simultaneously, they would become resistant to those antibiotic agents, and the therapeutic options would be very limited.

The co-occurrence of multiple resistant plasmids in one isolate often results in the resistance to almost all available antibiotics, and also promotes the dissemination of resistance determinants. Several studies also reported some co-existence of resistant-genes in *Enterobacteriaceae*, like *fosA3* and bla_{KPC-2} (Tang et al., 2020), or *mcr-1* and bla_{NDM-5} (Sun et al., 2016), these co-existences make the strain become extensively drug-resistant to multiple antibiotics. Notably, although there are several reports about the co-existence of *mcr-1* and bla_{NDM-5} in one plasmid or two separated plasmids, most of these plasmids were harbored by *E. coli* strains of animal origin or environmental origin, which is uncommon in *K. pneumoniae* (Yang et al., 2016; Quan et al., 2017; Mao et al., 2018; Wang et al., 2018, 2021; Chen et al., 2019; Liu and Song, 2019; Han et al., 2020; Yuan et al., 2021).

In this study, our aim was to characterize an XDR *K. pneumoniae* isolated from a clinical patient, which is not only highly resistant to carbapenems, but also resistant to all the alternative antibiotics, including tigecycline, ceftazidime–avibactam, Fosfomycin, and polymyxin. We applied whole-genome-sequencing (WGS) to explore the potential molecular mechanisms mediating this multidrug-resistance, and observed three key resistant plasmids. We also made a detailed analysis of the plasmid-backbone and the conjugation region to evaluate the potential movability, and applied the conjugation assay to further determine the dissemination risk of these resistant determinants. In addition to the plasmids, we described other related MEGs through the genetic comparisons as well. Overall, our goal was to report and describe a clinical multi-drug resistant *K. pneumoniae* clearly, and emphasize the possible risk of these strains.

MATERIALS AND METHODS

Bacterial Strains

To explore the molecular epidemic feature of carbapenem-resistant *K. pneumoniae* in China mainland, we randomly collected 137 carbapenem-resistant *K. pneumoniae* isolates from blood samples of individual patients at nine hospitals in eight Chinese provinces, from January 2015 to December 2018. The isolates were cultivated with LB medium. We applied WGS to analyze the presence of resistance elements among these isolates, and observed *K. pneumoniae* strain 1678 co-harboring multiple resistance determinants including *fosA3*, *mcr-1,* and bla_{NDM-5}, that were uncommon in other *K. pneumoniae. K. pneumoniae* strain 1678 was isolated from the blood samples of a 71-year-old patient in 2018, in a tertiary hospital in Shanghai, China. Plasmid transformation and conjugation were performed with *Escherichia coli* TOP10 and J53 (sodium-azide^R) used as recipients for the selection of *tetA-*, *fosA3-*, bla_{NDM-5}, or *mcr-1*-positive transformants and related transconjugants, respectively.

Antimicrobial Susceptibility Test

The minimum inhibitory concentration (MIC) of the original isolate 1678 and all the transformants and transconjugants were determined by both broth microdilution and the polymyxin MIC was determined by the E-test methods following the Clinical and Laboratory Standards Institute guidelines. Briefly, for the broth microdilution and agar dilution method, pick 1–2 bacterial clones diluted with saline to 0.5McF, and then dilute such bacterial suspension to 0.5×10^{-2} McF with CAMHB broth. The cells were inoculated in prefabricated commercial 96-well antibiotic culture plates or antibiotic agars, 100 μL

per well, and incubated overnight for 18 h at 37°C. E-test method using a colistin strip (concentration range, 0.016–256 μg/ml) (bioMérieux) was performed with Mueller–Hinton agar (MHA) (BD) plates in accordance with recommendations of the manufacturers. Notably, the Fosfomycin MIC was tested by the agar dilution using agar media supplemented with 25 μg/mL of glucose-6- phosphate. *Escherichia coli* ATCC25922 was used as a quality control strain for MIC determination. The interpretative breakpoints were based on CLSI2021 (Clinical and Laboratory Standards Clinical and Laboratory Standards Institute, 2021a; Clinical and Laboratory Standards Clinical and Laboratory Standards Institute, 2021b).

Quantitation of mRNA Expression

To explore whether the tigecycline-resistant phenotype was related with the overexpression of AcrAB and OqxAB efflux pumps, we applied q-RT-PCR (quantitative-real-time-PCR) to measure the relative gene expression. All the primers were listed in **Supplementary Table 1**. RNA manipulation and real-time PCR were performed as described previously (Zheng et al., 2018). All bacterial samples were cultured in LB medium that did not contain any antibiotics. RNA was isolated as per the protocol of the MiniBEST Universal RNA extraction kit (TaKaRa, Tokyo, Japan). RNA samples for real-time PCR were pre-treated with DNase I (TaKaRa, Tokyo, Japan). Real-time PCR was conducted on a 7,500 system (Applied Biosystems, Foster City, CA, United States) using SYBR Premix ExTag (Takara, Tokyo, Japan). The expression of target genes was standardized relative to the 16S rRNA housekeeping gene *rrsE*. The expression levels of the target genes were compared with those of *K. pneumoniae* ATCC 13,883 (tigecycline susceptible). The relative expression levels of genes were calculated using the $\Delta\Delta CT$ method. All assays were performed in triplicate with three independent RNA preparations.

Whole Genome Sequencing and Bioinformatics Analysis

The genomic DNA of 1678 was extracted using a commercial DNA extraction kit (Qiagen, Germany) and was sequenced using short- and long-read massively parallel sequencing. The paired-end short Illumina reads were used to correct the long PacBio reads utilizing *proovread*, and then the corrected PacBio reads were assembled *de novo* utilizing *SMARTdenovo*[1]. Resistant plasmid replicons were identified using the PlasmidFinder database using the minimum coverage and minimum identities of 90%[2]. Acquired antibiotic resistance genes were identified using ResFinder[3] with the default threshold. To determine whether the plasmids could self-transmission, we used the oriTfinder[4] to conduct a detailed analysis of the conjugation module, including the origin of transfer site (*oriT*), relaxase gene, type IV coupling protein (T4CP) gene, and the type IV secretion system gene cluster (T4SS). The related insertion sequences (IS) and transposons (Tn) were determined through the ISFinder[5]. BLAST Ring Image Generator (BRIG) was used to compare key resistant plasmids with other representative plasmids to further generate circular plasmid maps. Easyfig software was used to generate comparison of gene environment surrounding the vital resistant genes.

Transformation Assay

In order to test whether these plasmids could mediate the corresponding resistant phenotype, we extracted and transformed each single resistant plasmid to *E. coli* Top 10, and then tested the antibiotic susceptibility of all transformants. The plasmid extraction and transformation processes were performed as previously described (Yin et al., 2017).

We used the phenol-chloroform extraction method to extract the plasmids in 1678. Then, we mixed 4 μl extracted plasmids and *E. coli* Top 10 competent cells together, placed it on ice for 30 min, put it in a 42°C water bath for 90 s, and then took it out and placed it on ice for 2 min. After that, we used LB broth to resuscitate the strain, and screened the transformants on appropriate antibiotic plates. Successful transformants were determined by PCR. All the transformants were selected in appropriate antibiotics [Amp, 100 mg/L (bla_{NDM-5}); Fosfomycin, 16 mg/L (*fosA3*); colistin, 4 mg/L (*mcr-1*); tetracycline, 30 mg/L (*tetA*)].

Conjugation Assay

We applied conjugation assay (Zhou et al., 2020) to evaluate whether these resistant plasmids could be transferred or co-transferred from *K. pneumoniae* 1678 (donor isolate) to *E. coli* J53 (recipient isolate). The donors and recipients were cultured to the logarithmic phase, mixed in 1:1 ratio, centrifuged at 8,000 × *g* for 1 min, and then resuspended in 20 μl $MgSO_4$ (10 mM). The resuspension was spotted on the Luria Bertani (LB) plate and incubated at 37°C overnight. Subsequently, the serial dilutions were plated in media with appropriate antibiotics [Amp, 100 mg/L (bla_{NDM-5}); Fosfomycin, 16 mg/L (*fosA3*); colistin, 4 mg/L (*mcr-1*); sodium azide, 100 mg/L (J53 recipient)]. The conjugation frequency was calculated as the number of transconjugants per donor. All transconjugants were confirmed by PCR for the presence of *fosA3*, bla_{NDM-5}, and *mcr-1* genes. All the primers were listed in **Supplementary Table 1**.

S1-Pulsed-Field Gel Electrophoresis Assay

The S1-pulsed-field gel electrophoresis (S1-PFGE) was performed to further determine the existence of plasmids in the original isolate *K. pneumoniae* 1678, and its transformants and transconjugants. PFGE plugs of all these strains were prepared and digested as previously described (Ai et al., 2021). Briefly, the isolates were embedded in 10 g/L of Seakem Gold gel, and digested with endonuclease S1 nuclease (Takara, Dalian, China). PFGE analysis was performed with a CHEF mapper system (Bio-Rad). The digested DNA fragments were separated for 19 h at 6 V/cm, 14°C on a 1.0% agarose gel (Bio-Rad) with

[1]https://github.com/ruanjue/smartdenovo

[2]https://cge.cbs.dtu.dk/services/PlasmidFinder/

[3]https://cge.cbs.dtu.dk/services/ResFinder/

[4]https://tool-mml.sjtu.edu.cn/oriTfinder/oriTfinder.html

[5]https://www-is.biotoul.fr/

pulse times of 4–40 s. *XbaI*-digested Salmonella H9812 DNA was used as the DNA marker. The nucleic acid dye Gel-red (Yeasen, China) was used to stain the DNA in the gels.

Nucleotide Sequence Accession Numbers of *Klebsiella pneumoniae* 1678

The complete nucleotide sequences of the chromosome and plasmids p1678-2, p1678-3, p1678-4, p1678-5, and p187–6 were submitted to GenBank under accession numbers CP080445, CP080446, CP080447, CP080448, CP080449, and CP080450, respectively.

RESULTS

Klebsiella pneumoniae 1678 Was a Typical Extensively Drug-Resistant Isolate

In order to clarify the antibiotic-resistant phenotype of *Klebsiella pneumoniae* 1678, we tested the susceptibility of 26 antibiotics in this strain (**Table 1**), especially including Fosfomycin, tigecycline, colistin, and ceftazidime–avibactam that were known for their robust bactericidal effect against CRKP. Our results indicated the *K. pneumoniae* 1678 was a representative multi-drug resistant strain, which not only exhibited high-level resistance to all β-lactam antibiotics and carbapenems, but was even resistant to tigecycline, Fosfomycin, colistin, and ceftazidime–avibactam (**Table 1**). These resistance profiles indicated the treatment option for the infection caused by *K. pneumoniae* 1678 would be limited.

Klebsiella pneumoniae 1678 Co-harboring *fosA3*, bla_{NDM-5}, and *mcr-1*

To further investigate the related mechanism that mediated the extensively drug-resistant resistant (XDR) characteristic of *K. pneumoniae* 1678, we used WGS to deeply describe the genomic information of the XDR bacteria. According to the MLST analysis, the *K. pneumoniae* 1678 was typed as ST485. We found more than 20 resistant elements and 5 resistant plasmids in this isolate (**Table 2**). Moreover, three key resistance genes were focused, which played a significant role in the formation of resistance to Fosfomycin (*fosA3*), carbapenems, ceftazidime–avibactam (bla_{NDM-5}), and colistin (*mcr-1*). In addition to the molecular detection of these crucial resistant elements, we also extracted and transformed each resistant plasmid to *E. coli* Top 10 (**Figure 1A**) and tested whether these plasmids could mediate the corresponding resistant phenotype. Antibiotic susceptibility results of all transformants well proved the role of the resistant plasmids (**Table 2**).

Tigecycline Resistance Was Mediated by the Overexpression of RND-Type Efflux Transporters

The mechanisms underlying tigecycline resistance are complex. Previous studies demonstrated the mutation of plasmid-borne *tet(A)* could be an important factor causing tigecycline resistance in *K. pneumoniae*. Accordingly, we compared the amino-acid sequence of the Tet(A) protein of *K. pneumoniae* 1678 and the mutated Tet(A) confirmed before (**Supplementary Figure 1**). We found the Tet(A) carried by *K. pneumoniae* 1678 owned the same mutated characteristic which Xu (Xu et al., 2021) described (**Supplementary Figures 1**, **3**). Moreover, we also detected the mRNA expression of the *tet(A)* gene in the *E. coli* transformants to ensure the *tet(A)* gene could be expressed normally (**Supplementary Figure 2**). However, we could not detect the tigecycline resistant phenotype, but only the resistant to tetracycline in the *tet(A)*-transformants (**Table 2**), which indicated that this mutation may not contribute to tigecycline resistance in *K. pneumoniae* 1678.

In addition to the mutation of Tet(A) protein, the overexpression of the RND-type efflux pumps AcrAB and OqxAB has been shown to play a crucial role in tigecycline resistance in *K. pneumoniae* (Bialek-Davenet et al., 2015; Li et al., 2017). Our qRT-PCR experiments indicated that *K. pneumoniae* 1678 overexpressed the AcrAB–TolC pathway genes *acrA/B* and *tolC* (>sixfold greater than the tigecycline susceptible *K. pneumoniae* ATCC 13883 reference strain) (**Figure 2A**), and was also observed to overexpress *oqxA* and *oqxB* (range 6.432- to 10.435-fold compared with the reference strain levels) (**Figure 2B**). Moreover, the activating regulator of AcrAB (*ramA*) and OqxAB (*rarA*) also exhibited the same expression level (**Figure 2**). What is more, the mutation in RamR protein was also analyzed, for it is the negative regulator of RamA (Zheng et al., 2018), and we found an amino acid mutation (L44M) compared with the reference sequence (Accession number: ADI49705.1), but the phenotype is unproved. We assumed this may do a potential favor for the overexpression of AcrAB. These results showed the overexpression of RND-type efflux transporters contributed to the tigecycline resistance of *K. pneumoniae* 1678.

Comparative Genomics of the Plasmids Carrying Resistance Genes

We have confirmed that the key resistant genes were all located on plasmids. As plasmids are often transmissible between bacteria, and some have spread globally, we made detailed analysis of these resistant plasmids, aiming to further clarify the resistance mechanism and potential dissemination threats of *K. pneumoniae* 1678. p1678-3 was a typical IncFII-type plasmid, harboring a completed conjugation system, and shared 81% identity with pFOS-HK151325, the first *fosA3* plasmid from a clinical *E. coli* identified in China (**Figure 3A**). Moreover, p1678-3 was also highly similar to pKP32558-4 (89% identity, CP076034.1, *K. pneumoniae*) and p116753-KPC (95% identity, MN891682.1, *K. pneumoniae*). The genetic differences between p1678-3 and these plasmids were most concentrated in the surrounding genes of *fosA3* gene, which may be related to the mobility insertion of IS elements (**Figure 3A**).

The wide dissemination of bla_{NDM} genes is largely mediated by certain plasmids, particularly those of the IncX3 type, which p1678-4 plasmid belonged to. Moreover, the genetic context of the p1678-4 plasmid (**Figure 4A**) was nearly identical to that of the human *K. pneumoniae* plasmid pNDM-MGR194 (2015, IncX3, bla_{NDM-5}, KF220657.1) previously reported in India (Krishnaraju et al., 2015) and was also highly similar to p2B8067

TABLE 1 | Antimicrobial drug susceptibility profiles.

Antibiotics	MIC (mg/L)/antimicrobial susceptibility												
				Transformants				Transconjugants					
	1678	Top10	J53	p1678–6-TOP10 **(TetA)**	p1678-3 Top10 **(FosA3)**	p1678-4-Top10 **(NDM-5)**	p1678-5-Top10 **(MCR-1)**	p1678-3-J53 **(FosA3)**	p1678-4-J53 **(NDM-5)**	p1678-5-J53 **(MCR-1)**	p1678-3 and 5-J53 **(FosA3+MCR-1)**	p1678-4 and 5-J53 **(NDM-5+MCR-1)**	p1678-3 and 4 and 5-J53 **(FosA3+NDM-5+MCR-1)**
MEM	**>16/R**	≤0.06/S	≤0.06/S	≤0.06/S	≤0.06/S	**16/R**	≤0.06/S	≤0.06/S	**16/R**	≤0.06/S	≤0.06/S	**16/R**	**16/R**
IPM	**16/R**	≤0.25/S	≤0.25/S	≤0.25/S	≤0.25/S	**4/R**	≤0.25/S	≤0.25/S	**4/R**	≤0.25/S	≤0.25/S	**8/R**	**8/R**
ETP	**>2/R**	≤0.015/S	≤0.015/S	≤0.015/S	≤0.015/S	**>2/R**	≤0.015/S	≤0.015/S	**>2/R**	≤0.015/S	≤0.015/S	**>2/R**	**>2/R**
Caz/AVI	**>16/4/R**	≤0.5/4/S	≤0.5/4/S	≤0.5/4/S	≤0.5/4/S	**>16/4/R**	≤0.5/4/S	≤0.5/4/S	**>16/4/R**	≤0.5/4/S	≤0.5/4/S	**>16/4/R**	**>16/4/R**
TGC	**8/R**	≤0.25/S	≤0.25/S	**≤0.25/S**	≤0.25/S	≤0.25/S	≤0.25/S	≤0.25/S	≤0.25/S	≤0.25/S	≤0.25/S	≤0.25/S	≤0.25/S
POL	**16/R**	0.25/S	0.25/S	0.25/S	0.25/S	0.25/S	**16/R**	0.25/S	0.25/S	**16/R**	**16/R**	**16/R**	**16/R**
FOS	**>256/R**	0.25/S	0.25/S	0.25/S	**>256/R**	0.25/S	0.25/S	**>256/R**	0.25/S	0.25/S	**>256/R**	0.25/S	**>256/R**
AMP	**>32/R**	≤8/S	≤8/S	≤8/S	**>32/R**	**>32/R**	≤8/S	**>32/R**	**>32/R**	≤8/S	**>32/R**	**>32/R**	**>32/R**
CZO	**>32/R**	≤2/S	≤2/S	≤2/S	**>32/R**	**>32/R**	≤2/S	**>32/R**	**>32/R**	≤2/S	**>32/R**	**>32/R**	**>32/R**
CAZ	**>128/R**	≤0.25/S	≤0.25/S	≤0.25/S	**>128/R**	**>128/R**	≤0.25/S	**>128/R**	**>128/R**	≤0.25/S	**>128/R**	**>128/R**	**>128/R**
FEP	**>16/R**	≤0.5/S	≤0.5/S	≤0.5/S	≤0.5/S	**>16/R**	≤0.5/S	≤0.5/S	**>16/R**	≤0.5/S	≤0.5/S	**>16/R**	**>16/R**
CSL	**>64/32/R**	≤16/8/S	≤16/8/S	≤16/8/S	≤16/8/S	**>64/32/R**	≤16/8/S	≤16/8/S	**>64/32/R**	≤16/8/S	≤16/8/S	**>64/32/R**	**>64/32/R**
SAM	**>32/16/R**	≤16/4/S	≤16/4/S	≤16/4/S	≤16/4/S	**>32/16/R**	≤16/4/S	≤16/4/S	**>32/16/R**	≤16/4/S	≤16/4/S	**>32/16/R**	**>32/16/R**
FOX	**>32/R**	≤8/S	≤8/S	≤8/S	≤8/S	**>32/R**	≤8/S	≤8/S	**>32/R**	≤8/S	≤8/S	**>32/R**	**>32/R**
CXM	**>16/R**	8/S	8/S	8/S	**>16/R**	**>16/R**	8/S	**>16/R**	**>16/R**	8/S	**>16/R**	**>16/R**	**>16/R**
CTX	**>64/R**	≤0.12/S	≤0.12/S	≤0.12/S	**64/R**	**>64/R**	≤0.12/S	**64/R**	**>64/R**	≤0.12/S	**64/R**	**>64/R**	**>64/R**
TZP	**>128/4/R**	≤16/4/S	≤16/4/S	≤16/4/S	≤16/4/S	**>128/4/R**	≤16/4/S	≤16/4/S	**>128/4/R**	≤16/4/S	≤16/4/S	**>128/4/R**	**>128/4/R**
AMC	**>32/16/R**	≤8/4/S	≤8/4/S	≤8/4/S	≤8/4/S	**>32/16/R**	≤8/4/S	≤8/4/S	**>32/16/R**	≤8/4/S	≤8/4/S	**>32/16/R**	**>32/16/R**
LVX	**>8/R**	≤0.12/S	≤0.12/S	≤0.12/S	≤0.12/S	≤0.12/S	≤0.12/S	≤0.12/S	≤0.12/S	≤0.12/S	≤0.12/S	≤0.12/S	≤0.12/S
MFX	**>2/R**	≤0.25/S	≤0.25/S	≤0.25/S	≤0.25/S	≤0.25/S	≤0.25/S	≤0.25/S	≤0.25/S	≤0.25/S	≤0.25/S	≤0.25/S	≤0.25/S
TCY	**>16/R**	≤2/S	≤2/S	**16/R**	≤2/S	≤2/S	≤2/S	≤2/S	≤2/S	≤2/S	≤2/S	≤2/S	≤2/S
GEN	**16/R**	≤1/S	≤1/S	≤1/S	≤1/S	≤1/S	≤1/S	≤1/S	≤1/S	≤1/S	≤1/S	≤1/S	≤1/S
AMK	≤16/S	≤16/S	≤16/S	≤16/S	≤16/S	≤16/S	≤16/S	≤16/S	≤16/S	≤16/S	≤16/S	≤16/S	≤16/S
ATM	**>16/R**	≤4/S	≤4/S	≤4/S	**>16/R**	≤4/S	≤4/S	**>16/R**	≤4/S	≤4/S	≤4/S	≤4/S	**>16/R**
NIT	**64/I**	≤16/S	≤16/S	≤16/S	≤16/S	≤16/S	≤16/S	≤16/S	≤16/S	≤16/S	≤16/S	≤16/S	≤16/S
SXT	**>4/76/R**	≤0.5/9.5/S	≤0.5/9.5/S	≤0.5/9.5/S	≤0.5/9.5/S	≤0.5/9.5/S	≤0.5/9.5/S	≤0.5/9.5/S	≤0.5/9.5/S	≤0.5/9.5/S	≤0.5/9.5/S	≤0.5/9.5/S	≤0.5/9.5/S

MEM, Meropenem; IPM, Imipenem; ETP, Ertapenem; Caz/AVI, ceftazidime–avibactam; TGC, Tigecycline; POL, Polymixin B; FOS, Fosfomycin; AMP, Ampicillin; CZO, Cefazolin; CAZ, Ceftazidime; FEP, Cefepime; CSL, Cefoperazone/Sulbactam; SAM, Ampicillin/Sulbactam; FOX, Cefoxitin; CXM, Cefuroxime; CTX, Cefotaxime; TZP, Piperacillin/Tazobactam; AMC, Amoxicillin/Clavulanic acid; LVX, Levofloxacin; MFX, Moxifloxacin; TCY, Tetracycline; GEN, Gentamicin; AMK, Amikacin; ATM, Aztreonam; NIT, Nitrofurantoin; SXT, Trimethoprim/Sulfamethoxazole.

The other resistance phenotype like LVX, MFX, GEN, NIT, or SXT resistance did not present in these transformants or transconjugants in table because these elements are located on p1678-2 plasmid, not p16783-3(fosA3), p1678-4(bla_{NDM-5}), p1678-5(mcr-1), and p1678-6(tetA). The bold values indicated important resistance genes and resistance phenotypes.

TABLE 2 | General features, antimicrobial resistance genes of plasmids in *K. pneumoniae* 1678.

Characteristics	Results				
	p1678-2	**p1678-3**	**p1678-4**	**p1678-5**	**p1678-6**
Accension number	CP080446	CP080447	CP080448	CP080449	CP080450
Length(bp)	90,943	76,526	46,161	33,309	24,774
GC content (%)	54	52	47	42	54
No. of ORF	116	92	59	42	29
Incompatibility group	IncFIIK(IncQ1	**IncFII**	**IncX3**	**IncX4**	IncR
Conjugal ability	No	**Yes**	**Yes**	**Yes**	No
Resistant genes					
	bla_{OXA-1}	***fosA3***	***bla*$_{NDM-5}$**	***mcr-1***	*TetA*
	aac(3)-Iid	$bla_{CTX-M-55}$			
	aph(3′)-Ia	$bla_{TEM-141}$			
	sul2, sul1				
	sul2, sul1;				
	aac(6′)-Ib-cr				
	aph(3′)-Ia				
	aac(3)-Iid				
	mph(A)				
	aadA16				
	qnrB52				
	ARR-3				
	catB3				

The bold values indicated important resistance genes and resistance phenotypes.

(2021, IncX3, bla_{NDM-7}, CP070442.1). These results indicated that no matter the variants of bla_{NDM}, the IncX3 plasmid was a major vehicle in mediating the dissemination of bla_{NDM}. Similar to the IncFII plasmids described before (Bi et al., 2018), IncX3 plasmid also could be self-transferred among *Enterobacteriaceae*, supported with the results of the conjugation mode analysis of p1678-4 plasmid (**Table 2**).

p1678-5 plasmid was a 33,309-bp circular molecule with *repA* belonging to IncX4, harboring *mcr-1* resistance element (**Figure 5A**). Previous studies have demonstrated most plasmids carrying *mcr-1* are transferable, and IncX4 was dominant *mcr-1*-carrying plasmid types (Xiaomin et al., 2020). According to the genomic comparation, we found p1678-5 was almost identical to both pQDFD216-1 (CP053212.1) plasmid identified in *E. coli* and plasmid 16BU137 (MT316509.1) from *K. pneumoniae.* These results showed IncX4 plasmids harboring *mcr-1* could disseminate in different species of *Enterobacteriaceae*, and the completed conjugative element also can be found in p1678-5 plasmid (**Table 2**). In addition, we also make a comparison between p1678-5 and the first *mcr-1* plasmid pHNSHP45 (NZ_KP347127.1, IncI2) (Liu et al., 2016), and found low identity between two plasmids (**Supplementary Figure 4**).

Resistant Plasmids Could Be High-Efficient Self-Transferred or Co-transferred

We have known these three resistance plasmids were all bioinformatic predicted to carry essential conjugative modules (*oriT*, Relaxase, T4CP, and T4SS) and most of these types of plasmids have proved to be movable (Partridge et al., 2018). However, it is not common for such three plasmids to co-exist in one *K. pneumoniae*, and the transferring and co-transferring pattern was unclear. Here, we applied conjugation assay to imitate and evaluate the dissemination ability of these three plasmids in *K. pneumoniae* 1678. We found all these three plasmids could transfer to *E. coli* J53 with high conjugation frequencies ($1.42 \times 10^{-4} - 7.9 \times 10^{-3}$), especially for the *mcr-1* plasmid (p1678-5) (**Table 3**). In addition to the self-transferring of a single plasmid, we also observed co-transfer of two plasmids and even three plasmids and the co-conjugation frequencies of two plasmids only decrease 1-log compared to a single plasmid (**Table 3**). Although the co-conjugation frequencies of three plasmids was low, the potential clinical threat could not be ignored, since the clonal spread will accelerate the spread of these resistance genes. Moreover, the plasmid pattern of S1-PFGE further proved the transferring profile of the *K. pneumoniae* 1678 (**Figure 1B**), and the antibiotic MICs of these transconjugants also confirmed the spread of resistance phenotype of *K. pneumoniae* 1678 (**Table 1**).

Mobile Genetic Elements Associated With *fosA3*, *bla*$_{NDM-5}$, and *mcr-1*

The capture, accumulation, and dissemination of resistance genes are not only due to the spread of plasmids, but also to the actions of other MGEs, such as IS and Tn. To comprehensively evaluate the dissemination potential of these resistance genes in *K. pneumoniae* 1678, we also analyze the MGEs surrounding them. IS*26* seems to be the key element in the mobilization of *fosA3,* since it not only composes a composite transposon surrounding *fosA3* in the p1678-3 plasmids, but also surrounding the *fosA3* of pFOS-HK151325 plasmid (Yang et al., 2019) (2013, JX627737, *E. coli*, China), of pFOS18 plasmid (Yang et al., 2019) (2015, KJ653815, *K. pneumoniae*, China), and of p06607 plasmid (Yang et al., 2019) (2010, AB522970, first *fosA3* plasmid emerged in the world). Moreover, the same IS*26*-composite transposons were also observed to frequently contain additionally a bla_{CTX-M} gene. Compared to the first *fosA3* plasmid, there are more than 10 ORFs inserted around *fosA3* in p1678-3 plasmid, with some new IS, some elements associated with transcriptional regulation, and other resistance elements (**Figure 3B**).

The genetic contexts of bla_{NDM} share two common features. The insertion sequence IS*Aba125* (intact or truncated) is always upstream of bla_{NDM}, while a bleomycin resistance gene, ble_{MBL}, is always downstream. Further downstream of ble_{MBL}, there are usually located *trpF* and *dsbC* genes (**Figure 4B**). Although the bla_{NDM}-1 in *Acinetobacter* spp. is located within IS*Aba125*-based composite transposon Tn*125*(pNDM-BJ01, JQ001791) (Wu et al., 2019), it was always interrupted or truncated in *Enterobacteriaceae*. In p1678-4, Tn*125* was truncated by IS*5*, IS*26,* and IS*300* (**Figure 4B**). These new genetic contexts in p1678-4 may form a new mechanism involved in the mobilization of bla_{NDM-5}.

Similar to other *mcr-1*-carrying IncX4-type plasmids (Xiaomin et al., 2020), the typical IS*26-parA-mcr-1.1-pap2*

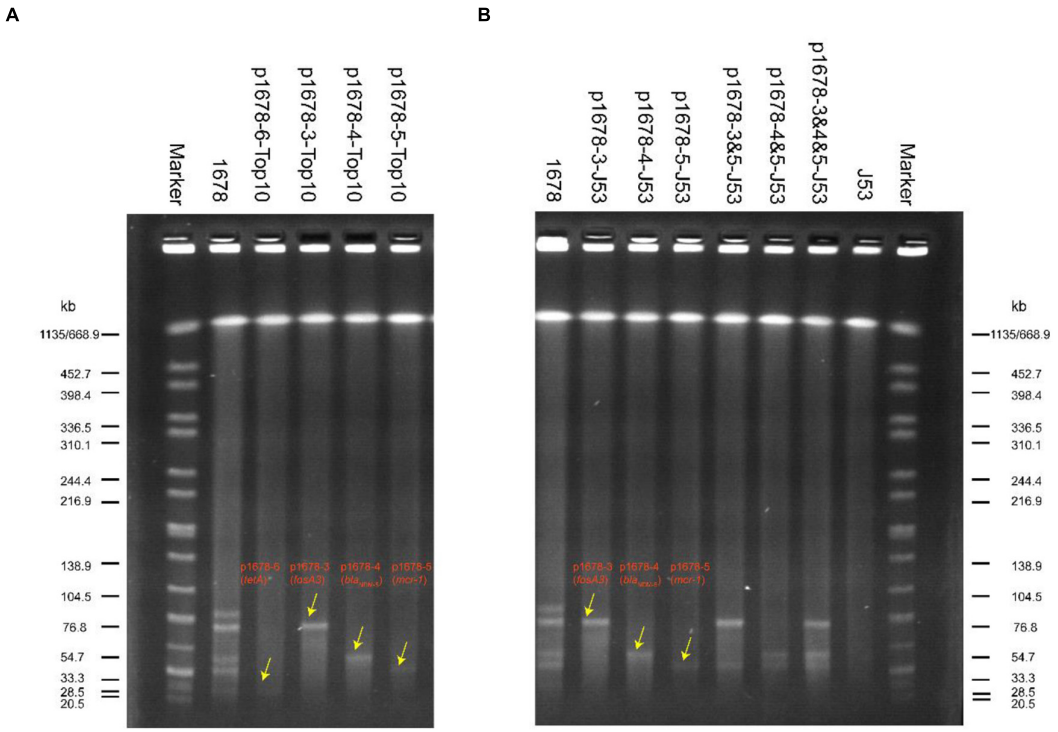

FIGURE 1 | SI-PFGE profiles of original *K. pneumoniae* 1678 and its transformants **(A)** and transconjugants **(B)**. Lane marker was *Xbal*-digested DNA of Salmonella Braenderup H9812; Lane 1678 and Lane J53 were used as positive reference and negative control, respectively; transformants: p1678-6-Top10 (*tetA*), p1678-3-Top10 (*fosA3*), p1678-4-Top10(bla_{NDM-5}), and p1678-5-Top10(*mcr-1*). Transconjugants: p1678-3-J53(*fosA3*), p1678-4-J53(bla_{NDM-5}), p1678-5-J53(*mcr-1*), p1678-3 and 5-J53 (*fosA3* and *mcr-1*), p1678-4 and 5-J53 ($bla_{NDM-5}$and *mcr-1*), and p1678-3 and 4 and 5-J53 (*fosA3*, bla_{NDM-5}, and *mcr-1*).

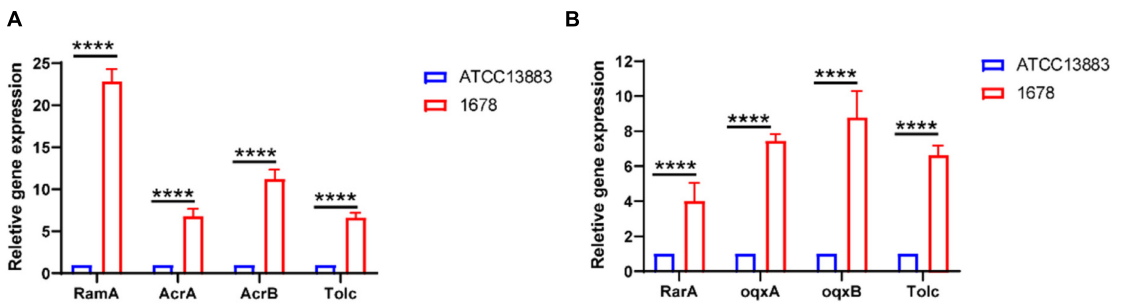

FIGURE 2 | Overexpression of AcrAB and OqxAB in clinical *K. pneumoniae* 1678 isolate. The expression levels of AcrA/B **(A)**, OqxA/B **(B)**, and related transcriptional regulators was determined by qRT-PCR. The *K. pneumoniae* ATCC13883 is used as the reference strain (expression = 1.0). The data represent the mean standard deviation for three independent biological replicates. Differences between different strains, regarding related gene expression, were statistically analyzed using a two-tailed Student's *t*-test with Bonferroni correction. ****$p < 0.0001$.

cassette was identified in p1678-5, with *pap2* gene partitional truncated (**Figure 5B**). Although IS*Apl1* has been described as the most common IS element adjacent to *mcr-1* at one or both ends, we did not observe it surrounding the *mcr-1* gene.

DISCUSSION

Extensively drug-resistant *K. pneumoniae* constitutes the major sources of nosocomial infections with extraordinary drug resistance. The prevalent resistance plasmids are responsible for the sudden increase in the population of multidrug resistance among *K. pneumoniae* isolates (Tzouvelekis et al., 2012; Chen et al., 2014). In this study, we described a multi-drug resistant *K. pneumoniae* 1678 co-harboring three self-transmissible resistant plasmids, which mediated the resistance for carbapenems, Fosfomycin, colistin, and ceftazidime–avibactam. The co-existing of these plasmids not only conferred the multi-drug resistant phenotype to *K. pneumoniae*

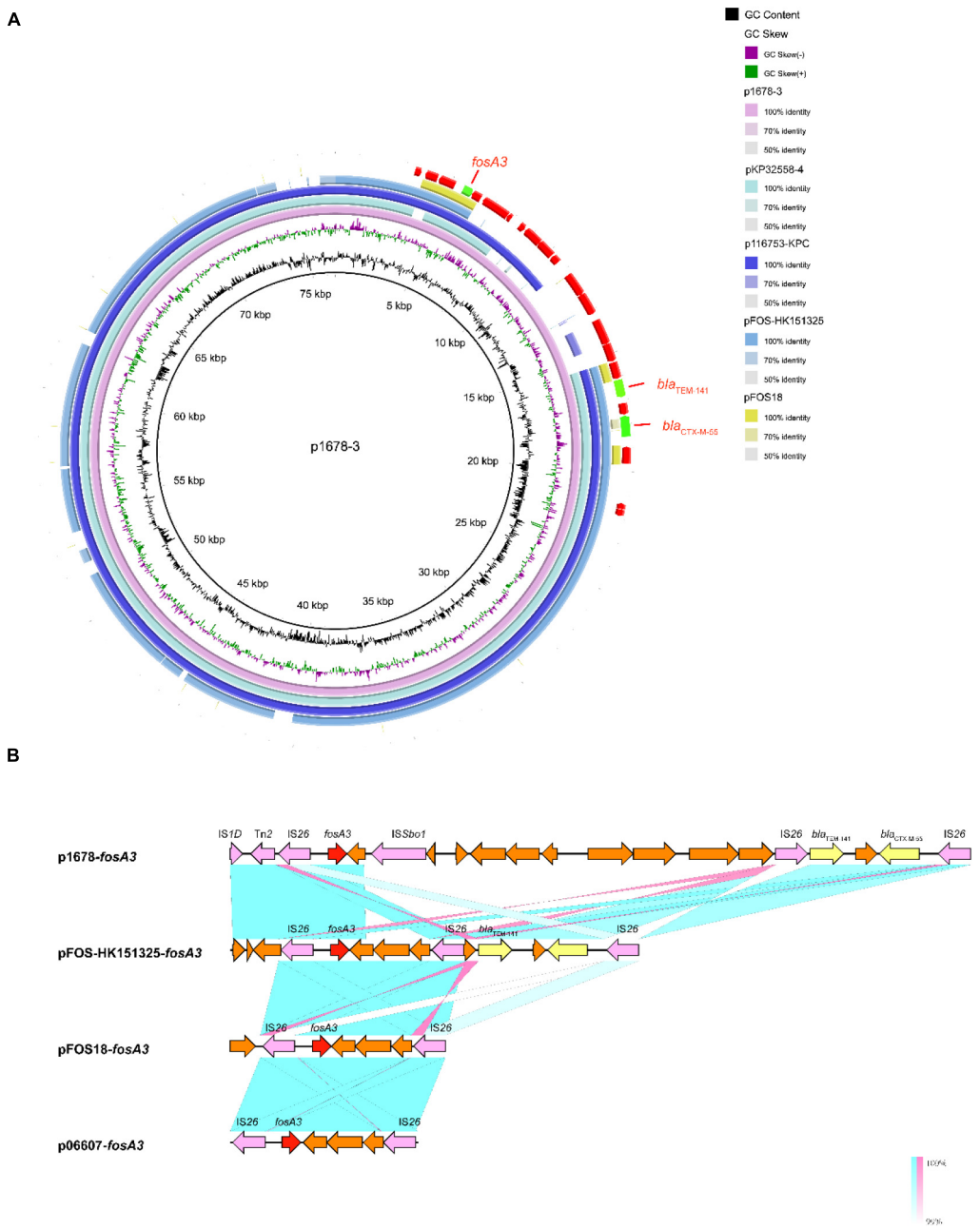

FIGURE 3 | Comparative analysis of pl687-3 plasmids with other reference plasmids. **(A)** p1678-3 (CP080447) was used as the reference plasmid to perform genome alignment with pFOS-HK151325 (JX627737, first *fosA3* plasmid from a clinical *E. coli* identified in China) and pFOS18 (KJ653815, first *fosA3* plasmid from a clinical *K. pneumoniae* identified in China). Moreover, p1678-3 was also compared with another two similar plasmids pKP32558-4 (CP076034.1, *K. pneumoniae*) and p116753-KPC (MN891682.1, *K. pneumoniae*). The red arrows represent CDs. **(B)** Linear comparison of the *fosA3* region. The *fosA3* region was compared with the regions extracted from pFOS-HK151325, pFOS18, and p06607 (AB522970, first *fosA3* plasmid).

1678, but also held the potential threat to co-transfer to other isolates.

Tigecycline has been considered as an effective antibiotic against CRKP *in vitro*, and is also considered as one of the last-resort antibiotics against CRKP infections (Chopra, 2002; Doi, 2019). Unfortunately, tigecycline resistance has been reported frequently in clinics (Fang et al., 2020). In this study, we found *K. pneumoniae* 1678 was resistant to tigecycline. We identified the *tet(A)* gene in this isolate, and also confirmed the mutations on Tet(A) protein (**Supplementary Figure 1**). Several studies had verified the plasmid-borne mutated *tet(A)* gene or the synergy of TetA and RND-type efflux transporters play an important role in causing tigecycline resistance (Bialek-Davenet et al., 2015; Foong et al., 2020; Xu et al., 2021). However, we found the

TABLE 3 | Conjugation frequency of resistant plasmids identified in *K. pneumoniae* 1678.

Plasmid	Resistance gene	No. of independent determinations	Conjugation frequencies	
			Mean	Range
p1678-3	*fosA3*	3	2.25×10^{-4}	$1.97 \times 10^{-4} - 2.75 \times 10^{-4}$
p1678-4	bla_{NDM-5}	3	1.84×10^{-4}	$1.42 \times 10^{-4} - 2.37 \times 10^{-4}$
p1678-5	*mcr-1*	3	5.41×10^{-3}	$2.94 \times 10^{-3} - 7.9 \times 10^{-3}$
Co-transfer of plasmids				
Co-transfer of p1678-3 and p1678-5	*fosA3* + *mcr-1*	3	1.78×10^{-5}	$1.29 \times 10^{-5} - 2.77 \times 10^{-5}$
Co-transfer of p1678-4 and p1678-5	bla_{NDM-5} + *mcr-1*	3	2.25×10^{-5}	$1.62 \times 10^{-5} - 2.92 \times 10^{-5}$
Co-transfer of p1678-3 and p1678-4 and p1678-5	*fosA3* + bla_{NDM-5} + *mcr-1*	3	9.63×10^{-8}	$8.08 \times 10^{-8} - 10.38 \times 10^{-8}$

p1678-6 plasmid, harboring mutated *tet(A)* gene, could not result in tigecycline resistance. According to the genetic comparison of p1678-6 plasmid with other *tet(A)*-plasmid (tigecycline-resistant), we found p1678-6 plasmid shared low identity with them. Further to analyze the genetic components surrounding *tet(A)* gene, we found the IS and Tn elements in p1678-6 plasmid also different. As the IS elements sometimes would affect promoter activity (Partridge et al., 2018), we assumed the expression discrepancy of *tet(A)* gene in p1687-6 plasmid with other tigecycline-resistant-*tet(A)* plasmids may be accounted for in this antibiotic-susceptibility phenomenon. Although the Tet(A) protein did not contribute to the tigecycline resistance, we observed the overexpression of the efflux pumps AcrAB and OqxAB in *K. pneumoniae* 1678, another key factor mediating the tigecycline resistance (Bialek-Davenet et al., 2015; Li et al., 2017). Hence, in this study, the overexpression of RND-type efflux pumps played a crucial role in tigecycline resistance in *K. pneumoniae* 1678.

Except for resistant to tigecycline, the resistant to Fosfomycin, colistin, carbapenems, and ceftazidime–avibactam in *K. pneumoniae* 1678 were all associated with the typical resistant plasmids. Both *fosA3* and $bla_{CTX-M-55}$ gene were located on p1678-3 plasmid, a typical IncFII plasmid. Previous studies have demonstrated that Fosfomycin-modifying enzymes were present on plasmids belonging to the IncF, IncN, IncA/C, IncHI2, and IncX1 family, whereas IncF was the predominant plasmid incompatibility type (Yang et al., 2019; Zurfluh et al., 2020). Although there existed several FosA variants, FosA3 was the most frequently found Fosfomycin-modifying enzyme worldwide, and many studies have confirmed the dissemination of the *fosA3* gene is closely associated with that of the ESBL gene bla_{CTX-M} (Yang et al., 2019), which was consistent with the findings in the p1678-3 plasmid. Our results also showed the p1678-3 plasmid had the completed conservative 35-kb conjugation module of IncF plasmids (Bi et al., 2018), and the self-transmissibility of this plasmid was also confirmed through conjugation assay. As we know, Fosfomycin was a potential regimen for treating extensively drug-resistant bacteria especially for carbapenemase-producing *Enterobacteriaceae* (CRE), once these isolates uptake the plasmids like p1678-3, the infection treatment would become limited.

bla_{NDM-5} plasmid (p1678-4) and *mcr-1* plasmid (p1678-5) all belong to IncX-type plasmid, holding a smaller size than IncF plasmid, which sometimes makes it easier for movement. p1678-4 plasmid belongs to IncX3 type, the major vehicle in mediating the dissemination of bla_{NDM} (Wu et al., 2019). Several NDM variants have been reported, which commonly contain between 1 and 5 amino acid substitutions compared to NDM-1. Notably, NDM-5 variant, containing the V88L substitution has repeatedly been reported to exhibit enhanced carbapenemase activity (Wu et al., 2019). MICs of ertapenem against strains producing NDM-5 were 4- or 8-fold higher than those against strains producing NDM-1 (Wu et al., 2019). Moreover, the novel antibiotic agent ceftazidime–avibactam used alone also makes no defense against NDM-5 carbapenemase (Yang et al., 2020). All this information indicated that the spread and pandemic of such IncX3-type p1678-4 plasmid could pose a huge risk to public health.

Like tigecycline, Fosfomycin, and ceftazidime–avibactam, colistin also is a robust antibiotic against infections caused by CRE (Doi, 2019). However, CRKP 1678 also harbored the pandemic IncX4 *mcr-1* plasmid (p1678-5), which conferred resistance to colistin. Most plasmids carrying *mcr-1* are reported to be transferable, and IncI2 and IncX4 are dominant *mcr-1*-carrying plasmid types. In previous studies, IncI2 and IncX4 plasmids harboring *mcr-1* were detected in different species of *Enterobacteriaceae,* owing to the high transfer rate (10^{-1}–10^{-3}) of *mcr-1* plasmid (Xiaomin et al., 2020). In this study, we also confirmed the p1678-5 plasmid could be transferred from *K. pneumoniae* to *E. coli* in high *in vitro* transfer rate.

According to the related genetic analysis and *in vitro* high conjugation rate, the threat of each single resistant plasmids was verified clearly in *K. pneumoniae* 1678. Once clinical isolate, especially for CRE, uptake one of these plasmids, the infection treatment would be tougher. Previous studies had reported the co-transfer of resistant element, but it is usually associated with one conjugative plasmid (Costa et al., 2021; Gu et al., 2021; Magi et al., 2021). Previous studies found the *mcr-1* plasmid also could co-transfer with bla_{NDM} plasmid to one recipient, but these plasmids did not transfer from the same donor like the observation in our study (Liang et al., 2021). Notably, in this study we found the *mcr-1* plasmid (p1678-5) could be co-transferred with *fosA3* plasmid (p1678-3) or bla_{NDM-5} plasmid (p1678-4) in 10^{-5} conjugation frequency. Moreover, we also observed these three plasmids could be transferred together, though the transfer rate was not high, the potential risk should be taken seriously. Furthermore, as

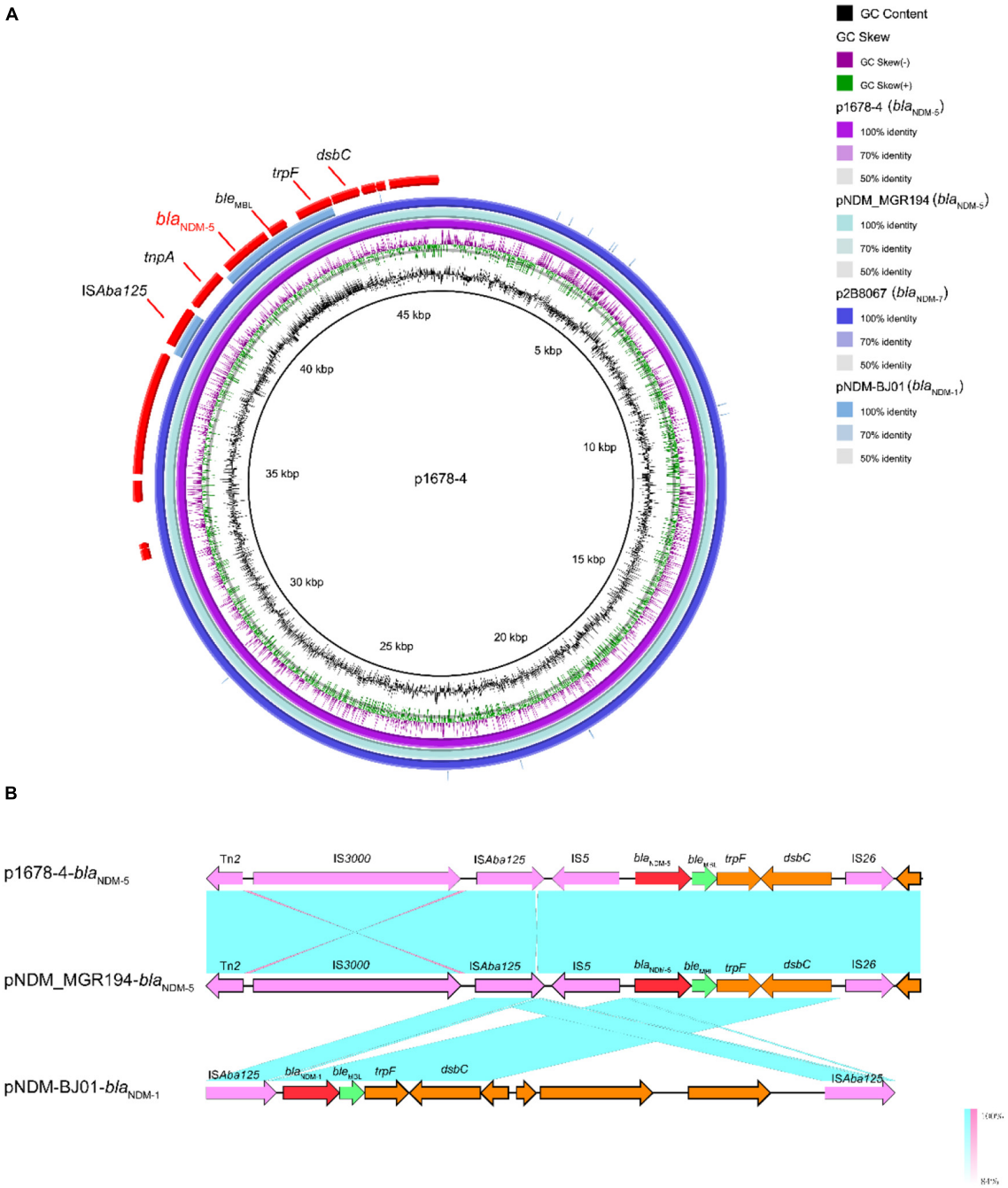

FIGURE 4 | Comparative analysis of pl687-4 plasmids with other reference plasmids. **(A)** p1678-4 (CP080448) was used as the reference plasmid to perform genome alignment with pNDM-MGR194 (bla_{NDM-5}, KF220657.1), p2B8067 (bla_{NDM-7}, CP070442.1), and pNDM-BJ01 (bla_{NDM-1}, JQ001791). The red arrows represent CDs. **(B)** Linear comparison of the bla_{NDM-5} region. The bla_{NDM-5} region was compared with the bla_{NDM} regions extracted from pNDM-MGR194 (bla_{NDM-5} reference plasmid) and pNDM-BJ01 (classical bla_{NDM}-Tn*125* transposon).

the overexpression of RND-type efflux transporters (mediating tigecycline resistance) were not rare in *K. pneumoniae* (Bialek-Davenet et al., 2015), once these movable resistant plasmids co-transmit to such isolate, like *K. pneumoniae 1678* in this study, the therapeutic option would be extremely limited. Tigecycline, Fosfomycin, colistin, carbapenems, and ceftazidime–avibactam are considered as the most effective antibiotics to defend XDR isolates, the co-transferring and co-existing of these typical high-risk plasmids would arise a huge peril to clinical treatment since these antibiotics may all be useless.

The dissemination of resistance genes is not only *via* plasmids, but also *via* other mobile structures like transposons and

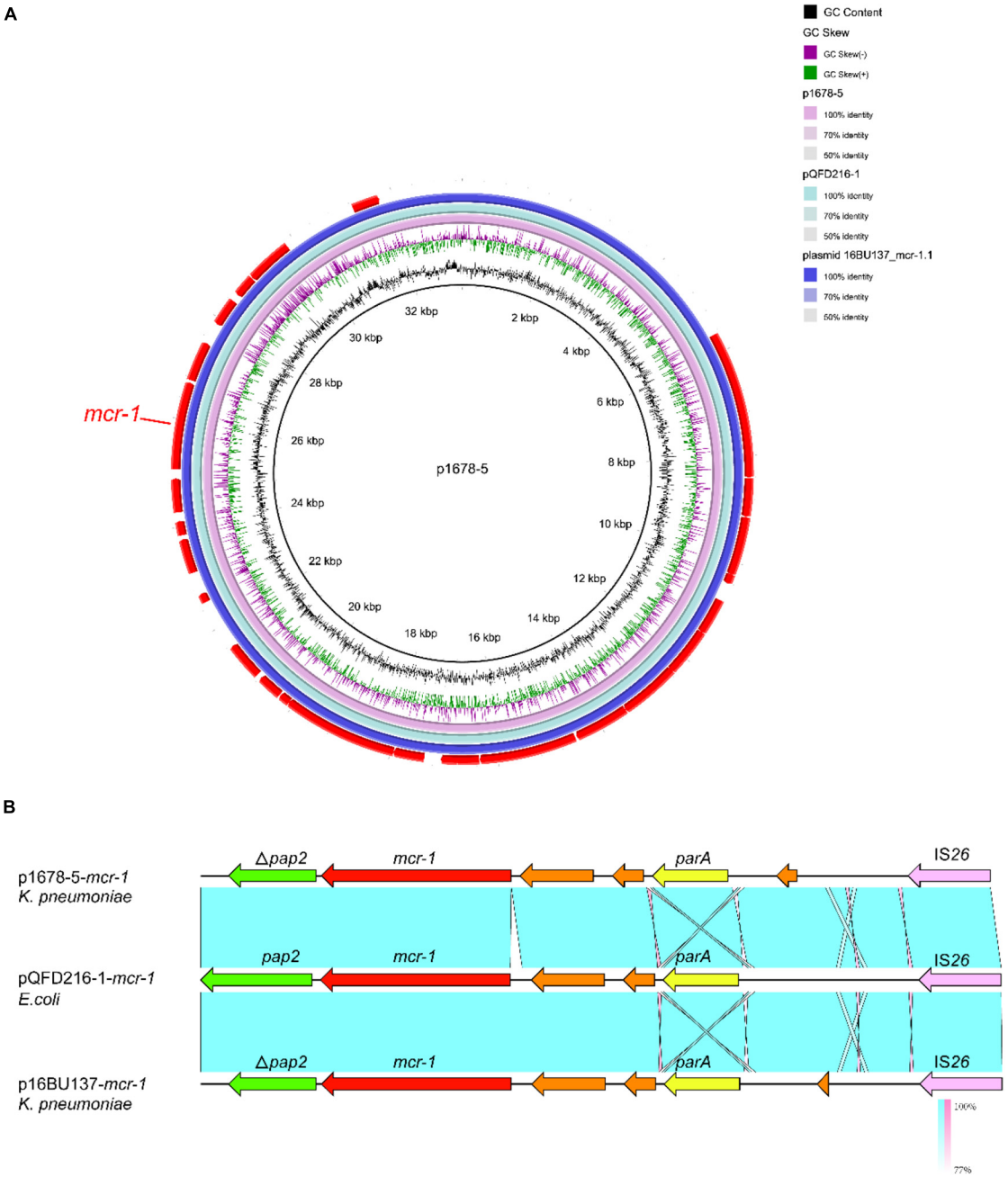

FIGURE 5 | Comparative analysis of pl687-5 plasmids with other reference plasmids. **(A)** p1678-5 (CP080449) was used as the reference plasmid to perform genome alignment with pQDFD216-1 (CP053212.1, *E. coli*) and plasmid 16BU137 (MT316509.1, *K. pneumoniae*). The red arrows represent CDs. **(B)** Linear comparison of the *mcr-1* region. The *mcr-1* region was compared with the *mcr-1* regions extracted from pQDFD216-1 and pQDFD216-1.

insertion elements. IS*26* plays a key role in the dissemination and mobilization of *fosA3*. This IS*26*-array forms two composite transposons and several IS*26*-based transposition units, and both conformations are capable of transposition and exhibit multiple movement modes. In addition to transposition, gene excision and rearrangement of gene modules *via* homologous recombination between IS*26* scattered in the plasmid and/or genome, also drive the evolutionary process of bacteria (Partridge et al., 2018), which could explain the structure of multiple ORF insertions observed in p1678-3 plasmid. The insertion sequence IS*Aba125* is always upstream of bla_{NDM}, providing the −35 region of a promoter for the expression of bla_{NDM} (Wu et al., 2019). In p1678-4, the Tn*125* was truncated by IS*26* and IS*3000*, forming other composite transposons. The mobilization of bla_{NDM} associated with IS*26* or IS*3000* transposons was also common (Wu et al., 2019). These results indicated that although Tn*125* transposon

was interrupted, the movability of bla_{NDM-5} remained. Previous studies have indicated that IS*Apl1* (always associated with the IncI2 plasmid) is a highly active insertion element and a key component required for the mobilization of the gene-cassette containing the *mcr-1* gene (Xiaomin et al., 2020). However, the IS*Apl1* was absent in the p1678-5 plasmid, and in all the *mcr-1*-carrying IncX4-type plasmids, IS*Apl1* in front of *mcr-1* was lost (Du et al., 2020). The loss of the composite transposon IS*Apl1* might increase the stability of the *mcr* gene in IncX4 plasmids, and promote the widespread dissemination of the *mcr-1* gene.

In this study, we report the coexistence and co-transferring of FosA3-, NDM-5, and MCR-1-encoding plasmids in a *K. pneumoniae* isolate. The co-occurrence of *fosA3*, bla_{NDM-5}, and *mcr-1,* and the overexpression of RND-type efflux pumps caused 1678 to be highly resistant not only to commonly used antibiotics (e.g., carbapenems, cephalosporins), but also to Fosfomycin, colistin, ceftazidime–avibactam, and tigecycline, which were considered as the last line for defending XDR Gram-negative organisms. Moreover, the high rate of transmission or co-transmission of these plasmids and various mobile elements surrounding resistant genes greatly increased the risk of spread of these resistant phenotypes. The main limitation in this study is we did not apply the conjugation assay between clinical isolates, which means we could not evaluate the dissemination ability of plasmids more accurately, and the *K. pneumoniae* 1678 did not exhibit any hyper-virulent phenotype. However, future studies are still necessary to evaluate the prevalence of such multi-drug resistant isolates.

DATA AVAILABILITY STATEMENT

The datasets presented in this study can be found in online repositories. The names of the repository/repositories and accession number(s) can be found in the article/ **Supplementary Material**.

AUTHOR CONTRIBUTIONS

FY conceptualized and designed the study. YZ performed data analysis and interpretation. YZ, WA, and YC wrote the original draft. YG, XCW, BW, LR, YX, HZ, and XYW contributed to the interpretation of data. All authors contributed to the manuscript drafting.

FUNDING

This study was supported by grants from Shanghai Pulmonary Hospital Development of Discipline-Department of Clinical Laboratory Medicine.

SUPPLEMENTARY MATERIAL

The Supplementary Material for this article can be found online at: https://www.frontiersin.org/articles/10.3389/fmicb.2021.811263/full#supplementary-material

REFERENCES

Ai, W., Zhou, Y., Wang, B., Zhan, Q., Hu, L., Xu, Y., et al. (2021). First report of coexistence of bla (SFO-1) and bla (NDM-1) β-lactamase genes as well as colistin resistance gene mcr-9 in a transferrable plasmid of a clinical isolate of *Enterobacter* hormaechei. *Front. Microbiol.* 12:676113. doi: 10.3389/fmicb.2021.676113

Bi, D., Zheng, J., Li, J., Sheng, Z., Zhu, X., Ou, H., et al. (2018). In silico typing and comparative genomic analysis of IncFIIK plasmids and insights into the evolution of replicons, plasmid backbones, and resistance determinant profiles. *Antimicrob. Agents* 62:e00764-18. doi: 10.1128/AAC.00764-18

Bialek-Davenet, S., Lavigne, J. P., Guyot, K., Mayer, N., Tournebize, R., Brisse, S., et al. (2015). Differential contribution of AcrAB and OqxAB efflux pumps to multidrug resistance and virulence in *Klebsiella pneumoniae*. *J. Antimicrob. Chemother.* 70, 81–88. doi: 10.1093/jac/dku340

Chen, L., Mathema, B., Chavda, K. D., Deleo, F. R., Bonomo, R. A., and Kreiswirth, B. N. (2014). Carbapenemase-producing *Klebsiella pneumoniae*: molecular and genetic decoding. *Trends Microbiol.* 22, 686–696. doi: 10.1016/j.tim.2014.09.003

Chen, Y., Liu, Z., Zhang, Y., Zhang, Z., Lei, L., and Xia, Z. (2019). Increasing prevalence of ESBL-producing multidrug resistance *Escherichia coli* from diseased pets in beijing. China from 2012 to 2017. *Front. Microbiol.* 10:2852. doi: 10.3389/fmicb.2019.02852

Chopra, I. (2002). New developments in tetracycline antibiotics: glycylcyclines and tetracycline efflux pump inhibitors. *Drug Resist Updat.* 5, 119–125. doi: 10.1016/s1368-7646(02)00051-1

Costa, A., Figueroa-Espinosa, R., Gaudenzi, F., Lincopan, N., Fuga, B., Ghiglione, B., et al. (2021). Co-occurrence of NDM-5 and RmtB in a clinical isolate of *Escherichia coli* belonging to CC354 in Latin America. *Front. Cell Infect. Microbiol.* 11:654852. doi: 10.3389/fcimb.2021.654852

Doi, Y. (2019). Treatment options for carbapenem-resistant gram-negative bacterial infections. *Clin. Infect. Dis.* 69(Suppl. 7), S565–S575. doi: 10.1093/cid/ciz830

Du, C., Feng, Y., Wang, G., Zhang, Z., Hu, H., Yu, Y., et al. (2020). Co-occurrence of the mcr-1.1 and mcr-3.7 genes in a multidrug-resistant *Escherichia* coli isolate from China. *Infect. Drug Resist.* 13, 3649–3655. doi: 10.2147/IDR.S268787

Fang, L. X., Chen, C., Cui, C. Y., Li, X. P., Zhang, Y., Liao, X. P., et al. (2020). Emerging high-level tigecycline resistance: novel tetracycline destructases spread via the mobile tet(X). *Bioessays* 42:e2000014. doi: 10.1002/bies.202000014

Foong, W. E., Wilhelm, J., Tam, H., and Pos, K. M. (2020). Tigecycline efflux in *Acinetobacter baumannii* is mediated by TetA in synergy with RND-type efflux transporters. *J. Antimicrob. Chemoth.* 75, 1135–1139. doi: 10.1093/jac/dkaa015

Gu, Y., Lü, Z., Cao, C., Sheng, H., Li, W., Cui, S., et al. (2021). Cunning plasmid fusion mediates antibiotic resistance genes represented by ESBLs encoding genes transfer in foodborne *Salmonella*. *Int. J. Food Microbiol.* 355:109336. doi: 10.1016/j.ijfoodmicro.2021.109336

Han, H., Liu, W., Cui, X., Cheng, X., and Jiang, X. (2020). Co-existence of mcr-1 and bla (NDM-5) in an *Escherichia coli* strain isolated from the pharmaceutical industry. *WWTP. Infect Drug Resist.* 13, 851–854. doi: 10.2147/IDR.S245047

Hirabayashi, A., Dao, T. D., Takemura, T., Hasebe, F., Trang, L. T., Thanh, N. H., et al. (2021). A transferable incC-incx3 hybrid plasmid cocarrying bla(NDM-4), tet(X), and tmexCD3-toprJ3 confers resistance to carbapenem and tigecycline. *mSphere* 6:e0059221. doi: 10.1128/mSphere.00592-21

Clinical and Laboratory Standards Institute (2021a). *Methods for Dilution Antimicrobial Susceptibility Tests for Bacteria That Grow Aerobically,* 11th Edn. Wayne, PA: CLSI.

Clinical and Laboratory Standards Institute (2021b). *Performance Standards for Antimicrobial Susceptibility Testing*, 28th Edn. Wayne, PA: CLSI.

Krishnaraju, M., Kamatchi, C., Jha, A. K., Devasena, N., Vennila, R., Sumathi, G., et al. (2015). Complete sequencing of an IncX3 plasmid carrying blaNDM-5

allele reveals an early stage in the dissemination of the blaNDM gene. *Indian J. Med. Microbiol.* 33, 30–38. doi: 10.4103/0255-0857.148373

Li, R., Han, Y., Zhou, Y., Du, Z., Wu, H., Wang, J., et al. (2017). Tigecycline susceptibility and molecular resistance mechanisms among clinical *klebsiella pneumoniae* strains isolated during non-tigecycline treatment. *Microb. Drug Resist.* 23, 139–146. doi: 10.1089/mdr.2015.0258

Liang, Z., Pang, J., Hu, X., Nie, T., Lu, X., Li, X., et al. (2021). Low prevalence of mcr-1 among clinical *Enterobacteriaceae* isolates and co-transfer of mcr-1 and bla(NDM-1) from separate donors. *Microb. Drug Resist.* 27, 476–484. doi: 10.1089/mdr.2020.0212

Liu, B. T., and Song, F. J. (2019). Emergence of two *Escherichia coli* strains co-harboring mcr-1 and bla (NDM) in fresh vegetables from China. *Infect. Drug Resist.* 12, 2627–2635. doi: 10.2147/IDR.S211746

Liu, Y. Y., Wang, Y., Walsh, T. R., Yi, L. X., Zhang, R., Spencer, J., et al. (2016). Emergence of plasmid-mediated colistin resistance mechanism MCR-1 in animals and human beings in China: a microbiological and molecular biological study. *Lancet Infect. Dis.* 16, 161–168. doi: 10.1016/S1473-3099(15)00424-7

Magi, G., Tontarelli, F., Caucci, S., Sante, L. D., Brenciani, A., Morroni, G., et al. (2021). High prevalence of carbapenem-resistant *Klebsiella pneumoniae* ST307 recovered from fecal samples in an Italian hospital. *Future Microbiol.* 16, 703–711. doi: 10.2217/fmb-2020-0246

Mao, J., Liu, W., Wang, W., Sun, J., Lei, S., and Feng, Y. (2018). Antibiotic exposure elicits the emergence of colistin- and carbapenem-resistant *Escherichia coli* coharboring MCR-1 and NDM-5 in a patient. *Virulence* 9, 1001–1007. doi: 10.1080/21505594.2018.1486140

Mcconville, T. H., Annavajhala, M. K., Giddins, M. J., Macesic, N., Herrera, C. M., Rozenberg, F. D., et al. (2020). CrrB positively regulates high-level polymyxin resistance and virulence in *Klebsiella pneumoniae*. *Cell Rep.* 33:108313. doi: 10.1016/j.celrep.2020.108313

Partridge, S. R., Kwong, S. M., Firth, N., and Jensen, S. O. (2018). Mobile genetic elements associated with antimicrobial resistance. *Clin. Microbiol. Rev.* 31:e00088-17. doi: 10.1128/CMR.00088-17

Petrosillo, N., Taglietti, F., and Granata, G. (2019). Treatment options for colistin resistant *Klebsiella pneumoniae*: present and future. *J. Clin. Med.* 8:934. doi: 10.3390/jcm8070934

Quan, J., Li, X., Chen, Y., Jiang, Y., Zhou, Z., Zhang, H., et al. (2017). Prevalence of mcr-1 in *Escherichia coli* and *Klebsiella pneumoniae* recovered from bloodstream infections in China: a multicentre longitudinal study. *Lancet Infect. Dis.* 17, 400–410. doi: 10.1016/S1473-3099(16)30528-X

Sun, J., Chen, C., Cui, C., Zhang, Y., Liu, X., Cui, Z., et al. (2019). Plasmid-encoded tet(X) genes that confer high-level tigecycline resistance in *Escherichia coli*. *Nat. Microbiol.* 4, 1457–1464. doi: 10.1038/s41564-019-0496-4

Sun, J., Yang, R., Zhang, Q., Feng, Y., Fang, L., Xia, J., et al. (2016). Co-transfer of blaNDM-5 and mcr-1 by an IncX3–X4 hybrid plasmid in *Escherichia coli*. *Nat. Microbiol.* 1:176. doi: 10.1038/nmicrobiol.2016.176

Tang, Y., Zhou, Y., Meng, C., Huang, Y., and Jiang, X. (2020). Co-occurrence of a novel VIM-1 and FosA3-encoding multidrug-resistant plasmid and a KPC-2-encoding pKP048-like plasmid in a clinical isolate of *Klebsiella pneumoniae* sequence type 11. *Infect. Genet. Evolu.* 85:104479. doi: 10.1016/j.meegid.2020.104479

Tzouvelekis, L. S., Markogiannakis, A., Psichogiou, M., Tassios, P. T., and Daikos, G. L. (2012). Carbapenemases in *Klebsiella pneumoniae* and other *Enterobacteriaceae*: an evolving crisis of global dimensions. *Clin. Microbiol. Rev.* 25, 682–707. doi: 10.1128/CMR.05035-11

Wang, M. G., Yu, Y., Wang, D., Yang, R. S., Jia, L., Cai, D. T., et al. (2021). The emergence and molecular characteristics of new delhi metallo β-lactamase-producing *Escherichia coli* from ducks in guangdong. *China. Front. Microbiol.* 12:677633. doi: 10.3389/fmicb.2021.677633

Wang, R., Liu, Y., Zhang, Q., Jin, L., Wang, Q., Zhang, Y., et al. (2018). The prevalence of colistin resistance in *Escherichia coli* and *Klebsiella pneumoniae* isolated from food animals in China: coexistence of mcr-1 and bla(NDM) with low fitness cost. *Int. J. Antimicrob Agents* 51, 739–744. doi: 10.1016/j.ijantimicag.2018.01.023

Wu, W., Feng, Y., Tang, G., Qiao, F., Mcnally, A., and Zong, Z. (2019). NDM metallo-β-lactamases and their bacterial producers in health care settings. *Clin. Microbiol. Rev.* 32:e00115-18. doi: 10.1128/CMR.00115-18

Xiaomin, S., Yiming, L., Yuying, Y., Zhangqi, S., Yongning, W., and Shaolin, W. (2020). Global impact of mcr-1-positive *Enterobacteriaceae* bacteria on "one health". *Crit. Rev. Microbiol.* 46, 565–577. doi: 10.1080/1040841X.2020.1812510

Xu, J., Zhu, Z., Chen, Y., Wang, W., and He, F. (2021). The plasmid-borne tet(A) gene is an important factor causing tigecycline resistance in ST11 carbapenem-resistant *Klebsiella pneumoniae* under selective pressure. *Front. Microbiol.* 12:644949. doi: 10.3389/fmicb.2021.644949

Yahav, D., Giske, C. G., Grāmatniece, A., Abodakpi, H., Tam, V. H., and Leibovici, L. (2020). New β-lactam-β-lactamase inhibitor combinations. *Clin. Microbiol. Rev.* 34, e115–e120. doi: 10.1128/CMR.00115-20

Yang, R. S., Feng, Y., Lv, X. Y., Duan, J. H., Chen, J., Fang, L. X., et al. (2016). Emergence of NDM-5- and MCR-1-producing *Escherichia coli* clones ST648 and ST156 from a single muscovy duck (cairina moschata). *Antimicrob Agents Chemother.* 60, 6899–6902. doi: 10.1128/AAC.01365-16

Yang, T., Lu, P., and Tseng, S. (2019). Update on fosfomycin-modified genes in *Enterobacteriaceae*. *J. Microbiol. Immunol. Infect.* 52, 9–21. doi: 10.1016/j.jmii.2017.10.006

Yang, Y., Guo, Y., Yin, D., Zheng, Y., Wu, S., Zhu, D., et al. (2020). In vitro activity of cefepime-zidebactam, ceftazidime-avibactam, and other comparators against clinical isolates of *Enterobacter*ales, *Pseudomonas aeruginosa*, and *Acinetobacter baumannii*: results from china antimicrobial surveillance network (CHINET) in 2018. *Antimicrob Agents Chemother.* 65:e01726-20. doi: 10.1128/AAC.01726-20

Yin, D., Dong, D., Li, K., Zhang, L., Liang, J., Yang, Y., et al. (2017). Clonal dissemination of OXA-232 carbapenemase-producing *Klebsiella pneumoniae* in neonates. *Antimicrob Agents Chemother.* 61:e00385-17. doi: 10.1128/AAC.00385-17

Yuan, J., Wang, X., Shi, D., Ge, Q., Song, X., Hu, W., et al. (2021). Extensive antimicrobial resistance and plasmid-carrying resistance genes in mcr-1-positive E. coli sampled in swine, in Guangxi. South China. *BMC Vet. Res.* 17:86. doi: 10.1186/s12917-021-02758-4

Yusuf, E., Bax, H. I., Verkaik, N. J., and van Westreenen, M. (2021). An update on eight "new" antibiotics against multidrug-resistant gram-negative bacteria. *J. Clin. Med.* 10:51068. doi: 10.3390/jcm10051068

Zhanel, G. G., Lawson, C. D., Adam, H., Schweizer, F., Zelenitsky, S., Lagacé-Wiens, P. R., et al. (2013). Ceftazidime-avibactam: a novel cephalosporin/β-lactamase inhibitor combination. *Drugs* 73, 159–177. doi: 10.1007/s40265-013-0013-7

Zheng, J., Lin, Z., Sun, X., Lin, W., Chen, Z., Wu, Y., et al. (2018). Overexpression of OqxAB and MacAB efflux pumps contributes to eravacycline resistance and heteroresistance in clinical isolates of*Klebsiella pneumoniae*. *Emerging Microbes Infect.* 7, 1–11. doi: 10.1038/s41426-018-0141-y

Zhou, Y., Tang, Y., Fu, P., Tian, D., Yu, L., Huang, Y., et al. (2020). The type I-E CRISPR-cas system influences the acquisition of bla KPC-IncF plasmid in *Klebsiella pneumonia*. *Emerging Microbes Infect.* 9, 1011–1022. doi: 10.1080/22221751.2020.1763209

Zurfluh, K., Treier, A., Schmitt, K., and Stephan, R. (2020). Mobile fosfomycin resistance genes in *Enterobacteriaceae*-an increasing threat. *Microbiologyopen* 9:e1135. doi: 10.1002/mbo3.1135

Conflict of Interest: The authors declare that the research was conducted in the absence of any commercial or financial relationships that could be construed as a potential conflict of interest.

Publisher's Note: All claims expressed in this article are solely those of the authors and do not necessarily represent those of their affiliated organizations, or those of the publisher, the editors and the reviewers. Any product that may be evaluated in this article, or claim that may be made by its manufacturer, is not guaranteed or endorsed by the publisher.

frontiers in Microbiology

ORIGINAL RESEARCH
published: 06 January 2022
doi: 10.3389/fmicb.2021.765113

Genomic Characterization of Carbapenem-Non-susceptible *Pseudomonas aeruginosa* Clinical Isolates From Saudi Arabia Revealed a Global Dissemination of GES-5-Producing ST235 and VIM-2-Producing ST233 Sub-Lineages

Michel Doumith[1,2], Sarah Alhassinah[1,2], Abdulrahman Alswaji[1,2], Maha Alzayer[1,2], Essa Alrashidi[1,2], Liliane Okdah[1,2], Sameera Aljohani[1,2,3], NGHA AMR Surveillance Group, Hanan H. Balkhy[4] and Majed F. Alghoribi[1,2,3]**

[1] Infectious Diseases Research Department, King Abdullah International Medical Research Center, Riyadh, Saudi Arabia, [2] King Saud bin Abdulaziz University for Health Sciences, Riyadh, Saudi Arabia, [3] Department of Pathology and Laboratory Medicine, King Abdulaziz Medical City (KAMC), Ministry of National Guard Health Affairs (MNGHA), Riyadh, Saudi Arabia, [4] World Health Organization, Geneva, Switzerland

Carbapenem-resistant *P. aeruginosa* has become a major clinical problem due to limited treatment options. However, studies assessing the trends in the molecular epidemiology and mechanisms of antibiotic resistance in this pathogen are lacking in Saudi Arabia. Here, we reported the genome characterization in a global context of carbapenem non-susceptible clinical isolates from a nationally representative survey. The antibiotic resistance profiles of the isolates (n = 635) collected over 14 months between March 2018 and April 2019 from different geographical regions of Saudi Arabia showed resistance rates to relevant β-lactams, aminoglycosides and quinolones ranging between 6.93 and 27.56%. Overall, 22.52% (143/635) of the isolates exhibited resistance to both imipenem and meropenem that were mainly explained by porin loss and efflux overexpression. However, 18.18% of resistant isolates harbored genes encoding GES (69.23%), VIM (23.07%), NDM (3.85%) or OXA-48-like (3.85%) carbapenemases. Most common GES-positive isolates produced GESs −5, −15 or −1 and all belonged to ST235 whereas the VIM-positive isolates produced mainly VIM-2 and belonged to ST233 or ST257. GES and VIM producers were detected at different sampling periods and in different surveyed regions. Interestingly, a genome-wide comparison revealed that the GES-positive ST235 and VIM-2-positive ST233 genomes sequenced in this study and those available through public databases from various locations worldwide, constituted each a phylogenetically closely related sub-lineage. Profiles of virulence determinants, antimicrobial resistance genes and associated mobile elements confirmed relatedness within each of these two different

OPEN ACCESS

Edited by:
Mullika Traidej Chomnawang, Mahidol University, Thailand

Reviewed by:
Piyatip Khuntayaporn, Mahidol University, Thailand
Rosa Del Campo, Ramón y Cajal Institute for Health Research, Spain

***Correspondence:**
Michel Doumith
doumithmi@ngha.med.sa
Majed F. Alghoribi
alghoribima@ngha.med.sa

Specialty section:
This article was submitted to Antimicrobials, Resistance and Chemotherapy, a section of the journal Frontiers in Microbiology

Received: *26 August 2021*
Accepted: *13 December 2021*
Published: *06 January 2022*

Citation:
Doumith M, Alhassinah S, Alswaji A, Alzayer M, Alrashidi E, Okdah L, Aljohani S, NGHA AMR Surveillance Group, Balkhy HH and Alghoribi MF (2022) Genomic Characterization of Carbapenem-Non-susceptible Pseudomonas aeruginosa Clinical Isolates From Saudi Arabia Revealed a Global Dissemination of GES-5-Producing ST235 and VIM-2-Producing ST233 Sub-Lineages. Front. Microbiol. 12:765113. doi: 10.3389/fmicb.2021.765113

sub-lineages. Sequence analysis located the bla_{GES} gene in nearly all studied genomes (95.4%) in the same integrative conjugative element that also harbored the *acc(6′)-Ib*, *aph(3′)-XV*, *aadA6*, *sul1*, *tet(G),* and *catB* resistance genes while bla_{VIM-2} in most (98.89%) ST233-positive genomes was co-located with *aac(6′)-I1*, *dfrB-5,* and *aac(3′)-Id* in the same class I integron. The study findings revealed the global spread of GES-5 ST235 and VIM-2 ST233 sub-lineages and highlighted the importance of routine detection of rare β-lactamases.

Keywords: high-risk clones, multidrug resistance, resistome, mobile element, β-lactamase, epidemiology

INTRODUCTION

P. aeruginosa is a major cause of healthcare associated infections and a serious public health threat due to its ability to resist antibiotics (Gellatly and Hancock, 2013). *P. aeruginosa* is genetically equipped with an outstanding intrinsic antibiotic resistance machinery and is adept at acquiring antibiotic resistance determinants (Lister et al., 2009; López-Causapé et al., 2018). Resistance to carbapenems in the species is due primarily to chromosomal modifications that inactivate or down-regulate the carbapenem-specific OprD porin or modify the expression levels of efflux systems and in particular the MexAB-OprM pump (López-Causapé et al., 2018). In recent years, this pathogen has been increasingly reported as a carrier of acquired carbapenemases and in particular those belonging to the VIM, IMP and GES families (Yoon and Jeong, 2021). *P. aeruginosa* has a non-clonal structure, nonetheless high-risk clones including sequence type (ST)235, ST111, ST233, ST244, ST357, ST308, ST175, ST277, ST654, and ST298 are widespread and frequently associated with outbreaks (Oliver et al., 2015; Miyoshi-Akiyama et al., 2017; del Barrio-Tofiño et al., 2020; Kocsis et al., 2021). ST235 is certainly the most relevant high-risk clone, showing a worldwide dissemination and an association with various β-lactamases, including GES, IMP, KPC, OXA-48, and VIM carbapenemases (Treepong et al., 2018; del Barrio-Tofiño et al., 2020). Other high-risk clones such as ST233, ST357, and ST111 have been also associated with acquired carbapenemases, notably the metallo-β-lactamase VIM, IMP, and NDM types (del Barrio-Tofiño et al., 2020). Using whole genome sequencing, we investigated the mechanisms of resistance to antibiotics in *P. aeruginosa* clinical isolates collected as part of a nationally representative survey from Saudi Arabia and contextualized against a global collection. In addition to porin impairment and overexpression of efflux, sequence analyses showed that resistance to carbapenems was partly due to the clonal spread of GES-5-producing ST235 and VIM-2-producing ST233 sub-lineages. More importantly, a genome-wide comparison revealed that these two sub-lineages were disseminated worldwide.

MATERIALS AND METHODS

Isolates and Phenotypic Characterization

P. aeruginosa isolates (n = 635) were collected between March-2018 and April-2019 as part of an antimicrobial resistance surveillance program that was initiated in 2018 by the Infectious Diseases Research Department (IDRD) at the National Guard Health Affairs (NGHA) to monitor the prevalence and trends of resistance in a variety of clinically important pathogens. The program involves the monthly collection of the first 10–30 non-duplicate consecutive isolates of each surveyed bacteria identified in the laboratories of NGHA medical cities located in Riyadh, Jeddah, Al Madinah, Dammam and Al Ahsa. The collection included in this study comprised 162 isolates referred from King Abdulaziz Medical City—Riyadh (Centre—Riyadh province, 1,500 bed facility), 275 from King Abdulaziz Medical City—Jeddah (West—Makkah province, 750 bed), 67 from Prince Mohammed Bin Abdul Aziz Hospital—Al Madinah (West—Al Madinah province, 215 bed), 86 from King Abdulaziz Hospital—Al Ahsa (East—Eastern province, 300 bed) and 45 from Imam Abdulrahman Al Faisal Hospital—Dammam (East—Eastern Province, 100 bed). Isolates were recovered from urine (208/635, 32.8%), respiratory (204/635, 32.1%), blood (101/635, 15.9%), wound (67/635, 10.6%) and other specimens (55/635, 8.7%); they were referred at an overall average of 45 (range 19–80) isolates per month (**Table 1**). Species identification and antimicrobial susceptibility testing were determined with the VITEK II system. Minimum inhibitory concentrations (MICs) of colistin were confirmed using the micro-broth dilution method. MICs were interpreted according to CLSI breakpoints.

Species Confirmation and β-Lactamase Screening

Species identity of the isolates was confirmed with a PCR targeting the species-specific *oprL* gene. Presence of genes encoding IMP, GES, KPC, NDM, OXA-48-like, VIM, BEL, PER, and VEB β-lactamases were screened by PCR using the primers described in **Supplementary Table 1**.

Whole Genome Sequencing and Bioinformatics

Genomic DNA from all isolates (n = 45) was extracted with the MagnaPure compact system (Roche, Switzerland) and prepared for sequencing with the Nextera XT DNA library preparation kit (Illumina, United Kingdom) according to the manufacturer's instructions. Sequencing was performed on the Miseq instrument using the 2 × 300 paired-end protocol. Of these, nine isolates were further sequenced on the Oxford Nanopore MinION using the ligation sequencing kit according to

TABLE 1 | Resistance rates to clinically relevant antibiotics among collected isolates.

Regions		Central	Western		Eastern		
City		Riyadh	Jeddah	Al Madinah	Al Ahsa	Dammam	Total
Isolates		162	275	67	86	45	635
Antibiotics	IMI	35.80	28.00	20.90	23.26	13.33	27.56
	MEM	33.95	21.45	20.90	19.77	6.67	23.31
	IMI and MEM	33.33	20.00	20.90	19.77	6.67	22.52
	IMI or MEM	36.42	29.45	20.90	23.26	13.33	28.35
	CAZ	19.14	13.45	11.94	12.79	6.67	14.17
	FEB	10.49	6.90	8.96	11.90	4.44	8.53
	PIP/TAZ	33.75	6.79	19.40	15.29	4.65	16.33
	AMK	9.26	6.18	11.94	2.33	4.44	6.93
	GM	10.49	7.66	13.43	2.35	4.44	8.06
	TOB	10.56	7.14	15.15	0.00	0.00	7.61
	CIP	19.75	16.73	20.90	10.47	4.44	16.22
	CST	2.53	4.52	9.09	1.23	0.00	3.83

Breakpoints amikacin (AMK) ≥ 64 mg/L; cefepime (FEB) ≥ 32 mg/L; ceftazidime (CAZ) ≥ 32 mg/L; ciprofloxacin (CIP) ≥ 2 mg/L; colistin (COL) ≥ 4 mg/L; piperacillin/tazobactam (PIP/TAZ) ≥ 128/4 mg/L; imipenem (IMI) and meropenem (MER) ≥ 8 mg/L; tobramycin (TOB) and gentamicin (GEN) ≥ 16 mg/L.

the manufacturer's instructions (Oxford Nanopore Technologies, United Kingdom). Genome assemblies using the Illumina reads alone or in combination with the Nanopore long-reads were generated using Unicycler 0.4.8 (Wick et al., 2017). Multilocus sequence type (MLST) was determined *in silico* using the mlst-v2.18.1 software. Genes, mutations associated with antimicrobial resistance, and virulence factors were detected with Abricate 0.9.8[1] or Genefinder.[2] In order to put the analysis into an international context, all *P. aeruginosa* paired-end Illumina sequenced genomes (n = 16,337) deposited before December 2020 in the NCBI sequence read archive database[3] were retrieved and the quality of corresponding reads was assessed with the FastQC software. Relatedness of recovered genomes with read coverage above 20x and those generated in this study was inferred using a single nucleotide polymorphisms (SNPs)-based approach by mapping reads against the publically available sequences of strain PAO1 (NC_002516) or the fully closed genome of strain ST235-MPA32 generated in this study. SNPs were first identified with Snippy 4.4.5[4] to create a full core genome alignment that was latter checked for recombination events using Gubbins 2.4.1 (Croucher et al., 2015). Filtered alignments were then used to construct the phylogenetic trees using RaXML with the default option of Gubbins. Phylogenetic trees were annotated using iTOL v6 and Microreact tools (Argimón et al., 2016; Letunic and Bork, 2021). SNP locations were determined using the annotated genome of the reference strain PAO1 (AE004091.2). Genome assemblies were annotated with prokka 1.14.6 and their gene contents were compared with Roary (Page et al., 2015). The integrative and conjugative elements (ICE) and direct environments of carbapenemases and extended-spectrum β-lactamases in fully closed genomes was determined manually. Presence of these elements in each sequenced genome was later determined by checking the depth of coverage of reads mapped across the full sequence of each mobile element.

[1]https://github.com/tseemann/abricate

[2]https://github.com/phe-bioinformatics/gene_finder

[3]https://www.ncbi.nlm.nih.gov/sra

[4]https://github.com/tseemann/snippy

RESULTS

Isolates and Phenotypic Testing

P. aeruginosa clinical isolates were referred over a 14-month period from five hospitals located in the eastern, western and central regions of Saudi Arabia. Susceptibility testing showed that 143/635 (22.52%) isolates were resistant to both imipenem and meropenem (MIC ≥ 8 mg/L) (**Table 1**). Otherwise, the isolates were variably resistant to ciprofloxacin (16.22%, range 4.44–20.90%), ceftazidime (14.17%, range 6.67–19.14%), cefepime (8.53%, 4.44–11.90%), piperacillin/tazobactam (16.33%, range 4.65–33.75%), amikacin (6.93%, range 2.33–11.94%), gentamicin (8.06%, range 2.35–13.43%) and tobramycin (7.61%, range 0–15.15%) but remained highly sensitive to colistin (96.17%, range 90.91–100%) (**Table 1**). Resistance to carbapenems was highest in respiratory isolates (40.69%) followed by blood (27.72%), urine (12.02%) then wound (8.96%) swab isolates. Extensively drug-resistant isolates, remaining only sensitive to colistin, accounted for 3.78% (24/635) of all isolates and were predominantly obtained from respiratory specimens (14/24, 58.33%). Regional and individual hospital variations in susceptibility patterns and frequencies were observed for most tested antibiotics (**Table 1**). Characteristically, hospitals hosting critical patients (i.e., Jeddah and Riyadh) experienced the highest levels of resistance across all tested antibiotics.

Screening for β-Lactamase Genes in Carbapenem-Resistant Isolates

PCR screening detected genes encoding GES (n = 18), VIM (n = 6), NDM (n = 1), and OXA-48-like (n = 1) β-lactamases, explaining resistance to imipenem and meropenem in 18.18%

(26/143) of carbapenem-resistant isolates. Genes encoding VEB ($n = 6$) and PER ($n = 2$) extended-spectrum β-lactamases (ESBLs) were detected in only eight isolates, including three of the six VIM-positive isolates. Most common GES- and VIM-positive isolates were referred from all regions at different sampling periods (i.e., 11 out of 14 sampling months) of the survey.

Genomic Characterization of Carbapenem-Resistant Isolates

To further investigate the molecular mechanisms of resistance to carbapenems, all carbapenemase and ESBL producers identified by PCR ($n = 31$) and a set of randomly selected isolates exhibiting resistance to imipenem and meropenem but with no acquired β-lactamases ($n = 14$) were whole genome sequenced on the Illumina Miseq system.

GES-Carbapenemase Positive Isolates

Sequence analyses showed that all genomes carrying genes encoding GES type β-lactamases, including GESs -5 ($n = 16$), −15 ($n = 1$) and −1 ($n = 1$), belonged to ST235. The later accounted for 5.03% (822/16,337) of all genomes retrieved from the public databases, and of which, the majority (71.29%, 586/822) carried genes encoding acquired carbapenemases, including IMP alone ($n = 264$) or in combination with NDM ($n = 1$) or OXA-48-like ($n = 1$), VIM alone ($n = 133$) or in combination with OXA-48-like ($n = 3$), GES ($n = 174$), KPC ($n = 9$), and OXA-48-like ($n = 1$) (**Table 2**). Full genome SNP-based phylogeny against the *P. aeruginosa* strain PAO1 reference genome grouped nearly all published GES-positive ST235 genomes and those generated in this study in a distinct cluster with the exception of three GES-20 producers which grouped apart (**Figure 1**). In contrast, the two other common VIM and IMP carbapenemases were distributed across multiple clusters suggesting that they were acquired through multiple events. The phylogenetic tree constructed based on SNP calls relative to the fully closed ST235 MPA32-genome confirmed the clustering of the GES-positive genomes in a well distinct clade (**Figure 2**). Clustered GES-positive genomes originated from at least six different countries, including Australia, China, Germany, Japan, Indonesia and Pakistan (**Figure 1**). Phylogeny showed that these producers were related to each other, with at most 120 SNPs to distinguish between them. More specifically, the GES-positive genomes ($n = 18$) from this study clustered tightly with others from Germany ($n = 26$) in a distinct subgroup with at most 45 SNPs to distinguish them from each other. GES-positive genomes were separated from the remaining ST235 genomes by at least 29 SNPs, of which, 14 were non-synonymous in genes classified as transcriptional regulators, metabolic genes and hypothetical proteins whereas four were located in the promoter or potential regulatory regions of genes encoding the porin OprO, global transcriptional regulator IscR or hypothetical proteins (**Supplementary Table 2**). Of these, only IscR has been shown to regulate genes involved in iron homeostasis, resistance to oxidants and pathogenicity (Romsang et al., 2014; Saninjuk et al., 2019). Comparison of the gene contents of ST235 genomes identified 4,373 core and 1,086 soft-core genes that were shared among 98.94–100% and 94.87–98.94% of genomes studied, respectively. Other 25,228 genes were found to be present within one to a maximum of 536 genomes (i.e., < 94.87%) thus showing a relatively wide genetic variability in the accessory genome of this ST. Overall there were a very limited number of genes ($n = 27$) which presence or absence distinguished the GES-positive cluster from the remaining ST235 but these mainly encoded phage or hypothetical proteins. Only one gene showing homology to the transcriptional repressor NrdR lacked in all GES producers but was present in the majority of remaining ST235 genomes. The latter, shown to regulate the ribonucleotide synthesis may grant the adaptability to thrive in different environments (Crespo et al., 2015). Otherwise, the presence of genomic features encoding the virulence factors gathered in the virulence factor database (VFDB) were comparable across all ST235 genomes. The majority of the genes and gene clusters previously shown to be involved in the species virulence were identified in nearly all (i.e., 98–100%) ST235 genomes with the exception of *wzz* and *wzy* genes that are involved in the B-band lipopolysaccharide O antigen synthesis and the pyoverdine outer membrane receptor *fpvA*. In accordance with previous studies, all ST235 genomes including those carrying bla_{GES} carried the ExoU toxin-encoding gene (Sato et al., 2003; Treepong et al., 2018).

Sequence examination of the fully reconstructed genomes of two GES-5 producers co-located the β-lactamase gene with *acc(6′)-Ib*, *aph(3′)-XV*, *aadA6*, *florR*, *sul1, tetG,* and *catB* genes in a type I integron that was embedded in a 95 kb integrative conjugative elements (ICE) inserted in the chromosome downstream the tRNA-Gly gene (**Figure 3**). Mapping of the short reads to the full sequence of this element confirmed its presence in nearly all publically available (166/174, 95.4%) and newly sequenced (18/18, 100%) GES-positive genomes. Of the remaining, five (5/174, 2.87%) genomes carrying bla_{GES-1} ($n = 1$) and bla_{GES-5} ($n = 4$) lacked the region located between position ∼65.1 and ∼72.1 kb and comprising the *floR* and *tetG* genes whereas the three genome carrying bla_{GES-20} (3/174, 1.73%) and clustering apart had the entire element missing (**Figure 3**). One GES-negative isolate (i.e., RPA66) sequenced in this study belonged to ST235 clustered also away, thus confirming the relatedness of the GES-producing ST235 isolates (**Supplementary Tables 3**, **4**).

VIM-Carbapenemase Positive Isolates

Sequence analysis showed that the majority of VIM-positive genomes (5/6, 83.3%) carried bla_{VIM-2} and belonged to ST233 ($n = 3$) or ST357 ($n = 2$). The remaining isolate (1/6, 16.7%) harbored bla_{VIM-28} and belonged to ST111. Isolates carrying bla_{VIM-2} were from three hospitals located in the three different regions included in the study (**Supplementary Table 3**). Here also, nearly all published ST233 genomes (90/94, 95.74%), which originated from at least four different countries, including Germany, Japan, Spain and United States, harbored bla_{VIM-2} and were highly related with at most 47 SNPs to distinguish them from each other. Isolates from this study clustered in two sub groups according to their geographical origins, nevertheless with 29 SNPs to distinguish them from each other (**Figure 4**). Sequence analysis located the bla_{VIM-2} of all newly sequenced

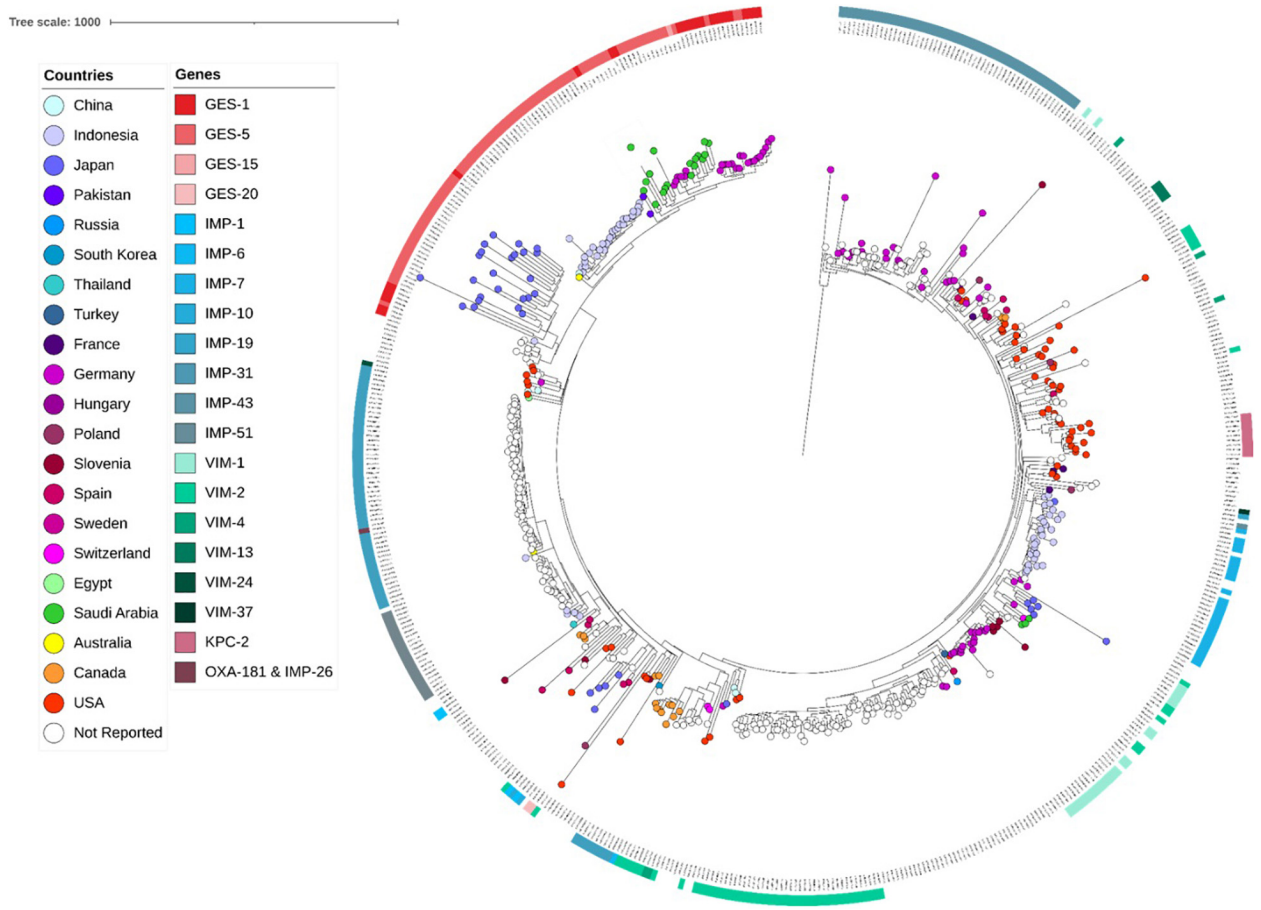

FIGURE 1 | Core genome SNP-based maximum likelihood phylogeny of ST235 genomes retrieved from the public domain and those generated in this study using the genome sequences of strain PAO1 as reference.

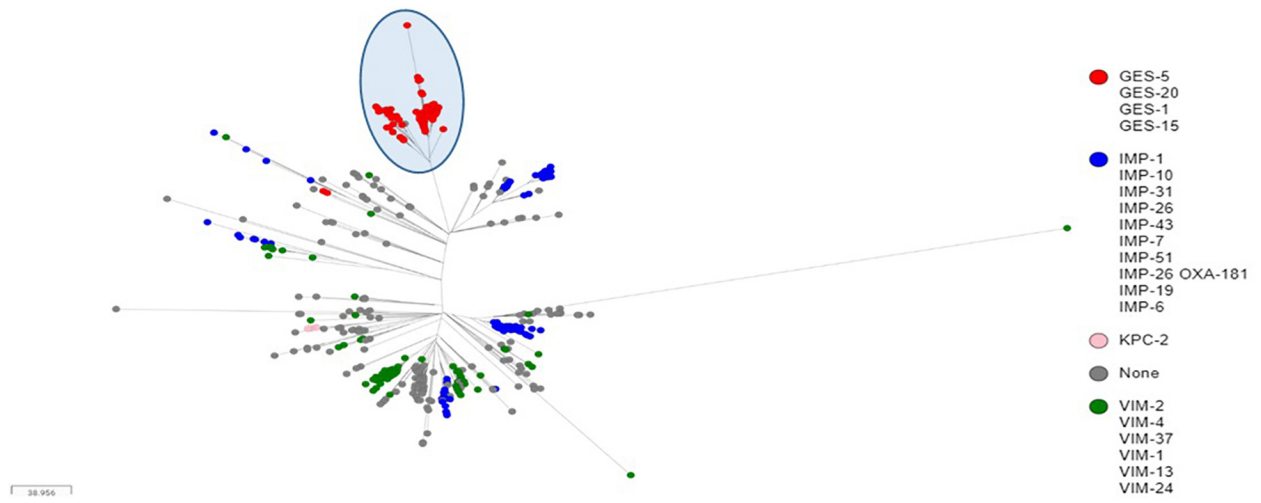

FIGURE 2 | Core genome SNP-based maximum likelihood phylogeny of ST235 genomes retrieved from the public domain and those generated in this study using the MPA32 closed genome as reference. The cluster of GES-positive ST235 genomes were highlighted in a blue circle.

TABLE 2 | Distribution of carbapenemase-encoding genes among publically available genomes belonging to the major carbapenemase-positive STs identified in isolates from this study.

ST	β-lactamase type	β-lactamase variant	Nb
ST233 (*n* = 94)	VIM	VIM-2	90
	None		4
ST235 (*n* = 822)	IMP (*n* = 264)	IMP-1	5
		IMP-6	1
		IMP-7	25
		IMP-10	2
		IMP-14	1
		IMP-19	1
		IMP-26	114
		IMP-31	63
		IMP-43	1
		IMP-51	51
	VIM (*n* = 133)	VIM-1	33
		VIM-2	87
		VIM-4	7
		VIM-13	4
		VIM-24	1
		VIM-27	1
	GES (*n* = 174)	GES-1	28
		GES-5	142
		GES-15	1
		GES-20	3
	KPC	KPC-2	9
	OXA-48-like	OXA-232	1
	VIM and OXA	VIM-2 OXA-232	3
	IMP and NDM	IMP-51 NDM-1	1
	IMP and OXA	IMP-26 OXA-181	1
	None		236
ST244 (*n* = 254)	VIM (*n* = 14)	VIM-2	13
		VIM-6	1
	IMP (*n* = 4)	IMP-34	1
		IMP-39	3
	KPC	KPC-2	2
	OXA-48-like	OXA-181	2
	None		232
ST357 (*n* = 229)	IMP (*n* = 46)	IMP-7	42
		IMP-13	2
		IMP-15	1
		IMP-16	1
	NDM	NDM-1	21
	KPC	KPC-2	1
	OXA-48-like	OXA-181	1
	VIM (*n* = 12)	VIM-2	8
		VIM-5	3
		VIM-18	1
	None		148
ST773 (*n* = 23)	VIM	VIM-2	4
	NDM	NDM-1	8
	None		11

ST233 isolates in a 4.4 kb class I integron comprising *aac(6′)-I1*, *dfrB-5,* and *aac(3′)-Id* resistance genes (100% identity, accession number AY943084.1), and which, in turn, was embedded in a transposon similar to those found in published *P. aeruginosa* genomes (e.g., CP056774.1 from nucleotide positions 5,258,523–5,270,622) (**Figure 5**). Screening of publically available bla_{VIM-2}-positive ST233 genomes showed that nearly all (89/90, 98.89%) had reads covering the entire 4.4 kb integron cassette and of which the majority (72/90, 80%) had also reads covering more than 95% of the entire 12 kb transposon. On the other hand, only a handful of publically available ST357 genomes harbored the bla_{VIM-2} (8/229, 3.49%) and had mainly IMP carbapenemases (46/229, 20.09%) and in particular the IMP-7 variant (42/46, 95.45%). The bla_{VIM-2} of newly sequenced ST357 genomes was detected in an integron type I mobile element embedded in a complex transposon containing all the resistance genes identified in this isolate (**Figure 5**). In contrast, the bla_{VIM-28} in the ST111 isolate was located on a 350 kb plasmid in a integron type I in association with *aac(6′)-I*.

Other Carbapenemase-Positive Isolates

Of the remaining carbapenemase-positive isolates, one carried $bla_{OXA-232}$ and belonged to ST244 while one had bla_{NDM-1} and belonged to ST773. Genome assemblies located the $bla_{OXA-232}$ gene on a 6.1 kb ColKP3-type non-conjugative plasmid similar to previously published plasmid pColKP3 (accession number CP036323). Otherwise, the bla_{NDM-1} was co-located with *floR2*, *rmtB*, *sul1,* and *tet(G)* in an ICE element of approximately ∼117 kb that was highly similar to the clc-like ICE recently identified in *P. aeruginosa* (accession number MK497171) (**Figure 3**).

Molecular Mechanisms of Resistance

β-Lactams

In addition to the acquisition of carbapenemases, sequence analysis identified alterations in the outer membrane protein OprD leading to function loss in the majority (82.22%, 37/45) of sequenced genomes. Porin alterations included large deletions at the beginning or end of the coding region (*n* = 11) and frameshifts produced by small insertions or deletions creating premature translational termination at various positions (*n* = 26) (**Supplementary Table 4**). Genes encoding the MexAB-OprM efflux system were highly conserved across all sequenced isolates. However, inactivation of either MexR (*n* = 4), NalC (*n* = 1), or NalD (*n* = 9), previously shown to up-regulate the expression of this efflux pump, was identified in nearly third (14/45, 31.1%) of sequenced isolates and mainly in the non-carbapenemase producers (9/14, 64.3%) (**Supplementary Tables 3**, **4**). Inactivation of these regulators was due to various insertions, deletions, or substitutions resulting in frameshift of the reading frame, and creating premature stop codons (**Supplementary Tables 3**, **4**). Overall, the acquisition of carbapenemase genes with porin inactivation and efflux upregulation explained resistance to imipenem and meropenem in all sequenced genomes. Carbapenemase-producing isolates (*n* = 26) were resistant to all tested non-carbapenem β-lactams

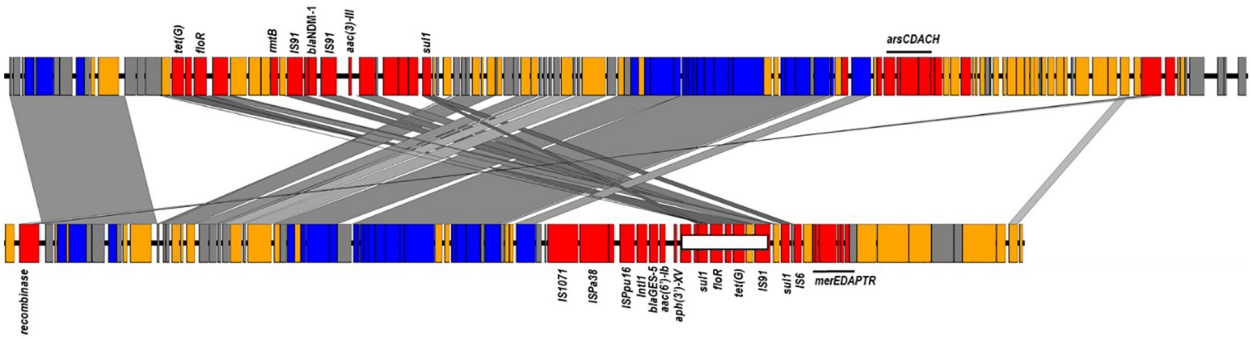

FIGURE 3 | ICEs harboring bla$_{NDM-1}$ and bla$_{GES-5}$ identified in ST773 and ST235 sequenced genomes. Colors showed in red genes encoding antimicrobial and heavy metal resistance, insertion sequences and transposon-related genes; blue, transfer and conjugative functions; yellow, other known functions and gray, hypothetical proteins. The region carrying the floR and tetG genes missing in some genomes were shown in a white box.

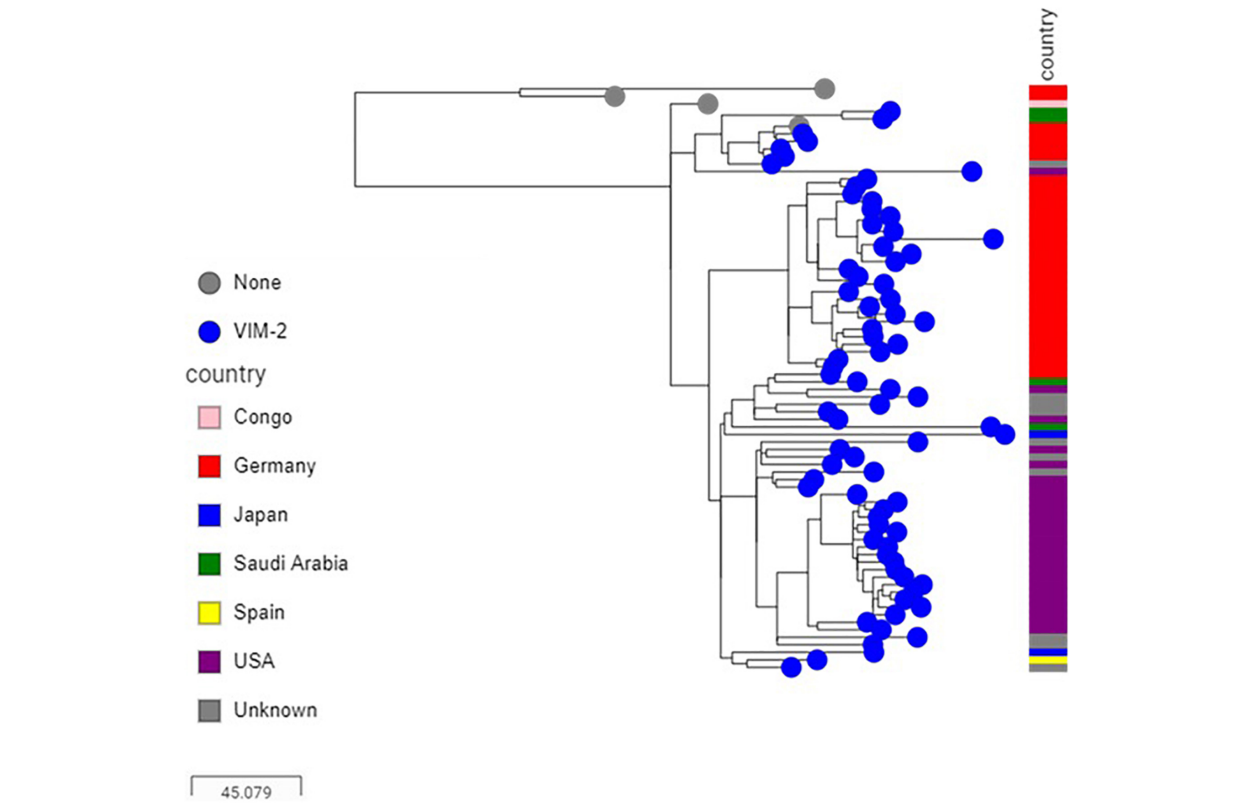

FIGURE 4 | Core genome SNP-based maximum likelihood phylogeny of ST233 genomes retrieved from the public domain and those generated in this study using the genome sequence of strain PAO1 as reference.

(i.e., piperacillin/tazobactam, cefipime, and ceftazidime) with the exception of those producing GES-5, which remained in majority (10/18, 55.56%) sensitive or intermediately resistant to ceftazidime (MIC 16 mg/L) and cefepime (MIC 8–16 mg/L). Resistance in some of these producers suggested an overexpression of the chromosomal AmpC but none had mutations in the coding sequences of AmpR, AmpRh1, AmpRh2, AmpD, PBPs, and GalU or in the *ampR-ampC* intergenic region to explain resistance. Of the remaining non-carbapenemase producers (n = 20), only six were resistant to ceftazidime (MIC $\geq$ 64 mg/L) and harbored GES-1 (n = 1), VEB (n = 4), or PER (n = 1) ESBL variants (**Supplementary Tables 3**, **4**).

Other Antibiotics

Scanning genome sequences identified alterations in GyrA (T83I/T83A and D87Y) and ParC (S87L) in all isolates (33/45, 73.33%) showing high level of resistance to ciprofloxacin (MIC $\geq$ 4 mg/L). Only three of the seven isolates exhibiting

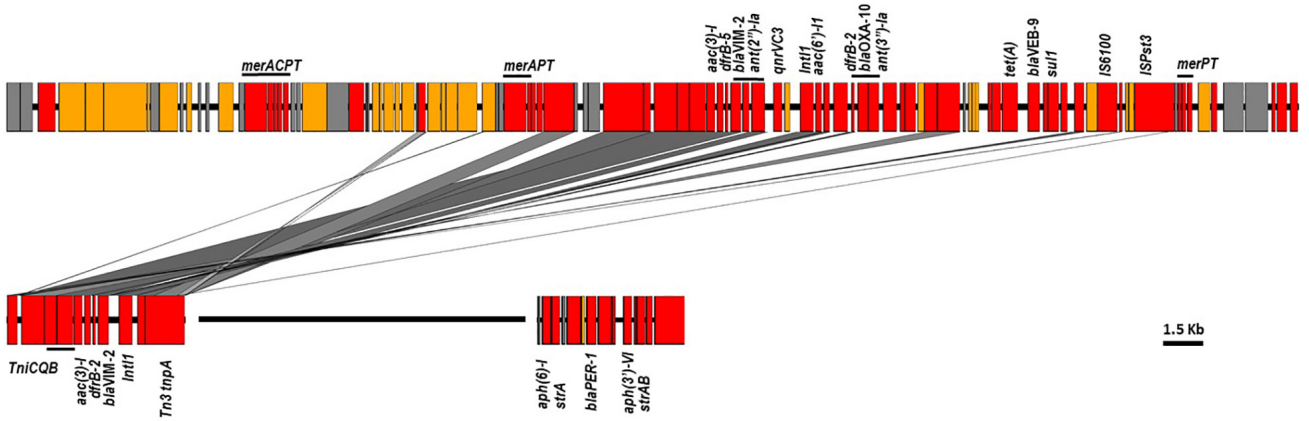

FIGURE 5 | The bla_{VIM-2}, bla_{VEB-9}, and bla_{PER-1} environments in ST357 (top) and ST233 (bottom) sequenced genomes. Colors showed in red genes encoding antimicrobial and heavy metal resistance, insertion sequences and transposon-related genes; blue, transfer and conjugative functions; yellow, other known functions and gray, hypothetical proteins.

low levels of resistance (MIC 1–2 mg/L) carried the plasmid-encoded ciprofloxacin resistance determinant *crpP* or had the MexAB-OprM efflux pump overexpressed (**Supplementary Tables 3**, **4**). However, the presence of *crpP* was detected in nearly half of the isolates (22/45, 48.89%) including in two sensitive isolates (MIC $\leq$ 0.25 mg/L). Resistance to all three tested aminoglycosides was associated in the majority of cases (n = 18) with the presence of the aminoglycoside-modifying enzyme Aac(6′)-Ib-cr and overexpression of the MexXY-OprM efflux system due to inactivation of its repressor MexZ by a deletion of 11 nucleotides creating a translational frameshift at position 290. Presence of the acquired *aac(6′)-I*, *aac(3′)-I*, *ant(2″)-Ia,* or the 16S rRNA methyltransferase *rmtB* genes explained resistance in 11 isolates while one isolate carried *acc(3′)-I* and had the MexXY-OprM overexpressed due to inactivation of MexZ by a substitution creating a premature stop codon at position 162 (**Supplementary Tables 3**, **4**). Resistance in three isolates did not correlate with the genomic data. Otherwise, the borderline resistance to colistin (MIC 4 mg/L) in few isolates (n = 6) were not associated with any mutations in the PmrA/PmrB or PhoP/PhoQ two-component systems (**Supplementary Tables 3**, **4**).

DISCUSSION

Susceptibility testing of *P. aeruginosa* clinical isolates from a large, nationally representative collection of Saudi Arabia showed an overall resistance rates to relevant aminoglycosides, quinolones, and β-lactams ranging from 6.93 to 27.56%. Resistance to either imipenem or meropenem varied greatly among recruited hospitals (28.35%, range 13.33–36.42%) with the highest levels of resistance observed in central region (i.e., Riyadh tertiary hospital). Sequence analysis identified loss of porin OprD and efflux overexpression at the origin of resistance in the majority (i.e., 81.56%) of sequenced isolates. Of the four efflux systems of the resistance nodulation division (RND) family, MexAB-OprM, MexEF-OprN, MexCD-OprJ, and MexXY-OprM that are known to contribute to antimicrobial resistance in the species, sequence analyses suggested that overexpression of the MexAB-OprM efflux, mainly through inactivation of its regulatory genes, constitute the main system acting synergistically with low outer membrane permeability to confer intrinsic multi-drug resistance (Poole et al., 1993, 1996; Köhler et al., 1997; Mine et al., 1999). More importantly, resistance to carbapenems was partly (i.e., 18.18%) associated with the acquisition of acquired carbapenemases, notably those encoding the GES and VIM type enzymes. GES-5 producers, which all belonged to ST235, were by far the most dominant among resistant isolates carrying acquired carbapenemases; they were also widespread, being identified in all regions surveyed during the study period. A previous study suggested that the ST235 lineage emerged in Europe but have since evolved globally and acquired locally diverse antimicrobial resistance determinants (Abril et al., 2019). The genome-wide sequence analysis identified a high genomic diversity among ST235 isolates and confirmed local acquisitions of carbapenemase-encoding genes. However, the GES-positive ST235 genomes sequenced in this study and all those publically available were similar and belonged to the same phylogenetic group. Moreover, the GES-encoding genes in nearly all these genomes (95.4%) was located in an identical ICE, thus supporting the early acquisition of the β-lactamase gene in this sub-lineage. The association of this ST with various β-lactamases has been in part linked to the presence of type IV secretion systems promoting foreign DNA capture, leading to the insertion of genetic element as transposon, integron, or genomic islands harboring resistance genes (Miyoshi-Akiyama et al., 2017; Treepong et al., 2018). Gene by gene comparisons identified only one gene showing homology to the regulator of deoxyribonucleotide reduction NdrD that was missing in the GES-positive genomes but present in the majority of remaining genomes. However, the significance of the absence of this gene need to be further investigated. Similar findings were also observed for the VIM-2-positive ST233 isolates where genome comparisons revealed that sequenced genomes and those

publically available were phylogenetically similar to each other. In contrast to ST235, nearly all ST233 genomes (90/94, 95.75%) in the public domain carried the VIM-2-encoding gene. Here also the environment of the β-lactamase gene, which was co-located in the same class I integron in all genomes, supported an ancestral acquisition and subsequent spreading, rather than multiple acquisition events.

The molecular basis of extended-spectrum β-lactamase (ESBL) and carbapenemase production in *P. aeruginosa* isolated from Saudi Arabia was reported in a limited number of studies but none has been based on whole-genome sequencing. Overall, these reports indicated that VIM-type enzymes were the most prevalent metallo-β-lactamase in isolates from the Kingdom (Al-Agamy et al., 2009; Shaaban et al., 2018). Detection of genes encoding the VIM-2 variant in ST233 isolates has been reported in several countries worldwide, including in a handful of isolates from Saudi Arabia and neighboring Bahrain and Egypt (Zafer et al., 2015; Zowawi et al., 2018). A recent study reported the identification of VIM-2 in isolates belonging to ST654 and GES in ST235 isolates from one hospital located in the western region (Al-Zahrani and Al-Ahmadi, 2021). Although VEB-like enzymes were the most common reported ESBLs in *P. aeruginosa* isolates from Saudi Arabia, few studies reported the detection of GES encoding genes in isolates from the Kingdom (Al-Agamy et al., 2012, 2016; Tawfik et al., 2012).

Overall, the study findings clearly showed a worldwide dissemination of the GES-5-producing ST235 and VIM-2-producing ST233 sub-lineages. Moreover, a recent study reporting the spread of ST235 isolates producing GES-type enzymes across multiple regions in Japan, confirmed the potential of these lineages to disseminate broadly (Hishinuma et al., 2018). The study results also emphasize the fact that the spread of strains producing rare carbapenemases, such as GES-type enzymes, could be underestimated because the genes encoding these β-lactamases are outside the scope of all commercially available assays that are mainly focused on the detection of most common NDM, VIM, OXA-48-like, KPC and IMP carbapenemase genes, and thus highlighting the importance of screening for these β -lactamases.

DATA AVAILABILITY STATEMENT

The datasets presented in this study can be found in online repositories. The names of the repository/repositories and accession number(s) can be found below: https://www.ncbi.nlm.nih.gov/bioproject/PRJNA751257.

AUTHOR CONTRIBUTIONS

MD, HB, SAJ, LO, and MFA contributed to the design of the study. The NGHA antimicrobial surveillance group collected the samples on a monthly basis. EA led the initial laboratory processing of the samples. SAH performed the β-lactamase screening by PCR. MAZ, SAH, and LO performed the genome sequencing. MD and AA performed the genomic data analysis. MD led the writing and revision of the manuscript. All authors commented and contributed on the final version of the manuscript.

FUNDING

This work was supported by the KAIMRC research funds under grant RC19/095/R.

ACKNOWLEDGMENTS

The research team would like to thank NGHA hospitals in Riyadh, Jeddah, Al Madinah, Al Ahsa, and Dammam for supporting the collection of isolates.

NGHA AMR SURVEILLANCE GROUP

Majed F. Alghoribi, Liliane Okdah, Essa Alrashidi, Alhanouf Alshahrani, Sameera Aljohani, Bassam Alalwan, Abdulfattah Al-Amri, Mai M. Kaaki, Mohamed Doud, Haitham S. Dadah, Fahad Alnashmy, and Michel Doumith.

SUPPLEMENTARY MATERIAL

The Supplementary Material for this article can be found online at: https://www.frontiersin.org/articles/10.3389/fmicb.2021.765113/full#supplementary-material

REFERENCES

Abril, D., Marquez-Ortiz, R. A., Castro-Cardozo, B., Moncayo-Ortiz, J. I., Olarte Escobar, N. M., Corredor Rozo, Z. L., et al. (2019). Genome plasticity favours double chromosomal Tn4401b-blaKPC-2 transposon insertion in the *Pseudomonas aeruginosa* ST235 clone. *BMC Microbiol.* 19:45. doi: 10.1186/s12866-019-1418-6

Al-Agamy, M. H., Jeannot, K., El-Mahdy, T. S., Samaha, H. A., Shibl, A. M., Plésiat, P., et al. (2016). Diversity of Molecular Mechanisms Conferring Carbapenem Resistance to *Pseudomonas aeruginosa* Isolates from Saudi Arabia. *Can. J. Infect. Dis. Med. Microbiol.* 2016:4379686. doi: 10.1155/2016/4379686

Al-Agamy, M. H., Shibl, A. M., Tawfik, A. F., Elkhizzi, N. A., and Livermore, D. M. (2012). Extended-spectrum and metallo-beta-lactamases among ceftazidime-resistant *Pseudomonas aeruginosa* in Riyadh, Saudi Arabia. *J. Chemother.* 24, 97–100. doi: 10.1179/1120009X12Z.00000000015

Al-Agamy, M. H. M., Shibl, A. M., Tawfik, A. F., and Radwan, H. H. (2009). High prevalence of metallo-beta-lactamase-producing *Pseudomonas aeruginosa* from Saudi Arabia. *J. Chemother.* 21, 461–462. doi: 10.1179/joc.2009.21.4.461

Al-Zahrani, I. A., and Al-Ahmadi, B. M. (2021). Dissemination of VIM-producing *Pseudomonas aeruginosa* associated with high-risk clone ST654 in a tertiary and quaternary hospital in Makkah, Saudi Arabia. *J. Chemother.* 33, 12–20. doi: 10.1080/1120009X.2020.1785741

Argimón, S., Abudahab, K., Goater, R. J. E., Fedosejev, A., Bhai, J., Glasner, C., et al. (2016). Microreact: visualizing and sharing data for genomic epidemiology and phylogeography. *Microb. Genomics* 2:e000093. doi: 10.1099/mgen.0.000093

Crespo, A., Pedraz, L., and Torrents, E. (2015). Function of the *Pseudomonas aeruginosa* NrdR Transcription Factor: global Transcriptomic Analysis and Its Role on Ribonucleotide Reductase Gene Expression. *PLoS One* 10:e0123571. doi: 10.1371/journal.pone.0123571

Croucher, N. J., Page, A. J., Connor, T. R., Delaney, A. J., Keane, J. A., Bentley, S. D., et al. (2015). Rapid phylogenetic analysis of large samples of recombinant bacterial whole genome sequences using Gubbins. *Nucleic Acids Res.* 43:e15. doi: 10.1093/nar/gku1196

del Barrio-Tofiño, E., López-Causapé, C., and Oliver, A. (2020). *Pseudomonas aeruginosa* epidemic high-risk clones and their association with horizontally-acquired β-lactamases: 2020 update. *Int. J. Antimicrob. Agents* 56:106196. doi: 10.1016/j.ijantimicag.2020.106196

Gellatly, S. L., and Hancock, R. E. W. (2013). *Pseudomonas aeruginosa*: new insights into pathogenesis and host defenses. *Pathog. Dis.* 67, 159–173. doi: 10.1111/2049-632X.12033

Hishinuma, T., Tada, T., Kuwahara-Arai, K., Yamamoto, N., Shimojima, M., and Kirikae, T. (2018). Spread of GES-5 carbapenemase-producing *Pseudomonas aeruginosa* clinical isolates in Japan due to clonal expansion of ST235. *PLoS One* 13:e0207134. doi: 10.1371/journal.pone.0207134

Kocsis, B., Gulyás, D., and Szabó, D. (2021). Diversity and Distribution of Resistance Markers in *Pseudomonas aeruginosa* International High-Risk Clones. *Microorganisms* 9:359. doi: 10.3390/microorganisms9020359

Köhler, T., Michéa-Hamzehpour, M., Henze, U., Gotoh, N., Kocjancic Curty, L., and Pechère, J. (1997). Characterization of MexE–MexF–OprN, a positively regulated multidrug efflux system of *Pseudomonas aeruginosa*. *Mol. Microbiol.* 23, 345–354. doi: 10.1046/j.1365-2958.1997.2281594.x

Letunic, I., and Bork, P. (2021). Interactive Tree Of Life (iTOL) v5: an online tool for phylogenetic tree display and annotation. *Nucleic Acids Res.* 49, W293–W296. doi: 10.1093/nar/gkab301

Lister, P. D., Wolter, D. J., and Hanson, N. D. (2009). Antibacterial-Resistant *Pseudomonas aeruginosa*: clinical impact and complex regulation of chromosomally encoded resistance mechanisms. *Clin. Microbiol. Rev.* 22, 582–610. doi: 10.1128/CMR.00040-09

López-Causapé, C., Cabot, G., del Barrio-Tofiño, E., and Oliver, A. (2018). The Versatile Mutational Resistome of *Pseudomonas aeruginosa*. *Front. Microbiol.* 9:685. doi: 10.3389/fmicb.2018.00685

Mine, T., Morita, Y., Kataoka, A., Mizushima, T., and Tsuchiya, T. (1999). Expression in *Escherichia coli* of a New Multidrug Efflux Pump, MexXY, from *Pseudomonas aeruginosa*. *Antimicrob. Agents Chemother.* 43, 415–417. doi: 10.1128/AAC.43.2.415

Miyoshi-Akiyama, T., Tada, T., Ohmagari, N., Viet Hung, N., Tharavichitkul, P., Pokhrel, B. M., et al. (2017). Emergence and Spread of Epidemic Multidrug-Resistant *Pseudomonas aeruginosa*. *Genome Biol. Evol.* 9, 3238–3245. doi: 10.1093/gbe/evx243

Oliver, A., Mulet, X., López-Causapé, C., and Juan, C. (2015). The increasing threat of *Pseudomonas aeruginosa* high-risk clones. *Drug Resist. Update* 2, 41–59. doi: 10.1016/j.drup.2015.08.002

Page, A. J., Cummins, C. A., Hunt, M., Wong, V. K., Reuter, S., Holden, M. T. G., et al. (2015). Roary: rapid large-scale prokaryote pan genome analysis. *Bioinformatics* 31, 3691–3693. doi: 10.1093/bioinformatics/btv421

Poole, K., Gotoh, N., Tsujimoto, H., Zhao, Q., Wada, A., Yamasaki, T., et al. (1996). Overexpression of the mexC-mexD-oprJ efflux operon in nfxB -type multidrug-resistant strains of *Pseudomonas aeruginosa*. *Mol. Microbiol.* 21, 713–725. doi: 10.1046/j.1365-2958.1996.281397.x

Poole, K., Krebes, K., McNally, C., and Neshat, S. (1993). Multiple antibiotic resistance in *Pseudomonas aeruginosa*: evidence for involvement of an efflux operon. *J. Bacteriol.* 175, 7363–7372. doi: 10.1128/jb.175.22.7363-7372.1993

Romsang, A., Duang-Nkern, J., Leesukon, P., Saninjuk, K., Vattanaviboon, P., and Mongkolsuk, S. (2014). The Iron-Sulphur Cluster Biosynthesis Regulator IscR Contributes to Iron Homeostasis and Resistance to Oxidants in *Pseudomonas aeruginosa*. *PLoS One* 9:e86763. doi: 10.1371/journal.pone.0086763

Saninjuk, K., Romsang, A., Duang-nkern, J., Vattanaviboon, P., and Mongkolsuk, S. (2019). Transcriptional regulation of the *Pseudomonas aeruginosa* iron-sulfur cluster assembly pathway by binding of IscR to multiple sites. *PLoS One* 14:e0218385. doi: 10.1371/journal.pone.0218385

Sato, H., Frank, D. W., Hillard, C. J., Feix, J. B., Pankhaniya, R. R., Moriyama, K., et al. (2003). The mechanism of action of the *Pseudomonas aeruginosa*-encoded type III cytotoxin, ExoU. *EMBO J.* 22, 2959–2969. doi: 10.1093/emboj/cdg290

Shaaban, M., Al-Qahtani, A., Al-Ahdal, M., and Barwa, R. (2018). Molecular characterization of resistance mechanisms in *Pseudomonas aeruginosa* isolates resistant to carbapenems. *J. Infect. Dev. Ctries.* 11, 935–943. doi: 10.3855/jidc.9501

Tawfik, A. F., Shibl, A. M., Aljohi, M. A., Altammami, M. A., and Al-Agamy, M. H. (2012). Distribution of Ambler class A, B and D β-lactamases among *Pseudomonas aeruginosa* isolates. *Burns* 38, 855–860. doi: 10.1016/j.burns.2012.01.005

Treepong, P., Kos, V. N., Guyeux, C., Blanc, D. S., Bertrand, X., Valot, B., et al. (2018). Global emergence of the widespread *Pseudomonas aeruginosa* ST235 clone. *Clin. Microbiol. Infect.* 24, 258–266. doi: 10.1016/j.cmi.2017.06.018

Wick, R. R., Judd, L. M., Gorrie, C. L., and Holt, K. E. (2017). Unicycler: resolving bacterial genome assemblies from short and long sequencing reads. *PLoS Comput. Biol.* 13:e1005595. doi: 10.1371/journal.pcbi.1005595

Yoon, E.-J., and Jeong, S. H. (2021). Mobile Carbapenemase Genes in *Pseudomonas aeruginosa*. *Front. Microbiol.* 12:614058. doi: 10.3389/fmicb.2021.614058

Zafer, M. M., Al-Agamy, M. H., El-Mahallawy, H. A., Amin, M. A., and El Din Ashour, S. (2015). Dissemination of VIM-2 producing *Pseudomonas aeruginosa* ST233 at tertiary care hospitals in Egypt. *BMC Infect. Dis.* 15:122. doi: 10.1186/s12879-015-0861-8

Zowawi, H. M., Syrmis, M. W., Kidd, T. J., Balkhy, H. H., Walsh, T. R., Al Johani, S. M., et al. (2018). Identification of carbapenem-resistant *Pseudomonas aeruginosa* in selected hospitals of the Gulf Cooperation Council States: dominance of high-risk clones in the region. *J. Med. Microbiol.* 67, 846–853. doi: 10.1099/jmm.0.000730

Conflict of Interest: HB has participated in this work during her tenure as Professor of pediatric infectious diseases at King Saud bin Abdulaziz University for Health Sciences.

The remaining authors declare that the research was conducted in the absence of any commercial or financial relationships that could be construed as a potential conflict of interest.

Publisher's Note: All claims expressed in this article are solely those of the authors and do not necessarily represent those of their affiliated organizations, or those of the publisher, the editors and the reviewers. Any product that may be evaluated in this article, or claim that may be made by its manufacturer, is not guaranteed or endorsed by the publisher.

frontiers in Microbiology

ORIGINAL RESEARCH
published: 12 January 2022
doi: 10.3389/fmicb.2021.794134

The Role of *nmcR*, *ampR*, and *ampD* in the Regulation of the Class A Carbapenemase NmcA in *Enterobacter ludwigii*

Ryuichi Nakano[1], Yuki Yamada[2], Akiyo Nakano[1], Yuki Suzuki[1], Kai Saito[1], Ryuji Sakata[3], Miho Ogawa[3], Kazuya Narita[2], Akio Kuga[4], Akira Suwabe[5] and Hisakazu Yano[1]*

[1] Department of Microbiology and Infectious Diseases, Nara Medical University, Kashihara, Japan, [2] Division of Central Clinical Laboratory, Iwate Medical University Hospital, Yahaba, Japan, [3] Department of Bacteriology, BML Inc., Kawagoe, Japan, [4] Hamamatsu Pharmaceutical Association, Hamamatsu, Japan, [5] Department of Laboratory Medicine, Iwate Medical University School of Medicine, Yahaba, Japan

Various carbapenemases have been identified in the Enterobacteriaceae. However, the induction and corresponding regulator genes of carbapenemase NmcA has rarely been detected in the *Enterobacter cloacae* complex (ECC). The NmcA-positive isolate ECC NR1491 was first detected in Japan in 2013. It was characterized and its induction system elucidated by evaluating its associated regulator genes *nmcR*, *ampD*, and *ampR*. The isolate was highly resistant to all β-lactams except for third generation cephalosporins (3GC). Whole-genome analysis revealed that bla_{NmcA} was located on a novel 29-kb putatively mobile element called EludIMEX-1 inserted into the chromosome. The inducibility of β-lactamase activity by various agents was evaluated. Cefoxitin was confirmed as a strong concentration-independent β-lactamase inducer. In contrast, carbapenems induced β-lactamase in a concentration-dependent manner. All selected 3GC-mutants harboring substitutions on *ampD* (as *ampR* and *nmcR* were unchanged) were highly resistant to 3GC. The *ampD* mutant strain NR3901 presented with a 700 × increase in β-lactamase activity with or without induction. Similar upregulation was also observed for *ampC* and *nmcA*. NR1491 (pKU412) was obtained by transforming the *ampR* mutant (135Asn) clone plasmid whose expression increased by ∼100×. Like NR3901, it was highly resistant to 3GC. Overexpression of *ampC*, rather than *nmcA*, may have accounted for the higher MIC in NR1491. The *ampR* mutant repressed *nmcA* despite induction and it remains unclear how it stimulates *nmcA* transcription via induction. Future experiments should analyze the roles of *nmcR* mutant strains.

Keywords: carbapenemase, NmcA, AmpC β-lactamase, *Enterobacter* cloacae complex, induction, regulator genes

OPEN ACCESS

Edited by:
Mullika Traidej Chomnawang, Mahidol University, Thailand

Reviewed by:
Valentine Usongo, Health Canada, Canada
Subhasree Roy, National Institute of Cholera and Enteric Diseases (ICMR), India

****Correspondence:***
Ryuichi Nakano
rnakano@naramed-u.ac.jp

Specialty section:
This article was submitted to Antimicrobials, Resistance and Chemotherapy, a section of the journal Frontiers in Microbiology

Received: *13 October 2021*
Accepted: *23 December 2021*
Published: *12 January 2022*

Citation:
Nakano R, Yamada Y, Nakano A, Suzuki Y, Saito K, Sakata R, Ogawa M, Narita K, Kuga A, Suwabe A and Yano H (2022) The Role of nmcR, ampR, and ampD in the Regulation of the Class A Carbapenemase NmcA in Enterobacter ludwigii. Front. Microbiol. 12:794134. doi: 10.3389/fmicb.2021.794134

INTRODUCTION

The *Enterobacter cloacae* complex (ECC) have become clinically significant opportunistic bacteria and are now common nosocomial pathogens causing pneumonia, urinary tract infections, and septicemia (Davin-Regli and Pages, 2015). Six *Enterobacter* species are assigned to the ECC: *E. cloacae*, *E. asburiae*, *E. hormaechei*, *E. kobei*, *E. ludwigii*, and *E. nimipressuralis* (Mezzatesta et al., 2012).

Multidrug resistance (MDR) has been observed for the last-resort carbapenems and has led to an increased global interest in Enterobacteriaceae in general and carbapenem-resistant ECC, in particular (Annavajhala et al., 2019). ECC are innately resistant to penicillins, first- and second-generation cephalosporins, and cephamycin due to the chromosomally encoded AmpC β-lactamase genes (serine β-lactamase, Ambler class C). AmpC β-lactamase expression is low but inducible in response to β-lactam exposure and is closely linked to a peptidoglycan recycling system, with the β-lactams imipenem, cefoxitin, and clavulanic acid strong *ampC* inducers (Jacoby, 2009). Regulation of AmpC β-lactamase expression is complex and involves AmpR (a transcriptional regulator of the LysR family), AmpD (a cytosolic amidase), and AmpG (a transmembrane permease) (Guerin et al., 2015). AmpR usually represses *ampC* in the absence of β-lactam inducers, whereas mutations at specific sites in AmpR derepresses AmpC synthesis and results in constitutive AmpC β-lactamase overexpression. Asp135Asn AmpR substitution is correlated with substantial increases in β-lactamase activity in several Gram-negative organisms including ECC, *Citrobacter freundii*, and *Pseudomonas aeruginosa* (Kuga et al., 2000; Caille et al., 2014; Nakano et al., 2017). Mutations that inactivate AmpD permanently induce and increase muropeptide concentrations in the cytoplasm and change the conformation of AmpR so that it becomes a transcriptional activator (Kuga et al., 2000). Specifically, AmpR mutations require site-specific substitution to induce AmpC β-lactamase overexpression whereas AmpD mutations need loss-of-function point mutations (missense mutation) or disruption of the protein carboxy terminus, nonsense mutations, frameshifts, and truncations (Schmidtke and Hanson, 2006). Among the ECC clinical isolates, high-level resistance to third generation cephalosporins (3GC) is caused by constitutive *ampC* overexpression mainly from *ampD* mutations and, more rarely, from *ampR* mutations (Kaneko et al., 2005; Guerin et al., 2015).

Carbapenem resistance in ECC is conferred either through constitutive AmpC β-lactamase overexpression combined with defective outer membrane (porin) permeability or via the acquisition of carbapenemase genes (Annavajhala et al., 2019), with the latter scenario being more common. Carbapenemases hydrolyze most β-lactams including carbapenems and are classified as serine β-lactamases (Ambler class A; KPC type and D; OXA-48 type) or metallo-β-lactamases (Ambler class B; IMP type, VIM type, and NDM type) (Diene and Rolain, 2014; Nakano et al., 2014; Ando et al., 2018). The distributions of these enzymes differ with geographical location: the KPC type occurs in the United States, NDM in the Indian subcontinent, and IMP in Japan (Chavda et al., 2016; Aoki et al., 2018; Peirano et al., 2018). Chromosomally encoded carbapenemase NmcA (Ambler class A) has been sporadically detected in ECC (Walther-Rasmussen and Hoiby, 2007).

NmcA was originally detected in the carbapenem-resistant *E. cloacae* strain NOR-1 isolated in France in 1990 (Nordmann et al., 1993). NmcA has occasionally been detected in *E. cloacae*, *E. asburiae*, and *E. ludwigii* from Europe, North America, and South America (Pottumarthy et al., 2003; Radice et al., 2004; Antonelli et al., 2015; Boyd et al., 2017). A recent study revealed that bla_{NmcA} is associated with a novel 29-kb putative Xer-dependent integrative mobile element (EludIMEX-1) inserted into the ECC chromosome (Antonelli et al., 2015). This enzyme hydrolyses different β-lactam agents except for 3GC and has particularly high hydrolytic activity against carbapenems (Nordmann et al., 1993; Mariotte-Boyer et al., 1996). The inducibility of NmcA is similar to AmpC β-lactamase (Pottumarthy et al., 2003), where the LysR family transcriptional regulator gene *nmcR* upstream of bla_{NmcA} regulates *nmcA* in the same manner as the *ampR–ampC* regulatory system does for AmpC. Additionally, AmpD co-regulates *nmcA* (Naas et al., 2001).

Here, we describe the characteristics of an *nmcA*-positive ECC isolate first observed in Japan. We also elucidate the *nmcA* induction system by evaluating *nmcA* expression in *ampD* and *ampR* mutant strains.

MATERIALS AND METHODS

Bacterial Strains and Antimicrobial Susceptibility Testing

The carbapenem-resistant ECC strain NR1491 was isolated from the urine of a patient in a Japanese hospital in 2013. The species was identified as *E. cloacae* by MicroScan WalkAway plus (Beckman Coulter, Inc., Brea, CA, United States). To evaluate the effects of *ampR* mutation on antimicrobial susceptibility and β-lactamase expression, *ampR* clone plasmids were constructed and used to transform NR1491. The *ampR* clone plasmids (pKU411 and pKU412) used in this study were already previously constructed (Kuga et al., 2000). An *in vitro* ceftazidime-resistant mutant strain NR3901 was isolated from NR1491. Characteristics of the bacterial strains and plasmids used in the present study are listed in **Table 1**.

The minimum inhibitory concentrations (MICs) of the various antimicrobial agents were determined for each

TABLE 1 | Bacterial strains and plasmids used in the present study.

Strain or plasmid	Relevant characteristics	Source or references
Strains		
E. ludwigii NR1491	Clinical isolate from Japan, resistance to carbapenems	This study
pKU411/NR1491	*E. ludwigii* transformed with pKU411	This study
pKU412/NR1491	*E. ludwigii* transformed with pKU412	This study
NR3901	Ceftazidime-resistant mutant of *E. ludwigii* NR1491, AmpD mutant (69delG)	This study
Plasmids		
pKU411	Wild type *ampR* (135Asp) of *E. cloacae* GN7471 cloned into pMW218	Kuga et al., 2000
pKU412	Mutant *ampR* (135Asn) of *E. cloacae* GN7471 cloned into pMW218	Kuga et al., 2000

strain by the agar dilution method according to CLSI guidelines (CLSI, 2018).

Whole-Genome Sequencing and Analysis

The genomic DNA of NR1491 was prepared with a Qiagen Genomic-tip 500/G kit (Qiagen, Hilden, Germany) and subjected to whole-genome sequencing on the MiSeq X10 platform (Illumina, San Diego, CA, United States). Reads were trimmed in Trimmomatic and assembled to contigs with the SPAdes v. 3.8.1 genome assembler in caution mode (Bankevich et al., 2012).

Species were precisely identified based on their average nucleotide identity (ANI) and *in silico* DNA–DNA hybridization between strain NR1491 (GenBank accession no. BKZO00000000.1), the *E. cloacae* type strain ATCC 13047 (GenBank accession no. MTFV00000000.1), the *E. ludwigii* type strain EN-119 (GenBank accession no. JTLO00000000.1), and the *E. ludwigii* type strain AOUC-8/14 (GenBank accession no. LGIV00000000.1). Earlier studies recommended ANI of ∼95–96% as a species demarcation cutoff (Goris et al., 2007; Chun and Rainey, 2014).

Antimicrobial resistance genes were identified in the genome sequence with the ResFinder database[1] using thresholds of 90% identity and 60% minimum length. β-lactamase genes including carbapenemases and extended-spectrum β-lactamases (ESBLs) were also assessed by PCR. PCR detection of carbapenemases (bla_{IMP}, bla_{VIM}, bla_{KPC}, $bla_{OXA-48-like}$, bla_{NDM}, bla_{GES}, $bla_{IMI/NmcA}$, and bla_{SME}) (Poirel et al., 2011; Hong et al., 2012; Nakano et al., 2018) and ESBLs (bla_{TEM}, bla_{SHV}, and bla_{CTX-M}) (Dallenne et al., 2010) were performed as previously described. The sequence surrounding bla_{NmcA}, a carbapenemase-encoding gene, was elucidated by PCR and Sanger sequencing to close the gaps between the contigs. Sequence alignment and analysis were performed with BLAST[2] at NCBI (National Centre for Biotechnology Information, Bethesda, MD, United States). Multilocus sequence typing (MLST) of the *E. cloacae* isolates was performed as previously described (Miyoshi-Akiyama et al., 2013). Sequence types were assigned at the PubMLST database.[3] The presence of mobile genetic elements was investigated using the MobileElementFinder (Johansson et al., 2021) and INTEGRALL (Moura et al., 2009). The plasmid content was assessed using PlasmidFinder (Carattoli et al., 2014).

Selection of Third-Generation Cephalosporin-Resistant Mutants and Detection of Sequence Alterations

Third-generation cephalosporin-resistant mutants were obtained by plating $\sim 10^9$ CFU mL^{-1} late-logarithmic-phase NR1491 grown in Luria-Bertani (LB) broth and on LB agar plates containing ceftazidime or cefotaxime at 2×, 4×, 8×, 16×, and 32× MIC. The mutation frequencies were determined by dividing the colony density in CFU mL^{-1} on LB agar plates containing the antibiotic agents by the total colony density in CFU mL^{-1}.

[1]https://cge.cbs.dtu.dk/services/ResFinder/

[2]https://blast.ncbi.nlm.nih.gov/Blast.cgi

[3]http://pubmlst.org/ecloacae/

The DNA sequences of the selected mutants were determined by Sanger sequencing of *nmcR*, *ampR*, and *ampD* amplicons. The primers used are listed in **Supplementary Table 1** (Radice et al., 2004). The nucleotides and amino acids of the selected mutants were compared with those of *E. ludwigii* NR1491 and EN-119.

β-Lactamase Induction Assays

β-lactamase activity was measured in terms of the protein content in the extract and compared among cultures in 50 mM phosphate buffer (pH 7.0) at 30°C by spectrophotometry as previously described (Nakano et al., 2004). The protein concentrations were determined by the Bradford assay (Bradford, 1976). One unit of β-lactamase activity was defined as the amount of β-lactamase hydrolyzing 1 μmol cephalothin in 1 min at 30°C. The β-lactamase induction assays were performed by subjecting mid-logarithmic phase bacteria in Mueller-Hinton broth to β-lactams at 1/16×, 1/8×, 1/4×, 1/2×, and 1× MICs for 2 h (Kuga et al., 2000). The antibiotics cefpodoxime, clavulanic acid, cefoxitin, imipenem, and meropenem were used as inducers. The induction ratios were calculated in terms of the ratio of β-lactamase activity mg^{-1} protein in induced cells to the β-lactamase activity per mg^{-1} protein in uninduced cells.

Measurement of *ampC* and *nmcA* mRNA Levels by qRT-PCR

The mRNA expression levels of *ampC* and *nmcA* with and without induction were determined by qRT-PCR as previously described (Nakano et al., 2017). Total RNA was extracted with the RNeasy protect bacteria mini kit and the RNase-free DNase set (Qiagen, Hilden, Germany) according to the manufacturer's instructions. The qRT-PCR was performed in a StepOnePlus real-time PCR system (Applied Biosystems, Foster City, CA, United States) with a Power SYBR Green RNA-to-CT 1-Step kit (Thermo Fisher Scientific, Waltham, MA, United States) and 100 ng total RNA in a 20-μL reaction, according to the manufacturer's instructions. The primers used are listed in **Supplementary Table 1** (Doumith et al., 2009). The relative gene expression levels were calculated by the $2^{-\Delta\Delta CT}$ method. The mRNA of the housekeeping gene *rpoB* was chosen as the endogenous reference for relative quantification. The results are presented as the mRNA expression level compared with that of NR1491. The experiment was performed in triplicate. The final relative expression levels of *ampC* and *nmcA* were determined by calculating the averages for their transcripts. The coefficient of variation (SD/mean) among experiments was $< 10\%$.

Nucleotide Sequence Accession Numbers

The nucleotide sequences of the genetic regions surrounding bla_{NmcA} and the whole-genome DNA sequences of NR1491 were deposited in the GenBank database under accession numbers LC482123 and BKZO00000000.1, respectively.

RESULTS

Identification of *bla*$_{NmcA}$-Harboring *Enterobacter ludwigii* NR1491

The draft NR1491 genome (GenBank accession no. BKZO00000000.1) was obtained by MiSeq (Illumina, Sa, Diego, CA, United States), and average nucleotide identity (ANI) analysis using *E. cloacae* strain ATCC13047, *E. ludwigii* type strain EN-119, and *E. ludwigii* AOUC-8/14 as reference genomes. Their respective ANI values were 87.82, 98.96, and 98.97%.[4] NR1491 was identified as *E. ludwigii* belonging to ST258.

Antimicrobial Susceptibility and Resistance Genes

Antimicrobial susceptibility assays showed that *E. ludwigii* NR1491 was highly resistant to cephalothin, cefmetazole, carbapenems, and fosfomycin (> 512 μg mL^{-1}) but susceptible to 3GC, piperacillin–tazobactam, cefepime, aztreonam, levofloxacin (≤0.06 μg mL^{-1}), and gentamicin (0.5 μg mL^{-1}) (**Table 2**). However, the MIC of cefotaxime increased when the agent was combined with clavulanic acid.

Whole-genome analysis with ResFinder revealed the following resistance-encoding genes: *bla*$_{NmcA}$ (carbapenemase), ACT-12 (AmpC β-lactamase), and *fosA2* (glutathione transferase; fosfomycin resistance). It also disclosed that the regulator genes *nmcR* and *ampR* were upstream of *bla*$_{NmcA}$ and *ampC*, respectively. The entire nucleotide sequences of *bla*$_{NmcA}$ and *nmcR* and the intercistronic region were determined by Sanger sequencing. The sequences were identical to that of *E. cloacae* NOR-1 (accession no. Z21956). PCR demonstrated that no other acquired β-lactamase gene was harbored. The regulatory gene sequences of *bla*$_{NmcA}$ (*nmcR*, *ampR*, and *ampD*) were compared with that of the reference strains of ECC (NOR-1, EN-119, and AOUC-8/14); there are no mutations in these genes. Whole-genome analysis indicated that the insertion sequence (IS) elements and an integron were not encoded on the chromosome; the strain did not harbor a plasmid.

Genetic Environment Analysis of *bla*$_{NmcA}$

The genetic environment of *bla*$_{NmcA}$ was determined to be a 48,089-bp nucleotide fragment characterized by whole-genome and Sanger sequencing and deposited into GenBank under accession no. LC482123. A BLASTn analysis showed that the fragment was highly similar to *E. ludwigii* AOUC-8/14 (accession no. KR919803) (44,766/44,874 nucleotides; 99.76% identity). The *bla*$_{NmcA}$ was located on a novel putatively mobile 29-kb element designated EludIMEX-1 inserted into the same chromosome location as that in *E. ludwigii* AOUC-8/14. Two imperfect 29-bp inverted repeat XerC/XerD binding sites associated with EludIMEX were identified at the chromosome–EludIMEX-1 junctions. The genetic regions were compared with the corresponding regions of *E. ludwigii* P101 (GenBank accession no. CP006580); the schematic representations are depicted in **Figure 1**. There were highly homologous regions (> 99%

[4]https://www.ezbiocloud.net/tools/ani

TABLE 2 | Susceptibility and β-lactamase activity of *E. ludwigii* NR1491 and the mutant strains.

Strain	Gene on plasmid	AmpD characteristic	MICs (μg mL^{-1})[a]										β-Lactamase activity of (Unit mg^{-1} of protein)[c]		Fold increase in activity		Expression[e]			
			PIP	PIP/TAZ[b]	CEF	CPD	CTX	CTX/CLA[b]	CAZ	FPM	CFX	AZT	IPM	MER	Basal	Induced[d]	Induced/basal	Mutant/WT	Basal			Induced[d]		
																			ampC	*nmcA*	*ampC*	*nmcA*	*ampC*	*nmcA*
NR1491	–	Wild type	4	2	>512	4	0.25	4	1	0.125	512	1	64	16	0.03	2.97	97.5	–	1	1	14.7	14.6		
NR1491 (pKU411)	Wild type AmpR (135D)		4	2	>512	2	0.25	2	1	0.125	512	1	64	16	0.03	2.94	101.1	1	0.7	1.1	14.6	15.3		
NR1491 (pKU412)	Mutant AmpR (135N)	Wild type	32	8	>512	512	32	16	64	0.25	>512	32	32	16	3.06	4.54	1.5	100.3	96.4	1.0	205.6	2.3		
NR3901	–	Mutant (69delG)	128	64	>512	256	32	16	64	0.5	>512	256	32	16	21.54	21.48	1.0	706.5	698.5	695.0	680.4	679.4		

[a]*Antibiotics: PIP, piperacillin; TAZ, tazobactam; CEF, cephalothin; CPD, cefpodoxime; CTX, cefotaxime; CLA, clavulanic acid; CAZ, ceftazidime; FEP, cefepime; CFX, cefoxitin; AZT, aztreonam; IPM, imipenem; MER, meropenem.*

[b]*MICs were determined in the presence of tazobactam (4 μg mL^{-1}) or clavulanic acid (4 μg mL^{-1}).*

[c]*β-lactamase activities are the geometric means for three independent cultures. The standard deviations were within 10%.*

[d]*Induction was carried out with 32 μg mL^{-1} cefoxitin.*

[e]*Relative to the expression of NR1491 which was assigned a value of 1. Standard deviations were within 10%.*

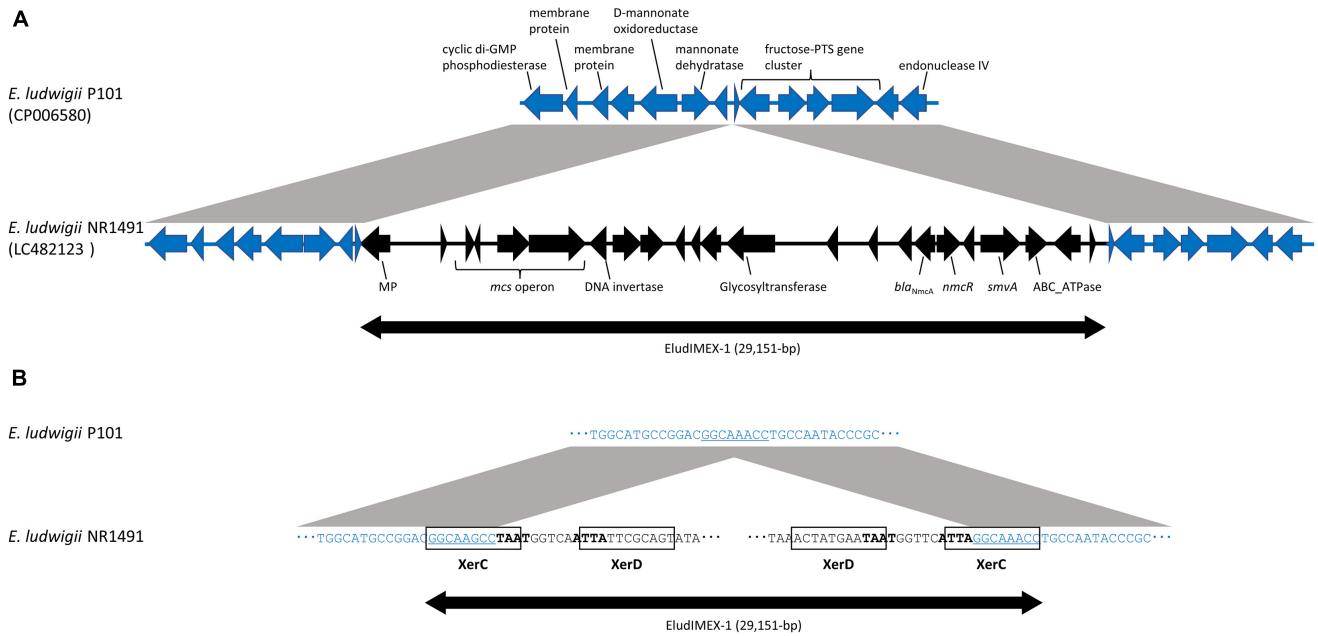

FIGURE 1 | Schematic representations and nucleotide sequences of the genetic elements surrounding EludIMEX-1 of *E. ludwigii* NR1491 (GenBank accession no. LC482123) and the corresponding region of *E. ludwigii* P101 (GenBank accession no. CP006580). **(A)** Schematic representation of the genetic region of *E. ludwigii* NR1491 (black arrow) and *E. ludwigii* P101 (blue arrow). The gray regions between the NR1491 and P101 indicate > 99% nucleotide sequence identity. Insertion of the EludIMEX-1 element (double-headed arrow) in *E. ludwigii* NR1491 was observed. **(B)** Nucleotide sequences at the junctions of EludIMEX-1 (a part of left and right of the junctions) of *E. ludwigii* NR1491 and the corresponding region of *E. ludwigii* P101. The XerC/XerD binding sites are boxed, the conserved regions are boldfaced, and the consensus repeat sequences in XerC binding site of *E. ludwigii* NR1491 and corresponding sequences of *E. ludwigii* P101 are indicated using underlined letters.

nucleotide sequence identity) and the insertion of EludIMEX-1. bla_{NmcA} was putatively integrated into the *E. ludwigii* chromosome via a Xer-dependent recombination mechanism mediated by EludIMEX-1, as described previously.

BLASTn analysis of NR1491 indicated that there were 10 strains of NmcA-positive ECC with > 99% nucleotide sequence identities (**Supplementary Table 2**). The query coverage includes the gene regions of the EludIMEX-1 element and the surrounding regions with consensus repeat sequences and a binding site. The EludIMEX-1 was integrated into the chromosome at the same site, in these strains. The genotypes of these strains were including ST258 (n = 2) same with NR1491, ST282 (n = 2), ST257, ST260, ST374, ST714 (AOUC-8/14), ST748, and ST1724.

Antibiotic Inducibility of β-Lactamase

The antibiotic inducibility of β-lactamase was analyzed in NR1491 (**Figure 2**). Cefpodoxime and clavulanic acid were slightly inducer in a concentration-dependent manner. They yielded only a maximum 3.3 × induction of the MIC. Conversely, cefoxitin, imipenem, and meropenem were strong β-lactamase inducers. The carbapenems imipenem and meropenem induced β-lactamase in a concentration-dependent manner to 159× and 202×, respectively, at half their MIC. In contrast, the cefoxitin induction rate was concentration-independent and remained virtually unchanged (98–113 ×) across the tested concentrations (1/16–1 × MIC).

Properties of the Selected Third Generation Cephalosporins-Resistant Mutants

The 3GC-resistant mutants were selected with cefotaxime and ceftazidime at 2×, 4×, 8×, 16×, and 32× MIC. The

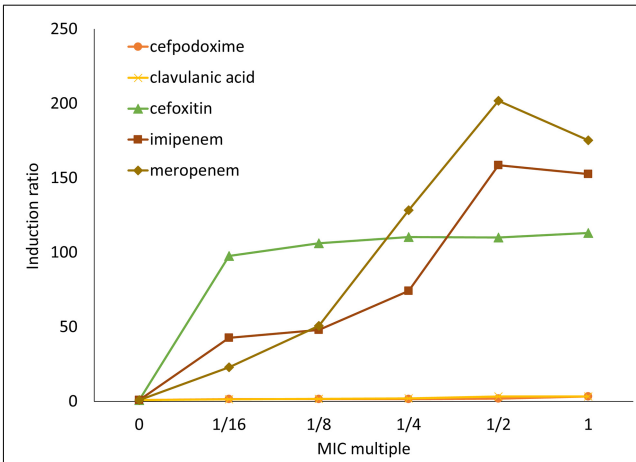

FIGURE 2 | Induction ratios of β-lactamase activity in response to antibiotics on *E. ludwigii* NR1491. β-lactamase inducers were cefpodoxime (○), clavulanic acid (×), cefoxitin (△), imipenem (□), and meropenem (◇).

antibiotic-resistant mutants were consistently obtained at a mutation frequency of $\sim10^{-6}$–10^{-7} both for cefotaxime and ceftazidime (**Table 3**).

To investigate the molecular mechanism of 3GC resistance in these mutants, 48 clones were randomly selected from each condition. The regulator genes *ampR, nmcR,* and *ampD* were sequenced and compared to those of the parent *E. ludwigii* NR1491 and wild type EN-119 strains. Sequence data revealed that only *ampD* was altered in all cases whereas neither *ampR* nor *nmcR* was changed. Of the 48 3GC-resistant mutants, 34 had possible loss-of-function caused by missense mutations including 18 amino acid substitutions at 16 positions in *ampD* (**Table 3**). Premature termination of the AmpD protein was found in 14 mutants. Seven had nonsense mutation at six positions, five had frameshift mutations (three deletions and two insertions), and two had missense mutations in which the start codon (ATG) was changed to Ile (ATA) at position 1. Its effect was transcriptional decay. These mutations were scattered throughout the entire *ampD* sequence. Moreover, the nucleotide substitutions and mutation types and locations did not differ among selective agents and concentrations. However, certain mutants had the same missense mutation positions. Eight were I78N, seven were T123P, and four were S100L. These mutation positions may have been influential to AmpD activity. These mutants were resistant to 3GC presumably as a consequence of loss of AmpD function via the introduction of substitution mutations or decay of the transcript containing the premature stop codon.

For the mutants, the MICs were determined for the selected β-lactams (**Table 3**). Compared with the MICs for the parent strain NR1491, the MICs of 3GC (cefotaxime and ceftazidime) and aztreonam for the mutants had increased by ≥ 16 ×. Thus, these strains were reclassified from susceptible to resistant. The MICs of cefepime increased by only 1–4 × relative to NR1491 and were beyond the clinical resistance breakpoint. In contrast, the MICs of the carbapenems were almost always the same as those for NR1491.

Effects of Regulator Genes on β-Lactamase Expression

To evaluate the effects of *ampR* and *ampD* on NR1491 drug susceptibility, β-lactamase activity and mRNA expression of AmpC and NmcA with and without induction were analyzed in the *ampR* mutant NR1491 (pKU412) and the *ampD* mutant NR3901 (**Table 2**). Induction was carried out with 32 μg mL^{-1} cefoxitin. The β-lactamase activity of NR1491 increased by ∼100 × and AmpC and NmcA were upregulated by ∼14.7× and 14.6×, respectively, in response to induction. *ampC* and *nmcA* expression levels were equally influenced by the induction.

NR3901 bore an *ampD* mutant (69delG) and was isolated by selection with 32 μg mL^{-1} ceftazidime. The MICs of 3GC and aztreonam increased by ≥ 64 × and they were reclassified as highly resistant. The β-lactamase activity of NR3901 increased by ∼706.5 and ∼704.5 × with and without induction, respectively, compared with the NR1491 basal condition. The *ampC* and *nmcA* expression levels in NR3901 both increased by ∼700 × in the presence and absence of induction. The *ampC* and *nmcA* expression levels in NR1491 both increased by ∼15 × in response to induction. Hence, *ampD* equally induced *ampC* and *nmcA* expression. NR3901 was highly drug-resistant because it acquired the *ampD* mutation which derepressed *ampC* and *nmcA* expression.

NR1491 (pKU412) was obtained by transfecting the *ampR* mutant (135Asn) clone plasmid pKU412 into NR1491. The MICs of NR1491 (pKU412) were elevated as they were for NR3901. The β-lactamase activity had increased by ∼100 × at basal condition. *ampC* expression also increased by ∼100 × whereas that of *nmcA* did not change. AmpR may induce AmpC β-lactamase but does not affect *nmcA* expression. NR1491 (pKU412) induction

TABLE 3 | Amino acid and nucleotide changes in AmpD of ceftazidime- or cefotaxime-resistant mutants of *E. ludwigii* NR1491 and their antimicrobial susceptibilities.

Mutation	Selective agents (μg mL^{-1})[a]	No. of selected strains	Amino acid and nucleotide changes detected in AmpD (no. of strains)[b]	MIC range (μg mL^{-1})[a]										
				PIP	PIP /TAZ	CPD	CTX	CTX /CLA	CAZ	FPM	CFX	AZT	IPM	MER
Missense	CTX (1, 2, 4, 8, 16) CAZ (2, 4, 8, 16, 32)	36	M1I (2), N35K (2), L56P, L56Q, T55P, H75Y, I78N (8), I78S, G82V, W95G, G98D, S100L (4), L117R, E118G, T123P (7), T137P, G166A, D170Y	16–128	8–32	128–256	8–32	8–16	16–64	0.125–0.5	512–> 512	32–256	16–64	8–16
Non-sense	CTX (1, 8, 16) CAZ (8, 32)	7	W7*, E26*, E83*, Q86*, Y102*(2), Q103*	128	32	256–512	16	8–16	64	0.25–0.5	512	256	16–32	8–16
Frameshift	CTX (8, 16) CAZ (4, 16, 32)	5	69delG, 129_130insT, 270_271insT, 372delC, 401_404del	128	16–32	256–512	16–32	8–16	64	0.5	512–> 512	256	32	16

[a]*Antibiotics: PIP, piperacillin; TAZ, tazobactam; CEF, cephalothin; CPD, cefpodoxime; CTX, cefotaxime; CLA, clavulanic acid; CAZ, ceftazidime; FEP, cefepime; CFX, cefoxitin; AZT, aztreonam; IPM, imipenem; MER, meropenem.*

[b]*Nucleotide and deduced amino acid differences in AmpD were compared with E. ludwigii NR1491 and EN-119. *, stop codon; del, deletion; ins, insertion.*

resulted in a 1.5 × increase which suggests partial derepression. *ampC* expression increased by ∼200 × after induction. However, *nmcA* expression only doubled despite NR1491 expression increasing by ∼15 ×. Plasmid pKU411 comprising the wild type *ampR* (135Asp)-harboring strain NR1491 (pKU411) was compared with the *ampR* mutant strain and used to verify it. The MICs and β-lactamase activity of NR1491 (pKU411) were nearly the same as those for NR1491.

DISCUSSION

The incidence of CPE is increasing globally. However, it has seldom (0.34%) been detected in Japan (Ohno et al., 2017). The most common carbapenemase genotype detected in Japan is IMP. Here, we isolated NmcA carbapenemase-producing ECC. NmcA carbapenemase has occasionally been reported for ECC in Europe, North America, and South America (Radice et al., 2004; Antonelli et al., 2015; Boyd et al., 2017). To the best of our knowledge, this is the first reported clinical isolation of an NmcA carbapenemase producer in Japan.

ANI revealed that NR1491 was, in fact, *E. ludwigii* belonging to ST258. A previous study reported that bla_{NmcA} was highly associated with *E. ludwigii.* ST258 is a genotype of the NmcA carbapenemase producer (Boyd et al., 2017). The genetic environment of bla_{NmcA} was nearly identical to that of *E. ludwigii* AOUC-8/14. Thus, bla_{NmcA} was putatively integrated into the chromosome by EludIMEX-1 via a Xer-dependent recombination mechanism as previously described for *E. ludwigii* AOUC-8/14 (Antonelli et al., 2015). Interestingly, *E. ludwigii* AOUC-8/14 was isolated from a Japanese tourist in Italy. These strains may have been concealed in Japan and unintentionally isolated in the present study. Comparative genome analysis revealed that there were 10 strains including AOUC-8/14, which have high homology regions with NR1491. These EludIMEX-1 was integrated in the chromosome at the same site as in NR1491. The genotypes of these strains were different; the EludIMEX-1 insertion event has possibility occurred in these STs strains.

As with bla_{NmcA}, NR1491 coexists with the regulator gene *nmcR*. A β-lactamase induction assay on NR1491 showed that it was weakly induced by clavulanic acid which was already known to be an inhibitor of Class A β-lactamases. Thus, it is inhibitory against NmcA β-lactamase (Mariotte-Boyer et al., 1996). On the other hand, clavulanic acid also induces chromosomally mediated AmpC β-lactamases in several Enterobacteriaceae (Drawz and Bonomo, 2010). Here, clavulanic acid induced β-lactamases via transcriptional regulator genes and not by inhibiting NmcA. The MIC of cefotaxime was increased in combination with clavulanic acid while imipenem and meropenem induced β-lactamase in a concentration-dependent manner. Previous study of its kinetic parameters show that NmcA demonstrated unusually strong hydrolytic activity toward imipenem and meropenem (Mariotte-Boyer et al., 1996). Therefore, NmcA producers are highly resistant to carbapenems as their inducers are upregulated and they are potently hydrolytic to carbapenems. Cefoxitin is a strong, stable, dose-independent β-lactamase inducer (100 × induction). The catalytic efficiency ($k_{\mathrm{cat}}/K_{\mathrm{m}}$) of cefoxitin is lower than those of the carbapenems but its MIC is comparatively higher (Mariotte-Boyer et al., 1996) possibly because of its high and stable inducibility.

To elucidate the mechanism of β-lactamase induction in NR1491, 3GC-resistant mutants were selected with cefotaxime and ceftazidime. The mutation frequencies were 10^{-6}–10^{-7} as previously described (Naas et al., 2001). Forty-eight randomly selected clones had variable susceptibilities to 3GC, piperacillin–tazobactam, and aztreonam (**Table 3**). A DNA sequence analysis revealed that all mutants presented with nucleotide substitutions (frameshift, missense, or nonsense) in *ampD* alone. In contrast, *ampR* and *nmcR* were unchanged. The mutants were resistant to 3GC and probably had loss of AmpD function. Premature AmpD termination with a stop codon or frameshift induced strong 3GC resistance. The MICs of the *ampD* mutant strains with missense mutation had different 3GC resistance levels. The degree of 3GC resistance depended on the position of the substitution at the core residues of the active site of AmpD.

In the present study, no mutants of the transcriptional regulator genes *ampR* and *nmcR* were obtained. We investigated the effects of *ampR* in the presence of a mutant or wild type *ampR* clone plasmid. AmpR is a member of the lysR family and regulates the expression of chromosomal AmpC β-lactamase. Nevertheless, *ampR* mutants cause constitutive AmpC overproduction (75–470× increase) irrespective of induction (Kuga et al., 2000). In the enzyme activity assay, NR1491 (pKU412) increased β-lactamase activity by 100 × at the basal level compared with NR1491, also upregulating *ampC*. β-lactamase activity in the NR1491 strain with wild type *ampR* was increased by 100 × by induction and *ampC* and *nmcA* were each upregulated 15×. Whereas NR1491 with wild type *ampR* upregulated *nmcA* 15×, *nmcA* expression in NR1491 (pKU412) only doubled. Mutant *ampR* may negatively regulate *nmcA* expression. Putative *ampR* binding sequences in the *E. cloacae ampR–ampC* intergenic region were highly conserved with *nmcR–*bla_{NmcA} and cross-reaction may have occurred (Naas and Nordmann, 1994). Earlier studies suggested that *ampR* is a global transcriptional regulator affecting the expression of several genes as well as *ampC* (Balasubramanian et al., 2012). NmcR was described as a positive regulator both in the absence and especially in the presence of a β-lactam inducer. In the absence of inducer, *ampR* is a negative regulator of *ampC* expression. In its presence, it positively regulates *ampC* expression (Naas and Nordmann, 1994). These findings suggest that even with available induction, mutant *ampR* represses the expression of *nmcA*. We believe this is the first study to describe the association between *ampR* and *nmcA* expression.

NmcR mutant strain has not been identified yet; therefore, the effect of *nmcR* mutations on the expression of *nmcA* could not be assessed. Point mutations in *nmcR* may be required to enhance its efficacy as an activator of *nmcA* in the same way as mutant *ampR* (such as that with a change in Asp135Asn). Alternatively, it may repress *nmcA* expression in the same way as wild type *ampR*. In a previous study, *ampR* mutants were obtained from the *ampD* mutant strain at a very low frequency (Kuga et al., 2000). The *ampD* mutant strain NR3901 selected *nmcR* mutants using ceftazidime at double and quadruple the

MIC (128 and 256 μg mL^{-1}). Nevertheless, no *nmcR* mutants were obtained (data not shown). *nmcR* mutants may be selected using *ampD*-mutant *E. coli* strains carrying bla_{NmcA} and *nmcR* cloning plasmids. NR1491 co-harbors *ampC* on the chromosome. The observed differences in β-lactamase substrate specificity may influence selection conditions, and further investigation is needed to clarify whether *nmcR* mutation increases resistance by upregulating *nmcA*. This study has certain limitations. The analysis included only one strain and the conclusions were based on the results from this strain. Therefore, further studies are required to clarify the mechanisms of *nmcR* by selecting the *nmcR* mutant strains using other NmcA-producing ECC or IMI (closely related carbapenemase NmcA) producing *E. coli*. Moreover, the *ampR* mutation in NR1491 resulted in strong 3GC resistance via *ampC* overexpression. However, it remains unclear as to how mutant *ampR* stimulates *nmcA* transcription through induction. Future research should aim to elucidate the function of *ampR*.

NR3901 with an *ampD* mutation presented with a 700 × increase in β-lactamase activity as well as upregulated *ampC* and *nmcA*. Consequently, the MICs of 3GC were elevated. It indicates that *ampD* mutation has a similar influence on the expression of both *ampC* and *nmcA*, suggesting that structurally unrelated genes could be under the control of an identical regulatory system (Naas et al., 2001). The MICs for NR3901 and NR1491 (pKU412) bearing the *ampR* mutant plasmid were nearly equal. The upregulated *nmcA* in NR3901 had no effect on MIC compared with NR1491 (pKU412). Moreover, the MICs of the carbapenems for NR3901 were almost always the same as those of the parent strain despite the *ampD* mutant constitutively upregulating *ampC* and *nmcA*. High-level *nmcA* expression may elevate the MICs of carbapenems; in fact, the MICs were same as those of the parent strain. NmcA metabolism and its associated physiology may be connected with MICs. However, further experimentation is required to clarify this mechanism.

Here, we detected the NmcA-producing strain NR1491 in a hospital patient. Examination of MIC patterns showed high resistance to carbapenems but susceptibility to 3GC. The *ampD* mutant strains were identified among clinical isolates of ceftazidime-resistant *E. cloacae* as previously reported (Kaneko et al., 2005). Therefore, *ampD*-mutant NmcA producers may occur and interfere with the clinical detection of their wild type counterparts. We characterized NmcA producers that were highly resistant to carbapenems and yet susceptible to cefepime, whether they acquired the *ampD* mutation. In future works, it would be informative to compare these strains with the Big Five carbapenemases (KPC, IMP, NDM, VIM, and OXA).

CONCLUSION

In the present study, we identified the *E. ludwigii* isolate NR1491 in Japan that produces NmcA. The bla_{NmcA} was located on a novel 29-kb putatively mobile element designated EludIMEX-1 identical in structure to that previously described in Europe. Induction studies revealed that the *ampD* mutants equally upregulated β-lactamases *nmcA* and *ampC* and were highly resistant to 3GC. However, the observed increase in the MIC value of 3GC was caused mainly by *ampC* overexpression. The *ampR* mutants also upregulated *ampC*, however, that of *nmcA* seemed to be repressed. Further research is necessary to elucidate the functions of *ampR* and *nmcR*.

DATA AVAILABILITY STATEMENT

The datasets presented in this study can be found in online repositories. The names of the repository/repositories and accession number(s) can be found in the article/ **Supplementary Material**.

AUTHOR CONTRIBUTIONS

RN conceived and designed the experiments, performed the experiments, analyzed and interpreted the data, and wrote the manuscript. YY contributed reagents and materials and performed the experiments. AN, YS, KS, RS, MO, and KN performed the experiments, validation, and interpreted the data. AK contributed reagents and materials, conceived, and designed the experiments. AS and HY supervision and project administration. All authors contributed to manuscript, read, and approved the submitted version.

FUNDING

This work was supported by JSPS KAKENHI (Grants Nos. 17K10027 and 21K10403).

SUPPLEMENTARY MATERIAL

The Supplementary Material for this article can be found online at: https://www.frontiersin.org/articles/10.3389/fmicb.2021.794134/full#supplementary-material

REFERENCES

Ando, S., Nakano, R., Kuchibiro, T., Yamasaki, K., Suzuki, Y., Nakano, A., et al. (2018). Emergence of VIM-2-producing *Citrobacter freundii* in Japan. *Infect. Dis. (Lond.).* 50, 862–863. doi: 10.1080/23744235.2018.1498592

Annavajhala, M. K., Gomez-Simmonds, A., and Uhlemann, A. C. (2019). Multidrug-resistant Enterobacter cloacae complex emerging as a global, diversifying threat. *Front. Microbiol.* 10:44. doi: 10.3389/fmicb.2019.00044

Antonelli, A., D'andrea, M. M., Di Pilato, V., Viaggi, B., Torricelli, F., and Rossolini, G. M. (2015). Characterization of a novel putative xer-dependent integrative mobile element carrying the blaNMC-A carbapenemase gene, inserted into the chromosome of members of the *Enterobacter cloacae* complex. *Antimicrob. Agents Chemother.* 59, 6620–6624. doi: 10.1128/AAC.01452-15

Aoki, K., Harada, S., Yahara, K., Ishii, Y., Motooka, D., Nakamura, S., et al. (2018). Molecular characterization of IMP-1-producing *Enterobacter cloacae* complex isolates in Tokyo. *Antimicrob. Agents Chemother.* 62, e2091–e2017. e02091-17, doi: 10.1128/AAC.02091-17

Balasubramanian, D., Schneper, L., Merighi, M., Smith, R., Narasimhan, G., Lory, S., et al. (2012). The regulatory repertoire of *Pseudomonas aeruginosa* AmpC β-lactamase regulator AmpR includes virulence genes. *PLoS One* 7:e34067. doi: 10.1371/journal.pone.0034067

Bankevich, A., Nurk, S., Antipov, D., Gurevich, A. A., Dvorkin, M., Kulikov, A. S., et al. (2012). SPAdes: a new genome assembly algorithm and its applications to single-cell sequencing. *J. Comput. Biol.* 19, 455–477. doi: 10.1089/cmb.2012.0021

Boyd, D. A., Mataseje, L. F., Davidson, R., Delport, J. A., Fuller, J., Hoang, L., et al. (2017). *Enterobacter cloacae* complex isolates harboring blaNMC-A or blaIMI-type class A carbapenemase genes on novel chromosomal integrative elements and plasmids. *Antimicrob. Agents Chemother.* 61:e02578-16. doi: 10.1128/AAC.02578-16

Bradford, M. M. (1976). A rapid and sensitive method for the quantitation of microgram quantities of protein utilizing the principle of protein-dye binding. *Anal. Biochem.* 72, 248–254. doi: 10.1006/abio.1976.9999

Caille, O., Zincke, D., Merighi, M., Balasubramanian, D., Kumari, H., Kong, K. F., et al. (2014). Structural and functional characterization of *Pseudomonas aeruginosa* global regulator AmpR. *J. Bacteriol.* 196, 3890–3902. doi: 10.1128/JB.01997-14

Carattoli, A., Zankari, E., Garcia-Fernandez, A., Voldby Larsen, M., Lund, O., Villa, L., et al. (2014). PlasmidFinder and pMLST: in silico detection and typing of plasmids. *Antimicrob. Agents Chemother.* 58, 3895–3903.

Chavda, K. D., Chen, L., Fouts, D. E., Sutton, G., Brinkac, L., Jenkins, S. G., et al. (2016). Comprehensive genome analysis of carbapenemase-producing *Enterobacter* spp.: new insights into phylogeny, population structure, and resistance mechanisms. *mBio* 7:e02093-16. doi: 10.1128/mBio.02093-16

Chun, J., and Rainey, F. A. (2014). Integrating genomics into the taxonomy and systematics of the bacteria and archaea. *Int. J. Syst. Evol. Microbiol.* 64, 316–324. doi: 10.1099/ijs.0.054171-0

CLSI (2018). *Performance Standards for Antimicrobial Susceptibility Testing*, 28th Edn. Wayne, PA: Clinical and Laboratory Standards Institute.

Dallenne, C., Da Costa, A., Decre, D., Favier, C., and Arlet, G. (2010). Development of a set of multiplex PCR assays for the detection of genes encoding important β-lactamases in *Enterobacteriaceae*. *J. Antimicrob. Chemother.* 65, 490–495. doi: 10.1093/jac/dkp498

Davin-Regli, A., and Pages, J. M. (2015). *Enterobacter* aerogenes and *Enterobacter cloacae*; versatile bacterial pathogens confronting antibiotic treatment. *Front. Microbiol.* 6:392. doi: 10.3389/fmicb.2015.00392

Diene, S. M., and Rolain, J. M. (2014). Carbapenemase genes and genetic platforms in gram-negative bacilli: *Enterobacteriaceae*, *Pseudomonas* and *Acinetobacter* species. *Clin. Microbiol. Infect.* 20, 831–838. doi: 10.1111/1469-0691.12655

Doumith, M., Ellington, M. J., Livermore, D. M., and Woodford, N. (2009). Molecular mechanisms disrupting porin expression in ertapenem-resistant *Klebsiella* and *Enterobacter* spp. clinical isolates from the UK. *J. Antimicrob. Chemother.* 63, 659–667. doi: 10.1093/jac/dkp029

Drawz, S. M., and Bonomo, R. A. (2010). Three decades of β-lactamase inhibitors. *Clin. Microbiol. Rev.* 23, 160–201.

Goris, J., Konstantinidis, K. T., Klappenbach, J. A., Coenye, T., Vandamme, P., and Tiedje, J. M. (2007). DNA-DNA hybridization values and their relationship to whole-genome sequence similarities. *Int. J. Syst. Evol. Microbiol.* 57, 81–91. doi: 10.1099/ijs.0.64483-0

Guerin, F., Isnard, C., Cattoir, V., and Giard, J. C. (2015). Complex regulation pathways of AmpC-mediated β-lactam resistance in *Enterobacter cloacae* complex. *Antimicrob. Agents Chemother.* 59, 7753–7761. doi: 10.1128/AAC.01729-15

Hong, S. S., Kim, K., Huh, J. Y., Jung, B., Kang, M. S., and Hong, S. G. (2012). Multiplex PCR for rapid detection of genes encoding class A carbapenemases. *Ann. Lab. Med.* 32, 359–361. doi: 10.3343/alm.2012.32.5.359

Jacoby, G. A. (2009). AmpC β-lactamases. *Clin. Microbiol. Rev.* 22, 161–182.

Johansson, M. H. K., Bortolaia, V., Tansirichaiya, S., Aarestrup, F. M., Roberts, A. P., and Petersen, T. N. (2021). Detection of mobile genetic elements associated with antibiotic resistance in *Salmonella enterica* using a newly developed web tool: mobile element finder. *J. Antimicrob. Chemother.* 76, 101–109. doi: 10.1093/jac/dkaa390

Kaneko, K., Okamoto, R., Nakano, R., Kawakami, S., and Inoue, M. (2005). Gene mutations responsible for overexpression of AmpC β-lactamase in some clinical isolates of *Enterobacter cloacae*. *J. Clin. Microbiol.* 43, 2955–2958. doi: 10.1128/JCM.43.6.2955-2958.2005

Kuga, A., Okamoto, R., and Inoue, M. (2000). ampR gene mutations that greatly increase class C β-lactamase activity in *Enterobacter cloacae*. *Antimicrob. Agents Chemother.* 44, 561–567. doi: 10.1128/AAC.44.3.561-567.2000

Mariotte-Boyer, S., Nicolas-Chanoine, M. H., and Labia, R. (1996). A kinetic study of NMC-A β-lactamase, an Ambler class A carbapenemase also hydrolyzing cephamycins. *FEMS Microbiol Lett* 143, 29–33. doi: 10.1111/j.1574-6968.1996.tb08457.x

Mezzatesta, M. L., Gona, F., and Stefani, S. (2012). *Enterobacter cloacae* complex: clinical impact and emerging antibiotic resistance. *Future Microbiol.* 7, 887–902. doi: 10.2217/fmb.12.61

Miyoshi-Akiyama, T., Hayakawa, K., Ohmagari, N., Shimojima, M., and Kirikae, T. (2013). Multilocus sequence typing (MLST) for characterization of *Enterobacter cloacae*. *PLoS One* 8:e66358. doi: 10.1371/journal.pone.0066358

Moura, A., Soares, M., Pereira, C., Leitao, N., Henriques, I., and Correia, A. (2009). INTEGRALL: a database and search engine for integrons, integrases and gene cassettes. *Bioinformatics* 25, 1096–1098. doi: 10.1093/bioinformatics/btp105

Naas, T., Massuard, S., Garnier, F., and Nordmann, P. (2001). AmpD is required for regulation of expression of NmcA, a carbapenem-hydrolyzing β-lactamase of *Enterobacter cloacae*. *Antimicrob. Agents Chemother.* 45, 2908–2915. doi: 10.1128/AAC.45.10.2908-2915.2001

Naas, T., and Nordmann, P. (1994). Analysis of a carbapenem-hydrolyzing class A β-lactamase from *Enterobacter cloacae* and of its LysR-type regulatory protein. *Proc. Natl. Acad. Sci. U.S.A.* 91, 7693–7697. doi: 10.1073/pnas.91.16.7693

Nakano, A., Nakano, R., Suzuki, Y., Saito, K., Kasahara, K., Endo, S., et al. (2018). Rapid Identification of blaIMP-1 and blaIMP-6 by multiplex amplification refractory mutation system PCR. *Ann. Lab. Med.* 38, 378–380.

Nakano, R., Nakano, A., Hikosaka, K., Kawakami, S., Matsunaga, N., Asahara, M., et al. (2014). First report of metallo-β-lactamase NDM-5-producing *Escherichia coli* in Japan. *Antimicrob. Agents Chemother.* 58, 7611–7612.

Nakano, R., Nakano, A., Yano, H., and Okamoto, R. (2017). Role of AmpR in the high expression of the plasmid-encoded AmpC β-lactamase CFE-1. *mSphere* 2:e00192-17. doi: 10.1128/mSphere.00192-17

Nakano, R., Okamoto, R., Nakano, Y., Kaneko, K., Okitsu, N., Hosaka, Y., et al. (2004). CFE-1, a novel plasmid-encoded AmpC β-lactamase with an ampR gene originating from *Citrobacter freundii*. *Antimicrob. Agents Chemother.* 48, 1151–1158. doi: 10.1128/AAC.48.4.1151-1158.2004

Nordmann, P., Mariotte, S., Naas, T., Labia, R., and Nicolas, M. H. (1993). Biochemical properties of a carbapenem-hydrolyzing β-lactamase from *Enterobacter cloacae* and cloning of the gene into *Escherichia coli*. *Antimicrob. Agents Chemother.* 37, 939–946. doi: 10.1128/AAC.37.5.939

Ohno, Y., Nakamura, A., Hashimoto, E., Matsutani, H., Abe, N., Fukuda, S., et al. (2017). Molecular epidemiology of carbapenemase-producing *Enterobacteriaceae* in a primary care hospital in Japan, 2010-2013. *J. Infect. Chemother.* 23, 224–229.

Peirano, G., Matsumura, Y., Adams, M. D., Bradford, P., Motyl, M., Chen, L., et al. (2018). Genomic epidemiology of global carbapenemase-producing *Enterobacter* spp., 2008-2014. *Emerg. Infect. Dis.* 24, 1010–1019. doi: 10.3201/eid2406.171648

Poirel, L., Walsh, T. R., Cuvillier, V., and Nordmann, P. (2011). Multiplex PCR for detection of acquired carbapenemase genes. *Diagn. Microbiol. Infect. Dis.* 70, 119–123. doi: 10.1016/j.diagmicrobio.2010.12.002

Pottumarthy, S., Moland, E. S., Juretschko, S., Swanzy, S. R., Thomson, K. S., and Fritsche, T. R. (2003). NmcA carbapenem-hydrolyzing enzyme in *Enterobacter cloacae* in North America. *Emerg. Infect. Dis.* 9, 999–1002. doi: 10.3201/eid0908.030096

Radice, M., Power, P., Gutkind, G., Fernandez, K., Vay, C., Famiglietti, A., et al. (2004). First class a carbapenemase isolated from *enterobacteriaceae* in

Argentina. *Antimicrob. Agents Chemother.* 48, 1068–1069. doi: 10.1128/AAC.48.3.1068-1069.2004

Schmidtke, A. J., and Hanson, N. D. (2006). Model system to evaluate the effect of ampD mutations on AmpC-mediated β-lactam resistance. *Antimicrob. Agents Chemother.* 50, 2030–2037. doi: 10.1128/AAC.01458-05

Walther-Rasmussen, J., and Hoiby, N. (2007). Class A carbapenemases. *J. Antimicrob. Chemother.* 60, 470–482.

Conflict of Interest: RS and MO were employed by the company BML Inc.

The remaining authors declare that the research was conducted in the absence of any commercial or financial relationships that could be construed as a potential conflict of interest.

Publisher's Note: All claims expressed in this article are solely those of the authors and do not necessarily represent those of their affiliated organizations, or those of the publisher, the editors and the reviewers. Any product that may be evaluated in this article, or claim that may be made by its manufacturer, is not guaranteed or endorsed by the publisher.

frontiers in Microbiology

ORIGINAL RESEARCH
published: 13 January 2022
doi: 10.3389/fmicb.2021.752535

Structural Insights for Core Scaffold and Substrate Specificity of B1, B2, and B3 Metallo-β-Lactamases

Yeongjin Yun[1†], Sangjun Han[1†], Yoon Sik Park[1], Hyunjae Park[1], Dogyeong Kim[1], Yeseul Kim[1], Yongdae Kwon[1], Sumin Kim[1], Jung Hun Lee[2], Jeong Ho Jeon[2], Sang Hee Lee[2] and Lin-Woo Kang[1]**

[1] Department of Biological Sciences, Konkuk University, Seoul, South Korea, [2] National Leading Research Laboratory of Drug Resistance Proteomics, Department of Biological Sciences, Myongji University, Yongin, South Korea

Metallo-β-lactamases (MBLs) hydrolyze almost all β-lactam antibiotics, including penicillins, cephalosporins, and carbapenems; however, no effective inhibitors are currently clinically available. MBLs are classified into three subclasses: B1, B2, and B3. Although the amino acid sequences of MBLs are varied, their overall scaffold is well conserved. In this study, we systematically studied the primary sequences and crystal structures of all subclasses of MBLs, especially the core scaffold, the zinc-coordinating residues in the active site, and the substrate-binding pocket. We presented the conserved structural features of MBLs in the same subclass and the characteristics of MBLs of each subclass. The catalytic zinc ions are bound with four loops from the two central β-sheets in the conserved αβ/βα sandwich fold of MBLs. The three external loops cover the zinc site(s) from the outside and simultaneously form a substrate-binding pocket. In the overall structure, B1 and B2 MBLs are more closely related to each other than they are to B3 MBLs. However, B1 and B3 MBLs have two zinc ions in the active site, while B2 MBLs have one. The substrate-binding pocket is different among all three subclasses, which is especially important for substrate specificity and drug resistance. Thus far, various classes of β-lactam antibiotics have been developed to have modified ring structures and substituted R groups. Currently available structures of β-lactam-bound MBLs show that the binding of β-lactams is well conserved according to the overall chemical structure in the substrate-binding pocket. Besides β-lactam substrates, B1 and cross-class MBL inhibitors also have distinguished differences in the chemical structure, which fit well to the substrate-binding pocket of MBLs within their inhibitory spectrum. The systematic structural comparison among B1, B2, and B3 MBLs provides in-depth insight into their substrate specificity, which will be useful for developing a clinical inhibitor targeting MBLs.

Keywords: metallo-β-lactamase (MBL), β-lactams, metal coordination, substrate specificity, β-lactamase inhibitor, antibiotic resistance

OPEN ACCESS

Edited by:
Mary Marquart, University of Mississippi Medical Center, United States

Reviewed by:
Sung-Kun (Sean) Kim, Northeastern State University, United States
Gerhard Schenk, The University of Queensland, Australia
Zainab Edoo, Institut Pasteur de Lille, France

***Correspondence:**
Sang Hee Lee
sangheelee@mju.ac.kr
Lin-Woo Kang
lkang@konkuk.ac.kr

[†] These authors have contributed equally to this work

Specialty section:
This article was submitted to Antimicrobials, Resistance and Chemotherapy, a section of the journal Frontiers in Microbiology

Received: *03 August 2021*
Accepted: *22 December 2021*
Published: *13 January 2022*

Citation:
Yun Y, Han S, Park YS, Park H, Kim D, Kim Y, Kwon Y, Kim S, Lee JH, Jeon JH, Lee SH and Kang L-W (2022) Structural Insights for Core Scaffold and Substrate Specificity of B1, B2, and B3 Metallo-β-Lactamases. Front. Microbiol. 12:752535. doi: 10.3389/fmicb.2021.752535

INTRODUCTION

The increasing incidence of multidrug-resistant (MDR) bacteria is a global health concern (Laxminarayan et al., 2013; Berendonk et al., 2015; Lee et al., 2016). β-lactams constitute 60% of current antibiotics; thus far, they have been the most applicable and useful class of antibiotics (Ozturk et al., 2015). However, the frequent clinical use of β-lactams has caused selective pressure, resulting in the rapid appearance of bacterial resistance to β-lactams. The most common mechanism of β-lactam resistance among MDR bacteria is the production of β-lactamases, which hydrolyze β-lactams into inactive forms (Paterson et al., 2020; Bahr et al., 2021). The evolution and catalytic mechanisms of various β-lactamases have been studied (Hall and Barlow, 2004; Sidjabat et al., 2018; Lee et al., 2019; Park et al., 2020; Pedroso et al., 2020). β-lactamases can be divided into serine β-lactamases and metallo- β-lactamases (MBLs). MBLs hydrolyze most β-lactams, including last resort antibiotics carbapenems. There are currently no effective and clinically available inhibitors against MBLs (Fisher et al., 2005). MBLs are further classified into the B1, B2, and B3 subclasses depending on their sequence, structure, and zinc ion site(s) and have diverse substrate profile or specificity for β-lactams (Crowder et al., 2006; Palacios et al., 2019; Behzadi et al., 2020; Park et al., 2020).

The substrate profile of MBLs is related to the antimicrobial susceptibility of MBL producers and is essential for the adequate treatment of patients with MBL-producing MDR bacteria (Lutgring et al., 2020). However, the main interest of antibiotic resistance study has been the efficacy and effectiveness of specific antibiotics and inhibitors on MDR bacteria in clinical use. The previous study of the substrate profile showed that B1 and B3 MBLs have a broad substrate spectrum, and B2 MBLs degrade only carbapenems (Bahr et al., 2021). Even in a subclass, there are many different types of MBLs and a growing number of variants, which also could have diverse hydrolytic activities on β-lactams; thus far, 710 MBLs of 509 B1, 22 B2, and 179 B3 members were reported (Naas et al., 2017). Independent research groups have studied the substrate profile and enzyme kinetics of MBLs with varied assay conditions. There are only limited numbers of MBL structures available for the study of structure-function relationships. The complexity and insufficiency of MBL data have prohibited the systematic study of the structure-based substrate specificity of MBLs. Herein, we compared several tens of B1, B2, and B3 MBLs in sequence and structure and proposed structural insights on the substrate specificity of MBLs. The specificity of the substrate-binding pocket of MBLs was also verified by B1 and cross-class MBL inhibitors binding to the same substrate-binding pocket. The cross-class inhibitors showed the complementary chemical structures to fit into the varied substrate-binding pockets of different subclasses of MBLs. The structural insights of MBLs will provide a valuable platform to understand the structure-function relationships of current and newly found putative MBLs and develop a broad-spectrum MBL inhibitor.

Scaffold of Metallo-β-Lactamases

The amino acid sequences of MBLs varied; the sequence identity among them could be as low as 10%. Within the same subclass, the B1, B2, and B3 MBLs had average sequence identities of 31.8, 60.2, and 33.0%, respectively (**Supplementary Table 1**). Although there was low sequence conservation, the MBL scaffold had the distinctive αβ/βα sandwich fold (**Figure 1A**) and was well conserved, as indicated by an RMSD value of 1.77 Å in approximately 220 residues (**Supplementary Table 2**). In the superimposed crystal structures of MBLs, there were conserved secondary structures of 5 α-helices and 13 β-strands as the core scaffold. The four loops of L1–4 coordinated the catalytic zinc ion(s), and the three external loops (eLs) eL1–3 formed the substrate-binding pocket (**Figure 1B**). The overall structure of the B1, B2, and B3 MBLs showed RMSD values of 1.45 in 205 residues, 0.65 in 223 residues, and 1.51 in 231 residues, respectively, among the members of the same subclass (**Supplementary Tables 3–5**).

The MBL structure can be divided into two parts at the interface between the two β-sheets (**Figure 1A**). The active site is located at the center between the two β-sheets, wherein the zinc ions are coordinated with various residues depending on each subclass (**Figures 1B**, **2**; Ullah et al., 1998; Fonseca et al., 2011b; King and Strynadka, 2011; Pedroso et al., 2020). The zinc-coordinating residues come from the L1–4 loops protruding from the two β-sheets. The zinc ions directly coordinate a catalytic water molecule, which is deprotonated to a hydroxide ion to attack the β-lactam ring of the substrate (**Supplementary Figure 1**). The central L1–4 loops are surrounded by the external loops eL1–3, which form the substrate-binding pocket and play an important role in the substrate specificity of MBLs (**Figures 1B**, **3**).

Representative Metallo-β-Lactamases in Each Subclass

Although many MBLs from the three different subclasses have been studied in parallel, these comparisons were mainly related to the catalytic zinc ion(s) and the sequence and structure of the coordinating residues. There is only limited comparative information about the structure of the core scaffold, the substrate-binding pocket, and the relationship between drug resistance and structure. In this study, we performed a systematic comparison of the sequence and structure of MBLs, both with protein alone and in complex with substrate antibiotics. First, the sequences and structures of MBLs were compared within the same subclass. Second, the representative MBL structures from each subclass were compared with those from the other subclasses. Finally, the β-lactam or inhibitor-bound B1, B2, and B3 MBL structures were studied based on the characteristics of each subclass.

For structural comparison, 11, 2, and 8 MBLs were selected from the B1, B2, and B3 subclasses, respectively (**Figure 2** and **Supplementary Figures 2–4**). These MBLs included the New Delhi metallo- β-lactamase (NDM-1) (PDB ID: 3S0Z, Guo et al., 2011), BlaB-1 (1M2X, Garcia-Saez et al., 2003a), VIM-2 (4NQ2, Aitha et al., 2014), DIM-1 (4ZEJ, Booth et al., 2015), IMP-1 (5EV6, Hinchliffe et al., 2016), TMB-1 (5MMD, Skagseth et al., 2017), SPS-1 (6CQS, Cheng et al., 2018), ECV-1 (6T5K, Frohlich et al., 2020), MYO-1 (6T5L, Frohlich et al., 2020), FIM-1 (6V3Q), and GIM-1 (2YNT, Borra et al., 2013)

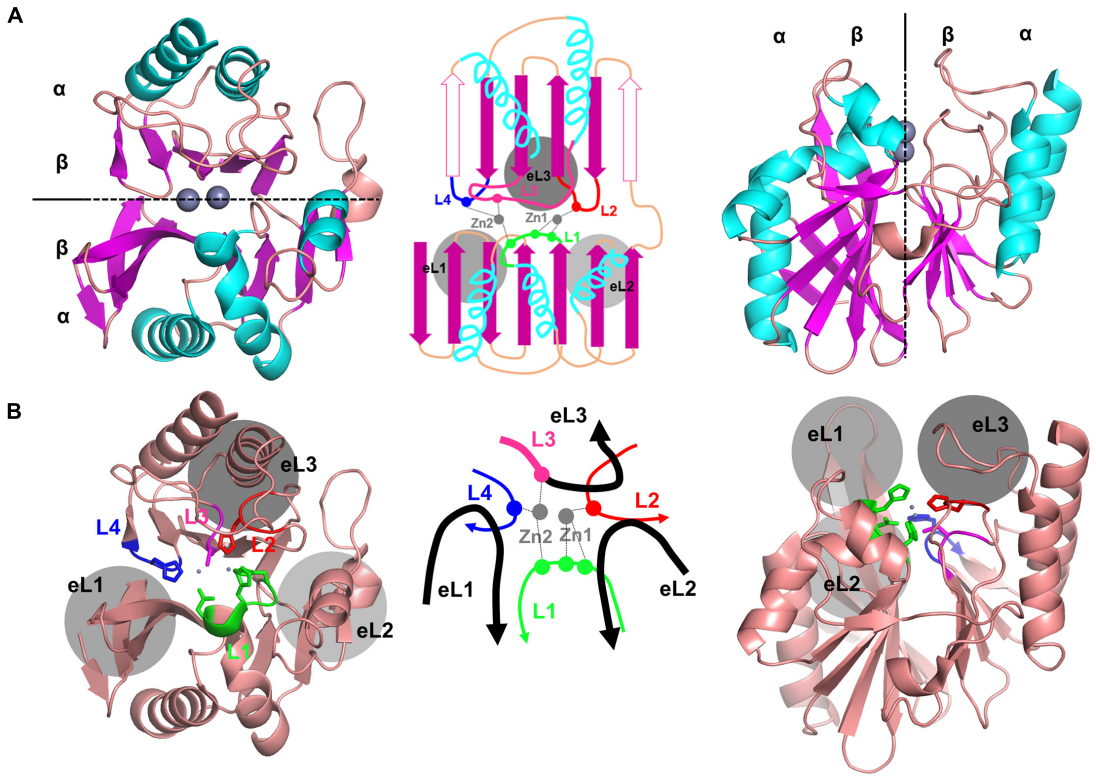

FIGURE 1 | The crystal structure of NDM-1, showing the representative core scaffold of MBLs. **(A)** The αβ/βα sandwich fold of NDM-1, which is the core scaffold of MBLs, is shown at the top (left) and side (right). The schematic representation is shown in the middle. The central two β-sheets and the five α-helices in the main scaffold are shown in purple and cyan, respectively. The two zinc ions are shown in gray. Certain β-strands in the second β-sheet exist as α-helices in some MBLs, which are shown as open purple arrows in the schematic representation (middle). **(B)** The overall structure of NMD-1 with the zinc-coordinating central loops L1–4 and the substrate-binding pocket forming the external loops eL1–3. The schematic representation of the central and external loops with zinc ions is shown in the middle. L3 is the N-terminal part of eL3.

in B1; CphA (1X8G, Garau et al., 2005) and SfhI (5EW0, Hinchliffe et al., 2016) in B2; and Adelaide imipenemase (AIM-1) (4AWZ, Leiros et al., 2012), GOB-18 (5K0W, Moran-Barrio et al., 2016), FEZ-1 (1K07, Garcia-Saez et al., 2003b), Rm3 (5IQK, Salimraj et al., 2016), SMB-1 (3VPE, Wachino et al., 2013), L1 (2AIO, Spencer et al., 2005), BJP-1 (5NJW, Di Pisa et al., 2018), and LRA-12 (5AEB, Rodriguez et al., 2017) in B3. Among them, NDM-1 in the B1 subclass (Khan et al., 2017), CphA in the B2 subclass (Hernandez Valladares et al., 1997), and AIM-1 in the B3 subclass (Yong et al., 2012) were selected as the representative MBLs of each subclass for structural comparison (**Figure 3**). NDM-1 is found in the clinically important *Klebsiella pneumoniae*, *Enterobacter cloacae*, *Pseudomonas* spp., and *Acinetobacter baumannii,* and is mostly found in plasmids. NMD-1 hydrolyzes a wide range of β-lactams (Khan et al., 2017) and NDM-1 producers are resistant to imipenem, meropenem, ertapenem, gentamicin, amikacin, tobramycin, and ciprofloxacin; meanwhile, NDM-1 producers are susceptible to colistin and tigecycline (Kumarasamy et al., 2010). CphA was originally found in *Aeromonas hydrophila* and has a narrow substrate specificity for carbapenems (Hernandez Valladares et al., 1997). AIM-1 was found in *P. aeruginosa* and hydrolyzes a wide range of substrates, such as imipenem, meropenem, penicillin G, piperacillin, cephalothin, cefoxitin, and cefepime; however, it has no activity against aztreonam (Yong et al., 2012; Selleck et al., 2016).

When we performed structural sequence alignment, the internal sequence identity among MBLs within the same subclass was higher than that between the MBLs of different subclasses. NDM-1 was compared with 10 other MBLs in B1; CphA was compared with SfhI in B2: and AIM-1 was compared with seven other MBLs in B3 (**Supplementary Table 1**). The RMSD value was 1.45 Å in approximately 205 residues when comparing NDM-1 with the selected members in B1. The RMSD values comparing NDM-1 for B2 and B3 MBLs were 1.42 Å in approximately 195 residues and 2.25 Å in approximately 176 residues, respectively (**Supplementary Tables 2–5**). These results show that the overall scaffold is more similar between B1 and B2 MBLs than between B3 MBLs and the other two subclasses.

B1 Subclass

Members of the B1 subclass exist in large numbers and contain many clinically important MDLs, such as NDMs, Verona integrin-encoded MBLs (VIMs), imipenemases (IMPs), and German imipenemases (GIMs). In the B1 subclass, 11 MBLs, including NDM-1 (PDB ID: 3S0Z, Guo et al., 2011), VIM-2

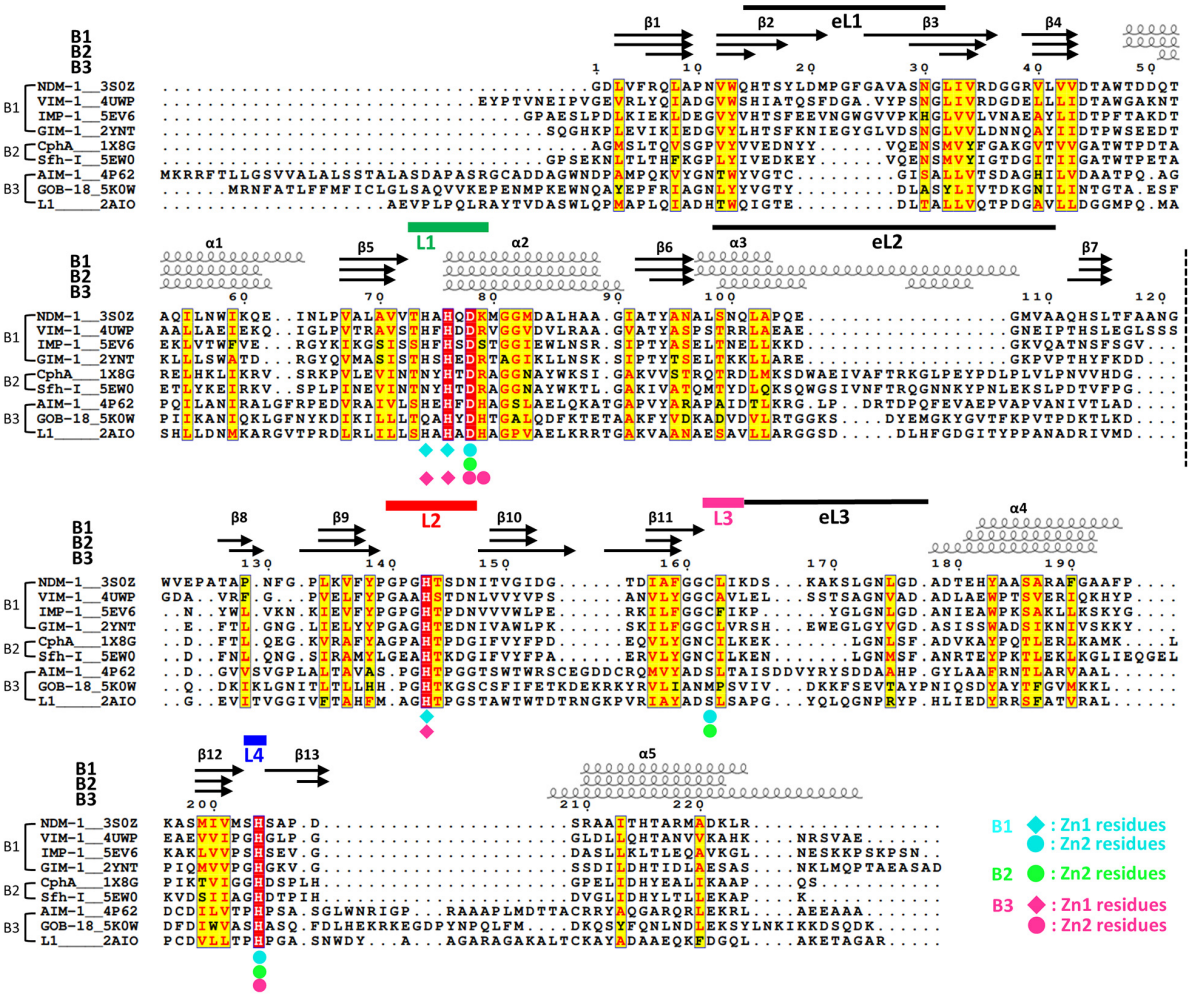

FIGURE 2 | The structural sequence alignment of MBLs. The secondary structures of NDM-1, CphA, and AIM-1 are shown at the top. The labels B1, B2, and B3 show the representative member of each subclass. The numbering of secondary structures is based on the core scaffold of 13 β-strands and 5 α-helices. In some B3 MBLs, including AIM-1, an additional α-helix (α3′) exists after α3. The first and second halves of the αβ/βα sandwich fold are divided by a dashed line between the β7 and β8 strands. The zinc-coordinating residues of the B1, B2, and B3 subclasses are shown as diamonds and circles in cyan, green, and pink, respectively. The four zinc-coordinating loops L1, L2, L3, and L4 are shown as thick green, red, pink, and blue lines, respectively. The three external loops eL1, eL2, and eL3 are shown as thin black lines.

(4NQ2, Aitha et al., 2014), IMP-1 (5EV6, Hinchliffe et al., 2016), and GIM-1 (2YNT, Borra et al., 2013), were chosen as representative B1 MBLs (**Supplementary Figure 2**).

When the crystal structures of the representative B1 members were superimposed, the RMSD values among structures were between 1.06 and 1.76 Å in 205 residues. This finding shows that the overall scaffold is well conserved within the B1 subclass (**Supplementary Table 3**). The two central β-sheets in a core scaffold generally consist of seven β-strands and six β-strands in the first and second β-sheets, respectively (**Figure 1A**). Even though the terminal β-strands located at the ends of β-sheets are often changed to an α-helix or loop in certain members, the overall scaffold is well conserved (**Figure 3A**). The N-terminal sequences also varied; before the β1 strand, additional secondary structures could exist, such as an additional α-helix or β-strand (**Supplementary Figure 5**). Among the 13 β-strands, β2 and β3 are long, and β1 is only half the length of β2. The protruding tips of β2 and β3 of eL1 have a flexible conformation (Raczynska et al., 2020).

The two zinc ions are coordinated with four loops in the active site: short L1, long L2, extralong L3, and short L4 (**Figure 3A**). The first zinc ion, Zn1, is coordinated with three His residues (two from L1 and one from L2), and the second zinc ion, Zn2, is coordinated with Asp, Cys, and His residues from L1, L3, and L4, respectively. All six residues are strictly conserved in the sequences of B1 MBLs; among the 11 MBLs in B1, only SPS-1 loses one His residue in L1 (**Supplementary Figure 2**). All the zinc-coordinating residues exist at the tip of the secondary structures of the helix and strand; they are tightly wrapped in the center with three external loops (eL1–3) from the outside. The stable zinc-coordinating residues contain two metal ions at the catalytic positions.

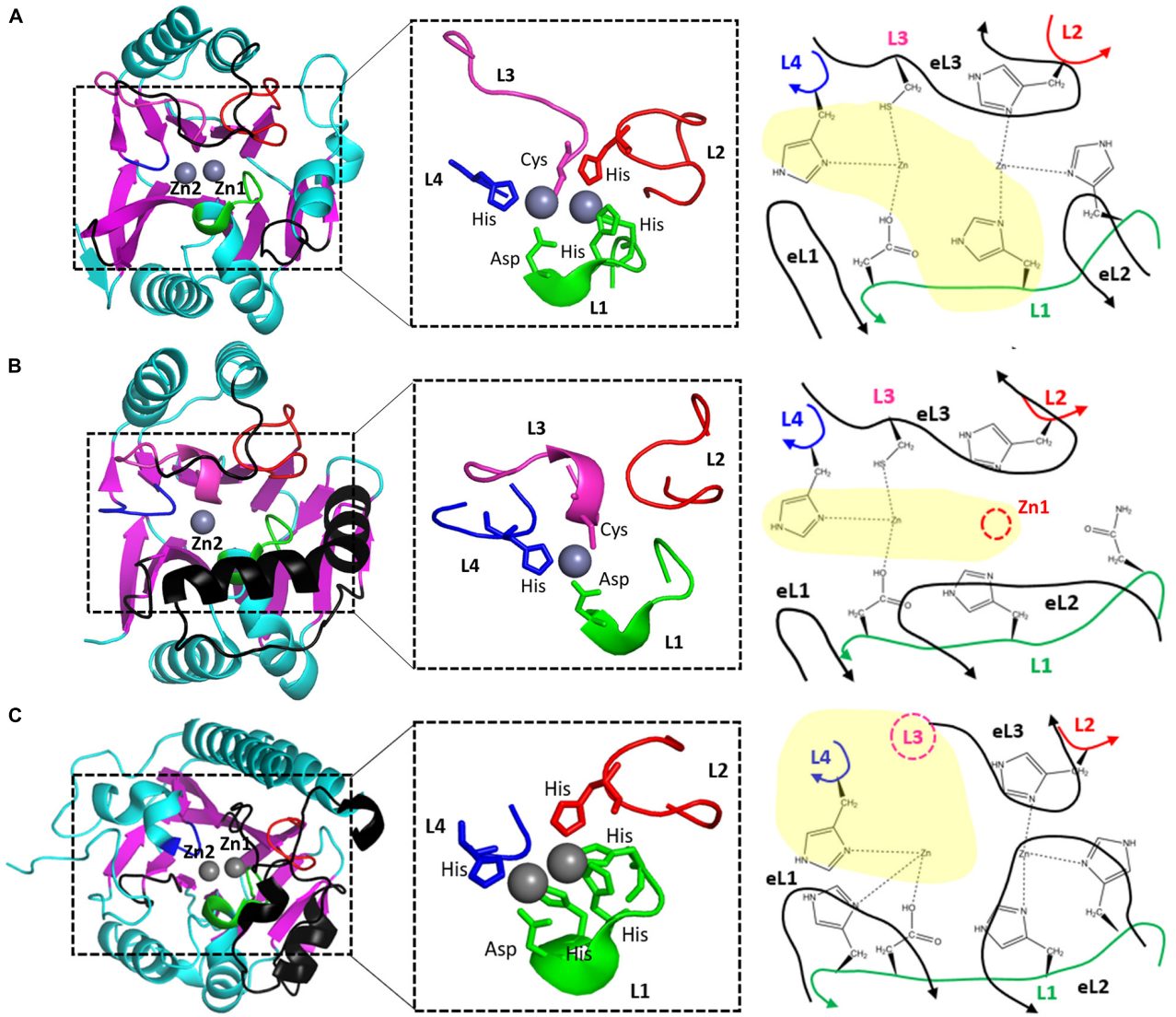

FIGURE 3 | The zinc coordination of **(A)** NDM-1, **(B)** CphA, and **(C)** AIM-1 as the representative B1, B2, and B3 MBLs. The schematic representations of zinc coordination are shown on the right. The four zinc-coordinating loops L1, L2, L3, and L4 are shown as green, red, pink, and blue lines, respectively. The three external loops eL1, eL2, and eL3 are shown as black lines. L3 is the N-terminal part of eL3 and is shown in black. The missing Zn1 ion and Zn2-coordinating residue from L3 are shown as red and pink dashed circles, respectively.

The three external loops eL1, eL2, and eL3, including L3, surround the zinc binding sites and form the substrate-binding pocket as three protruding fingers (**Figure 1B**). eL1 forms the left wall with long and flexible β2 and β3 (**Figure 4A**). At the bottom and right side of the pocket, eL2 provides a large hole in the central bottom of the pocket, which allows the flexible binding of bulky substrates. eL3 is extruded and shows a natural curvy-loop conformation to form the entire upper lip of the substrate-binding pocket.

B2 Subclass

B2 MBLs, existing in 3% among all known MBLs, include CphA (Garau et al., 2005), SfhI from *Serratia fonticola* (Hinchliffe et al., 2016), ImiS from *Aeromonas sobria* (Walsh et al., 1996), and AsbM1 from *Aeromonas sobria* (Yang and Bush, 1996) and preferentially hydrolyze carbapenems (Fonseca et al., 2011a). Among them, only two crystal structures of CphA (PDB ID: 1X8G, Garau et al., 2005) and SfhI (5EW0, Hinchliffe et al., 2016) were determined, and the RMSD value between them was 0.65 (**Supplementary Table 4**). B2 MBLs have a zinc ion in the Zn2 site, which is coordinated with Asp, Cys, and His residues and loses the other zinc ions at the Zn1 site (**Figure 3B** and **Supplementary Figure 3**).

In the B2 subclass, both structures of CphA and SfhI showed a well-conserved core scaffold of MBLs with two central β-sheets of seven β-strands and six β-strands (**Figure 3B**). β2 and β3 are shorter in the B2 subclass compared with the B1 subclass in their lengths, and the resulting lengths of β1, β2, and β3 are similar

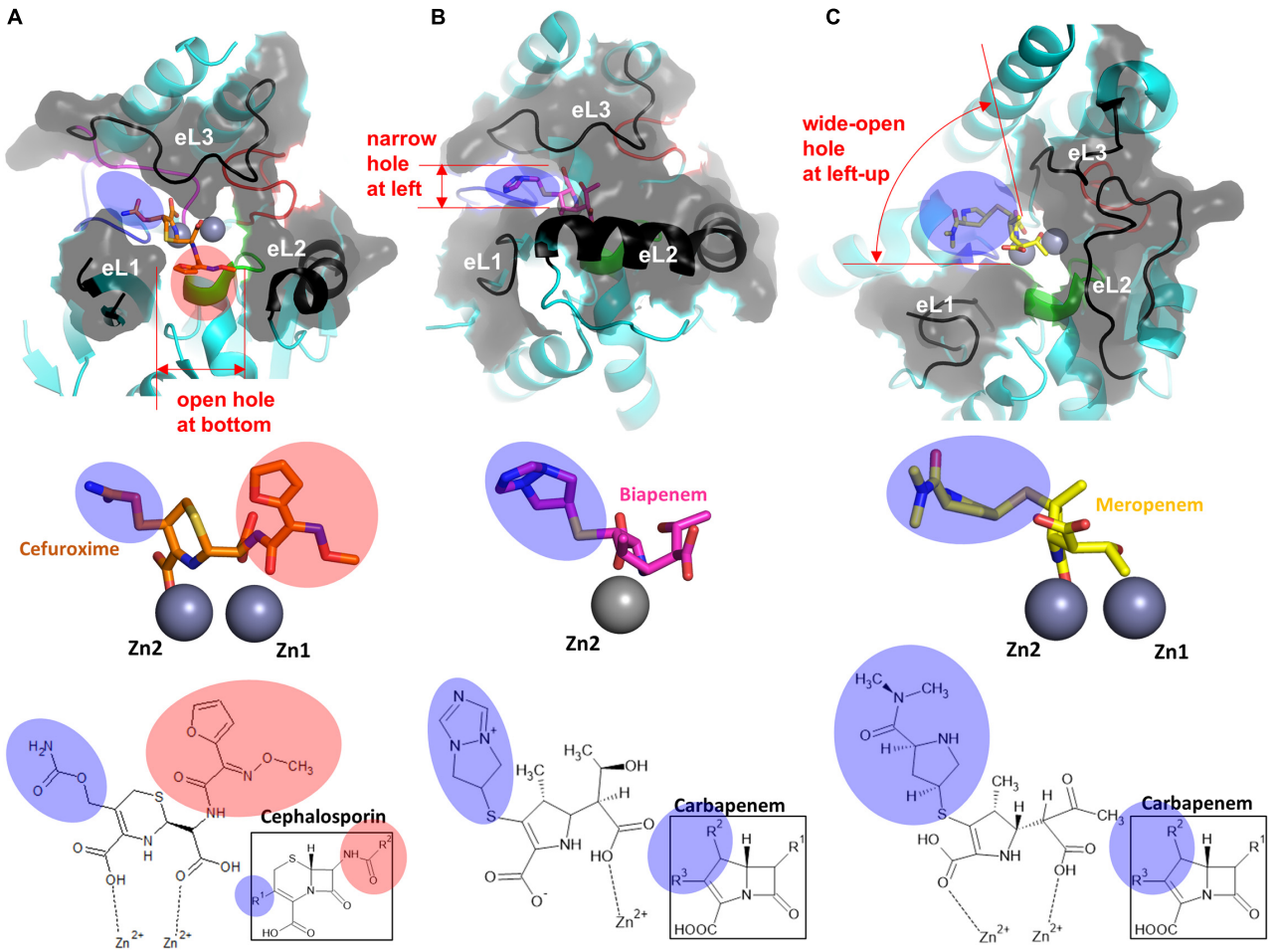

FIGURE 4 | The structure of the substrate-binding pocket forming eL1–3 of each subclass. The surface representation of eL1, eL2, and eL3 of **(A)** cefuroxime-bound NDM-1 (PDB ID: 3SPU), **(B)** biapenem-bound CphA (PDB ID: 1X8I), and **(C)** meropenem-bound SMB-1 (PDB ID: 5AXO) is shown at the top. The enlarged view of the hydrolyzed β-lactams with the zinc ion(s) is shown in the middle. The zinc ion(s)-bound chemical structures of β-lactams, including the core structures of each β-lactam group, are shown at the bottom. The substituted R groups at the four-member β-lactam ring are shaded in pink, and those at the five or six-membered dihydropyrrole ring or dihydrothiazine ring next to the β-lactam ring are shaded in blue.

(**Figure 2** and **Supplementary Figure 6**). The helix α3 is long and bent in the middle, and the end of long α3 is positioned close to eL1 (**Supplementary Figure 6**).

CphA lost the Zn1 ion and maintained only the Zn2 ion. All three Zn2-coordinating residues in CphA of Asp, Cys, and His from L1, L3, and L4, respectively, are conserved in B2 MBLs (**Supplementary Figure 3**). In the Zn1 site, the first His residue among the three conserved His residues is changed to an Asn residue with a shorter side chain, which is insufficient to coordinate Zn1 compared to the canonical His residue (**Figure 3B**). The remaining two His residues were not sufficient to bind the Zn1 ion in CphA.

Although the overall structures of the zinc-coordinating L1–4 loops in the active site of CphA are conserved with NMD-1, all three external loops forming the substrate-binding pocket are different (**Figure 4B**). eL1 is shorter because of the shorter β2 and β3 and provides a shallow left boundary of the substrate-binding pocket. eL2, consisting of long and bent helix α3, forms a solid wall in the lower lip of the substrate-binding pocket, which could restrain substrate binding and accordingly affect the substrate specificity of CphA. eL3 of the upper lip of the substrate-binding pocket is slightly shorter than that found in B1 MBLs but adopts a similar conformation.

B3 Subclass

B3 MBLs include SMB-1 (Wachino et al., 2013), AIM-1 (Leiros et al., 2012), L1 (Spencer et al., 2005), GOB-1 (Moran-Barrio et al., 2016), MIM-1 (Selleck et al., 2020), SAM-1 (Selleck et al., 2020), CSR-1 (Pedroso et al., 2020), SIE-1 (Wilson et al., 2021), SPR-1 (Vella et al., 2013), and LRA-8 (Pedroso et al., 2017). When the crystal structures of the eight selected B3 MBLs were superimposed, the RMSD values among the structures were between 0.90 and 1.73 Å, with an average value of 1.51 Å in 231 residues. These values suggest that the overall structures are well conserved within the B3 subclass (**Supplementary Table 5**). The B3 MBLs showed significant structural differences in the

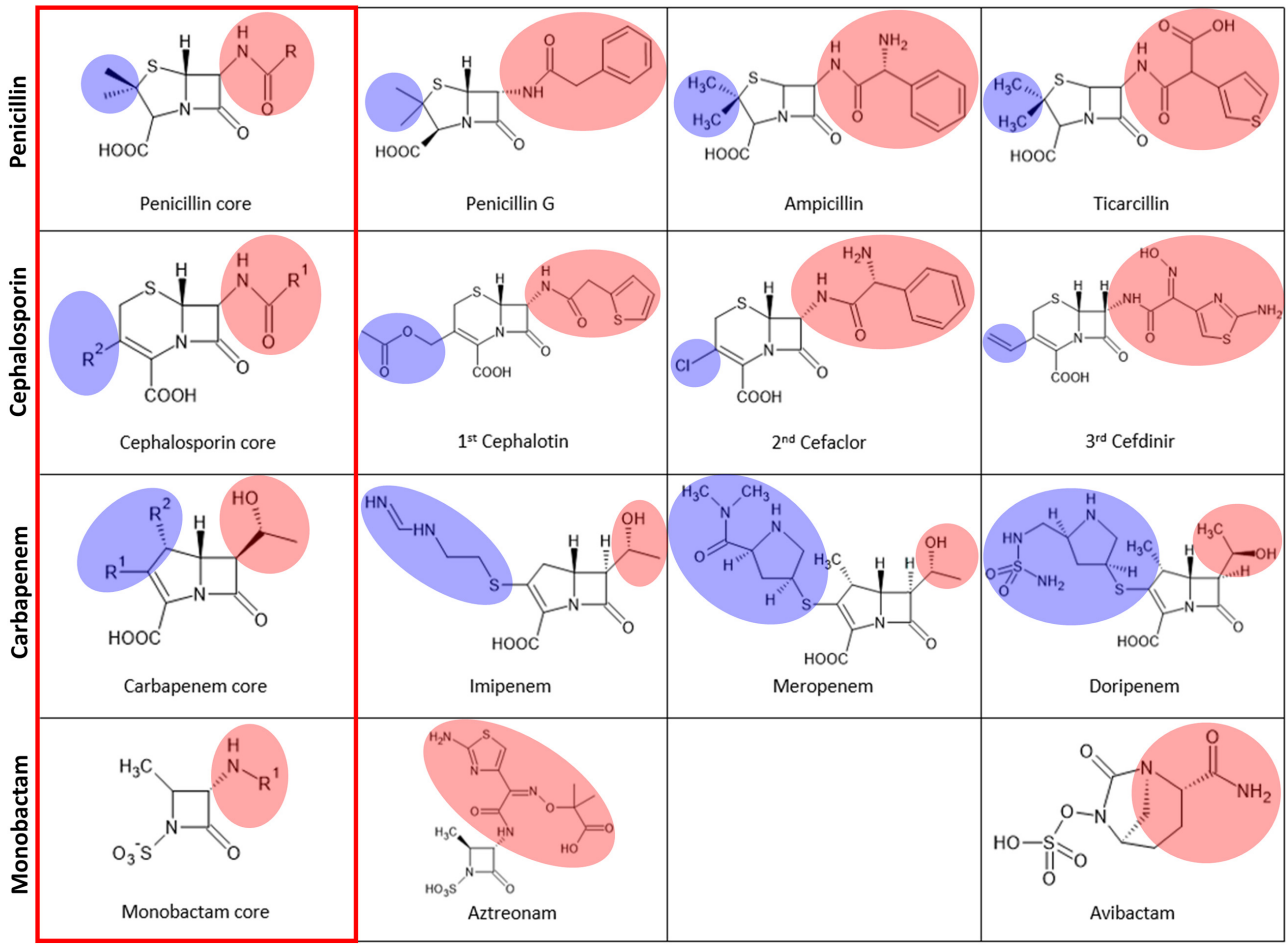

FIGURE 5 | The chemical structures of the four major classes of β-lactams. The left column, labeled with a red rectangle, shows the core scaffold of each type of β-lactam. The substituted R groups at the four-member β-lactam ring are shaded in pink, and those at the five or six-membered dihydropyrrole ring or dihydrothiazine ring next to the β-lactam ring are shaded in blue.

core scaffold compared to B1 and B2 MBLs (**Figure 3C**). In the central β-sheets of the core scaffold, β1, β2, and β3 from the first β-sheet are very short and a long N-terminal tail provides a flexible conformation of eL1; the second β-sheet consists of five β-strands instead of six β-strands, and the C-terminal β13 is changed to the helix (**Supplementary Figure 7**). The additional helix α3′ exists immediately after α3 and before β7. The long N-terminal tail forming eL1 showed varied relative positions in the different B3 MBL structures of L1, GOB-1, CSR-1, and AIM-1, which could affect the catalytic activity (Pedroso et al., 2020).

Although two zinc ions are bound in B3 MBLs, their coordination is different from that of B1 MBLs (Pedroso et al., 2020). In canonical B3 MBLs, the Zn1 ion is coordinated with three His residues like B1 MBLs. However, the Zn2 site of B3 MBLs was different from those of both B1 and B2 MBLs. The L3 of B3 MBLs was shorter than those of B1 and B2 MBLs without the Zn2 ion coordinating Cys residue, and its conformation was also different (**Figure 4C**). A compensatory His residue from the L1 loop is additionally involved to bind the Zn2 ion from the bottom position (**Figure 3C**). In the Zn1 site, the first His residue from the L1 loop is sometimes replaced with a Gln residue (**Supplementary Figure 4**). Compared to the corresponding Asn residue of B2 MBLs, the longer Gln side chain in B3 MBLs could be sufficient to coordinate and hold the Zn1 ion. Recently, B3 MBL variants with different zinc coordination residues in both zinc sites were also found, which implies the active site of B3 MBLs appears to be more diverse than those of B1 and B2 MBLs (Pedroso et al., 2020).

eL1, eL2, and eL3 of B3 MBLs were different from those of B1 and B2 MBLs (**Figure 3C**). In AIM-1, eL1 includes a long N-terminal tail loop, which exists close to the Zn2 site and forms the left wall of the substrate-binding pocket (**Figure 3C** and **Supplementary Figure 7**). Although the secondary structures of eL1 are different in B1 and B3 MBLs, the superimposed positions are similar. eL2 has the characteristic additional helix α3′, which is close to the long α3 in B2 members but has a different orientation (**Figure 3C**). The most significant change occurred in eL3. Without a Zn2-coordinating residue from L3, eL3 stretches straight outward from the second β-sheet, which causes eL3 to shift to the right side and generates a large hole in the upper and

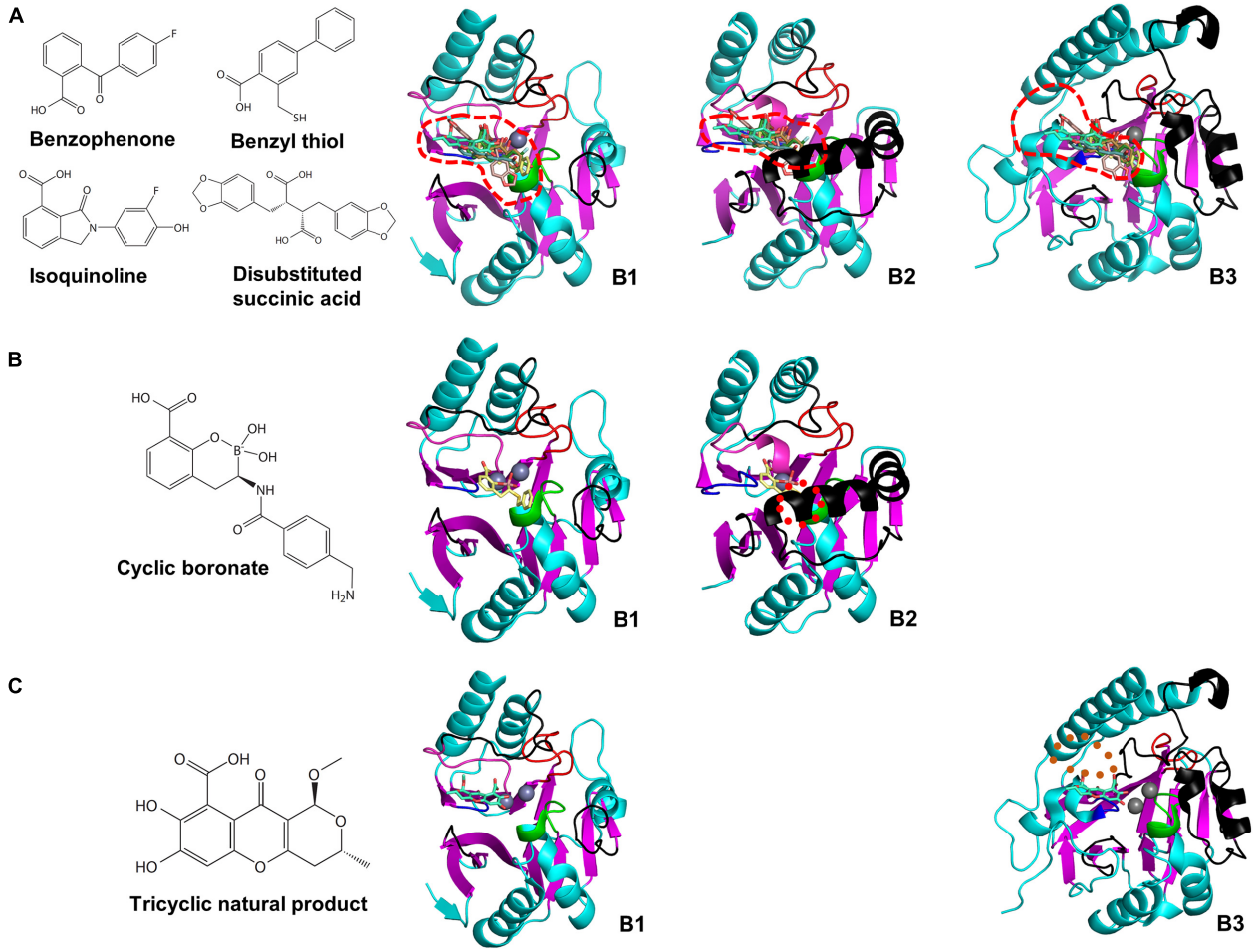

FIGURE 6 | The chemical structures of B1 MBL inhibitors and their superimposed structures on the representative B1, B2, and B3 MBLs. The chemical structures of **(A)** benzophenone, benzyl thiol, isoquinoline, disubstituted succinic acid, **(B)** cyclic boronate, and **(C)** tricyclic natural product, and their superimposed structures on the B1, B2, and B3 MBLs of NDM-1, CphA, and AIM-1, respectively. The substrate-binding pockets of the B1, B2, and B3 MBLs are represented by red dashed lines. The red dotted circle represents the clashed region between the superimposed cyclic boronate and the substrate-binding pocket of B2 MBL. The brown dotted oval represents the space between the tricyclic natural product and substrate-binding pocket of B3 MBL.

left lip. Generally, B3 MBLs have the upper left open space in the substrate-binding pocket to accommodate bulky R groups on β-lactam substrates (**Figure 4C** and **Supplementary Figure 7**).

Comparison Among the Metallo-β-Lactamases of the Three Subclasses

MBLs have zinc ion(s) in the active site on the top of two central β-sheets, and the substrate-binding pocket is formed mainly from the external loops protruding above the canonical αβ/βα MBL scaffold. Structural comparison among the MBLs B1 NDM-1, B2 CphA, and B3 AIM-1 revealed the characteristic structural features of each subclass in the core scaffold, zinc coordination, and substrate-binding pocket.

In the active site, both the Zn1 and Zn2 sites of NDM-1 and CphA were well superimposed (**Figure 3**). Although CphA does not have the Zn1 ion, the corresponding position of the Zn1 site was well superimposed. However, the zinc binding sites of AIM-1 were shifted to the lower left position compared to those of NDM-1 due to the change in the core scaffold. Within B3 MBLs, the correlation of the metal-metal distance in the active site was observed (Wilson et al., 2021). Interestingly, even in the shifted or different zinc positions, the interatomic distance between the two zinc ions was almost the same as that observed between NDM-1 and AIM-1 (3.45 Å). The average distance in all the selected B1 and B3 MBLs was 3.56 Å (**Supplementary Table 6**), which is sufficient to bind and coordinate the catalytic water molecule to hydrolyze the β-lactam ring of the substrates in the active site.

The shape of the substrate-binding pocket, which is mainly formed by the core scaffold and external loops, is important for substrate binding according to substrate specificity. Compared to the conserved coordination geometry of zinc binding sites in each subclass and the interatomic distance between the Zn1 and Zn2 ions, the structure of the substrate-binding pocket varies among the three subclasses: B1 MBLs have a long eL1, short eL2, and long

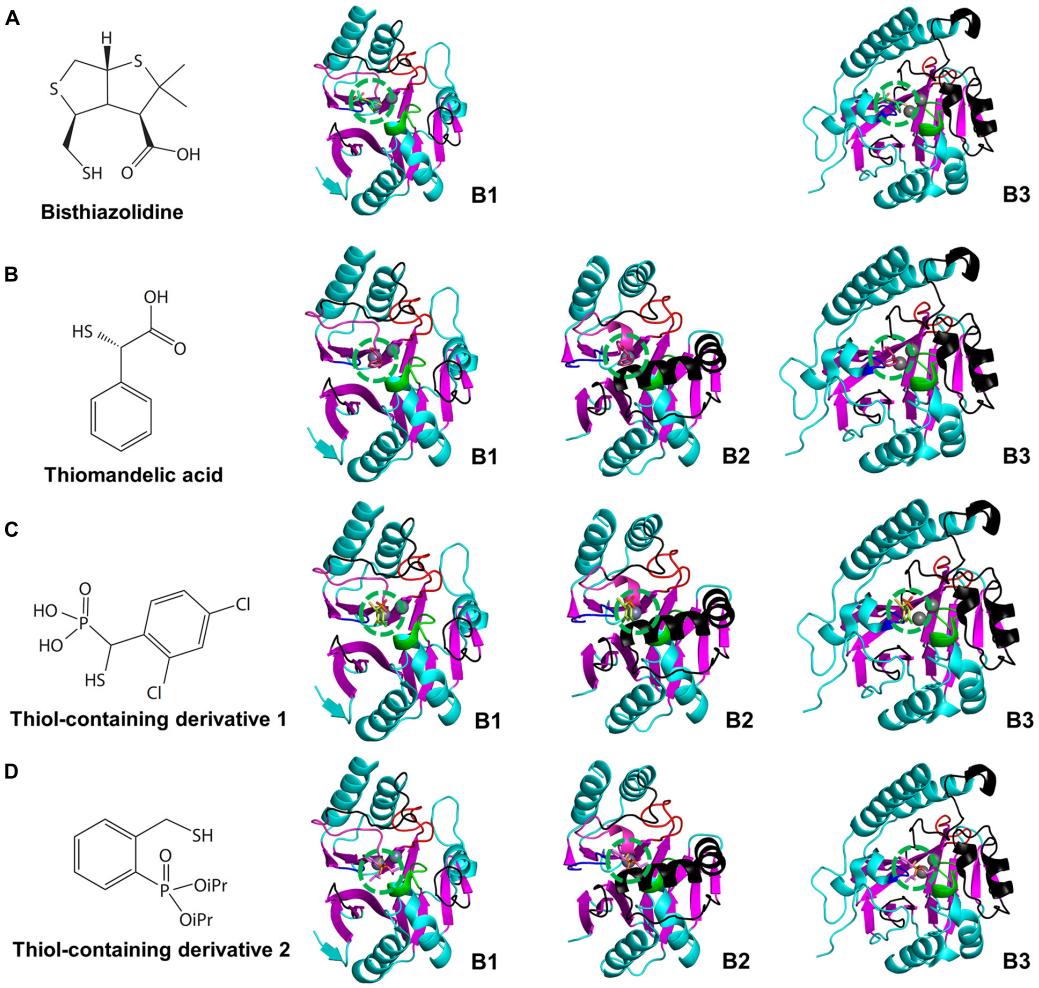

FIGURE 7 | The chemical structures of cross-class MBL inhibitors and their superimposed structures on the representative B1, B2, and B3 MBLs. The chemical structures of **(A)** bisthiazolidine, **(B)** thiomandelic acid, **(C,D)** thiol-containing derivatives and their superimposed structures on the B1, B2, and B3 MBLs of NDM-1, CphA, and AIM-1, respectively. The binding sites of the cross-class inhibitors are represented by green dashed circles. The binding sites are well conserved on top of the zinc-binding site(s). The superimposed cross-class MBL inhibitors with small globular shapes show limited steric hindrances with the substrate-binding pockets of the B1, B2, and B3 MBLs. In (D), iPR represents isopropyl group.

eL3; B2 MBLs have a short eL1, long eL2, and long eL3; and B3 MBLs have long eL1, long eL2, and short eL3 (**Figures 3**, **4**).

B1 MBLs have an open space in the left and central bottom positions in the substrate-binding pocket (**Figure 4A**). B2 MBLs have a narrow open space on the left side horizontal to the Zn1 and Zn2 sites. Furthermore, the bottom is blocked by the long eL2, forming a narrow substrate-binding pocket (**Figure 4B**). In B3 MBLs, both zinc ions are extensively exposed to solutions, and the left and upper sides of the substrate-binding pocket are wide open (**Figure 4C**). Only the short eL3 provides a shallow barrier on the upper and right sides of the substrate-binding pocket.

β-Lactam-Bound Metallo-β-Lactamases

The structures of β-lactam-bound MBLs were superimposed to study substrate recognition in the varied substrate-binding pockets of MBLs: the hydrolyzed product β-lactam-bound MBL structures were used instead of substrate β-lactam-bound MBL structures due to unavailability (**Figure 4**). The bound β-lactams showed a well-conserved conformation in the active site (**Supplementary Figure 8**). The cleavable C-N bond of β-lactams was faced toward the zinc site(s) within the distance of direct interactions, in which the β-lactam ring can be easily attacked by a catalytic hydroxide ion bound to zinc ion(s) (**Supplementary Figures 1, 8**). In the bound structures, the existing carboxyl and carbonyl groups of the core β-lactams were directly bound to the zinc ion(s) in the active sites of MBLs. Accordingly, there is little space to accommodate additional structural motifs in the β-lactam positions.

All B1, B2, and B3 MBLs have open space on the left side between potentially flexible eL1 and eL3; B2 MBLs have a narrow pocket, B1 MBLs have a medium-sized pocket, and B3 MBLs have a wide-open pocket. The left side of the substrate-binding pocket can accommodate the various R groups at the five- or six-membered ring side of the core β-lactam scaffold with a

carboxylate (blue shade). The bottom pocket between eL1 and eL2 is noticeably wide only in B1 MBLs and is limited in B2 and B3 MBLs. The bottom side of the substrate-binding pocket binds the R groups on the β-lactam ring side (red shade) and allows only limited structural substitutions.

Thus far, various modifications have been introduced in the different R positions in the core β-lactam scaffold for better efficacy in all classes of β-lactams, including penicillins, carbapenems, cephalosporins, and monobactams (**Figure 5**). Modifications, especially bulky ones, can cause steric hindrance in the varied substrate-binding pockets in B1, B2, and B3 MBLs. Among the five β-lactams in the six substrate-bound structures, penicillin G and cephalosporin have an additional bulky motif at the β-lactam ring side (red shade), and meropenem and biapenem have one at the other five- or six-member ring side (blue shade). This motif is bound to the open space on the bottom (red shade) and left side (blue shade) of the substrate-binding pocket, respectively (**Figures 4**, **5**). The available room on the bottom and left side of the pockets of B1, B2, and B3 MBLs is important for binding a specific β-lactam antibiotic for substrate specificity.

Inhibitor-Bound Metallo-β-Lactamases

We selected the MBL inhibitors having the co-crystal structure and the inhibitory mechanism of metal ion-binding (**Supplementary Table 7**; Ju et al., 2018). The inhibitor-bound MBLs were superimposed to study the inhibitory spectrum in the varied substrate-binding pockets. The inhibitors are divided into B1 and cross-class inhibitors, which have inhibitory activity on B1 MBLs (**Figure 6**) and MBLs of more than a subclass (**Figure 7**), respectively, based on limited enzyme assay results. The B1 MBL inhibitors include benzophenone (Christopeit et al., 2015), benzyl thiol (Cain et al., 2018), isoquinoline (Li et al., 2017), disubstituted succinic acid (Toney et al., 2001), cyclic boronate (Brem et al., 2016), tricyclic natural product (Payne et al., 2002), and biphenyl tetrazole (Toney et al., 1998) and the cross-class inhibitors, bisthiazolidine (Hinchliffe et al., 2016), thiomandelic acid (Mollard et al., 2001; Karsisiotis et al., 2013), and thiol-containing derivatives (Lassaux et al., 2010). The B1 inhibitors were developed against clinically relevant B1 MBLs, and their inhibitory activities were primarily measured on only B1 MBLs; accordingly, some B1 inhibitors might inhibit other subclass MBLs. Among them, cyclic boronate and tricyclic natural product have selective inhibitory activity on B1 MBLs. Based on the proposed structural characteristics of B1, B2, and B3 subclasses, the structure of cyclic boronate is well fitted within the substrate-binding pocket of B1 MBL, but the steric hindrance is shown with that of B2 MBL (**Figure 6B**). The structure of the tricyclic natural product is also well fitted in that of B1 MBL, but the loosen interaction is shown within the wide-open substrate-binding pocket of B3 (**Figure 6C**).

The cross-class MBL inhibitors show relatively smaller and globular shapes rather than the elongated shapes of the B1 inhibitors, which fit well within the center of the substrate-binding pocket on top of the zinc-binding site (**Figure 7**). The central pocket is conserved and free from the steric hindrance with eL1-3 within MBLs of all subclasses. Significantly, the thiol-containing derivatives showing similarity with the thiomandelic acid were co-crystallized with the B2 subclass CphA, which has the narrow substrate-binding pocket. The thiol-containing derivatives showed comparable inhibitory effects on MBLs of all three subclasses (**Supplementary Table 7**). In addition to the inhibitors co-crystallized with MBLs, potent MBL inhibitors having trifluoromethyl ketones and alcohols, dicarboxylic acids, thiols, sulfates, hydroxamates, tetrazoles, and sulfonamides as scaffolds have been studied with molecular modeling and docking methods (McGeary et al., 2014, 2017; Arjomandi et al., 2016; Yusof et al., 2016).

DISCUSSION

The varied substrate-binding pockets of B1, B2, and B3 MBLs makes it difficult to develop a broad-spectrum inhibitor against all subclasses of MBLs. However, the zinc sites are relatively well conserved in all MBLs; the relative distance between two zinc ions is almost the same in all MBLs, except for the loss of Zn1 in the B2 subclass. Considering the conserved zinc sites and the opposingly varied substrate-binding pockets of MBLs, the catalytic value of k_{cat} could be affected mainly by the catalytic hydroxide ion bound at the zinc ion(s). The K_m value for the affinity for the substrate could be more affected by the substrate-binding pockets formed by the external loops.

From the systematic structure analysis of all MBLs, a strategy to develop a broad-spectrum inhibitor could involve targeting a metal-binding inhibitor to the zinc ion(s) in the active site. This could involve an inhibitor that had a sufficiently small size or flexible structure to fit into the diverse substrate-binding pockets of all subclasses of MBLs. Aspergillomarasmine A might have a similar working mechanism, as it has a flexible scaffold with metal chelator activity and successfully inhibits MBLs (King et al., 2014; Mojica et al., 2021); however, its clinical efficacy remains to be determined. Zinc ions are abundant in living organisms. Approximately 1,600 proteins have been proposed as zinc proteins in human, and these proteins have catalytic and structural roles (Andreini et al., 2006). The human zinc-binding proteins are potential off-targets, and the resulting side effects should be considered. It is necessary to identify the window span for inhibitors with a high affinity for many MBLs and a low affinity for off-targets in humans.

The structural comparison among the selected MBLs of the three subclasses and the β-lactam-bound structures demonstrates the conserved features and unique characteristics of each subclass. The proposed unique characteristics of the substrate-binding pocket in B1, B2, and B3 MBLs were further verified with narrow and broad-spectrum MBL inhibitors. The cross-class inhibitors are found to bind to the central substrate-binding pocket, which is commonly available in all subclasses, with the complementary chemical structures.

Different from traditional MBLs, there are also non-canonical MBLs such as SPS-1 (Cheng et al., 2018) and SPM-1 (Brem et al., 2015) that belong to the B1 and B3 subclasses, respectively. SPS-1

has a long eL2 (**Supplementary Figure 2**), which showed a long bent α3 helix forming eL2 similar to that of the B2 members (**Supplementary Figure 9A**). SPM-1 showed two different open and close conformations in the α3 (**Supplementary Figure 9B**). These findings imply that despite decades of β-lactam-related research by international groups, the current classification and structural information of B1, B2, and B3 MBLs could be still incomplete and limited. Even the directed evolution study of AIM-1 showed the substrate preference relevant amino acids are not necessarily near the catalytic center of the enzyme (Hou et al., 2017). Cautions should be exerted when making a conclusion related to MBLs based on the currently available structural information.

This study systematically compared MBLs of all three subclasses altogether in sequence, structure, and substrate specificity. The MBL structures are scrutinized in the core scaffold, zinc-coordination loops of L1-4, and substrate-binding pocket-forming external loops of eL1-3 for the structure-function relationships in terms of substrate specificity. Because all MBLs have the common comprising moieties, the sequences and structures of characteristic moieties could be compared simultaneously among multiple MBLs. The multiple comparative statistics in the sequence identities and RMSD values among MBLs are used to verify the conservation and difference among MBLs of the same and different subclasses. The characteristic structural differences are used to explain the substrate specificity of MBLs. However, the currently available structural information of MBLs is limited. For example, there is no structure of any unbroken substrate β-lactam-bound MBL and only hydrolyzed product β-lactam-bound MBLs are available. There are many MBLs and variants with uncharacterized activities on substrates and unknown structures, making it hard to generalize the current understandings as the canonical structural features and substrate specificity of classified MBLs. Consequently, the systematic comparative study of several tens of multiple MBLs in the sequence, structure, and structure-function relationships is still limited, but could be used as a valuable platform to understand and predict the mechanism and substrate specificity of existing or newly found MBLs. The structural insights of MBLs are also valuable to develop a broad-spectrum inhibitor against MBLs.

DATA AVAILABILITY STATEMENT

The datasets presented in this study can be found in online repositories. The names of the repository/repositories and accession number(s) can be found in the article/ **Supplementary Material**.

AUTHOR CONTRIBUTIONS

YY, SH, YSP, HP, DK, YSK, YDK, SK, JHL, JHJ, SHL, and L-WK: investigation and writing. YY, SH, YSP, and L-WK: methodology. JHL, JHJ, SHL, and L-WK: funding acquisition. All authors have read and agreed to the published version of the manuscript.

FUNDING

This work was supported by the Bio and Medical Technology Development Program of the National Research Foundation of Korea (NRF) funded by the Ministry of Science and ICT (NRF-2017M3A9E4078014 and NRF-2017M3A9E4078017). This work was supported by the project "Development of Biomedical Materials Based on Marine Proteins" (Project No. 20170305), funded by the Ministry of Oceans and Fisheries, South Korea (JHL).

SUPPLEMENTARY MATERIAL

The Supplementary Material for this article can be found online at: https://www.frontiersin.org/articles/10.3389/fmicb.2021.752535/full#supplementary-material

REFERENCES

Aitha, M., Marts, A. R., Bergstrom, A., Moller, A. J., Moritz, L., Turner, L., et al. (2014). Biochemical, mechanistic, and spectroscopic characterization of metallo-beta-lactamase VIM-2. *Biochemistry* 53, 7321–7331. doi: 10.1021/bi500916y

Andreini, C., Banci, L., Bertini, I., and Rosato, A. (2006). Counting the zinc-proteins encoded in the human genome. *J. Proteome Res.* 5, 196–201. doi: 10.1021/pr050361j

Arjomandi, O. K., Hussein, W. M., Vella, P., Yusof, Y., Sidjabat, H. E., Schenk, G., et al. (2016). Design, synthesis, and in vitro and biological evaluation of potent amino acid-derived thiol inhibitors of the metallo-beta-lactamase IMP-1. *Eur. J. Med. Chem.* 114, 318–327. doi: 10.1016/j.ejmech.2016.03.017

Bahr, G., Gonzalez, L. J., and Vila, A. J. (2021). Metallo-beta-lactamases in the age of multidrug resistance: from structure and mechanism to evolution, dissemination, and inhibitor design. *Chem. Rev.* 121, 7957–8094. doi: 10.1021/acs.chemrev.1c00138

Behzadi, P., Garcia-Perdomo, H. A., Karpinski, T. M., and Issakhanian, L. (2020). Metallo-ss-lactamases: a review. *Mol. Biol. Rep.* 47, 6281–6294. doi: 10.1007/s11033-020-05651-9

Berendonk, T. U., Manaia, C. M., Merlin, C., Fatta-Kassinos, D., Cytryn, E., Walsh, F., et al. (2015). Tackling antibiotic resistance: the environmental framework. *Nat. Rev. Microbiol.* 13, 310–317. doi: 10.1038/nrmicro3439

Booth, M. P., Kosmopoulou, M., Poirel, L., Nordmann, P., and Spencer, J. (2015). Crystal structure of DIM-1, an acquired subclass B1 metallo-beta-lactamase from *Pseudomonas* stutzeri. *PLoS One* 10:e0140059. doi: 10.1371/journal.pone.0140059

Borra, P. S., Samuelsen, O., Spencer, J., Walsh, T. R., Lorentzen, M. S., and Leiros, H. K. (2013). Crystal structures of *Pseudomonas aeruginosa* GIM-1: active-site plasticity in metallo-beta-lactamases. *Antimicrob. Agents Chemother.* 57, 848–854. doi: 10.1128/AAC.02227-12

Brem, J., Cain, R., Cahill, S., McDonough, M. A., Clifton, I. J., Jimenez-Castellanos, J. C., et al. (2016). Structural basis of metallo-beta-lactamase, serine-beta-lactamase and penicillin-binding protein inhibition by cyclic boronates. *Nat. Commun.* 7:12406. doi: 10.1038/ncomms12406

Brem, J., Struwe, W. B., Rydzik, A. M., Tarhonskaya, H., Pfeffer, I., Flashman, E., et al. (2015). Studying the active-site loop movement of the sao paolo metallo-beta-lactamase-1. *Chem. Sci.* 6, 956–963. doi: 10.1039/c4sc01752h

Cain, R., Brem, J., Zollman, D., McDonough, M. A., Johnson, R. M., Spencer, J., et al. (2018). In silico fragment-based design identifies subfamily B1

metallo-beta-lactamase inhibitors. *J. Med. Chem.* 61, 1255–1260. doi: 10.1021/acs.jmedchem.7b01728

Cheng, Z., VanPelt, J., Bergstrom, A., Bethel, C., Katko, A., Miller, C., et al. (2018). A noncanonical metal center drives the activity of the sediminispirochaeta smaragdinae metallo-beta-lactamase SPS-1. *Biochemistry* 57, 5218–5229. doi: 10.1021/acs.biochem.8b00728

Christopeit, T., Carlsen, T. J., Helland, R., and Leiros, H. K. (2015). Discovery of novel inhibitor scaffolds against the metallo-beta-lactamase VIM-2 by surface plasmon resonance (SPR) based fragment screening. *J. Med. Chem.* 58, 8671–8682. doi: 10.1021/acs.jmedchem.5b01289

Crowder, M. W., Spencer, J., and Vila, A. J. (2006). Metallo-beta-lactamases: novel weaponry for antibiotic resistance in bacteria. *Acc. Chem. Res.* 39, 721–728. doi: 10.1021/ar0400241

Fisher, J. F., Meroueh, S. O., and Mobashery, S. (2005). Bacterial resistance to beta-lactam antibiotics: compelling opportunism, compelling opportunity. *Chem. Rev.* 105, 395–424. doi: 10.1021/cr030102i

Di Pisa, F., Pozzia, C., Benvenuti, M., Docquier, J.-D., De Luca, F., and Mangani, S. (2018). Boric acid and acetate anion binding to subclass B3 metallo-β-lactamase BJP-1 provides clues for mechanism of action and inhibitor design. *Inorg. Chim. Acta* 470, 331–341.

Fonseca, F., Bromley, E. H., Saavedra, M. J., Correia, A., and Spencer, J. (2011b). Crystal structure of *Serratia fonticola* Sfh-I: activation of the nucleophile in mono-zinc metallo-beta-lactamases. *J. Mol. Biol.* 411, 951–959. doi: 10.1016/j.jmb.2011.06.043

Fonseca, F., Arthur, C. J., Bromley, E. H., Samyn, B., Moerman, P., Saavedra, M. J., et al. (2011a). Biochemical characterization of Sfh-I, a subclass B2 metallo-beta-lactamase from *Serratia fonticola* UTAD54. *Antimicrob. Agents Chemother.* 55, 5392–5395. doi: 10.1128/AAC.00429-11

Frohlich, C., Sorum, V., Huber, S., Samuelsen, O., Berglund, F., Kristiansson, E., et al. (2020). Structural and biochemical characterization of the environmental MBLs MYO-1, ECV-1 and SHD-1. *J. Antimicrob. Chemother.* 75, 2554–2563. doi: 10.1093/jac/dkaa175

Garau, G., Bebrone, C., Anne, C., Galleni, M., Frere, J. M., and Dideberg, O. (2005). A metallo-beta-lactamase enzyme in action: crystal structures of the monozinc carbapenemase CphA and its complex with biapenem. *J. Mol. Biol.* 345, 785–795. doi: 10.1016/j.jmb.2004.10.070

Garcia-Saez, I., Hopkins, J., Papamicael, C., Franceschini, N., Amicosante, G., Rossolini, G. M., et al. (2003a). The 1.5-A structure of *Chryseobacterium meningosepticum* zinc beta-lactamase in complex with the inhibitor, D-captopril. *J. Biol. Chem.* 278, 23868–23873. doi: 10.1074/jbc.M301062200

Garcia-Saez, I., Mercuri, P. S., Papamicael, C., Kahn, R., Frere, J. M., Galleni, M., et al. (2003b). Three-dimensional structure of FEZ-1, a monomeric subclass B3 metallo-beta-lactamase from *Fluoribacter gormanii*, in native form and in complex with D-captopril. *J. Mol. Biol.* 325, 651–660. doi: 10.1016/s0022-2836(02)01271-8

Guo, Y., Wang, J., Niu, G., Shui, W., Sun, Y., Zhou, H., et al. (2011). A structural view of the antibiotic degradation enzyme NDM-1 from a superbug. *Protein Cell* 2, 384–394. doi: 10.1007/s13238-011-1055-9

Hall, B. G., and Barlow, M. (2004). Evolution of the serine beta-lactamases: past, present and future. *Drug Resist. Updat.* 7, 111–123. doi: 10.1016/j.drup.2004.02.003

Hernandez Valladares, M., Felici, A., Weber, G., Adolph, H. W., Zeppezauer, M., Rossolini, G. M., et al. (1997). Zn(II) dependence of the *Aeromonas hydrophila* AE036 metallo-beta-lactamase activity and stability. *Biochemistry* 36, 11534–11541. doi: 10.1021/bi971056h

Hinchliffe, P., Gonzalez, M. M., Mojica, M. F., Gonzalez, J. M., Castillo, V., Saiz, C., et al. (2016). Cross-class metallo-beta-lactamase inhibition by bisthiazolidines reveals multiple binding modes. *Proc. Natl. Acad. Sci. U.S.A.* 113, E3745–E3754. doi: 10.1073/pnas.1601368113

Hou, C. D., Liu, J. W., Collyer, C., Mitic, N., Pedroso, M. M., Schenk, G., et al. (2017). Insights into an evolutionary strategy leading to antibiotic resistance. *Sci. Rep.* 7:40357. doi: 10.1038/srep40357

Ju, L. C., Cheng, Z., Fast, W., Bonomo, R. A., and Crowder, M. W. (2018). The continuing challenge of metallo-beta-lactamase inhibition: mechanism matters. *Trends Pharmacol. Sci.* 39, 635–647. doi: 10.1016/j.tips.2018.03.007

Karsisiotis, A. I., Damblon, C. F., and Roberts, G. C. (2013). Solution structures of the *Bacillus cereus* metallo-beta-lactamase BcII and its complex with the broad spectrum inhibitor R-thiomandelic acid. *Biochem. J.* 456, 397–407. doi: 10.1042/BJ20131003

Khan, A. U., Maryam, L., and Zarrilli, R. (2017). Structure, genetics and worldwide spread of new Delhi metallo-beta-lactamase (NDM): a threat to public health. *BMC Microbiol.* 17:101. doi: 10.1186/s12866-017-1012-8

King, A. M., Reid-Yu, S. A., Wang, W., King, D. T., De Pascale, G., Strynadka, N. C., et al. (2014). Aspergillomarasmine a overcomes metallo-beta-lactamase antibiotic resistance. *Nature* 510, 503–506. doi: 10.1038/nature13445

King, D., and Strynadka, N. (2011). Crystal structure of New Delhi metallo-beta-lactamase reveals molecular basis for antibiotic resistance. *Protein Sci.* 20, 1484–1491. doi: 10.1002/pro.697

Kumarasamy, K. K., Toleman, M. A., Walsh, T. R., Bagaria, J., Butt, F., Balakrishnan, R., et al. (2010). Emergence of a new antibiotic resistance mechanism in India, Pakistan, and the UK: a molecular, biological, and epidemiological study. *Lancet Infect. Dis.* 10, 597–602. doi: 10.1016/S1473-3099(10)70143-2

Lassaux, P., Hamel, M., Gulea, M., Delbruck, H., Mercuri, P. S., Horsfall, L., et al. (2010). Mercaptophosphonate compounds as broad-spectrum inhibitors of the metallo-beta-lactamases. *J. Med. Chem.* 53, 4862–4876. doi: 10.1021/jm100213c

Laxminarayan, R., Duse, A., Wattal, C., Zaidi, A. K., Wertheim, H. F., Sumpradit, N., et al. (2013). Antibiotic resistance-the need for global solutions. *Lancet Infect. Dis.* 13, 1057–1098. doi: 10.1016/S1473-3099(13)70318-9

Lee, J. H., Park, K. S., Karim, A. M., Lee, C. R., and Lee, S. H. (2016). How to minimise antibiotic resistance. *Lancet Infect. Dis.* 16, 17–18. doi: 10.1016/S1473-3099(15)00467-3

Lee, J. H., Takahashi, M., Jeon, J. H., Kang, L. W., Seki, M., Park, K. S., et al. (2019). Dual activity of PNGM-1 pinpoints the evolutionary origin of subclass B3 metallo-beta-lactamases: a molecular and evolutionary study. *Emerg. Microbes Infect.* 8, 1688–1700. doi: 10.1080/22221751.2019.1692638

Leiros, H. K., Borra, P. S., Brandsdal, B. O., Edvardsen, K. S., Spencer, J., Walsh, T. R., et al. (2012). Crystal structure of the mobile metallo-beta-lactamase AIM-1 from *Pseudomonas aeruginosa*: insights into antibiotic binding and the role of Gln157. *Antimicrob. Agents Chemother.* 56, 4341–4353. doi: 10.1128/AAC.00448-12

Li, G. B., Abboud, M. I., Brem, J., Someya, H., Lohans, C. T., Yang, S. Y., et al. (2017). NMR-filtered virtual screening leads to non-metal chelating metallo-beta-lactamase inhibitors. *Chem. Sci.* 8, 928–937. doi: 10.1039/c6sc04524c

Lutgring, J. D., Balbuena, R., Reese, N., Gilbert, S. E., Ansari, U., Bhatnagar, A., et al. (2020). Antibiotic Susceptibility of NDM-producing enterobacterales collected in the United States in 2017 and 2018. *Antimicrob. Agents Chemother.* 64, e499–e420. doi: 10.1128/AAC.00499-20

McGeary, R. P., Schenk, G., and Guddat, L. W. (2014). The applications of binuclear metallohydrolases in medicine: recent advances in the design and development of novel drug leads for purple acid phosphatases, metallo-beta-lactamases and arginases. *Eur. J. Med. Chem.* 76, 132–144. doi: 10.1016/j.ejmech.2014.02.008

McGeary, R. P., Tan, D. T. C., Selleck, C., Monteiro Pedroso, M., Sidjabat, H. E., and Schenk, G. (2017). Structure-activity relationship study and optimisation of 2-aminopyrrole-1-benzyl-4,5-diphenyl-1H-pyrrole-3-carbonitrile as a broad spectrum metallo-beta-lactamase inhibitor. *Eur. J. Med. Chem.* 137, 351–364. doi: 10.1016/j.ejmech.2017.05.061

Mojica, M. F., Rossi, M. A., Vila, A. J., and Bonomo, R. A. (2021). The urgent need for metallo-beta-lactamase inhibitors: an unattended global threat. *Lancet Infect. Dis.* 22, e28–e34. doi: 10.1016/S1473-3099(20)30868-9

Mollard, C., Moali, C., Papamicael, C., Damblon, C., Vessilier, S., Amicosante, G., et al. (2001). Thiomandelic acid, a broad spectrum inhibitor of zinc beta-lactamases: kinetic and spectroscopic studies. *J. Biol. Chem.* 276, 45015–45023. doi: 10.1074/jbc.M107054200

Moran-Barrio, J., Lisa, M. N., Larrieux, N., Drusin, S. I., Viale, A. M., Moreno, D. M., et al. (2016). Crystal Structure of the metallo-beta-lactamase GOB in the periplasmic dizinc form reveals an unusual metal site. *Antimicrob. Agents Chemother.* 60, 6013–6022. doi: 10.1128/AAC.01067-16

Naas, T., Oueslati, S., Bonnin, R. A., Dabos, M. L., Zavala, A., Dortet, L., et al. (2017). Beta-lactamase database (BLDB) - structure and function. *J. Enzyme Inhib. Med. Chem.* 32, 917–919. doi: 10.1080/14756366.2017.1344235

Ozturk, H., Ozkirimli, E., and Ozgur, A. (2015). Classification of *Beta-lactamases* and penicillin binding proteins using ligand-centric network models. *PLoS One* 10:e0117874. doi: 10.1371/journal.pone.0117874

Palacios, A. R., Mojica, M. F., Giannini, E., Taracila, M. A., Bethel, C. R., Alzari, P. M., et al. (2019). The reaction mechanism of metallo-beta-lactamases is tuned by the conformation of an active-site mobile loop. *Antimicrob. Agents Chemother.* 63:5489. doi: 10.1128/AAC.01754-18

Park, Y. S., Kim, T. Y., Park, H., Lee, J. H., Nguyen, D. Q., Hong, M. K., et al. (2020). Structural study of metal binding and coordination in ancient metallo-beta-lactamase PNGM-1 variants. *Int. J. Mol. Sci.* 21:4926. doi: 10.3390/ijms21144926

Paterson, D. L., Isler, B., and Stewart, A. (2020). New treatment options for multiresistant gram negatives. *Curr. Opin. Infect. Dis.* 33, 214–223. doi: 10.1097/QCO.0000000000000627

Payne, D. J., Hueso-Rodriguez, J. A., Boyd, H., Concha, N. O., Janson, C. A., Gilpin, M., et al. (2002). Identification of a series of tricyclic natural products as potent broad-spectrum inhibitors of metallo-beta-lactamases. *Antimicrob. Agents Chemother.* 46, 1880–1886. doi: 10.1128/AAC.46.6.1880-1886.2002

Pedroso, M. M., Selleck, C., Enculescu, C., Harmer, J. R., Mitic, N., Craig, W. R., et al. (2017). Characterization of a highly efficient antibiotic-degrading metallo-beta-lactamase obtained from an uncultured member of a permafrost community. *Metallomics* 9, 1157–1168. doi: 10.1039/c7mt00195a

Pedroso, M. M., Waite, D. W., Melse, O., Wilson, L., Mitic, N., McGeary, R. P., et al. (2020). Broad spectrum antibiotic-degrading metallo-beta-lactamases are phylogenetically diverse. *Protein Cell* 11, 613–617. doi: 10.1007/s13238-020-00736-4

Raczynska, J. E., Imiolczyk, B., Komorowska, M., Sliwiak, J., Czyrko-Horczak, J., Brzezinski, K., et al. (2020). Flexible loops of New Delhi metallo-beta-lactamase modulate its activity towards different substrates. *Int. J. Biol. Macromol.* 158, 104–115. doi: 10.1016/j.ijbiomac.2020.04.219

Rodriguez, M. M., Herman, R., Ghiglione, B., Kerff, F., D'Amico Gonzalez, G., Bouillenne, F., et al. (2017). Crystal structure and kinetic analysis of the class B3 di-zinc metallo-beta-lactamase LRA-12 from an Alaskan soil metagenome. *PLoS One* 12:e0182043. doi: 10.1371/journal.pone.0182043

Salimraj, R., Zhang, L., Hinchliffe, P., Wellington, E. M., Brem, J., Schofield, C. J., et al. (2016). Structural and biochemical characterization of Rm3, a subclass B3 metallo-beta-lactamase identified from a functional metagenomic study. *Antimicrob. Agents Chemother.* 60, 5828–5840. doi: 10.1128/AAC.00750-16

Selleck, C., Larrabee, J. A., Harmer, J., Guddat, L. W., Mitic, N., Helweh, W., et al. (2016). AIM-1: an antibiotic-degrading metallohydrolase that displays mechanistic flexibility. *Chemistry* 22, 17704–17714. doi: 10.1002/chem.201602762

Selleck, C., Pedroso, M. M., Wilson, L., Krco, S., Knaven, E. G., Miraula, M., et al. (2020). Structure and mechanism of potent bifunctional beta-lactam- and homoserine lactone-degrading enzymes from marine microorganisms. *Sci. Rep.* 10:12882. doi: 10.1038/s41598-020-68612-z

Sidjabat, H. E., Gien, J., Kvaskoff, D., Ashman, K., Vaswani, K., Reed, S., et al. (2018). The use of SWATH to analyse the dynamic changes of bacterial proteome of carbapanemase-producing *Escherichia coli* under antibiotic pressure. *Sci. Rep.* 8:3871. doi: 10.1038/s41598-018-21984-9

Skagseth, S., Christopeit, T., Akhter, S., Bayer, A., Samuelsen, O., and Leiros, H. S. (2017). Structural insights into TMB-1 and the role of residues 119 and 228 in substrate and inhibitor binding. *Antimicrob. Agents Chemother.* 61, e2602–e2616. doi: 10.1128/AAC.02602-16

Spencer, J., Read, J., Sessions, R. B., Howell, S., Blackburn, G. M., and Gamblin, S. J. (2005). Antibiotic recognition by binuclear metallo-beta-lactamases revealed by X-ray crystallography. *J. Am. Chem. Soc.* 127, 14439–14444. doi: 10.1021/ja0536062

Toney, J. H., Fitzgerald, P. M., Grover-Sharma, N., Olson, S. H., May, W. J., Sundelof, J. G., et al. (1998). Antibiotic sensitization using biphenyl tetrazoles as potent inhibitors of *Bacteroides* fragilis metallo-beta-lactamase. *Chem. Biol.* 5, 185–196. doi: 10.1016/s1074-5521(98)90632-9

Toney, J. H., Hammond, G. G., Fitzgerald, P. M., Sharma, N., Balkovec, J. M., Rouen, G. P., et al. (2001). Succinic acids as potent inhibitors of plasmid-borne IMP-1 metallo-beta-lactamase. *J. Biol. Chem.* 276, 31913–31918. doi: 10.1074/jbc.M104742200

Ullah, J. H., Walsh, T. R., Taylor, I. A., Emery, D. C., Verma, C. S., Gamblin, S. J., et al. (1998). The crystal structure of the L1 metallo-beta-lactamase from *Stenotrophomonas* maltophilia at 1.7 A resolution. *J. Mol. Biol.* 284, 125–136. doi: 10.1006/jmbi.1998.2148

Vella, P., Miraula, M., Phelan, E., Leung, E. W., Ely, F., Ollis, D. L., et al. (2013). Identification and characterization of an unusual metallo-beta-lactamase from *Serratia proteamaculans*. *J. Biol. Inorg. Chem.* 18, 855–863. doi: 10.1007/s00775-013-1035-z

Wachino, J., Yamaguchi, Y., Mori, S., Kurosaki, H., Arakawa, Y., and Shibayama, K. (2013). Structural insights into the subclass B3 metallo-beta-lactamase SMB-1 and the mode of inhibition by the common metallo-beta-lactamase inhibitor mercaptoacetate. *Antimicrob. Agents Chemother.* 57, 101–109. doi: 10.1128/AAC.01264-12

Walsh, T. R., Gamblin, S., Emery, D. C., MacGowan, A. P., and Bennett, P. M. (1996). Enzyme kinetics and biochemical analysis of ImiS, the metallo-beta-lactamase from *Aeromonas sobria* 163a. *J. Antimicrob. Chemother.* 37, 423–431. doi: 10.1093/jac/37.3.423

Wilson, L. A., Knaven, E. G., Morris, M. T., Monteiro Pedroso, M., Schofield, C. J., Bruck, T. B., et al. (2021). Kinetic and structural characterization of the first B3 metallo-beta-lactamase with an active-site glutamic acid. *Antimicrob. Agents Chemother.* 65:e0093621. doi: 10.1128/AAC.00936-21

Yang, Y., and Bush, K. (1996). Biochemical characterization of the carbapenem-hydrolyzing beta-lactamase AsbM1 from *Aeromonas sobria* AER 14M: a member of a novel subgroup of metallo-beta-lactamases. *FEMS Microbiol. Lett.* 137, 193–200. doi: 10.1111/j.1574-6968.1996.tb08105.x

Yong, D., Toleman, M. A., Bell, J., Ritchie, B., Pratt, R., Ryley, H., et al. (2012). Genetic and biochemical characterization of an acquired subgroup B3 metallo-beta-lactamase gene, blaAIM-1, and its unique genetic context in *Pseudomonas aeruginosa* from Australia. *Antimicrob. Agents Chemother.* 56, 6154–6159. doi: 10.1128/AAC.05654-11

Yusof, Y., Tan, D. T. C., Arjomandi, O. K., Schenk, G., and McGeary, R. P. (2016). Captopril analogues as metallo-beta-lactamase inhibitors. *Bioorg. Med. Chem. Lett.* 26, 1589–1593. doi: 10.1016/j.bmcl.2016.02.007

Conflict of Interest: The authors declare that the research was conducted in the absence of any commercial or financial relationships that could be construed as a potential conflict of interest.

Publisher's Note: All claims expressed in this article are solely those of the authors and do not necessarily represent those of their affiliated organizations, or those of the publisher, the editors and the reviewers. Any product that may be evaluated in this article, or claim that may be made by its manufacturer, is not guaranteed or endorsed by the publisher.

frontiers in Microbiology

OPINION
published: 21 February 2022
doi: 10.3389/fmicb.2022.808993

Comamonas thiooxydans Expressing a Plasmid-Encoded IMP-1 Carbapenemase Isolated From Continuous Ambulatory Peritoneal Dialysis of an Inpatient in Japan

Yuki Suzuki[1], Ryuichi Nakano[1], Akiyo Nakano[1], Hikari Tasaki[2], Tomoko Asada[1], Saori Horiuchi[1], Kai Saito[1], Mako Watanabe[1], Yasumistu Nomura[1], Daisuke Kitagawa[1], Sang-Tae Lee[3], Koji Ui[3], Akira Koizumi[3], Yuji Nishihara[4], Takahiro Sekine[4], Ryuji Sakata[5], Miho Ogawa[5], Masahito Ohnishi[3], Kazuhiko Tsuruya[2], Kei Kasahara[4] and Hisakazu Yano[1]*

[1] Department of Microbiology and Infectious Diseases, Nara Medical University, Kashihara, Japan, [2] Department of Nephrology, Nara Medical University, Kashihara, Japan, [3] Central Clinical Laboratory, Nara Medical University, Kashihara, Japan, [4] Center for Infectious Diseases, Nara Medical University, Kashihara, Japan, [5] Department of Bacteriology, BML Inc., Kawagoe, Japan

Keywords: ***Comamonas thiooxydans*, IMP-1, metallo-β-lactamase, plasmid-mediated, whole genome sequence**

Edited by:
Che-Hsin Lee, National Sun Yat-sen University, Taiwan

Reviewed by:
Huiluo Cao, The University of Hong Kong, Hong Kong SAR, China

***Correspondence:**
Ryuichi Nakano
rnakano@naramed-u.ac.jp

Specialty section:
This article was submitted to Antimicrobials, Resistance and Chemotherapy, a section of the journal Frontiers in Microbiology

Received: *04 November 2021*
Accepted: *28 January 2022*
Published: *21 February 2022*

Citation:
Suzuki Y, Nakano R, Nakano A, Tasaki H, Asada T, Horiuchi S, Saito K, Watanabe M, Nomura Y, Kitagawa D, Lee S-T, Ui K, Koizumi A, Nishihara Y, Sekine T, Sakata R, Ogawa M, Ohnishi M, Tsuruya K, Kasahara K and Yano H (2022) Comamonas thiooxydans Expressing a Plasmid-Encoded IMP-1 Carbapenemase Isolated From Continuous Ambulatory Peritoneal Dialysis of an Inpatient in Japan. Front. Microbiol. 13:808993. doi: 10.3389/fmicb.2022.808993

INTRODUCTION

Comamonas thiooxydans is a Gram-negative, rod-shaped, glucose-non-fermentative bacteria. The genus *Comamonas* is present in multiple natural environments; it has been isolated from sulfur springs, the termite gut, and water in natural and industrial environments (Chou et al., 2007; Narayan et al., 2010; Zhang et al., 2013; Hatayama, 2014). Although there are a few reports describing infections caused by *Comamonas* spp., including intra-abdominal infections and bacteremia (Almuzara et al., 2013; Zhou et al., 2018), *C. thiooxydans* has rarely been associated with human infections in clinical settings, with only one case of urinary tract infection reported to date (Guo et al., 2021).

Antibiotic resistance, particularly to carbapenems, is a threat to global health. Infections caused by carbapenemase-producing Gram-negative bacteria have limited treatment options and have high mortality (Tzouvelekis et al., 2014). Carbapenemase genes are frequently located on plasmids and mobile genetic elements that can be transmitted between species (Ludden et al., 2017). Recently, carbapenemase-producing Gram-negative bacteria have been reported from multiple species (Endo et al., 2012; Bonomo et al., 2018; Suzuki et al., 2019).

In this study, we isolated carbapenem-resistant *C. thiooxydans* from an inpatient in a hospital in Japan and investigated its molecular characteristics by whole-genome sequencing (WGS).

BACTERIAL ISOLATION AND ANTIMICROBIAL SUSCEPTIBILITY

Carbapenem-resistant *Comamonas* sp. strain NR4028 was isolated from a patient undergoing continuous ambulatory peritoneal dialysis at Nara Medical University Hospital in 2019. The isolate was identified as *Comamonas teststeroni* by matrix-assisted laser desorption/ionization time-of-flight mass spectrometry (MALDI-TOF MS) using a Vitek MS system (bioMérieux, Marcy-l'Étoile, France). The antimicrobial susceptibility of multiple

antimicrobial agents was determined using the agar dilution method (Clinical Laboratory Standards Institute, 2015), and quality control was performed using *Escherichia coli* ATCC 25922. The minimum inhibitory concentrations for the isolate were: ceftazidime 256 μg/ml, cefepime 64 μg/ml, imipenem 1 μg/ml, meropenem 16 μg/ml, levofloxacin 32 μg/ml, gentamycin 256 μg/ml, and colistin 2 μg/ml.

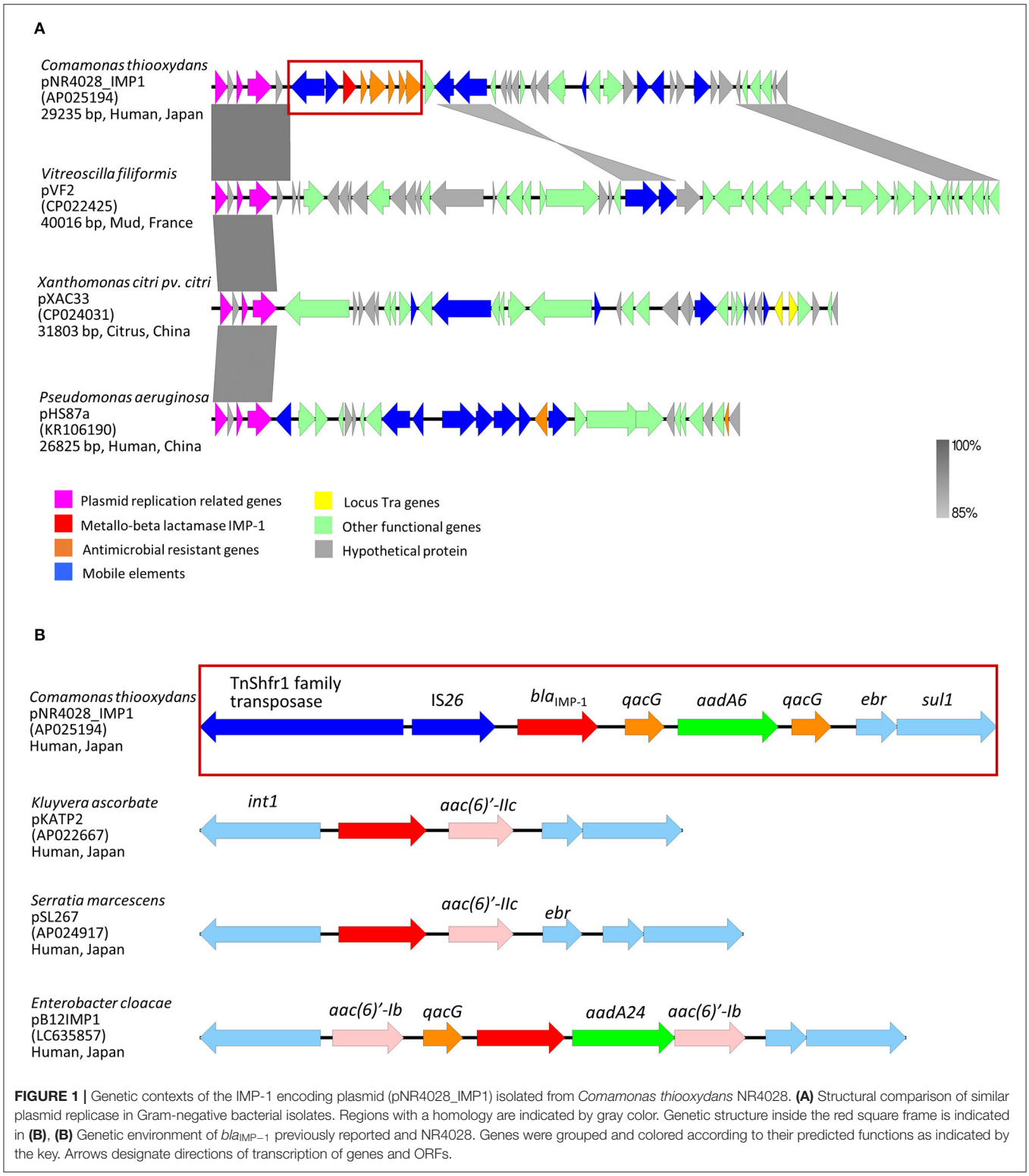

FIGURE 1 | Genetic contexts of the IMP-1 encoding plasmid (pNR4028_IMP1) isolated from *Comamonas thiooxydans* NR4028. **(A)** Structural comparison of similar plasmid replicase in Gram-negative bacterial isolates. Regions with a homology are indicated by gray color. Genetic structure inside the red square frame is indicated in **(B)**, **(B)** Genetic environment of bla_{IMP-1} previously reported and NR4028. Genes were grouped and colored according to their predicted functions as indicated by the key. Arrows designate directions of transcription of genes and ORFs.

WGS

Genomic DNA was extracted using QIAGEN Genomic-tip 500/G (Qiagen, Germany) and sequenced using MiSeq (Illumina, United States), MinION (Oxford Nanopore Technologies, United Kingdom), and Sanger sequencing. After read trimming and quality filtering, hybrid *de novo* assembly was performed using Unicycler v0.4.9 (Wick et al., 2017). The assembled sequences were annotated using DFAST v1.4.0 with standard settings (Tanizawa et al., 2018). For species identification, average nucleotide identity (ANI) analysis was performed using *C. testosteroni* ATCC 11996 (GenBank accession no. AHIL01000000), *C. testosteroni* TK102 (GenBank accession no. CP006704), *C. thiooxydans* ZDHYF418 (GenBank accession no. CP063057), *C. thiooxydans* PHE2-6 (GenBank accession no. LKFB01000000), and *C. thiooxydans* DSM 17888 (GenBank accession no. LIOM01000000) as the reference genome (https://www.ezbiocloud.net/tools/ani). ANI values were 94.44, 92.54, 98.49, 96.66, and 96.83%, respectively. It was indicated that NR4028 had the highest homology with *C. thiooxydans* strains, and the species was determined as *C. thiooxydans*. Acquired resistance genes were identified using ResFinder version 4.1 (Bortolaia et al., 2020) on the Center for Genomic Epidemiology (CGE) server (http://www.genomicepidemiology.org/). Comparison of the plasmid sequence of *C. thiooxydans* NR4028 was performed using BLASTn (https://blast.ncbi.nlm.nih.gov/Blast.cgi) and visualized with Easyfig version 2.2.5. (Sullivan et al., 2011).

The genome sequence revealed three circular contigs with a total length of 5,620,102 bp and a G + C content of 61.2%. The genome of *C. thiooxydans* NR4028 consisted of one chromosome (5,588,008 bp; accession number AP025193) and two plasmids (29,235 bp, named pNR4028_IMP1; accession number AP025194, and 2,859 bp; accession number AP025195). ResFinder version 4.1 identified three antimicrobial resistance genes (bla_{IMP-1}, *aadA6*, and *sul1*) on the plasmid pNR4028_IMP1. This IMP-1-encoding plasmid structure was different from the previously reported, and **Figure 1** shows a map of pNR4028_IMP1.

CONJUGATION ASSAY

To determine the transferability of the IMP-1 gene, we used the filter mating method, with *C. thiooxydans* NR4028 as the donor and sodium azide-resistant *E. coli* J53 and rifampicin-resistant *Pseudomonas aeruginosa* PAO1 as the recipient, as previously described (Nakano et al., 2004). However, we did not observe transfer of the bla_{IMP-1} gene-encoding plasmid to either *E. coli* J53 or to *P. aeruginosa* PAO1.

DISCUSSION

C. thiooxydans is prevalent in the natural environment; however, it can also cause infection and/or colonization in human clinical settings. *C. thiooxydans* producing IMP-8 has been reported from China by Guo et al. (2021) with IMP-8 encoded by a chromosomal gene. *C. thiooxydans* NR4028 possessed plasmid-encoded IMP-1, a common carbapenemase gene in Japan, and resistanct to meropenem.

Figure 1 indicades the comparison of the plasmid structure of *C. thiooxydans* NR4028 with similar plasmid replicase genes and the genetic environment of resistance genes in IMP-1-encoded plasmids. The plasmid *repA* replicase gene that was present in this isolate was different from that circulating in Enterobacterales, but had high homology to those of plasmids in non-fermenting gram-negative bacteria, including *Vitreoscilla filiformis* (CP022425), *Xanthomonas* spp. (CP024031), and *P. aeruginosa* (KR106190) (Bi et al., 2016) (**Figure 1A**). Therefore, IMP-1 may spread among the less common bacterial species, as mentioned above. We found a genetic structure of this plasmid and genetic environment that are different from those previously described (Wajima et al., 2020; Mori et al., 2021). IMP-type carbapenemase genes are frequently located in class 1 integrons; however, in this case, IS*26* was located upstream of bla_{IMP-1} (**Figure 1B**). It is possible that the integrase gene was lost as a consequence of the insertion of the IS element.

This plasmid pNR4028_IMP1 was found to have a unique genetic structure. The IMP-1-encoding plasmid was about 30 kbp in length and did not have a locus Tra region, which is an essential region for conjugation. Due to the lost of the locus Tra region in this plasmid, it is suggested that the IMP-1-encoding plasmid could not be transferred to recipients by conjugation. However, it is necessary to characterize this unique plasmid by conducting transformation experiments with the plasmid or cloning the resistance genes, including IS*26* in the future.

In conclusion, to the best of our knowledge, this is the first report of plasmid-encoded IMP-1 producing *C. thiooxydans*. This plasmid has a unique structure; therefore, the dissemination of both this species and this plasmid should be monitored.

AUTHOR CONTRIBUTIONS

YS: conceptualization, methodology, investigation, and writing of the original draft. RN: critical revision. AN, HT, TA, SH, KS, MW, YNo, DK, S-TL, KU, AK, YNi, RS, MOg, MOh, and TS: validation and data curation. KT, KK, and HY: supervision and project administration. All authors contributed to the manuscript and approved the submitted version.

FUNDING

This study was supported by JSPS KAKENHI grant 21K17897.

ACKNOWLEDGMENTS

We thank the staff of the Department of Microbiology and Infectious Diseases, and the Microbiology Laboratory of Nara Medical University Hospital for technical support.

REFERENCES

Almuzara, M. N., Cittadini, R., Vera Ocampo, C., Bakai, R., Traglia, G., Ramirez, M. S., et al. (2013). Intra-abdominal infections due to *Comamonas kerstersii*. *J. Clin. Microbiol*. 51, 1998–2000. doi: 10.1128/JCM.00659-13

Bi, D., Xie, Y., Tai, C., Jiang, X., Zhang, J., Harrison, E. M., et al. (2016). A site-specific integrative plasmid found in *Pseudomonas aeruginosa* clinical isolate HS87 along with A plasmid carrying an aminoglycoside-resistant gene. *Plos One*. 11, e0148367. doi: 10.1371/journal.pone.0148367

Bonomo, R. A., Burd, E. M., Conly, J., Limbago, B. M., Poirel, L., Segre, J. A., et al. (2018). Carbapenemase-producing organisms: a global scourge. *Clin. Infect. Dis*. 66, 1290–1297. doi: 10.1093/cid/cix893

Bortolaia, V., Kaas, R. S., Ruppe, E., Roberts, M. C., Schwarz, S., Cattoir, V., et al. (2020). ResFinder 4.0 for predictions of phenotypes from genotypes. *J. Antimicrob. Chemother*. 75, 3491–3500. doi: 10.1093/jac/dkaa345

Chou, J. H., Sheu, S. Y., Lin, K. Y., Chen, W. M., Arun, A. B., and Young, C. C. (2007). *Comamonas odontotermitis* sp. nov., isolated from the gut of the termite Odontotermes formosanus. *Int. J. Syst. Evol. Microbiol*. 57, 887–891. doi: 10.1099/ijs.0.64551-0

Clinical and Laboratory Standards Institute. (2015). *Methods for Dilution Antimicrobial Susceptibility Tests for Bacteria That Grow Aerobically; Approved Standard-A10, M07*. ed. 10 Wayne, PA: CLSI.

Endo, S., Sasano, M., Yano, H., Inomata, S., Ishibashi, N., Aoyagi, T., et al. (2012). IMP-1-producing carbapenem-resistant *Acinetobacter ursingii* from Japan. *J. Antimicrob. Chemother*. 67, 2533–2534. doi: 10.1093/jac/dks249

Guo, X., Wang, Q., Xu, H., He, X., Guo, L., Liu, S., et al. (2021). Emergence of IMP-8-Producing *Comamonas thiooxydans* causing urinary tract infection in China. *Front. Microbiol*. 12, 585716. doi: 10.3389/fmicb.2021.585716

Hatayama, K. (2014). *Comamonas humi* sp. *nov*., isolated from soil. *Int. J. Syst. Evol. Microbiol*. 64, 3976–3982. doi: 10.1099/ijs.0.067439-0

Ludden, C., Reuter, S., Judge, K., Gouliouris, T., Blane, B., Coll, F., et al. (2017). Sharing of carbapenemase-encoding plasmids between Enterobacteriaceae in UK sewage uncovered by MinION sequencing. *Microb. Genom*. 3, e000114. doi: 10.1099/mgen.0.000114

Mori, N., Tada, T., Oshiro, S., Kuwahara-Arai, K., Kirikae, T., and Uehara, Y. (2021). A transferrable IncL/M plasmid harboring a gene encoding IMP-1 metallo-β-lactamase in clinical isolates of Enterobacteriaceae. *BMC Infect. Dis*. 21, 1061. doi: 10.1186/s12879-021-06758-5

Nakano, R., Okamoto, R., Nakano, Y., Kaneko, K., Okitsu, N., Hosaka, Y., et al. (2004). CFE-1, a novel plasmid-encoded AmpC β-lactamase with an ampR gene originating from *Citrobacter freundii*. *Antimicrob. Agents Chemother*. 48, 1151–1158. doi: 10.1128/AAC.48.4.1151-1158.2004

Narayan, K. D., Pandey, S. K., and Das, S. K. (2010). Characterization of Comamonas thiooxidans sp. nov., and comparison of thiosulfate oxidation with Comamonas testosteroni and Comamonas composti. *Curr. Microbiol*. 61, 248–253. doi: 10.1007/s00284-010-9602-9

Sullivan, M. J., Petty, N. K., and Beatson, S. A. (2011). Easyfig: a genome comparison visualizer. *Bioinformatics*. 27, 1009–1010. doi: 10.1093/bioinformatics/btr039

Suzuki, Y., Endo, S., Nakano, R., Nakano, A., Saito, K., Kakuta, R., et al. (2019). Emergence of IMP-34- and OXA-58-producing carbapenem-resistant *Acinetobacter colistiniresistens*. *Antimicrob. Agents Chemother*. 63, e02633–e02618. doi: 10.1128/AAC.02633-18

Tanizawa, Y., Fujisawa, T., and Nakamura, Y. (2018). DFAST: A flexible prokaryotic genome annotation pipeline for faster genome publication. *Bioinformatics*. 34, 1037–1039. doi: 10.1093/bioinformatics/btx713

Tzouvelekis, L. S., Markogiannakis, A., Piperaki, E., Souli, M., and Daikos, G. L. (2014). Treating infections caused by carbapenemase-producing Enterobacteriaceae. *Clin. Microbiol. Infect*. 20, 862–872. doi: 10.1111/1469-0691.12697

Wajima, T., Hirai, Y., Otake, T., Momose, Y., Nakaminami, H., and Noguchi, N. (2020). First isolation of an IMP-1 metallo-β-lactamase-producing *Kluyvera ascorbata* in Japan. *J. Glob. Antimicrob. Resist*. 23, 228–231. doi: 10.1016/j.jgar.2020.09.026

Wick, R. R., Judd, L. M., Gorrie, C. L., and Holt, K. E. (2017). Unicycler: Resolving bacterial genome assemblies from short and long sequencing reads. *PLOS Comput. Biol*. 13, e1005595. doi: 10.1371/journal.pcbi.1005595

Zhang, J., Wang, Y., Zhou, S., Wu, C., He, J., and Li, F. (2013). Comamonas guangdongensis sp. nov., isolated from subterranean forest sediment, and emended description of the genus Comamonas. *Int. J. Syst. Evol. Microbiol*. 63, 809–814. doi: 10.1099/ijs.0.040188-0

Zhou, Y. H., Ma, H. X., Dong, Z. Y., and Shen, M. H. (2018). *Comamonas kerstersii* bacteremia in a patient with acute perforated appendicitis: A rare case report. *Med. (Baltim.)*. 97, e9296. doi: 10.1097/MD.0000000000009296

Conflict of Interest: RS and MOg are employed by BML Inc.

The remaining authors declare that the research was conducted in the absence of any commercial or financial relationships that could be construed as a potential conflict of interest.

Publisher's Note: All claims expressed in this article are solely those of the authors and do not necessarily represent those of their affiliated organizations, or those of the publisher, the editors and the reviewers. Any product that may be evaluated in this article, or claim that may be made by its manufacturer, is not guaranteed or endorsed by the publisher.

frontiers in Microbiology

ORIGINAL RESEARCH
published: 11 March 2022
doi: 10.3389/fmicb.2022.703113

A Longitudinal Nine-Year Study of the Molecular Epidemiology of Carbapenemase-Producing *Enterobacterales* Isolated From a Regional Hospital in Taiwan: Predominance of Carbapenemase KPC-2 and OXA-48

Tran Thi Thuy Duong[1†], Ya-Min Tsai[2†], Li-Li Wen[2], Hui-Chuan Chiu[2], Pek Kee Chen[1], Tran Thi Dieu Thuy[1], Pei-Yun Kuo[1], Jazon Harl Hidrosollo[1], Shining Wang[1], Yen-Zhen Zhang[1], Wei-Hung Lin[3,4], Ming-Cheng Wang[3,5] and Cheng-Yen Kao[1]*

[1] Institute of Microbiology and Immunology, School of Life Sciences, National Yang Ming Chiao Tung University, Taipei, Taiwan, [2] Department of Clinical Laboratory, En Chu Kong Hospital, New Taipei City, Taiwan, [3] Institute of Clinical Medicine, College of Medicine, National Cheng Kung University, Tainan, Taiwan, [4] Division of Nephrology, Department of Internal Medicine, National Cheng Kung University Hospital, College of Medicine, National Cheng Kung University, Tainan, Taiwan, [5] Institute of Clinical Pharmacy and Pharmaceutical Sciences, College of Medicine, National Cheng Kung University, Tainan, Taiwan

OPEN ACCESS

Edited by:
Che-Hsin Lee,
National Sun Yat-sen University,
Taiwan

Reviewed by:
Miriam Cordovana,
Bruker Daltonik GmbH, Germany
Chih-Ho Lai,
Chang Gung University, Taiwan
Alainna Jamal,
University of Toronto, Canada

***Correspondence:**
Cheng-Yen Kao
kaocy@ym.edu.tw

[†] These authors have contributed equally to this work

Specialty section:
This article was submitted to Antimicrobials, Resistance and Chemotherapy, a section of the journal Frontiers in Microbiology

Received: 30 April 2021
Accepted: 23 February 2022
Published: 11 March 2022

Citation:
Duong TTT, Tsai Y-M, Wen L-L, Chiu H-C, Chen PK, Thuy TTD, Kuo P-Y, Hidrosollo JH, Wang S, Zhang Y-Z, Lin W-H, Wang M-C and Kao C-Y (2022) A Longitudinal Nine-Year Study of the Molecular Epidemiology of Carbapenemase-Producing Enterobacterales Isolated From a Regional Hospital in Taiwan: Predominance of Carbapenemase KPC-2 and OXA-48. Front. Microbiol. 13:703113. doi: 10.3389/fmicb.2022.703113

Enterobacterales clinical isolates are now being resistant to clinically achievable concentrations of most commonly used antibiotics that makes treatment of hospitalized patients very challenging. We hereby determine the molecular characteristics of carbapenemase genes in carbapenem-resistant *Enterobacterales* (CRE) isolates in Taiwan. A total of 455 CRE isolates were identified between August 2011 to July 2020. Minimum inhibitory concentrations for selected carbapenems were tested using Vitek 2, and carbapenemase genes were determined using polymerase chain reaction in combination with sequencing. Phenotypic detection of carbapenemase was determined by modified carbapenem inactivation method (mCIM) and EDTA-modified carbapenem inactivation method (eCIM) to validate our PCR screening results. Pulsed-field gel electrophoresis (PFGE) was used to determine the clonality of carbapenemase-producing *Enterobacterales* (CPE) isolates, and the transferability of carbapenemase-carrying plasmids was determined by conjugation assays. A slight increase in carbapenem-resistant *E. coli* (CREC) was observed, however, the prevalence of carbapenem-resistant *K. pneumoniae* (CRKP) was steady, during 2011–2020. The dominant species among our CRE was *K. pneumoniae* (270/455, 59.3%), followed by *E. coli* (81/455, 17.8%), *Morganella morganii* (32/455, 7.0%), and *Enterobacter cloacae* (25/455, 5.5%). From 2011 to 2020, the total percentage of CPE increased steadily, accounting for 61.0% of CRE in 2020. Moreover, 122 of 455 CRE isolates (26.8%) were CPE. Among the CPE isolates, the dominant carbapenemase gene was $bla_{\text{OXA}-48-\text{like}}$ (54/122, 44.3%), and the second most common carbapenemase gene was $bla_{\text{KPC}-2}$ (47/122, 38.5%). The sensitivity and specificity for mCIM to detect carbapenemase

in the 455 isolates were both 100% in this study. The PFGE results showed that 39 carbapenemase-producing *E. coli* and 69 carbapenemase-producing *K. pneumoniae* isolates carrying bla_{KPC-2} and/or bla_{NDM-5} could be classified into 5 and 12 clusters, respectively. In conclusion, our results showed an increase in CPE isolates in Taiwan. Moreover, the distribution of carbapenemase and antimicrobial susceptibility in CPE were associated with PFGE typing.

Keywords: carbapenem-resistant *Enterobacterales* (CRE), KPC-2, OXA-48, NDM, pulsed-field gel electrophoresis (PFGE), carbapenemase

INTRODUCTION

Enterobacterales are Gram-negative, facultatively anaerobic, non-spore-forming rods, and one of the most common causes of nosocomial infections. Successive studies have demonstrated increasing antibiotic resistance among clinical *Enterobacterales* isolates, and high proportions of *Enterobacterales* isolates are now non-susceptible to clinically achievable concentrations of most commonly used antibiotics, such as broad-spectrum cephalosporins (Iredell et al., 2016; De Oliveira et al., 2020). Carbapenems are considered effective antimicrobial options for the treatment of critically ill patients with a variety of bacterial infections due to their broadest spectrum among β-lactam antibiotics and their relative resistance to hydrolysis by most β-lactamases (Barry et al., 1985). However, carbapenem resistance rates in *Enterobacterales* isolates have increased worldwide over the past decade (Logan and Weinstein, 2017; Lutgring, 2019).

The presence of innate resistance mechanisms and the acquisition of clusters of foreign resistance genes (e.g., plasmid, transposon, or integron) that promote survival of *Enterobacterales* under antibiotic treatment and host selection pressures are associated with the rapid emergence of multidrug-resistant (MDR) or extensively drug-resistant (XDR) *Enterobacterales* worldwide (Iredell et al., 2016; Kopotsa et al., 2019). Reduced expression or mutations in porins, overexpression of efflux pumps, and the presence of β-lactamases, play a critical role in resistance to carbapenems (Poirel et al., 2004; Iredell et al., 2016; Sugawara et al., 2016; De Oliveira et al., 2020). The first reported plasmid-mediated carbapenemase gene, *K. pneumoniae* carbapenemase (bla_{KPC}), was identified in *K. pneumoniae* in 2001 (Yigit et al., 2001) and became the predominant carbapenemase in *K. pneumoniae* (Chen L. et al., 2014; Chen et al., 2018). bla_{NDM} is the second most common carbapenemase found among carbapenem-resistant *Enterobacterales* (CRE) in China and is more prevalent in *E. coli* (Zhang et al., 2018). Therefore, the study aimed to investigate the molecular epidemiology of CRE in a regional hospital in Taiwan during 2011–2020.

MATERIALS AND METHODS

Identification of Carbapenem-Resistant *Enterobacterales* Isolates

Enterobacterales were isolated at En Chu Kong Hospital (ECKH), from 2011 August to 2020 July. En Chu Kong hospital, located at Sanxia district, New Taipei city, is an approximate 500-bed capacity regional teaching hospital (include three buildings: Fuxing building, Zhongshan building, and outpatient department building). The ECKH provides comprehensive medical services from fetus to the elderly, from acute trauma to hospice care, and from precision medicine to community health. These isolates were identified in the clinical laboratory by colony morphology, Gram stain, biochemical tests, and the Vitek 2 system (bioMérieux, Marcy-l'Étoile, France) according to the manufacturer's recommendations. Non-duplicate 27,585 *E. coli* and 11,582 *K. pneumoniae* were collected in this study. The susceptibility of *Enterobacterales* isolates to third-generation cephalosporins (ceftazidime or ceftriaxone, 30 μg/disc, BD BBL™ Sensi-Disc™, Sparks, MD, United States) was determined by the disk diffusion method on Mueller-Hinton (MH) agar plates according to the Clinical and Laboratory Standards Institute (CLSI) guidelines (M100-S30) (CLSI, 2020). Third-generation cephalosporin-resistant isolates were also tested for susceptibility to carbapenems, including imipenem, ertapenem, meropenem, and doripenem (10 μg/disc, BD BBL, United States). A total of 455 CRE isolates were identified and stored at −80°C in tryptic soy broth (TSB) containing 20% glycerol (v/v) until use.

Carbapenemase Gene Detection

Bacterial genomic DNA was isolated from bacteria grown overnight at 37°C in 3°ml LB broth. The bacterial culture was centrifuged at 12,000 rpm for 1 min, and the supernatant was removed. Crude DNA extracts were obtained by suspending the pellet in 300 μl distilled water and boiling at 95°C for 10min, followed by centrifugation at 12,000 rpm for 5 min. The DNA-containing supernatant was transferred to a new eppendorf tube, and DNA samples were stored at 4°C until testing. PCR amplification for detection of β-lactamase genes (bla_{KPC}, bla_{NDM}, bla_{IMP}, bla_{VIM}, bla_{OXA-48}, bla_{GES}, bla_{IMI}, bla_{SME}, bla_{SPM}, bla_{SIM}, bla_{DIM}, and bla_{GIM}) was performed on a GeneExplorer Thermal Cycler (BIOER, China) with the Fast-Run™ 2× Taq Master Mix (Protech, Taipei, Taiwan). Primers and PCR procedures used for the detection of β-lactamase genes have been described in previous studies (Yigit et al., 2001; Ellington et al., 2007; Doyle et al., 2012; Mlynarcik et al., 2016). PCR products were analyzed by electrophoresis using 1.2% agarose gels in 0.5× Tris-borate-EDTA (TBE) buffer. Gels were stained with ethidium bromide (EtBr), and PCR products were visualized using UV transilluminator. Clinical *K. pneumoniae* isolates carrying bla_{KPC}, bla_{NDM}, bla_{IMP}, bla_{VIM}, and bla_{OXA-48}

were used as PCR positive controls. The PCR products of bla_{GES}, bla_{IMI}, bla_{SME}, bla_{SPM}, bla_{SIM}, bla_{DIM}, or bla_{GIM}, with relevant expected sizes were verified by sequencing due to the lack of relative control strains.

Phenotypic Detection of Carbapenemase-Producing *Enterobacterales*

The modified carbapenem inactivation method (mCIM) and EDTA-modified carbapenem inactivation method (eCIM) were performed on CRE isolates according to the previous study to detect the presence of carbapenemase (Sfeir et al., 2019; Tsai et al., 2020). Briefly, a 1-μl loopful of bacteria was resuspended in a 2-ml tube containing TSB. Another 1-μl loopful of bacteria was resuspended in a 2-ml tube containing TSB supplemented with EDTA at a final concentration of 5 mM. A meropenem disk was placed in each tube, and the tubes were incubated at 35°C for 4 h ± 15 min. The disks were then removed and placed onto MH agar plates freshly plated with a 0.5 McFarland suspension of a carbapenem-susceptible *E. coli* strain ATCC 25922. Plates were incubated at 35°C for 16 to 20 h, and mCIM and eCIM results were interpreted as previously described (Sfeir et al., 2019). In accordance with CLSI guidelines (CLSI, 2020), *K. pneumoniae* ATCC BAA-1706 (carbapenemase negative), *K. pneumoniae* ATCC BAA-1705 (bla_{KPC} positive), and *K. pneumoniae* ATCC BAA-2146 (bla_{NDM} positive) were used as internal controls for mCIM and eCIM testing. The mCIM and eCIM tests were replicated by two independent investigators to ensure reproducibility.

Determination of Minimum Inhibitory Concentrations

Minimum inhibitory concentrations (MICs) for cefmetazole, cefotaxime, ceftazidime, cefepime, imipenem, ertapenem, meropenem, amikacin, gentamicin, ciprofloxacin, levofloxacin, tigecycline, colistin, and trimethoprim for CPE isolates were determined with Vitek 2 using the card AST-N322 according to the manufacturer's instructions. *E. coli* ATCC 25922 was used as a quality control strain. Antibiotic susceptibility (except tigecycline) was interpreted according to CLSI guidelines (M100-S30) (Zhang et al., 2018). The results of tigecycline susceptibility were interpreted according to the breakpoints of the U.S. Food and Drug Administration (FDA) (≥ 8.0 μg/ml, resistant; 4.0 μg/ml, intermediate; ≤ 2.0 μg/ml, susceptible).

Pulsed-Field Gel Electrophoresis (PFGE)

Pulsed-field gel electrophoresis was performed to determine the clonality of CPE isolates according to a previous study (Li et al., 2018). Briefly, PFGE of *Xba*I-digested genomic DNA was performed using a CHEF Mapper XA instrument (Bio-Rad Laboratories, Inc., Hercules, CA, United States) with the following parameters: separation on a 1% agarose gel (Seakem Gold agarose; FMC Bio Products) in 0.5× TBE buffer for 19 h at 14°C with pulse times ranging from 5 to 35 s at 6 V/cm. Gels were stained with EtBr and photographed with UV transillumination. PFGE profiles were analyzed and compared using the GelCompar II software, version 2.0 (Unimed Healthcare, Inc., Houston, TX, United States). The PFGE patterns were interpreted according to a previous study (Bando et al., 2009) and the isolates having > 80% pattern similarity were assigned to the same cluster.

Conjugation Experiments

The liquid mating-out assay was performed to transfer carbapenemase genes from CPE isolates to the rifampicin- and streptomycin-resistant *E. coli* C600 strain as previously described (Kao et al., 2016). All isolates tested were sensitive to rifampicin or streptomycin at the concentration of 256 μg/ml. Therefore, transconjugants were selected on LB plates with 256 μg/ml rifampicin (Sigma-Aldrich, United States) or 256 μg/ml streptomycin (Sigma-Aldrich, United States) in combination with 1 μg/ml meropenem. The conjugation assay was performed in triplicate to determine the transferability of the plasmid.

Statistical Analysis

A Cochran–Armitage test was used to evaluate trends in CREC, CRKP, CPE, CPEC, and CPKP over time. Statistical analyses were performed using the JMP software (SAS Institute Inc., Cary, NC, United States). A p-value < 0.05 is statistically significant.

RESULTS

Identification of Carbapenem-Resistant *Enterobacterales*

The dominant species among our CRE was *K. pneumoniae* (270/455, 59.4%), followed by *E. coli* (80/455, 17.6%), *Morganella morganii* (32/455, 7.0%), and *Enterobacter cloacae* (25/455, 5.5%) (**Table 1**). Thus, 0.003% (80/27,585) *E. coli* and 2.323% (270/11,582) *K. pneumoniae* showed resistance to carbapenem. A slight increase in carbapenem-resistant *E. coli* (CREC) was observed during 2011–2020 ($p > 0.05$) (**Figure 1A**). In contrast, the prevalence of carbapenem-resistant *K. pneumoniae* (CRKP) was steady ($p > 0.05$) (**Figure 1B**). In addition, 205 (44.9%) and 169 (37.0%) CRE strains were isolated from urine and sputum, respectively (**Table 1**). CRKP was most frequently isolated from sputum (127/270, 47.0%), followed by urine (107/270, 39.6%). In contrast, CREC was most frequently isolated from urine (54/80, 67.5%), followed by sputum (12/80, 15.0%) (**Table 1**).

Distribution of Carbapenemase Genes in Carbapenem-Resistant *Enterobacterales*

PCR was used to detect the presence of carbapenemase genes, and the results showed that 122 of 455 CRE isolates (26.8%) were CPE (**Table 2**). No carbapenemase genes were detected in carbapenem-resistant *Providencia rettgeri*, *Providencia stuartii*, and *Serratia marcescens*. In addition, no GES-, IMI-, SME-, SPM-, SIM-, DIM-, and GIM-producers were identified in our CRE isolates. Overall, the dominant carbapenemase gene was $bla_{OXA-48-like}$ (54/122, 44.3%) among CPE isolates, and the second most common carbapenemase gene was bla_{KPC-2}

TABLE 1 | Source of clinical specimens and bacterial species of 455 non-duplicate CRE.

	Clinical specimens' source											No. of isolates
	Urine	Sputum	Wound pus	Bronchial washing	Abscess	Blood	Vaginal discharge	Ear discharge	Catheter tip	Body fluid	Nasal	
Citrobacter freundii	1	0	0	0	0	1	0	0	0	0	0	2
Citrobacter koseri	3	2	1	0	0	1	0	0	0	0	0	7
Citrobacter youngae	1	0	0	0	0	0	0	0	0	0	0	1
Enterobacter aerogenes	1	6	1	0	0	0	0	0	0	0	1	9
Enterobacter cloacae	10	9	0	1	1	3	0	0	1	0	0	25
Escherichia coli	54	12	3	3	2	5	1	0	0	0	0	80
Escherichia hermannii	0	1	0	0	0	0	0	0	0	0	0	1
Klebsiella oxytoca	1	1	0	0	0	0	0	0	0	0	0	2
Klebsiella pneumoniae	107	127	8	15	0	11	0	0	0	2	0	270
Morganella morganii	13	4	9	2	0	3	0	1	0	0	0	32
Providencia rettgeri	6	0	0	0	0	2	0	0	0	0	0	8
Providencia stuartii	6	5	1	0	0	0	0	0	0	0	0	12
Serratia marcescens	2	2	1	0	0	1	0	0	0	0	0	6
no. of isolates	205	169	24	21	3	27	1	1	1	2	1	455

(47/122, 38.5%) (**Table 2**). In addition, we found metallo-carbapenemases NDM, IMP, and VIM in 23 (18 bla_{NDM-5}, 3 bla_{NDM-1}, and 2 bla_{NDM-4}), 9 (9 bla_{IMP-8}), and 4 (bla_{VIM-1}) CPE isolates, respectively (**Table 2**). Importantly, 15 CPE isolates carrying more than one carbapenemase gene were identified during 2017–2020. Seven *E. coli* isolates and 3 *K. pneumoniae* isolates had both $bla_{OXA-48-like}$ and bla_{KPC-2} (**Table 2**). Coexistence of bla_{KPC-2}/bla_{NDM-5} and $bla_{OXA-48-like}$/bla_{NDM-5} was found in 2 and 2 carbapenem-resistant *E. coli*, respectively. One *Klebsiella oxytoca* isolate had both bla_{VIM-1} and bla_{NDM-1} (**Table 2**).

Among the CRE isolates, 39 (39/80, 48.8%) *E. coli* and 69 (69/270, 25.6%) *K. pneumoniae* isolates were CPE. The dominant carbapenemase gene was $bla_{OXA-48-like}$ (20/39, 51.3%) among carbapenemase-producing *E. coli* (CPEC) isolates, and the second most common carbapenemase gene was bla_{NDM-5} (17/39, 43.6%). In contrast, bla_{KPC-2} was found dominant among carbapenemase-producing *K. pneumoniae* (CPKP) isolates (34/69, 49.3%), followed by $bla_{OXA-48-like}$ (27/69, 39.1%) (**Table 2**).

Modified Carbapenem Inactivation Method/EDTA-Modified Carbapenem Inactivation Method Phenotypic Detection of Carbapenemase Producer

It was previously reported that eCIM in combination with the mCIM is efficient for identifying CPE (Sfeir et al., 2019). Therefore, phenotypic detection mCIM/eCIM was performed on our 455 CRE isolates to validate PCR results for carbapenemase gene detection. In this study, the sensitivity and specificity for the mCIM to detect carbapenemase in 455 CRE isolates were both 100% which is consistent with our previous report (Tsai et al., 2020).

Interestingly, we found that four isolates containing metallo-carbapenemase NDM-5 and non-metallo-carbapenemases (OXA-48 or KPC-2) showed inconsistent mCIM/eCIM results (**Table 3**). *E. coli* isolate 488, an NDM-5 and OXA-48 producer, showed a false-negative result in mCIM/eCIM (**Table 3**). In contrast, *E. coli* isolate 514 with bla_{NDM-5} and bla_{OXA-48} showed a positive mCIM/eCIM result (**Table 3**). In addition, *E. coli* 571 and 572 with bla_{KPC-2}/bla_{NDM-5} also showed positive results by mCIM/eCIM (**Table 3**).

Increase in Carbapenemase-Producing *E. coli* and *K. pneumoniae* During 2011–2020

From 2011 to 2020, the total percentage of CPE increased steadily, accounting for 61.0% of CRE in 2020 (16.7% in August 2011–July 2012) ($p < 0.0001$) (**Figure 1C**). *E. coli* and *K. pneumoniae* isolates were dominant in our CPE collection (**Table 2**), so we aimed to further characterize the molecular epidemiology of CPEC and CPKP isolates. Among CPEC isolates, we found a dramatic increase in bla_{NDM-5} and bla_{KPC-2}/$bla_{OXA-48-like}$ in 2020 ($p < 0.0001$) (**Figure 1D**). In contrast to CPEC, bla_{KPC-2} and $bla_{OXA-48-like}$ were predominant in CPKP isolates in 2020 ($p < 0.0001$) (**Figure 1E**).

Pulsed-Field Gel Electrophoresis Typing of Carbapenemase-Producing *E. coli* and *K. pneumoniae*

The clonality of 39 CPEC and 69 CPKP isolates carrying carbapenemase KPC-2, NDM, and OXA-48 was further determined by PFGE (**Figure 2**). The PFGE patterns of 30 *E. coli* CPE isolates were assigned to five clusters based on > 80% pattern similarity (**Figure 2A**). All isolates in cluster 1 ($n = 3$) contained bla_{KPC-2}, isolates in cluster 2 ($n = 5$) contained bla_{oxa-48}, and isolates in cluster 5 ($n = 7$) contained both bla_{KPC-2} and bla_{oxa-48} (**Figure 2A**). In contrast, isolates from clusters 3 ($n = 12$) and 4 ($n = 3$) contained bla_{NDM-5} (two isolates contained bla_{NDM-5} and bla_{KPC-2}; one isolate contained bla_{NDM-5} and bla_{oxa-48})

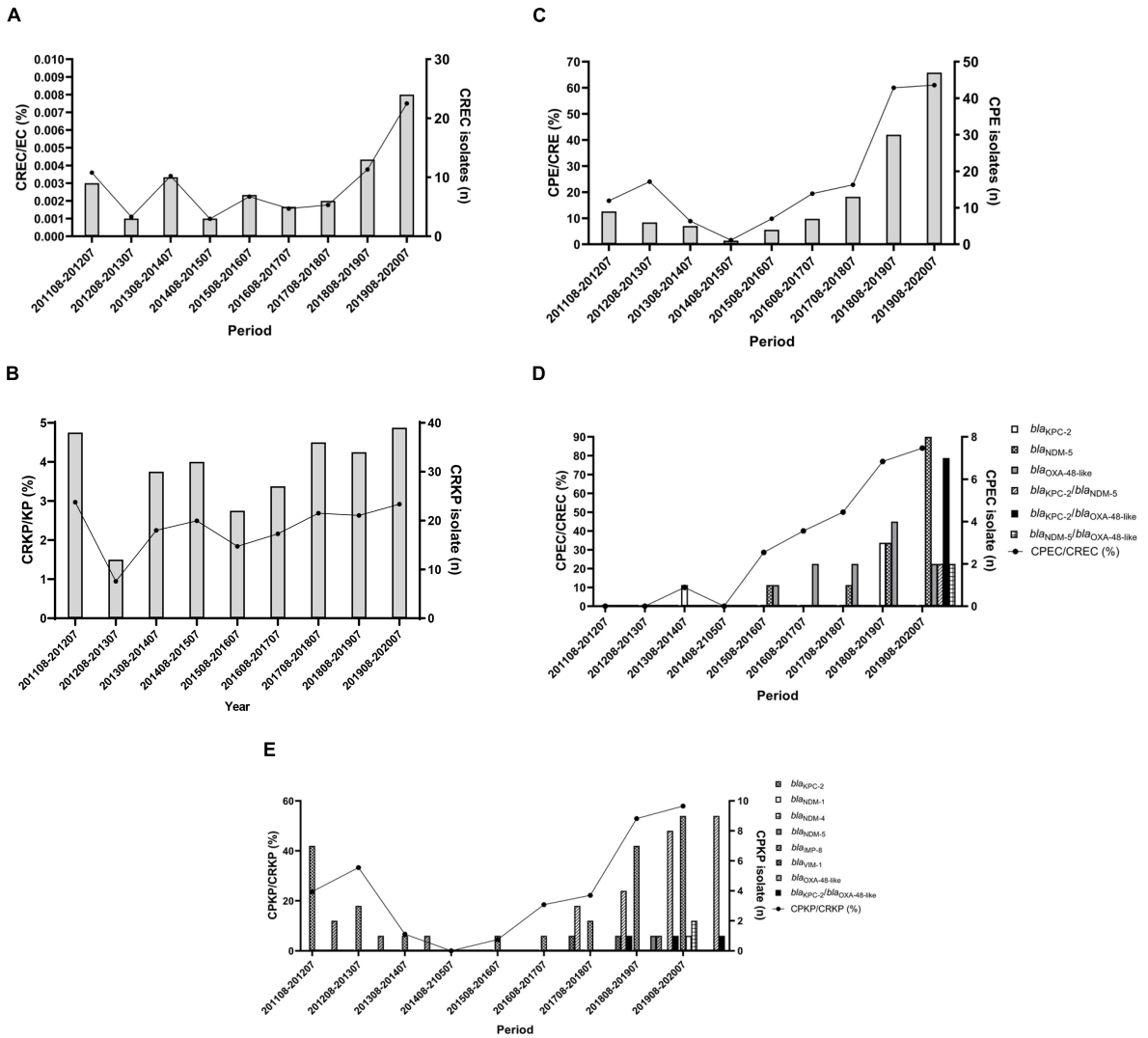

FIGURE 1 | Distribution of carbapenemase-producing *Enterobacterales* during 2011–2020. **(A)** Annual proportions and numbers of carbapenem-resistant *E. coli* among all *E. coli*. **(B)** Annual proportions and numbers of carbapenem-resistant *K. pneumoniae* among all *K. pneumoniae*. **(C)** Annual proportions and numbers of carbapenemase-producers among CRE. **(D,E)** Annual proportions and numbers of carbapenemase-producers among carbapenem-resistant *E. coli* **(D)** and *K. pneumoniae* **(E)**. The percentage of isolates is plotted as a line graph on the primary axis while the number of isolates is plotted as bars on the secondary axis.

(**Figure 2A**). Interestingly, isolates belonging to clusters 2 or 5 were resistant to gentamycin (**Figure 2A**). Although all 39 CPEC were resistant to ciprofloxacin (MIC $\geq$ 4 μg/ml) and levofloxacin (MIC $\geq$ 8 μg/ml), these isolates were sensitive to tigecycline (MIC $\leq$ 0.5 μg/ml) and colistin (MIC $\leq$ 0.5 μg/ml) (**Figure 2A**).

The PFGE patterns of 69 CPKP isolates were assigned to 12 clusters based on > 80% pattern similarity (**Figure 2B**). All isolates in clusters 2 (n = 3), 3 (n = 7), 4 (n = 3), 5 (n = 11), and 6 (n = 5) contained $bla_{\mathrm{KPC-2}}$, whereas isolates in clusters 8 (n = 2), 9 (n = 6), 10 (n = 2), and 11 (n = 4) contained $bla_{\mathrm{oxa-48}}$ (**Figure 2B**). Clusters 1 (n = 2) and 12 (n = 2) isolates contained $bla_{\mathrm{NDM-4}}$ and $bla_{\mathrm{IMP-8}}$, respectively (**Figure 2B**). Only isolates in cluster 12 were susceptible to both ciprofloxacin and levofloxacin (**Figure 2B**). In addition, 6 and 11 CPKP were resistant to colistin (MIC $\geq$ 4 μl/ml) and tigecycline (MIC $\geq$ 8 μl/ml), respectively (**Figure 2B**). The PFGE results indicate that the distribution of carbapenemase and antimicrobial susceptibility in CPE were associated with PFGE typing (**Figure 2**).

Carbapenemase Transfer and Plasmid Analysis

A total of 37 CPEC and 53 CPKP isolates carrying carbapenemase were further analyzed with conjugation assays to determine whether there were horizontally spread carbapenemase-carrying plasmids in Taiwan (18 CPE isolates showed resistance to rifampicin were excluded in this assay). Transfer of carbapenemase gene by conjugation to *E. coli* C600 was successful in 4 NDM-5-producing CPEC (isolates 257, 462, 500, and

TABLE 2 | The distribution of carbapenemase genes among 455 non-duplicate CRE.

	Carbapenemase genes											No. of isolates
	bla_{KPC-2}	bla_{NDM-1}	bla_{NDM-4}	bla_{NDM-5}	bla_{IMP-8}	bla_{VIM-1}	$bla_{OXA-48-like}$	bla_{KPC-2} bla_{NDM-5}	bla_{KPC-2} $bla_{OXA-48-like}$	bla_{NDM-5} $bla_{OXA-48-like}$	bla_{NDM-1} bla_{VIM-1}	
Citrobacter freundii	0	0	0	0	1	0	0	0	0	0	0	1
Citrobacter koseri	0	0	0	0	0	0	4	0	0	0	0	4
Citrobacter youngae	0	0	0	0	0	0	1	0	0	0	0	1
Enterobacter aerogenes	0	1	0	0	0	1	0	0	0	0	0	2
Enterobacter cloacae	0	0	0	0	2	0	1	0	0	0	0	3
Escherichia coli	4	0	0	13	0	0	11	2	7	2	0	39
Escherichia hermannii	0	0	0	0	1	0	0	0	0	0	0	1
Klebsiella oxytoca	0	0	0	0	0	0	0	0	0	0	1	1
Klebsiella pneumoniae	31	1	2	1	5	2	24	0	3	0	0	69
Morganella morganii	0	0	0	0	0	0	1	0	0	0	0	1
no. of isolates	35	2	2	14	9	3	42	2	10	2	1	122

TABLE 3 | Characteristics of three isolates that contained both metallo-carbapenemases and non-metallo-carbapenemases.

		MIC (μ g/ml)			Disc zone (mm)						Phenotypic detection	
Isolate	**Carbapenemase**	**IPM**	**ETP**	**MEM**	**IPM**	**ETP**	**MEM**	**DOP**	**mCIM**	**eCIM**	**mCIM**	**eCIM**
E. coli 488[a]	bla_{OXA-48}/bla_{NDM-5}	≥16	≥8	8	6	6	6	6	6	6	+	−
E. coli 514	bla_{OXA-48}/bla_{NDM-5}	≥16	≥8	≥16	16	12	15	16	6	23	+	+
E. coli 571	bla_{KPC-2}/bla_{NDM-5}	≥16	≥8	≥16	13	9	12	14	6	20	+	+
E. coli 572	bla_{KPC-2}/bla_{NDM-5}	8	≥8	8	12	8	12	11	6	20	+	+

[a] *The characteristics of isolate E. coli 488 were reported in our previous study (Tsai et al., 2020). IPM, imipenem; ETP, ertapenem; MEM, meropenem; DOP, doripenem.*

505) and 1 IMP-8-producing CPKP (isolate 21). However, all bla_{KPC-2}- and bla_{OXA-48}-carrying plasmids did not show transferability.

DISCUSSION

In this study, we isolated 455 CRE isolates from a regional teaching hospital in Taiwan (2011 August to 2020 July) and present their characteristics. Our results showed that 122 of 455 CRE isolates were CPE (**Table 2**). No carbapenemase genes were detected in our carbapenem-resistant *P. rettgeri*, *P. stuartii*, and *S. marcescens*. However, we could not rule out the presence of other carbapenemases in these isolates.

The dominant carbapenemase gene among our CPE isolates was bla_{OXA-48}, and the second most common carbapenemase gene was bla_{KPC-2} (**Table 2**). Chiu et al. (2018) showed a sharp increase in the annual prevalence rate of OXA-48-like producers among Taiwanese CPE isolates between 2012 and 2015. In 2017, bla_{OXA-48} was detected in 18.2% of CPE in Taiwan (Jean et al., 2018). Moreover, Wu et al. (2021) reported that the bla_{KPC-2} was the most common carbapenemase gene in CRKP isolated from patients with bacteremia at a hospital in northern Taiwan from 2013 to 2018. A 22-year (1998–2019) observation to determine the evolution of carbapenemase genes in *K. pneumoniae* in Taiwan discovered that the endemicity has changed from bla_{IMP-8}, bla_{NDM-1}, and bla_{VIM-1} to the most common bla_{KPC-2} and rapidly emerging bla_{OXA-48} (Lai and Yu, 2021). These results are consistent with our finding that the distribution of $bla_{OXA-48-like}$ was dramatically increased after 2018. Therefore, whether there is a circulation of OXA-48-producing plasmids/isolates in Taiwan is worth continually monitoring. Surprisingly, a very low conjugation rate of carbapenemase genes-carrying plasmids was observed in this study. Therefore, taxonomic relatedness and recipient strain used for conjugation tests may limit the conjugation in liquid matings (Chen Y. T. et al., 2014; Alderliesten et al., 2020).

Interestingly, the data from Surveillance of Multicentre Antimicrobial Resistance in Taiwan (SMART) with a multicenter collection of bacteremic isolates of *E. coli* (n = 423) and

A

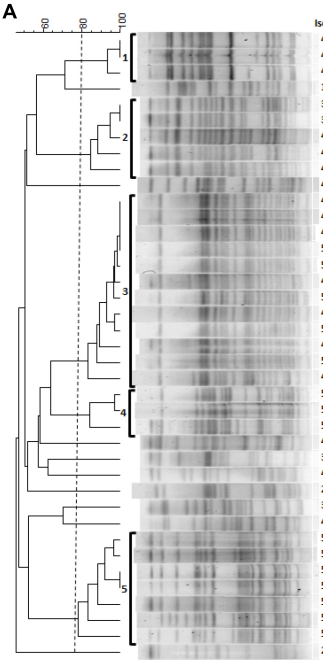

Isolate	Source	Year	Carbapenemase	MICs (mg/L) CMZ	CTX	CAZ	CEF	ETP	IMP	MEM	AMK	GEN	TMP
439	Wound pus	2019	KPC-2	32	8	16	8	≥8	≥16	≥16	≥64	4	≤20
449	blood	2019	KPC-2	16	4	4	2	4	8	≥16	32	4	≤20
446	sputum	2019	KPC-2	32	16	16	8	≥8	≥16	≥16	≥64	4	≤20
100	sputum	2013	KPC-2	8	≥64	16	≥64	≥8	≥16	≥16	16	≥16	≥320
303	blood	2016	OXA-48	≥64	≥64	≥64	≥64	4	2	1	4	≥16	≥320
329	urine	2017	OXA-48	≥64	≥64	≥64	≥64	4	2	4	8	≥16	≥320
485	bw	2019	OXA-48	≤1	≥64	16	≥64	2	2	1	4	≥16	≥320
450	urine	2019	OXA-48	≥64	≥64	16	8	4	1	0.5	16	≥16	≥320
433	bw	2018	OXA-48	≤1	≥64	16	4	2	1	1	4	≥16	≥320
488	Wound pus	2019	NDM-5/OXA-48	≥64	≥64	≥64	≥64	≥8	≥16	8	≥64	≥16	≥320
479	blood	2019	NDM-5	≥64	≥64	≥64	≥64	≥8	≥16	≥16	4	≤1	≥320
487	urine	2019	NDM-5	≥64	≥64	≥64	≥64	≥8	≥16	≥16	≤2	≤1	≥320
493	sputum	2019	NDM-5	≥64	≥64	≥64	≥64	≥8	≥16	≥16	≤2	≤1	≥320
505	urine	2019	NDM-5	≥64	≥64	≥64	≥64	≥8	≥16	8	≤2	≤1	≥320
500	sputum	2019	NDM-5	≥64	≥64	≥64	≥64	≥8	≥16	≥16	≤2	≤1	≥320
469	urine	2019	NDM-5	≥64	≥64	≥64	≥64	≥8	≥16	≥16	≤2	≤1	≥320
572	urine	2020	KPC-2/NDM-5	≥64	≥64	≥64	≥64	≥8	8	8	16	≤1	≥320
462	urine	2019	NDM-5	≥64	≥64	≥64	≥64	≥8	≥16	≥16	4	≤1	≥320
514	urine	2019	NDM-5/OXA-48	≥64	≥64	≥64	≥64	≥8	≥16	8	8	≤1	≥320
465	urine	2019	NDM-5	≥64	≥64	≥64	≥64	≥8	≥16	≥16	4	≤1	≥320
538	urine	2020	NDM-5	8	≥64	≥64	≥64	4	≥16	≥16	8	≤1	≥320
406	urine	2018	NDM-5	≥64	≥64	≥64	≥64	≥8	≥16	≥16	≤2	≤1	≥320
571	urine	2020	KPC-2/NDM-5	≥64	≥64	≥64	16	≥8	≥16	≥16	32	4	≥320
587	urine	2020	NDM-5	≥64	≥64	≥64	8	≥8	≥16	≥16	32	4	≥320
590	urine	2020	NDM-5	≥64	≥64	≥64	16	≥8	≥16	≥16	≥64	4	≥320
476	urine	2019	OXA-48	≥64	32	≥64	≤1	4	≤0.25	1	≤2	≥16	≥320
392	sputum	2018	OXA-48	4	≥64	16	32	≥8	2	2	≤2	≤1	≤20
434	urine	2018	OXA-48	32	32	≥64	≤1	≥8	1	1	16	≥16	≤20
257	sputum	2015	NDM-5	≥64	≥64	≥64	≥64	≥8	≥16	≥16	≤2	≤1	≥320
356	urine	2017	OXA-48	≤1	≥64	16	4	4	4	1	≤2	≤1	≤20
475	urine	2019	OXA-48	≥64	≥64	≥64	8	≥8	≥16	2	16	≤1	≥320
540	sputum	2020	KPC-2/OXA-48	≥64	≥64	≥64	≥64	≥8	≥16	≥16	8	≥16	≥320
541	urine	2020	KPC-2/OXA-48	32	≥64	≥64	≥64	≥8	8	≥16	≤2	≥16	≥320
542	urine	2020	KPC-2/OXA-48	≥64	≥64	≥64	≥64	≥8	8	≥16	16	≥16	≥320
543	urine	2020	KPC-2/OXA-48	≥64	≥64	≥64	≥64	≥8	≥16	≥16	8	≥16	≥320
537	urine	2020	KPC-2/OXA-48	≥64	≥64	≥64	≥64	≥8	≥16	≥16	8	≥16	≥320
529	urine	2020	KPC-2/OXA-48	≥64	≥64	≥64	≥64	≥8	≥16	≥16	4	≥16	≥320
563	urine	2020	KPC-2/OXA-48	≥64	≥64	≥64	≥64	≥8	4	≥16	8	≥16	≥320
276	wound pus	2016	OXA-48	32	16	16	≤1	≥8	2	4	≤2	≥16	≥320

B

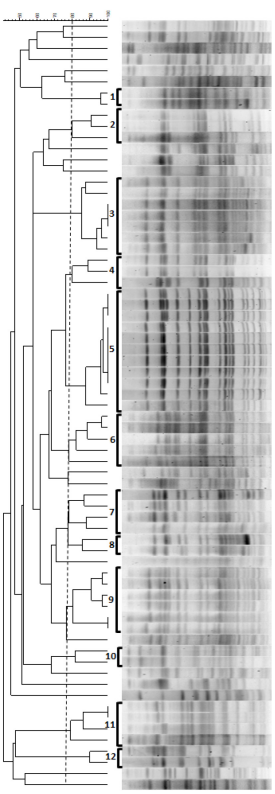

Isolate	Source	Year	Carbapenemase	MICs (mg/L) CMZ	CTX	CAZ	CEF	ETP	IMP	MEM	AMK	GEN	CIP	LVX	TIG	COL	TMP
CRE-363	363	sputum	2018	OXA-48	4	≥64	≥64	≤1	≥8	8	4	16	≤1	≥4	≥8	1	≤0.5	≥320
CRE-409	409	sputum	2018	OXA-48	4	16	≥64	≤1	≥8	≥16	4	16	≤1	≥4	≥8	2	≤0.5	≥320
CRE-480	480	blood	2019	NDM-1	32	≥64	≥64	≥64	≥8	8	≥16	≤2	≤1	≥4	≥8	≤0.5	≤0.5	≥320
CRE-391	391	sputum	2018	OXA-48	32	4	4	≤1	4	≥16	4	≤2	≤1	≥4	≥8	≤0.5	≤0.5	≥320
CRE-339	339	sputum	2017	VIM-1	4	≥64	≥64	2	≤0.5	≥16	≥16	≤2	≤1	1	1	≤0.5	≤0.5	≤20
CRE-591	591	urine	2020	KPC-2/OXA-48	≥64	≥64	16	32	≥8	≥16	≥16	8	≥16	≥4	≥8	4	≤0.5	≥320
CRE-525	525	sputum	2020	NDM-4	≥64	≥64	≥64	≥64	≥8	≥16	≥16	≤2	≤1	≥4	≥8	≥8	≤0.5	≥320
CRE-545	545	sputum	2020	NDM-4	≥64	≥64	≥64	≥64	≥8	≥16	≥16	≥64	8	≥4	≥8	4	≤0.5	≤20
CRE-337	337	sputum	2017	KPC-2	≥64	≥64	≥64	≥64	≥8	≥16	≥16	≤2	≤1	≥4	≥8	1	≤0.5	≤20
CRE-349	349	wound pus	2017	KPC-2/OXA-48	≥64	≥64	≥64	≥64	≥8	≥16	≥16	≤2	≤1	≥4	≥8	1	≤0.5	≥320
CRE-474	474	sputum	2019	KPC-2	≥64	≥64	≥64	≥64	≥8	≥16	≥16	≤2	≤1	≥4	≥8	2	≤0.5	80
CRE-440	440	urine	2019	KPC-2/OXA-48	≥64	≥64	≥64	≥64	≥8	8	≥16	≥64	≥16	≥4	≥8	2	≤0.5	≥320
CRE-429	429	wound pus	2018	NDM-5	≥64	≥64	≥64	≥64	≥8	≥16	≥16	≤2	≥16	≥4	≥8	≥8	1	≥320
CRE-565	565	urine	2020	KPC-2	≥64	≥64	≥64	≥64	≥8	≥16	≥16	≥64	≥16	≥4	≥8	2	≤0.5	≥320
CRE-557	557	sputum	2020	KPC-2	≥64	≥64	≥64	≥64	≥8	≥16	≥16	≤2	8	≥4	≥8	≥8	≤0.5	≥320
CRE-579	579	sputum	2020	KPC-2	≥64	≥64	≥64	≥64	≥8	≥16	≥16	≤2	≤1	≥4	≥8	4	≤0.5	≥320
CRE-512	512	sputum	2019	KPC-2	≥64	≥64	≥64	≥64	≥8	≥16	≥16	≤2	8	≥4	≥8	≥8	≤0.5	≥320
CRE-516	516	urine	2019	KPC-2	≥64	≥64	≥64	≥64	≥8	≥16	≥16	≤2	8	≥4	≥8	≥8	≤0.5	≥320
CRE-554	554	sputum	2020	KPC-2	≥64	≥64	≥64	≥64	≥8	≥16	≥16	≤2	8	≥4	≥8	≥8	≤0.5	≥320
CRE-549	549	urine	2020	KPC-2	≥64	8	16	≤1	≥8	2	2	≤2	8	≥4	≥8	≥8	≤0.5	≥320
CRE-570	570	urine	2020	KPC-2	≥64	≥64	≥64	≥64	≥8	≥16	≥16	≤2	8	≥4	≥8	4	≤0.5	≥320
CRE-365	365	urine	2018	KPC-2	≥64	≥64	≥64	≥64	≥8	≥16	≥16	≤2	≥16	≥4	≥8	2	≥16	≤20
CRE-367	367	urine	2018	KPC-2	4	≥64	≥64	≥64	≥8	≥16	≥16	≤2	≥16	≥4	≥8	2	≤0.5	≥320
CRE-117	117	urine	2013	KPC-2	≥64	≥64	≥64	≥64	≥8	≥16	≥16	≥64	≥16	≥4	≥8	2	≤0.5	≥320
CRE-23	23	Sputum	2012	KPC-2	≥64	≥64	≥64	≥64	≥8	≥16	≥16	≤2	≤1	≥4	≥8	2	≤0.5	≤20
CRE-26	26	bw	2012	KPC-2	≥64	≥64	≥64	≥64	≥8	≥16	≥16	≤2	≤1	≥4	≥8	1	≤0.5	≤20
CRE-91	91	sputum	2013	KPC-2	≥64	≥64	≥64	≥64	≥8	≥16	≥16	≤2	≤1	≥4	≥8	2	≤0.5	≥320
CRE-20	20	sputum	2012	KPC-2	≥64	≥64	32	≥64	≥8	≥16	≥16	≤2	≤1	≥4	≥8	2	≤0.5	≤20
CRE-39	39	sputum	2012	KPC-2	8	≥64	≥64	8	≥8	≥16	≥16	≤2	≤1	≥4	≥8	2	≤0.5	≤20
CRE-45	45	urine	2012	KPC-2	32	≥64	≥64	8	≥8	≥16	≥16	≤2	≤1	≥4	≥8	≥8	≤0.5	≤20
CRE-49	49	bw	2012	KPC-2	8	8	≥64	2	≥8	≥16	≥16	≤2	≤1	≥4	≥8	2	≤0.5	≤20
CRE-64	64	urine	2012	KPC-2	8	≥64	≥64	8	≥8	≥16	≥16	≤2	≤1	≥4	≥8	2	≤0.5	≤20
CRE-89	89	urine	2013	KPC-2	≥64	≥64	≥64	≥64	≥8	≥16	≥16	≤2	≤1	≥4	≥8	≥8	≤0.5	40
CRE-31	31	urine	2012	KPC-2	≥64	≥64	≥64	≥64	≥8	≥16	≥16	≤2	≤1	≥4	≥8	4	≤0.5	≤20
CRE-271	271	blood	2015	KPC-2	≥64	≥64	≥64	≥64	≥8	≥16	≥16	≤2	≥16	≥4	≥8	2	≤0.5	80
CRE-470	470	sputum	2019	KPC-2	≥64	≥64	≥64	≥64	≥8	≥16	≥16	≥64	≥16	≥4	≥8	≤0.5	≥16	≤20
CRE-471	471	urine	2019	KPC-2	≥64	≥64	≥64	≥64	≥8	≥16	≥16	≤2	≥16	≥4	≥8	≤0.5	≥16	80
CRE-451	451	bw	2019	KPC-2	≥64	≥64	≥64	≥64	≥8	≥16	≥16	4	≥16	≥4	≥8	≤0.5	≥16	80
CRE-452	452	sputum	2019	KPC-2	≥64	≥64	≥64	≥64	≥8	≥16	≥16	4	≥16	≥4	≥8	1	≥16	80
CRE-491	491	urine	2019	KPC-2	≥64	≥64	≥64	≥64	≥8	≥16	≥16	≤2	≤1	≥4	≥8	2	≥16	≥320
CRE-438	438	Sputum	2019	KPC-2	≥64	≥64	≥64	≥64	≥8	≥16	≥16	≤2	≤1	≥4	≥8	≤0.5	≤0.5	40
CRE-458	458	sputum	2019	KPC-2	≥64	2	4	≤1	4	4	1	≤2	≥16	≥4	≥8	2	≤0.5	≥320
CRE-105	105	urine	2013	IMP-8	≥64	≥64	≥64	16	4	8	1	≤2	≥16	≥4	≥8	2	≤0.5	≥320
CRE-489	489	urine	2019	OXA-48	≥64	≥64	≥64	8	1	0.5	≤0.25	≤2	≥16	≥4	≥8	4	≤0.5	≥320
CRE-327	327	bw	2017	OXA-48	≥64	≥64	16	≥64	≥8	2	4	≤2	≤1	≥4	≥8	2	≤0.5	80
CRE-578	578	urine	2020	OXA-48	≥64	≥64	16	≥64	≥8	2	1	≥64	≥16	≥4	≥8	2	≤0.5	80
CRE-316	316	urine	2017	OXA-48	≥64	≥64	16	≥64	≥8	≥16	≥16	≤2	≥16	≥4	≥8	2	2	≥320
CRE-444	444	sputum	2019	OXA-48	≥64	≥64	≥64	≥64	≥8	1	2	≥64	≥16	≥4	≥8	1	≤0.5	≥320
CRE-468	468	urine	2019	OXA-48	≥64	≥64	≥64	≥64	≥8	≥16	≥16	≤2	≤1	≥4	≥8	≤0.5	≤0.5	≤20
CRE-448	448	urine	2019	OXA-48	4	≥64	≥64	≤1	4	≥16	4	16	≤1	≥4	4	≤0.5	≤0.5	≥320
CRE-473	473	sputum	2019	OXA-48	≥64	8	≥64	≤1	≥8	≥16	1	16	≤1	≥4	≥8	1	≤0.5	≥320
CRE-416	416	sputum	2018	OXA-48	≥64	≥64	≥64	≤1	≥8	4	4	16	≤1	≥4	≥8	1	≤0.5	≥320
CRE-417	417	urine	2018	OXA-48	≥64	≥64	≥64	≤1	≥8	2	1	16	≤1	≥4	≥8	≤0.5	≤0.5	≥320
CRE-553	553	urine	2020	OXA-48	≥64	8	≥64	≤1	≥8	4	4	16	≤1	≥4	≥8	1	≤0.5	≥320
CRE-573	573	urine	2020	OXA-48	≥64	8	≥64	≤1	≥8	2	4	16	≤1	≥4	≥8	2	≤0.5	≥320
CRE-456	456	sputum	2019	IMP-8	≥64	16	≥64	≤1	2	0.5	≤0.25	≤2	≤1	≥4	≥8	2	≤0.5	≥320
CRE-460	460	blood	2019	OXA-48	≥64	≥64	≥64	32	≥8	2	1	≤2	≥16	≥4	≥8	1	≤0.5	≥320
CRE-547	547	sputum	2020	OXA-48	≤1	≥64	≥64	32	≥8	≥16	4	≤2	≥16	≥4	≥8	1	≤0.5	≥320
CRE-372	372	urine	2018	OXA-48	≥64	4	32	≤1	4	2	1	16	≥16	≥4	≥8	1	≤0.5	≥320
CRE-483	483	urine	2019	OXA-48	≥64	8	16	≤1	≥8	4	≥16	≥64	8	≥4	≥8	1	≤0.5	≥320
CRE-63	63	urine	2012	IMP-8	≥64	≥64	≥64	8	2	8	1	≤2	≥16	≥4	≥8	4	≤0.5	≥320
CRE-499	499	blood	2019	OXA-48	≤1	≥64	4	2	4	2	≥16	≤2	≥16	≥4	≥8	2	≤0.5	≥320
CRE-502	502	sputum	2019	OXA-48	8	16	≥64	2	≥8	2	4	≤2	≥16	≥4	≥8	≥8	≤0.5	≥320
CRE-503	503	sputum	2019	OXA-48	4	32	≥64	2	4	2	4	≤2	≥16	≥4	≥8	≥8	≤0.5	≥320
CRE-472	472	urine	2019	OXA-48	≤1	≥64	16	≥64	4	2	1	≤2	≤1	≥4	≥8	≤0.5	≤0.5	≤20
CRE-21	21	sputum	2012	IMP-8	≥64	8	≥64	2	≤0.5	≥16	1	≤2	≥16	≤0.25	1	≤0.5	≤0.5	≥320
CRE-47	47	blood	2012	IMP-8	≥64	8	≥64	2	2	4	1	≤2	≥16	0.5	1	≤0.5	≤0.5	≥320
CRE-336	336	bw	2017	OXA-48	≥64	≥64	≥64	≥64	8	4	4	≤2	≤1	≥4	≥8	≤0.5	≤0.5	≥320
CRE-412	412	sputum	2018	VIM-1	≤1	≥64	16	2	≤0.5	≤0.25	≤0.25	≤2	≤1	≥4	4	1	≤0.5	≥320

FIGURE 2 | PFGE, the origin of isolate, year, MICs of antibiotics, and carbapenemase genes in 39 *E. coli* **(A)** and 69 *K. pneumoniae* **(B)** isolates. **(A)** All CPEC had the following MICs of antibiotics: ampicillin ≥ 32 μg/ml, piperacillin > 128 μg/ml, cefazolin ≥ 64 μg/ml, ciprofloxacin ≥ 4 μg/ml, levofloxacin ≥ 8 μg/ml, tigecycline ≤ 0.5 μg/ml, and colistin ≤ 0.5 μg/ml. **(B)** All CPKP had MICs of the antibiotics as follows, ampicillin ≥ 32 μg/ml and cefazolin ≥ 64 μg/ml. bw, bronchial washing; CMZ, cefmetazole; CTX, cefotaxime; CAZ, ceftazidime; CEF, cefepime; IPM, imipenem; ETP, ertapenem; MEM, meropenem; AMK, amikacin; GEN, gentamicin; CIP, ciprofloxacin; LVX, levofloxacin; TIG, tigecycline; COL, colistin; TMP, trimethoprim.

K. pneumoniae (n = 372) showed the carbapenem resistance rates were 1.2% (5/423) in *E. coli* and 7.5% (28/372) in *K. pneumoniae* (Liu et al., 2020). Moreover, carbapenemase genes were detected in 67.8% *K. pneumoniae* isolates (19/28). Among the CRKP isolates, 57.1% (16/28) harbored bla_{KPC} (Liu et al., 2020). However, in 2019, we found OXA-48-like was the dominant carbapenemase in CRKP. These results suggested the difference in the distribution of carbapenemase genes in CRKP isolated from different specimens and regions. Moreover, previous studies showed that most KPC-2 producers in CRKP were ST11 (Liu et al., 2020; Wu et al., 2021). Therefore, the ST type of OXA-48-like producing CRKP is worth further investigating.

We also found a dramatic increase in $bla_{\mathrm{NDM-5}}$ and $bla_{\mathrm{KPC-2/blaOXA-48-like}}$ from 2018 to 2020 in CREC when compared to the years before 2018 (**Figure 1**). Huang et al. (2021) reported an increase of NDM-producing *E. coli* in northern Taiwan during 2016 to 2018. Importantly, in all five $bla_{\mathrm{NDM-5}}$-positive isolates, the $bla_{\mathrm{NDM-5}}$ gene was located in a ∼46 kb IncX3 plasmid that were nearly identical to each other (Huang et al., 2021). These five $bla_{\mathrm{NDM-5}}$-containing plasmids are similar to pP785-NDM5 from China (Ho et al., 2018). These results suggest the dissemination of a specific IncX3 $bla_{\mathrm{NDM-5}}$-containing plasmid in Taiwan. Seven CPEC isolates having $bla_{\mathrm{KPC-2/blaOXA-48-like}}$ were collected from August 2019 to July 2020 in this study. The clonality of these seven strains remain unclear and worth investigating to determine whether is a specific CPEC clone outbreak in the hospital.

In addition, we found 15 CPE isolates carrying more than one carbapenemase gene during 2017–2020 (**Table 2**). Whether these carbapenemase genes were located on a single plasmid is worth investigating. We also found that four isolates containing metallo-carbapenemase NDM-5 and non-metallo-carbapenemases (OXA-48 or KPC-2) showed inconsistent mCIM/eCIM results (**Table 3**). These results raised the possibility that different expression levels of carbapenemase genes were present in these isolates, thus affecting the phenotypic detection of mCIM/eCIM. In addition, it remains to be investigated whether the genotypes of the carbapenemase genes in these isolates affect their enzymatic activity.

The emergence of CRE strains that also exhibit resistance to colistin and tigecycline has become a major clinical concern, as these two antibiotics are used as first-line for the treatment of CRE infections (Doi, 2019). Our results showed that all CPEC were sensitive to colistin and tigecycline (**Figure 2A**), while 6 and 11 CPKP were resistant to colistin (MIC $\geq$ 4 μl/ml) and tigecycline (MIC $\geq$ 8 μl/ml), respectively (**Figure 2B**). The mechanisms responsible for colistin and tigecycline resistance of these CPKP isolates remain to be studied. In addition, all CPKP isolates (n = 5) in cluster 6 were resistant to colistin and 5 of 7 isolates in cluster 3 were resistant to tigecycline (**Figure 2B**). The characteristics of the isolates in clusters 3 and 6 are worthy of future study.

Hentschke et al. (2010) demonstrated the induction of AcrAB-mediated multidrug resistance by prior treatment with multiple antibiotics. Kanwar et al. (2018) also revealed the occurrence of treatment-emergent colistin-resistant KPC-producing *K. pneumoniae* after 8 days of colistin-based combination therapy due to disruption of *mgrB*. Studies with clinical isolates provided evidence of an association between the emergence of colistin and tigecycline resistance in CRKP and frequent antibiotic use (van Duin et al., 2014; Du et al., 2018; Kanwar et al., 2018). Therefore, it is worth investigating whether the patient received long-term antibiotics, including tigecycline or colistin, after the diagnosis of CRKP infection, inducing resistance in this study.

Salipante et al. (2015) reported that whole-genome sequencing (WGS) has significantly improved resolving power for strain typing compared to PFGE. However, the present barriers to the universal adoption of WGS by clinical laboratories include relatively high costs of instrumentation and a lack of bioinformatic expertise (Salipante et al., 2015). Therefore, in this study, we performed PFGE to determine the clonality of 39 CPEC and 69 CPKP isolates carrying carbapenemase KPC-2, NDM, and OXA-48.

In conclusion, our longitudinal collection of isolates showed the increase of CPE in CRE isolates in Taiwan during 2011–2020, and the dominant carbapenemase gene was $bla_{\mathrm{OXA-48-like}}$, followed by $bla_{\mathrm{KPC-2}}$, among our CPE isolates. Moreover, we found the carbapenemase distribution and antimicrobial susceptibility in CPE were associated with PFGE typing. Although the analysis of our study was restricted to a single hospital as opposed to population-based, the continued epidemiological surveillance and control of antimicrobial prescribing and consumption would reduce the prevalence of drug-resistant organisms and the spread of antibiotic resistance.

DATA AVAILABILITY STATEMENT

The original contributions presented in the study are included in the article/supplementary material, further inquiries can be directed to the corresponding author.

AUTHOR CONTRIBUTIONS

Y-MT, H-CC, and L-LW contributed to the collection of isolates. TD, PC, Y-MT, H-CC, P-YK, TT, JH, SW, Y-ZZ, W-HL, and M-CW performed the experiments and interpreted the results of bacterial identification, antibiotic susceptibility tests, mCIM/eCIM tests, carbapenemases detection, and conjugation assays. C-YK was responsible for data analysis, manuscript writing, designed the study, and responsible for overall management and planning. All authors read and approved the final manuscript.

FUNDING

This work was supported by the Ministry of Science and Technology, Taiwan (Grant Number 109-2320-B-

-036-MY3); the En Chu Kong Hospital, Taiwan (Grant Number ECKH_W11001); the Yen Tjing Ling Medical Foundation, Taiwan (Grant Number CI-110-13); and the National Yang-Ming University-Far Eastern Memorial Hospital Joint Research Program, Taiwan (Grant Number 110DN14).

REFERENCES

Alderliesten, J. B., Duxbury, S. J. N., Zwart, M. P., de Visser, J., Stegeman, A., and Fischer, E. A. J. (2020). Effect of donor-recipient relatedness on the plasmid conjugation frequency: a meta-analysis. *BMC Microbiol.* 20:135. doi: 10.1186/s12866-020-01825-4

Bando, S. Y., Andrade, F. B., Guth, B. E., Elias, W. P., Moreira-Filho, C. A., and Pestana de Castro, A. F. (2009). Atypical enteropathogenic *Escherichia coli* genomic background allows the acquisition of non-EPEC virulence factors. *FEMS Microbiol. Lett.* 299, 22–30. doi: 10.1111/j.1574-6968.2009.01735.x

Barry, A. L., Jones, R. N., Thornsberry, C., Ayers, L. W., and Kundargi, R. (1985). Imipenem (N-formimidoyl thienamycin): in vitro antimicrobial activity and beta-lactamase stability. *Diagn. Microbiol. Infect. Dis.* 3, 93–104. doi: 10.1016/0732-8893(85)90017-3

Chen, C. M., Guo, M. K., Ke, S. C., Lin, Y. P., Li, C. R., and VyNguyen, H. T. (2018). Emergence and nosocomial spread of ST11 carbapenem-resistant *Klebsiella pneumoniae* co-producing OXA-48 and KPC-2 in a regional hospital in Taiwan. *J. Med. Microbiol.* 67, 957–964. doi: 10.1099/jmm.0.000771

Chen, L., Mathema, B., Chavda, K. D., DeLeo, F. R., Bonomo, R. A., and Kreiswirth, B. N. (2014). Carbapenemase-producing *Klebsiella pneumoniae*: molecular and genetic decoding. *Trends Microbiol.* 22, 686–696. doi: 10.1016/j.tim.2014.09.003

Chen, Y. T., Lin, J. C., Fung, C. P., Lu, P. L., Chuang, Y. C., Wu, T. L., et al. (2014). KPC-2-encoding plasmids from *Escherichia coli* and *Klebsiella pneumoniae* in Taiwan. *J. Antimicrob. Chemother.* 69, 628–631.

Chiu, S. K., Ma, L., Chan, M. C., Lin, Y. T., Fung, C. P., Wu, T. L., et al. (2018). Carbapenem nonsusceptible *klebsiella pneumoniae* in taiwan: dissemination and increasing resistance of carbapenemase producers during 2012-2015. *Sci. Rep.* 8:8468. doi: 10.1038/s41598-018-26691-z

CLSI (2020). *Performance Standards for Antimicrobial Susceptibility Testing.* Wayne: CLSI.

De Oliveira, D. M. P., Forde, B. M., Kidd, T. J., Harris, P. N. A., Schembri, M. A., and Beatson, S. A. (2020). Antimicrobial resistance in ESKAPE Pathogens. *Clin. Microbiol. Rev.* 33, 181–119.

Doi, Y. (2019). Treatment Options for Carbapenem-resistant Gram-negative Bacterial Infections. *Clin. Infect. Dis.* 69, S565–S575. doi: 10.1093/cid/ciz830

Doyle, D., Peirano, G., Lascols, C., Lloyd, T., Church, D. L., and Pitout, J. D. (2012). Laboratory detection of *Enterobacteriaceae* that produce carbapenemases. *J. Clin. Microbiol.* 50, 3877–3880.

Du, X., He, F., Shi, Q., Zhao, F., Xu, J., Fu, Y., et al. (2018). The rapid emergence of tigecycline resistance in blaKPC-2 harboring *klebsiella pneumoniae*, as mediated in vivo by mutation in teta during tigecycline treatment. *Front. Microbiol.* 9:648. doi: 10.3389/fmicb.2018.00648

Ellington, M. J., Kistler, J., Livermore, D. M., and Woodford, N. (2007). Multiplex PCR for rapid detection of genes encoding acquired metallo-beta-lactamases. *J. Antimicrob. Chemother.* 59, 321–322. doi: 10.1093/jac/dkl481

Hentschke, M., Wolters, M., Sobottka, I., Rohde, H., and Aepfelbacher, M. (2010). ramR mutations in clinical isolates of *Klebsiella pneumoniae* with reduced susceptibility to tigecycline. *Antimicrobial. Agents Chemother.* 54, 2720–2723. doi: 10.1128/AAC.00085-10

Ho, P. L., Wang, Y., Liu, M. C., Lai, E. L., Law, P. Y., Cao, H., et al. (2018). IncX3 Epidemic plasmid carrying blaNDM-5 in *Escherichia coli* from swine in multiple geographic areas in china. *Antimicrobial. Agents Chemother.* 62, e2295–e2217. doi: 10.1128/AAC.02295-17

Huang, Y. S., Sai, W. C., Li, J. J., Chen, P. Y., Wang, J. T., Chen, Y. T., et al. (2021). Increasing New Delhi metallo-beta-lactamase-positive *Escherichia coli* among carbapenem non-susceptible *Enterobacteriaceae* in Taiwan during 2016 to 2018. *Sci. Rep.* 11:2609. doi: 10.1038/s41598-021-82166-8

Iredell, J., Brown, J., and Tagg, K. (2016). Antibiotic resistance in *Enterobacteriaceae*: mechanisms and clinical implications. *BMJ* 352:6420.

Jean, S. S., Lee, N. Y., Tang, H. J., Lu, M. C., Ko, W. C., and Hsueh, P. R. (2018). Carbapenem-resistant *enterobacteriaceae* infections: taiwan aspects. *Front. Microbiol.* 9:2888. doi: 10.3389/fmicb.2018.02888

Kanwar, A., Marshall, S. H., Perez, F., Tomas, M., Jacobs, M. R., Hujer, A. M., et al. (2018). Emergence of resistance to colistin during the treatment of bloodstream infection caused by *klebsiella pneumoniae* carbapenemase-producing *klebsiella pneumoniae*. *Open Forum. Infect. Dis.* 5:54. doi: 10.1093/ofid/ofy054

Kao, C. Y., Udval, U., Huang, Y. T., Wu, H. M., Huang, A. H., Bolormaa, E., et al. (2016). Molecular characterization of extended-spectrum beta-lactamase-producing *Escherichia coli* and Klebsiella spp. isolates in Mongolia. *J. Microbiol. Immunol. Infect.* 49, 692–700. doi: 10.1016/j.jmii.2015.05.009

Kopotsa, K., Osei Sekyere, J., and Mbelle, N. M. (2019). Plasmid evolution in carbapenemase-producing *Enterobacteriaceae*: a review. *Ann. NY Acad. Sci.* 1457, 61–91. doi: 10.1111/nyas.14223

Lai, C. C., and Yu, W. L. (2021). *Klebsiella pneumoniae* harboring carbapenemase genes in taiwan: its evolution over 20 Years, 1998-2019. *Int. J. Antimicrob. Agents* 58:106354. doi: 10.1016/j.ijantimicag.2021.106354

Li, H. Y., Kao, C. Y., Lin, W. H., Zheng, P. X., Yan, J. J., Wang, M. C., et al. (2018). Characterization of CRISPR-Cas systems in clinical *klebsiella pneumoniae* isolates uncovers its potential association with antibiotic susceptibility. *Front. Microbiol.* 9:1595. doi: 10.3389/fmicb.2018.01595

Liu, P. Y., Lee, Y. L., Lu, M. C., Shao, P. L., Lu, P. L., Chen, Y. H., et al. (2020). National surveillance of antimicrobial susceptibility of bacteremic gram-negative bacteria with emphasis on community-acquired resistant isolates: report from the 2019 surveillance of multicenter antimicrobial resistance in taiwan (SMART). *Antimicrobial. Agents Chemother.* 64, e1089–e1020. doi: 10.1128/AAC.01089-20

Logan, L. K., and Weinstein, R. A. (2017). The epidemiology of carbapenem-resistant *enterobacteriaceae*: the impact and evolution of a global menace. *J. Infect. Dis.* 215, S28–S36. doi: 10.1093/infdis/jiw282

Lutgring, J. D. (2019). Carbapenem-resistant *Enterobacteriaceae*: An emerging bacterial threat. *Semin. Diagn. Pathol.* 36, 182–186. doi: 10.1053/j.semdp.2019.04.011

Mlynarcik, P., Roderova, M., and Kolar, M. (2016). Primer evaluation for pcr and its application for detection of carbapenemases in *enterobacteriaceae*. *Jundishapur J. Microbiol.* 9:e29314. doi: 10.5812/jjm.29314

Poirel, L., Heritier, C., Spicq, C., and Nordmann, P. (2004). In vivo acquisition of high-level resistance to imipenem in *Escherichia coli*. *J. Clin. Microbiol.* 42, 3831–3833.

Salipante, S. J., SenGupta, D. J., Cummings, L. A., Land, T. A., Hoogestraat, D. R., and Cookson, B. T. (2015). Application of whole-genome sequencing for bacterial strain typing in molecular epidemiology. *J. Clin. Microbiol.* 53, 1072–1079. doi: 10.1128/JCM.03385-14

Sfeir, M. M., Hayden, J. A., Fauntleroy, K. A., Mazur, C., Johnson, J. K., Simner, P. J., et al. (2019). EDTA-Modified carbapenem inactivation method: a phenotypic method for detecting metallo-beta-lactamase-producing *enterobacteriaceae*. *J. Clin. Microbiol.* 57, e1757–e1718. doi: 10.1128/JCM.01757-18

Sugawara, E., Kojima, S., and Nikaido, H. (2016). *Klebsiella pneumoniae* major porins ompk35 and ompk36 allow more efficient diffusion of beta-lactams than their *escherichia coli* homologs ompf and OMpC. *J. Bacteriol.* 198, 3200–3208. doi: 10.1128/JB.00590-16

Tsai, Y. M., Wang, S., Chiu, H. C., Kao, C. Y., and Wen, L. L. (2020). Combination of modified carbapenem inactivation method (mCIM) and EDTA-CIM (eCIM) for phenotypic detection of carbapenemase-producing *Enterobacteriaceae*. *BMC Microbiol.* 20:315. doi: 10.1186/s12866-020-02010-3

van Duin, D., Cober, E. D., Richter, S. S., Perez, F., Cline, M., Kaye, K. S., et al. (2014). Tigecycline therapy for carbapenem-resistant *Klebsiella pneumoniae*

(CRKP) bacteriuria leads to tigecycline resistance. *Clin. Microbiol. Infect.* 20, 1117–1120. doi: 10.1111/1469-0691.12714

Wu, A. Y., Chang, H., Wang, N. Y., Sun, F. J., and Liu, C. P. (2021). Clinical and molecular characteristics and risk factors for patients acquiring carbapenemase-producing and non-carbapenemase-producing carbapenem-nonsusceptible-Enterobacterales bacteremia. *J. Microbiol. Immunol. Infect.* 9, 235–238. doi: 10.1016/j.jmii.2021.10.008

Yigit, H., Queenan, A. M., Anderson, G. J., Domenech-Sanchez, A., Biddle, J. W., and Steward, C. D. (2001). Novel carbapenem-hydrolyzing beta-lactamase, KPC-1, from a carbapenem-resistant strain of *Klebsiella pneumoniae*. *Antimicrob. Agents Chemother.* 45, 1151–1161. doi: 10.1128/AAC.45.4.1151-1161.2001

Zhang, Y., Wang, Q., Yin, Y., Chen, H., Jin, L., Gu, B., et al. (2018). Epidemiology of carbapenem-resistant *enterobacteriaceae* infections: report from the china CRE Network. *Antimicrob. Agents Chemother.* 62, e1882–e1817. doi: 10.1128/AAC.01882-17

Conflict of Interest: The authors declare that the research was conducted in the absence of any commercial or financial relationships that could be construed as a potential conflict of interest.

Publisher's Note: All claims expressed in this article are solely those of the authors and do not necessarily represent those of their affiliated organizations, or those of the publisher, the editors and the reviewers. Any product that may be evaluated in this article, or claim that may be made by its manufacturer, is not guaranteed or endorsed by the publisher.

frontiers | Frontiers in Microbiology

ORIGINAL RESEARCH
published: 19 May 2022
doi: 10.3389/fmicb.2022.825389

Emergence of bla_{NDM-1}-Carrying *Aeromonas caviae* K433 Isolated From Patient With Community-Acquired Pneumonia

Xinhua Luo[1†], Kai Mu[2,3†], Yujie Zhao[4], Jin Zhang[1], Ying Qu[1], Dakang Hu[1], Yifan Jia[1], Piaopiao Dai[1], Jian Weng[5], Dongguo Wang[6†] and Lianhua Yu[1*]*

[1] Department of Clinical Laboratory Medicine, Taizhou Municipal Hospital Affiliated With Taizhou University, Taizhou, China, [2] Beijing Institute of Radiation Medicine, Beijing, China, [3] Beijing Key Laboratory of New Molecular Diagnosis Technologies for Infectious Diseases, Beijing, China, [4] Department of Clinical Laboratory Medicine, Ningbo Medical Center Li Huili Hospital, Ningbo, China, [5] Taizhou Center for Disease Control and Prevention, Taizhou, China, [6] Department of Central Laboratory, Taizhou Municipal Hospital Affiliated With Taizhou University, Taizhou, China

OPEN ACCESS

Edited by:
Mary Marquart,
University of Mississippi Medical Center, United States

Reviewed by:
Milena Dropa,
University of São Paulo, Brazil
Ahmed Mahrous Soliman,
Kafrelsheikh University, Egypt
Costas C. Papagiannitsis,
University of Thessaly, Greece

***Correspondence:**
Lianhua Yu
yulianhua64@126.com
Dongguo Wang
wdgtzs@163.com

[†] These authors have contributed equally to this work

Specialty section:
This article was submitted to Antimicrobials, Resistance and Chemotherapy, a section of the journal Frontiers in Microbiology

Received: 30 November 2021
Accepted: 16 February 2022
Published: 19 May 2022

Citation:
Luo X, Mu K, Zhao Y, Zhang J, Qu Y, Hu D, Jia Y, Dai P, Weng J, Wang D and Yu L (2022) Emergence of bla_{NDM-1}-Carrying Aeromonas caviae K433 Isolated From Patient With Community-Acquired Pneumonia. Front. Microbiol. 13:825389. doi: 10.3389/fmicb.2022.825389

To demonstrate the detailed genetic characteristics of a bla_{NDM-1}-carrying multidrug-resistant *Aeromonas caviae* strain, the complete genome of the *A. caviae* strain K433 was sequenced by Illumina HiSeq and Oxford nanopore platforms, and mobile genetic elements associated with antibiotic resistance genes were analyzed by a series of bioinformatics methods. *A. caviae* K433 which was determined to produce class B carbapenemase, was resistant to most antibiotics tested except amikacin. The genome of K433 consisted of a chromosome cK433 (6,482-kb length) and two plasmids: pK433-qnrS (7.212-kb length) and pK433-NDM (200.855-kb length), the last being the first investigated bla_{NDM}-carrying plasmid from *Aeromonas* spp. By comparison of the backbone and MDR regions from the plasmids studied, they involved a highly homologous sequence structure. This study provides in-depth genetic insights into the plasmids integrated with bla_{NDM}-carrying genetic elements from *Aeromonas* spp.

Keywords: ***Aeromonas*** **spp., IMEs, mobile genetic elements,** bla_{NDM}**, multidrug resistance**

INTRODUCTION

Aeromonas spp. was first recognized as a human pathogen in 1954 when it was isolated from a blood sample (Parker and Shaw, 2011). In the following years, there were more confirmed cases of *Aeromonas* spp. causing human infections with varying degrees of severity, mainly, gastroenteritis (Parker and Shaw, 2011). *Aeromonas* spp. is ubiquitous in water, which can form biofilms, and then colonize the water system, drinking water may be a potential source of infection. *Aeromonas* spp. was mainly found in marine environments and freshwater (Figueira et al., 2011; Martino et al., 2014), and their spread is related to contact and ingestion of contaminated water or food.

In 2018, *Aeromonas* spp. was investigated in a wastewater treatment plant effluent in Tokyo, Japan, and two strains harboring the bla_{KPC-2} gene were detected (Sekizuka et al., 2019). Besides KPC, *Aeromonas caviae* producing VIM was reported in an Israeli hospital in 2014 (Adler et al., 2014), *Aeromonas hydrophila* carrying GES-24 carbapenemase was discovered in 2018 from a hospitalized patient in Okinawa, Japan (Uechi et al., 2018), and *A. caviae* from India was confirmed to carry OXA-181-carbapenemase (Anandan et al., 2017). *Aeromonas* spp. simultaneously harboring $bla_{CTX-M-15}$, bla_{SHV-12}, bla_{PER-1}, and bla_{FOX-2}, was isolated from Adriatic Sea of Croatia (Maravić et al., 2013). In the past 10 years, carbapenemase-producing

bacteria have been isolated from non-human sources, including the aquatic environment. The carbapenemase-producing bacteria from the aquatic environment are particularly susceptible to human activities. Bidirectional movement of the carbapenemase-producing bacteria between the aquatic environment and humans has been occurring all the time (Hammer-Dedet et al., 2020). The fewest members of metallo-beta-lactamases B2 are composed of different species of *Aeromonas*, such as *A. hydrophila*, *Aeromonas Veronii*, and *Serratia Fonticola*, named CphA, ImiS, and SFH-I in the literature, respectively (Mojica et al., 2022). Just due to the pooling of carbapenemase-producing *Aeromonas* spp. from water, acquired resistance genes appear from time-to-time in the clinic, which deserves attention.

Although the aforementioned genes involving carbapenemase or other beta-lactamase were reported in *Aeromonas* spp., bla_{NDM} has not been reported in *A. caviae* to date. Since the bla_{NDM} gene was first discovered in India in 2009 (Yong et al., 2009), it has rapidly spread all over the world (Dortet et al., 2014). Although bla_{NDM} was originally determined in a *Klebsiella pneumoniae* plasmid (Yong et al., 2009), it has also been reported in the recent years that bla_{NDM} has been found in the chromosomes of *Enterobacteriaceae* (Girlich et al., 2015; Shen et al., 2017; Sakamoto et al., 2018; Reynolds et al., 2019; Kong et al., 2020). The strains carrying metallo-beta-lactamases are capable of hydrolyzing all beta-lactam antibiotics except aztreonam, which has raised great concerns worldwide.

In this work, we first discovered a multidrug-resistant *A. caviae* strain carrying bla_{NDM-1}. The whole genome of the strain was sequenced and the mobile genetic elements of the strain containing drug-resistant genes were thoroughly and genetically studied.

MATERIALS AND METHODS

Bacterial Strain and *16S rRNA* Gene

A. caviae strain K433 was isolated from a patient's sputum in the Taizhou Municipal Hospital affiliated with the Taizhou University of China in 2018. EC600 (highly resistant to rifampicin) and *Escherichia coli* DH5α were used as hosts for conjugal and plasmid transfers, respectively. Strain K433 was initially identified by Vitek 2. Later, it was confirmed by PCR amplification and sequencing of *16S rRNA* with primers: Forward, 5′-AGAGTTTGATCATGGCTCAG-3′; Reverse: 5′-GGTTACCTTGTTACGACTT-3′ (Demarta et al., 1999). Moreover, bacterial species identification was also performed using genome sequence-based average nucleotide identity (ANI) analysis[1] (Richter and Rosselló-Móra, 2009).

Phenotypic Assays

Detection of Class a Serine Carbapenemase and Class B Metallo β-Lactamase

The activities of class A serine carbapenemase and class B metallo β-lactamase could be suppressed by 3-aminophenyl boronic acid (APB) and ethylenediamine tetra-acetic acid (EDTA) (Pournaras et al., 2013). We chose APB combined with EDTA to detect the carbapenemase of strain K433 according to the previous report (Tsakris et al., 2010).

The interpretation of the results was as follows: (1) if the diameter of the inhibition zone of the imipenem disc with APB solution differs from that of the single-imipenem disc by ≥5 mm, it could be judged that the tested strain produced class A carbapenemase; (2) if the diameter of the inhibition zone of the imipenem disc with EDTA solution differed from that of the single-imipenem disc by ≥5 mm, it might be that the tested strain produced class B carbapenemase; (3) If APB + EDTA were added concurrently, the diameters of the inhibition zone of the imipenem discs with APB + EDTA differed from that of the single-imipenem disc by ≥5 mm, it could be confirmed that the tested strain simultaneously produced class A carbapenemase + class B metallo β-lactamase; (4) if the difference between the inhibition zone diameter of the imipenem disc containing enzyme inhibitor and the single-imipenem disc was less than 5 mm, it could be determined that the bacteria did not produce class A carbapenemase or class B metallo β-lactamase.

Antibiotic Susceptibility Test

The method used for testing bacterial resistance was BioMérieux VITEK2, and the results were determined in accordance with the 2020 Clinical and Laboratory Standards Association (CLSI) guidelines (Clinical and Laboratory Standards Institute [CLSI], 2020).

12 antibiotics, namely, cefepime, aztreonam, imipenem, meropenem, amikacin, ciprofloxacin, levofloxacin, tigecycline, minocycline, tigecycline/clavulanic acid, and piperacillin/tazobactam, were tested. *E. coli* ATCC 25922 was used as the quality control strain.

Conjugal Transfer and Plasmid Transfer

Bacterial plasmid DNA of strain K433 was extracted using a plasmid extraction kit (TaKaRa, Dalian, China) in accordance with the manufacturer's instructions. The plasmid was transferred in an attempt from the *A. caviae* K433 isolate into EC600 and *E. coli* DH5a through conjugal transfer and electroporation, respectively. For the selection of transconjugants and/or transformants containing the bla_{NDM} marker, 2 μg/ml imipenem and 1,000 μg/ml rifampicin were used according to specific circumstances.

Sequencing and Sequence Assembly

Genomic DNA was extracted from strain K433 using a Gentra Puregene Yeast/Bact. Kit (Qiagen, Valencia, CA, United States). Libraries were prepared separately using the TruePrepTM DNA Library Prep Kit V2 and the SQU-LSK109 Ligation Sequencing kit. After the preparation of the library was completed, it was separately sequenced on an Illumina HiSeq X Ten platform (Illumina Inc., San Diego, CA, United States) and GridION X5 platform (Oxford Nanopore, United Kingdom). To improve the reliability of data processing, raw data from the HiSeq X Ten platform and the GridION X5 platform were trimmed to obtain

[1] http://www.ezbiocloud.net/tools/ani

the high-quality clean reads (clean data) by Canu v1.8.[2]. The paired-end short Illumina reads and the long Nanopore reads were "*de novo*" assembled using Unicycler v0.4.5.[3]

Sequence Annotation and Comparison

Open reading frames and pseudogenes were predicted using RAST2.0 (Brettin et al., 2015), BLASTP/BLASTN (Boratyn et al., 2013), UniProtKB/Swiss-Prot (Boutet et al., 2016), and RefSeq databases (O'Leary et al., 2016). Annotation of drug resistance genes, mobile genetic elements, and other features were performed using online databases, such as CARD (Liang et al., 2017), ResFinder (Zankari et al., 2012), ISfinder (Siguier et al., 2006), INTEGRALL (Moura et al., 2009), and the Tn Number Registry (Roberts et al., 2008). Multiple and pairwise sequence comparisons were performed using MUSCLE 3.8.31 (Edgar, 2004) and BLASTN. The genome map was drawn using Inkscape 0.48.1.[4]

Nucleotide Sequence Accession Numbers

Nucleotide sequence accession numbers for chromosome K433 (ck433), plasmid K433-qnrS (pK433-qnrS), and plasmid K433-NDM (pK433-NDM) were CP084031, OK017455, and OK287926, respectively.

It was collected for comparative analysis between pK433-NDM and related plasmids, including p13ZX28-272, p13ZX28-TC-98, p13ZX36-200, pCP077202, pCP077203, and pCP077204, which nucleotide sequence accession numbers were MN101850, MN101852, MN101853, CP077202, CP077203, and CP077204, respectively.

RESULTS

Antimicrobial Susceptibility Test, Enzymatic Properties, and Transferrable Features

Through the *16S rRNA* sequence and genome sequence-based ANI analysis, strain K433 was identified to be *A. caviae* eventually. The results of the antimicrobial susceptibility tests on strain K433 were shown in **Table 1**. Through detection of enzymatic properties, the strain K433 was confirmed to harbor only class B metallo β-lactamase. After bacterial conjugative transfer and electroporation assays, no transconjugant or transformant carrying pK433-NDM could be recovered despite repeated trials.

Overview of the Genome of K433

Strain K433 carried a 6,482-kb-long chromosome cK433, a 200.855-kb-long plasmid pK433-NDM, and a 7.212-kb-long plasmid pK433-qnrS (**Supplementary Table 1**). Plasmid pK433-NDM involved the region of bla_{MOX-6} gene, and a 42.3-kb-long MDR region where bla_{NDM} was inserted (**Supplementary Figure 1**). Plasmid pK433-qnrS only contained drug-resistance gene *qnrS2* (**Supplementary Figure 2**). All resistance genes were listed in **Table 2**.

TABLE 1 | Antimicrobial drug susceptibility profiles of *Aeromonas caviae* K433.

Antibiotics	MIC values (μg/mL)	Antimicrobial susceptibility
Ceftazidime	32	R
Cefepime	16	R
Aztreonam	16	R
imipenem	8	R
Meropenem	8	R
Amikacin	4	S
Ciprofloxacin	≥4	R
Levofloxacin	≥8	R
tigecycline	≥8	R
Minocycline	≥16	R
Ticarcilin/clavulanic acid	≥128	R
Piperacillin/tazobactam	≥128	R

Characteristics of IMEs on Chromosome cK433

Integrative and mobilizable elements (IMEs) were extremely closely related to the acquisition or loss of bacterial resistance to antibiotics (Bellanger et al., 2014; Delavat et al., 2017). Three IMEs were found on cK433, including IME*1*, IME*2*, and IME*3* regions (**Figure 1**).

IME*1*, flanked by a pair of *attL/attR* (14 bp in length), had a backbone (containing *int*) with insertion of two accessory modules: 43.9-kb *strAB*–$bla_{CTX-M-3}$ region and truncated IS*630*-family IS element. The 43.9-kb *strAB*–$bla_{CTX-M-3}$ region, including In792 [gene cassette array (GCA): *aac(6')-Ib-cr–arr3*], was inserted between the *orf339* and *wyl* gene at the left end of the backbone region, and truncated IS*630*-family IS element was inserted between the *hns* and *orf114* gene at the right end of the backbone region (**Figure 1A**). Meanwhile, the unit transposon Tn*6320* (carrying bla_{TEM-1} and $bla_{CTX-M-3}$) was inserted into the *qacED1* gene of In792. Tn*5393n* was inserted between the *virD2* and *lepB* gene at the right end of In792, following, IS*Aeca7* was inserted into Δ*tnpA* gene, which was divided into two parts on the left end of Tn*5393n*, then, two identical IS*6100*s were inserted between the 3′-CS and the right end of In792, forming the current complex IME*1* structure just like "Russian nesting dolls."

IME*2* consisted of the backbone region and *tetA-tetR* module which was related to tetracycline drug resistance (**Figure 1B**). IME*3* contained the backbone region, IS*Ave3* and In27 [GCA: *dfrA12–gcuF–aadA2*] which was truncated by *chrA-orf98* unit, IS*26-mph(A)*-IS*6100* unit, and two intersecting Tn*4352* (**Figure 1C**).

Comparison of Plasmids pK433-NDM, pCP077202, pCP077203, and pCP077204

According to the BLASTN alignments of the complete sequence of plasmid pK433-NDM in the NCBI GenBank database, we

[2]https://canu.readthedocs.io/en/latest/index.html

[3]https://github.com/rrwick/Unicycler

[4]https://inkscape.org/en

TABLE 2 | Resistance genes in the strain of K433.

Sequence	Resistance locus	Resistance phenotype	Nucleotide position	Region located
Chromosome K433	*aac(6')-Ib-cr*	Fluoroquinolone and aminoglycoside resistance	1358857.1359456	IME1
	arr3	Rifampicin resistance	1359553.1360005	
	bla_{TEM-1}	β-lactam resistance	1364218.1365078	
	$bla_{CTX-M-3}$	β-lactam resistance	1365860.1366735	
	sul1	Sulfonamide resistance	1368946.1369785	
	floR	Phenicol resistance	1375626.1376840	
	strA	Aminoglycoside resistance	1384020.1384823	
	strB	Aminoglycoside resistance	1384823.1385659	
	tetA(E)	Tetracycline resistance	4241253.4242470	IME2
	dfrA12	Trimethoprim resistance	4646267.4646764	IME3
	aadA2	Aminoglycoside resistance	4647172.4647963	
	qacED1	Quaternary ammonium	4648127.4648474	
	sul1	Sulfonamide resistance	4648468.4649307	
	chrA	Chromate resistance	4649794.4650999	
	mph(A)	Macrolide resistance	4654618.4655523	
	aphA-1	Aminoglycoside resistance	4656500.4657315 4658360.4659175	
pK433-NDM	bla_{MOX-6}	β-lactam resistance	57439.58587	bla_{MOX-6} region
	mer locus	Mercuric resistance	93469.97431	MDR region
	mph(A)	Macrolide resistance	100351.101256	
	chrA	Chromate resistance	104875.106080	
	sul1	Sulfonamide resistance	106567.107406 119294.120133	
	bla_{OXA}	β-lactam resistance	107877.108671	
	bla_{NDM-1}	β-lactam resistance	114445.115257	
	ble_{MBL}	Bleomycin resistance	115261.115626	
	qacED1	Quaternary ammonium	120127.120474	
	dfrA12	Trimethoprim resistance	120981.121478	
	aacC2	Aminoglycoside resistance	123848.124708	
	tmrB	Tunicamycin resistance	124721.125263	
	bla_{TEM-1}	β-lactam resistance	129680.130540	
pK433-qnrS	*qnrS2*	Quinolone resistance	2300.2956	–

found that the top three plasmids ranked by coverage value were pCP077202 (59%), pCP077203 (26%), and pCP077204 (24%), and their identities were both 100%. These three plasmids (pCP077202, pCP077203, and pCP077204) collected from GenBank all belonged to *Aeromonas* spp. in the United States and had a close correlation with plasmid pK433-NDM. Plasmids pCP077202, pCP077203, and pCP077204 were from the same strain with 161.381-, 85.67-, and 80.98-kb length, respectively. The sequence composition and structure of pK433-NDM and pCP077203 were highly similar (>95% identity) around the first 35 kb length in the plasmid maintenance region (**Figure 2**). Both plasmids pK433-NDM and pCP077202 contained the MDR region, in which there was also a high similarity with the composition and structure located on the MDR region upstream and downstream of the plasmid maintenance regions (>95% identity) (**Figure 2**). The comparison of MDR regions for 42.3 kb long pK433-NDM and 40.2 kb long pCP077202 is illustrated in **Figure 3**. The composition and structure of the sequence approximate 32 kb long on the left end of plasmid maintenance regions of pK433-NDM (23111.55424) and pCP077204 (5096.36653) were also highly similar (>95% identity). However, no plasmid replication gene was found in plasmid pCP077204 and pCP077202.

Comparison of MDR Regions From Plasmids pK433-NDM, pCP077202, pKP-14-6-NDM-1, p13ZX28-272, p13ZX36-200, and p13ZX28-TC-98

All the aforementioned plasmids except pK433-NDM were obtained from GenBank. pKP-14-6-NDM-1 was isolated from *K. pneumoniae* and p13ZX28-272, p13ZX36-200, and p13ZX28-TC-98 were all achieved from *E. coli*. The coverage and identity of the MDR region from aforementioned plasmids were listed in **Supplementary Table 2**. Compared with MDR regions from plasmids pK433-NDM and pCP077202, it seemed that In37 [Variable region 1 (VR1) containing *aacA4cr*, bla_{OXA-1}, and *catB1* and VR2 containing bla_{PER-1}] of MDR region from pCP077202 was replaced by In384 [VR1 containing *dfrA12*, VR2 containing bla_{NDM-1} and ble_{MBL}, and VR3 containing bla_{OXA}] of MDR region from pK433-NDM, and the remaining regions had a high degree of identity (>95%) with MDR region

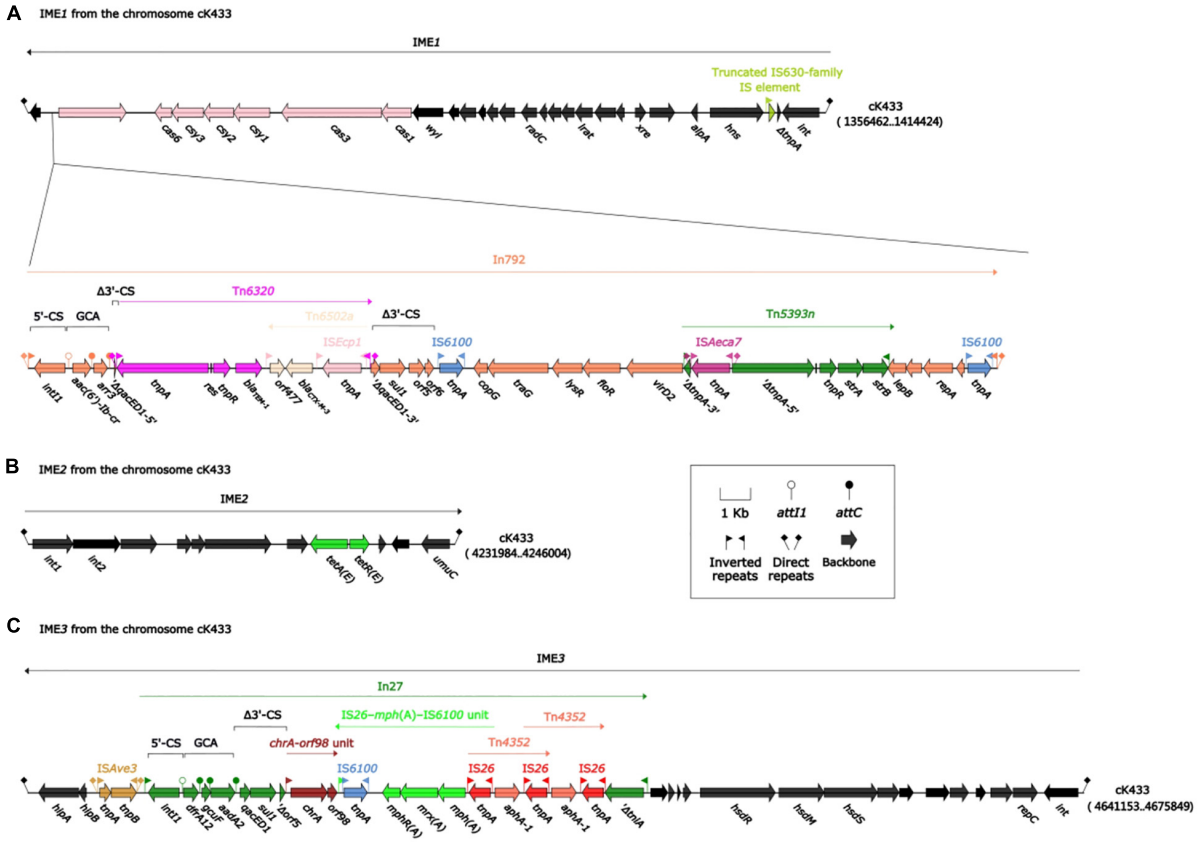

FIGURE 1 | Mobile genetic elements associated with resistant genes on chromosome cK433. IMEs were abbreviation integrative and mobilizable elements. Three IMEs (IME*1*, IME*2*, and IME*3*) were to be discovered on chromosome cK433. **(A)** IME*1*, comprising the backbone region, *cas-csy* module and In792; **(B)** IME*2*, consisting of backbone region and *tetA-tetR* module; **(C)** IME*3*, involving the backbone region, IS*Ave3* and In27.

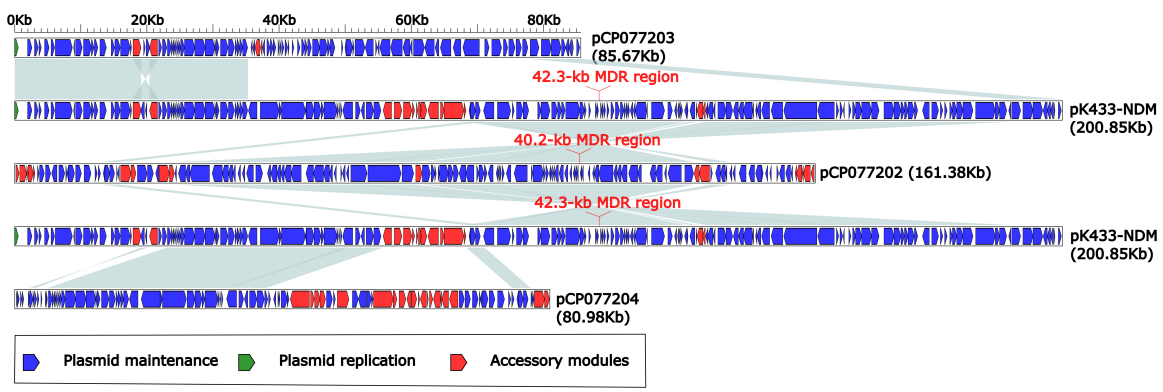

FIGURE 2 | Comparison of plasmids pK433-NDM, pCP077202, pCP077203, and pCP077204. Plasmids pCP077202, pCP077203, and pCP077204 were obtained from GenBank, which came from *Aeromonas* spp. in the United States. Plasmids pCP077202, pCP077203, and pCP077204 had 161.381, 85.67, and 80.98 kb lengths, respectively. The shadow of light blue represented >95% identity.

from pK433-NDM. (**Figure 3**). However, the MDR region from pK433-NDM carried the *bla*$_{NDM-1}$ gene located in the truncated composite transposon Tn*125*, while the MDR region from pCP077202 did not, which was the significant difference between them. Compared with MDR regions from pK433-NDM and pK-14-6-NDM-1, both involved *bla*$_{NDM}$ gene and were highly consistent with *aaC2-tmrB* region and In384 (>95% identity), and also ΔTn*21*, *chrA-orf98* unit and IS*26-mph(A)*-IS*6100* unit (>95% identity). Compared with MDR regions from pK-14-6-NDM-1 and p13ZX28-272, the regions containing *bla*$_{NDM}$

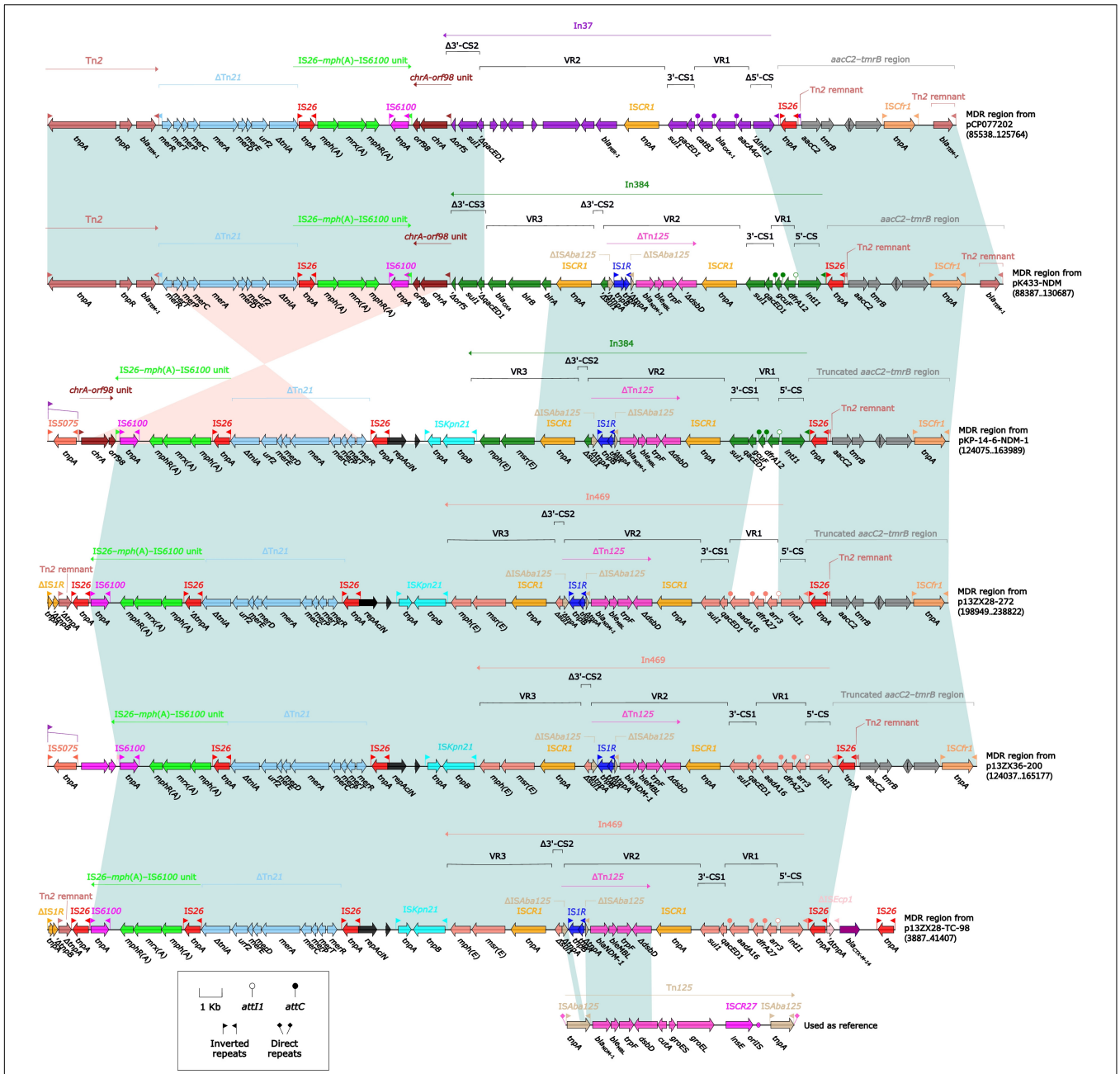

FIGURE 3 | Comparison of MDR regions from plasmids pK433-NDM, pCO077202, pKP-14-6-NDM-1, p13ZX28-272, p13ZX36-200, and p13ZX28-TC-98. pK433-NDM and pCO077202 came from *Aeromonas* spp. pKP-14-6-NDM-1 was isolated from *Klebsiella pneumoniae*, and p13ZX28-272, p13ZX36-200, and p13ZX28-TC-98 were all achieved from *Escherichia coli*.

gene showed high consistency except for the insertion type of integron (In469 from p13ZX28-272 replaced by In384 from pK-14-6-NDM-1). Compared with p13ZX28-272, p13ZX36-200, and p13ZX28-TC-98, MDR regions of pK-14-6-NDM-1 and p13ZX28-272 showed the highest identity (>95%) but revealed different coverage, which was listed in **Supplementary Table 2**. Interestingly, In469 and In384 in pK433-NDM, pK-14-6-NDM-1, p13ZX28-272, p13ZX36-200, and p13ZX28-TC-98 all contained the identical IS*CR1* and ΔTn*125* structure, which suggested IS*CR1* prompted the accumulation of ΔTn*125* between these plasmids.

DISCUSSION

Various types of antibiotic resistance genes have been discovered over and over again in *Aeromonas* spp. from nature, which is commonly resistant to quinolone and β-lactam drugs

(Piotrowska et al., 2017). It is very likely that *Aeromonas* spp. is naturally an important repository of acquired β-lactamase genes from wastewater or sludge, which was to be found in plentiful genes harboring classes A, B, C, and D β-lactamase (Piotrowska et al., 2017). However, only a tiny amount of class B carbapenemases were found, such as AsbM1, IMP-19, VIM, ImiS, ImiH, and CphA (Janda and Abbott, 2010; Piotrowska et al., 2017). So far, NDM had never been reported. To our knowledge, this is the first study involving NDM carbapenemase from an *A. caviae* strain (K433), which was isolated from inpatient's source with multidrug-resistance in our hospital. This study not only provided the first evidence of nosocomial infection and colonization of an NDM-producing *A. caviae*, but also revealed the strong transmission ability of NDM.

Reported firstly in 2009, NDM-1 has caused a major public health problem because of its high resistance profile to carbapenems and its global prevalence (Yong et al., 2009). To date, 40 variants of NDM carbapenemases have been reported.[5] The bacterial strains harboring bla_{NDM} exhibited significantly increased MICs for carbapenems, cephalosporins, penicillins, ticarcilin/clavulanic acid, and piperacillin/tazobactam except for aztreonam, just as shown in the susceptibility test of *A. caviae* K433 (**Table 1**). Strain K433 was resistant to almost all the antibiotics (including imipenem, meropenem, and tigecycline) except amikacin. Among the reported mechanisms of tigecycline resistance, the bacterial efflux pump system plays a major role. The overexpression of characteristic efflux pumps AdeABC, AdeFGH, and AdeIJK, together with the deletion and mutation of the two-component regulatory systems adeR and adeS, can lead to tigecycline resistance (Nguyen et al., 2014). In addition, the reasons for the decreased sensitivity to tigecycline include the inactivation of tigecycline by the modification enzyme Tet(X), the alteration of the cell membrane permeability because of the mutation of the *plsC* gene, and the decreased affinity between tigecycline and the ribosome due to the mutation of the *rpsJ* gene, etc. (Beabout et al., 2015). Recently, studies have reported that tigecycline resistance can be transmitted in bacteria by conjugation of plasmids carrying resistance genes (Partridge et al., 2018). In this study, we have not detected the *tet(X)* gene or other tigecycline resistance genes in strain K433. The possible mechanisms of tigecycline resistance in K433 were the overexpression of bacterial efflux pump system or/and the altering of cell membrane permeability, etc.

After high-throughput sequencing, it was determined that *A. caviae* K433 carried two plasmids: (pK433-NDM and pK433-qnrS), and one 6,482-kb-long chromosome cK433, carrying three IMEs: (IME*1*, IME*2*, and IME*3*) (**Figure 1**). IMEs and ICEs (integrative and conjugative elements) (Botelho and Schulenburg, 2021) are two different types of mobile genetic elements. They are often integrated into bacterial chromosomes to prompt the spread of resistance genes. IMEs cannot be self-transmitted, and they move between cells with the help of other conjugative elements that encode proteins involving in the complete conjugation function. IMEs usually have *attL*, *int*, *rlx*, *oriT*, and *attR*, but do not contain conjugative transfer genes (Luo et al., 2021). As for other properties of chromosome cK433, further study is needed.

It was utterly different between pK433-NDM and pK433-qnrS. Plasmid pK433-qnrS (7212 kb in length) had only *qnrS2-repC-repA-mob* gene cassettes (**Supplementary Figure 2**), while plasmid pK433-NDM (200.855 kb in length) possessed the backbone, including plasmid maintenance and replication regions, and variable regions: 42.3-kb MDR region, bla_{MOX-6} region, IS*Aeme19* and IS*AS17* (**Supplementary Figure 1**). We speculated that such a length of plasmid and the complex structure of the MDR region may result in the failures of plasmid conjugative transfer and electroporation experiment for pK433-NDM. There were six units or modules in the MDR region from pK433-NDM, revealing Tn*2*, ΔTn*21*, IS*26-mph(A)*-IS*6100* unit, *chA-orf98* unit, In384, and *aaC2-tmrB* region (**Figure 3**). The biggest differences between the MDR regions from pCP077202 and pK433-NDM were that In384 from pK433-NDM replaced the position of In37 from pCP077202, and, In37 involved 2 variable regions (VR), In384 contained 3 variable regions, then, VR2 carried ΔTn*125* with bla_{NDM} (**Figure 3**). Such a complex plasmid structure would greatly enhance the resistance to the drugs, such as carbapenems, cephalosporins, and penicillins (**Table 1**). Except that the MDR region was somewhat comparable, the backbone regions of plasmids: pCP077202, pCP077203, and pCP077204 which came from the same strain were more or less identified with the pK433-NDM, but there were some repeat backbone regions between the pCP077202, pCP077203, and pCP077204 (**Figure 2**). In general, these plasmids from different *Aeromonas* spp. had more similar structures and compositions despite of coming from different countries, different times, and even different races (**Figure 2**). As for the comparative analysis of the MDR regions from the pK433-NDM, p13ZX28-272, p13ZX28TC-98, pKP14-6-NDM-1, and p13ZX36-200, we found that the MDR regions from different plasmids almost had the identical structure, harboring ΔTn*125* with bla_{NDM} gene. It suggested that after the In384 carrying ΔTn*125* with bla_{NDM} gene was replaced by the In469 which also carried the ΔTn*125* with bla_{NDM} gene, it might be evolved even more epidemic; simultaneously, we also speculated that part of the plasmid structure and composition of *A. caviae* cK433 might come from other popular plasmids, and there was a potential risk of transmission, which must be actively prevented.

CONCLUSION

This study characterized the genome structure and constitution of the bla_{NDM}-carrying multidrug-resistant *A. caviae* strain K433. Plasmids pK433-NDM and pK433-qnrS and chromosome cK433 were discovered. In total, three drug-resistant-gene-associated IMEs (IME*1*, IME*2*, and IME*3*) were inserted into complex gene structures, including integrons, transposons, and other mobile genetic modules or units, and studied in cK433. Four plasmids: pK433-NDM, pCP077202, pCP077203, and pCP077204 were compared with the backbone and MDR regions. It showed a highly homologous sequence structure between pK433-NDM and plasmids from the same strain: pCP077202,

[5]http://www.bldb.eu/Enzymes.php

pCP077203, and pCP077204, in the backbone regions. It also indicated a highly homologous sequence structure between the MDR regions of pK433-NDM, pCP077202, pKP-14-6-NDM-1, p13ZX28-272, p13ZX36-200, and p13ZX28-TC-98. This study would provide a further theoretical basis for genetic evolution for plasmids involving bla_{NDM}-carrying genetic elements from *Aeromonas* spp.

DATA AVAILABILITY STATEMENT

The original contributions presented in the study are publicly available. This data can be found here: PRJNA765169, OK287926, and OK017455.

AUTHOR CONTRIBUTIONS

LY and DW conceptualized and designed the study. All authors participated and acquired the data. XL, KM, LY, and DW analyzed and interpreted the data. XL and KM drafted the manuscript. LY and DW critically revised the manuscript. All authors read and approved the final manuscript.

FUNDING

This work was supported by the Foundation of the Public Welfare Program of Natural Science Foundation of Zhejiang (LGF19H200006) and the Zhejiang Health Department of China (2020KY364).

SUPPLEMENTARY MATERIAL

The Supplementary Material for this article can be found online at: https://www.frontiersin.org/articles/10.3389/fmicb.2022.825389/full#supplementary-material

REFERENCES

Adler, A., Assous, M. V., Paikin, S., Shulman, A., Miller-Roll, T., Hillel, S., et al. (2014). Emergence of VIM-producing *Aeromonas caviae* in Israeli hospitals. *J. Antimicrob. Chemother.* 69, 1211–1214. doi: 10.1093/jac/dkt505

Anandan, S., Gopi, R., Devanga Ragupathi, N. K., Muthuirulandi Sethuvel, D. P., Gunasekaran, P., Walia, K., et al. (2017). First report of *bla*(OXA-181)-mediated carbapenem resistance in *Aeromonas caviae* in association with pKP3-A: threat for rapid dissemination. *J. Glob. Antimicrob. Resist.* 10, 310–314. doi: 10.1016/j.jgar.2017.07.006

Beabout, K., Hammerstrom, T. G., Perez, A. M., Magalhães, B. F., Prater, A. G., Clements, T. P., et al. (2015). The ribosomal S10 protein is a general target for decreased tigecycline susceptibility. *Antimicrob. Agents Chemother.* 59, 5561–5566. doi: 10.1128/aac.00547-15

Bellanger, X., Payot, S., Leblond-Bourget, N., and Guédon, G. (2014). Conjugative and mobilizable genomic islands in bacteria: evolution and diversity. *FEMS Microbiol. Rev.* 38, 720–760. doi: 10.1111/1574-6976.12058

Boratyn, G. M., Camacho, C., Cooper, P. S., Coulouris, G., Fong, A., Ma, N., et al. (2013). BLAST: a more efficient report with usability improvements. *Nucleic Acids Res.* 41, W29–W33. doi: 10.1093/nar/gkt282

Botelho, J., and Schulenburg, H. (2021). The role of integrative and conjugative elements in antibiotic resistance evolution. *Trends Microbiol.* 29, 8–18. doi: 10.1016/j.tim.2020.05.011

Boutet, E., Lieberherr, D., Tognolli, M., Schneider, M., Bansal, P., Bridge, A. J., et al. (2016). UniProtKB/swiss-prot, the manually annotated section of the uniprot knowledgebase: how to use the entry view. *Methods Mol. Biol.* 1374, 23–54. doi: 10.1007/978-1-4939-3167-5_2

Brettin, T., Davis, J. J., Disz, T., Edwards, R. A., Gerdes, S., Olsen, G. J., et al. (2015). RASTtk: a modular and extensible implementation of the RAST algorithm for building custom annotation pipelines and annotating batches of genomes. *Sci. Rep.* 5:8365. doi: 10.1038/srep08365

Clinical and Laboratory Standards Institute [CLSI] (2020). *Performance Standards for Antimicrobial Susceptibility Testing. 30 th ed. CLSI Supplement M100*. Wayne, PA: CLSI.

Delavat, F., Miyazaki, R., Carraro, N., Pradervand, N., and van der Meer, J. R. (2017). The hidden life of integrative and conjugative elements. *FEMS Microbiol. Rev.* 41, 512–537. doi: 10.1093/femsre/fux008

Demarta, A., Tonolla, M., Caminada, A. P., Ruggeri, N., and Peduzzi, R. (1999). Signature region within the 16S rDNA sequences of *Aeromonas popoffii*. *FEMS Microbiol. Lett.* 172, 239–246. doi: 10.1111/j.1574-6968.1999.tb13474.x

Dortet, L., Poirel, L., and Nordmann, P. (2014). Worldwide dissemination of the NDM-type carbapenemases in Gram-negative bacteria. *Biomed Res. Int.* 2014:249856. doi: 10.1155/2014/249856

Edgar, R. C. (2004). MUSCLE: a multiple sequence alignment method with reduced time and space complexity. *BMC Bioinformatics* 5:113. doi: 10.1186/1471-2105-5-113

Figueira, V., Vaz-Moreira, I., Silva, M., and Manaia, C. M. (2011). Diversity and antibiotic resistance of *Aeromonas* spp. in drinking and waste water treatment plants. *Water Res.* 45, 5599–5611. doi: 10.1016/j.watres.2011.08.021

Girlich, D., Dortet, L., Poirel, L., and Nordmann, P. (2015). Integration of the *bla*NDM-1 carbapenemase gene into *Proteus* genomic island 1 (PGI1-PmPEL) in a *Proteus mirabilis* clinical isolate. *J. Antimicrob. Chemother.* 70, 98–102. doi: 10.1093/jac/dku371

Hammer-Dedet, F., Jumas-Bilak, E., and Licznar-Fajardo, P. (2020). The hydric environment: a hub for clinically relevant carbapenemase encoding genes. *Antibiotics* 9:699. doi: 10.3390/antibiotics9100699

Janda, J. M., and Abbott, S. L. (2010). The genus *Aeromonas*: taxonomy, pathogenicity, and infection. *Clin. Microbiol. Rev.* 23, 35–73. doi: 10.1128/cmr.00039-09

Kong, L. H., Xiang, R., Wang, Y. L., Wu, S. K., Lei, C. W., Kang, Z. Z., et al. (2020). Integration of the *bla*NDM-1 carbapenemase gene into a novel SXT/R391 integrative and conjugative element in *Proteus vulgaris*. *J. Antimicrob. Chemother.* 75, 1439–1442. doi: 10.1093/jac/dkaa068

Liang, Q., Yin, Z., Zhao, Y., Liang, L., Feng, J., Zhan, Z., et al. (2017). Sequencing and comparative genomics analysis of the IncHI2 plasmids pT5282-mphA and p112298-catA and the IncHI5 plasmid pYNKP001-dfrA. *Int. J. Antimicrob. Agents* 49, 709–718. doi: 10.1016/j.ijantimicag.2017.01.021

Luo, X., Yin, Z., Zeng, L., Hu, L., Jiang, X., Jing, Y., et al. (2021). Chromosomal integration of huge and complex *bla* (NDM)-carrying genetic elements in Enterobacteriaceae. *Front. Cell Infect. Microbiol.* 11:690799. doi: 10.3389/fcimb.2021.690799

Maravić, A., Skoèibušić, M., Samanić, I., Fredotović, Z., Cvjetan, S., Jutronić, M., et al. (2013). *Aeromonas* spp. simultaneously harbouring *bla*(CTX-M-15), *bla*(SHV-12), *bla*(PER-1) and *bla*(FOX-2), in wild-growing Mediterranean mussel (*Mytilus galloprovincialis*) from Adriatic Sea Croatia. *Int. J. Food Microbiol.* 166, 301–308. doi: 10.1016/j.ijfoodmicro.2013.07.010

Martino, M. E., Fasolato, L., Montemurro, F., Novelli, E., and Cardazzo, B. (2014). *Aeromonas* spp.: ubiquitous or specialized bugs? *Environ. Microbiol.* 16, 1005–1018. doi: 10.1111/1462-2920.12215

Mojica, M. F., Rossi, M. A., Vila, A. J., and Bonomo, R. A. (2022). The urgent need for metallo-β-lactamase inhibitors: an unattended global threat. *Lancet Infect. Dis.* 22, e28–e34. doi: 10.1016/s1473-3099(20)30868-9

Moura, A., Soares, M., Pereira, C., Leitão, N., Henriques, I., and Correia, A. (2009). INTEGRALL: a database and search engine for integrons, integrases and gene cassettes. *Bioinformatics* 25, 1096–1098. doi: 10.1093/bioinformatics/btp105

Nguyen, F., Starosta, A. L., Arenz, S., Sohmen, D., Dönhöfer, A., and Wilson, D. N. (2014). Tetracycline antibiotics and resistance mechanisms. *Biol. Chem.* 395, 559–575. doi: 10.1515/hsz-2013-0292

O'Leary, N. A., Wright, M. W., Brister, J. R., Ciufo, S., Haddad, D., McVeigh, R., et al. (2016). Reference sequence (RefSeq) database at NCBI: current status, taxonomic expansion, and functional annotation. *Nucleic Acids Res.* 44, D733–D745. doi: 10.1093/nar/gkv1189

Parker, J. L., and Shaw, J. G. (2011). *Aeromonas* spp. clinical microbiology and disease. *J. Infect.* 62, 109–118. doi: 10.1016/j.jinf.2010.12.003

Partridge, S. R., Kwong, S. M., Firth, N., and Jensen, S. O. (2018). Mobile genetic elements associated with antimicrobial resistance. *Clin. Microbiol. Rev.* 31, e88–e17. doi: 10.1128/cmr.00088-17

Piotrowska, M., Przygodzińska, D., Matyjewicz, K., and Popowska, M. (2017). Occurrence and variety of β-lactamase genes among *Aeromonas* spp. isolated from urban wastewater treatment plant. *Front. Microbiol.* 8:863. doi: 10.3389/fmicb.2017.00863

Pournaras, S., Zarkotou, O., Poulou, A., Kristo, I., Vrioni, G., Themeli-Digalaki, K., et al. (2013). A combined disk test for direct differentiation of carbapenemase-producing enterobacteriaceae in surveillance rectal swabs. *J. Clin. Microbiol.* 51, 2986–2990. doi: 10.1128/jcm.00901-13

Reynolds, M. E., Phan, H. T. T., George, S., Hubbard, A. T. M., Stoesser, N., Maciuca, I. E., et al. (2019). Occurrence and characterization of *Escherichia coli* ST410 co-harbouring *bla*NDM-5, *bla*CMY-42 and *bla*TEM-190 in a dog from the UK. *J Antimicrob Chemother* 74, 1207–1211. doi: 10.1093/jac/dkz017

Richter, M., and Rosselló-Móra, R. (2009). Shifting the genomic gold standard for the prokaryotic species definition. *Proc. Natl. Acad. Sci. U.S.A.* 106, 19126–19131. doi: 10.1073/pnas.0906412106

Roberts, A. P., Chandler, M., Courvalin, P., Guédon, G., Mullany, P., Pembroke, T., et al. (2008). Revised nomenclature for transposable genetic elements. *Plasmid* 60, 167–173. doi: 10.1016/j.plasmid.2008.08.001

Sakamoto, N., Akeda, Y., Sugawara, Y., Takeuchi, D., Motooka, D., Yamamoto, N., et al. (2018). Genomic characterization of carbapenemase-producing *Klebsiella pneumoniae* with chromosomally carried *bla* (NDM-1). *Antimicrob. Agents Chemother.* 62, e1520–e1518. doi: 10.1128/aac.01520-18

Sekizuka, T., Inamine, Y., Segawa, T., Hashino, M., Yatsu, K., and Kuroda, M. (2019). Potential KPC-2 carbapenemase reservoir of environmental *Aeromonas hydrophila* and *Aeromonas caviae* isolates from the effluent of an urban wastewater treatment plant in Japan. *Environ. Microbiol. Rep.* 11, 589–597. doi: 10.1111/1758-2229.12772

Shen, P., Yi, M., Fu, Y., Ruan, Z., Du, X., Yu, Y., et al. (2017). Detection of an *Escherichia coli* sequence type 167 strain with two tandem copies of *bla*NDM-1 in the chromosome. *J. Clin. Microbiol.* 55, 199–205. doi: 10.1128/jcm.01581-16

Siguier, P., Perochon, J., Lestrade, L., Mahillon, J., and Chandler, M. (2006). ISfinder: the reference centre for bacterial insertion sequences. *Nucleic Acids Res.* 34, D32–D36. doi: 10.1093/nar/gkj014

Tsakris, A., Poulou, A., Pournaras, S., Voulgari, E., Vrioni, G., Themeli-Digalaki, K., et al. (2010). A simple phenotypic method for the differentiation of metallo-beta-lactamases and class A KPC carbapenemases in Enterobacteriaceae clinical isolates. *J. Antimicrob. Chemother.* 65, 1664–1671. doi: 10.1093/jac/dkq210

Uechi, K., Tada, T., Sawachi, Y., Hishinuma, T., Takaesu, R., Nakama, M., et al. (2018). A carbapenem-resistant clinical isolate of *Aeromonas hydrophila* in Japan harbouring an acquired gene encoding GES-24 β-lactamase. *J. Med. Microbiol.* 67, 1535–1537. doi: 10.1099/jmm.0.000842

Yong, D., Toleman, M. A., Giske, C. G., Cho, H. S., Sundman, K., Lee, K., et al. (2009). Characterization of a new metallo-beta-lactamase gene, *bla*(NDM-1), and a novel erythromycin esterase gene carried on a unique genetic structure in *Klebsiella pneumoniae* sequence type 14 from India. *Antimicrob. Agents Chemother.* 53, 5046–5054. doi: 10.1128/aac.00774-09

Zankari, E., Hasman, H., Cosentino, S., Vestergaard, M., Rasmussen, S., Lund, O., et al. (2012). Identification of acquired antimicrobial resistance genes. *J. Antimicrob. Chemother.* 67, 2640–2644. doi: 10.1093/jac/dks261

Conflict of Interest: The authors declare that the research was conducted in the absence of any commercial or financial relationships that could be construed as a potential conflict of interest.

Publisher's Note: All claims expressed in this article are solely those of the authors and do not necessarily represent those of their affiliated organizations, or those of the publisher, the editors and the reviewers. Any product that may be evaluated in this article, or claim that may be made by its manufacturer, is not guaranteed or endorsed by the publisher.

Advantages of publishing in Frontiers

OPEN ACCESS
Articles are free to read for greatest visibility and readership

FAST PUBLICATION
Around 90 days from submission to decision

HIGH QUALITY PEER-REVIEW
Rigorous, collaborative, and constructive peer-review

TRANSPARENT PEER-REVIEW
Editors and reviewers acknowledged by name on published articles

Frontiers
Avenue du Tribunal-Fédéral 34
1005 Lausanne | Switzerland

Visit us: www.frontiersin.org
Contact us: frontiersin.org/about/contact

REPRODUCIBILITY OF RESEARCH
Support open data and methods to enhance research reproducibility

DIGITAL PUBLISHING
Articles designed for optimal readership across devices

FOLLOW US
@frontiersin

IMPACT METRICS
Advanced article metrics track visibility across digital media

EXTENSIVE PROMOTION
Marketing and promotion of impactful research

LOOP RESEARCH NETWORK
Our network increases your article's readership